

Miguel Orszag

Quantum Optics

Including Noise Reduction,
Trapped Ions, Quantum Trajectories,
and Decoherence

With 75 Figures
and 79 Problems with Hints for Solutions



Springer

Professor Dr. Miguel Orszag
Facultad de Física
Pontifical Catholic University of Chile
Casilla 306
22 Santiago
Chile
E-mail: morszag@chopin.fis.puc.cl

ISSN 1439-2674
ISBN 3-540-65008-3 Springer-Verlag Berlin Heidelberg New York

Library of Congress Cataloging-in-Publication Data.

Orszag, Miguel, 1944-, Quantum optics / Miguel Orszag. p. cm. Includes bibliographical references and index. ISBN 3-540-65008-3 (alk. paper) 1. Quantum optics. I. Title. QC446.2.078 1999 535'.15-dc21 99-33296 CIP

This work is subject to copyright. All rights are reserved, whether the whole or part of the material is concerned, specifically the rights of translation, reprinting, reuse of illustrations, recitation, broadcasting, reproduction on microfilm or in any other way, and storage in data banks. Duplication of this publication or parts thereof is permitted only under the provisions of the German Copyright Law of September 9, 1965, in its current version, and permission for use must always be obtained from Springer-Verlag. Violations are liable for prosecution under the German Copyright Law.

© Springer-Verlag Berlin Heidelberg 2000
Printed in Germany

The use of general descriptive names, registered names, trademarks, etc. in this publication does not imply, even in the absence of a specific statement, that such names are exempt from the relevant protective laws and regulations and therefore free for general use.

Data conversion by Steingraeber Satztechnik GmbH, Heidelberg
Cover design: *design & production* GmbH, Heidelberg

SPIN: 10691798 56/3144/mf - 5 4 3 2 1 0 - Printed on acid-free paper

Quantum Optics

Springer
Berlin
Heidelberg
New York
Barcelona
Hong Kong
London
Milan
Paris
Singapore
Tokyo

Advanced Texts in Physics

This program of advanced texts covers a broad spectrum of topics which are of current and emerging interest in physics. Each book provides a comprehensive and yet accessible introduction to a field at the forefront of modern research. As such, these texts are intended for senior undergraduate and graduate students at the MS and PhD level; however, research scientists seeking an introduction to particular areas of physics will also benefit from the titles in this collection.

To all those who gave me their support and wisdom.

My parents

Ladislao Orszag (1911–1984)

Isabel Posa (1908–1999)

and

Martita.

Preface

This graduate text originated from lectures given by the author at the Universidad Católica de Chile in Santiago, as well as at the University of New Mexico. Also, material has been drawn from short summer courses given in Rio de Janeiro and Caracas.

Chapter 1 is devoted to some basic ideas of the interaction of radiation and matter, starting from Einstein's ideas of emission and absorption, and ending with elementary laser theory.

The quantum mechanical description of the atom-radiation interaction is dealt with in Chap. 2, and includes Rabi's oscillations and Bloch's equations.

Chapter 3 contains the basic quantization of the electromagnetic field, while Chaps. 4, 5 and 6 study special states of the electromagnetic field and the quantum theory of coherence.

The Jaynes-Cummings model, which describes in a fully quantized manner, the atom-radiation interaction, is studied in Chap. 8, along with the phenomena of collapse and revival. We also introduce the dressed state description, which is useful when studying resonance fluorescence (Chap. 10).

Real physical systems are open, that is, one must always consider dissipative mechanisms, including electromagnetic losses in cavity walls or atomic decay. All these effects can be considered in great detail, by studying system-reservoir interactions, leading to the master and Fokker-Planck equations. These reservoirs can also be phase dependent, an effect that can modify the decay rate of an atom (Chap. 9). As we mentioned before, Chap. 10 is entirely devoted to resonance fluorescence, and the study and observation of photon antibunching.

The invention of the laser, in the 1960s, opened up a new area of research, baptized quantum optics. This discovery spurred the growth of new research fields such as non-linear optics and non-linear spectroscopy. First the semiclassical theory, and then the quantum theory of the laser was well developed by the late 1960s. The quantum theory of the laser, based on the master equation and the Langevin equation approach, is extensively treated in Chaps. 11 and 12, respectively. We have also added some more recent material, including the micromaser and the effect of pump statistics, as a form of noise reduction scheme. Although pump statistics did not play any role in the original laser theory, recent experiments and theoretical calculations have

shown that one could reduce considerably the photon number fluctuations if one is careful enough in pumping the atoms in an orderly way.

We further study quantum noise reduction in correlated emission lasers and the generation of squeezed states, typically from a parametric oscillator. These subjects are studied in Chaps. 13 and 14 respectively. In Chap. 14 we also introduce the input–output theory, which is very appropriate for describing the parametric oscillator and other non-linear optical systems.

Quantum phase, which started with Dirac, is a controversial subject, even today (Chap. 15). Most of the time optical experiments deal with direct or indirect measurement of a phase. For this reason, I felt it was important to include it in this book, even if it may not be a mature subject.

The last five chapters deal with more recent topics in quantum and atom optics. The Monte Carlo method and the stochastic Schrödinger equation (Chap. 16) are recent tools that have been used to attack optical problems with losses. Theoretically, it takes a different point of view from the more traditional way via the master or Fokker–Planck equations, and it is convenient for practical simulations.

Measurements in optics, and physics in general, play a central role. This was recognized early in the history of quantum mechanics. We introduce the reader to the notions of quantum standard limits and quantum non-demolition measurements (Chap. 18). A detailed example is studied in connection with the QND measurement of the photon number in a cavity. Continuous measurements are also studied. A related subject, decoherence (Chap. 20), is quite relevant for quantum computing. This intriguing phenomenon is connected with dissipation and measurement.

Finally, although a bit outside the scope of quantum optics, we have included the topics of atom optics (Chap. 17) and trapped ions (Chap. 19). These are fast-growing areas of research.

Over the years I have collaborated with many colleagues and students, who directly or indirectly contributed to this work; in particular: G.S. Agarwal, Claus Benkert, Janos Bergou, Wilhelm Becker, Luiz Davidovich, Mary Fuka, Mark Hillery, T. Kist, María Loreto Ladron de Guevara, Jack. K. McIver, Douglas Mundarain, L.M. Narducci, Ricardo Ramírez, Juan Carlos Retamal, Luis Roa, Jaime Röessler, Bernd Rohwedder, Carlos Saavedra, Wolfgang Schleich, Marlan O. Scully, D.F. Walls, Herbert Walther, K. Wodkiewicz, Nicim Zagury, F.X. Zhao, Sh.Y Zhu. I thank them all.

I want to thank Prof. Juan Carlos Retamal and Mr E. Massoni for reading and correcting the whole manuscript, Dr. H. Lotsch for the encouragement to write this book, as well as Dr. H.J. Kölsch, Dr. Victoria Wicks, Ms Jacqueline Lenz, Ms Friedhilde Meyer and the whole editorial team at Springer for a great job, and Prof. Hernan Chuaqui and Mr Jaime Fernandez for invaluable help with the computer generated figures and photography.

Finally, last but not least, I would like to thank my wife Marta Montoya (Martita) for her love and constant support during this project.

*No te escapes
Ahora
Ma ayudarás. Un dedo,
una palabra,
un signo
tuyo
y cuando
dedos, signos, palabras
caminen y trabajen
algo
aparecerá en el aire inmóvil,
un
solidario sonido en la ventana,
una estrella en la terrible paz nocturna,
entonces
tu dormirás tranquilo,
tu vivirás tranquilo:
será parte
del sonido que acude a tu ventana,
de la luz que rompió la soledad.*

From: Odas Elementales, Pablo Neruda [P.1]

Contents

1. Einstein's Theory of Atom–Radiation Interaction	1
1.1 The A and B Coefficients	1
1.2 Thermal Equilibrium	3
1.3 Photon Distribution and Fluctuations	3
1.4 Light Beam Incident on Atoms	4
1.5 Elementary Laser Theory	5
1.5.1 Threshold and Population Inversion	6
1.5.2 Steady State	6
1.5.3 Linear Stability Analysis	7
Problems	9
2. Atom–Field Interaction: Semiclassical Approach	11
2.1 Broad-Band Radiation Spectrum	14
2.2 Rabi Oscillations	15
2.3 Bloch's Equations	16
2.4 Decay to an Unobserved Level	17
2.5 Decay Between Levels	18
2.6 Optical Nutation	18
Problems	19
3. Quantization of the Electromagnetic Field	21
3.1 Fock States	24
3.2 Density of Modes	25
3.3 Commutation Relations	26
Problems	27
4. States of the Electromagnetic Field I	29
4.1 Further Properties	30
4.1.1 Coherent States are Minimum Uncertainty States	30
4.1.2 Coherent States are not Orthogonal	30
4.1.3 Coherent States are Overcomplete	31
4.1.4 The Displacement Operator	31
4.1.5 Photon Statistics	32
4.1.6 Coordinate Representation	33

4.2 Mixed State. Thermal Radiation	33
Problems	35
5. States of the Electromagnetic Field II	39
5.1 Squeezed States. General Properties and Detection	39
5.1.1 The Squeeze Operator and the Squeezed State	41
5.1.2 The Squeezed State is an Eigenstate of A	42
5.1.3 Calculation of Moments with Squeezed States	42
5.1.4 Quadrature Fluctuations	43
5.1.5 Photon Statistics	44
5.2 Multimode Squeezed States	44
5.3 Detection of Squeezed States	45
5.3.1 Ordinary Homodyne Detection	46
5.3.2 Balanced Homodyne Detection	47
5.3.3 Heterodyne Detection	48
Problems	48
6. Quantum Theory of Coherence	51
6.1 One-Atom Detector	52
6.2 The n -Atom Detector	55
6.3 General Properties of the Correlation Functions	56
6.4 Young's Interference and First-Order Correlation	58
6.5 Second-Order Correlations. Photon Bunching and Antibunching	60
6.5.1 Classical Second-Order Coherence	60
6.5.2 Quantum Theory of Second-Order Coherence	62
6.6 Photon Counting	65
6.6.1 Some Simple Examples	68
6.6.2 Quantum Mechanical Photon Count Distribution	68
6.6.3 Particular Examples	69
Problems	70
7. Phase Space Description	71
7.1 Q -Representation. Antinormal Ordering	71
7.1.1 Normalization	71
7.1.2 Average of Antinormally Ordered Products	72
7.1.3 Some Examples	72
7.1.4 The Density Operator in Terms of the Function Q	73
7.2 Characteristic Function	74
7.3 P -Representation: Normal Ordering	74
7.3.1 Normalization	74
7.3.2 Averages of Normally Ordered Products	75
7.3.3 Some Interesting Properties	75
7.3.4 Some Examples	75
7.4 The Wigner Distribution: Symmetric Ordering	77

7.4.1 Moments	77
Problems	78
8. Atom-Field Interaction	81
8.1 Atom-Field Hamiltonian and the Dipole Approximation	81
8.2 A Two-Level Atom Interacting with a Single Field Mode	83
8.3 The Dressed State Picture. Quantum Rabi Oscillations	85
8.4 Collapse and Revivals	88
Problems	92
9. System-Reservoir Interactions	93
9.1 Quantum Theory of Damping	93
9.2 General Properties	96
9.3 Expectation Values of Relevant Physical Quantities	97
9.4 Time Evolution of the Density Matrix Elements	98
9.5 The Glauber-Sudarshan Representation and the Fokker-Planck Equation	100
9.6 Time-Dependent Solution. The Method of the Eigenfunctions	101
9.6.1 General Solution	103
9.7 Langevin's Equations	103
9.7.1 Calculation of the Correlation Function $\langle F(t')F(t'')^\dagger \rangle_B$	105
9.7.2 Differential Equation for the Photon Number	105
9.8 Other Master Equations	105
9.8.1 Two-Level Atom in a Thermal Bath	105
9.8.2 Damped Harmonic Oscillator in a Squeezed Bath	107
9.8.3 Application. Spontaneous Decay in a Squeezed Vacuum	109
Problems	110
10. Resonance Fluorescence	113
10.1 Background	113
10.2 Heisenberg's Equations	114
10.3 Spectral Density and the Wiener-Kinchine Theorem	118
10.4 Emission Spectra from Strongly Driven Two-Level Atoms ...	120
10.5 Intensity Correlations	123
Problems	127
11. Quantum Laser Theory. Master Equation Approach	129
11.1 Heuristic Discussion of Injection Statistics	131
11.2 Master Equation for Generalized Pump Statistics	131
11.3 The Quantum Theory of the Laser. Random Injection ($p = 0$)	133
11.3.1 Photon Statistics	134
11.3.2 The Fokker-Planck Equation. Laser Linewidth	137
11.3.3 Alternative Derivation of the Laser Linewidth	138

11.4 Quantum Theory of the Micromaser.	
Random Injection ($p = 0$)	140
11.4.1 The Micromaser.....	141
11.4.2 Trapping States	144
11.5 Quantum Theory of the Laser and the Micromaser	
with Pump Statistics ($p \neq 0$)	146
Problems	150
12. Quantum Laser Theory. Langevin Approach	151
12.1 Quantum Langevin Equations	151
12.1.1 Generalized Einstein Relations	152
12.1.2 Atomic Noise Moments	153
12.2 <i>C</i> -Number Langevin Equations.....	157
12.2.1 Adiabatic Approximation.....	158
12.3 Phase and Intensity Fluctuations	159
12.4 Discussion	160
Problems	162
13. Quantum Noise Reduction I	163
13.1 Correlated Emission Laser (CEL) Systems:	
The Quantum Beat Laser	164
13.1.1 The Model	164
13.1.2 The Solution.....	167
13.1.3 The Master Equation	167
13.1.4 Photon Statistics	169
13.2 Other CEL Systems	171
Problems	172
14. Quantum Noise Reduction II	173
14.1 Introduction to Non-linear Optics	173
14.1.1 Multiple Photon Transitions	173
14.2 Parametric Processes Without Losses	177
14.3 Input–Output Theory	179
14.4 The Degenerate Parametric Oscillator	183
14.5 Experimental Results	185
Problems	187
15. Quantum Phase	191
15.1 The Dirac Phase	191
15.2 The Louisell Phase	192
15.3 The Susskind–Glogower Phase	192
15.4 The Pegg–Barnett Phase	195
15.4.1 Applications	198
15.5 Phase Fluctuations in a Laser	200
Problems	203

16. Quantum Trajectories	205
16.1 Monte Carlo Wavefunction Method	206
16.1.1 The Monte Carlo Method is Equivalent, on Average, to the Master Equation	207
16.2 The Stochastic Schrödinger Equation	209
16.3 Stochastic Schrödinger Equations and Dissipative Systems ..	211
16.4 Simulation of a Monte Carlo SSE	213
16.5 Simulation of the Homodyne SSDE	218
16.6 Numerical Results and Localization	221
16.6.1 Evolution of Quantum Jumps	222
16.6.2 Diffusion-like Evolution	224
16.6.3 Analytical Proof of Localization	225
16.7 Conclusions	228
Problems	229
17. Atom Optics	231
17.1 Optical Elements	231
17.2 Atomic Diffraction from an Optical Standing Wave	232
17.2.1 Theory	233
17.2.2 Particular Cases	236
17.3 Atomic Focusing	239
17.3.1 The Model	240
17.3.2 Initial Conditions and Solution	241
17.3.3 Quantum and Classical Foci	242
17.3.4 Thin versus Thick Lenses	243
17.3.5 The Quantum Focal Curve	244
17.3.6 Aberrations	245
Problems	246
18. Measurements, Quantum Limits and all That	247
18.1 Quantum Standard Limit	247
18.1.1 Quantum Standard Limit for a Free Particle	247
18.1.2 Standard Quantum Limit for an Oscillator	248
18.1.3 Thermal Effects	249
18.2 Quantum Non-demolition (QND) Measurements	250
18.2.1 The Free System	250
18.2.2 Monitoring a Classical Force	252
18.2.3 Effect of the Measuring Apparatus or Probe	253
18.3 QND Measurement of the Number of Photons in a Cavity ..	253
18.3.1 The Model	253
18.3.2 The System-Probe Interaction	255
18.3.3 Measuring the Atomic Phase with Ramsey Fields	255
18.3.4 QND Measurement of the Photon Number	259
18.4 Quantum Theory of Continuous Photodetection Processes ..	261

18.4.1 Continuous Measurement in a Two-Mode System. Phase Narrowing	263
Problems	267
19. Trapped Ions	269
19.1 Paul Trap	269
19.1.1 Stability Analysis	272
19.2 The Trapped Ion in the Raman Scheme	276
19.2.1 The Model and the Effective Hamiltonian	276
19.2.2 The Lamb–Dicke Expansion and Raman Cooling	281
19.2.3 The Dynamical Evolution	282
19.2.4 QND Measurements of Vibrational States	285
19.2.5 Generation of Non-classical Vibrational States	288
Problems	289
20. Decoherence	291
20.1 Dynamics of the Correlations	293
20.2 How Long Does it Take to Decohere?	295
Problems	299
A. Operator Relations	301
A.1 Theorem 1.....	301
A.2 Theorem 2. The Baker–Campbell–Haussdorf Relation	302
A.3 Theorem 3. Similarity Transformation	303
B. The Method of Characteristics	305
C. Proof of Eq. (12.37)	309
D. Stochastic Processes in a Nutshell	311
D.1 Introduction	311
D.2 Probability Concepts.....	312
D.3 Stochastic Processes	313
D.3.1 The Chapman–Kolmogorov Equation	313
D.4 The Fokker–Planck Equation	316
D.4.1 The Wiener Process	317
D.4.2 General Properties of the Fokker–Planck Equation....	319
D.4.3 Steady State Solution	319
D.5 Stochastic Differential Equations	320
D.5.1 Ito versus Stratonovich Calculus.....	322
D.5.2 Ito’s Formula	324
D.6 Approximate Methods	325
E. Derivation of the Homodyne Stochastic Schrödinger Differential Equation	329

F. Fluctuations	333
Hints for Solutions of Problems.....	335
References	340
Index	355

1. Einstein's Theory of Atom–Radiation Interaction

In 1917, Einstein formulated a theory of spontaneous stimulated emission and absorption, based on purely phenomenological considerations [1.1]. His results paved the way for an understanding, in a qualitative way, of the basic ingredients of the atom–radiation interaction, and could be useful for describing the processes of absorption, light scattering by atoms, stimulated emission in a variety of laser and maser systems, etc. This happened after Planck found that the spectral distribution of blackbody radiation could be explained by quantizing the energy [1.2], and Einstein had explained the photoelectric effect [1.3] by postulating the existence of energy packets that were later called *photons*.

Einstein's theory is based on reasonable postulates, which will be justified more rigorously later, when we treat the same problem using quantum mechanics. The present arguments are of a heuristic nature [1.1]:

'Recently I found a derivation of Planck's radiation formula which is based upon the basic assumption of quantum theory and which is related to Wien's original consideration: in this derivation, the relationship between the Maxwell distribution and the chromatic black-body distribution plays a role. The derivation is of interest not only because it is simple, but especially because it seems to clarify somewhat the at present unexplained phenomena of emission and absorption of radiation by matter. I have shown, on the basis of a few assumptions, about emission and absorption of radiation by molecules, which are closely related to quantum theory, that molecules distributed in temperature equilibrium over states, in a way which is compatible with quantum theory, are in dynamic equilibrium with Planck's radiation. In this way, I deduced in a remarkably simple and general manner, Planck's formula.' [1.4]

1.1 The A and B Coefficients

We assume a closed cavity with N identical atoms, with two relevant bound-state energy levels, which we shall label E_b and E_a and which are quasi-

resonant with the thermal radiation produced by the cavity walls at a given temperature. Let

$$\hbar\omega = E_a - E_b. \quad (1.1)$$

We will also assume that there is an external source of electromagnetic energy, for example, a light beam crossing the cavity, and we may be interested in the scattering losses of such a beam.

The average energy density (over a cycle) can be written as

$$U(\omega) = U_T(\omega) + U_E(\omega). \quad (1.2)$$

The total energy density, will, in general be a function of position and frequency however, for the sake of simplicity, we consider it to be *only a slow varying function of frequency*. The labels T and E refer to thermal and external sources.

Energy-conserving processes are: spontaneous emission of a photon, stimulated emission and absorption, as shown in Fig. 1.1.

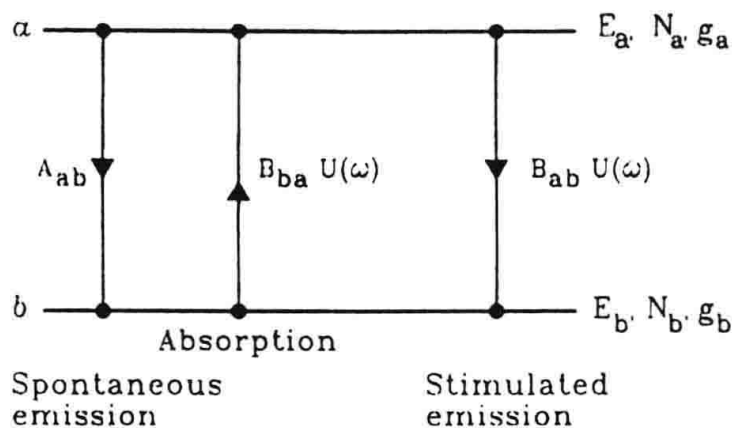


Fig. 1.1. The three processes in the atom-field interaction. Absorption, stimulated emission and spontaneous emission

Let A_{ab} be the probability per unit time for the atom to spontaneously decay from level a to b , emitting a photon of energy $\hbar\omega$. On the other hand, if the atom is in state b , there will be a probability/time for absorption which will be *proportional* to the electromagnetic energy present in the cavity, that is the absorption rate will be $B_{ba}U(\omega)$. The two processes described above are quite reasonable.

Now, Einstein proposed that in order to rediscover Planck's radiation law, *it is absolutely necessary to assume a third type of process called stimulated emission*, and the corresponding rate is defined as $B_{ab}U(\omega)$. For now, we will consider A_{ab} , B_{ba} , and B_{ab} , as phenomenological constants.

We can now write a rate equation. Calling N_b and N_a the populations of the lower and upper levels, respectively, and $N_b + N_a = N$, N being the total number of atoms, then

$$\frac{dN_b}{dt} = -\frac{dN_a}{dt} = \underbrace{A_{ab}N_a + B_{ab}U(\omega)N_a}_{,} - \underbrace{N_bB_{ba}U(\omega)}_{,} \quad (1.3)$$

where the terms grouped in the first curly bracket represent the emission and in the second, the absorption.

1.2 Thermal Equilibrium

We will consider the equilibrium condition in (1.3), that is,

$$\frac{dN_b}{dt} = 0, \quad (1.4)$$

so that if we have only thermal electromagnetic energy ($U_E = 0$) then

$$U_T(\omega) = \frac{A_{ab}}{B_{ab}[(B_{ba}g_b)/(B_{ab}g_a)\exp(\beta\hbar\omega) - 1]}, \quad (1.5)$$

where we have assumed a Boltzmann distribution for the level populations, weighted with their respective degeneracies g_b and g_a :

$$\frac{N_b}{N_a} = \frac{g_b \exp(-\beta E_b)}{g_a \exp(-\beta E_a)} = \frac{g_b}{g_a} \exp(\beta\hbar\omega). \quad (1.6)$$

Comparison of (1.5) with Planck's blackbody energy distribution:

$$U_T(\omega) \Big|_{\text{Planck}} = \frac{\hbar\omega^3}{\pi^2 c^3 (\exp(\beta\hbar\omega) - 1)} \quad (1.7)$$

gives us

$$\frac{B_{ba}}{B_{ab}} \frac{g_b}{g_a} = 1, \quad (1.8)$$

$$\frac{\hbar\omega^3}{\pi^2 c^3} = \frac{A_{ab}}{B_{ab}}. \quad (1.9)$$

From (1.8), (1.9), we can see that there are two equations for three coefficients, that is, only one of them is independent.

1.3 Photon Distribution and Fluctuations

If we quantize the thermal photons as

$$E_n = n\hbar\omega, \quad (1.10)$$

then the probability of finding n photons at temperature T [$\beta = (k_B T)^{-1}$] is given by the usual Boltzmann factor

$$P_n = \frac{\exp(-\beta E_n)}{\sum_n \exp(-\beta E_n)} = \exp(-\beta(n+1)\hbar\omega) [\exp(\beta\hbar\omega) - 1], \quad (1.11)$$

but since

$$\langle n \rangle = \frac{1}{\exp(\beta \hbar \omega) - 1}, \quad (1.12)$$

we finally get

$$P_n = \frac{\langle n \rangle^n}{(\langle n \rangle + 1)^{n+1}}, \quad (1.13)$$

which is the Bose-Einstein distribution for thermal photons.

We can also express P_n in terms of the level populations

$$P_n = \left(\frac{g_b N_a}{g_a N_b} \right)^n \left(1 - \frac{g_b N_a}{g_a N_b} \right) \quad (1.14)$$

thus showing that, if $g_b = g_a$, one cannot achieve population inversion by only thermal excitation of the atoms. ($N_a \leq N_b$ in order to have $0 \leq P_n \leq 1$). It is left to the reader to prove that

$$(\Delta n)^2 \equiv \langle n^2 \rangle - \langle n \rangle^2 = \langle n \rangle + \langle n \rangle^2. \quad (1.15)$$

In the next two sections, we will apply these simple ideas to atomic excitation by an external light source, and to elementary laser theory.

1.4 Light Beam Incident on Atoms

We assume here that we have a cavity filled with atoms interacting with an external light beam whose frequency is resonant with a pair of atomic levels, consistent with Einstein's description of the atom-radiation interaction. As we saw in a previous section, three important processes take place. One important fact is that stimulated emission from the excited atom tends to remain in the same electromagnetic mode, thus tending to amplify the incident radiation. On the other hand, spontaneous emission is isotropic in all spatial directions and independent of the direction of the incident beam [1.5].

If we neglect the spatial dependence of the radiation in the cavity (thin cavity), then $U = \text{constant}$ and one easily finds a solution for (1.3):

$$N_b(t) = \left(N_b^0 - \frac{N(A + BU)}{A + 2BU} \right) \exp[-(A + 2BU)t] + \frac{N(A + BU)}{A + 2BU} \quad (1.16)$$

where we have assumed $g_b = g_a = 1$, thus $B_{ba} = B_{ab} = B$ and N_b^0 is the initial population of the lower level.

In the particular case $N_b^0 = N$, that is, all the atoms are initially in the lower energy level, we have

$$\frac{N_a}{N} = \chi(1 - \exp(-\tau)) \quad (1.17)$$

with $\chi \equiv BU/(A + 2BU)$ and $\tau \equiv t(A + 2BU)$. In the steady state ($\tau \rightarrow \infty$), we have

$$\frac{N_a}{N} = \frac{1}{2 + A/BU}. \quad (1.18)$$

We notice again that even when the stimulated emission term (BU) is much stronger than the spontaneous emission term, by for example having a large energy on the external light beam, one can at best achieve equal population in the two levels.

If we now disconnect the external light source, (1.3) becomes

$$\frac{dN_a}{dt} = -N_a A; \quad (1.19)$$

thus $N_a(t) = N_a^0 \exp(-At)$, describing the exponential decay of the upper level population or spontaneous emission. The average lifetime of the upper level is $\tau_R = A^{-1}$.

1.5 Elementary Laser Theory

A simplified view of the process of amplification of light can be formulated based on Einstein's ideas on the fundamental processes in the atom-radiation interaction [1.6].

As in the previous sections, we consider two-level atoms, resonant with the electromagnetic field. Also, for the moment, we will neglect the effects of spontaneous emission. The corresponding rate equations are

$$\frac{dN_b}{dt} = -W_{ba}nN_b + W_{ab}nN_a, \quad (1.20)$$

$$\frac{dN_a}{dt} = W_{ba}nN_b - W_{ab}nN_a, \quad (1.21)$$

where n is the number of photons in the cavity and W_{ij} is the transition rate from level i to j .

We can also define the population difference $D = N_a - N_b$, which obeys

$$\frac{dD}{dt} = -2WnD \quad (1.22)$$

where we have set $W_{ba} = W_{ab} = W$, consistent with the previous arguments.

On the other hand, one also has a rate equation for the photons, namely,

$$\frac{dn}{dt} = WnD - \frac{n}{t_{cav}}, \quad (1.23)$$

where we have included the term $-n/t_{cav}$ to account for the photons coming out of the cavity (t_{cav} is the lifetime of the photons in the cavity).

The two coupled equations read

$$\frac{dD}{dt} = -2WnD - \frac{1}{T_1}(D - D_0), \quad (1.24)$$

$$\frac{dn}{dt} = WnD - \frac{n}{t_{cav}}.$$

In the first equation of (1.24), we have included a phenomenological term

$$-\frac{1}{T_1}(D - D_0)$$

which accounts for the spontaneous decay and pump action, T_1 being a characteristic lifetime associated with the decay of the population. Also D_0 is the equilibrium population in the absence of photons.

The equations given by (1.24) are called the laser rate equations. Although, as mentioned above, these equations, are a simplified version of the fully quantum mechanical laser theory, they do allow us to study some basic characteristics of laser action, such as the steady state, its stability and the laser threshold.

1.5.1 Threshold and Population Inversion

Assuming initially a low photon number (say 1), amplification of the number of photons will occur only if

$$\frac{dn}{dt} = \left(WD(0) - \frac{1}{t_{\text{cav}}} \right) > 0,$$

or, equivalently,

$$D(0) = D_0 > D_{\text{thresh}} = \frac{1}{Wt_{\text{cav}}}. \quad (1.25)$$

From the above analysis two conclusions can be drawn:

- (1) There is a laser threshold condition given in the inequalities (1.25). Laser action only takes place if the initial inversion is above the threshold value. Usually, the equilibrium population is equal to the initial one, so the inequality can be referred to the equilibrium value.
- (2) Clearly D_0 is positive which implies $N_a > N_b$, that is, population inversion is required, and it has to be enough to compensate for the cavity losses. One would like to have D_{thresh} as small as possible, which implies either t_{cav} or W large, or both. A large t_{cav} means that we need a high-quality optical cavity. On the other hand, high W implies that we need to choose a pair of levels with a large dipole moment.

1.5.2 Steady State

The steady state condition reads

$$2WnD + \frac{1}{T_1}(D - D_0) = 0, \quad (1.26)$$

$$n \left(WD - \frac{1}{t_{\text{cav}}} \right) = 0. \quad (1.27)$$

There are two possible solutions to the steady state equations:

(1) $n = 0, D = D_0$, which is the case of trivial equilibrium with the pump and no photons in the cavity;

(2)

$$D = \frac{1}{t_{\text{cav}} W} = D_{\text{thresh}}, \quad (1.28)$$

$$n = \frac{D_0 - D_{\text{thresh}}}{2WD_{\text{thresh}}T_1} = (D_0 - D_{\text{thresh}}) \frac{t_{\text{cav}}}{2T_1}. \quad (1.29)$$

A serious limitation of this model is that if $n(0) = 0$, then $n(t) = 0$, for all times. The laser does not get started even if $D_0 > D_{\text{thresh}}$. The reason for this limitation is the absence of quantum noise due to spontaneous emission, which was introduced in the present treatment in an *ad hoc* manner. Quantum laser theory does not have this limitation, since quantum noise and spontaneous emission appear in a natural way.

As we can see from (1.29), the only possibility of having a positive steady state photon number is if $D_0 > D_{\text{thresh}}$.

1.5.3 Linear Stability Analysis

If we call n_∞ and D_∞ the steady state values, then we can write these quantities as their steady state value plus a small deviation, that is,

$$n(t) = n_\infty + \varepsilon_n(t), \quad (1.30)$$

$$D(t) = D_\infty + \varepsilon_D(t). \quad (1.31)$$

Linearizing (1.24), up to order ε , we easily get

$$\begin{aligned} \frac{d\varepsilon_D}{dt} &= -2W(n_\infty \varepsilon_D + D_\infty \varepsilon_n) - \frac{1}{T_1} \varepsilon_D, \\ \frac{d\varepsilon_n}{dt} &= W(n_\infty \varepsilon_D + D_\infty \varepsilon_n) - \frac{\varepsilon_n}{t_{\text{cav}}}. \end{aligned} \quad (1.32)$$

We now look for a solution of the form

$$\begin{pmatrix} \varepsilon_D \\ \varepsilon_n \end{pmatrix} = \exp(\lambda t) \begin{bmatrix} \varepsilon_D(0) \\ \varepsilon_n(0) \end{bmatrix}, \quad (1.33)$$

and get two algebraic coupled equations

$$\left(\lambda + 2Wn_\infty + \frac{1}{T_1} \right) \varepsilon_D(0) + 2WD_\infty \varepsilon_n(0) = 0, \quad (1.34)$$

$$-Wn_\infty \varepsilon_D(0) + \left(\lambda - WD_\infty + \frac{1}{t_{\text{cav}}} \right) \varepsilon_n(0) = 0. \quad (1.35)$$

From (1.34), (1.35), we get the secular equation

$$\left(\lambda + 2Wn_{\infty} + \frac{1}{T_1} \right) \left(\lambda - WD_{\infty} + \frac{1}{t_{\text{cav}}} \right) + 2W^2 n_{\infty} D_{\infty} = 0. \quad (1.36)$$

In order to have a stable solution, one must have

$$\operatorname{Re}\{\lambda_j\} < 0 \quad \text{for } j = 1, 2.$$

Case (1) ($D = D_0, n = 0$):

$$\lambda_1 = -\frac{1}{T_1}, \quad (1.37)$$

$$\lambda_2 = WD_0 - \frac{1}{t_{\text{cav}}}, \quad (1.38)$$

therefore, the above solution is stable only if $WD_0 - 1/t_{\text{cav}} < 0$, that is for the laser below threshold. On the other hand, for $WD_0 - 1/t_{\text{cav}} > 0$, the $n = 0$ solution becomes unstable.

Case (2):

The two roots are

$$\lambda_{1,2} = \frac{1}{2} \left\{ -\frac{D_0}{D_{\text{thresh}} T_1} \pm \left[\left(\frac{D_0}{D_{\text{thresh}} T_1} \right)^2 - \frac{4W(D_0 - D_{\text{thresh}})}{T_1} \right]^{1/2} \right\}. \quad (1.39)$$

It is evident that the solution is stable only if $D_0 > D_{\text{thresh}}$.

This stability analysis is shown pictorially in Fig. 1.2.

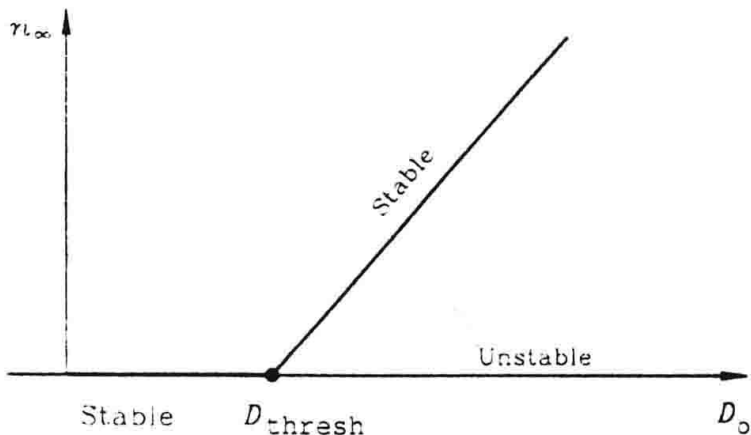


Fig. 1.2. Behaviour of the steady state photon number versus population

Problems

- 1.1. Prove the thermal photon distribution given by (1.13).
- 1.2. Prove that, for a thermal distribution, the correct expression for fluctuations of the photon number is given by (1.15).
- 1.3. Verify that for $U = \text{constant}$, the solution of (1.3) is given by (1.16).

2. Atom-Field Interaction: Semiclassical Approach

In this chapter, we study the resonant interaction between atoms and light. Bloch's equations are derived and, by adding a relaxation term, various decay effects are included.

We describe here various aspects that appear in the interaction between a collection of atoms or molecules and light. The basic phenomena may be understood using exactly soluble models and they are often excellent approximations of real experiments. The so-called semiclassical models, such as those presented in this chapter, describe a classical field interacting with quantum mechanical atoms. A fully quantum mechanical model is described later in Chap. 8. Furthermore, here we will deal with quasi-resonant phenomena, where the electromagnetic field frequency almost coincides with the energy difference between a pair of atomic levels. In this context, we will often use the concept of a 'two-level atom'.

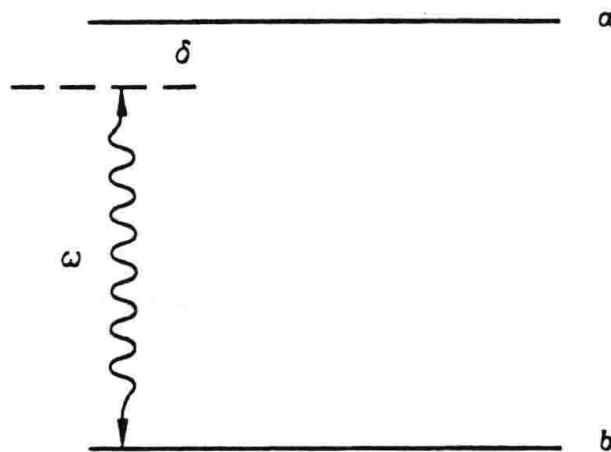


Fig. 2.1. Quasi-resonant interaction between a two-level atom and electromagnetic radiation, with a detuning δ

This situation is described in Fig. 2.1. The two-level atom is characterized by the ground state $|b\rangle$ and an excited state $|a\rangle$ with energies $\hbar\omega_b$ and $\hbar\omega_a$. The detuning δ is defined by:

$$\delta \equiv (\omega_a - \omega_b) - \omega = \omega_{ab} - \omega. \quad (2.1)$$

The strength of the interaction is usually measured by the so-called Rabi frequency which depends, at resonance, on the square root of the number of photons.

For the calculation of the transition rates, consider an atom interacting with a sinusoidal field:

$$\mathbf{E}(t) = \mathbf{e}E_0 \cos \omega t, \quad (2.2)$$

which is switched on at $t = 0$. \mathbf{e} represents the unit vector along the direction of polarization of the field. We will show that the presence of higher excited states can be neglected, when the transition frequencies are very different from ω .

We start with the time-dependent Schrödinger equation:

$$i\hbar \frac{\partial \psi}{\partial t} = (H_0 + H')\psi. \quad (2.3)$$

Here H_0 represents the time-independent Hamiltonian of the free atom and H' is the time-dependent atomic field interaction, which in the electric dipole approximation can be written as (e being negative for the electron)

$$H' = -e\mathbf{E} \cdot \mathbf{r} = -eE_0(\mathbf{e} \cdot \mathbf{r}) \cos \omega t. \quad (2.4)$$

Since H_0 is the Hamiltonian of the free atom, one can write

$$i\hbar \frac{\partial \Psi}{\partial t} = (H_0)\Psi, \quad (2.5)$$

with solutions of the form

$$\Psi = \psi_n(\mathbf{r}) \exp\left(\frac{-iE_n t}{\hbar}\right), \quad (2.6)$$

where $\psi_n(\mathbf{r})$ and E_n are the eigenfunctions and eigenvalues of H_0 :

$$H_0\psi_n(\mathbf{r}) = E_n\psi_n(\mathbf{r}). \quad (2.7)$$

The functions $\psi_n(\mathbf{r})$ satisfy the usual orthonormality conditions

$$\int d\mathbf{r} \psi_n^*(\mathbf{r}) \psi_m(\mathbf{r}) = \delta_{nm}. \quad (2.8)$$

The above wavefunctions will serve as a convenient basis in which to expand the wavefunction of the time-dependent problem

$$\psi(\mathbf{r}, t) = \sum_n C_n(t) \psi_n(\mathbf{r}) \exp(-i\omega_n t). \quad (2.9)$$

with

$$\omega_n \equiv \frac{E_n}{\hbar}.$$

Substituting (2.9) in (2.3) we get

$$\begin{aligned} i\hbar \sum_n \left(\frac{dC_n}{dt} - i\omega_n C_n \right) \psi_n(\mathbf{r}) \exp(-i\omega_n t) \\ = \sum_n E_n C_n \psi_n(\mathbf{r}) \exp(-i\omega_n t) \\ - eE_0(\mathbf{e} \cdot \mathbf{r}) \sum_n C_n \psi_n(\mathbf{r}) \exp(-i\omega_n t) \cos \omega t. \end{aligned} \quad (2.10)$$

The second term on the left-hand side cancels the first term on the right-hand side, thus getting, after multiplication by ψ_m^* on the left and integration,

$$i\hbar \frac{dC_m}{dt} = \frac{E_0}{2} \sum_n d_{mn} C_n(t) [\exp i(\omega_{mn} + \omega)t + \exp i(\omega_{mn} - \omega)t], \quad (2.11)$$

where

$$\begin{aligned} \omega_{mn} &= \omega_m - \omega_n = \frac{1}{\hbar}(E_m - E_n), \\ d_{mn} &= |e| \int d\mathbf{r} \psi_m^*(\mathbf{r})(\mathbf{e} \cdot \mathbf{r}) \psi_n(\mathbf{r}). \end{aligned} \quad (2.12)$$

Now let us assume that initially the atom is in the state $\psi_k(\mathbf{r})$; in other words:

$$\begin{aligned} C_k(t=0) &= 1, \\ C_n(t=0) &= 0, \quad n \neq k. \end{aligned} \quad (2.13)$$

As a first approximation, we replace $C_n(t)$ by $C_n(0)$ in (2.11), getting

$$i\hbar \frac{dC_m}{dt} = \frac{E_0}{2} d_{mk} [\exp i(\omega_{mk} + \omega)t + \exp i(\omega_{mk} - \omega)t], \quad (2.14)$$

and integrating

$$\begin{aligned} C_m(t) - C_m(0) &= -\frac{E_0}{2\hbar} d_{mk} \left[\frac{\exp i(\omega_{mk} + \omega)t - 1}{(\omega_{mk} + \omega)} \right. \\ &\quad \left. + \frac{\exp i(\omega_{mk} - \omega)t - 1}{(\omega_{mk} - \omega)} \right], \end{aligned} \quad (2.15)$$

and for $m \neq k$ we get

$$\begin{aligned} C_m(t) &= -i \frac{E_0}{\hbar} d_{mk} \left\{ \exp \left[i(\omega_{mk} + \omega) \frac{t}{2} \right] \frac{\sin \frac{1}{2}(\omega_{mk} + \omega)t}{(\omega_{mk} + \omega)} \right. \\ &\quad \left. + \exp \left[i(\omega_{mk} - \omega) \frac{t}{2} \right] \frac{\sin \frac{1}{2}(\omega_{mk} - \omega)t}{(\omega_{mk} - \omega)} \right\}. \end{aligned} \quad (2.16)$$

As we can easily see from the Fig. 2.2, the function:

$$\frac{1}{(\omega_{mk} - \omega)} \sin \frac{(\omega_{mk} - \omega)t}{2} \quad (2.17)$$

is sharply peaked around $\omega_{mk} \simeq \omega$, for large t .

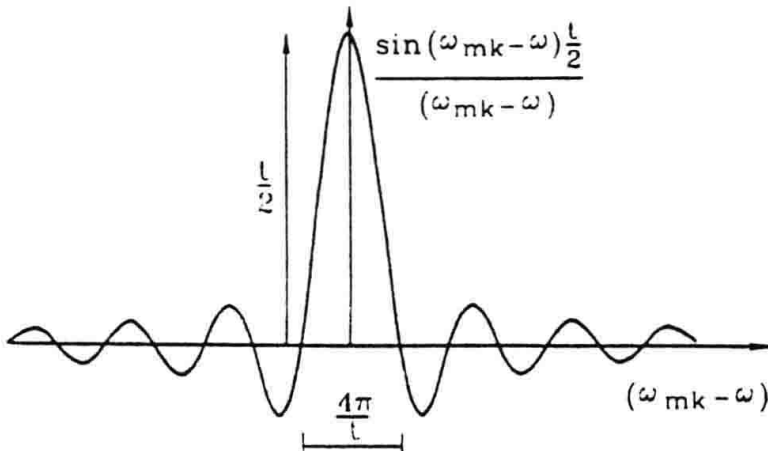


Fig. 2.2. The function $[\sin \frac{1}{2}(\omega_{mk} - \omega)t]/(\omega_{mk} - \omega)$ is sharply peaked around $\omega = \omega_{mk}$

As we can see from the above discussion, for those states with ω_{mk} very different from ω , the transition probability is indeed very small, thus justifying the two-level approximation [2.1].

In (2.17), ω_{mk} is negative for emission and positive for absorption, thus the main contribution comes from the first term in the first case and from the second term for absorption.

Now we return to the two-level model of Fig. 2.1, and assume that initially the atom is in its lower level b . The transition probability to a is

$$|C_a(t)|^2 = \frac{|d_{ab}|^2 E_0^2}{4\hbar^2} \left(\frac{\sin \frac{1}{2}(\omega_{ab} - \omega)t}{\frac{1}{2}(\omega_{ab} - \omega)} \right)^2. \quad (2.18)$$

The result given in (2.18) is approximate, and represents, for $|C_a(t)|^2 \ll 1$, the probability for stimulated absorption.

2.1 Broad-Band Radiation Spectrum

Now we modify our previous analysis by considering broad-band light, rather than monochromatic light. Since the average electromagnetic energy density per unit volume is $\frac{1}{2}\epsilon_0 E_0^2$, and since $U(\omega)$ is the spectral energy, such that $U(\omega)d\omega$ represents the field energy per unit volume and in the frequency interval ω and $\omega + d\omega$, we just replace E_0^2 by $2U(\omega)d\omega/\epsilon_0$ and integrate over the spectrum, getting

$$|C_a(t)|^2 = \frac{|d_{ab}|^2}{2\epsilon_0 \hbar^2} \int d\omega U(\omega) \left(\frac{\sin \frac{1}{2}(\omega_{ab} - \omega)t}{\frac{1}{2}(\omega_{ab} - \omega)} \right)^2; \quad (2.19)$$

and assuming $U(\omega)$ to be slowly varying with ω , we get the approximate result:

$$\begin{aligned} |C_a(t)|^2 &\simeq \frac{|d_{ab}|^2}{2\epsilon_0\hbar^2} U(\omega_{ab}) \int d\omega \left(\frac{\sin \frac{1}{2}(\omega_{ab} - \omega)t}{\frac{1}{2}(\omega_{ab} - \omega)} \right)^2, \\ &= \frac{\pi |d_{ab}|^2}{\epsilon_0\hbar^2} U(\omega_{ab})t. \end{aligned} \quad (2.20)$$

From (2.20) we see that the absorption probability per unit time is proportional to the energy density, as in Einstein's theory. In order to get the B coefficient, we have to average over all directions, since:

$$\begin{aligned} \overline{|d_{ab}|^2} &\sim \left| |e| \int d\mathbf{r} \psi_a^*(\mathbf{r}) (\overline{\mathbf{e} \cdot \mathbf{r}}) \psi_b(\mathbf{r}) \right|^2 \\ &\sim \left| |e| \int d\mathbf{r} \psi_a^*(\mathbf{r}) \mathbf{r} \psi_b(\mathbf{r}) \right|^2 \frac{1}{\cos^2 \theta} \\ &\sim \left| \left[|e| \int d\mathbf{r} \psi_a^*(\mathbf{r}) \mathbf{r} \psi_b(\mathbf{r}) \right] \right|^2 \frac{1}{3}, \end{aligned}$$

so finally

$$\frac{|C_a(t)|^2}{t} = \frac{\pi p_{ab}^2}{3\epsilon_0\hbar^2} U(\omega_{ab}) \equiv B_{ba} U(\omega_{ab}), \quad (2.21)$$

$$p_{ab}^2 = \left| |e| \int d\mathbf{r} \psi_a^*(\mathbf{r}) \mathbf{r} \psi_b(\mathbf{r}) \right|^2, \quad (2.22)$$

and we may write

$$B_{ba} = \frac{\pi p_{ab}^2}{3\epsilon_0\hbar^2}. \quad (2.23)$$

2.2 Rabi Oscillations

Instead of the general expansion given in (2.9), consider two levels only:

$$\psi(\mathbf{r}, t) = C'_b(t) \psi_b(\mathbf{r}) \exp(-i\omega_b t) + C'_a(t) \psi_a(\mathbf{r}) \exp(-i\omega_a t). \quad (2.24)$$

Making use of (2.11) for this particular case, we get

$$\begin{aligned} i\hbar \frac{dC'_b}{dt} &= \frac{E_0 d_{ba}}{2} C'_a(t) \{ \exp[-i(\omega_{ab} - \omega)t] + \exp[-i(\omega_{ab} + \omega)t] \}, \\ i\hbar \frac{dC'_a}{dt} &= \frac{E_0 d_{ab}}{2} C'_b(t) [\exp i(\omega_{ab} - \omega)t + \exp i(\omega_{ab} + \omega)t]. \end{aligned} \quad (2.25)$$

Defining

$$C_{b,a} = \exp \left(\pm i \frac{\delta t}{2} \right) C'_{b,a},$$

and performing the rotating-wave approximation to neglect the rapidly varying term $\exp i(\omega_{ab} + \omega)t$ versus the term $\exp i(\omega_{ab} - \omega)t$, we find

$$\frac{dC_b}{dt} = -\frac{i}{2}(-\delta C_b + \frac{E_0 d_{ba}}{\hbar} C_a), \quad (2.26)$$

$$\frac{dC_a}{dt} = -\frac{i}{2}(\delta C_a + \frac{E_0 d_{ab}}{\hbar} C_b). \quad (2.27)$$

We can write (2.26), (2.27) in the matrix form

$$\frac{d}{dt} \begin{bmatrix} C_b(t) \\ C_a(t) \end{bmatrix} = \frac{-i}{2} \begin{bmatrix} -\delta & \frac{E_0 d_{ba}}{\hbar} \\ \frac{E_0 d_{ab}}{\hbar} & \delta \end{bmatrix} \begin{bmatrix} C_b(t) \\ C_a(t) \end{bmatrix}. \quad (2.28)$$

The eigenvalues of (2.28) are $\mp R$, where

$$R \equiv \sqrt{\delta^2 + |R_0|^2}, \quad (2.29)$$

$$R_0 \equiv \frac{E_0 d_{ba}}{\hbar}.$$

Normally R_0 is referred to as the Rabi frequency [2.2, 2.3, 2.4].

The solution of (2.28) is:

$$\begin{bmatrix} C_b(t) \\ C_a(t) \end{bmatrix} = \begin{bmatrix} \cos \frac{Rt}{2} + \frac{i\delta}{R} \sin \frac{Rt}{2} & -i \frac{E_0 d_{ba}}{Rh} \sin \frac{Rt}{2} \\ -i \frac{E_0 d_{ab}}{Rh} \sin \frac{Rt}{2} & \cos \frac{Rt}{2} - \frac{i\delta}{R} \sin \frac{Rt}{2} \end{bmatrix} \begin{bmatrix} C_b(0) \\ C_a(0) \end{bmatrix}. \quad (2.30)$$

To take a simple example, if we start from the lower state [$C_b(0) = 1$], the transition probability for absorption is:

$$|C_a(t)|^2 = \left| \frac{R_0}{R} \right|^2 \sin^2 \frac{Rt}{2}. \quad (2.31)$$

2.3 Bloch's Equations

Equations (2.25) describe exactly the interaction between a two-level atom and the radiation field:

$$\begin{aligned} i \frac{dC'_b}{dt} &= R_0 C'_a(t) \exp(-i\omega_{ab}t) \cos \omega t, \\ i \frac{dC'_a}{dt} &= R_0^* C'_b(t) \exp(i\omega_{ab}t) \cos \omega t. \end{aligned} \quad (2.32)$$

A general treatment involves the density matrix.

Define

$$\rho_{bb} = |C'_b|^2, \quad (2.33)$$

$$\rho_{aa} = |C'_a|^2,$$

$$\rho_{ba} = C'_b C'^*_a = \rho_{ab}^*.$$

Of course, the property $\text{Tr}\rho = 1$ is automatically satisfied since:

$$\rho_{bb} + \rho_{aa} = |C'_b|^2 + |C'_a|^2 = 1.$$

We differentiate ρ_{ij} with respect to time, getting

$$\frac{d\rho_{ij}}{dt} = C'_i \frac{dC_j'^*}{dt} + C_j'^* \frac{dC'_i}{dt}, \quad (2.34)$$

and substituting (2.32) into (2.34), we get (making use of the rotating-wave approximation)

$$\begin{aligned} \frac{d\rho_{aa}}{dt} &= -\frac{d\rho_{bb}}{dt} \\ &= -\frac{i}{2} R_0^* \exp [i(\omega_{ab} - \omega)t] \rho_{ba} + \frac{i}{2} R_0 \exp [-i(\omega_{ab} - \omega)t] \rho_{ab}, \\ \frac{d\rho_{ba}}{dt} &= \frac{d\rho_{ab}^*}{dt} = \frac{i}{2} R_0 \exp [-i(\omega_{ab} - \omega)t] (\rho_{bb} - \rho_{aa}). \end{aligned} \quad (2.35)$$

Equations (2.35) are the **optical Bloch equations**.

In order to introduce dissipative effects, we can modify (2.11):

$$\begin{aligned} i\hbar \frac{dC_m}{dt} &= \frac{E_0}{2} \sum_n d_{mn} C_n(t) \{ \exp [i(\omega_{mn} + \omega)t] \\ &\quad + \exp [i(\omega_{mn} - \omega)t] \} \\ &\quad - i\hbar \frac{\gamma_m}{2} C_m, \end{aligned} \quad (2.36)$$

where we have added a relaxation term. In the absence of coupling, the relaxation term will generate a solution

$$|C_m(t)|^2 = |C_m(0)|^2 \exp(-\gamma_m t). \quad (2.37)$$

Obviously such a decay constant in Schrödinger's equation does not preserve the norm.

2.4 Decay to an Unobserved Level

The effect on the density matrix is as follows

$$\begin{aligned} \frac{d\rho_{ij}}{dt} &= C'_i \frac{dC_j'^*}{dt} + C_j'^* \frac{dC'_i}{dt} \\ &= ()_{\text{nondissipation}} - \frac{\gamma_i + \gamma_j}{2} \rho_{ij}. \end{aligned} \quad (2.38)$$

For population levels, this leads to an exponential decay $\rho_{ii}(t) \propto \exp(-\gamma_i t)$.

As the spontaneous decay process will emit a photon, we find that the number of spontaneously emitted photons will be proportional to $\gamma_i \rho_{ii}$, and the intensity of spontaneously emitted photons will be a measure of the decaying level.

2.5 Decay Between Levels

If we consider spontaneous emission between two levels (Fig. 2.1), then the upper state will decay as:

$$\frac{d}{dt} \rho_{aa} = -\gamma \rho_{aa}. \quad (2.39)$$

On the other hand, this event will increase the population in level b , so:

$$\frac{d}{dt} \rho_{bb} = \gamma \rho_{bb}. \quad (2.40)$$

The calculation of γ comes from a quantum electrodynamical theory called the Wigner-Weisskopf theory, which will be covered in a later chapter. It involves the interaction of an atom with an infinite number of harmonic oscillators, at zero temperature, which is in the vacuum state.

On the other hand, the off-diagonal term will decay as

$$\frac{d}{dt} \rho_{ab} = -\frac{\gamma}{2} \rho_{ab}. \quad (2.41)$$

Equation (2.41) can be proven with a fully quantum mechanical analysis.

The Bloch equations with losses can be written as

$$\begin{aligned} \frac{d\rho_{aa}}{dt} &= -\frac{i}{2} R_0^* \exp [i(\omega_{ab} - \omega)t] \rho_{ba} + \frac{i}{2} R_0 \exp [-i(\omega_{ab} - \omega)t] \rho_{ab} \\ -\gamma \rho_{aa} &= -\frac{d\rho_{bb}}{dt}, \\ \frac{d\rho_{ba}}{dt} &= \frac{d\rho_{ab}^*}{dt} = \frac{i}{2} R_0 \exp [-i(\omega_{ab} - \omega)t] (\rho_{bb} - \rho_{aa}) - \frac{\gamma'}{2} \rho_{ba}, \end{aligned} \quad (2.42)$$

where $T_1 = 1/\gamma$ is the longitudinal relaxation time and $T_2 = 2/\gamma'$ is the transverse relaxation time, and $\gamma' = \gamma + \gamma_{\text{coll}}$, and we have introduced the collision frequency γ_{coll} in an *ad hoc* manner.

2.6 Optical Nutation

An interesting case that has an exact solution is when $\omega_{ab} = \omega$ and initially $\rho_{aa} = \rho_{ba} = 0$. The solution in this case is

$$\begin{aligned} \rho_{aa}(t) &= \frac{|R_0|^2/2}{\gamma^2/2 + |R_0|^2} \left[1 - \left(\cos \lambda t + \frac{3\gamma}{4\lambda} \sin \lambda t \right) \exp -\frac{3\gamma t}{4} \right], \\ \lambda &\equiv \sqrt{|R_0|^2 - \frac{\gamma^2}{16}}. \end{aligned} \quad (2.43)$$

The result given in (2.43) is illustrated in Fig. 2.3. We notice that the oscillations occur when the Rabi frequency R_0 is much bigger than the damping γ .

An experimental demonstration of optical nutation was done by Gibbs [2.5]. The results are depicted in Fig. 2.4.

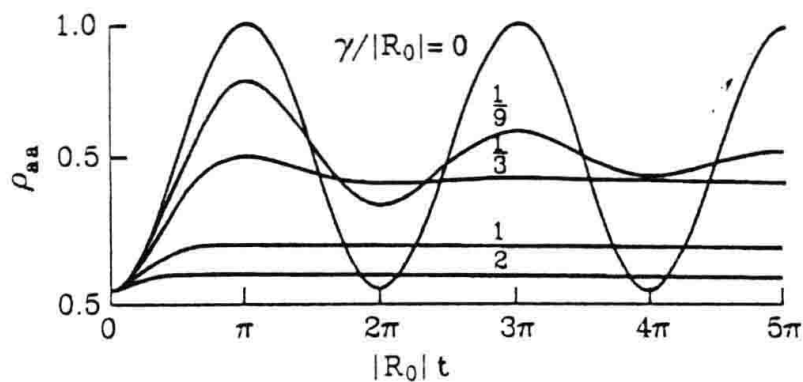


Fig. 2.3. Atomic population of the upper level versus time, for various ratios of γ/R_0 (after [1.5])

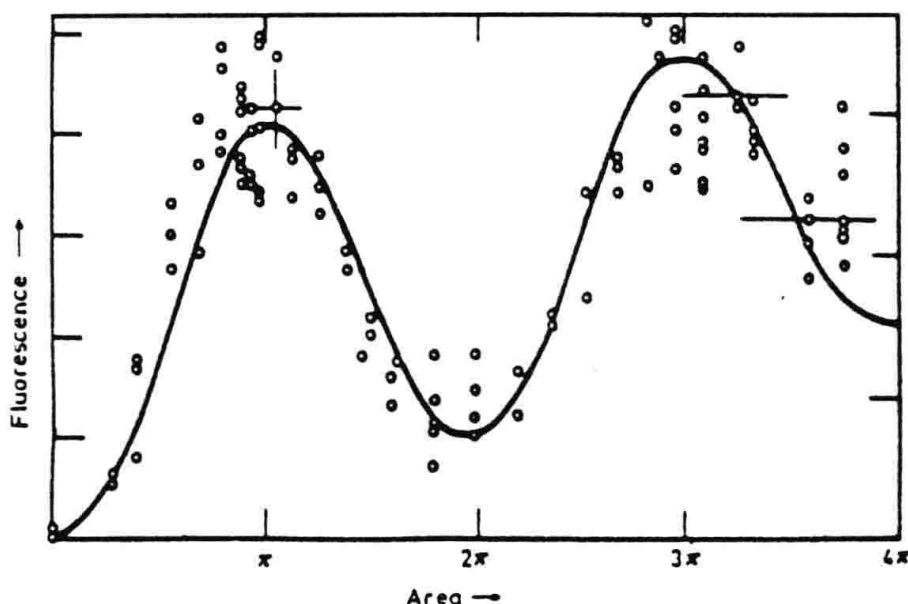


Fig. 2.4. Experimental evidence for Rabi oscillations. Rubidium atoms were excited by a Hg II laser

Problems

- 2.1. Prove that the solution given by (2.43) satisfies (2.35).

3. Quantization of the Electromagnetic Field

We start with the source-free Maxwell's equations

$$\nabla \cdot \mathbf{B} = 0, \quad (3.1)$$

$$\nabla \times \mathbf{E} = -\frac{\partial \mathbf{B}}{\partial t}, \quad (3.2)$$

$$\nabla \cdot \mathbf{E} = 0, \quad (3.3)$$

$$\nabla \times \mathbf{H} = \frac{\partial \mathbf{D}}{\partial t}, \quad (3.4)$$

together with

$$\begin{aligned} \mathbf{B} &= \mu_0 \mathbf{H}, \\ \mathbf{D} &= \epsilon_0 \mathbf{E}, \end{aligned} \quad (3.5)$$

where μ_0, ϵ_0 are the magnetic permeability and permittivity of free space, obeying the relation $\mu_0 \epsilon_0 = c^{-2}$. The equations (3.1), (3.2) are automatically satisfied when one defines the vector and scalar potentials (\mathbf{A} and V)

$$\begin{aligned} \mathbf{B} &= \nabla \times \mathbf{A}, \\ \mathbf{E} &= -\frac{\partial \mathbf{A}}{\partial t} - \nabla V. \end{aligned} \quad (3.6)$$

Since Maxwell's equations are gauge invariant, we choose the Coulomb gauge, which is particularly useful when dealing with non-relativistic electrodynamics:

$$\begin{aligned} \nabla \cdot \mathbf{A} &= 0, \\ V &= 0. \end{aligned} \quad (3.7)$$

With the above gauge, (3.3) is automatically satisfied and both \mathbf{B} and \mathbf{E} can be expressed in terms of \mathbf{A} only.

If we now substitute (3.6) into (3.4), we get the wave equation for the vector potential

$$\nabla^2 \mathbf{A} = \frac{1}{c^2} \frac{\partial^2 \mathbf{A}}{\partial t^2}. \quad (3.8)$$

Now, we perform the standard separation of variables

$$\mathbf{A}(\mathbf{r}, t) = \sum_m \sqrt{\frac{\hbar}{2\omega_m \epsilon_0}} [a_m(t) \mathbf{u}_m(\mathbf{r}) + a_m^\dagger(t) \mathbf{u}_m^*(\mathbf{r})], \quad (3.9)$$

which, after substitution into (3.8), gives

$$\begin{aligned} \nabla^2 \mathbf{u}_m(\mathbf{r}) + \frac{\omega_m^2}{c^2} \mathbf{u}_m(\mathbf{r}) &= 0, \\ \frac{\partial^2 a_m}{\partial t^2} + \omega_m^2 a_m &= 0, \end{aligned} \quad (3.10)$$

where ω_m^2/c^2 is the separation constant.

Obviously,

$$\begin{aligned} a_m(t) &= a_m \exp(-i\omega_m t), \\ a_m^\dagger(t) &= a_m^\dagger \exp(+i\omega_m t). \end{aligned} \quad (3.11)$$

Both $a_m(t)$ and $a_m^\dagger(t)$ are, for the time being, a pair of complex conjugate numbers. Later on, when we quantize the field, they will be interpreted as an operator and its harmonic conjugate.

Depending on the boundary conditions, the functions $\mathbf{u}_m(\mathbf{r})$ could be sinusoidal (cavity) or exponential (traveling waves). For plane waves:

$$\mathbf{u}_m(\mathbf{r}) = \frac{\mathbf{e}_m \exp i\mathbf{k}_m \cdot \mathbf{r}}{\sqrt{v}}, \quad (3.12)$$

where $k_m^2 = \omega_m^2/c^2$, v is the volume, and the Coulomb gauge condition implies $\mathbf{e}_m \cdot \mathbf{k}_m = 0$, which is the transversality condition for the m th mode, thus allowing two possible and mutually orthogonal polarizations, contained in a plane perpendicular to \mathbf{k}_m .

Therefore, the subscript m signifies the various modes, including the two polarization states. The allowed values of k are determined by the boundary conditions. If we take periodic boundary conditions for a cube of volume L^3 , then we require that

$$\mathbf{A}(\mathbf{r} + L\mathbf{i}) = \mathbf{A}(\mathbf{r} + L\mathbf{j}) = \mathbf{A}(\mathbf{r} + L\mathbf{k}) = \mathbf{A}(\mathbf{r}), \quad (3.13)$$

which implies

$$\mathbf{k}_m = \frac{2\pi}{L} (m_1 \mathbf{i} + m_2 \mathbf{j} + m_3 \mathbf{k}),$$

m_1, m_2, m_3 , being integer numbers.

The vectors $\mathbf{u}_m(\mathbf{r})$ satisfy the orthogonality condition

$$\int \mathbf{u}_m(\mathbf{r}) \mathbf{u}_n(\mathbf{r}) dv = \delta_{mn}. \quad (3.14)$$

The final form for the vector potential \mathbf{A} is

$$\begin{aligned} \mathbf{A}(\mathbf{r}, t) = \sum_m \sqrt{\frac{\hbar}{2\omega_m \epsilon_0 v}} \mathbf{e}_m &\{ a_m \exp[i(\mathbf{k}_m \cdot \mathbf{r} - \omega_m t)] \\ &+ a_m^\dagger \exp[-i(\mathbf{k}_m \cdot \mathbf{r} - \omega_m t)] \}. \end{aligned} \quad (3.15)$$

From (3.6) we can also write

$$\begin{aligned} \mathbf{E}(r, t) &= i \sum_m \sqrt{\frac{\hbar\omega_m}{2\varepsilon_0 v}} \mathbf{e}_m \left\{ a_m \exp [i(\mathbf{k}_m \cdot \mathbf{r} - \omega_m t)] \right. \\ &\quad \left. - a_m^\dagger \exp [-i(\mathbf{k}_m \cdot \mathbf{r} - \omega_m t)] \right\}, \end{aligned} \quad (3.16)$$

$$\begin{aligned} \mathbf{H}(r, t) &= -\frac{i}{c\mu_0} \sum_m \sqrt{\frac{\hbar\omega_m}{2\varepsilon_0 v}} \mathbf{e}_m \times \mathbf{k}_m \left\{ a_m \exp [i(\mathbf{k}_m \cdot \mathbf{r} - \omega_m t)] \right. \\ &\quad \left. - a_m^\dagger \exp [-i(\mathbf{k}_m \cdot \mathbf{r} - \omega_m t)] \right\}. \end{aligned} \quad (3.17)$$

The total energy of the multimode radiation field is given by

$$\begin{aligned} H &= \frac{1}{2} \int (\varepsilon_0 \mathbf{E}^2 + \mu_0 \mathbf{H}^2) dv \\ &= \frac{1}{2} \int \left(\varepsilon_0 \left(\frac{\partial \mathbf{A}}{\partial t} \right)^2 + \mu_0^{-1} (\nabla \times \mathbf{A})^2 \right) dv \\ &= \sum_m \hbar\omega_m (a_m a_m^\dagger + a_m^\dagger a_m) \equiv \sum_m H_m. \end{aligned} \quad (3.18)$$

In the last step to obtain (3.18), we used (3.17), (3.14). We preserved the order of a_m^\dagger, a_m , for future purposes. Now they are just numbers.

Now the quantization is trivial. The a_m obey the same differential equation as a harmonic oscillator, so the quantization rule is [3.1]

$$\begin{aligned} [a_m, a_n^\dagger] &= \delta_{nm}, \\ [a_m, a_n] &= 0, \\ [a_m^\dagger, a_n^\dagger] &= 0. \end{aligned} \quad (3.19)$$

We remind the reader that the standard connection between the a and a^\dagger operators, with the usual p and q is given by (one mode)

$$\begin{aligned} a &= \frac{1}{\sqrt{2\hbar\omega}} (\omega q + ip), \\ a^\dagger &= \frac{1}{\sqrt{2\hbar\omega}} (\omega q - ip), \end{aligned} \quad (3.20)$$

so that :

$$\frac{1}{2} (p^2 + (\omega q)^2) = \hbar\omega \left(a^\dagger a + \frac{1}{2} \right). \quad (3.21)$$

For many modes, and dropping the zero-point energy, the energy and momentum are given by:

$$H = \sum_m \hbar\omega_m (a_m^\dagger a_m), \quad (3.22)$$

$$G = \sum_m \hbar k_m a_m^\dagger a_m. \quad (3.23)$$

We notice that in the Schrödinger picture, the vector potential is [A.1]

$$\mathbf{A}(\mathbf{r}, 0) = \sum_m \sqrt{\frac{\hbar}{2\omega_m \epsilon_0 v}} \mathbf{e}_m \{ a_m \exp[i(\mathbf{k}_m \cdot \mathbf{r})] + a_m^\dagger \exp[-i(\mathbf{k}_m \cdot \mathbf{r})] \}. \quad (3.24)$$

Here we use the notation that a_m is a Schrödinger operator, while $a_m(t)$ is its Heisenberg version. Now we interpret a_m and a_m^\dagger as the annihilation and creation operators for this particular oscillator, or for this particular mode of the radiation field.

3.1 Fock States

The operator $N_m = a_m^\dagger a_m$ is the photon number of the m th mode. We define a basis which can be written as a product of state vectors for each mode, since they are independent, as follows

$$|n_1\rangle |n_2\rangle \dots |n_\infty\rangle = |n_1, n_2, \dots, n_\infty\rangle$$

such that both N_m and the Hamiltonian are diagonal in this basis.

For one mode

$$a^\dagger a |n\rangle = n |n\rangle, \quad (3.25)$$

$$H |n\rangle = \hbar\omega(a^\dagger a + \frac{1}{2}) |n\rangle = \hbar\omega(n + \frac{1}{2}) |n\rangle = E_n |n\rangle. \quad (3.26)$$

From the commutation rule (3.19) we can simply infer that

$$a^\dagger |n\rangle = \sqrt{n+1} |n+1\rangle, \quad (3.27)$$

$$a |n\rangle = \sqrt{n} |n-1\rangle.$$

Similarly, for a multimode field.

We also notice that the energy of the ground state is

$$\langle 0 | H | 0 \rangle = \frac{1}{2} \sum_m \hbar\omega_m, \quad (3.28)$$

which, of course, diverges, causing a conceptual difficulty with the whole quantization procedure.

In most practical situations, however, one does not measure absolute energies, but rather energy changes, so that the infinite zero-point energy does not generate any divergences.

To generate any Fock state of the k th mode $|n_k\rangle$ from the vacuum, we just have to apply (3.27) several times, getting

$$|n_k\rangle = \frac{(a_k^\dagger)^{n_k}}{\sqrt{n_k!}} |0\rangle \quad n_k = 0, 1, 2, \dots \quad (3.29)$$

These Fock or number states are orthogonal

$$\langle n_k | m_k \rangle = \delta_{nm}, \quad (3.30)$$

and complete

$$\sum_{n_k=0}^{\infty} |n_k\rangle\langle n_k| = 1. \quad (3.31)$$

3.2 Density of Modes

As we saw,

$$\mathbf{k}_m = \frac{2\pi}{L}(m_1\mathbf{i} + m_2\mathbf{j} + m_3\mathbf{k}), \quad (3.32)$$

so we may ask the following question: How many normal modes are contained in a cavity of volume $v = L^3$? Each set of integer numbers (m_1, m_2, m_3) corresponds to two travelling wave modes, since we have two polarizations. This corresponds to a point in Fig. 3.1.

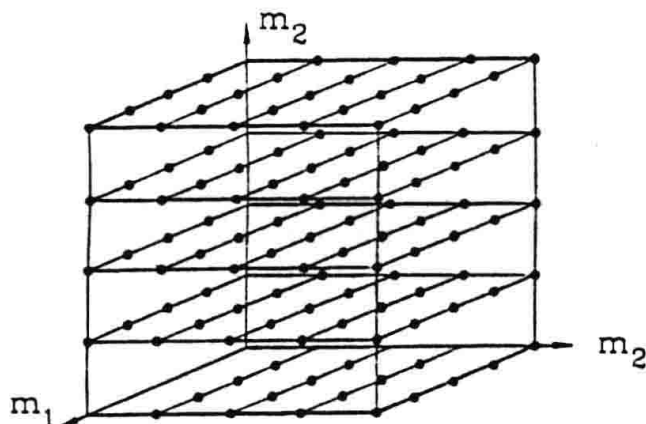


Fig. 3.1. Normal modes in a cavity

In an infinitesimal volume element $dm_1 dm_2 dm_3$, the number of modes is

$$dn = 2dm_1 dm_2 dm_3, \quad (3.33)$$

and, according to (3.32), we get

$$dn = 2 \left(\frac{L}{2\pi} \right)^3 dk_x dk_y dk_z = 2 \left(\frac{L}{2\pi} \right)^3 d\mathbf{k}. \quad (3.34)$$

Now, letting $L \rightarrow \infty$, the sums become integrals and

$$\frac{1}{L^3} \sum_m [] \xrightarrow{L \rightarrow \infty} \left(\frac{1}{2\pi} \right)^3 \iiint [] d\mathbf{k}. \quad (3.35)$$

If one goes to polar coordinates, we can also write

$$dn = 2 \left(\frac{L}{2\pi} \right)^3 dk_x dk_y dk_z = 2 \left(\frac{L}{2\pi} \right)^3 k^2 dk d\Omega, \quad (3.36)$$

where $d\Omega$ is an element of solid angle about \mathbf{k} . Since $\omega^2 = c^2 k^2$, one can write

$$dn = 2 \left(\frac{L}{2\pi c} \right)^3 \omega^2 d\omega d\Omega, \quad (3.37)$$

and the number of normal modes per unit volume, with angular frequencies between ω and $\omega + d\omega$, and per solid angle $d\Omega$, is

$$\frac{dn}{d\Omega L^3} = \frac{2\omega^2}{(2\pi c)^3} d\omega \equiv g(\omega) d\omega, \quad (3.38)$$

where $g(\omega)$ is the mode density.

3.3 Commutation Relations

Using the commutation relations (3.19), one can write [A.1]

$$[\mathbf{A}_i(\mathbf{r}), \mathbf{E}_j(\mathbf{r}')] = -\frac{i\hbar}{2v\varepsilon_0} \sum_{l,\sigma} (\mathbf{e}_{l\sigma})_i (\mathbf{e}_{l\sigma})_j [\exp(i\mathbf{k}_l \cdot \boldsymbol{\rho}) + cc], \quad (3.39)$$

$$\boldsymbol{\rho} = \mathbf{r} - \mathbf{r}'.$$

In this expression, we have replaced $m \rightarrow (l, \sigma)$, in order to separate the propagation vector index (l) from that of the polarization (σ).

Now, the three vectors $\mathbf{e}_{l1}, \mathbf{e}_{l2}, \hat{\mathbf{k}}_l$ are mutually orthogonal. So, in three-dimensional space, one may write:

$$|\mathbf{e}_{l1}\rangle \langle \mathbf{e}_{l1}| + |\mathbf{e}_{l2}\rangle \langle \mathbf{e}_{l2}| + |\hat{\mathbf{k}}_l\rangle \langle \hat{\mathbf{k}}_l| = 1, \quad (3.40)$$

so, taking i and j components of the above relation, one gets

$$\sum_{\sigma=1,2} (\mathbf{e}_{l\sigma})_i (\mathbf{e}_{l\sigma})_j = \delta_{ij} - \frac{(\mathbf{k}_l)_i (\mathbf{k}_l)_j}{k_l^2} = \delta_{ij} - (\hat{\mathbf{k}}_l)_i (\hat{\mathbf{k}}_l)_j. \quad (3.41)$$

We substitute the result of (3.41) into the commutation relation (3.39), getting:

$$[\mathbf{A}_i(\mathbf{r}), \mathbf{E}_j(\mathbf{r}')] = -\frac{i\hbar}{v\varepsilon_0} \sum_l [\delta_{ij} - (\hat{\mathbf{k}}_l)_i (\hat{\mathbf{k}}_l)_j] \exp(i\mathbf{k}_l \cdot \boldsymbol{\rho}), \quad (3.42)$$

where the sum over l now covers both positive and negative integers, since:

$$\widehat{\mathbf{k}_{-l}} = -\widehat{\mathbf{k}_l}. \quad (3.43)$$

Letting $L \rightarrow \infty$, and making use of (3.35), we can write

$$[\mathbf{A}_i(\mathbf{r}), \mathbf{E}_j(\mathbf{r}')] = -\frac{i\hbar}{\varepsilon_0} \delta_{ij}^T(\mathbf{r} - \mathbf{r}'), \quad (3.44)$$

where $\delta_{ij}^T(\mathbf{r} - \mathbf{r}')$ is the transverse δ function defined as

$$\delta_{ij}^T(\mathbf{r} - \mathbf{r}') = \frac{1}{(2\pi)^3} \int \int \int d\mathbf{k} [\delta_{ij} - (\hat{\mathbf{k}})_i (\hat{\mathbf{k}})_j] \exp(i\mathbf{k} \cdot \boldsymbol{\rho}). \quad (3.45)$$

Following the same procedure, the reader can show that

$$[\mathbf{A}_i(\mathbf{r}, t), \mathbf{A}_j(\mathbf{r}', t)] = 0, \quad (3.46)$$

$$[\mathbf{E}_i(\mathbf{r}, t), \mathbf{E}_j(\mathbf{r}', t)] = 0, \quad (3.47)$$

$$[\mathbf{B}_i(\mathbf{r}, t), \mathbf{B}_j(\mathbf{r}', t)] = 0. \quad (3.48)$$

Actually, to show the above commutation relation, one can work in the Schrödinger picture, with time-independent operators, and if the above is true, then it is also true in the Heisenberg picture, at equal times.

Problems

3.1. Prove that the $|n\rangle$ state can be expressed in terms of the vacuum state as

$$|n\rangle = \frac{(a^\dagger)^n}{\sqrt{n!}} |0\rangle.$$

3.2. Prove the following commutation relations

$$[a, a^{\dagger n}] = n(a^\dagger)^{n-1},$$

$$[a^n, a^\dagger] = n(a)^{n-1}.$$

3.3. The commutation relations of Problem 3.2 can be generalized. Prove that

$$[a, f(a, a^\dagger)] = \frac{\partial f}{\partial a^\dagger},$$

$$[a^\dagger, f(a, a^\dagger)] = -\frac{\partial f}{\partial a},$$

$$\exp(-\alpha a^\dagger a) f(a, a^\dagger) \exp(\alpha a^\dagger a) = f(a e^\alpha, a^\dagger e^{-\alpha})$$

(see Appendix A).

3.4. Show that

$$[\mathbf{A}_k(\mathbf{r}), \mathbf{E}_l(\mathbf{r}')] = -i\hbar \frac{\delta_{kl}^T(\mathbf{r} - \mathbf{r}')}{\epsilon_0}.$$

3.5. Show that

$$[\mathbf{E}_i(\mathbf{r}, t), \mathbf{B}_j(\mathbf{r}', t)] = \begin{cases} 0, & i = j \\ -i\hbar \frac{\partial}{x_k} \delta(\rho), & i, j, k = 1, 2, 3 \\ i\hbar \frac{\partial}{x_k} \delta(\rho). & i, j, k = 1, 3, 2. \end{cases}$$

and $\rho = \mathbf{r} - \mathbf{r}'$.

4. States of the Electromagnetic Field I

Coherent states, introduced by Glauber [4.1] and Sudarshan [4.2], are defined as the eigenstates of the annihilation operator. For a single mode

$$a |\alpha\rangle = \alpha |\alpha\rangle, \quad (4.1)$$

where α is a complex number. Expanding the coherent state in the Fock basis

$$|\alpha\rangle = \sum_{n=0}^{\infty} c_n |n\rangle, \quad (4.2)$$

we easily get

$$\begin{aligned} a |\alpha\rangle &= \sum_{n=1}^{\infty} c_n \sqrt{n} |n-1\rangle \\ &= \alpha \sum_{n=0}^{\infty} c_n |n\rangle, \end{aligned} \quad (4.3)$$

from which we get the following recursion relation

$$c_n \sqrt{n} = \alpha c_{n-1}. \quad (4.4)$$

The solution of (4.4) gives

$$c_n = \frac{\alpha^n}{\sqrt{n!}} c_0.$$

The coefficient c_0 is found from normalization:

$$\langle \alpha | \alpha \rangle = 1 = |c_0|^2 \sum_n \frac{|\alpha|^{2n}}{n!} = |c_0|^2 \exp |\alpha|^2 \quad (4.5)$$

so that we can now write the expansion

$$|\alpha\rangle = \exp \left(-\frac{|\alpha|^2}{2} \right) \sum_n \frac{\alpha^n}{\sqrt{n!}} |n\rangle. \quad (4.6)$$

4.1 Further Properties

4.1.1 Coherent States are Minimum Uncertainty States

We write the usual relation between a, a^\dagger and q, p :

$$\begin{aligned} a &= \frac{1}{\sqrt{2\hbar\omega}}(\omega x + ip), \\ a^\dagger &= \frac{1}{\sqrt{2\hbar\omega}}(\omega x - ip), \end{aligned} \tag{4.7}$$

with $[x, p] = i\hbar$, or equivalently $(\Delta x)^2(\Delta p)^2 \geq \hbar^2/4$.

By inverting the relations (4.7), and taking the expectation value over a coherent state, one gets

$$\begin{aligned} \langle x \rangle_\alpha &= \sqrt{\frac{\hbar}{2\omega}} \langle \alpha | (a + a^\dagger) | \alpha \rangle, \\ &= \sqrt{\frac{\hbar}{2\omega}} (\alpha + \alpha^*), \end{aligned} \tag{4.8}$$

and

$$\begin{aligned} \langle x^2 \rangle_\alpha &= \frac{\hbar}{2\omega} \langle \alpha | (a + a^\dagger)^2 | \alpha \rangle \\ &= \frac{\hbar}{2\omega} (1 + (\alpha + \alpha^*)^2), \end{aligned} \tag{4.9}$$

so

$$(\Delta x)_\alpha^2 = \langle x^2 \rangle_\alpha - \langle x \rangle_\alpha^2 = \frac{\hbar}{2\omega}. \tag{4.10}$$

In a similar way, one finds

$$(\Delta p)_\alpha^2 = \frac{\hbar\omega}{2}, \tag{4.11}$$

so that

$$(\Delta x)_\alpha^2(\Delta p)_\alpha^2 = \frac{\hbar^2}{4},$$

and the coherent states are minimum uncertainty states (MUS).

4.1.2 Coherent States are not Orthogonal

$$\begin{aligned} \langle \alpha | \beta \rangle &= \exp \left[-\frac{1}{2}(|\alpha|^2 + |\beta|^2) \right] \sum_{nm} \langle m | \frac{\alpha^n \beta^{*m}}{\sqrt{n!m!}} | n \rangle \\ &= \exp \left[-\frac{1}{2}(|\alpha|^2 + |\beta|^2) \right] \exp(\alpha^* \beta), \end{aligned}$$

or put it differently

$$|\langle \alpha | \beta \rangle|^2 = \exp(-|\alpha - \beta|^2). \tag{4.12}$$

4.1.3 Coherent States are Overcomplete

We now calculate $\int d^2\alpha |\alpha\rangle\langle\alpha|$ where $d^2\alpha = (d\operatorname{Re}\alpha)(d\operatorname{Im}\alpha)$:

$$\int d^2\alpha |\alpha\rangle\langle\alpha| = \sum_{nm} \frac{|n\rangle\langle m|}{\sqrt{n!m!}} \int d^2\alpha \exp(-|\alpha|^2) \alpha^n \alpha^{*m}. \quad (4.13)$$

It is convenient to write $\alpha = r \exp i\phi$, so

$$\begin{aligned} & \int d^2\alpha |\alpha\rangle\langle\alpha| \\ &= \sum_{nm} \frac{|n\rangle\langle m|}{\sqrt{n!m!}} \int r dr \exp(-r^2) r^{n+m} \int d\phi \exp(i(n-m)\phi), \end{aligned} \quad (4.14)$$

but

$$\int d\phi \exp[i(n-m)\phi] = 2\pi\delta_{nm}$$

so

$$\int d^2\alpha |\alpha\rangle\langle\alpha| = 2\pi \sum_n \frac{|n\rangle\langle n|}{n!} \int dr \exp(-r^2) r^{2n+1}, \quad (4.15)$$

and defining $\varepsilon \equiv r^2$, the integral of (4.15) can be written as

$$\frac{1}{2} \int \varepsilon^n e^{-\varepsilon} d\varepsilon = \frac{n!}{2}.$$

The last result combined with (4.15) gives us finally

$$\int d^2\alpha |\alpha\rangle\langle\alpha| = \pi. \quad (4.16)$$

4.1.4 The Displacement Operator

We define the displacement operator as [4.1]

$$D(\alpha) = \exp(\alpha a^\dagger - \alpha^* a). \quad (4.17)$$

We make use of the Baker–Campbell–Haussdorf (BCH) relation (see Appendix A)

$$e^{(A+B)} = e^A e^B e^{-\frac{1}{2}[A,B]}, \quad (4.18)$$

valid if $[A, [A, B]] = [B, [A, B]] = 0$.

We now use the BCH relation on the displacement operator and apply it to the vacuum state:

$$\begin{aligned}
D(\alpha) |0\rangle &= \exp(\alpha a^\dagger - \alpha^* a) |0\rangle \\
&= \exp(\alpha a^\dagger) \exp(-\alpha^* a) \exp\left(-\frac{|\alpha|^2}{2}\right) |0\rangle \\
&= \exp\left(-\frac{|\alpha|^2}{2}\right) \exp(\alpha a^\dagger) \exp(-\alpha^* a) |0\rangle \\
&= \exp\left(-\frac{|\alpha|^2}{2}\right) \exp(\alpha a^\dagger) |0\rangle \\
&= \exp\left(-\frac{|\alpha|^2}{2}\right) \sum_{n=0}^{\infty} \frac{\alpha^n}{n!} (a^\dagger)^n |0\rangle,
\end{aligned} \tag{4.19}$$

so, finally

$$D(\alpha) |0\rangle = |\alpha\rangle. \tag{4.20}$$

In the last step, we used the property

$$(a^\dagger)^n |0\rangle = \sqrt{n!} |n\rangle. \tag{4.21}$$

From (4.20) we can see that a coherent state is just the vacuum displaced by $D(\alpha)$.

One other property of the displacement operator can be derived using (Appendix A)

$$\exp(\varepsilon A) B \exp(-\varepsilon A) = B + \varepsilon [A, B] + \frac{\varepsilon^2}{2} [A, [A, B]] + \dots \tag{4.22}$$

Now we can easily calculate

$$\begin{aligned}
D^\dagger(\alpha) a D(\alpha) &= a + \alpha, \\
D^\dagger(\alpha) a^\dagger D(\alpha) &= a^\dagger + \alpha^*.
\end{aligned}$$

4.1.5 Photon Statistics

By simple inspection of the expansion of the coherent states in terms of Fock states (4.6), one gets

$$P_n \equiv |C_n|^2 = |\langle n | \alpha \rangle|^2 = \exp - |\alpha|^2 \frac{|\alpha|^{2n}}{n!}. \tag{4.23}$$

Equation (4.23) says that the probability of having n photons in a coherent state obeys Poisson statistics.

We can easily calculate the average photon number and variance:

$$\begin{aligned}
\langle n \rangle &= \langle \alpha | a^\dagger a | \alpha \rangle = |\alpha|^2, \\
\langle n^2 \rangle &= \langle \alpha | a^\dagger a a^\dagger a | \alpha \rangle = \langle \alpha | a^\dagger a | \alpha \rangle + \langle \alpha | a^{\dagger 2} a^2 | \alpha \rangle \\
&= |\alpha|^2 + |\alpha|^4,
\end{aligned} \tag{4.24}$$

so that $(\Delta n)^2 = \langle n^2 \rangle - \langle n \rangle^2 = \langle n \rangle$, which is expected from the Poisson statistics.

4.1.6 Coordinate Representation

We would like to find the quantity $\langle q' | \alpha \rangle$. Making use (3.20), we write [4.3]

$$a |\alpha\rangle = \frac{1}{\sqrt{2\hbar\omega}}(\omega q + ip) |\alpha\rangle, \quad (4.25)$$

and multiplying (4.25) by $\langle q' |$ on the left, we get

$$\begin{aligned} \langle q' | (\omega q + ip) |\alpha\rangle &= \sqrt{2\hbar\omega}\alpha\langle q' | \alpha\rangle \\ &= (\omega q' + \hbar\frac{\partial}{\partial q'})\langle q' | \alpha\rangle. \end{aligned} \quad (4.26)$$

A more convenient way of writing (4.26) is

$$\frac{d\langle q' | \alpha\rangle}{\langle q' | \alpha\rangle} = \left[\sqrt{\frac{2\omega}{\hbar}}\alpha - \frac{\omega}{\hbar}q' \right] dq'. \quad (4.27)$$

The solution of (4.27) is

$$\langle q' | \alpha\rangle = \left(\frac{\omega}{\pi\hbar} \right)^{\frac{1}{4}} \exp \left(-\frac{\omega}{2\hbar}q'^2 + \sqrt{\frac{2\omega}{\hbar}}\alpha q' - \frac{|\alpha|^2 + \alpha^2}{2} \right), \quad (4.28)$$

where the result given by (4.28) was obtained using the normalization condition $\int_{-\infty}^{+\infty} dq' |\langle q' | \alpha\rangle|^2 = 1$, and defining $\alpha = r \exp(i\phi)$, with $\phi = 0$.

4.2 Mixed State. Thermal Radiation

A pure state implies perfect knowledge of the state of our system. If that is not the case, we have the mixed case, where we know our state only probabilistically. In general we write

$$\rho = \sum_R p_R |R\rangle\langle R|, \quad (4.29)$$

and the expectation value of any operator O can be expressed as

$$\begin{aligned} \langle O \rangle &= \sum_S \langle S | \rho O | S \rangle \\ &= Tr(\rho O) \\ &= \sum_S \langle S | \sum_R p_R |R\rangle\langle R| O | S \rangle \\ &= \sum_R p_R \langle R | O | R \rangle, \end{aligned} \quad (4.30)$$

where $|S\rangle$ is an arbitrary set of orthogonal and complete states. A property of ρ is that $Tr\{\rho\} = \sum_S \sum_R P_R \langle S | R \rangle \langle R | S \rangle = \sum_R P_R = 1$, which just implies that probability conservation should also hold for mixed states.

An example of a mixed state is thermal radiation. For thermal equilibrium at temperature T , the probability P_n that one mode of the field is excited with n photons, is given by the usual Boltzmann factor

$$P_n = \frac{\exp(-E_n/K_B T)}{\sum_n \exp(-E_n/K_B T)}. \quad (4.31)$$

The zero-point energy cancels when the quantized energy is substituted and, using the shorthand notation

$$Z = \exp\left(-\frac{\hbar\omega}{K_B T}\right), \quad (4.32)$$

the probability can be written as

$$P_n = \frac{Z^n}{\sum_n Z^n}. \quad (4.33)$$

The denominator of the above expression can be easily summed as a geometrical series

$$\sum_n Z^n = \frac{1}{1 - Z},$$

giving

$$P_n = (1 - Z)Z^n = \left[1 - \exp\left(-\frac{\hbar\omega}{K_B T}\right)\right] \exp\left(-\frac{n\hbar\omega}{K_B T}\right). \quad (4.34)$$

Therefore, the density operator for a mixed one-mode thermal state is given by:

$$\begin{aligned} \rho_{\text{thermal}} &= \left[1 - \exp\left(-\frac{\hbar\omega}{K_B T}\right)\right] \sum_n \exp\left(-\frac{n\hbar\omega}{K_B T}\right) |n\rangle\langle n|, \\ &= \left[1 - \exp\left(-\frac{\hbar\omega}{K_B T}\right)\right] \sum_n \exp\left(-\frac{\hbar\omega a^\dagger a}{K_B T}\right) |n\rangle\langle n| \\ &= \left[1 - \exp\left(-\frac{\hbar\omega}{K_B T}\right)\right] \exp\left(-\frac{\hbar\omega a^\dagger a}{K_B T}\right) \\ &= \sum_n \frac{\langle n \rangle_{\text{th}}^n}{(1 + \langle n \rangle_{\text{th}})^{n+1}} |n\rangle\langle n|. \end{aligned} \quad (4.35)$$

In the last line, we used the relation

$$P_n = \frac{\langle n \rangle_{\text{th}}^n}{(1 + \langle n \rangle_{\text{th}})^{n+1}}, \quad (4.36)$$

which can be easily proven as follows

$$\begin{aligned}
\langle n \rangle_{\text{th}} &= \sum_n n P_n = (1 - Z) \sum_n n Z^n \\
&= (1 - Z) Z \frac{\partial}{\partial Z} \sum_n Z^n \\
&= \frac{Z}{1 - Z};
\end{aligned} \tag{4.37}$$

thus, the average photon number is

$$\langle n \rangle_{\text{th}} = \frac{1}{\exp(\hbar\omega/K_B T) - 1}. \tag{4.38}$$

From (4.38), the reader can easily verify (4.36), for the photon statistics of a one-mode thermal state.

The obvious extension of (4.35) is, for the multimode case,

$$\rho_{\text{thermal}} = \sum_{\{n_k\}} \Pi_k \frac{(\langle n_k \rangle_{\text{th}})^{n_k}}{(1 + \langle n_k \rangle_{\text{th}})^{n_k+1}} |\{n_k\}\rangle\langle\{n_k\}|. \tag{4.39}$$

Problems

4.1. Show that the eigenstate of the creation operator does not exist.

4.2. Show that

$$a^\dagger |\alpha\rangle\langle\alpha| = \left(\alpha^* + \frac{\partial}{\partial\alpha} \right) |\alpha\rangle\langle\alpha|,$$

and

$$|\alpha\rangle\langle\alpha| a = \left(\alpha + \frac{\partial}{\partial\alpha^*} \right) |\alpha\rangle\langle\alpha|.$$

4.3. Show that if a harmonic oscillator is initially in a coherent state

$$|\psi, 0\rangle = |\alpha\rangle,$$

then at later time t it will still be coherent:

$$|\psi, t\rangle = |\alpha \exp(-i\omega t)\rangle.$$

4.4. For a collection of oscillators in thermal equilibrium at temperature T , one can write

$$P(q, T) = \sum_{n=0}^{\infty} P_n |\psi_n(q)|^2 = \frac{\sum_n \exp(-\beta E_n) |\psi_n(q)|^2}{\sum_n \exp(-\beta E_n)},$$

$$P(p, T) = \sum_{n=0}^{\infty} P_n |\phi_n(p)|^2 = \frac{\sum_n \exp(-\beta E_n) |\phi_n(p)|^2}{\sum_n \exp(-\beta E_n)},$$

with $\beta = 1/K_B T$. Show that

$$P(q, T) = \frac{\exp(-q^2/2\sigma_q^2)}{\sqrt{2\pi\sigma_q^2}}.$$

$$P(p, T) = \frac{\exp(-p^2/2\sigma_p^2)}{\sqrt{2\pi\sigma_p^2}},$$

with

$$\sigma_q^2 = \frac{\hbar}{2m\omega} \coth\left(\frac{\hbar\omega}{2K_B T}\right),$$

$$\sigma_p^2 = \frac{\hbar m\omega}{2} \coth\left(\frac{\hbar\omega}{2K_B T}\right).$$

Also verify that

$$\sigma_q \sigma_p = \frac{K_B T}{\omega},$$

for $K_B T \gg \hbar\omega$ and

$$\sigma_q \sigma_p = \frac{\hbar}{4\pi}$$

for $K_B T \ll \hbar\omega$.

4.5. Show that for a pure state, the condition

$$\rho^2 = \rho$$

is necessary and sufficient. Also, verify that for a mixed state

$$\text{Tr}\{\rho^2\} < 1.$$

4.6. *Coherent state with an unknown phase.* Let $\alpha = |\alpha| \exp(i\varphi)$, with φ unknown and uniformly distributed. Show that

$$\begin{aligned} \rho &= \frac{1}{2\pi} \int_0^{2\pi} |\langle \alpha | \exp(i\varphi) \rangle|^2 |\alpha|^2 d\varphi \\ &= \sum_{n=0}^{\infty} \exp(-|\alpha|^2) \frac{|\alpha|^{2n}}{n!} |n\rangle \langle n|. \end{aligned}$$

We can see that the phase ignorance washes out the off-diagonal elements.

4.7. Define the characteristic function or 'momentum generating function' (see also Chap. 7) as:

$$C_A(\xi) = \sum_{n=0}^{\infty} \frac{(\mathrm{i}\xi)^n}{n!} \langle A^n \rangle.$$

Show that

$$\langle A^n \rangle = \left(\frac{\partial}{\partial(i\xi)} \right)^n C_A(\xi) \Big|_{\xi=0},$$

$$C_A(\xi) = \text{Tr}(\rho \exp(i\xi A)),$$

$$C_A(\xi) = \int P(A'/\rho) \exp(i\xi A') dA',$$

where A' is an eigenvalue of A and $P(A'/\rho)$ the corresponding probability density. Hint: To prove the last property, use the second relation for a continuous spectrum.

4.8. Let the operator A in Problem 4.7 be

$$A = \gamma a + \gamma^* a^\dagger.$$

For a harmonic oscillator in a coherent state $|\alpha\rangle$, show that

$$C_A(\xi) = \exp \left[-\frac{1}{2}\xi^2 \gamma \gamma^* + i(\alpha^* \gamma^* + \alpha \gamma) \right],$$

$$\langle A \rangle = \alpha^* \gamma^* + \alpha \gamma,$$

$$\sigma_A^2 = \langle A^2 \rangle - \langle A \rangle^2 = |\gamma|^2,$$

$$P(A'/\rho) = \frac{1}{\sqrt{2\pi\sigma_A^2}} \exp \left(-\frac{(A' - \langle A \rangle)^2}{2\sigma_A^2} \right).$$

The last property shows that the distribution is Gaussian.

5. States of the Electromagnetic Field II

In this chapter we deal with the general properties of squeezed states. We also describe two methods of detection of these states.

5.1 Squeezed States. General Properties and Detection

We define the quadrature operators X and Y [5.1]:

$$\begin{aligned} X &= \frac{a + a^\dagger}{2} = \sqrt{\frac{\omega}{2\hbar}} q, \\ Y &= \frac{a - a^\dagger}{2i} = \sqrt{\frac{1}{2\hbar\omega}} p. \end{aligned} \quad (5.1)$$

The name ‘quadrature’ appears naturally if one replaces the expressions (5.1) into the quantized electric field

$$\begin{aligned} E(1 \text{ mode}) &= i\sqrt{\frac{\hbar\omega}{2\varepsilon_0 v}} e_m [a \exp(-i\omega t + ik \cdot r) \\ &\quad - a^\dagger \exp(i\omega t - ik \cdot r)], \\ &= 2\sqrt{\frac{\hbar\omega}{2\varepsilon_0 v}} e_m [X \sin(\omega t - k \cdot r) \\ &\quad - Y \cos(\omega t - k \cdot r)]. \end{aligned} \quad (5.2)$$

X and Y thus appear as factor operators in front of the sin and cos functions.

X and Y are Hermitian operators obeying the commutation relation

$$[X, Y] = \frac{i}{2}, \quad (5.3)$$

or

$$\langle (\Delta X)^2 \rangle \langle (\Delta Y)^2 \rangle \geq \frac{1}{16}. \quad (5.4)$$

In the case of coherent states, according to (4.10), (4.11), one can write

$$\langle (\Delta X)^2 \rangle = \frac{1}{4}, \quad \langle (\Delta Y)^2 \rangle = \frac{1}{4}. \quad (5.5)$$

From the quadrature perspective, a coherent state is a minimum uncertainty state with equal fluctuations in both quadratures.

Furthermore, since

$$\langle(X + iY)\rangle_\alpha = \langle a \rangle_\alpha = \alpha, \quad (5.6)$$

so

$$\langle X \rangle_\alpha = \operatorname{Re}\{\alpha\}, \quad \langle Y \rangle_\alpha = \operatorname{Im}\{\alpha\}. \quad (5.7)$$

Pictorially, a coherent state can be represented, in the complex plane, as an error circle of diameter $\frac{1}{2}$ and its centre displaced by α . (Fig. 5.1).

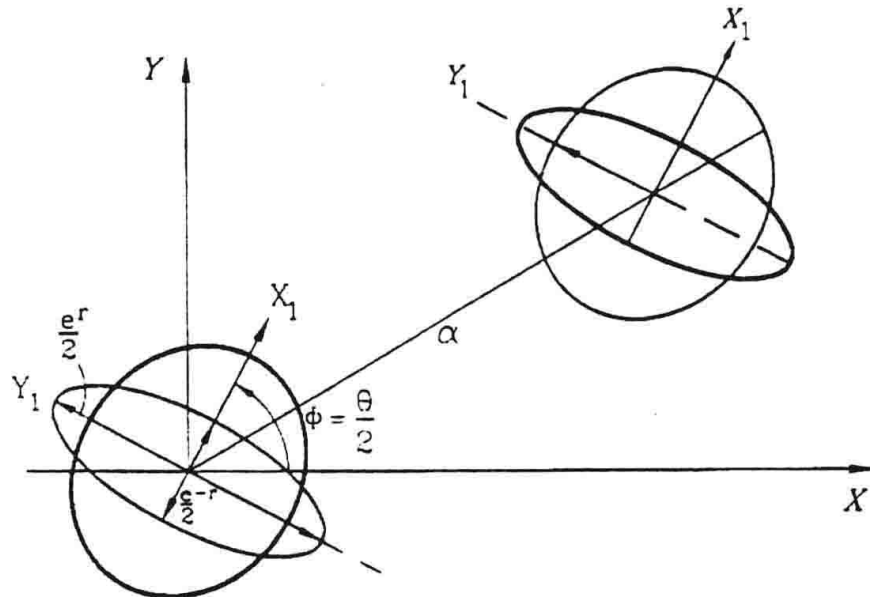


Fig. 5.1. Phase space representation of a coherent (*displaced circle*) and a squeezed state (*displaced ellipse*)

If there is a state for which either X or Y has a dispersion less than $\frac{1}{4}$, at the expense of the other quadrature, then its representation in the complex plane takes the form of an ellipse and we call this state a *squeezed state* [5.2], [5.3]. Of course we may generalize our treatment, not only to squeeze along the X or Y axis, but along any pair of axes

$$X_1 = \frac{ae^{-i\phi} + a^\dagger e^{i\phi}}{2}, \quad Y_1 = \frac{ae^{-i\phi} - a^\dagger e^{i\phi}}{2i}. \quad (5.8)$$

One can check easily that X_1, Y_1 obey the same commutation relation as X and Y :

$$[X_1, Y_1] = \frac{i}{2}, \quad (5.9)$$

$$\langle (\Delta X_1)^2 \rangle \langle (\Delta Y_1)^2 \rangle \geq \frac{1}{16}.$$

From (5.8), we show that

$$\begin{aligned}\Delta X_1 &= \Delta X \cos \phi + \Delta Y \sin \phi, \\ \Delta Y_1 &= -\Delta X \sin \phi + \Delta Y \cos \phi,\end{aligned}\quad (5.10)$$

where $\Delta O \equiv O - \langle O \rangle$. Then, we define a squeezed state by $\langle (\Delta X_1)^2 \rangle < \frac{1}{4}$ or $\langle (\Delta Y_1)^2 \rangle < \frac{1}{4}$, for some ϕ .

We denote by $\langle : X_1^2 : \rangle$ the normal ordered average. Then

$$\langle : X_1^2 : \rangle = \frac{1}{4} [\langle a^{\dagger 2} \rangle \exp(2i\phi) + \langle a^2 \rangle \exp(-2i\phi) + 2\langle a^\dagger a \rangle], \quad (5.11)$$

and

$$\langle X_1^2 \rangle = \frac{1}{4} [\langle a^{\dagger 2} \rangle \exp(2i\phi) + \langle a^2 \rangle \exp(-2i\phi) + 2\langle a^\dagger a \rangle + 1], \quad (5.12)$$

so that $\langle : \Delta X_1^2 : \rangle = \langle X_1^2 \rangle - \frac{1}{4}$, and for a squeezed state $\langle : \Delta X_1^2 : \rangle < 0$.

If we represent the density operator ρ as (we will see the details in Chap. 7)

$$\rho = \int P(\alpha) |\alpha\rangle\langle\alpha| d^2\alpha,$$

then

$$\langle : \Delta X_1^2 : \rangle = \int P(\alpha) (\Delta X_1^2)_\alpha d^2\alpha, \quad (5.13)$$

where $(\Delta X_1^2)_\alpha$ is just ΔX_1^2 with $a \rightarrow \alpha, a^\dagger \rightarrow \alpha^*$. Thus

$$(\Delta X_1^2)_\alpha = \frac{1}{4} [\Delta\alpha^* \exp(i\phi) + \Delta\alpha \exp(-i\phi)]^2, \quad (5.14)$$

and the squeezing condition can be written as

$$\langle : \Delta X_1^2 : \rangle = \frac{1}{4} \int P(\alpha) [\Delta\alpha^* \exp(i\phi) + \Delta\alpha \exp(-i\phi)]^2 d^2\alpha < 0, \quad (5.15)$$

and since $[\Delta\alpha^* \exp(i\phi) + \Delta\alpha \exp(-i\phi)]^2$ is real and positive, squeezing can only take place if $P(\alpha)$ is not a positive definite probability density.

5.1.1 The Squeeze Operator and the Squeezed State

We define a squeeze operator as

$$S(\xi) = \exp \left[\frac{1}{2} (\xi^* a^2 - \xi a^{\dagger 2}) \right], \quad (5.16)$$

which is a unitary transformation, and $\xi \equiv r \exp(i\theta)$ is called the *squeeze parameter*. With the help of (4.22), we can define a *generalized annihilation operator* as

$$\begin{aligned}A &= S(\xi) a S^\dagger(\xi) \\ &= a \cosh r + a^\dagger \exp i\theta \sinh r \\ &\equiv \mu a + \nu a^\dagger.\end{aligned}\quad (5.17)$$

As we can see, $\mu \equiv \cosh r$, $\nu \equiv \exp(i\theta) \sinh r$ and $[A, A^\dagger] = 1$.

The *coherent squeezed state* is defined as (one mode)[5.4]:

$$|\alpha, \xi\rangle = D(\alpha)S(\xi)|0\rangle. \quad (5.18)$$

Inverting (5.17), one can also write

$$\begin{aligned} a &= \mu A - \nu A^\dagger, \\ a^\dagger &= \mu A^\dagger - \nu^* A. \end{aligned} \quad (5.19)$$

5.1.2 The Squeezed State is an Eigenstate of A

$$\begin{aligned} A |\alpha, \xi\rangle &= AD(\alpha)S(\xi)|0\rangle \\ &= S(\xi)aS^\dagger(\xi)D(\alpha)S(\xi)|0\rangle. \end{aligned} \quad (5.20)$$

One can prove that

$$D(\alpha)S(\xi) = S(\xi)D(\beta), \quad (5.21)$$

with

$$\beta \equiv \alpha \cosh r + \alpha^* \exp(i\theta) \sinh r. \quad (5.22)$$

Replacing (5.21) in (5.20), we get

$$\begin{aligned} A |\alpha, \xi\rangle &= S(\xi)aD(\beta)|0\rangle = S(\xi)a|\beta\rangle \\ &= \beta S(\xi)|\beta\rangle = \beta S(\xi)D(\beta)|0\rangle = \beta D(\alpha)S(\xi)|0\rangle \\ &= \beta |\alpha, \xi\rangle. \end{aligned} \quad (5.23)$$

Pictorially, a squeezed state in phase space is the vacuum (represented by a circle at the origin) which is first squeezed into an ellipse, tilted by $\frac{\theta}{2}$ and then displaced by α (see Fig. 5.1).

5.1.3 Calculation of Moments with Squeezed States

With the help of (5.19), (5.21), we find

$$\begin{aligned} \langle \alpha, \xi | a | \alpha, \xi \rangle &= \langle \alpha, \xi | \mu A - \nu A^\dagger | \alpha, \xi \rangle \\ &= \mu \beta - \nu \beta^* \\ &= \alpha. \end{aligned} \quad (5.24)$$

In a similar way, one can find

$$\begin{aligned} \langle \alpha, \xi | a^\dagger a | \alpha, \xi \rangle &\equiv \langle n \rangle_{sq} \\ &= \langle 0 | S^\dagger(\xi)D^\dagger(\alpha)a^\dagger a D(\alpha)S(\xi)|0\rangle \\ &= \langle 0 | S^\dagger(\xi)D^\dagger(\alpha)a^\dagger D(\alpha)D^\dagger(\alpha)a D(\alpha)S(\xi)|0\rangle \\ &= \langle 0 | S^\dagger(\xi)(a^\dagger + \alpha^*)(a + \alpha)S(\xi)|0\rangle, \end{aligned} \quad (5.25)$$

and since $\langle 0 | S^\dagger(\xi)a^\dagger S(\xi) | 0 \rangle$, $\langle 0 | S^\dagger(\xi)aS(\xi) | 0 \rangle$ are linear combinations of a and a^\dagger averaged over the vacuum state, they will give no contribution, and

$$\begin{aligned}\langle n \rangle_{\text{sq}} &= \langle 0 | S^\dagger(\xi)(a^\dagger a)S(\xi) | 0 \rangle + |\alpha|^2 \\ &= \langle 0 | S^\dagger(\xi)a^\dagger S(\xi)S^\dagger(\xi)aS(\xi) | 0 \rangle + |\alpha|^2 \\ &= \langle 0 | [a^\dagger \cosh r - a \exp(-i\theta) \sinh r] \\ &\quad [a \cosh r - a^\dagger \exp(i\theta) \sinh r] | 0 \rangle + |\alpha|^2 \\ &= \sinh^2 r + |\alpha|^2.\end{aligned}\quad (5.26)$$

Finally, using a similar procedure, one can verify that

$$\langle a^2 \rangle_{\text{sq}} = \alpha^2 - \cosh r \sinh r \exp(i\theta). \quad (5.27)$$

5.1.4 Quadrature Fluctuations

We calculate

$$\begin{aligned}\langle \Delta X_1^2 \rangle_{\text{sq}} &= \langle 0 | S^\dagger(\xi)D^\dagger(\alpha)\Delta X_1 D(\alpha)D^\dagger(\alpha)\Delta X_1 D(\alpha)S(\xi) | 0 \rangle \quad (5.28) \\ &= \langle 0 | S^\dagger(\xi) \frac{1}{4} [\exp(-i\phi)(a + \alpha - \langle a \rangle) \\ &\quad + \exp(i\phi)(a^\dagger + \alpha^* - \langle a^\dagger \rangle)]^2 S(\xi) | 0 \rangle \\ &= \frac{1}{4} \langle 0 | S^\dagger(\xi) [\exp(-i\phi)a + \exp(i\phi)a^\dagger]^2 S(\xi) | 0 \rangle \\ &= \frac{1}{4} [\exp(-2i\phi)\langle \xi, 0 | a^2 | \xi, 0 \rangle + \exp(2i\phi)\langle \xi, 0 | a^{*2} | \xi, 0 \rangle \\ &\quad + 1 + 2\langle \xi, 0 | a^\dagger a | \xi, 0 \rangle].\end{aligned}$$

We take $\theta = 2\phi$, thus getting

$$\begin{aligned}\langle \Delta X_1^2 \rangle_{\text{sq}} &= \frac{1}{4} (1 + 2 \sinh^2 r - 2 \cosh r \sinh r) \quad (5.29) \\ &= \frac{e^{-2r}}{4}.\end{aligned}$$

Similarly

$$\langle \Delta Y_1^2 \rangle_{\text{sq}} = \frac{e^{2r}}{4}. \quad (5.30)$$

If we now go back to the original quadratures, we readily find

$$\begin{aligned}\langle (\Delta X)^2 \rangle_{\text{sq}} &= \frac{1}{4} \left(\exp(-2r) \cos^2 \frac{\theta}{2} + \exp(2r) \sin^2 \frac{\theta}{2} \right), \quad (5.31) \\ \langle (\Delta Y)^2 \rangle_{\text{sq}} &= \frac{1}{4} \left(\exp(-2r) \sin^2 \frac{\theta}{2} + \exp(2r) \cos^2 \frac{\theta}{2} \right).\end{aligned}$$

We notice, from the above expressions, that the variances are independent of the coherent amplitude α .

The squeezing condition for the quadrature operator X

$$\langle (\Delta X)^2 \rangle_{\text{sq}} < \frac{1}{4},$$

is satisfied if

$$\cos \theta > \tanh r,$$

and its minimum value is

$$\langle (\Delta X)^2 \rangle_{\text{sq}} = \frac{\exp(-2r)}{4},$$

for $\theta = 0$. The squeezing condition for Y is

$$\cos \theta < -\tanh r.$$

Finally, it is easy to verify that

$$\langle (\Delta X)^2 \rangle_{\text{sq}} \langle (\Delta Y)^2 \rangle_{\text{sq}} = \frac{1}{16} [\cosh^2(2r) \sin^2 \theta + \cos^2 \theta].$$

The above formula takes the minimum uncertainty value (MUS), for $\theta = 0$ or $\theta = \pi$:

$$\langle (\Delta X)^2 \rangle_{\text{sq}} \langle (\Delta Y)^2 \rangle_{\text{sq}} = \frac{1}{16}.$$

5.1.5 Photon Statistics

The photon distribution of a coherent squeezed state can be written as

$$P_n = |\langle n | \alpha, \xi \rangle|^2,$$

where

$$\begin{aligned} \langle n | \alpha, \xi \rangle &= \frac{1}{\sqrt{n! \cosh r}} \left[\frac{1}{2} \exp(i\theta) \tanh r \right]^{\frac{n}{2}} \\ &\times \exp \left[-\frac{1}{2} (|\alpha|^2 + \alpha^{*2} \exp i\theta \tanh r) \right] \\ &\times H_n \left[\frac{\alpha + \alpha^* \exp i\theta \tanh r}{(2 \exp i\theta \tanh r)^{\frac{1}{2}}} \right], \end{aligned}$$

where H_n is the Hermite polynomial of degree n [5.5, 5.6].

5.2 Multimode Squeezed States

In general, the squeezed states generated experimentally are not single mode, but rather they cover a certain frequency band.

We consider, here, for example, a two-mode squeezed state, defined as

$$|\alpha_+, \alpha_-, \xi\rangle = D_+(\alpha_+)D_-(\alpha_-)S_{+-}(\xi)|0\rangle, \quad (5.32)$$

where

$$D_{\pm}(\alpha_{\pm}) = \exp \left[\alpha_{\pm} a_{\pm}^{\dagger} - \alpha_{\pm}^* a_{\pm} \right], \quad (5.33)$$

are the coherent displacement operators for the two modes described by the destruction operators a_+ and a_- , and

$$S_{+-}(\xi) = \exp \left(\xi^* a_+ a_- - \xi a_+^{\dagger} a_-^{\dagger} \right), \quad (5.34)$$

which is the two-mode squeezing operator and $|0\rangle$ the two-mode vacuum state.

Similarly to (5.17), we have

$$S_{+-}(\xi) a_{\pm} S_{+-}(\xi)^{\dagger} = a_{\pm} \cosh r + a_{\pm}^{\dagger} \exp(i\theta) \sinh r. \quad (5.35)$$

The above properties enable us to calculate various expectation values of combinations of creation and destruction operators:

$$\begin{aligned} \langle a_{\pm} \rangle &= \alpha_{\pm}, \\ \langle a_+ a_- \rangle &= \alpha_+ \alpha_- - \exp(i\theta) \sinh r \cosh r = \langle a_- a_+ \rangle, \\ \langle a_+ a_+ \rangle &= \alpha_+^2, \\ \langle a_- a_- \rangle &= \alpha_-^2, \\ \langle a_+^{\dagger} a_+ \rangle &= |\alpha_+|^2 + \sinh^2 r, \\ \langle a_-^{\dagger} a_- \rangle &= |\alpha_-|^2 + \sinh^2 r. \end{aligned} \quad (5.36)$$

As we can see from the above results, the squeezing affects only the diagonal photon number for each mode and the off-diagonal two-mode expectation values.

5.3 Detection of Squeezed States

As we saw in the previous section, the quadrature fluctuations of squeezed light have a dependence on the phase θ of the squeezing parameter. In principle, we can detect the squeezed signal by four different methods:

- direct Photodetection
- ordinary homodyne detection
- balanced homodyne detection
- heterodyne detection.

The first method of direct photodetection, although simple, is not the most convenient one, because the advantage of the phase-dependent squeezed light is lost, and one can associate antibunching or sub-Poissonian photon counting statistics to an incoming squeezed signal. However, both effects can also be measured with non-squeezed light, so we really need a phase-sensitive method to display the characteristics of the squeezed input. Therefore, our discussion will be centred on the two homodyne detection methods and we will also mention some aspects of heterodyne detection.

5.3.1 Ordinary Homodyne Detection

In Fig. 5.2 we show the schematic arrangement of homodyne detection. In the case of ordinary homodyne detection ([5.7],[5.8],[5.9]), only three of the four ports are used, and in the case of balanced homodyne detection, all four ports are used.

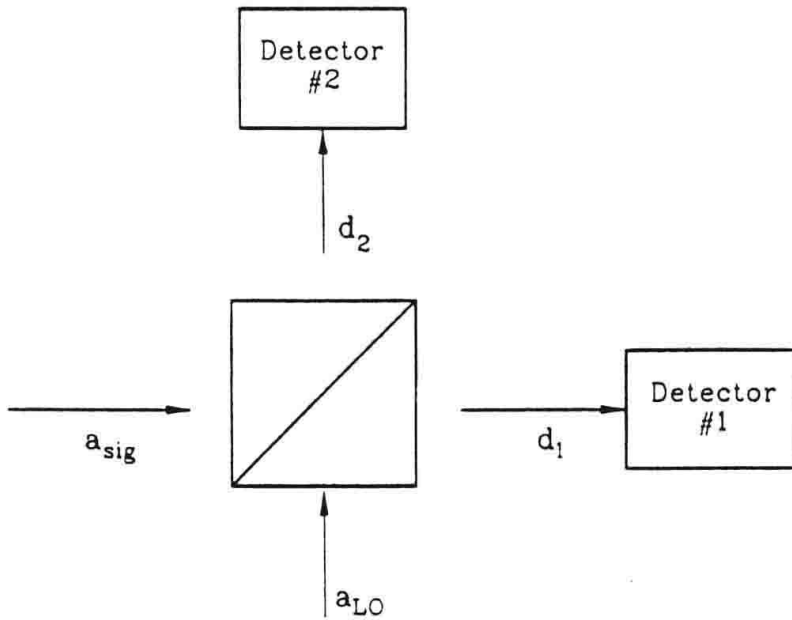


Fig. 5.2. Schematic arrangement of a homodyne detector

A lossless symmetric beam splitter mixes the squeezed signal a_{sig} with a local oscillator a_{LO} , with t and r being the transmission and reflection coefficients respectively, so one can write

$$\begin{pmatrix} d_1 \\ d_2 \end{pmatrix} = \begin{pmatrix} r & t \\ t & r \end{pmatrix} \begin{pmatrix} a_{\text{LO}} \\ a_{\text{sig}} \end{pmatrix}, \quad (5.37)$$

and the unitarity of the matrix $\begin{pmatrix} r & t \\ t & r \end{pmatrix}$ imposes the conditions

$$\begin{aligned} |r|^2 + |t|^2 &= 1, \\ rt^* + r^*t &= 0. \end{aligned} \quad (5.38)$$

If we write $r = |r| \exp(i\theta_r)$, $t = |t| \exp(i\theta_t)$, the second condition of (5.38) becomes

$$|r| |t| \{\exp[i(\theta_r - \theta_t)] + \exp[-i(\theta_r - \theta_t)]\} = 0,$$

or, since $|r|, |t| \neq 0$

$$\theta_r - \theta_t = \frac{\pi}{2}. \quad (5.39)$$

In ordinary homodyne detection $|r| \ll |t|$ while in balanced detection $|r| = |t| = 1/\sqrt{2}$.

Now we calculate the number of photons $\langle d_1 d_1 \rangle$ measured at detector #1, assumed 100% efficient, and also assuming that the local oscillator is in a coherent state $|\alpha_{\text{LO}} = |\alpha_{\text{LO}}| \exp(i\phi_{\text{LO}})\rangle$:

$$\begin{aligned}\langle d_1 d_1 \rangle &= \langle n_1 \rangle \\ &= \langle (t^* a_{\text{sig}}^\dagger + r^* a_{\text{LO}}^\dagger)(ta_{\text{sig}} + ra_{\text{LO}}) \rangle \\ &= |r|^2 |\alpha_{\text{LO}}|^2 + 2|r||t||\alpha_{\text{LO}}| \langle X_1(\phi) \rangle + |t|^2 \langle a_{\text{sig}}^\dagger a_{\text{sig}} \rangle,\end{aligned}\quad (5.40)$$

with

$$\begin{aligned}X_1(\phi) &= \frac{1}{2} [a_{\text{sig}} \exp(-i\phi) + a_{\text{sig}}^\dagger \exp(-i\phi)], \\ \phi &= \phi_{\text{LO}} + \theta_r - \theta_t = \frac{\pi}{2} + \phi_{\text{LO}}.\end{aligned}\quad (5.41)$$

Normally homodyne detectors use strong local oscillators, that is

$$|r|^2 |\alpha_{\text{LO}}|^2 \gg |t|^2 \langle a_{\text{sig}}^\dagger a_{\text{sig}} \rangle,\quad (5.42)$$

and one can approximately write

$$\langle d_1 d_1 \rangle = \langle n_1 \rangle = |r|^2 |\alpha_{\text{LO}}|^2 + 2|r||t||\alpha_{\text{LO}}| \langle X_1(\phi) \rangle.\quad (5.43)$$

One can also calculate the variance of n_1 . The result is

$$\langle \Delta n_1^2 \rangle = |r|^2 |\alpha_{\text{LO}}|^2 [|r|^2 + 4|t|^2 \langle \Delta X_1(\phi)^2 \rangle].\quad (5.44)$$

As we can see, with $r \ll t$, the fluctuations in the photon number at detector #1 are determined by the quadrature fluctuations of the phase-dependent squeezed signal.

5.3.2 Balanced Homodyne Detection

An alternative detection scheme that eliminates the large local oscillator term of the fluctuations in the direct homodyne case is to take the photocurrent difference between the two exit ports ([5.10],[5.11],[5.12]) that is (also in this balanced case $r = t = 1/\sqrt{2}$):

$$\begin{aligned}n_{12} &= d_1^\dagger d_1 - d_2^\dagger d_2 \\ &= i(a_{\text{sig}}^\dagger a_{\text{LO}} - a_{\text{sig}} a_{\text{LO}}^\dagger).\end{aligned}\quad (5.45)$$

We leave the reader to show that

$$\begin{aligned}\langle n_{12} \rangle &= 2|\alpha_{\text{LO}}| \langle X_1(\phi) \rangle, \\ \langle \Delta n_{12}^2 \rangle &= 4|\alpha_{\text{LO}}|^2 \langle \Delta X_1^2(\phi) \rangle,\end{aligned}\quad (5.46)$$

where again we have assumed that the local oscillator is coherent and much stronger than the input signal.

We notice that for a squeezed signal, $\langle \Delta X_1(\phi)^2 \rangle < \frac{1}{4}$, and therefore, the fluctuations of the photon number difference $\langle \Delta n_{12}^2 \rangle < |\alpha_{\text{LO}}|^2$ are sub-Poisson. This result would seem no different from the direct or ordinary homodyne detection scheme; however, here we have the phase dependence to check that the origin of the sub-Poissonian nature of the photocurrent is due to the squeezed field, on the one hand, and, on the other hand, we have been able to eliminate the large coherent amplitude of the local oscillator.

If we consider a more realistic detector, with a quantum efficiency η , the above result is modified [5.1] and, calling the photoncount m_{12} :

$$\begin{aligned}\langle m_{12} \rangle &= 2\eta |\alpha_{\text{LO}}| \langle X_1(\phi) \rangle, \\ \langle \Delta m_{12}^2 \rangle &= \eta |\alpha_{\text{LO}}|^2 \{1 + \eta [4\langle \Delta X_1^2(\phi) \rangle - 1]\}.\end{aligned}\quad (5.47)$$

These results coincide with (5.46) for $\eta = 1$.

5.3.3 Heterodyne Detection

Heterodyne detection is appropriate when dealing with a two-mode squeezed state. For more details, the interested reader is referred to [5.1].

Problems

5.1. Prove that for an ideal squeezed state

$$\begin{aligned}(\Delta n)^2 &= |\alpha|^2 \left[\exp(-2r) \cos^2 \left(\phi - \frac{\theta}{2} \right) + \exp(2r) \sin^2 \left(\phi - \frac{\theta}{2} \right) \right] \\ &\quad + 2 \sinh^2 r \cosh^2 r,\end{aligned}$$

where $\alpha = |\alpha| \exp i\phi$.

5.2. If we define

$$g^{(2)}(0) = \frac{\langle a^\dagger a^\dagger a a \rangle}{\langle a^\dagger a \rangle^2},$$

and

$$(Q)_{\text{Mandel}} = \frac{\langle \Delta n^2 \rangle - \langle n \rangle}{\langle n \rangle},$$

prove that for a squeezed vacuum

$$g^{(2)}(0)_{\text{sq}} = 3 + \frac{1}{\langle n \rangle},$$

$$(Q)_{\text{Mandel, sq}} = 2\langle n \rangle + 1,$$

so that the squeezed vacuum shows photon bunching and super-Poissonian statistics (Chap. 6).

5.3. Show that in balanced homodyne detection, with a quantum efficiency η , the average and fluctuations of the photocounts are

$$\langle m_{12} \rangle = 2\eta |\alpha_{\text{LO}}| \langle X_1(\phi) \rangle,$$

$$\langle \Delta m_{12}^2 \rangle = \eta |\alpha_{\text{LO}}|^2 \{ 1 + \eta [4\langle \Delta X_1^2(\phi) \rangle - 1] \}.$$

5.4. If $|X\rangle$ are eigenstates of X , show that, for $\theta = 0$

$$|\langle X | \alpha, r \rangle|^2 = \left(\frac{2 \exp 2r}{\pi} \right)^{1/2} \exp [-2(X - \text{Re}\{\alpha\})^2 \exp(2r)],$$

thus showing that squeezed states are Gaussian wavepackets.

5.6. Show that for a squeezed state, the maximum and minimum values of the Q_{Mandel} factor are given by [5.1]

$$Q_{\max} = \exp(2r) - 1, \quad \phi = \frac{\theta + \pi}{2},$$

$$Q_{\min} = \exp(-2r) - 1, \quad \phi = \frac{\theta}{2}.$$

6. Quantum Theory of Coherence

This theory was formulated originally by Glauber [6.1], where he considers the process of photon detection, which plays a central role. The basic process involved in the detection is the absorption of a photon and the corresponding generation of a photoelectron, measured via an electric current. This type of detector is insensitive to phases and spontaneous emission. This simple Glauber model is an ideal detector, sensitive to what we define as the positive frequency component of the field (proportional to the annihilation operator of the field)

$$\mathbf{E}^+(\mathbf{r}, t) = i \sum_{\mathbf{k}} \sqrt{\frac{\hbar \omega_{\mathbf{k}}}{2\epsilon_0}} a_{\mathbf{k}} u_{\mathbf{k}, \lambda}(\mathbf{r}) \exp(-i\omega_{\mathbf{k}} t), \quad (6.1)$$

$$u_{\mathbf{k}, \lambda}(\mathbf{r}) = \frac{e_{\lambda} \exp(i\mathbf{k} \cdot \mathbf{r})}{\sqrt{v}}, \quad (6.2)$$

$$\mathbf{E} = \mathbf{E}^+ + \mathbf{E}^-, \quad (6.3)$$

$$\mathbf{E}^- = (\mathbf{E}^+)^{\dagger}. \quad (6.4)$$

with e_{λ} being the polarization vector. Also, in this model, the detector atoms are in the ground state, so that only absorption takes place. Since it is only the annihilation part $\mathbf{E}^+(\mathbf{r}, t)$ of the field that takes place in the photodetection process, there is a real asymmetry between $\mathbf{E}^+(\mathbf{r}, t)$ and $\mathbf{E}^-(\mathbf{r}, t)$ in a way that the actual detection is more closely related to $\mathbf{E}^+(\mathbf{r}, t)$ than the total field \mathbf{E} . An ideal photodetector would also have an infinite bandwidth, responding to a field at time t , and a negligible spatial extension.

The transition probability from an initial state $|\psi_i\rangle$ to a final state $|\psi_f\rangle$ is proportional to

$$W_{if} = |\langle \psi_f | \mathbf{E}^+ | \psi_i \rangle|^2. \quad (6.5)$$

As we will see, this is a first-order approximation. In general, the final state of the field is not known, so we have to sum over all the possible final states:

$$\begin{aligned} I_i(\mathbf{r}, t) &= \sum_f |\langle \psi_f | \mathbf{E}^+ | \psi_i \rangle|^2 \\ &= \sum_f \langle \psi_i | \mathbf{E}^- | \psi_f \rangle \langle \psi_f | \mathbf{E}^+ | \psi_i \rangle \\ &= \langle \psi_i | \mathbf{E}^- \mathbf{E}^+ | \psi_i \rangle, \end{aligned} \quad (6.6)$$

giving us an average field intensity. In the last step, we made use of the completeness of the final states.

If the initial state is a mixed state, then we have to use the density matrix, and write

$$\langle I_i(\mathbf{r}, t) \rangle = \text{Tr} \{ \rho \mathbf{E}^-(\mathbf{r}, t) \mathbf{E}^+(\mathbf{r}, t) \}. \quad (6.7)$$

We now define the first-order coherence function:

$$G^{(1)}(x, x') = \text{Tr} \{ \rho \mathbf{E}^-(x) \mathbf{E}^+(x') \}, \quad (6.8)$$

where x and x' are $x = (\mathbf{r}, t)$ and $x' = (\mathbf{r}', t')$.

The first-order coherence function appears typically in interference experiments. In order to describe more sophisticated experiments, like the coincidence experiments of Hanbury, Brown and Twiss, it is useful to define an n th order coherence function

$$\begin{aligned} G^{(n)}(x_1, x_2, \dots, x_n; x_{n+1}, \dots, x_{2n}) \\ = \text{Tr}(\rho \mathbf{E}^-(x_1), \dots, \mathbf{E}^-(x_n) \mathbf{E}^+(x_{n+1}), \dots, \mathbf{E}^+(x_{2n})). \end{aligned} \quad (6.9)$$

We will discuss the analytical properties of these functions later.

One could in principle have a more general definition of coherence functions with unequal numbers of creation and annihilation operators. However, these functions are not particularly useful in typical photon-counting measurement.

6.1 One-Atom Detector

We now consider the detailed photodetection process. Imagine, for simplicity, as a first approach to the detection problem, that we have a one-atom photodetector, which can undergo photoabsorption transitions like the photoelectric effect. We will calculate the probability of occurrence for this type of transition within a given time interval. The Hamiltonian of the system is

$$H = H_{0,\text{at}} + H_{0,\text{f}} + H_I, \quad (6.10)$$

where $H_{0,\text{at}}$ is the free atom, $H_{0,\text{f}}$ the free field and H_I the interaction between both. H_I is in the Schrödinger picture and therefore time-independent. However, when one goes into the interaction picture, it becomes time-dependent:

$$\begin{aligned} H_I &= \exp \left[\frac{i(H_{0,\text{at}} + H_{0,\text{f}})t}{\hbar} \right] H_I \exp \left[-\frac{i(H_{0,\text{at}} + H_{0,\text{f}})t}{\hbar} \right] \\ &= -e \sum_{\gamma} q_{\gamma}(t) \cdot \mathbf{E}(\mathbf{r}, t), \end{aligned} \quad (6.11)$$

where \mathbf{r} represents the position of the atomic nucleus and q_{γ} the position of the γ electron, relative to the nucleus.

The Schrödinger equation for the system is

$$i\hbar \frac{\partial}{\partial t} |\psi(t)\rangle = H_1 |\psi(t)\rangle, \quad (6.12)$$

and its solution to first order is

$$\begin{aligned} |\psi(t)\rangle &= U(t, t_0) |\psi(t_0)\rangle \\ &\simeq \left\{ 1 + \frac{1}{i\hbar} \int_{t_0}^t dt' H_1(t') \right\} |\psi(t_0)\rangle. \end{aligned} \quad (6.13)$$

Now, suppose that initially the system is in state $|b\rangle|i\rangle$, where $|i\rangle$ is the initial state of the field and $|b\rangle$ the ground state of the atom. We ask for the probability of the system being in the excited state $|a\rangle$ and with a final state of the field $|f\rangle$. Using the Schrödinger equation with the interaction Hamiltonian H_1 , we can write

$$\begin{aligned} \langle a, f | U(t, t_0) | b, i \rangle &= \frac{1}{i\hbar} \int_{t_0}^t dt' \langle a, f | H_1(t') | b, i \rangle \\ &= \frac{ie}{\hbar} \sum_{\gamma} \int_{t_0}^t dt' \langle a | q_{\gamma}(t') | b \rangle \langle f | E(\mathbf{r}', t') | i \rangle. \end{aligned} \quad (6.14)$$

The atomic matrix element can be evaluated starting from

$$q_{\gamma}(t') = \exp \left[\frac{iH_{0,\text{at}}t'}{\hbar} \right] q_{\gamma}(0) \exp \left[-\frac{iH_{0,\text{at}}t'}{\hbar} \right], \quad (6.15)$$

and therefore

$$\begin{aligned} \langle a | \sum_{\gamma} q_{\gamma}(t') | b \rangle &= d_{ab} \exp(i\omega_{ab}t'), \\ d_{ab} &= \langle a | \sum_{\gamma} q_{\gamma}(0) | b \rangle. \end{aligned} \quad (6.16)$$

Thus, using (6.14), (6.16)

$$\begin{aligned} \langle a, f | U(t, t_0) | b, i \rangle &= \frac{ie}{\hbar} \sum_{\gamma} \int_{t_0}^t dt' \exp(i\omega_{ab}t') d_{ab} \cdot \langle f | E(\mathbf{r}', t') | i \rangle. \end{aligned} \quad (6.17)$$

We can now replace the electric field in the above expression, which consists of the sum of two operators. The emission operator $E^-(\mathbf{r}, t)$ contains the negative frequencies of the form $\exp(i\omega t)$ for $\omega > 0$, which will produce a rapidly oscillating term in (6.17), and can be safely neglected, when compared with the annihilation operator $E^+(\mathbf{r}, t)$.

We now calculate the square of the absolute value of (6.17) and sum over the final states, getting

$$\begin{aligned}
& \sum_f |\langle a, f | U(t, t_0) | b, i \rangle|^2 \\
&= \left(\frac{e}{\hbar}\right)^2 \int_{t_0}^t \int_{t_0}^t dt' dt'' \exp(i\omega_{ab}(t'' - t')) \\
&\quad \times \sum_{\mu, \nu} d_{ab, \mu}^* d_{ab, \nu} \langle i | E_\mu^-(\mathbf{r}, t') E_\nu^+(\mathbf{r}, t'') | i \rangle,
\end{aligned} \tag{6.18}$$

where, to derive the last result, we used the completeness of the final states and the relation $\langle f | E^+ | i \rangle = \langle i | E^- | f \rangle^*$.

Since the initial state $|i\rangle$ is rarely known, we must add over all initial states, and we finally get the transition probability

$$\begin{aligned}
p_{b \rightarrow a} &= \left[\sum_f |\langle a, f | U(t, t_0) | b, i \rangle|^2 \right]_{av(i)} \\
&= \left(\frac{e}{\hbar}\right)^2 \sum_{\mu, \nu} \int_{t_0}^t \int_{t_0}^t dt' dt'' \exp[i\omega_{ab}(t'' - t')] d_{ab, \mu}^* d_{ab, \nu} \\
&\quad \times \text{Tr} \{ \rho E_\mu^-(\mathbf{r}, t') E_\nu^+(\mathbf{r}, t'') \} \\
&= \left(\frac{e}{\hbar}\right)^2 \sum_{\mu, \nu} \int_{t_0}^t \int_{t_0}^t dt' dt'' \exp[i\omega_{ab}(t'' - t')] d_{ab, \mu}^* d_{ab, \nu} \\
&\quad \times G_{\mu, \nu}^{(1)}(\mathbf{r}t', \mathbf{r}t'').
\end{aligned} \tag{6.19}$$

So far, we have discussed the case of discrete final electronic states. Perhaps a more realistic model is to consider a continuum of states, characterized by a density of states $g(\omega_{ab})$, so (6.19) should be replaced by

$$p(t) = \int g(\omega_{ab}) p_{b \rightarrow a}(t) d\omega_{ab}. \tag{6.20}$$

For a broad-band detector, g is practically constant and the integral over frequencies gives us

$$\int_{-\infty}^{+\infty} d\omega_{ab} \exp(i\omega_{ab}(t'' - t')) = 2\pi\delta(t'' - t'), \tag{6.21}$$

and

$$p(t) = \sum_{\mu, \nu} S_{\mu, \nu} \int_{t_0}^t G_{\mu, \nu}^{(1)}(\mathbf{r}, t'; \mathbf{r}, t') dt', \tag{6.22}$$

with

$$S_{\mu, \nu} \equiv 2\pi \left(\frac{e}{\hbar}\right)^2 \sum_a R(a) d_{ab, \mu}^* d_{ab, \nu} \delta(\omega - \omega_{ab}).$$

We notice that in the last expression we have averaged over all final states, using $R(a)$ as a weight.

Differentiating (6.22), we get, for the rate of transition probability, or counting rate

$$w^{(1)} = \frac{dp(t)}{dt} = \sum_{\mu,\nu} S_{\mu\nu} G_{\mu\nu}^{(1)}(\mathbf{r}, t; \mathbf{r}, t). \quad (6.23)$$

If we finally put a polarization filter in front of the counter, then

$$w^{(1)} = sG^{(1)}(\mathbf{r}, t; \mathbf{r}, t) \quad (6.24)$$

with $s = S_{ii}$, i being the direction of the polarization.

The ideal photon counter is, thus, proportional to the first-order correlation function, evaluated at a single point and at a single time. A real detector, of course, has many atoms.

6.2 The n -Atom Detector

The photon counter we have discussed so far consisted of a single atom. We will see that a many-atom detector will be useful to study higher-order correlation functions of the field. The type of experiment we are thinking of is the coincidence type, where n -atom detectors are placed in positions $\mathbf{r}_1, \mathbf{r}_2, \dots, \mathbf{r}_n$. There will be a shutter opening at $t = 0$ and closing at time t . We ask for the probability $p_n(t)$ for each atom to absorb a photon, after a time interval t . It is clear that for this purpose we must apply n th-order perturbation theory.

The time evolution operator is

$$U(t, 0) = \sum_{n=0}^{\infty} \frac{(-i)^n}{n!} \int_0^t dt_1 \dots \int_0^t dt_n T [H_1(t_1) \dots H_1(t_n)] \quad (6.25)$$

$$\equiv \sum_{n=0}^{\infty} U^{(n)}(t, 0), \quad (6.26)$$

where T is Dyson's time ordering operator. Now we assume that there is no direct interaction among the atoms. Then the interaction Hamiltonian, assuming the field is linearly polarized in the x -direction, is

$$H_i(t) = -e \sum_j x_j(t) E(r_j, t) \equiv \sum_j H_{1,j}(t). \quad (6.27)$$

Replacing the Hamiltonian in Dyson's expansion, we get different types of terms. Those with repeated $H_{1,j}(t)$ correspond to atoms that absorbed more than one photon and do not contribute to $p_n(t)$. There are, on the other hand, $n!$ terms in which $H_{1,j}(t)$ appears only once, and they are all equal after time ordering. Thus, save for this factor,

$$\begin{aligned} U^{(n)}(t, 0) &\propto (-i)^n \int_0^t dt_1 \dots \int_0^t dt_n T [H_{1,1}(t_1) \dots H_{1,n}(t_n)] \quad (6.28) \\ &= \left(\frac{ie}{\hbar}\right)^n \int_0^t dt_1 \dots \int_0^t dt_n T \left[\prod_{j=1}^n x_j(t_j) E^{(+)}(\mathbf{r}_j, t_j) \right], \end{aligned}$$

where only the positive frequency part was considered, in an approximation similar to the one-atom detector case.

Taking the square modulus of the matrix elements of (6.28) between an initial and final state, summing over those final states and averaging over the initial ones, we readily get for the probability $p_n(t)$:

$$p_n(t) = s^n \int_0^t dt'_1 \dots \int_0^t dt'_n G^{(n)}(\mathbf{r}_1, t'_1, \dots, \mathbf{r}_n, t'_n; \mathbf{r}_n, t'_n, \dots, \mathbf{r}_1, t'_1), \quad (6.29)$$

where all detectors are broad-band with sensitivity s . Also

$$\begin{aligned} G^{(n)}(\mathbf{x}_1, \dots, \mathbf{x}_n; \mathbf{x}_{n+1}, \dots, \mathbf{x}_{2n}) \quad (6.30) \\ \equiv \text{Tr} \left\{ \rho E^{(-)}(\mathbf{x}_1) \dots E^{(-)}(\mathbf{x}_n) E^{(+)}(\mathbf{x}_{n+1}) \dots E^{(+)}(\mathbf{x}_{2n}) \right\}, \end{aligned}$$

where again $\mathbf{x}_j = (\mathbf{r}_j, t_j)$.

We have thus far considered n atoms undergoing absorption as part of a single detector, which in a way is similar to having n detectors, each consisting of a single atom. Now if instead the shutter in each atom is closed at different times, that is the j th atom's shutter closes at t_j , then instead of (6.29) we get

$$\begin{aligned} p_n(t_1, \dots, t_n) &= s^n \int_0^{t_1} dt'_1 \dots \int_0^{t_n} dt'_n G^{(n)} \quad (6.31) \\ &\times (\mathbf{r}_1, t'_1, \dots, \mathbf{r}_n, t'_n; \mathbf{r}_n, t'_n, \dots, \mathbf{r}_1, t'_1), \end{aligned}$$

and the n th fold coincidence rate is given by

$$\begin{aligned} w^{(n)}(t_1, \dots, t_n) &= \frac{\partial^n}{\partial t_1 \dots \partial t_n} p_n(t_1, \dots, t_n) \quad (6.32) \\ &= s^n G^{(n)}(\mathbf{r}_1, t_1, \dots, \mathbf{r}_n, t_n; \mathbf{r}_n, t_n, \dots, \mathbf{r}_1, t_1). \end{aligned}$$

Equation (6.32) tells us that a coincidence experiment with ideal detectors gives us a measure of the higher-order correlation functions. We remark here that the present theory is only approximate, to the lowest order. Higher-order corrections are, however, typically, extremely small.

6.3 General Properties of the Correlation Functions

The n th-order correlation function was defined as the expectation value

$$\begin{aligned} G^{(n)}(\mathbf{x}_1, \dots, \mathbf{x}_n; \mathbf{x}_{n+1}, \dots, \mathbf{x}_{2n}) \\ \equiv \text{Tr} \left\{ \rho E^{(-)}(\mathbf{x}_1) \dots E^{(-)}(\mathbf{x}_n) E^{(+)}(\mathbf{x}_{n+1}) \dots E^{(+)}(\mathbf{x}_{2n}) \right\}. \end{aligned}$$

As a first property, we notice that if there is an upper bound on the number of photons present in the field, then $G^{(n)}(x_1, \dots, x_n; x_{n+1}, \dots, x_{2n})$ must vanish identically for n larger than the upper bound M . To be more specific, if the field density operator is written as

$$\rho = \sum_{n,m} C_{n,m} |n\rangle\langle m|, \quad (6.33)$$

and if $C_{n,m} = 0$ for n or m larger than M , then

$$E^{(+)}(x_1) \dots E^{(+)}(x_p) \rho = 0, \quad (6.34)$$

for $p > M$, simply because the number of times the annihilation operator is applied to the density matrix is larger than the number of photons available in the field. Thus, $G^{(p)} = 0$ for $p > M$.

Another property can be derived from the identity

$$\text{Tr}(A^\dagger) = \text{Tr}(A)^* \quad (6.35)$$

which is valid for any linear operator A . Applying this identity to $G^{(n)}(x_1, \dots, x_n; x_{n+1}, \dots, x_{2n})$ we get

$$\begin{aligned} & \left[G^{(n)}(x_1, \dots, x_n; x_{n+1}, \dots, x_{2n}) \right]^* \\ &= \text{Tr} \left\{ E^{(-)}(x_{2n}) \dots E^{(-)}(x_{n+1}) E^{(+)}(x_n) \dots E^{(+)}(x_1) \rho \right\} \\ &= \text{Tr} \left\{ \rho E^{(-)}(x_{2n}) \dots E^{(-)}(x_{n+1}) E^{(+)}(x_n) \dots E^{(+)}(x_1) \right\} \\ &= \left[G^{(n)}(x_{2n}, \dots, x_{n+1}; x_n, \dots, x_1) \right], \end{aligned} \quad (6.36)$$

where we made use of the Hermitian character of ρ and the invariance of the trace under cyclic permutation. As a consequence of the commutation properties of $E^{(-)}$ and $E^{(+)}$, we can freely permute the arguments (x_1, x_2, \dots, x_n) and $(x_{n+1}, x_{n+2}, \dots, x_{2n})$ without changing $G^{(n)}$, but we cannot interchange any of the first n arguments with any of the remaining n , since the corresponding operators do not commute.

Another set of properties can be derived from the positive definite character of the operator $A^\dagger A$, so that:

$$\text{Tr}(A^\dagger A) \geq 0, \quad (6.37)$$

for any linear operator A . To show the above inequality, we write

$$\begin{aligned} \text{Tr}(\rho A^\dagger A) &= \sum_k p_k \langle k | A^\dagger A | k \rangle \\ &= \sum_{k,m} p_k \langle k | A^\dagger | m \rangle \langle m | A | k \rangle \\ &= \sum_{k,m} p_k |\langle m | A | k \rangle|^2 \geq 0, \end{aligned} \quad (6.38)$$

since p_k and $|\langle m | A | k \rangle|^2 \geq 0$. There are several interesting cases:

(a) $A = E^{(+)}(x_1)$. Then applying the inequality (6.37) we get

$$G^{(1)}(x_1, x_1) \geq 0. \quad (6.39)$$

(b) $A = E^{(+)}(x_1) \dots E^{(+)}(x_n)$. We get directly

$$G^{(n)}(x_1, \dots, x_n; x_n, \dots, x_1) \geq 0. \quad (6.40)$$

(c) $A = \sum_{j=1}^n \lambda_j E^{(+)}(x_j)$, where λ_j is a set of arbitrary complex numbers. In this case, we get

$$\sum_{i,j} \lambda_i^* \lambda_j G^{(1)}(x_i, x_j) \geq 0, \quad (6.41)$$

thus the set of correlation functions $G^{(1)}(x_i, x_j)$ forms a matrix coefficient for the quadratic form of the λ s. Such a matrix has a positive determinant; thus: For $n = 1$ we get (6.39); for $n = 2$ we get

$$G^{(1)}(x_1, x_1) G^{(1)}(x_2, x_2) \geq |G^{(1)}(x_1, x_2)|^2, \quad (6.42)$$

which is a simple generalization of Schwartz's identity.

6.4 Young's Interference and First-Order Correlation

Consider Young's experiment shown in Fig. 6.1.

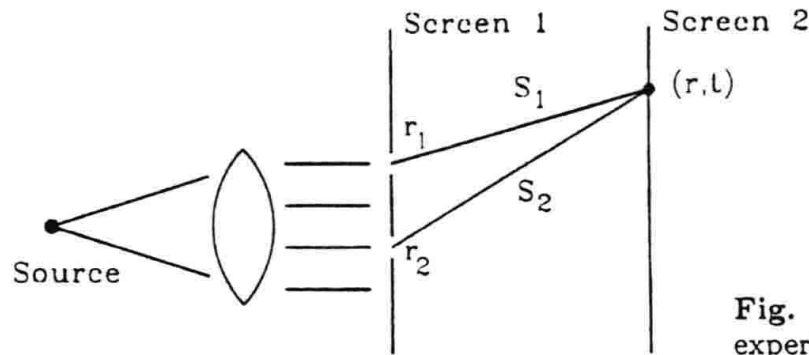


Fig. 6.1. Young's double slit experiment

We consider the positive frequency component of the field

$$\mathbf{E}^+(\mathbf{r}, t) = \mathbf{E}_1^+(\mathbf{r}, t) + \mathbf{E}_2^+(\mathbf{r}, t), \quad (6.43)$$

where $\mathbf{E}_i^+(\mathbf{r}, t)$ is the spherical wave field produced at the pinhole i , observed at screen 2:

$$\mathbf{E}_i^+(\mathbf{r}, t) = \mathbf{E}_i^+ \left(\mathbf{r}_i, t - \frac{s_i}{c} \right) \left(\frac{1}{s_i} \right) \exp(ks_i - \omega t), \quad (6.44)$$

and $\mathbf{E}_i^+(\mathbf{r}_i, t - s_i/c)$ is the field at the pinholes. Denoting

$$x_i = \left(\mathbf{r}_i, t - \frac{s_i}{c} \right), \quad i = 1, 2, \quad (6.45)$$

and $s_1 \approx s_2 = R$, then

$$\mathbf{E}^+(\mathbf{r}, t) = \frac{1}{R} [\mathbf{E}_1^+(\mathbf{x}_1) + \mathbf{E}_2^+(\mathbf{x}_2)], \quad (6.46)$$

and one can write the intensity as

$$\begin{aligned} I &= \eta \text{Tr} \{ \rho \mathbf{E}^-(\mathbf{r}, t) \mathbf{E}^+(\mathbf{r}, t) \} \\ &= \eta \left[G^{(1)}(\mathbf{x}_1, \mathbf{x}_1) + G^{(1)}(\mathbf{x}_2, \mathbf{x}_2) \right. \\ &\quad \left. + 2 \text{Re} \exp[ik(s_1 - s_2)] G^{(1)}(\mathbf{x}_1, \mathbf{x}_2) \right], \end{aligned} \quad (6.47)$$

where η scales as $1/R^2$. The first two terms are the intensities from each pinhole, with the other one blocked, and the third term is the interference.

Writing

$$G^{(1)}(\mathbf{x}_1, \mathbf{x}_2) = |G^{(1)}(\mathbf{x}_1, \mathbf{x}_2)| \exp(i\Psi), \quad (6.48)$$

then

$$I = \eta \left[G^{(1)}(\mathbf{x}_1, \mathbf{x}_1) + G^{(1)}(\mathbf{x}_2, \mathbf{x}_2) + 2 \cos(\phi) |G^{(1)}(\mathbf{x}_1, \mathbf{x}_2)| \right] \quad (6.49)$$

with $\phi = \Psi + k(s_1 - s_2)$.

In order to have a maximum interference term or maximum visibility, we have to maximize $|G^{(1)}(\mathbf{x}_1, \mathbf{x}_2)|$. However, this quantity is limited by the inequality

$$|G^{(1)}(\mathbf{x}_1, \mathbf{x}_2)| \leq \sqrt{G^{(1)}(\mathbf{x}_1, \mathbf{x}_1)G^{(1)}(\mathbf{x}_2, \mathbf{x}_2)}, \quad (6.50)$$

which leads us to the definition of the first-order normalized correlation function

$$g^{(1)}(\mathbf{x}_1, \mathbf{x}_2) = \frac{G^{(1)}(\mathbf{x}_1, \mathbf{x}_2)}{\sqrt{G^{(1)}(\mathbf{x}_1, \mathbf{x}_1)G^{(1)}(\mathbf{x}_2, \mathbf{x}_2)}}. \quad (6.51)$$

The condition of full first-order coherence is satisfied if

$$g^{(1)}(\mathbf{x}_1, \mathbf{x}_2) = \exp(i\Psi), \quad (6.52)$$

or

$$|g^{(1)}(\mathbf{x}_1, \mathbf{x}_2)| = 1. \quad (6.53)$$

One usually defines a quantity called the visibility, as

$$\begin{aligned} v &= \frac{I_{\max} - I_{\min}}{I_{\max} + I_{\min}} \\ &= \frac{2 |G^{(1)}(\mathbf{x}_1, \mathbf{x}_2)|}{G^{(1)}(\mathbf{x}_1, \mathbf{x}_1) + G^{(1)}(\mathbf{x}_2, \mathbf{x}_2)}, \end{aligned} \quad (6.54)$$

and for equal intensities in the two pinholes

$$v = |g^{(1)}(\mathbf{x}_1, \mathbf{x}_2)|. \quad (6.55)$$

For full first-order coherence, $v = 1$ and this corresponds to maximum visibility.

A more general definition of coherence is related to the factorization of the correlation functions. For first-order coherence, the first-order correlation function factorizes as

$$G^{(1)}(x_1, x_2) = \varepsilon(x_1)\varepsilon(x_2). \quad (6.56)$$

Obviously, for a state that is an eigenstate of $\mathbf{E}^+(\mathbf{x})$, that is an eigenstate of the annihilation operator, this factorization holds. This is precisely the case of the coherent states. In a similar way, n th-order optical coherence implies

$$G^{(n)}(x_1, x_2, \dots, x_n, \dots, x_{2n}) = \varepsilon(x_1)\varepsilon(x_2)\dots\varepsilon(x_{2n}), \quad (6.57)$$

which again is satisfied by coherent states.

To finish this section, we point out that in spite of the fact that the first-order correlation function can be evaluated quantum mechanically, the difference between the classical and the quantum predictions in first-order coherence may be difficult to detect. In both cases $0 \leq |g^{(1)}(x_1, x_2)| \leq 1$.

In second-order coherence effects, the differences are more striking.

6.5 Second-Order Correlations. Photon Bunching and Antibunching

The second-order normalized correlation function is defined as [6.6]

$$\begin{aligned} g^{(2)}(r_1 t_1, r_2 t_2; r_2 t_2, r_1 t_1) &= (6.58) \\ &= \frac{\langle \mathbf{E}^-(\mathbf{r}_1, t_1) \mathbf{E}^-(\mathbf{r}_2, t_2) \mathbf{E}^+(\mathbf{r}_2, t_2) \mathbf{E}^+(\mathbf{r}_1, t_1) \rangle}{\langle \mathbf{E}^-(\mathbf{r}_1, t_1) \mathbf{E}^+(\mathbf{r}_1, t_1) \rangle \langle \mathbf{E}^-(\mathbf{r}_2, t_2) \mathbf{E}^+(\mathbf{r}_2, t_2) \rangle}. \end{aligned}$$

In this section, we will consider only parallel light beams (z -direction), so that the space-time coordinates $(z_1, t), (z_2, t_2)$ enter in $g^{(2)}$ only as a phase difference:

$$\tau = t_2 - t_1 + \frac{z_1 - z_2}{c}. \quad (6.59)$$

We start the subject with a brief review of some classical aspects.

6.5.1 Classical Second-Order Coherence

We consider a beam of light described by a classical intensity $I_1(t)$, which is time-dependent and averaged over each cycle. In general, the intensity will show random fluctuations, if one is dealing, for example, with a source of chaotic light. We will assume that the light sources under study are stationary and ergodic, in such a way that ensemble averages are equal to time averages. Classically, the second-order correlation function may be defined as

$$g_{11}^{(2)}(t) = \frac{\langle I_1(t)I_1(0) \rangle}{\bar{I}_1^2}, \quad (6.60)$$

where the average is over a long series of pairs of intensity measurements separated by a fixed time t and $\bar{I}_1 = \langle I_1 \rangle$ is a time-independent average, due to the assumption of stationary sources.

In a different type of experiment, we may measure intensities at different positions $\mathbf{r}_1, \mathbf{r}_2$. Then the relevant second-order correlation function is

$$g_{12}^{(2)}(t) = \frac{\langle I_1(t)I_2(0) \rangle}{\bar{I}_1 \bar{I}_2}. \quad (6.61)$$

The classical correlation functions satisfy a series of inequalities:

(a) Since the intensity is positive

$$g_{12}^{(2)}(t) \geq 0. \quad (6.62)$$

(b) Since $\langle I_1^2 \rangle \geq \bar{I}_1^2$, then

$$g_{11}^{(2)}(0) \geq 1. \quad (6.63)$$

(c) In the more general case, and according to Cauchy's inequality,

$$\langle I_1^2 \rangle \langle I_2^2 \rangle \geq \langle I_1 I_2 \rangle^2. \quad (6.64)$$

Fixing the time t between the two measurements on the two beams, we have:

$$g_{11}^{(2)}(0) g_{22}^{(2)}(0) \geq [g_{12}^{(2)}(t)]^2, \quad (6.65)$$

and for a single beam $g_{11}^{(2)}(0) = g_{22}^{(2)}(0)$ and

$$g_{11}^{(2)}(0) \geq g_{12}^{(2)}(t). \quad (6.66)$$

In many cases, the fluctuations of the cycle-averaged intensities are too rapid for direct observation and the measurement reflects some average of the fluctuations over some typical response time of the detector. However, we do have fast detectors nowadays, so let us assume that its response time is much faster than the coherence time of the light, so that effectively we have instantaneous measurements of the intensity. If, furthermore, the ergodic hypothesis is satisfied, then the time average may be replaced by statistical averages, denoted by angle brackets. We take a model of chaotic light emitted by a collision-broadened light source. In this model, the elastic collisions break up the wave radiated by single atoms, in discrete sections, where each section has a constant phase that abruptly ends with a collision. Suppose that we have light of intensity I_0 from n radiating atoms, the phase of the field emitted from the i th atom being a random variable ϕ_i . Then, one can write

$$\begin{aligned} E(t) &= E_1(t) + E_2(t) + \cdots + E_n(t) \\ &= E_0 \{ \exp[i\phi_1(t)] + \exp[i\phi_2(t)] + \cdots + \exp[i\phi_n(t)] \}, \end{aligned}$$

where each atom is associated with the same amplitude and field frequency but with phases which are completely independent.

The instantaneous average value of the square of the intensity is

$$\overline{I_1^2(0)} = I_0^2 |\exp(i\phi_1) + \exp(i\phi_2) + \cdots + \exp(i\phi_n)|^4. \quad (6.67)$$

The only non-zero contributions come from the terms in which each factor is multiplied by its complex conjugate. These are

$$\begin{aligned} \overline{I_1^2(0)} &= I_0^2 \left[\sum_{i=1}^n |\exp(i\phi_i)|^4 + \sum_{i \neq j} |2 \exp i(\phi_i - \phi_j)|^2 \right] \\ &= I_0^2 [2n^2 - n]. \end{aligned} \quad (6.68)$$

If we further average, considering a Poissonian distribution of incoming atoms, with a mean \bar{n} , and $\bar{n}^2 = \bar{n}^2 + \bar{n}$, then

$$\langle \overline{I_1^2(0)} \rangle_{\text{Poisss}} = I_0^2 (2\bar{n}^2 + \bar{n}). \quad (6.69)$$

Also, since $\langle \overline{I_1(0)} \rangle_{\text{Poisss}} = \bar{n}I_0$, we have

$$g_{11}^{(2)}(0) = 2 + \frac{1}{\bar{n}}. \quad (6.70)$$

The standard theory of chaotic light considers a very large number of atoms radiating, that is, the limit $\bar{n} \rightarrow \infty$, $g_{11}^{(2)}(0) = 2$. More generally, one can consider a large number of radiating atoms and the summation over the phases is treated as a random walk. As a result of such a theory, one gets the probability distribution for the instantaneous intensity I_1 :

$$P(I) = \frac{1}{I_1} \exp - \frac{I_1}{I_1}, \quad (6.71)$$

giving $g_{11}^{(2)}(0) = 2$, in agreement with our previous result.

Normally, when we deal with a single beam of light, we skip the lower indices, and for chaotic light, we will just write $g^{(2)}(0) = 2$.

6.5.2 Quantum Theory of Second-Order Coherence

The quantum mechanical normalized second-order correlation function $g^2(\tau)$ is positive, so that the inequality

$$\infty \geq g^{(2)}(\tau) \geq 0, \quad (6.72)$$

is identical to the classical range. However, the classical inequalities given in (6.63), (6.66) are, in general, no longer true. Even for zero time delay, in the quantum mechanical case, the only true inequality is

$$\infty \geq g^{(2)}(0) \geq 0. \quad (6.73)$$

and since classically $g_2(0) |_{\text{class}} \geq 1$, there is an interesting range:

$$1 > g^{(2)}(0) \geq 0, \quad (6.74)$$

which is a purely quantum mechanical range.

For a single-mode field, the normalized correlation functions become simpler, and one can write

$$g^{(2)}(\tau) = \frac{\langle a^\dagger a^\dagger a a \rangle}{\langle a^\dagger a \rangle^2}, \quad (6.75)$$

which can also be written in terms of the photon-number operator

$$\begin{aligned} g^{(2)}(\tau) &= \frac{\langle n(n-1) \rangle}{\langle n \rangle^2} \\ &= 1 + \frac{\langle (\Delta n)^2 \rangle - \langle n \rangle}{\langle n \rangle^2}. \end{aligned} \quad (6.76)$$

We observe that for a single-mode field, there is no time dependence (the τ dependent phase factor cancels) in $g^{(2)}(\tau)$.

A few simple examples of $g^{(2)}(\tau)$ are:

(a) For an $|n\rangle$ state

$$g^{(2)}(\tau) = \frac{(n-1)}{n}, \quad n \geq 2 \quad (6.77)$$

and $g^{(2)}(\tau) = 0$ for $n = 0, 1$.

(b) For a coherent state $|\alpha\rangle$, $\langle(\Delta n)^2\rangle = \langle n \rangle$ and $g^{(2)}(\tau) = 1$. It is convenient to define the momentum generating function $Q(s)$ as

$$Q(s) = \sum_{n=0}^{\infty} (1-s)^n P(n), \quad (6.78)$$

where $P(n)$ is the probability of having n photons in the field. One immediately sees that

$$\begin{aligned} \langle n \rangle &= -\frac{d}{ds} Q(s) \Big|_{s=0}, \\ \langle(\Delta n)^2\rangle &= \langle n^2 \rangle - \langle n \rangle^2 \\ &= \left(\frac{d}{ds}\right)^2 Q(s) \Big|_{s=0} - \langle n \rangle(\langle n \rangle - 1), \end{aligned} \quad (6.79)$$

and also

$$g^{(2)} = \frac{1}{\langle n \rangle^2} \left(\frac{d}{ds}\right)^2 Q(s) \Big|_{s=0}. \quad (6.80)$$

In general, light with $g^{(2)} = 1$ is second-order coherent or Poissonian (as in the case of the coherent state), $g^{(2)} > 1$ super-Poissonian and $g^{(2)} < 1$ sub-Poissonian.

(c) Squeezed states. In Chap. 5 (see problem 5.1), we saw that

$$\begin{aligned} (\Delta n)^2 &= |\alpha|^2 \left[\exp(-2r) \cos^2 \left(\phi - \frac{\theta}{2} \right) + \exp(2r) \sin^2 \left(\phi - \frac{\theta}{2} \right) \right] \\ &\quad + 2 \sinh^2 r \cosh^2 r, \end{aligned} \quad (6.81)$$

with

$$\alpha = |\alpha| \exp i\phi. \quad (6.82)$$

With the above expression and (6.76), one can evaluate $g^{(2)}(0)$.

In Fig. 6.2 we show the second-order correlation function of the squeezing parameter r , with constant average photon number. We can see that for $\phi = \theta/2$ one can minimize $\langle \Delta n \rangle_{\text{sq}}^2$ and we can get sub-Poissonian light. On the other hand, for very many other combinations of the parameters, the light is super-Poissonian.

If $g^{(2)}(\tau) < g^{(2)}(0)$, there is a tendency for photons to arrive in pairs, a situation referred to as *photon bunching*. The reverse situation $g^{(2)}(\tau) > g^{(2)}(0)$ is called *photon antibunching*, and this occurs typically when an atom emits a photon and right after that there is an anticorrelation for a second photon to be emitted, considering that the atom requires a finite time to go back to its excited state to be ready to emit a second photon. For very long times, there is no longer any correlation and $g^{(2)}(\tau) \xrightarrow{\tau \rightarrow \infty} 1$. Thus, a field with $g^{(2)}(0) < 1$ will always be antibunched over some time scale, which is the quantum mechanical case with no classical analogue.

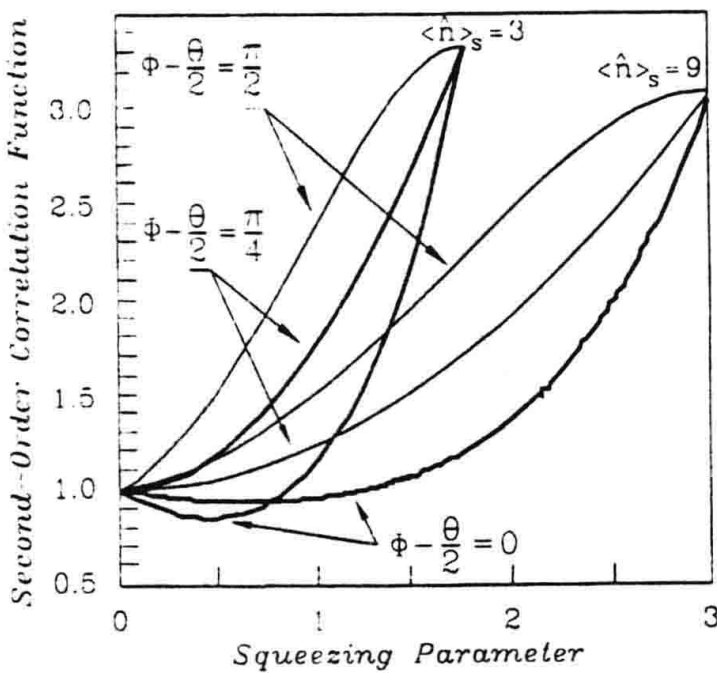


Fig. 6.2. The second-order correlation function of the coherent squeezed state (after [5.5])

Photon antibunching and sub-Poissonian statistics sometimes get mixed up in the literature, giving the wrong impression that they correspond to the same thing. Although they are related, they are not the same.

Mandel [6.2] derived a formula for stationary fields:

$$V(n) - \langle n \rangle = \frac{\langle n \rangle^2}{T^2} \int_{-T}^{+T} d\tau (T - |\tau|) [g^{(2)}(\tau) - 1], \quad (6.83)$$

with $V(n) = \langle n^2 \rangle - \langle n \rangle^2$. When a field has $g^{(2)}(\tau) < 1$ for all τ , then $V(n) - \langle n \rangle < 0$ and exhibits sub-Poissonian statistics. However, we may have the case $g^{(2)}(\tau) > g^{(2)}(0)$ (antibunching) which exhibits super-Poissonian statistics ($g^{(2)}(\tau), g^{(2)}(0) > 1$), for some time interval τ .

6.6 Photon Counting

The probability distribution $p(n, t, T)$ of registering n photoelectrons in the interval $t, t + T$ is given by the relation

$$p(n, T) = \int_0^\infty \frac{[\alpha \bar{I}(t)T]^n}{n!} \exp[-\alpha \bar{I}(t)T] P[\bar{I}(t)] d\bar{I}(t), \quad (6.84)$$

where α is the quantum efficiency of the detector and $\bar{I}(t)$ is the average intensity

$$\bar{I}(t) = \frac{1}{T} \int_t^{t+T} dt' I(t'). \quad (6.85)$$

$P(\bar{I}(t))$ is the probability density of $\bar{I}(t)$, considered as a random variable. This formula was derived by Mandel [6.3], using classical arguments. The two basic assumptions in this derivation are:

- (a) the probability of registering a photoelectric count in a short time interval Δt is linear with Δt and with the instantaneous intensity $I(t)$;
- (b) different photon counts are statistically independent.

However, since the photoelectric effect is a quantum mechanical phenomenon, the above assumptions were not completely satisfactory and Mandel *et al.* (6.84) introduced improvements, using first-order perturbation theory, with a semiclassical model, where the field is classical and the detector quantum mechanical [6.4]. He considered a model of a photodetector that consisted of a group of independent atoms interacting with the radiation field. The result showed that the probability of photoemission is proportional to $I(t)$:

$$P(t)\Delta t = \alpha I(t)\Delta t, \quad (6.86)$$

α again being the quantum efficiency which depends on the detector parameters. We also assume that the light falling on the detector is quasi-monochromatic, and that Δt is much smaller than the coherence time of the

light t_c . This coherence time gives the time scale over which intensity changes take place.

From the assumption that different photoelectric emissions are statistically independent events, it follows that the probability of having n photoelectric emissions in a finite time interval $t, t + T$ is a Poisson distribution:

$$p(n, t, T) = \frac{(\alpha \bar{I}(t, T)T)^n}{n!} \exp(-\alpha \bar{I}(t, T)T). \quad (6.87)$$

To see how (6.87) follows from (6.86) [6.5], we divide the interval $t, t + T$ in a large number N of subintervals, with $\Delta t = T/N$. Let z_k be a random variable taking the values 0 or 1, depending respectively, on whether or not there has been a photoemission in the interval $t + (k - 1)\Delta t, t + (k)\Delta t$, for $k = 1, 2, \dots, N$. The total number of photoemissions is then

$$n = \sum_{k=1}^N z_k. \quad (6.88)$$

Now, we define a generating function $G(\lambda, t, T)$ as

$$G(\lambda, t, T) = \sum_n (1 - \lambda)^n p(n, t, T). \quad (6.89)$$

If we assume that all the z_k are independent, we find that

$$\begin{aligned} G(\lambda, t, T) &= \langle (1 - \lambda)^n \rangle \\ &= \langle \prod_{k=1}^N (1 - \lambda)^{z_k} \rangle \\ &= \prod_{k=1}^N \langle (1 - \lambda)^{z_k} \rangle. \end{aligned} \quad (6.90)$$

Since z_k is either 0 or 1, $(1 - \lambda)^{z_k} = 1 - \lambda z_k$, and therefore

$$\begin{aligned} G(\lambda, t, T) &= \prod_{k=1}^N [1 - \lambda p(z_k = 1)] \\ &= \prod_{k=1}^N (1 - \lambda \alpha \bar{I}(t + k \Delta t) \Delta t) \\ &\xrightarrow{N \rightarrow \infty} \exp \left[-\alpha \lambda \int_t^{t+T} I(t') dt' \right] \\ &= \exp [-\alpha \lambda T \bar{I}(t)], \end{aligned} \quad (6.91)$$

and since

$$p(n, t, T) = \frac{(-1)^n}{n!} \frac{\partial^n}{\partial \lambda^n} G(\lambda, t, T) \Big|_{\lambda=1}, \quad (6.93)$$

we get (6.87).

The probability $p(n, t, T)$ represents the distribution of readings of the photon count obtained in a series of experiments, all of them with the same initial time t . Normally in experiments the situation is rather different. Measurements are not in parallel but in series, that is, one conducts only one counting measurement at a time, followed by successive counting periods, consecutively rather than simultaneously, and the outcome of such a sequence of measurements is an average of $p(n, t, T)$ over the starting times t . Thus, we write

$$p(n, T) = \left\langle \frac{[\alpha \bar{I}(t, T)T]^n}{n!} \exp[-\alpha \bar{I}(t, T)T] \right\rangle_t \quad (6.94)$$

where $\langle \rangle_t$ means an average over the initial times t .

The photon count distribution can be further simplified in the case of counting times $T \ll t_c$, in which case the intensity is basically a constant during the counting time, and we can write:

$$\bar{I}(t, T) = \bar{I}(t). \quad (6.95)$$

With the usual ergodic hypothesis that time averages can be replaced by ensemble averages, and considering the intensity distribution $P(\bar{I}(t))$, one can write

$$p(n, T) = \int d\bar{I}(t) P(\bar{I}(t)) \frac{(\alpha \bar{I}(t)T)^n}{n!} \exp(-\alpha \bar{I}(t)T),$$

which is precisely (6.84).

Our discussion shows that the fluctuations in the photoelectric emission may be regarded as being due to two causes

- (1) Intrinsic fluctuations in the detection process. This is due to the random ejection of photoelectrons, regardless of the intensity fluctuations of the light falling on the detector, resulting in a Poisson distribution.
- (2) Fluctuations in the intensity. As a result, usually the photoelectron distribution is *not* a Poissonian.

Making use of the expression for $p(n, T)$, we can calculate the average number of photon counts, as well as various moments. For the average

$$\begin{aligned} \langle n \rangle &= \sum_n np(n, T) \\ &= \int_0^\infty \sum_{n=0}^{\infty} d\bar{I}(t) P(\bar{I}(t)) n \frac{[\alpha \bar{I}(t)T]^n}{n!} \exp[-\alpha \bar{I}(t)T] \\ &= \int_0^\infty d\bar{I}(t) P(\bar{I}(t)) \alpha T \bar{I}(t) \sum_{n=1}^{\infty} \frac{[\alpha \bar{I}(t)T]^{n-1}}{(n-1)!} \exp[-\alpha \bar{I}(t)T] \\ &= \alpha T \langle \bar{I}(t) \rangle. \end{aligned} \quad (6.96)$$

Similarly, one finds

$$\begin{aligned} \langle n^2 \rangle &= \alpha^2 T^2 \langle \bar{I}(t)^2 \rangle + \alpha T \langle \bar{I}(t) \rangle, \\ \langle (\Delta n)^2 \rangle &= \langle n^2 \rangle - \langle n \rangle^2 = \alpha^2 T^2 [\langle \bar{I}(t)^2 \rangle - \langle \bar{I}(t) \rangle^2] + \alpha T \langle \bar{I}(t) \rangle. \end{aligned} \quad (6.97)$$

6.6.1 Some Simple Examples

- (1) Constant intensity $I(t) = I$. In this case the averaging procedure is unnecessary, and one gets the Poisson distribution

$$p(n, T) = \frac{\langle n \rangle^n}{n!} \exp(-\langle n \rangle). \quad (6.98)$$

with

$$\langle n \rangle = \alpha T \bar{I}, \quad (6.99)$$

- (2) $P(\bar{I}(t)) = \exp(-\bar{I}(t)/\bar{I})/\bar{I}$. This corresponds to a chaotic light source. The photon count probability is:

$$\begin{aligned} p(n, T) &= \frac{1}{\bar{I}} \int d\bar{I}(t) \exp\left(-\frac{\bar{I}(t)}{\bar{I}}\right) \left[\left\{ \frac{[\alpha \bar{I}(t)T]^n}{n!} \right\} \right] \\ &\quad \times \exp[-\alpha \bar{I}(t)T] \\ &= \frac{\langle n \rangle^n}{(1 + \langle n \rangle)^{n+1}}. \end{aligned} \quad (6.100)$$

Thus, for short counting times, the photon count distribution for chaotic light is similar to the photon distribution of single-mode thermal light. However, the difference is that this photon count distribution applies to any chaotic light, in general with many modes.

6.6.2 Quantum Mechanical Photon Count Distribution

A fully quantum mechanical description of photon counting was first derived by Kelly and Kleiner [6.6], [6.7]. The result is similar to the classical expression

$$p(n, T) = \left\langle : \frac{[\alpha \bar{I}(T)T]^n}{n!} \exp[-\alpha \bar{I}(T)T] : \right\rangle. \quad (6.101)$$

The only difference with the classical expression is the $::$ symbol, indicating normal ordering. In (6.101), $\bar{I}(T)$ is defined as

$$\begin{aligned} \bar{I}(T) &= \frac{1}{T} \int_0^T I(t) dt \\ &= \frac{1}{T} \int_0^T E^{(-)}(\mathbf{r}, t) E^{(+)}(\mathbf{r}, t) dt. \end{aligned} \quad (6.102)$$

For the case of a single radiation mode, the above formula simplifies to

$$p(n, T) = \text{Tr} \left\{ \rho : \frac{(\xi a^\dagger a)^n}{n!} \exp(-\xi a^\dagger a) : \right\}, \quad (6.103)$$

with

$$\xi \equiv \alpha \frac{\hbar \omega T}{2 \varepsilon_0 v}. \quad (6.104)$$

The parameter ξ is usually called the quantum efficiency of the detector. We also notice that in the case of a single mode, $p(n, T)$ is time independent.

Expanding the exponential in (6.103), one can write

$$p(m, T) = \sum_n P_n \left(\frac{\xi^m}{m!} \right) \sum_{l=0}^{\infty} (-1)^l \frac{\xi^l}{l!} \langle n | (a^\dagger)^{m+l} (a)^{m+l} | n \rangle, \quad (6.105)$$

where $P_n = \langle n | \rho | n \rangle$. By making use of (3.27), the above result can be simplified to

$$\begin{aligned} p(m, T) &= \sum_n P_n \left(\frac{\xi^m}{m!} \right) \sum_{l=0}^{n-m} (-1)^l \frac{\xi^l}{l!} \frac{n!}{(n-m-l)!}, \\ &= \sum_{n=m}^{\infty} P_n \binom{n}{m} \xi^m (1-\xi)^{n-m}. \end{aligned} \quad (6.106)$$

This form of the photocount distribution is the Bernoulli distribution, and has a physical interpretation as follows: the probability of a photon being counted during the period T is the quantum efficiency ξ , thus the probability of counting m out of n photons is proportional to the probability of counting m photons ξ^m times the probability of not counting $n-m$ photons $(1-\xi)^{n-m}$. Now, the only fixed number in this analysis is m , the number of detected photons after the given interval, so the total probability of counting m photons has to involve a sum from $n=m$ to ∞ , weighted by two factors. The first one is the probability of having n photons to start with, P_n , and the second factor is related to the indistinguishability of the photons.

6.6.3 Particular Examples

It is simple to calculate the following cases:

Coherent state

$$\begin{aligned} P_n &= \frac{(\bar{n})^n}{n!} \exp(-\bar{n}), \\ p(m, T) &= \frac{(\xi \bar{n})^m}{m!} \exp(-\xi \bar{n}). \end{aligned} \quad (6.107)$$

Filtered single-mode chaotic light

$$\begin{aligned} P_n &= \frac{(\bar{n})^n}{(1+\bar{n})^{1+n}}, \\ p(m, T) &= \frac{(\xi \bar{n})^m}{(1+\xi \bar{n})^{m+1}}. \end{aligned} \quad (6.108)$$

Problems

6.1. Prove (6.97).

7. Phase Space Description

In general, a full description of the state of the electromagnetic field is given by the density operator. However, there are various ways in which the field can be described by complex functions of α . These methods are of considerable practical interest, since one is dealing with functions rather than operators. The most common representations in phase space are the Glauber distribution, and the Q and Wigner representations. The Wigner distribution is the one that resembles more closely the classical probability. On the other hand, the P -distribution originates from representing the density operator as an ensemble of coherent states and the Q -representation is a description of the density matrix via its diagonal elements, again, in a coherent state basis.

7.1 Q -Representation. Antinormal Ordering

The definition of the Q -distribution function is

$$Q(\alpha, \alpha^*) \equiv \frac{1}{\pi} \langle \alpha | \rho | \alpha \rangle. \quad (7.1)$$

There are a number of properties associated to the Q -function.

7.1.1 Normalization

$$\begin{aligned} \text{Tr} \{ \rho \} &= 1 \\ &= \text{Tr} \left\{ \frac{1}{\pi} \int d^2\alpha |\alpha\rangle\langle\alpha| \rho \right\} \\ &= \frac{1}{\pi} \int d^2\alpha \langle\alpha | \rho | \alpha\rangle, \end{aligned}$$

which implies

$$\int d^2\alpha Q(\alpha, \alpha^*) = 1. \quad (7.2)$$

7.1.2 Average of Antinormally Ordered Products

We calculate averages of the type

$$\begin{aligned}\langle a^r(a^\dagger)^s \rangle &= \text{Tr} \{ a^r(a^\dagger)^s \rho \} \\ &= \text{Tr} \left\{ \frac{1}{\pi} \int d^2\alpha |\alpha\rangle\langle\alpha| (a^\dagger)^s \rho a^r \right\} \\ &= \frac{1}{\pi} \int d^2\alpha \text{Tr} \{ |\alpha\rangle\langle\alpha| (a^\dagger)^s \rho a^r \} \\ &= \frac{1}{\pi} \int d^2\alpha \langle\alpha| (a^\dagger)^s \rho a^r |\alpha\rangle,\end{aligned}$$

so, we finally write

$$\langle a^r(a^\dagger)^s \rangle = \int d^2\alpha (\alpha^*)^s \alpha^r Q(\alpha, \alpha^*). \quad (7.3)$$

7.1.3 Some Examples

Coherent state

$$\rho = |\alpha_0\rangle\langle\alpha_0|,$$

which gives

$$Q(\alpha, \alpha^*) = \frac{1}{\pi} |\langle\alpha_0|\alpha\rangle|^2 = \frac{1}{\pi} \exp(-|\alpha - \alpha_0|^2). \quad (7.4)$$

Number state

$$\rho = |n\rangle\langle n|,$$

$$Q(\alpha, \alpha^*) = \frac{1}{\pi} |\alpha| |n\rangle\langle n| = \frac{1}{\pi} \exp(-|\alpha|^2) \left\{ \frac{(|\alpha|^2)^n}{n!} \right\}. \quad (7.5)$$

We notice that the Q -function is independent of the phase of α , and the maximum is located at $|\alpha|^2 = n$.

Thermal state

$$\rho = \left(1 - \exp\left(-\frac{\hbar\omega}{kT}\right) \right) \sum_n |n\rangle\langle n| \exp\left(-\frac{n\hbar\omega}{k_B T}\right), \quad (7.6)$$

$$Q(\alpha, \alpha^*) = \frac{1 - \exp(-\hbar\omega/kT)}{\pi} \sum_n \exp\left(-\frac{n\hbar\omega}{k_B T}\right) [\exp(-|\alpha|^2)] \frac{|\alpha|^{2n}}{n!},$$

so, that

$$Q(\alpha, \alpha^*) = \frac{1 - \exp(-\hbar\omega/kT)}{\pi} \exp\left\{-|\alpha|^2 \left(1 - \exp\left(-\frac{\hbar\omega}{k_B T}\right)\right)\right\}. \quad (7.7)$$

It is simple to show that

$$\langle \alpha^p \rangle = \langle \alpha^{*p} \rangle = 0, \quad (7.8)$$

by observing that

$$\langle \alpha^p \rangle = \langle a^p \rangle \propto \langle n | a^p | n \rangle = 0.$$

Also,

$$\langle aa^\dagger \rangle = \langle |\alpha|^2 \rangle = \left(1 - \exp\left(-\frac{\hbar\omega}{k_B T}\right) \right)^{-1}. \quad (7.9)$$

In the particular limit $k_B T \rightarrow 0$, we get $\langle aa^\dagger \rangle = \langle |\alpha|^2 \rangle = 1$, which is the correct answer, since at $T = 0$, $\langle n \rangle = 0$.

7.1.4 The Density Operator in Terms of the Function *Q*

We pose the following question: Is it possible to construct the density matrix, once the *Q*-function is known? Starting from a coherent state

$$| \alpha \rangle = \exp(-|\alpha|^2) \sum_n \frac{\alpha^n}{n!} | n \rangle,$$

and using the definition of the *Q*-function, (7.1), we write

$$\begin{aligned} Q(\alpha, \alpha^*) &\equiv \frac{1}{\pi} \langle \alpha | \rho | \alpha \rangle \\ &= \frac{\exp(-|\alpha|^2)}{\pi} \sum_{n,m} \frac{\langle n | \rho | m \rangle}{\sqrt{n!m!}} \alpha^m \alpha^{*n} \\ &\equiv \sum_{n,m} Q_{n,m} \alpha^m \alpha^{*n}. \end{aligned} \quad (7.10)$$

From (7.10), we get

$$\begin{aligned} Q(\alpha, \alpha^*) \exp(|\alpha|^2) &= \sum_{n',m',r} \frac{Q_{n',m'} \alpha^{m'+r} \alpha^{*n'+r}}{r!} \\ &= \frac{1}{\pi} \sum_{n,m} \frac{\langle n | \rho | m \rangle \alpha^m \alpha^{*n}}{\sqrt{n!m!}}. \end{aligned}$$

Comparing equal powers of α and α^* , we get

$$\sum_r \frac{Q_{n-r,m-r}}{r!} \pi \sqrt{n!m!} = \langle n | \rho | m \rangle, \quad (7.11)$$

thus answering the question posed at the beginning of this section.

7.2 Characteristic Function

There are three characteristic functions, defined in a normal, antinormal and symmetric (Wigner) way

$$\begin{aligned} X_N(\eta) &= \text{Tr} \{ \rho \exp(\eta a^\dagger) \exp(-\eta^* a) \}, \\ X_A(\eta) &= \text{Tr} \{ \rho \exp(-\eta^* a) \exp(\eta a^\dagger) \}, \\ X_W(\eta) &= \text{Tr} \{ \rho \exp(\eta a^\dagger - \eta^* a) \}. \end{aligned} \quad (7.12)$$

The antinormal characteristic function is related to the Q -distribution:

$$\begin{aligned} X_A(\eta) &= \text{Tr} \{ \rho \exp(-\eta^* a) \exp(\eta a^\dagger) \} \\ &= \frac{1}{\pi} \int d^2\alpha \langle \alpha | \exp(\eta a^\dagger) \rho \exp(-\eta^* a) | \alpha \rangle \\ &= \int d^2\alpha \exp(-\eta^* \alpha + \eta \alpha^*) Q(\alpha), \end{aligned} \quad (7.13)$$

thus, the two functions are Fourier transforms of each other, in two-dimensional space.

7.3 P -Representation: Normal Ordering

The Glauber-Sudarshan P -function is defined as

$$\rho = \int d^2\alpha P(\alpha, \alpha^*) |\alpha\rangle\langle\alpha|. \quad (7.14)$$

If one allows $P(\alpha, \alpha^*)$ to be singular, this representation always exists for any density operator. However, for certain quantum states, $P(\alpha, \alpha^*)$ may become negative, thus in general, this function cannot be interpreted as a probability density.

7.3.1 Normalization

Starting from

$$\begin{aligned} \text{Tr} \{ \rho \} &= 1 \\ &= \int d^2\alpha P(\alpha, \alpha^*) \sum_n \langle n | \alpha \rangle \langle \alpha | n \rangle \\ &= \int d^2\alpha P(\alpha, \alpha^*) \langle \alpha | \alpha \rangle, \end{aligned}$$

we conclude that

$$\int d^2\alpha P(\alpha, \alpha^*) = 1. \quad (7.15)$$

7.3.2 Averages of Normally Ordered Products

Here, we compute the normally ordered averages

$$\begin{aligned}\langle a^{\dagger r} a^s \rangle &= \text{Tr} \{ a^{\dagger r} a^s \rho \} \\ &= \text{Tr} \{ a^s \rho a^{\dagger r} \} \\ &= \int d^2\alpha P(\alpha, \alpha^*) \text{Tr} \{ a^s | \alpha \rangle \langle \alpha | a^{\dagger r} \},\end{aligned}$$

so, we get

$$\langle a^{\dagger r} a^s \rangle = \int d^2\alpha P(\alpha, \alpha^*) \alpha^s \alpha^{*r}. \quad (7.16)$$

As we can see, the average of a normally ordered product can be written as a *c*-number integral in the two-dimensional complex plane.

7.3.3 Some Interesting Properties

The *Q*-function is a Gaussian Convolution of *P*. From the definition of the *Q*-function

$$\begin{aligned}Q(\alpha) &= \frac{1}{\pi} \langle \alpha | \rho | \alpha \rangle \\ &= \frac{1}{\pi} \int \langle \alpha | \beta \rangle \langle \beta | P(\beta) d^2\beta | \alpha \rangle,\end{aligned}$$

or

$$Q(\alpha) = \frac{1}{\pi} \int \exp(-|\alpha - \beta|^2) P(\beta) d^2\beta. \quad (7.17)$$

P* is the Fourier Transform of *X_N

$$\begin{aligned}X_N(\eta) &= \text{Tr} \{ \rho \exp(\eta a^\dagger) \exp(-\eta^* a) \} \\ &= \text{Tr} \left\{ \int d^2\alpha P(\alpha, \alpha^*) | \alpha \rangle \langle \alpha | \exp(\eta a^\dagger) \exp(-\eta^* a) \right\},\end{aligned}$$

or, finally

$$X_N(\eta) = \left\{ \int d^2\alpha P(\alpha, \alpha^*) \exp(\eta \alpha^* - \eta^* \alpha) \right\}. \quad (7.18)$$

7.3.4 Some Examples

Coherent State

$$\begin{aligned}\rho &= |\alpha_0\rangle\langle\alpha_0|, \\ P(\alpha, \alpha^*) &= \delta(\alpha - \alpha_0).\end{aligned} \quad (7.19)$$

Thermal State. To obtain $P(\alpha, \alpha^*)$, we first calculate X_A and X_N . Since

$$\rho = \left[1 - \exp \left(-\frac{\hbar\omega}{k_B T} \right) \right] \sum_n |n\rangle \langle n| \exp \left(-\frac{n\hbar\omega}{k_B T} \right),$$

one can define

$$s = \left(1 - \exp \left(-\frac{\hbar\omega}{k_B T} \right) \right), \quad (7.20)$$

$$\eta \equiv x + iy,$$

$$\alpha = r + ik;$$

then

$$\begin{aligned} X_A(\eta) &= \frac{s}{\pi} \int d^2\alpha \exp(\eta\alpha^* - \eta^*\alpha) \exp(-s|\alpha|^2) \\ &= \frac{s}{\pi} \int dr \int dk \exp \left[-s \left(r - \frac{iy}{s} \right)^2 - s \left(k + \frac{ix}{s} \right)^2 \right] \\ &\quad \times \exp \left(-\frac{x^2 + y^2}{s} \right) \end{aligned}$$

or

$$X_A(\eta) = \exp \left(-\frac{|\eta|^2}{s} \right). \quad (7.21)$$

Now, we proceed to calculate the normally ordered characteristic function. By definition

$$\begin{aligned} X_N(\eta) &= \text{Tr} \{ \rho \exp(\eta a^\dagger) \exp(-\eta^* a) \} \\ &= \text{Tr} \{ \rho \exp(-\eta^* a) \exp(\eta a^\dagger) \} \exp |\eta|^2, \end{aligned}$$

so that

$$X_N(\eta) = X_A(\eta) \exp |\eta|^2, \quad (7.22)$$

so, for the thermal state, we get

$$X_N(\eta) = \exp \left(-\frac{|\eta|^2 (1-s)}{s} \right). \quad (7.23)$$

Finally, we calculate $P(\alpha)$ as the Fourier transform of the normally ordered characteristic function

$$\begin{aligned} P(\alpha) &= \frac{1}{\pi^2} \int d^2\eta \exp(\alpha\eta^* - \alpha^*\eta) \exp \left[-\frac{|\eta|^2 (1-s)}{s} \right] \\ &= \frac{1}{\pi^2} \int dx \int dy \exp \left[2i(kx - ry) - \frac{(1-s)}{s}(x^2 + y^2) \right] \\ &= \frac{s}{\pi(1-s)} \exp \left(-\frac{|\alpha|^2 s}{1-s} \right), \end{aligned}$$

or, written in a different way

$$P(\alpha) = \frac{1}{\pi} \left[\exp\left(\frac{\hbar\omega}{k_B T}\right) - 1 \right] \exp \left\{ -|\alpha|^2 \left[\exp\left(\frac{\hbar\omega}{k_B T}\right) - 1 \right] \right\}. \quad (7.24)$$

For this system, P is a well-behaved function, a Gaussian [7.1].

When $T \rightarrow 0$, $P(\alpha)$ becomes a very sharp function of α . At the other extreme, that is when $T \rightarrow \infty$,

$$P(\alpha) \rightarrow \frac{\hbar\omega}{k_B T} \exp\left(-|\alpha|^2 \frac{\hbar\omega}{k_B T}\right),$$

which is the same as the high-temperature limit of the Q -function, and basically corresponds to a classical Boltzmann distribution.

Number state. This is a case where one cannot find a functional form solution for the P -function, but only a solution in terms of derivatives of the delta function. The result is (for an $|n\rangle$ state)

$$P(\alpha) = \frac{\exp |\alpha|^2}{n!} \left(\frac{\partial^2}{\partial \alpha \partial \alpha^*} \right)^n \delta^2(\alpha). \quad (7.25)$$

For a squeezed state, $P(\alpha)$ is negative. This was shown in (5.15).

7.4 The Wigner Distribution: Symmetric Ordering

The first quasi-probability distribution was introduced by Wigner [7.2] to study quantum corrections to classical statistical mechanics. We will designate the Wigner distribution by W . The original idea was to reformulate Schrödinger's equation, and it found many applications in quantum chemistry, statistical mechanics and quantum optics. In our context, we define the Wigner function $W(\alpha, \alpha^*)$ as the Fourier transform of the symmetric characteristic function X_W

$$W(\alpha, \alpha^*) = \frac{1}{\pi^2} \int d^2\eta \exp(-\eta\alpha^* + \eta^*\alpha) X_W(\eta, \eta^*). \quad (7.26)$$

7.4.1 Moments

The moments of $W(\alpha, \alpha^*)$ are equal to the averages of symmetrically ordered products of creation and annihilation operators. These products, denoted by $\{a^r a^{s*}\}_{\text{sym}}$, are defined as the expansion coefficient of $\eta^s (-\eta^{*r})$ in $(\eta a^\dagger - \eta^* a)^{r+s}$. We give here some examples:

$$\begin{aligned} \{a^2 a^{+2}\}_{\text{sym}} &= \frac{1}{6} (a^{+2} a^2 + a^\dagger a a^\dagger a + a^\dagger a^2 a^\dagger + a a^{+2} a + a a^\dagger a a^\dagger + a^2 a^{+2}), \\ \{a a^{+2}\}_{\text{sym}} &= \frac{1}{3} (a^{+2} a + a^\dagger a a^\dagger + a a^{+2}), \\ &\text{etc.} \end{aligned}$$

With the above definition, one can write

$$\exp(\eta a^\dagger - \eta^* a) = \sum_{r,s} \frac{\eta^s (-\eta^*)^r}{r! s!} \{a^r a^{\dagger s}\}_{\text{sym}}. \quad (7.27)$$

Now, by partial integration of (7.26), we get

$$\int d^2\alpha \alpha^r \alpha^{*s} W(\alpha, \alpha^*) = \left(\frac{\partial}{\partial \eta} \right)^s \left(-\frac{\partial}{\partial \eta^*} \right)^r X_W(\eta, \eta^*), \quad (7.28)$$

and making use of (7.12), we readily get

$$\langle \{a^r a^{\dagger s}\}_{\text{sym}} \rangle = \int d^2\alpha \alpha^r \alpha^{*s} W(\alpha, \alpha^*).$$

Problems

7.1 Normal ordering. Let

$$A = \sum_{n,m} A_{nm} a^{\dagger n} a^m$$

be normally ordered. Show that

$$\langle A \rangle = \frac{1}{\pi} \int P(\alpha) \sum_{n,m} A_{nm} \alpha^{*n} \alpha^m d^2\alpha.$$

7.2. Show that if

$$A = (a^\dagger a)^2,$$

then its normal and antinormal ordered version are

$$[(a^\dagger a)^2]_{\text{normal}} = a^{\dagger 2} a^2 + (a^\dagger a),$$

$$[(a^\dagger a)^2]_{\text{antinormal}} = a^2 a^{\dagger 2} - 3(a a^\dagger) + 1.$$

7.3. Let us assume that an operator A is normally ordered. Then, we substitute:

$$a \rightarrow z, \quad a^\dagger \rightarrow z^*$$

and define the result as

$$A^{(n)}(z, z^*).$$

Similarly, if A is antinormally ordered, we define a $A^{(a)}(z, z^*)$. For example, from the previous problem, we can write

$$A^{(n)}(z, z^*) = |z|^4 + |z|^2,$$

$$A^{(a)}(z, z^*) = |z|^4 - 3|z|^2 + 1.$$

Now, we define the \mathcal{N} and \mathcal{A} operators whose effect on a given operator is to rearrange it so as to transform it to normal and antinormal form respectively. For example

$$\mathcal{N}(a^{\dagger 2}a^2 + (a^{\dagger}a)) = a^{\dagger 2}a^2 + (a^{\dagger}a),$$

$$\mathcal{A}(a^{\dagger 2}a^2 + (a^{\dagger}a)) = a^2a^{\dagger 2} + (aa^{\dagger}).$$

Show that

$$aa^{\dagger n}a^m = \mathcal{N}\left(a + \frac{\partial}{\partial a^{\dagger}}\right)a^{\dagger n}a^m.$$

Hint: use the commutation relation

$$[a, a^{\dagger n}] = na^{\dagger n-1}.$$

7.4. If $F^{(n)}(a^{\dagger}, a)$ is a normally ordered operator, show, using the notation of Problem 7.3, that

$$aF^{(n)}(a^{\dagger}, a) = \mathcal{N}\left(a + \frac{\partial}{\partial a^{\dagger}}\right)F^{(n)}(a^{\dagger}, a),$$

$$F^{(n)}(a^{\dagger}, a)a^{\dagger} = \mathcal{N}\left(a^{\dagger} + \frac{\partial}{\partial a}\right)F^{(n)}(a^{\dagger}, a).$$

7.5. Show, using the same notation as in Problems 7.3 and 7.4, that for a product of two normally ordered operators (the product is of course not normally ordered)

$$F^{(n)}(a^{\dagger}, a)G^{(n)}(a^{\dagger}, a) = \mathcal{N}F^{(n)}\left(a^{\dagger}, a + \frac{\partial}{\partial a^{\dagger}}\right)F^{(n)}(a^{\dagger}, a).$$

8. Atom–Field Interaction

In this chapter, we study the atom–field interaction in the usual and dressed picture. We also address the problems of Rabi oscillations and collapse and revivals.

8.1 Atom–Field Hamiltonian and the Dipole Approximation

The Hamiltonian for an atom interacting with an electromagnetic field may be written as

$$H = \frac{1}{2m} [\mathbf{p} - e\mathbf{A}(\mathbf{r}, t)]^2 + eV(\mathbf{r}) + H_r, \quad (8.1)$$

where \mathbf{p} is the momentum of the electron, $V(\mathbf{r})$ is the Coulomb potential, \mathbf{A} is the vector potential of the field and H_r is the free radiation field. We now make use of the unitary transformation [8.1]:

$$|\psi(t)\rangle = \exp \left[\frac{i\epsilon\mathbf{r}}{\hbar} \cdot \mathbf{A}(\mathbf{r}, t) \right] |\chi(t)\rangle \equiv U |\chi(t)\rangle, \quad (8.2)$$

so the Schrödinger equation can be written as

$$\begin{aligned} i\hbar \frac{\partial |\psi(t)\rangle}{\partial t} &= H |\chi(t)\rangle \\ i\hbar U \frac{\partial |\chi(t)\rangle}{\partial t} + i\hbar \frac{\partial U}{\partial t} |\chi(t)\rangle &= HU |\chi(t)\rangle. \end{aligned} \quad (8.3)$$

Multiplying (8.3) by $U^\dagger = U^{-1}$ on the left, we get

$$i\hbar \frac{\partial |\chi(t)\rangle}{\partial t} = H' |\chi(t)\rangle, \quad (8.4)$$

$$H' \equiv U^\dagger HU - i\hbar U^\dagger \frac{\partial U}{\partial t}. \quad (8.5)$$

The second term in (8.5) can be written as

$$-i\hbar U^\dagger \frac{\partial U}{\partial t} = e\mathbf{r} \cdot \frac{\partial \mathbf{A}}{\partial t} = -e\mathbf{r} \cdot \mathbf{E}(\mathbf{r}, t), \quad (8.6)$$

where in the last equation we used (3.6), (3.7), and H' becomes

$$H' = U^\dagger H U - e\mathbf{r} \cdot \mathbf{E}(\mathbf{r}, t). \quad (8.7)$$

We have to calculate $U^\dagger H U$:

$$U^\dagger H U = \frac{1}{2m} U^\dagger \mathbf{p}^2 U - \frac{e}{m} \mathbf{A} \cdot U^\dagger \mathbf{p} U + \frac{e^2}{2m} \mathbf{A}^2 + eV(\mathbf{r}) + H_r, \quad (8.8)$$

where we have used the fact that only the \mathbf{p} -dependent terms are affected by the transformation, and that $\sum_{l=1}^3 [\mathbf{p}_l, \mathbf{A}_l] = -i\hbar \sum_l \partial \mathbf{A}_l / \partial x_l = 0$ in the Coulomb gauge, thus $\mathbf{p} \cdot \mathbf{A} = \mathbf{A} \cdot \mathbf{p}$. Since

$$[p_i, U] = -i\hbar \frac{\partial U}{\partial x_i} = cU \frac{\partial(r \cdot A)}{\partial x_i}, \quad (8.9)$$

therefore

$$\begin{aligned} -\frac{e}{m} \mathbf{A} \cdot (U^\dagger \mathbf{p} U) &= -\frac{e}{m} \mathbf{A} \cdot U^\dagger [U \mathbf{p} + cU \nabla(r \cdot \mathbf{A})] \\ &= -\frac{e}{m} \mathbf{A} \cdot \mathbf{p} - \frac{e^2}{m} \mathbf{A} \cdot \nabla(r \cdot \mathbf{A}). \end{aligned} \quad (8.10)$$

Next, we calculate

$$\begin{aligned} \sum_{i=1}^3 [p_i^2, U] &= \sum_i (p_i [p_i, U] + [p_i, U] p_i) \\ &= \sum_i ([p_i, [p_i, U]] + 2[p_i, U] p_i). \end{aligned} \quad (8.11)$$

Now, from (8.9), one can write

$$\begin{aligned} [p_i, [p_i, U]] &= c \left[p_i, U \frac{\partial(r \cdot \mathbf{A})}{\partial x_i} \right] = -ie\hbar \frac{\partial}{\partial x_i} \left[U \frac{\partial(r \cdot \mathbf{A})}{\partial x_i} \right] \\ &= U \left\{ -ie\hbar \frac{\partial^2(r \cdot \mathbf{A})}{\partial^2 x_i} + e^2 \left[\frac{\partial(r \cdot \mathbf{A})}{\partial x_i} \right]^2 \right\}, \end{aligned} \quad (8.12)$$

so

$$[\mathbf{p}^2, U] = U \left\{ -ie\hbar \nabla^2(r \cdot \mathbf{A}) + e^2 [\nabla(r \cdot \mathbf{A})]^2 + 2e \nabla(r \cdot \mathbf{A}) \cdot \mathbf{p} \right\}. \quad (8.13)$$

With (8.9), (8.13) we get for $U^\dagger H U$:

$$\begin{aligned} U^\dagger H U &= \frac{e^2}{2m} \mathbf{A}^2 + eV(\mathbf{r}) + H_r + \frac{\mathbf{p}^2}{2m} + \frac{e\hbar}{2im} \nabla^2(r \cdot \mathbf{A}) \\ &\quad + \frac{e^2}{2m} [\nabla(r \cdot \mathbf{A})]^2 + \frac{e}{m} \nabla(r \cdot \mathbf{A}) \cdot \mathbf{p} - \frac{e}{m} \mathbf{A} \cdot \mathbf{p} - \frac{e^2}{m} \mathbf{A} \cdot [\nabla(r \cdot \mathbf{A})]. \end{aligned} \quad (8.14)$$

Now

$$\frac{\partial}{\partial x_i} (\mathbf{r} \cdot \mathbf{A}) = \mathbf{A}_i + \mathbf{r} \cdot \frac{\partial \mathbf{A}}{\partial x_i}, \quad (8.15)$$

$$\sum_i \left[\frac{\partial}{\partial x_i} (\mathbf{r} \cdot \mathbf{A}) \right]^2 = \mathbf{A}^2 + \sum_{i,j} 2A_i x_j \frac{\partial A_j}{\partial x_i} + \sum_{i,j,k} x_j x_k \frac{\partial A_j}{\partial x_i} \frac{\partial A_k}{\partial x_i},$$

$$\nabla^2(\mathbf{r} \cdot \mathbf{A}) = \sum_{i,j} x_i \frac{\partial^2 \mathbf{A}}{\partial x_j^2}.$$

In the last term we used $\nabla \cdot \mathbf{A} = 0$.

Finally, one can write

$$\begin{aligned} U^\dagger HU &= eV(\mathbf{r}) + \frac{\mathbf{p}^2}{2m} + H_r + \frac{e}{m} \sum x_i \frac{\partial A_i}{\partial x_j} p_j \\ &\quad + \frac{e\hbar}{2mi} \sum_{i,j} x_i \frac{\partial^2 A_i}{\partial x_j^2} + \frac{e^2}{2m} \sum_{i,j,k} x_i x_j \frac{\partial A_i}{\partial x_k} \frac{\partial A_j}{\partial x_k} \\ &= H' + e\mathbf{r} \cdot \mathbf{E}. \end{aligned} \quad (8.16)$$

The standard dipole approximation assumes that, in the case of plane waves,

$$\begin{aligned} \mathbf{A} &= \mathbf{A}_0 \exp(-i\omega t + i\mathbf{k} \cdot \mathbf{r}) \\ &\approx \mathbf{A}_0 \exp(-i\omega t + i\mathbf{k} \cdot \mathbf{r}_0) = \mathbf{A}(\mathbf{r}_0), \end{aligned} \quad (8.17)$$

where \mathbf{r}_0 is the position of the atomic nucleus, provided the radiation wavelength is several orders of magnitude larger than the atomic size. In that case, all the derivatives of the vector potential can be neglected, and one gets:

$$H' = eV(\mathbf{r}) + \frac{\mathbf{p}^2}{2m} + H_r - e\mathbf{r} \cdot \mathbf{E}(\mathbf{r}, t) \quad (8.18)$$

or

$$H' = \hbar \sum_i \omega_i |i\rangle \langle i| + H_r - e\mathbf{r} \cdot \mathbf{E}(\mathbf{r}, t),$$

where $|i\rangle$ are the unperturbed atomic states with eigenenergies $\hbar\omega_i$.

8.2 A Two-Level Atom Interacting with a Single Field Mode

In the case of a two-level atom interacting with one mode of the field, the interaction Hamiltonian in the dipole approximation can be written as:

$$H_1 = -e\mathbf{r} \cdot \mathbf{E}(\mathbf{r}). \quad (8.19)$$

We can assume one mode for instance when we have a high-quality electromagnetic cavity. Thus, for this particular case, it is more convenient to have stationary rather than travelling waves. The one-mode electric field can be written as

$$E(z, t) = \epsilon(a + a^\dagger) \sin kz, \quad (8.20)$$

where $\epsilon \equiv \sqrt{\hbar\omega/\epsilon_0 v}$ is the field per photon, and the Hamiltonian can be written as

$$H_1 = \hbar g(\sigma_+ + \sigma_-)(a + a^\dagger), \quad (8.21)$$

with $g \equiv -(\epsilon d/\hbar) \sin kz$, $d = e\mathbf{r}_{ab} \cdot \mathbf{e}$ and the σ are the usual Pauli spin matrices defined as

$$\begin{aligned}\sigma_+ &= \begin{bmatrix} 0 & 1 \\ 0 & 0 \end{bmatrix}, & \sigma_- &= \begin{bmatrix} 0 & 0 \\ 1 & 0 \end{bmatrix}, \\ \sigma_x &= \begin{bmatrix} 0 & 1 \\ 1 & 0 \end{bmatrix}, & \sigma_y &= \begin{bmatrix} 0 & -i \\ i & 0 \end{bmatrix}, \\ \sigma_z &= \begin{bmatrix} 1 & 0 \\ 0 & -1 \end{bmatrix}.\end{aligned}\quad (8.22)$$

As in the semiclassical case, we have assumed that the dipole induced by the field has only non-diagonal matrix elements, that is the two states considered here have opposite parity so that $\tau_{aa} = \tau_{bb} = 0$; thus the \mathbf{r} operator is proportional to $(\sigma_+ + \sigma_-)$. The complete Hamiltonian is

$$H = \frac{\hbar\omega_{ab}}{2}\sigma_z + \hbar\omega a^\dagger a + \hbar g(\sigma_+ + \sigma_-)(a + a^\dagger). \quad (8.23)$$

We notice, in the above expression, that the zero energy level was taken halfway between the two atomic levels, so that the unperturbed atomic energies are $\pm 1/2\hbar\omega_{ab}$.

The four terms appearing in the interaction part of the Hamiltonian have the following simple interpretation:

$a\sigma_+$: one photon is absorbed and the atom is excited from state b to state a .

$a^\dagger\sigma_-$: emission of a photon and de-excitation of the atom.

These two processes are energy-conserving. We will show that for a very weak coupling constant, they vary slowly in time. On the other hand, the terms $a^\dagger\sigma_+$ and $a\sigma_-$ do not conserve the energy. They represent:

$a^\dagger\sigma_+$: one photon is emitted and the atom is excited;

$a\sigma_-$: one photon is absorbed and the atom gets de-excited.

These processes are shown in Fig. 8.1. The straight arrows represent atomic levels and the wavy arrows photons. Lines towards (away from) the interaction point correspond to destruction (creation) of states.

To see the time dependence of all these processes, we go to the interaction picture:

$$\begin{aligned}H_1^{(I)} &= \hbar g \exp(i\omega t a^\dagger a)(a + a^\dagger) \exp(-i\omega t a^\dagger a) \\ &\times \exp\left[it \begin{pmatrix} \frac{\omega_{ab}}{2} & 0 \\ 0 & -\frac{\omega_{ab}}{2} \end{pmatrix} \right] \begin{bmatrix} 0 & 1 \\ 1 & 0 \end{bmatrix} \exp\left[-it \begin{pmatrix} \frac{\omega_{ab}}{2} & 0 \\ 0 & -\frac{\omega_{ab}}{2} \end{pmatrix} \right].\end{aligned}\quad (8.24)$$

Making use of the properties:

$$\exp(i\omega t a^\dagger a)(a + a^\dagger) \exp(-i\omega t a^\dagger a) = a \exp(-i\omega t) + a^\dagger \exp(i\omega t),$$

$$\begin{aligned}&\exp\left[it \begin{pmatrix} \frac{\omega_{ab}}{2} & 0 \\ 0 & -\frac{\omega_{ab}}{2} \end{pmatrix} \right] \begin{bmatrix} 0 & 1 \\ 1 & 0 \end{bmatrix} \exp\left[-it \begin{pmatrix} \frac{\omega_{ab}}{2} & 0 \\ 0 & -\frac{\omega_{ab}}{2} \end{pmatrix} \right] \\ &= \sigma_+ \exp(i\omega_{ab}t) + \sigma_- \exp(-i\omega_{ab}t)\end{aligned}$$

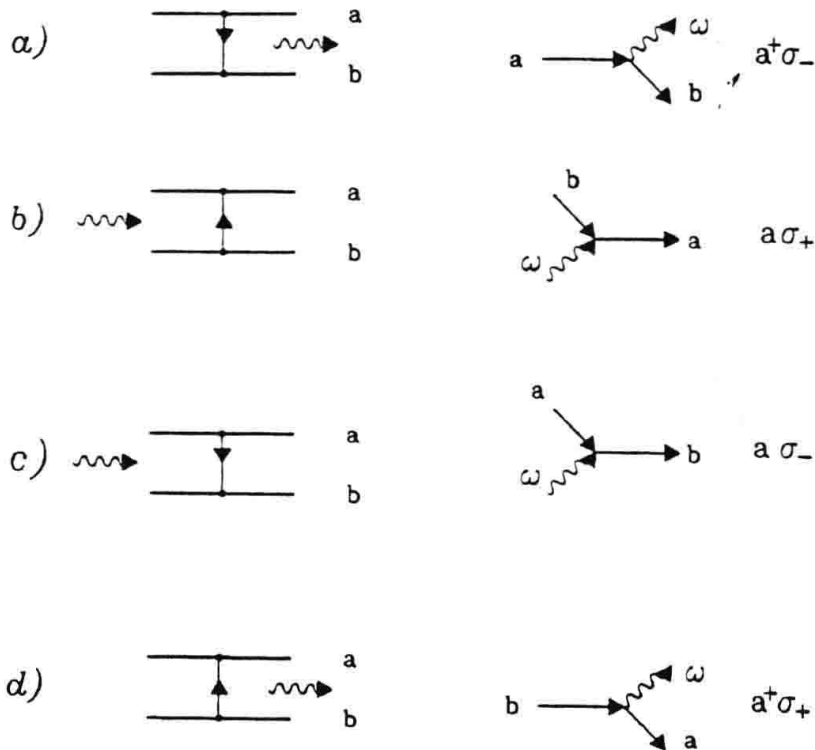


Fig. 8.1. Four processes in the atom–field interaction. The processes a and b conserve the energy

we get

$$H_1^{(I)}(t) = \hbar g \{ \sigma_+ a \exp[-i(\omega - \omega_{ab})t] + \sigma_- a^\dagger \exp[i(\omega - \omega_{ab})t] \\ + \sigma_- a \exp[-i(\omega + \omega_{ab})t] + a^\dagger \sigma_+ \exp[i(\omega + \omega_{ab})t] \}. \quad (8.25)$$

The rotating-wave approximation, as in the semiclassical theory, consists in neglecting the rapidly oscillating terms $\sigma_- a \exp[-i(\omega + \omega_{ab})t] + a^\dagger \sigma_+ \exp[i(\omega + \omega_{ab})t]$. Going back to the Schrödinger picture, the Hamiltonian in the dipole and rotating-wave approximations is

$$H = H_0 + H_1 = \frac{\hbar\omega_{ab}}{2} \sigma_z + \hbar\omega a^\dagger a + \hbar g(a\sigma_+ + \sigma_- a^\dagger). \quad (8.26)$$

This is the Jaynes–Cummings Hamiltonian and it will be very useful in describing various physical effects.

8.3 The Dressed State Picture. Quantum Rabi Oscillations

We begin by taking the unperturbed eigenstates $|a, n\rangle, |b, n+1\rangle$ of H_0 :

$$H_0 |a, n\rangle = \hbar \left(\frac{\omega_{ab}}{2} + n\omega \right), \quad (8.27)$$

$$H_0 |b, n+1\rangle = \hbar \left(-\frac{\omega_{ab}}{2} + (n+1)\omega \right). \quad (8.28)$$

Now, the interaction couples only $|a, n\rangle$ to $|b, n+1\rangle$, for each n , and no other states. Therefore we can consider the subspace $\epsilon_n = \{|a, n\rangle, |b, n+1\rangle\}$ and the total Hamiltonian can be written as [8.2], [8.3]

$$H = \sum_n H_n, \quad (8.29)$$

where H_n acts only in ϵ_n , and can be written as

$$H_n = \hbar\omega \left(n + \frac{1}{2} \right) \begin{bmatrix} 1 & 0 \\ 0 & 1 \end{bmatrix} + \frac{\hbar}{2} \begin{bmatrix} \delta & 2g\sqrt{n+1} \\ 2g\sqrt{n+1} & -\delta \end{bmatrix} \quad (8.30)$$

One can easily diagonalize the above Hamiltonian, getting the following eigenvalues

$$E_{1n} = \hbar\omega \left(n + \frac{1}{2} \right) + \frac{\hbar}{2} R_n, \quad (8.31)$$

$$E_{2n} = \hbar\omega \left(n + \frac{1}{2} \right) - \frac{\hbar}{2} R_n, \quad (8.32)$$

with

$$\delta = \omega_{ab} - \omega, \quad (8.33)$$

$$R_n = \sqrt{\delta^2 + 4g^2(n+1)}.$$

The corresponding eigenstates are

$$\begin{aligned} |1n\rangle &= \cos \theta_n |a, n\rangle + \sin \theta_n |b, n+1\rangle, \\ |2n\rangle &= -\sin \theta_n |a, n\rangle + \cos \theta_n |b, n+1\rangle, \end{aligned} \quad (8.34)$$

with

$$\cos \theta_n = \frac{2g\sqrt{n+1}}{\sqrt{(R_n - \delta)^2 + 4g^2(n+1)}}. \quad (8.35)$$

Also, it is simple to prove that

$$\sin 2\theta_n = \frac{2g\sqrt{n+1}}{R_n}, \quad (8.36)$$

$$\cos 2\theta_n = \frac{\delta}{R_n},$$

$$\tan 2\theta_n = \frac{2g\sqrt{n+1}}{\delta}.$$

We can write

$$\begin{aligned} \begin{bmatrix} |1n\rangle \\ |2n\rangle \end{bmatrix} &= \begin{bmatrix} \cos \theta_n & \sin \theta_n \\ -\sin \theta_n & \cos \theta_n \end{bmatrix} \begin{bmatrix} |a, n\rangle \\ |b, n+1\rangle \end{bmatrix} \\ &\equiv R(\theta_n) \begin{bmatrix} |a, n\rangle \\ |b, n+1\rangle \end{bmatrix}. \end{aligned} \quad (8.37)$$

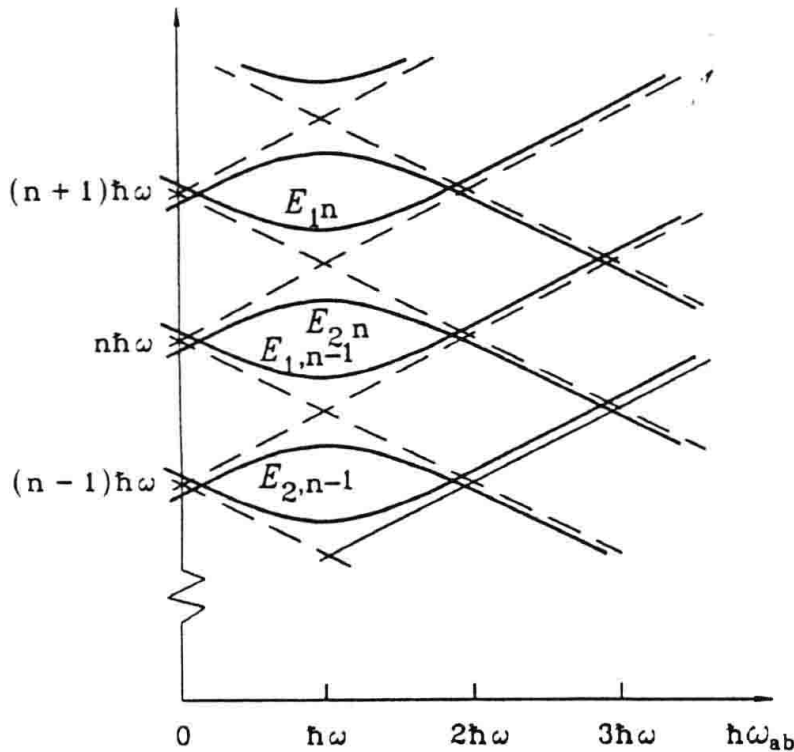


Fig. 8.2. Energy levels of the dressed and bare states versus ω_{ab} , for different n subspaces

These are the dressed states, as opposed to the bare states $|a, n\rangle$ and $|b, n+1\rangle$. Diagrammatically, the dressed state eigenvalues are pictured in Fig. 8.2, where we plot energy versus ω_{ab} for different n -values.

In the particularly simple case $\delta = 0$ and $\sin \theta_n = \cos \theta_n = 1/\sqrt{2}$, the states and eigenvalues are

$$|1n\rangle = [|a, n\rangle + |b, n+1\rangle] \frac{1}{\sqrt{2}}, \quad (8.38)$$

$$|2n\rangle = (- |a, n\rangle + |b, n+1\rangle) \frac{1}{\sqrt{2}}, \quad (8.39)$$

and

$$E_{1n} = \hbar\omega \left(n + \frac{1}{2} \right) + \hbar g \sqrt{n+1}, \quad (8.40)$$

$$E_{2n} = \hbar\omega \left(n + \frac{1}{2} \right) - \hbar g \sqrt{n+1}. \quad (8.41)$$

Finally in this section, we will look into the problem of the quantum Rabi oscillations. If one writes

$$|\psi(t)\rangle = \exp \left(-\frac{iHt}{\hbar} \right) |\psi(0)\rangle, \quad (8.42)$$

and introduces a unit operator in terms of the dressed states, we readily get

$$|\psi(t)\rangle = \sum_{n=0}^{\infty} \sum_{j=1}^2 \exp\left(-\frac{iE_j t}{\hbar}\right) |j, n\rangle \langle j, n | \psi(0)\rangle, \quad (8.43)$$

where E_j are the eigenvalues corresponding to the dressed states. Now, we can write the state vector in terms of both dressed and bare bases, as follows

$$\begin{aligned} |\psi(t)\rangle &= \sum_n [C_{an} |a, n\rangle + C_{bn+1} |b, n+1\rangle] \\ &= \sum_n [C_{1n} |1n\rangle + C_{2n} |2n\rangle]. \end{aligned} \quad (8.44)$$

In the rotating frame at frequency $(n + \frac{1}{2})\omega$, we can write (8.43) as

$$\begin{pmatrix} C_{1n}(t) \\ C_{2n}(t) \end{pmatrix} = \begin{pmatrix} \exp(i\frac{R_n}{2}t) & 0 \\ 0 & \exp(-i\frac{R_n}{2}t) \end{pmatrix} \begin{pmatrix} C_{1n}(0) \\ C_{2n}(0) \end{pmatrix} \quad (8.45)$$

and also making use of (8.37), we can write

$$\begin{bmatrix} C_{an}(t) \\ C_{bn+1}(t) \end{bmatrix} = R^{-1}(\theta_n) \begin{bmatrix} \exp(i\frac{R_n}{2}t) & 0 \\ 0 & \exp(-i\frac{R_n}{2}t) \end{bmatrix} \times R(\theta_n) \begin{bmatrix} C_{an}(0) \\ C_{bn+1}(0) \end{bmatrix} \quad (8.46)$$

or

$$\begin{bmatrix} C_{an}(t) \\ C_{bn+1}(t) \end{bmatrix} = \begin{bmatrix} \cos \frac{R_n}{2}t + i\delta R_n^{-1} \sin \frac{R_n}{2}t & 2ig\sqrt{n+1}R_n^{-1} \sin \frac{R_n}{2}t \\ 2ig\sqrt{n+1}R_n^{-1} \sin \frac{R_n}{2}t & \cos \frac{R_n}{2}t - i\delta R_n^{-1} \sin \frac{R_n}{2}t \end{bmatrix} \begin{bmatrix} C_{an}(0) \\ C_{bn+1}(0) \end{bmatrix}.$$

If initially the atom is in the upper state and $\delta = 0$, we get

$$|C_{an}(t)|^2 = \cos^2 g\sqrt{n+1}t, \quad (8.47)$$

$$|C_{bn+1}(t)|^2 = \sin^2 g\sqrt{n+1}t. \quad (8.48)$$

This is the quantum Rabi oscillation.

8.4 Collapse and Revivals

With the Jaynes-Cummings Hamiltonian, one has, in principle, the time evolution of the system. Of course, there are also the initial conditions [8.4]. The simplest case is when one knows precisely the energy level of the atom, which is suddenly brought into a cavity with a definite photon number. Usually in experiments one can only specify for example the statistics of the cavity field, that is the probability of having a given number of photons. We will deal with the general case. Consider the state vector $\psi(n, t)$ which evolves from an initial state with exactly n photons. When this field has an unknown

photon number, specified only by a probability P_m for having m photons, then at time t the probability of being in a given state k ($k = a, b$) is

$$P_k(t) = \sum_{m=0}^{\infty} P_m |\langle m, \psi_k | \psi(m, t) \rangle|^2 = \sum_{m=0}^{\infty} P_m |C_{k,m}(t)|^2, \quad (8.49)$$

and the photon distribution is

$$\begin{aligned} p_n(t) &= \sum_{\substack{m=0 \\ k=a,b}}^{\infty} P_m |\langle n, \psi_k | \psi(m, t) \rangle|^2 \\ &= P_n |C_{a,n}(t)|^2 + P_{n-1} |C_{b,n}(t)|^2. \end{aligned} \quad (8.50)$$

One would expect that the superposition of periodic solutions might produce destructive interference, thus a collapse. This indeed occurs [8.5].

An interesting example is the case of a two-level atom that encounters a cavity at temperature T , whose photon number distribution is the one-mode Bose-Einstein distribution, with a probability for m photons given by

$$\begin{aligned} P_m(T) &= \frac{1}{1 + \bar{n}} \left(\frac{\bar{n}}{1 + \bar{n}} \right)^m, \\ \bar{n} &= \left[\exp \left(\frac{\hbar\omega}{k_B T} \right) - 1 \right]^{-1}, \\ \langle \Delta n^2 \rangle &= \langle n \rangle^2 + \langle n \rangle. \end{aligned} \quad (8.51)$$

In Fig. 8.3 we show the population inversion $w(t) = P_a(t) - P_b(t)$ for an initially excited two-level atom interacting with a single-mode thermal field. The time axis has been scaled to an adimensional time $\tau = gt\sqrt{n}/2$. The first curve shows the Rabi oscillations when the atom enters an empty cavity. The subsequent curves show an increasing average photon number. As we can observe, there is a wide range of Rabi frequencies, for which there is no trace of population inversion. The collapse time, for large \bar{n} , is of the order of [8.6]

$$t_c^{-1} \cong g\sqrt{\bar{n}}. \quad (8.52)$$

The time scale of Fig. 8.3 has been chosen in such a way that in each case, the collapse occurs at $\tau = 2$.

A particular and interesting example where the collapse can be studied in detail is the case when the initial field is a coherent state, where one can study also the revivals [8.7]. In this case, the probability for an excited atom is

$$\begin{aligned} P_a(t) &= \sum_n P_n |C_{a,n}(t)|^2 \\ &= \exp - |\alpha|^2 \sum_n \frac{|\alpha|^{2n}}{n!} \cos^2(g\sqrt{n+1}t), \end{aligned} \quad (8.53)$$

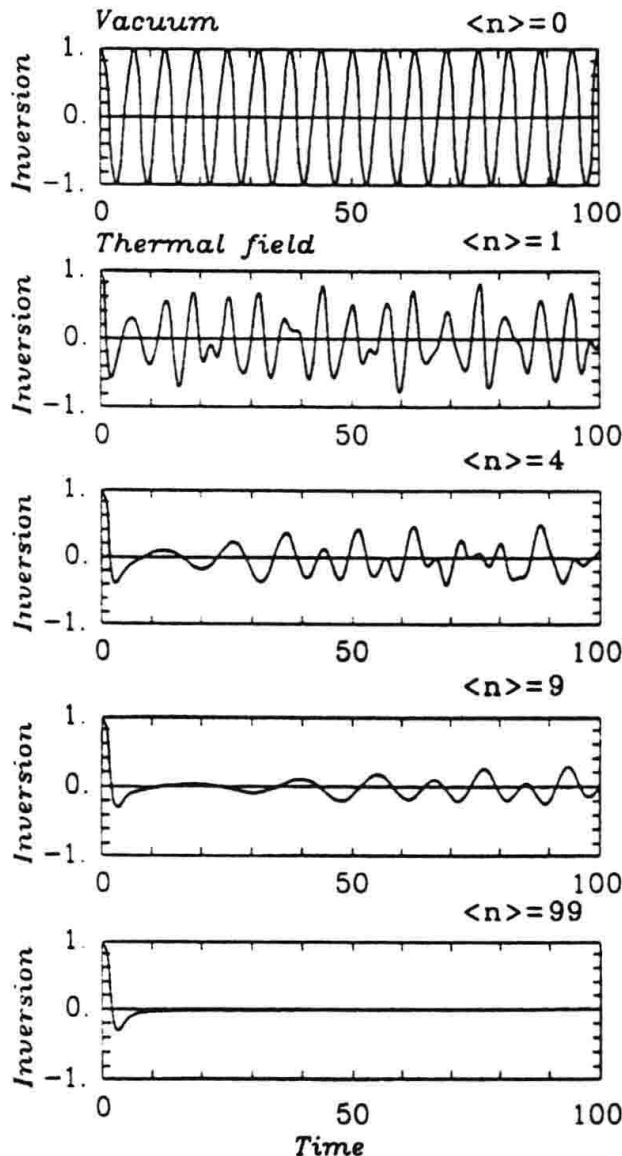


Fig. 8.3. The population inversion for a two-level atom initially in the upper state interacting with a thermal field and mean photon numbers $\langle n \rangle_{\text{th}} = 0, 1, 4, 9, 99$ (after [8.4])

which, for short times ($gt \ll |\alpha|$), can be approximated to

$$P_a(t) = \frac{1}{2} + \frac{1}{2} \cos(2gt|\alpha|) \exp[-(gt)^2]. \quad (8.54)$$

This case is described in Fig. 8.4. As we can see, as the field becomes more intense, the Rabi oscillations persist for longer intervals, until the destructive interference between the oscillations takes over. Basically the relevant range of Rabi frequencies is $g\sqrt{n + \Delta n} \rightarrow g\sqrt{n - \Delta n}$, the inverse of which is the collapse time, so

$$t_c^{-1} \approx g, \quad (8.55)$$

which is independent of the average photon number. Also, the effect of revival is quite remarkable, that is, after a certain time, the Rabi oscillations

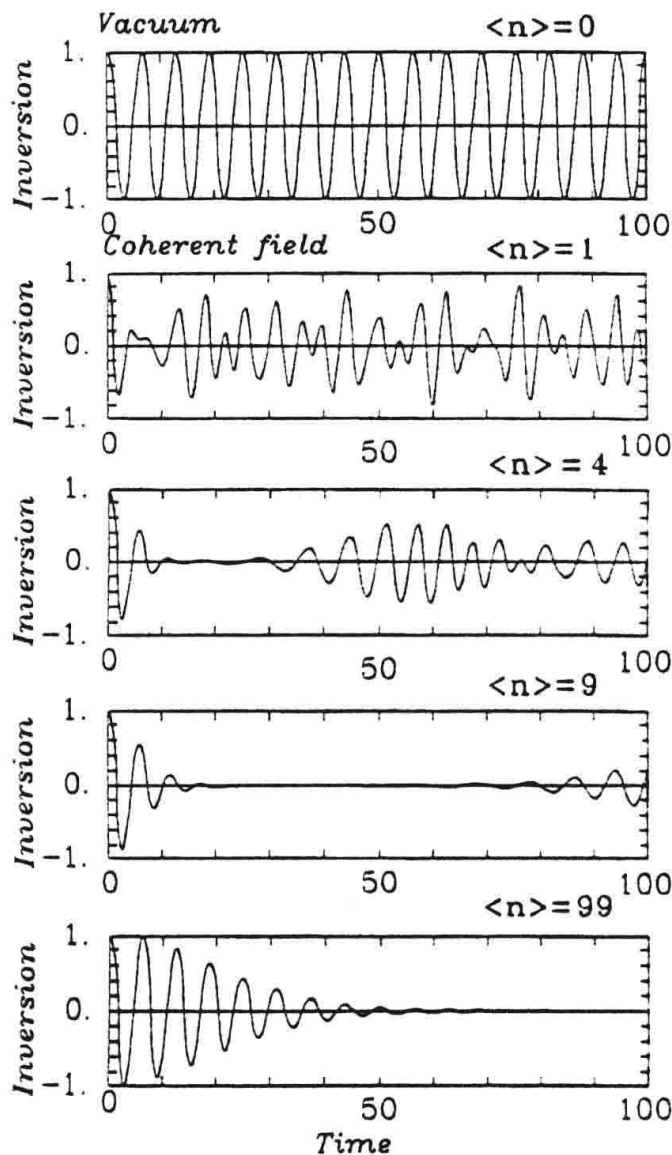


Fig. 8.4. Population inversion of a two-level atom interacting with a single-mode coherent field, for $\langle n \rangle_{\text{th}} = 0, 1, 4, 9, 99$. We observe a collapse and then a revival (After [8.4])

reappear. This was studied first by Eberly *et al.* [8.7] and others [8.8], [8.9], [8.10]. The revival time is $t_r = t_c 2\pi \sqrt{\bar{n}}$.

As we can see, the behaviour of a two-level atom interacting with a single electromagnetic mode (coherent) is surprisingly rich. We have Rabi oscillations that collapse and remain quiescent, revive, and then collapse again.

The Jaynes-Cummings model, in its linear and non-linear version, has been used extensively in connection with the trapped ions with quantized vibrational motion [8.11, 8.12, 8.13, 8.14, 8.15].

Problems

- 8.1. Starting from the Hamiltonian H_n , find the eigenvalues $E_{i,n}$ for $i = 1, 2$, and the dressed states $|1n\rangle, |2n\rangle$, that is, verify (8.31)–(8.35).
- 8.2. Prove (8.47).
- 8.3. Show that the summation for the probability of the excited atom (8.54) reduces to (8.54), when $gt \ll |\alpha|$.

9. System–Reservoir Interactions

Losses play an important role in physics, and in general they cannot be avoided. For example, the decay of an atom can be described as a small or relevant system (the atom) interacting with a large reservoir consisting of an infinite number of harmonic oscillators or electromagnetic modes. It appears quite surprising that starting from time-reversible dynamics, one ends up in an irreversible situation, such as the natural decay of an excited atom. Of course, as we shall see this is closely related to the type of approximation (Markov) used.

Here we present a quantum theory of damping where the system consists of a single harmonic oscillator coupled to a reservoir of a large number of oscillators. Using the density matrix approach, we eliminate the reservoir variables, obtaining a differential equation for the reduced density matrix in the Schrödinger picture. We also study the problem in the Heisenberg picture, thus introducing the concepts of Langevin equations and noise operators. [9.1], [9.2].

9.1 Quantum Theory of Damping

The main purpose, in this section, is to study the fluctuations and relaxations of quantum systems. We will find that the expectation values of some relevant operators do relax as their classical counterparts. Also, and very importantly, relaxation phenomena are always accompanied by statistical fluctuations. In other words, a pure state does not relax and a system connected to a bath or reservoir, even if starting from a pure state, will always become a mixed state.

The method that we are going to use is the following. Starting from Liouville's equation, under a certain approximation scheme, and tracing over the reservoir variables, we end up with a differential equation for a reduced density matrix, the so-called master equation, which is still an operator equation. Then, we use the phase space techniques learned in Chap. 7 to get a c number differential equation, for example, for the Glauber P -distribution. This is the Fokker–Planck equation.

Consider a harmonic oscillator

$$\begin{aligned} H_{0,A} &= \hbar\omega a^\dagger a, \\ [a, a^\dagger] &= 1, \end{aligned} \tag{9.1}$$

which we define as the system, and a set of harmonic oscillators:

$$\begin{aligned} H_{0,B} &= \sum_j \hbar\omega_j b_j^\dagger b_j, \\ [b_j, b_k^\dagger] &= \delta_{jk}, \end{aligned}$$

which is the bath or reservoir. We further assume a very general type of system–reservoir coupling of the type XX_j , which contain terms like $ab_j^\dagger, a^\dagger b_j, a^\dagger b_j^\dagger, ab_j$, and using rotating-wave approximation arguments, already discussed previously, we only keep the counter-rotating terms. Therefore, the complete Hamiltonian reads

$$\begin{aligned} H &= H_0 + H_1 \\ &= \hbar\omega a^\dagger a + \sum_j \hbar\omega_j b_j^\dagger b_j + \sum_j g_j (a^\dagger b_j + ab_j^\dagger), \end{aligned} \tag{9.2}$$

where the g_j are taken as reals.

Now, we define ρ_{AB} as the density matrix of the complete system, whereas $\rho_A = \text{Tr}_B(\rho_{AB}) = \sum_B \langle B | \rho_{AB} | B \rangle$ and $\rho_B = \text{Tr}_A(\rho_{AB}) = \sum_A \langle A | \rho_{AB} | A \rangle$ are the reduced density matrices for the systems A and B , respectively, and are obtained simply by tracing over the other variable. The Liouville equation for the complete system is

$$i\hbar \frac{d\rho_{AB}}{dt} = [H, \rho_{AB}]. \tag{9.3}$$

It is convenient to work in the interaction picture. The density matrix is

$$\widetilde{\rho_{AB}} = \exp\left(\frac{i}{\hbar} H_0 t\right) \rho_{AB} \exp\left(-\frac{i}{\hbar} H_0 t\right),$$

and, differentiating with respect to time, we get

$$\begin{aligned} \frac{d\widetilde{\rho_{AB}}}{dt} &= \frac{i}{\hbar} [H_0, \widetilde{\rho_{AB}}] + \exp\left(\frac{i}{\hbar} H_0 t\right) \frac{\partial \rho_{AB}}{\partial t} \exp\left(-\frac{i}{\hbar} H_0 t\right) \\ &= \frac{i}{\hbar} \left\{ [H_0 - \tilde{H}, \widetilde{\rho_{AB}}] \right\} \\ &= -\frac{i}{\hbar} [\tilde{H}_1, \widetilde{\rho_{AB}}], \end{aligned} \tag{9.4}$$

where

$$\begin{aligned}
\tilde{H}_1(t) &= \exp\left(\frac{i}{\hbar}H_0t\right) H_1 \exp\left(-\frac{i}{\hbar}H_0t\right), \\
&= \exp(i\omega t a^\dagger a + i \sum_j \omega_j t b_j^\dagger b_j) \\
&\quad \times \sum_j \hbar g_j (a^\dagger b_j + a b_j^\dagger) \exp(-i\omega t a^\dagger a - i \sum_j \omega_j t b_j^\dagger b_j) \\
&= \sum_j \hbar g_j \left\{ a^\dagger b_j \exp[i(\omega - \omega_j)t] + a b_j^\dagger \exp[-i(\omega - \omega_j)t] \right\} \\
&= \hbar(G(t)a^\dagger + G^\dagger(t)a),
\end{aligned} \tag{9.5}$$

and

$$G(t) \equiv \sum_j g_j b_j \exp[i(\omega - \omega_j)t]. \tag{9.6}$$

Next, we formally integrate the Liouville equation

$$\widetilde{\rho_{AB}}(t) = \widetilde{\rho_{AB}}(0) + \frac{1}{i\hbar} \int_0^t [\tilde{H}_1(t'), \widetilde{\rho_{AB}}(t')] dt' \tag{9.7}$$

and, substituting back in (9.4), we get

$$\frac{d\widetilde{\rho_{AB}}}{dt} = \frac{1}{i\hbar} [H_1, \widetilde{\rho_{AB}}(0)] - \frac{1}{\hbar^2} \int_0^t [\tilde{H}_1(t), [\tilde{H}_1(t'), \widetilde{\rho_{AB}}(t')]] dt'. \tag{9.8}$$

We trace over the reservoir variables to get

$$\frac{d\widetilde{\rho_A}}{dt} = -\frac{1}{\hbar^2} \int_0^t \text{Tr}_B [\tilde{H}_1(t), [\tilde{H}_1(t'), \widetilde{\rho_{AB}}(t')]] dt'. \tag{9.9}$$

In the last step, we assumed that

$$\text{Tr}_B [\tilde{H}_1(t), \widetilde{\rho_{AB}}(0)] = 0. \tag{9.10}$$

To justify (9.10), assume that at $t = 0$ there is no correlation between the system and the bath, or $\widetilde{\rho_{AB}}(0) = \widetilde{\rho_A}(0) \otimes \widetilde{\rho_B}(0)$, where

$$\widetilde{\rho_B}(0) = \frac{\prod_j \exp(-\hbar\omega_j b_j^\dagger b_j / K_B T)}{\text{Tr}_B \prod_j \exp(-\hbar\omega_j b_j^\dagger b_j / K_B T)}. \tag{9.11}$$

Now, $\tilde{H}_1(t)$ contains linear terms in b_j and b_j^\dagger and $\text{Tr}_B b_j \exp(-\hbar\omega_j b_j^\dagger b_j / K_B T) = 0$.

The final step in finding the master equation for the damped harmonic oscillator is to evaluate the double commutator appearing in (9.9). Also, a fundamental step is to assume that $\widetilde{\rho_{AB}}(t) = \widetilde{\rho_A}(t) \otimes \widetilde{\rho_B}(0)$, which is the Markovian assumption. After a straightforward calculation, one finds

$$\begin{aligned}
\frac{d\widetilde{\rho_A}}{dt} &= -i\Delta\omega [a^\dagger a, \widetilde{\rho_A}(t)] + A [a, \widetilde{\rho_A}(t)a^\dagger] + A [a\widetilde{\rho_A}(t), a^\dagger] \\
&\quad + B [a^\dagger, \widetilde{\rho_A}(t)a] + B [a^\dagger \widetilde{\rho_A}(t), a].
\end{aligned} \tag{9.12}$$

where to derive (9.12) we used the following properties

$$\begin{aligned}\text{Tr}_B(b_j^\dagger b_k \widetilde{\rho}_B(0)) &= \delta_{jk} \langle n_j \rangle, \\ \text{Tr}_B(b_j b_j \widetilde{\rho}_B(0)) &= 0, \\ \Delta\omega &= P \int_0^\infty \frac{g(\omega_j)^2 D(\omega_j)}{\omega - \omega_j} d\omega_j,\end{aligned}\tag{9.13}$$

and $D(\omega)$ is the density function that converts $\sum_j \rightarrow \int D(\omega_j) d\omega_j$, and

$$\int_0^t dt' \exp \pm i(\omega - \omega_j)t \approx \pi \delta(\omega - \omega_j) \pm P \left(\frac{1}{\omega - \omega_j} \right),\tag{9.14}$$

$$\begin{aligned}A &\equiv \pi g(\omega)^2 D(\omega)(1 + \langle n(\omega) \rangle), \\ B &\equiv \pi g(\omega)^2 D(\omega) \langle n(\omega) \rangle.\end{aligned}\tag{9.15}$$

A more standard form of the master equation (9.12) is

$$\begin{aligned}\frac{d\widetilde{\rho}_A}{dt} &= -i\Delta\omega [a^\dagger a, \widetilde{\rho}_A(t)] \\ &\quad - \frac{\gamma}{2}(1 + \langle n(\omega) \rangle)(\widetilde{\rho}_A(t)a^\dagger a + a^\dagger a \widetilde{\rho}_A(t) - 2a \widetilde{\rho}_A(t) a^\dagger) \\ &\quad - \frac{\gamma}{2}\langle n(\omega) \rangle(\widetilde{\rho}_A(t)aa^\dagger + aa^\dagger \widetilde{\rho}_A(t) - 2a^\dagger \widetilde{\rho}_A(t)a).\end{aligned}\tag{9.16}$$

For the particular case $T = 0$ or $\langle n(\omega) \rangle = 0$ and $\Delta\omega \approx 0$, we get the simpler version of (9.16):

$$\begin{aligned}\frac{d\widetilde{\rho}_A}{dt} &= -\frac{\gamma}{2}(\widetilde{\rho}_A(t)a^\dagger a + a^\dagger a \widetilde{\rho}_A(t) - 2a \widetilde{\rho}_A(t) a^\dagger) \\ \gamma &\equiv 2(A - B) = 2\pi g(\omega)^2 D(\omega).\end{aligned}\tag{9.17}$$

9.2 General Properties

Equation (9.12) is called the master equation for the damped harmonic oscillator, and has the following properties.

- (1) Hermiticity. It is simple to verify that the Hermitian conjugate of the master equation gives back the same equation.
- (2) Normalization. It is not obvious that after tracing over the bath variables and making the Markov approximation, ρ_A is still normalized. However it is quite simple to prove that if $\text{Tr}_A \rho_A(0) = 1$, then $\text{Tr}_A \rho_A(t) = 1$, for all times.

9.3 Expectation Values of Relevant Physical Quantities

The calculation, for example, of $\langle a^\dagger \rangle(t)$ can be done in any picture, since they all give the same answer. However, we must be careful to calculate both a^\dagger and ρ_A in the same picture:

$$\langle a^\dagger \rangle(t) = \text{Tr}_A(\tilde{\rho}_A(t)a^\dagger(t)), \quad (9.18)$$

and

$$\tilde{a}^\dagger(t) = \exp(i\omega a^\dagger at)a^\dagger \exp(-i\omega a^\dagger at) = a^\dagger \exp(i\omega t).$$

Now we differentiate (9.18) with respect to time. We readily get

$$\begin{aligned} \frac{d}{dt}\langle a^\dagger \rangle(t) &= \frac{d}{dt}\{\text{Tr}_A[\tilde{\rho}_A(t)a^\dagger] \exp(i\omega t)\} \\ &= \text{Tr}_A\left[\frac{\partial \tilde{\rho}_A(t)}{\partial t}a^\dagger \exp(i\omega t) + i\omega \text{Tr}_A(\tilde{\rho}_A(t)a^\dagger \exp(i\omega t))\right], \end{aligned} \quad (9.19)$$

and making use of the master equation (9.12) it is simple to obtain

$$\frac{d}{dt}\langle a^\dagger \rangle(t) = i(\omega + \Delta\omega)\langle a^\dagger \rangle(t) - (A - B)\langle a^\dagger \rangle(t). \quad (9.20)$$

The solution of (9.20) is

$$\begin{aligned} \langle a^\dagger \rangle(t) &= \langle a^\dagger \rangle(0) \exp[i(\omega + \Delta\omega)t] \exp\left(-\frac{\gamma}{2}t\right), \\ \gamma &\equiv 2(A - B) = 2\pi g(\omega)^2 D(\omega). \end{aligned} \quad (9.21)$$

Using the same procedure as that described above, one can also find $\langle a^\dagger a \rangle(t)$. The differential equation and solution are

$$\begin{aligned} \frac{d}{dt}\langle a^\dagger a \rangle(t) &= -\gamma(\langle a^\dagger a \rangle(t) - \langle n(\omega) \rangle), \\ \langle a^\dagger a \rangle(t) &= \langle a^\dagger a \rangle(0) \exp(-\gamma t) + \langle n(\omega) \rangle [1 - \exp(-\gamma t)]. \end{aligned} \quad (9.22)$$

An interesting property is that $\langle a^\dagger a \rangle(t) \xrightarrow{t \rightarrow \infty} \langle n(\omega) \rangle$, which has a simple interpretation. After a long time, the oscillator in contact with a heat bath gets thermalized, with the same average photon number as the thermal average, at the oscillator's frequency.

Once we know $\langle a^\dagger \rangle(t)$ and $\langle a \rangle(t)$, we can calculate the average position and momentum of the oscillator. The results are

$$\begin{aligned} \langle q \rangle(t) &= \left(\frac{\hbar}{2\omega}\right)^{1/2} [\langle a \rangle(t) + \langle a^\dagger \rangle(t)], \\ \langle p \rangle(t) &= i\left(\frac{\hbar\omega}{2}\right)^{1/2} [-\langle a \rangle(t) + \langle a^\dagger \rangle(t)], \end{aligned} \quad (9.23)$$

which can be written as

$$\langle q \rangle(t) = \exp\left(-\frac{\gamma}{2}t\right) \left[\langle q \rangle(0) \cos \omega t + \frac{\langle p \rangle(0)}{\omega} \sin \omega t \right]. \quad (9.24)$$

$$\langle p \rangle(t) = \exp\left(-\frac{\gamma}{2}t\right) [-\omega \langle q \rangle(0) \sin \omega t + \langle p \rangle(0) \cos \omega t], \Delta\omega = 0.$$

Finally, if we assume an initial minimum uncertainty state (mus), it is simple to show that

$$\Delta p \Delta q = \frac{\hbar}{2} \{1 + 2\langle n(\omega) \rangle [1 - \exp(-\gamma t)]\}. \quad (9.25)$$

The result given by (9.25) shows again that for $t \rightarrow \infty$, $\Delta p \Delta q \rightarrow \frac{1}{2}\hbar[1 + 2\langle n(\omega) \rangle]$, which is the uncertainty product for a thermal photon at frequency ω .

We notice here that the particular example of the damped harmonic oscillator is a simple one, in the sense that the expectation values we found are only coupled with moments of the same order, and not higher. This is not generally the case where the moment equations are coupled with higher orders and one has to use some kind of approximate truncation scheme.

9.4 Time Evolution of the Density Matrix Elements

We are interested in the time evolution of $(\tilde{\rho}_A(t))_{nn} \equiv p_n(t)$. If we assume $\Delta\omega = 0$, and take the matrix elements of (9.12), we readily get

$$\frac{dp_n}{dt} = 2A(n+1)p_{n+1} + 2Bnp_{n-1} - p_n(2An + 2B(n+1)). \quad (9.26)$$

Each term in the right-hand side of (9.26) has an interpretation in terms of energy transitions, as described in Fig. 9.1, where the arrows arriving at one of the energy levels increase dp_n/dt and those leaving the level decrease the rate.

A common technique used in solving this type of difference-differential equation, is that of the generating function. We define

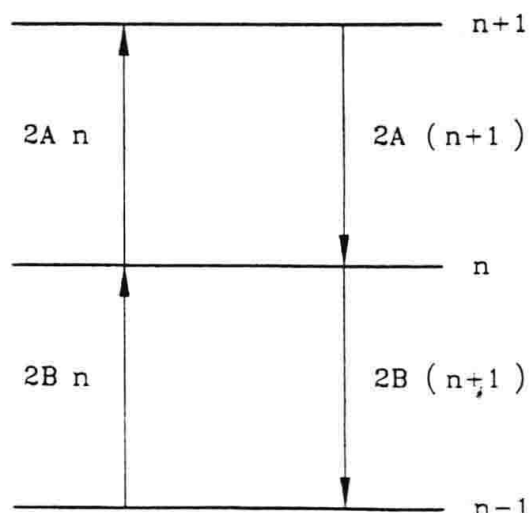


Fig. 9.1. Graphical representation of the time evolution equation for p_n , where each arrow pointing towards the n th level increases p_n , and vice versa

$$Q(x, t) = \sum_{n=0}^{\infty} (1-x)^n p_n(t), \quad (9.27)$$

where p_n can be easily calculated as

$$p_n = \frac{(-1)^n}{n!} \frac{\partial^n}{\partial x^n} Q(x, t) \Big|_{x=1}. \quad (9.28)$$

Multiplying (9.26) by $(1-x)^n$ and summing over n , we get

$$\frac{\partial Q}{\partial t} = -2BxQ - 2(A-B)x \frac{\partial Q}{\partial x} - 2Bx^2 \frac{\partial Q}{\partial x}. \quad (9.29)$$

In deriving (9.29) we made use of relations like

$$\sum p_{n+1}(n+1)(1-x)^n = -\frac{\partial Q}{\partial x}, \quad (9.30)$$

$$\sum p_n(n)(1-x)^n = -(1-x) \frac{\partial Q}{\partial x}, \text{ etc.}$$

In order to solve (9.29), we make use of the method of characteristics [9.3] (see Appendix B). Equation (9.29) can be conveniently written as

$$\begin{aligned} \frac{dt}{1} &= \frac{dx}{2[(A-B) + Bx]}, \\ \frac{dx}{2[(A-B) + Bx]} &= -\frac{dQ}{2BQ}. \end{aligned} \quad (9.31)$$

The simultaneous solution of the system of differential equations is:

$$\begin{aligned} t + \frac{\ln H}{2(A-B)} &= \frac{1}{2(A-B)} \ln \left[\frac{x}{2(A-B) + 2Bx} \right], \\ -\ln Q + \ln K &= \ln [2(A-B) + 2Bx], \end{aligned} \quad (9.32)$$

or explicitly

$$K = Q [2(A-B) + 2Bx], \quad (9.33)$$

$$H = \frac{x \exp[-2(A-B)t]}{2(A-B) + 2Bx} \quad (9.34)$$

where K and H are integration constants to be determined from the initial conditions, satisfying the general integral of the differential equation

$$K = g(H), \quad (9.35)$$

g being an arbitrary function.

Now we consider the initial state of the oscillator to be a coherent state, that is

$$p_n(0) = \frac{\bar{n}^n}{n!} \exp(-\bar{n}), \quad (9.36)$$

so that

$$Q(x, 0) = \sum_{n=0}^{\infty} (1-x)^n \frac{\bar{n}^n}{n!} \exp -\bar{n} = \exp -\bar{n}x. \quad (9.37)$$

Making use of (9.35), (9.33), (9.34), one can write

$$Q(x, t) = \frac{1}{2(A-B) + 2Bx} g \left(\frac{x \exp [-2(A-B)t]}{2(A-B) + 2Bx} \right), \quad (9.38)$$

and making use of the initial condition (9.37), we obtain

$$Q(x, t) = \frac{1}{1 + [B/(A-B)]x \{1 - \exp [-(2A-B)t]\}} \quad (9.39)$$

$$\times \exp \left[-x \frac{\bar{n} \exp [-(2A-B)t]}{1 + [B/(A-B)]x \{1 - \exp [-(2A-B)t]\}} \right]. \quad (9.40)$$

In the limit $n \rightarrow \infty$,

$$Q(x, \infty) = \frac{1}{1 + [B/(A-B)]x} = \frac{1}{1 + x \langle n(\omega) \rangle} = \sum_{n=0}^{\infty} (1-x)^n p_n(\infty),$$

and with the use of (9.28), we get

$$p_n(\infty) = \frac{\langle n(\omega) \rangle^n}{[1 + \langle n(\omega) \rangle]^{n+1}}. \quad (9.41)$$

As we can see, the oscillator, initially in a coherent state, gets thermalized when $t \rightarrow \infty$, or

$|\alpha\rangle \Rightarrow$ one more element of the reservoir.

9.5 The Glauber–Sudarshan Representation and the Fokker–Planck Equation

It is convenient, for the purposes of this section, to define the Bargmann [9.4] states as

$$|\alpha\rangle = \exp \left(\frac{|\alpha|^2}{2} \right) |\alpha\rangle. \quad (9.42)$$

It is simple to show, from the definition of the coherent states, that

$$a^\dagger |\alpha\rangle = \frac{\partial}{\partial \alpha} |\alpha\rangle, \quad (9.43)$$

$$\langle \alpha | a = \frac{\partial}{\partial \alpha^*} \langle \alpha |.$$

We now write the density operator in the P -representation

$$\rho = \int d^2\alpha |\alpha\rangle \langle \alpha| \exp(-|\alpha|^2) P(\alpha). \quad (9.44)$$

Then

$$\begin{aligned} a^\dagger \rho &= \int d^2\alpha \frac{\partial}{\partial \alpha} (\|\alpha\rangle) \langle \alpha \| \exp(-|\alpha|^2) P(\alpha), \\ &= \int d^2\alpha (\|\alpha\rangle \langle \alpha \|) \exp(-|\alpha|^2) \left(\alpha^* - \frac{\partial}{\partial \alpha} \right) P(\alpha). \end{aligned} \quad (9.45)$$

Thus we have the following correspondence

$$\begin{aligned} a^\dagger \rho &\rightarrow \left(\alpha^* - \frac{\partial}{\partial \alpha} \right) P(\alpha), \\ \rho a &\rightarrow \left(\alpha - \frac{\partial}{\partial \alpha^*} \right) P(\alpha), \\ \rho a^\dagger &\rightarrow \alpha^* P(\alpha), \\ a \rho &\rightarrow \alpha P(\alpha), \\ a^\dagger a \rho &\rightarrow \left(\alpha^* - \frac{\partial}{\partial \alpha} \right) \alpha P(\alpha), \\ a a^\dagger \rho &\rightarrow \alpha \left(\alpha^* - \frac{\partial}{\partial \alpha} \right) P(\alpha) \\ \rho a^\dagger a &\rightarrow \left(\alpha - \frac{\partial}{\partial \alpha^*} \right) \alpha^* P(\alpha), \\ \rho a a^\dagger &\rightarrow \alpha^* \left(\alpha - \frac{\partial}{\partial \alpha^*} \right) P(\alpha). \end{aligned} \quad (9.46)$$

If we now apply the above rules to the master equation (9.16), for $\Delta\omega = 0$, we get the Fokker-Planck equation for the damped harmonic oscillator:

$$\frac{\partial P(\alpha, \alpha^*, t)}{\partial t} = \frac{\gamma}{2} \left(\frac{\partial}{\partial \alpha} \alpha P + \frac{\partial}{\partial \alpha^*} \alpha^* P \right) + \gamma \langle n \rangle \frac{\partial^2 P}{\partial \alpha \partial \alpha^*}. \quad (9.47)$$

9.6 Time-Dependent Solution. The Method of the Eigenfunctions

We try to solve the Fokker-Planck equation (9.47), using the following ansatz [9.5], [9.6]

$$P(\alpha, \alpha^*, t) = \exp(-\lambda t) Q(\alpha, \alpha^*). \quad (9.48)$$

By replacing the above ansatz in the Fokker-Planck equation, we get the following result

$$LQ = -\lambda Q, \quad (9.49)$$

$$L \equiv \frac{\gamma}{2} \left(\alpha \frac{\partial}{\partial \alpha} + \alpha^* \frac{\partial}{\partial \alpha^*} + 2 \right) + \gamma \langle n \rangle \frac{\partial^2}{\partial \alpha \partial \alpha^*}.$$

Now we perform the following change of variables

$$\alpha = \sqrt{\langle n \rangle} (x + iy), \quad (9.50)$$

$$Q(\alpha) = \exp \frac{1}{2}(x^2 + y^2) N(x, y).$$

With the above transformation, the eigenvalue equation (9.49) becomes just the well-known Schrödinger equation for the two-dimensional isotropic harmonic oscillator. The eigenfunctions and eigenvalues are

$$N_{n_x, n_y} = K_{n_x, n_y} \exp \left[-\frac{1}{2}(x^2 + y^2) \right] H_{n_x}(x) H_{n_y}(y). \quad (9.51)$$

$$\epsilon = \frac{4\lambda}{\gamma} + 2 = n_x + 1 + n_y + 1,$$

where n_x and n_y are integer numbers, so the solution now becomes

$$P_{n_x, n_y} = K_{n_x, n_y} \exp \left\{ -\frac{1}{2}(x^2 + y^2) \right\} H_{n_x}(x) H_{n_y}(y) \quad (9.52)$$

$$\times \exp \left[-\frac{\gamma}{2}(n_x + n_y)t \right].$$

We calculate the normalization constant K_{n_x, n_y} from the normalization of the P -distribution

$$\int \frac{d^2\alpha}{\pi} P(\alpha, t) = 1,$$

and the properties of the Hermite polynomials

$$\int_{-\infty}^{\infty} dx H_n(x) H_m(x) \exp \left(-\frac{1}{2}x^2 \right) = \delta_{nm} 2^n n! \sqrt{\pi}, \quad (9.53)$$

$$H_0(x) = 1.$$

We write

$$\begin{aligned} & \frac{1}{\pi} K_{n_x, n_y} \langle n \rangle \int dx \exp(-\frac{1}{2}x^2) H_{n_x}(x) \\ & \times \int dy H_{n_y}(y) \exp(-\frac{1}{2}y^2) \exp(-\frac{\gamma}{2}(n_x + n_y)t) \\ & = \frac{1}{\pi} K_{n_x, n_y} \langle n \rangle \delta_{n_x, 0} \delta_{n_y, 0} \exp \left[-\frac{\gamma}{2}(n_x + n_y)t \right] \sqrt{\pi} \sqrt{\pi} = 1, \end{aligned}$$

so that $K_{00} = 1/\langle n \rangle$ and $P_{00} = (1/\langle n \rangle) \exp[-\frac{1}{2}(x^2 + y^2)]$ which correspond to the time-independent steady state solution with the eigenvalue $\lambda = 0$. Going back to the α variables,

$$\lim_{t \rightarrow \infty} P(\alpha, \alpha^*, t) = P_{00} = \frac{1}{\langle n \rangle} \exp \left[-\frac{|\alpha|^2}{\langle n \rangle} \right],$$

which corresponds, as it should, to the P -representation of the thermal density matrix.

9.6.1 General Solution

We now concentrate on the general solution of the Fokker–Planck equation, using conditional probability densities such as $P(\alpha, t | \alpha', 0)$ with the initial condition

$$P(\alpha, 0 | \alpha', 0) = \delta^2(\alpha - \alpha'). \quad (9.54)$$

Of course we notice that since

$$P(\alpha, t) = \int \frac{d^2\alpha'}{\pi} P(\alpha, t | \alpha', 0) P(\alpha', 0),$$

the solution will have the form

$$P(\alpha, t | \alpha', 0) = \sum_{n_x n_y} \frac{P_{n_x n_y}(x, y, t) P_{n_x n_y}(x', y', 0)}{\langle n \rangle P_{00}(x', y')} \quad (9.55)$$

Now we explain why $P(\alpha, t | \alpha', 0)$ given by (9.55) is the general solution of the Fokker–Planck equation (9.47). In the first place it consists of linear superposition of $P_{n_x n_y}(x, y, t)$ solutions. So we have only to verify that it satisfies the initial conditions. Making use of another property of the Hermite polynomials,

$$\sum_{m=0}^{\infty} \frac{1}{2^m m! \sqrt{\pi}} \exp(-x^2) H_m(x) H_m(x') = \delta(x - x'),$$

we find

$$K_{n_x, n_y} = \frac{1}{\sqrt{2^{n_x} n_x! \sqrt{\pi} 2^{n_y} n_y! \sqrt{\pi}}},$$

and the initial condition (9.54) is satisfied.

9.7 Langevin's Equations

We now study the damped harmonic oscillator problem, in the Heisenberg picture, with the initial reservoir operators interpreted as the quantum version of a stochastic or Langevin force. From the Hamiltonian (9.2), the Heisenberg equations for a and b_j are [9.7]

$$\frac{da(t)}{dt} = -i\omega a(t) - i \sum_j g_j b_j(t), \quad (9.56)$$

$$\frac{db_j(t)}{dt} = -i\omega_j b_j(t) - ig_j^* a(t).$$

Integrating formally the second of (9.56), we get

$$b_j(t) = b_j(t_0) \exp[-i\omega_j(t - t_0)] - ig_j^* \int_{t_0}^t dt' a(t') \exp[-i\omega_j(t - t')]. \quad (9.57)$$

We insert (9.57) back in (9.56), to get

$$\begin{aligned}\frac{da(t)}{dt} = & -i\omega a(t) - i \sum_j g_j b_j(t_0) \exp[-i\omega_j(t-t_0)] \\ & - \sum_j |g_j|^2 \int_{t_0}^t dt' a(t') \exp[-i\omega_j(t-t')].\end{aligned}\quad (9.58)$$

The second term on the right-hand side of (9.58) represents the fluctuating term, independent of the system oscillator variable, and the third term is the back-reaction to the oscillator.

We now want to eliminate the fast time-varying terms and introduce a rotating frame by defining $A(t) = a(t) \exp(i\omega t)$ with $[A(t), A(t)^\dagger] = 1$, so (9.58) can be written now as

$$\begin{aligned}\frac{dA(t)}{dt} = & - \sum_j |g_j|^2 \int_{t_0}^t dt' A(t') \exp[-i(\omega_j - \omega)(t-t')] + F(t), \\ F(t) = & \text{noise operator} \\ = & -i \sum_j g_j b_j(t_0) \exp[-i\omega_j(t-t_0)] \exp i\omega t.\end{aligned}\quad (9.59)$$

Since, for a thermal bath, $\langle b_j \rangle = 0$, therefore $\langle F(t) \rangle_B = 0$.

We follow the same procedure as in the previous section, that is, make the Markov approximation, convert the discrete sum into an integral and arrive at the following result

$$\frac{dA(t)}{dt} = -\frac{\gamma}{2} A(t) + F(t). \quad (9.60)$$

On the average (9.60) behaves classically:

$$\frac{d\langle A(t) \rangle}{dt} = -\frac{\gamma}{2} \langle A(t) \rangle. \quad (9.61)$$

Equation (9.60) is called generically the Langevin equation for the damped harmonic oscillator. The original idea came from the study of Brownian motion, where the particles in a liquid suffer from the rapid impact of the liquid molecules on the Brownian particle, having as a net effect, a rapidly time-varying force.

We have to point out that, in spite of the fact that averaging (9.60) over the bath variables makes the fluctuating force disappear, $F(t)$ plays the very important role of preserving the commutation relations, in other words if the equation $dA(t)/dt = -(1/2)\gamma A(t)$ were true, then we would have $A(t) = A(t_0) \exp(-(1/2)\gamma t)$ and therefore $[A(t), A(t)^\dagger] \rightarrow 0$, thus violating quantum mechanics.

9.7.1 Calculation of the Correlation Function $\langle F(t')F(t'')^\dagger \rangle_B$

According to the definition of $F(t)$, we can write

$$\begin{aligned}
& \langle F(t')F(t'')^\dagger \rangle_B \\
&= \sum_i \sum_j g_i g_j^* \langle b_i b_j^\dagger \rangle \exp[i\omega(t' - t'')] \exp[i(\omega_j t'' - \omega_i t')] \\
&= \sum_i |g_i|^2 \langle b_i b_i^\dagger \rangle \exp[i\omega(t' - t'')] \exp[-i\omega_i(t' - t'')] \\
&= \int d\omega' D(\omega') |g(\omega')|^2 [\langle n(\omega') \rangle + 1] \exp[i(\omega - \omega')(t' - t'')] \\
&= \gamma [\langle n(\omega) \rangle + 1] \delta(t' - t'').
\end{aligned} \tag{9.62}$$

In a similar calculation, one gets

$$\langle F(t')^\dagger F(t'') \rangle_B = \gamma \langle n(\omega) \rangle \delta(t' - t''). \tag{9.63}$$

9.7.2 Differential Equation for the Photon Number

The Heisenberg equation for the photon number can be written as

$$\begin{aligned}
\frac{dA^\dagger A}{dt} &= - \sum_j |g_j|^2 A^\dagger(t) \int_{t_0}^t dt' A(t') \exp[i(\omega - \omega_j)(t - t')] \\
&\quad - i \sum_j g_j A^\dagger(t) b_j(t_0) \exp[i(\omega - \omega_j)(t - t_0)] + \text{adj.}
\end{aligned} \tag{9.64}$$

Making the Markov approximation, and transforming the sum into an integral, we get the following Langevin equation

$$\begin{aligned}
\frac{dA^\dagger A}{dt} &= -\gamma A^\dagger A + F'_{A^\dagger A}, \\
F'_{A^\dagger A} &= i \sum_j g_j^* A(t) b_j^\dagger(t_0) \exp[-i(\omega - \omega_j)(t - t_0)] + \text{adj.}
\end{aligned} \tag{9.65}$$

It is simple to show that $\langle F'_{A^\dagger A} \rangle = \gamma \langle n \rangle$, so that it is more convenient to define a noise operator with zero average $F_{A^\dagger A} = F'_{A^\dagger A} - \gamma \langle n \rangle$, so that

$$\frac{dA^\dagger A}{dt} = -\gamma A^\dagger A + \gamma \langle n \rangle + F_{A^\dagger A}. \tag{9.66}$$

9.8 Other Master Equations

9.8.1 Two-Level Atom in a Thermal Bath

We attack here a different problem, but it is formally similar to the damped harmonic oscillator. Consider a two-level atom interacting with a reservoir of

harmonic oscillators. Physically, this could, for example, represent an atom decaying irreversibly when interacting with infinite vacuum modes of the electromagnetic field. The Hamiltonian of this problem is

$$H = \frac{\hbar\omega}{2}\sigma_z + \hbar \sum_l \omega_l b_l^\dagger b_l + \hbar \sum_l (g_l b_l^\dagger \sigma + g_l^* b_l \sigma^\dagger). \quad (9.67)$$

The master equation for the atom can be derived exactly as in the case of the damped harmonic oscillator. The result gives back (9.16), with the substitution

$$\begin{aligned} a &\rightarrow \sigma \\ a^\dagger &\rightarrow \sigma^\dagger. \end{aligned}$$

It then reads

$$\begin{aligned} \frac{d\tilde{\rho}_A}{dt} = & -\frac{\gamma}{2}(1 + \langle n(\omega) \rangle)(\tilde{\rho}_A(t)\sigma^\dagger\sigma + \sigma^\dagger\sigma\tilde{\rho}_A(t) - 2\sigma\tilde{\rho}_A(t)\sigma^\dagger) \\ & -\frac{\gamma}{2}\langle n(\omega) \rangle(\tilde{\rho}_A(t)\sigma\sigma^\dagger + \sigma\sigma^\dagger\tilde{\rho}_A(t) - 2\sigma^\dagger\tilde{\rho}_A(t)\sigma). \end{aligned} \quad (9.68)$$

Making use of the Pauli matrix properties

$$\begin{aligned} \sigma\sigma^\dagger &= \frac{1}{2}(1 - \sigma_z), \\ \sigma^\dagger\sigma &= \frac{1}{2}(1 + \sigma_z). \end{aligned}$$

one can write a different version of the master equation (9.68)

$$\begin{aligned} \frac{d\tilde{\rho}_A}{dt} = & \gamma(1 + \langle n(\omega) \rangle)\sigma\tilde{\rho}_A(t)\sigma^\dagger + \gamma\langle n(\omega) \rangle\sigma^\dagger\tilde{\rho}_A(t)\sigma \\ & -\tilde{\rho}_A\gamma\left[\frac{1}{2} + \langle n(\omega) \rangle\right] - \frac{\gamma}{4}(\tilde{\rho}_A\sigma_z + \sigma_z\tilde{\rho}_A). \end{aligned} \quad (9.69)$$

The master equation written in the form (9.69) is suitable to calculate $\langle \sigma_z \rangle$:

$$\frac{d\langle \sigma_z \rangle}{dt} = \frac{d}{dt} \text{Tr} \{ \tilde{\rho}_A \sigma_z \} = \text{Tr} \left\{ \frac{d\tilde{\rho}_A}{dt} \sigma_z \right\}, \quad (9.70)$$

where we have used the fact that $\tilde{\sigma}_z = \sigma_z$.

By introducing the master equation in (9.70), and after some simple algebra, one arrives at

$$\frac{d\langle \sigma_z \rangle}{dt} = -\gamma - 2\gamma \left[\frac{1}{2} + \langle n(\omega) \rangle \right] \langle \sigma_z \rangle. \quad (9.71)$$

The solution of (9.71) is

$$\begin{aligned} \langle \sigma_z \rangle(t) = & \langle \sigma_z \rangle(0) \exp(-2\gamma t) \left[\frac{1}{2} + \langle n(\omega) \rangle \right] \\ & - \frac{1}{2 \left[\frac{1}{2} + \langle n(\omega) \rangle \right]} \left\{ 1 - \exp(-2\gamma t) \left[\frac{1}{2} + \langle n(\omega) \rangle \right] \right\}. \end{aligned} \quad (9.72)$$

We now take the aa matrix element of (9.68) and get

$$\frac{d}{dt} P_a(t) = \frac{d}{dt} \rho_{aa}(t) = -\gamma P_a(t), \quad (9.73)$$

and the solution is $P_a(t) = P_a(0) \exp(-\gamma t)$, which is the well-known result of E. Wigner and V. Weisskopf [9.8], predicting the exponential decay of an atom initially in an excited state. We notice that here the single atom is interacting with an infinite reservoir of electromagnetic modes in the vacuum, and the predicted behaviour here is very different from the Rabi flopping of the atom interacting with a single mode in a good cavity.

9.8.2 Damped Harmonic Oscillator in a Squeezed Bath

We start with (9.9), and write it out in detail, using the Hamiltonian of (9.5), thus getting

$$\begin{aligned} \frac{d\rho_A}{dt} = & - \int_0^t dt' \text{Tr}_B \{ [a^\dagger G(t) + G^\dagger(t)a] \\ & \times [a^\dagger G(t') + G^\dagger(t')a] \rho_B \otimes \rho(t') \\ & - [a^\dagger G(t) + G^\dagger(t)a] \rho_B \otimes \rho(t') [a^\dagger G(t') + G^\dagger(t')a] \\ & - [a^\dagger G(t') + G^\dagger(t')a] \rho_B \otimes \rho(t') [a^\dagger G(t) + G^\dagger(t)a] \\ & + \rho_B \otimes \rho(t') [a^\dagger G(t') + G^\dagger(t')a] [a^\dagger G(t) + G^\dagger(t)a] \}. \end{aligned} \quad (9.74)$$

Using the properties

$$\begin{aligned} \langle G(t')G(t) \rangle &= \langle G(t)G(t') \rangle, \\ \langle G^\dagger(t')G(t) \rangle &= \langle G^\dagger(t)G(t') \rangle^*, \\ \langle G(t')G^\dagger(t) \rangle &= \langle G(t)G^\dagger(t') \rangle^*, \\ \langle G^\dagger(t')G^\dagger(t) \rangle &= \langle G^\dagger(t)G^\dagger(t') \rangle, \end{aligned} \quad (9.75)$$

we can write

$$\begin{aligned} \frac{d\rho_A(t)}{dt} = & I_1 [a^\dagger a^\dagger \rho_A + \rho_A a^\dagger a^\dagger - 2a^\dagger \rho_A a^\dagger] \\ & + I_2 [aa\rho_A + \rho_A aa - 2a\rho_A a] \\ & + I_3 [a^\dagger a\rho_A + \rho_A a^\dagger a - 2a\rho_A a^\dagger] \\ & + I_4 [aa^\dagger \rho_A + \rho_A aa^\dagger - 2a^\dagger \rho_A a] \end{aligned} \quad (9.76)$$

where we defined

$$\begin{aligned} I_1 &= \int dt' \langle G(t)G(t') \rangle, \\ I_2 &= \int dt' \langle G^\dagger(t)G^\dagger(t') \rangle, \end{aligned} \quad (9.77)$$

$$I_3 = \int dt' \langle G(t)G^\dagger(t') \rangle,$$

$$I_4 = \int dt' \langle G^\dagger(t)G(t') \rangle.$$

We will calculate one of them in detail, for example I_1 :

$$\begin{aligned} I_1 &= \int dt' \langle G(t)G(t') \rangle, \\ &= \int dt' \sum_{k,k'} g_k g_{k'} \exp [i(\omega - \omega_k)t] \exp [i(\omega - \omega_{k'})t'] \langle b_k b_{k'} \rangle, \\ &= \int_0^t dt' \sum_{k,k'} g_k g_{k'} \exp [i\omega(t + t')] \exp [-i(\omega_k t + \omega_{k'} t')] \langle b_k b_{k'} \rangle. \end{aligned} \quad (9.78)$$

Now, we consider the two-mode squeezing correlation

$$\langle b_k b_{k'} \rangle = \langle b_k b_{-k} \rangle \delta_{k',-k} = M \quad (9.79)$$

placed symmetrically around the system frequency ω , so

$$\omega_{\pm k} = \omega \pm \Omega.$$

Then, converting the sum into a frequency integral, with a density D , we can write

$$I_1 = M \int_0^\infty d\Omega D(\omega + \Omega) g^2(\omega + \Omega) \int_0^t dt' \exp [-i\Omega(t - t')].$$

If we assume that the functions D and g are slowly varying with frequency, then the time-dependent result after the frequency integration is sharply peaked and we can set $t \rightarrow \infty$, without much error, getting a $\delta(\Omega)$ and a small frequency shift. The result then reads

$$I_1 = \frac{\gamma}{2} M + i\delta_1, \quad (9.80)$$

with

$$\gamma = 2\pi D(\omega)g(\omega)^2, \quad (9.81)$$

$$\delta_1 = P \int_{-\infty}^{\infty} \frac{d\Omega}{\Omega} D(\Omega + \omega) g^2(\Omega + \omega) M.$$

In a similar way, we obtain the other integrals

$$I_2 = \frac{\gamma}{2} M^* - i\delta_1, \quad (9.82)$$

$$I_3 = \frac{\gamma}{2} (N + 1) + i\delta_2, \quad (9.83)$$

$$I_4 = \frac{\gamma}{2} N - i\delta_2, \quad (9.84)$$

with

$$\langle b_k^\dagger b_{k'} \rangle = N \delta_{k,k'}. \quad (9.85)$$

If we compare the above results with the average corresponding to the two-mode squeezed vacuum, we readily get

$$N = \sinh^2 r, \quad (9.86)$$

$$M = -\exp(i\theta) \sinh r \cosh r,$$

obeying the relation

$$\sqrt{N(N+1)} = \sqrt{\sinh^2 r \cosh^2 r} = |M|. \quad (9.87)$$

Ignoring the small frequency shifts δ_1 and δ_2 , we finally write the master equation for the damped harmonic oscillator in a squeezed vacuum:

$$\begin{aligned} \frac{d\rho}{dt} = & \frac{\gamma}{2}(N+1)(2a\rho a^\dagger - a^\dagger a\rho - \rho a^\dagger a) \\ & + \frac{\gamma}{2}(N)(2a^\dagger \rho a - a a^\dagger \rho - \rho a a^\dagger) \\ & + \frac{\gamma}{2}(M)[2a^\dagger \rho a^\dagger - a^\dagger a^\dagger \rho - \rho a^\dagger a^\dagger] \\ & + \frac{\gamma}{2}(M^*)(2a\rho a - a a \rho - \rho a a). \end{aligned} \quad (9.88)$$

In the particular case of a thermal reservoir $N \rightarrow \langle n \rangle$, $M \rightarrow 0$, and we recover (9.16).

This master equation is expected to give a correct description of a system driven by noise that comes from the squeezed vacuum, provided the squeezing is reasonably constant over the bandwidth of the system.

The above condition has to be satisfied, since if D, k, M are slowly varying functions of Ω , then the frequency integral approaches a δ -function in time and we are justified in setting the upper limit to ∞ .

9.8.3 Application. Spontaneous Decay in a Squeezed Vacuum

Once more, in the master equation [9.9], [9.10], we replace

$$a \rightarrow \sigma, a^\dagger \rightarrow \sigma^\dagger, \quad (9.89)$$

in order to study atomic decay, getting

$$\begin{aligned} \frac{d\rho}{dt} = & \frac{\gamma}{2} \cosh^2 r (2\sigma\rho\sigma^\dagger - \sigma^\dagger\sigma\rho - \rho\sigma^\dagger\sigma) \\ & + \frac{\gamma}{2} \sinh^2 r (2\sigma^\dagger\rho\sigma - \sigma\sigma^\dagger\rho - \rho\sigma\sigma^\dagger) \\ & - \gamma \exp(i\theta) \sinh r \cosh r (\sigma^\dagger\rho\sigma^\dagger) \\ & - \gamma \exp(-i\theta) \sinh r \cosh r (\sigma\rho\sigma). \end{aligned} \quad (9.90)$$

In the above equation, we used the property $\sigma^2 = \sigma^{\dagger 2} = 0$.

If we take the expectation value of

$$\sigma_x = \frac{\sigma + \sigma^\dagger}{2}, \quad (9.91)$$

$$\sigma_x = \frac{\sigma - \sigma^\dagger}{2i},$$

$$\sigma_z = (2\sigma^\dagger\sigma - 1).$$

we get the following differential equations

$$\langle \dot{\sigma}_x \rangle = -\frac{\gamma}{2} \exp(2r) \langle \sigma_x \rangle \equiv -\gamma_x \langle \sigma_x \rangle, \quad (9.92)$$

$$\langle \dot{\sigma}_y \rangle = -\frac{\gamma}{2} \exp(-2r) \langle \sigma_y \rangle \equiv -\gamma_y \langle \sigma_x \rangle, \quad (9.93)$$

$$\langle \dot{\sigma}_z \rangle = -\gamma(2 \sinh^2 r + 1) \langle \sigma_z \rangle - \gamma \equiv -\gamma_z \langle \sigma_z \rangle - \gamma. \quad (9.94)$$

As we can see, for large squeezing, both γ_x and γ_z become large, and γ_y becomes very small. On a time scale short compared to γ_y^{-1} , but larger than γ_x^{-1} and γ_z^{-1} , we get

$$\langle \sigma_x \rangle \rightarrow 0, \quad \langle \sigma_z \rangle \rightarrow -\frac{1}{2 \sinh^2 r + 1}. \quad (9.95)$$

Problems

9.1. The Dirac delta-function can be defined as

$$\delta(\omega_0 - \omega) = \frac{2}{\pi} \text{Lim}_{t \rightarrow \infty} \frac{\sin^2 \left\{ \left[\frac{1}{2}(\omega_0 - \omega)t \right] \right\}}{(\omega_0 - \omega)^2 t}.$$

Prove that

$$(a) \quad \int_{-\infty}^{\infty} \delta(\omega_0 - \omega) d\omega = 1$$

$$(b) \quad \int_{\omega_1}^{\omega_2} \delta(\omega_0 - \omega) f(\omega) d\omega = f(\omega_0).$$

with $\omega_1 < \omega_0 < \omega_2$.

9.2. Prove that the following are acceptable definitions or representations of the Dirac delta-function

$$(a) \quad \delta(\omega_0 - \omega) = \frac{1}{2\pi} \text{Lim}_{T_1, T_2 \rightarrow \infty} \int_{T_1}^{T_2} \exp(i(\omega_0 - \omega)t) dt,$$

$$(b) \quad \delta(\omega_0 - \omega) = \text{Lim}_{T \rightarrow \infty} \left[\frac{\sin(\omega_0 - \omega)T}{(\omega_0 - \omega)\pi} \right],$$

$$(c) \quad \delta(\omega_0 - \omega) = \frac{1}{\pi} \text{Lim}_{\varepsilon \rightarrow 0} \frac{\varepsilon}{(\omega_0 - \omega)^2 + \varepsilon^2}.$$

9.3. Write down the Fokker–Planck equation of the damped harmonic oscillator in a squeezed bath, starting from (9.88).

9.4. The master equation

$$\dot{\rho} = \frac{\mathcal{A}}{2}(2a^\dagger \rho a - aa^\dagger \rho - \rho aa^\dagger) - \frac{C}{2}(a^\dagger a \rho + \rho a^\dagger a - 2a \rho a^\dagger)$$

represents the laser theory in the lowest-order approximation, where \mathcal{A} is the gain and C the cavity loss.

Prove that the corresponding Fokker–Planck equation is

$$\frac{\partial P}{\partial t} = -\frac{\mathcal{A} - C}{2} \left(\frac{\partial}{\partial \alpha} \alpha + \frac{\partial}{\partial \alpha^*} \alpha^* \right) P + \mathcal{A} \frac{\partial^2 P}{\partial \alpha \partial \alpha^*}.$$

9.5. Generalizing the results of Problem 9.4, we now take second-order laser theory. For the following master equation

$$\begin{aligned} \frac{d\rho_f}{dt} = & -\frac{\mathcal{A}}{2} \left\{ aa^\dagger \left[\rho_f - \left(\frac{g}{\gamma} \right)^2 (aa^\dagger \rho_f + 3\rho_f aa^\dagger) \right] \right. \\ & + \left[\rho_f - \left(\frac{g}{\gamma} \right)^2 (\rho_f aa^\dagger + 3aa^\dagger \rho_f) \right] aa^\dagger \\ & \left. - 2a^\dagger \left[\rho_f a - 2 \left(\frac{g}{\gamma} \right)^2 (aa^\dagger \rho_f + \rho_f aa^\dagger) a \right] \right\} \\ & - \frac{C}{2} (a^\dagger a \rho_f + \rho_f a^\dagger a - 2a \rho_f a^\dagger), \end{aligned}$$

show that the corresponding Fokker–Planck equation is

$$\begin{aligned} \frac{\partial P}{\partial t} = & -\frac{1}{2} \frac{\partial}{\partial \alpha} \left\{ \left[(\mathcal{A} - C) - 4A \frac{g^2}{\gamma^2} |\alpha|^2 \right] \alpha P - \mathcal{A} \frac{\partial P}{\partial \alpha^*} \right\} \\ & -\frac{1}{2} \frac{\partial}{\partial \alpha^*} \left\{ \left[(\mathcal{A} - C) - 4A \frac{g^2}{\gamma^2} |\alpha|^2 \right] \alpha^* P - \mathcal{A} \frac{\partial P}{\partial \alpha} \right\}. \end{aligned}$$

Notice that we regain the results of Problem 9.4 when we neglect the g^2 terms.

9.6. For the damped harmonic oscillator show that if one assumes initially a minimum uncertainty state, then at time t

$$\Delta q(t) \Delta p(t) = \frac{\hbar}{2} [1 + 2\langle n(\omega) \rangle (1 - \exp(-\gamma t))].$$

10. Resonance Fluorescence

The theory of spontaneous emission was originally developed by Weisskopf and Wigner [10.1]. However, the sidebands for coherent single-mode fields were found by Mollow in the 1960s [10.2]. The physical origin of the sidebands in the resonance fluorescence spectrum can be nicely seen using dressed states [10.3].

10.1 Background

We assume a two-level atom driven by a continuous monochromatic field. The atom scatters the light in all directions, as shown in Fig. 10.1. For a weak incident field, the spectrum, as we shall see in some detail, exhibits a single peak much narrower than the natural linewidth of the atomic transition. As we increase the field, this spectrum splits into three peaks consisting of a central peak at the laser frequency and two sidebands symmetrically placed at $\pm R_n$ with respect to the centre.

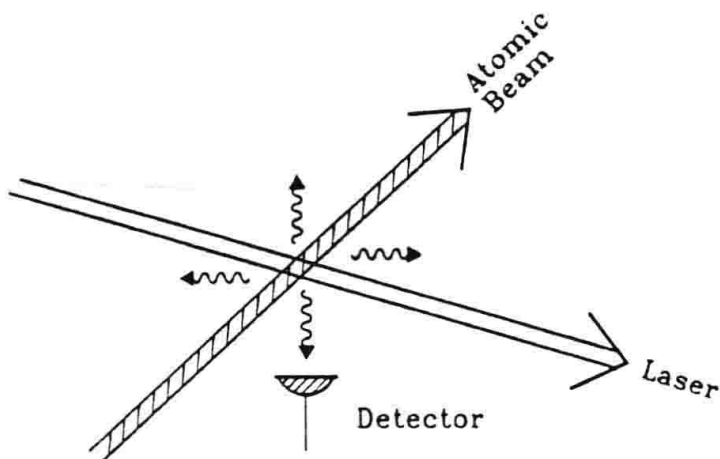


Fig. 10.1. Diagram showing the interaction between an atomic beam and a laser generating resonance fluorescence

When the light intensity is very weak and the atom is initially in the ground state $|b\rangle$, it absorbs and scatters a single photon, whose frequency is identical to the laser frequency ω_L , in other words

$$S(\omega) = S_0 \delta(\omega - \omega_L), \quad (10.1)$$

which is just Rayleigh scattering. In practice, however, the laser is not perfectly monochromatic, so that the scattered spectrum will have a narrow but finite (non-zero) linewidth.

Now, if we increase the laser power, the sidebands that appear in the spectrum can be understood intuitively, using the dressed picture description of the atom-field interaction, as we did in Chap. 8. In the resonant case, we saw that

$$E_{1n} = \hbar \left(n + \frac{1}{2} \right) + \hbar g \sqrt{n+1}, \quad (10.2)$$

$$E_{2n} = \hbar \left(n + \frac{1}{2} \right) - \hbar g \sqrt{n+1}.$$

thus the energy separation between the two levels is

$$R_n(\delta=0) = 2g\sqrt{n+1}. \quad (10.3)$$

This is described in the Fig. 10.2. As we can see from the dressed level picture, besides the transition at the laser frequency ω_L , it is also possible to have transitions at $\omega = \omega_L \pm R_n$, which correspond to the two sidebands. The details of the heights and widths of the peaks requires a full quantum theory, including atomic losses.

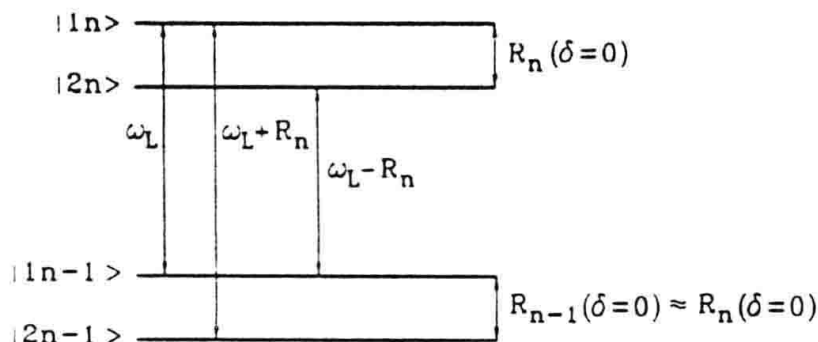


Fig. 10.2. Energy diagram showing the origin of the three frequencies in resonance fluorescence, corresponding to the central peak and the two sidebands

10.2 Heisenberg's Equations

We begin with the Hamiltonian [10.4]

$$H = H_A + H_r - e\mathbf{r} \cdot \mathbf{E}, \quad (10.4)$$

describing the interaction of the radiation field with a single-electron atom. If we consider many modes for the field, we can generalize the Jaynes-Cummings model, described in Chap. 8, as

$$H = H_r + \frac{\hbar\omega_{ab}}{2}\sigma_z - i\hbar \sum_{\mathbf{k},\lambda} g_{\mathbf{k},\lambda}(\sigma_+ + \sigma_-)(a_{\mathbf{k},\lambda} - a_{\mathbf{k},\lambda}^\dagger), \quad (10.5)$$

where H_r is the free multimode radiation energy, and the interaction terms are now slightly different, since we are taking travelling waves rather than standing waves. Thus we use the quantized field \mathbf{E} described in Chap. 3. Also, \mathbf{k} is the wavevector and λ the polarization, and

$$g_{\mathbf{k},\lambda} \equiv \sqrt{\frac{\omega_{\mathbf{k}}}{2\hbar\varepsilon_0 v}} \mathbf{e}_r \cdot \mathbf{e}_{\mathbf{k},\lambda}, \quad (10.6)$$

with

$$[\sigma_+, \sigma_-] = \sigma_z, \quad (10.7)$$

$$[\sigma_z, \sigma_{\pm}] = \pm 2\sigma_{\pm}. \quad (10.8)$$

Also, one has

$$[a_{\mathbf{k},\lambda}, a_{\mathbf{k}',\lambda'}^\dagger] = \delta_{\mathbf{k},\mathbf{k}'}^{(3)} \delta_{\lambda,\lambda'}. \quad (10.9)$$

The Heisenberg equations of motion for the operators are

$$\dot{a}_{\mathbf{k},\lambda} = -i\omega_{\mathbf{k}} a_{\mathbf{k},\lambda} + g_{\mathbf{k},\lambda}(\sigma_+ + \sigma_-), \quad (10.10)$$

$$\dot{\sigma}_- = -i\omega_{ab}\sigma_- + \sum_{\mathbf{k},\lambda} g_{\mathbf{k},\lambda} \sigma_z (a_{\mathbf{k},\lambda} - a_{\mathbf{k},\lambda}^\dagger), \quad (10.11)$$

$$\dot{\sigma}_z = 2 \sum_{\mathbf{k},\lambda} g_{\mathbf{k},\lambda} (\sigma_- - \sigma_+) (a_{\mathbf{k},\lambda} - a_{\mathbf{k},\lambda}^\dagger). \quad (10.12)$$

Both $a_{\mathbf{k},\lambda}$ and σ_- have basically a positive frequency temporal dependence and σ_z varies slowly with time. Thus making use of the rotating-wave approximation, we can neglect the σ_+ and $a_{\mathbf{k},\lambda}^\dagger$ terms from the first two equations respectively and the counter-rotating terms $\sigma_- a_{\mathbf{k},\lambda}$ and $\sigma_+ a_{\mathbf{k},\lambda}^\dagger$ from the third one, writing a simplified version of (10.10), (10.11), (10.12) as

$$\dot{a}_{\mathbf{k},\lambda} = -i\omega_{\mathbf{k}} a_{\mathbf{k},\lambda} + g_{\mathbf{k},\lambda} \sigma_-, \quad (10.13)$$

$$\dot{\sigma}_- = -i\omega_{ab}\sigma_- + \sum_{\mathbf{k},\lambda} g_{\mathbf{k},\lambda} \sigma_z (a_{\mathbf{k},\lambda}), \quad (10.14)$$

$$\dot{\sigma}_z = -2 \sum_{\mathbf{k},\lambda} g_{\mathbf{k},\lambda} (\sigma_- a_{\mathbf{k},\lambda}^\dagger + \sigma_+ a_{\mathbf{k},\lambda}). \quad (10.15)$$

We can rewrite the last two equations as

$$\dot{\sigma}_- = -i\omega_{ab}\sigma_- - \frac{i}{\hbar} \mathbf{d} \cdot \sigma_z \mathbf{E}^+(t), \quad (10.16)$$

$$\dot{\sigma}_z = -\frac{2i}{\hbar} \mathbf{d} \cdot [\sigma_- \mathbf{E}^-(t) - \sigma_+ \mathbf{E}^+(t)], \quad (10.17)$$

with

$$\mathbf{E}^+(t) = i \sum_{\mathbf{k}, \lambda} \sqrt{\frac{\hbar \omega_{\mathbf{k}}}{2 \varepsilon_0 v}} a_{\mathbf{k}, \lambda}(t) \mathbf{e}_{\mathbf{k}, \lambda}, \quad d = e r_{ab}. \quad (10.18)$$

Integrating (10.13), we get

$$\begin{aligned} a_{\mathbf{k}, \lambda}(t) &= a_{\mathbf{k}, \lambda}(0) \exp(-i \omega_{\mathbf{k}} t) \\ &\quad + g_{\mathbf{k}, \lambda} \int_0^t dt_1 \sigma_-(t_1) \exp[i \omega_{\mathbf{k}}(t_1 - t)]. \end{aligned} \quad (10.19)$$

Thus, replacing the above result in (10.18), we get

$$\mathbf{E}^+(t) = \mathbf{E}_0^+(t) + \mathbf{E}_{RR}^+(t), \quad (10.20)$$

where

$$\mathbf{E}_0^+(t) = i \sum_{\mathbf{k}, \lambda} \sqrt{\frac{\hbar \omega_{\mathbf{k}}}{2 \varepsilon_0 v}} a_{\mathbf{k}, \lambda}(0) \exp(-i \omega_{\mathbf{k}} t) \mathbf{e}_{\mathbf{k}, \lambda}, \quad (10.21)$$

$$\mathbf{E}_{RR}^+(t) = i \sum_{\mathbf{k}, \lambda} \sqrt{\frac{\hbar \omega_{\mathbf{k}}}{2 \varepsilon_0 v}} g_{\mathbf{k}, \lambda} \int_0^t dt_1 \sigma_-(t_1) \exp[i \omega_{\mathbf{k}}(t_1 - t)] \mathbf{e}_{\mathbf{k}, \lambda}. \quad (10.22)$$

The first term $\mathbf{E}_0^+(t)$ is the solution of the homogeneous Maxwell equation and corresponds to the field at the position of the atom as if the atom were not there. On the other hand, the second term $\mathbf{E}_{RR}^+(t)$ represents the influence of the atom or, in other words, the radiation reaction field of the electric point dipole.

Substituting (10.21), (10.22) into (10.20), we get

$$\begin{aligned} \mathbf{E}^+(t) &= i \sum_{\mathbf{k}, \lambda} \sqrt{\frac{\hbar \omega_{\mathbf{k}}}{2 \varepsilon_0 v}} a_{\mathbf{k}, \lambda}(0) \exp(-i \omega_{\mathbf{k}} t) \mathbf{e}_{\mathbf{k}, \lambda} \\ &\quad + i \sum_{\mathbf{k}, \lambda} \sqrt{\frac{\hbar \omega_{\mathbf{k}}}{2 \varepsilon_0 v}} g_{\mathbf{k}, \lambda} \int_0^t dt_1 \sigma_-(t_1) \exp[i \omega_{\mathbf{k}}(t_1 - t)] \mathbf{e}_{\mathbf{k}, \lambda}, \end{aligned} \quad (10.23)$$

but, using (3.36), that is, changing the sum into an integral with the corresponding density of modes

$$\sum_{\mathbf{k}, \lambda} \rightarrow \sum_{\lambda=1,2} \int dk k^2 \int \sin \theta d\theta \int d\varphi \frac{v}{(2\pi)^3}, \quad (10.24)$$

we can write

$$\begin{aligned} (\mathbf{E}_{RR}^+(t))_z &= i \sum_{\mathbf{k}, \lambda} \frac{\omega_{\mathbf{k}}}{2 \varepsilon_0 v} (\mathbf{d} \cdot \mathbf{e}_{\mathbf{k}, \lambda}) \mathbf{e}_{\mathbf{k}, \lambda} \int_0^t dt_1 \sigma_-(t_1) \exp[i \omega_{\mathbf{k}}(t_1 - t)] \\ &= 2i \int dk k^2 \int d\varphi \frac{\omega_{\mathbf{k}}}{2 \varepsilon_0 v} \frac{v}{(2\pi)^3} |\mathbf{d}| \int \cos^2 \theta \sin \theta d\theta \\ &\quad \times \int_0^t dt_1 \sigma_-(t_1) \exp[i \omega_{\mathbf{k}}(t_1 - t)], \end{aligned} \quad (10.25)$$

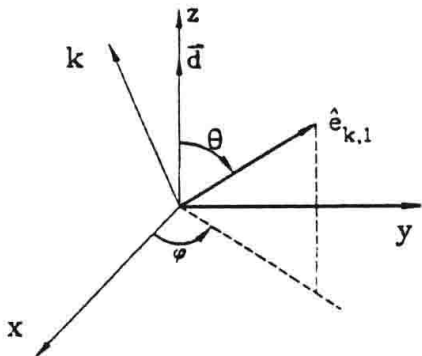


Fig. 10.3. The atomic dipole and k -vector of the electric field in polar coordinates

where we chose the dipole moment along the z -axis, so that $\mathbf{d} \cdot \mathbf{e}_{k,\lambda} = |\mathbf{d}| \cos \theta$, as shown in Fig. 10.3.

If we take the lowest-order approximation for $\sigma_-(t)$ and perform the θ integral, we get

$$\begin{aligned} [\mathbf{E}_{RR}^+(t)]_z &= \frac{2i|\mathbf{d}|\sigma_-(0)\exp(-i\omega_{ab}t)}{3(2\pi)^2\varepsilon_0 c^3} \\ &\times \int d\omega \omega^3 \int dt_1 \exp i(\omega - \omega_{ab})(t_1 - t). \end{aligned} \quad (10.26)$$

We now calculate the above time integral, with the change of variable $-\tau = t_1 - t$:

$$\begin{aligned} &\int dt_1 \exp [i(\omega - \omega_{ab})(t_1 - t)] \\ &= \int_0^t d\tau \exp [i(\omega - \omega_{ab})\tau] \xrightarrow[t \rightarrow \infty]{} \pi\delta(\omega - \omega_{ab}). \end{aligned} \quad (10.27)$$

The final result for the $[\mathbf{E}_{RR}^+(t)]_z$ field is

$$[\mathbf{E}_{RR}^+(t)]_z = \frac{1}{4\pi\varepsilon_0} \frac{2i|\mathbf{d}|\sigma_-(0)\omega_{ab}^3}{3c^3} \sigma_-(t), \quad (10.28)$$

(in CGS units $1/4\pi\varepsilon_0 = 1$), and the differential equations for the Heisenberg operators now become

$$\dot{\sigma}_- = -i(\omega_{ab} - i\beta)\sigma_- - \frac{i}{\hbar}\mathbf{d} \cdot \sigma_z \mathbf{E}_0^+(t), \quad (10.29)$$

$$\dot{\sigma}_z = -2\beta(1 + \sigma_z) - \frac{2i}{\hbar}\mathbf{d} \cdot [\sigma_- \mathbf{E}_0^-(t) - \sigma_+ \mathbf{E}_0^+(t)], \quad (10.30)$$

with

$$\beta \equiv \frac{1}{4\pi\varepsilon_0} \frac{2|\mathbf{d}|^2\omega_{ab}^3}{3\hbar c^3}. \quad (10.31)$$

10.3 Spectral Density and the Wiener–Khinchine Theorem

If one has a random process $y(t)$, an interesting characteristic of this process is its spectrum. We may define a Fourier transform

$$y(t) = \int_{-\infty}^{\infty} \tilde{y}(\omega) \exp(-i\omega t) d\omega, \quad (10.32)$$

which, in principle, can be inverted as

$$\tilde{y}(\omega) = \frac{1}{2\pi} \int_{-\infty}^{\infty} y(t) \exp(i\omega t) dt. \quad (10.33)$$

We also define a spectral density or just plain spectrum, as the expectation value of $|\tilde{y}(\omega)|^2$:

$$S(\omega) = \langle |\tilde{y}(\omega)|^2 \rangle, \quad (10.34)$$

whose physical meaning is the fluctuation strength associated with a definite frequency component.

However, a word of caution: If one is dealing with a stationary process, invariant under a translation of the time origin, then $y(t)$ does not go to zero for $t \rightarrow \pm\infty$, and therefore this function is not square integrable and the Fourier transform does not exist in the usual sense. We will consider them as symbolic formulas, which can be given rigorous mathematical meaning in an enlarged functional space.

However, Wiener observed that the functions

$$\Gamma(\tau) = \lim_{T \rightarrow \infty} \frac{1}{2T} \int_{-T}^{T} y^*(t)y(t+\tau) dt, \quad (10.35)$$

and

$$\sigma(\omega) = \frac{1}{2\pi} \int_{-\infty}^{\infty} \Gamma(\tau) \frac{\exp(i\omega\tau) - 1}{i\tau} d\tau \quad (10.36)$$

do exist.

One can define an alternative spectrum as

$$S(\omega) = \frac{d\sigma(\omega)}{d\omega} = \frac{1}{2\pi} \int_{-\infty}^{\infty} \exp(i\omega\tau) \Gamma(\tau) d\tau. \quad (10.37)$$

One can also invert the above formula, to get

$$\Gamma(\tau) = \int \exp(-i\omega\tau) S(\omega) d\omega. \quad (10.38)$$

In order to understand the relation between the two definitions of the spectra (10.34) and (10.37), we calculate the ensemble average of $\tilde{y}^*(\omega) \tilde{y}(\omega')$:

$$\langle \tilde{y}^*(\omega) \tilde{y}(\omega') \rangle = \frac{1}{(2\pi)^2} \int \int_{-\infty}^{\infty} \langle y^*(t) y(t') \rangle \exp i(\omega' t' - \omega t) dt dt', \quad (10.39)$$

and since $y(t)$ is stationary and ergodic (the time and ensemble averages are equal)

$$\langle y^*(t)y(t') \rangle = \Gamma(t' - t), \quad (10.40)$$

where Γ is the two-time correlation function.

Substituting (10.40) into (10.39), and changing the variable: $t' - t = \tau$, we get

$$\langle \tilde{y}^*(\omega) \tilde{y}(\omega') \rangle = \frac{1}{(2\pi)^2} \int_{-\infty}^{\infty} \exp(it(\omega' - \omega)) dt \int_{-\infty}^{\infty} d\tau \Gamma(\tau) \exp(i\omega'\tau), \quad (10.41)$$

which implies

$$\langle \tilde{y}^*(\omega) \tilde{y}(\omega') \rangle = \tilde{\Gamma}(\omega) \delta(\omega - \omega'), \quad (10.42)$$

with

$$\tilde{\Gamma}(\omega) = \frac{1}{(2\pi)} \int_{-\infty}^{\infty} d\tau \Gamma(\tau) \exp(i\omega\tau). \quad (10.43)$$

We notice that (10.42) tells us that the generalized Fourier components are uncorrelated.

On the other hand, (10.43) gives us a measure of the strength of the fluctuations, at a given frequency. Thus we may identify it with the spectrum

$$\tilde{\Gamma}(\omega) = S(\omega). \quad (10.44)$$

We also notice that the singularity in (10.42) can be easily removed by integrating, over a small range containing ω , in ω' :

$$S(\omega) = \lim_{\Delta\omega \rightarrow 0} \int_{\omega - \frac{\Delta\omega}{2}}^{\omega + \frac{\Delta\omega}{2}} d\omega' \langle \tilde{y}^*(\omega) \tilde{y}(\omega') \rangle, \quad (10.45)$$

which is equivalent to (10.34).

The pair of formulas (10.37) and (10.38) is known as the Wiener–Khintchine theorem, which tells us that for a stationary random process, the autocorrelation function and the power spectrum are a Fourier pair. If we apply these ideas to the correlation of a quantum field, we get

$$S(\omega) = \frac{1}{2\pi} \int_{-\infty}^{\infty} \exp(i\omega\tau) \langle E^-(t) E^+(t + \tau) \rangle_{ss} d\tau. \quad (10.46)$$

10.4 Emission Spectra from Strongly Driven Two-Level Atoms

The power delivered to the field can be expressed as the energy per unit time

$$\begin{aligned}
 P(t) &= \frac{d \text{ Energy}}{dt} \\
 &= \frac{d}{dt} \sum_{\mathbf{k}, \lambda} \hbar \omega_{\mathbf{k}} \langle a_{\mathbf{k}, \lambda}^{\dagger}(t) a_{\mathbf{k}, \lambda}(t) \rangle \\
 &= \sum_{\mathbf{k}, \lambda} g_{\mathbf{k}, \lambda} \hbar \omega_{\mathbf{k}} \left[\langle a_{\mathbf{k}, \lambda}^{\dagger}(0) \sigma_{-}(t) \rangle \exp(i\omega_{\mathbf{k}} t) + \langle \sigma_{+}(t) a_{\mathbf{k}, \lambda}(0) \rangle \exp(-i\omega_{\mathbf{k}} t) \right] \\
 &\quad + 2 \operatorname{Re} \left\{ \sum_{\mathbf{k}, \lambda} g_{\mathbf{k}, \lambda}^2 \hbar \omega_{\mathbf{k}} \int_0^t dt_1 \langle \sigma_{+}(t_1) \sigma_{-}(t) \rangle \exp[-i\omega_{\mathbf{k}}(t_1 - t)] \right\}.
 \end{aligned} \tag{10.47}$$

The first two terms in the above expression refer to the change in the energy of the field due to stimulated energy and absorption. On the other hand, the last term is the radiation scattered out of the incident beam as resonance fluorescence.

We shall concentrate in this last term:

$$\begin{aligned}
 &2 \operatorname{Re} \left\{ \sum_{\mathbf{k}, \lambda} \frac{\omega_{\mathbf{k}} \cos^2 \theta | \mathbf{d} |^2}{2v\varepsilon_0} \int_0^t dt_1 \langle \sigma_{+}(t_1) \sigma_{-}(t) \rangle \exp[i\omega_{\mathbf{k}}(t - t_1)] \right\} \\
 &= \frac{| \mathbf{d} |^2}{3\pi^2 c^3 \varepsilon_0} \operatorname{Re} \int \omega^4 d\omega \int_0^t dt_1 \langle \sigma_{+}(t_1) \sigma_{-}(t) \rangle \exp[i\omega(t - t_1)],
 \end{aligned} \tag{10.48}$$

where, in the last term, we took the limit $v \rightarrow \infty$. Defining

$$S_{\pm}(t) \equiv \sigma_{\pm}(t) \exp(\mp i\omega_L t), \tag{10.49}$$

we can write

$$\begin{aligned}
 P_s(t) &= \frac{1}{4\pi\varepsilon_0} \frac{4 | \mathbf{d} |^2}{3\pi c^3} \\
 &\times \operatorname{Re} \left\{ \int_0^{\infty} \omega^4 d\omega \int_0^t dt_1 \langle S_{+}(t_1) S_{-}(t) \rangle \exp[i(\omega - \omega_L)(t - t_1)] \right\},
 \end{aligned}$$

and assuming that the spectrum will be concentrated near $\omega \cong \omega_L$, we approximate

$$\begin{aligned}
 P_s(\infty) &= \frac{1}{4\pi\varepsilon_0} \frac{4 | \mathbf{d} |^2 \omega^4}{3\pi c^3} \\
 &\times \operatorname{Re} \left\{ \int_0^{\infty} d\omega \int_0^{\infty} d\tau \langle S_{+}(t_0) S_{-}(t_0 + \tau) \rangle \exp[i(\omega - \omega_L)\tau] \right\}.
 \end{aligned} \tag{10.50}$$

In the last step, we also took the stationary limit $t \rightarrow \infty$, and $\tau \equiv t - t_0$, so that the correlation function $\langle S_{+}(t_0) S_{-}(t_0 + \tau) \rangle$ only depends on τ , where t_0 is a time much longer than the radiative lifetime.

The power spectrum of the resonance fluorescence is defined as

$$\mathcal{S}(\omega) = 2 \operatorname{Re} \left\{ \int_0^\infty d\tau \langle S_+(t_0) S_-(t_0 + \tau) \rangle' \exp[i(\omega - \omega_L)\tau] \right\}. \quad (10.51)$$

As we can see, basically we have to calculate the atomic correlation function [10.4]

$$g(\tau) = \langle S_+(t_0) S_-(t_0 + \tau) \rangle. \quad (10.52)$$

On the other hand, we can write the Heisenberg equations for the atomic operators, using the above definition of $S_-(t)$, and assuming, for simplicity, that the incident field is linearly polarized parallel to the dipole d :

$$\dot{S}_-(t) = -i(\omega_{ab} - \omega_L - i\beta)S_-(t) - \frac{id}{\hbar}\sigma_z(t)E_0^+(t)\exp(i\omega_L t), \quad (10.53)$$

$$\begin{aligned} \dot{\sigma}_z(t) &= -2\beta[1 + \langle \sigma_z(t) \rangle] \\ &\quad - \frac{2i}{\hbar}d[S_-(t)E_0^-(t)\exp(-i\omega_L t) - S_+(t)E_0^+(t)\exp(i\omega_L t)]. \end{aligned} \quad (10.54)$$

Making use of (10.55), we can find a differential equation for $g(\tau)$. It is simple to verify that

$$\frac{dg(\tau)}{d\tau} = -i((\omega_{ab} - \omega_L - i\beta))g(\tau) + \frac{dE_0}{2\hbar}\langle S_-(t_0)\sigma_z(t_0 + \tau) \rangle, \quad (10.55)$$

where we took initially a coherent state for the driving field, so

$$E_0^+(t)|\psi\rangle = \frac{i}{2}E_0\exp(-i\omega_L t)|\psi\rangle. \quad (10.56)$$

In order to have a closed set of equations, we further define

$$h(\tau) = \langle S_+(t_0)\sigma_z(t_0 + \tau) \rangle, \quad (10.57)$$

and

$$f(\tau) = \langle S_+(t_0)S_+(t_0 + \tau) \rangle. \quad (10.58)$$

The equations satisfied by these three functions g, h, f are [10.4]

$$\left[\frac{d}{d\tau} + i(\Delta - i\beta) \right] g(\tau) = \frac{\Omega}{2} \quad (10.59)$$

$$\left(\frac{d}{d\tau} + 2\beta \right) h(\tau) = -2\beta\langle S_+(t_0) \rangle - \Omega g(\tau) - \Omega f(\tau), \quad (10.60)$$

$$\left[\frac{d}{d\tau} - i(\Delta + i\beta) \right] f(\tau) = \frac{\Omega}{2} \quad (10.61)$$

with

$$\Delta = \omega_{ab} - \omega_L, \quad (10.62)$$

$$\Omega = \frac{dE_0}{\hbar}. \quad (10.63)$$

In the derivation of the above equations, we made use of the approximation [10.4]

$$[S_+(t_0), E_0^-(t + \tau)] \approx 0. \quad (10.64)$$

We have to solve the above equations, with the following initial conditions

$$g(0) = \langle S_+(t_0)S_-(t_0) \rangle = \frac{1}{2} [1 + \langle \sigma_z(t_0) \rangle], \quad (10.65)$$

$$h(0) = \langle S_+(t_0)\sigma_z(t_0) \rangle = -\langle S_+(t_0) \rangle, \quad (10.66)$$

$$f(0) = \langle S_+(t_0)S_+(t_0) \rangle = 0, \quad (10.67)$$

where we have used the properties of the Pauli spin matrices.

The initial values $\langle \sigma_z(t_0) \rangle$ and $\langle S_+(t_0) \rangle$ can be easily obtained from the steady state solutions of the equations

$$\dot{\langle S_-(t) \rangle} = -i(\Delta - i\beta)\langle S_-(t) \rangle + \frac{i\Omega}{2}\langle \sigma_z(t) \rangle, \quad (10.68)$$

$$\dot{\langle \sigma_z(t) \rangle} = -2\beta(1 + \langle \sigma_z(t) \rangle) - \Omega(\langle S_+(t) \rangle + \langle S_-(t) \rangle), \quad (10.69)$$

obtained by taking the expectation values of (10.53) and (10.55). Equations (10.68), (10.69) are usually referred to as the optical Bloch equations.

By setting the time derivatives to zero, we readily get

$$g(0) = \frac{\Omega^2}{(4\Delta^2 + 4\beta^2 + 2\Omega^2)}, \quad (10.70)$$

$$h(0) = \frac{\Omega(\beta + i\Delta)}{(2\Delta^2 + 2\beta^2 + \Omega^2)}. \quad (10.71)$$

In the particular case of high intensity ($\Omega \gg \beta$) and zero detuning, we get

$$g(\tau) = \frac{1}{2} \left[\exp(-\beta\tau) + \exp\left(-\frac{3\beta\tau}{2}\right) \cos(\Omega\tau) \right] + \left(\frac{\beta}{\Omega}\right)^2, \quad (10.72)$$

and for the spectrum:

$$\begin{aligned} S(\omega) &= 2\pi \left(\frac{\beta}{\Omega}\right)^2 \delta(\omega - \omega_L) + \frac{\beta/2}{(\omega - \omega_L)^2 + \beta^2} \\ &\quad + \frac{3\beta/8}{(\omega - \omega_L - \Omega)^2 + 9\beta^2/4} + \frac{3\beta/8}{(\omega - \omega_L + \Omega)^2 + 9\beta^2/4}. \end{aligned} \quad (10.73)$$

These results were obtained by Burshtein [10.6], Newstein [10.5] and Mollow [10.2]. The more general case, for any Δ and Ω , can also be obtained either analytically or numerically. In Fig. 10.4 we show the resonance fluorescence

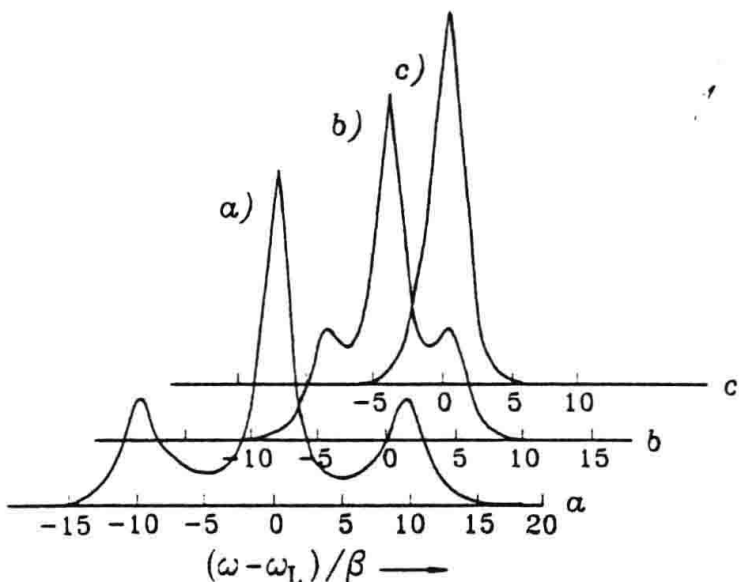


Fig. 10.4. Resonance fluorescence spectrum for the following parameters: $\Omega = 10\beta$ (a); $\Omega = 5\beta$ (b); $\Omega = 2\beta$ (c); in all cases we took $\Delta = 0$. (after [10.4])

spectrum, omitting the δ -component for (a) $\Omega = 10\beta$, (b) $\Omega = 5\beta$, (c) $\Omega = 2\beta$. In all cases we took $\Delta = 0$. It is quite striking how the sidebands appear as we increase the laser intensity at the positions $\omega_L \pm \Omega$, with their heights in the ratio 3:1, with respect to the central peak.

Experimentally, the three-peaked spectrum was observed by Schuda *et al.* [10.8], Walther *et al.* [10.9], Ezekiel *et al.* [10.7], and good agreement between theory and experiment was found.

10.5 Intensity Correlations

As we have already seen, from (10.28), the field radiated by a two-level atom is, to a good approximation, proportional to the atomic lowering operator at a retarded time

$$E^+(\mathbf{r}, t) \sim \sigma \left(t - \frac{r}{c} \right), \quad (10.74)$$

and, if for the moment, we ignore the vector character of the field, the spectrum is related to the first order correlation function:

$$G^{(1)}(\mathbf{r}, t; \mathbf{r}, t + \tau) = \langle E^-(\mathbf{r}, t) E^+(\mathbf{r}, t + \tau) \rangle. \quad (10.75)$$

Now, we may consider the intensity measurements registered by photodetectors at two different space-time points.

In Chap. 6, we defined the joint probability density

$$\begin{aligned} p(\mathbf{r}, t_1; \mathbf{r}, t_2) &\propto G^{(2)}(\mathbf{r}_1, t_1; \mathbf{r}_2, t_2) \\ &= \langle E^-(\mathbf{r}_1, t_1) E^+(\mathbf{r}_2, t_2) E^+(\mathbf{r}_1, t_1) E^-(\mathbf{r}_2, t_2) \rangle. \end{aligned} \quad (10.76)$$

A classical experiment dealing with this type of correlation is the Brown-Twiss experiment [10.10]. We show the experimental setup in Fig. 10.5.

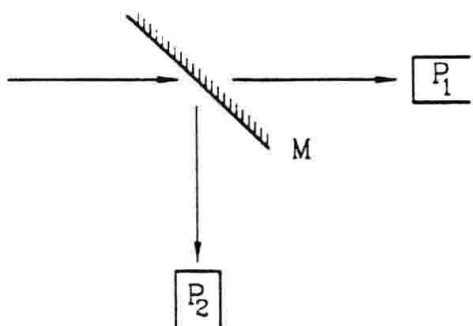


Fig. 10.5. Experimental setup to measure intensity correlations

A half-silvered mirror divides the incident beam into two identical beams, whose intensities are recorded in the photodetectors P_1 and P_2 . One takes the product of $I_1(t)$ and $I_2(t + \tau)$ and averages over a time t , keeping the value of τ fixed. Then one takes many different values for τ .

If the two beams are independent, this average should be independent of τ . However, the observation of a small bump in the experimental curve, as shown in Fig. 10.6, indicates that the photons have a distinct tendency to arrive in pairs, or photon bunching effect.

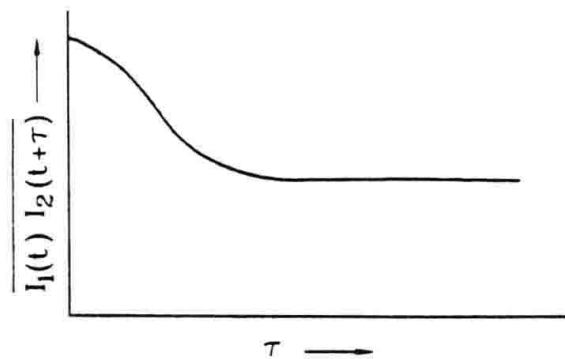


Fig. 10.6. Photon bunching effect near $\tau = 0$

One could regard the effect as a result of the boson nature of the photons. However, this is not quite true. In Chap. 6 we discussed the negative Brown-Twiss effect or photon antibunching effect displaying an anticorrelation for $\tau = 0$. Carmichael and Walls [10.11] were the first to predict that photon antibunching should be an observable effect in resonance fluorescence. In order to study this effect, we consider the joint probability density of photodetection at the same point but at two different times:

$$p(\mathbf{r}, t; \mathbf{r}, t + \tau) = p(\mathbf{r}, t, t + \tau) \propto G^{(2)}(\mathbf{r}, t; \mathbf{r}, t + \tau). \quad (10.77)$$

Once more, in the stationary regime $p(\mathbf{r}, t; \mathbf{r}, t + \tau)$ is independent of t , and is proportional the second-order atomic dipole correlation function

$$\begin{aligned} g^{(2)}(\tau) &= \langle \sigma_+(t_0)\sigma_+(t_0 + \tau)\sigma_-(t_0 + \tau)\sigma_-(t_0) \rangle, \\ &= \langle S_+(t_0)S_+(t_0 + \tau)S_-(t_0 + \tau)S_-(t_0) \rangle. \end{aligned} \quad (10.78)$$

On the other hand, from the properties of the Pauli spin matrices

$$S_+(t_0 + \tau)S_-(t_0 + \tau) = \sigma_+(t_0 + \tau)\sigma_-(t_0 + \tau) = \frac{1}{2} + \sigma_z(t_0 + \tau), \quad (10.79)$$

so we can write

$$\begin{aligned} g^{(2)}(\tau) &= \frac{1}{2}\langle S_+(t_0)S_-(t_0) \rangle + \frac{1}{2}\langle S_+(t_0)\sigma_z(t_0 + \tau)S_-(t_0) \rangle. \\ &= \frac{1}{2}g(0) + \frac{1}{2}G(\tau), \end{aligned} \quad (10.80)$$

where

$$G(\tau) \equiv \langle S_+(t_0)\sigma_z(t_0 + \tau)S_-(t_0) \rangle. \quad (10.81)$$

We now proceed in a similar way to the last section, namely, we calculate differential equations for $G(\tau)$ and other correlation functions. Define

$$F(\tau) \equiv \langle S_+(t_0)S_+(t_0 + \tau)S_-(t_0) \rangle, \quad (10.82)$$

$$H(\tau) \equiv \langle S_+(t_0)S_-(t_0 + \tau)S_-(t_0) \rangle. \quad (10.83)$$

Using the Heisenberg equations for the atomic operator, we readily find three differential equations for G, F, H

$$\frac{dG(\tau)}{d\tau} = -2\beta g(0) - 2\beta G(\tau) - \Omega(F(\tau) + H(\tau)), \quad (10.84)$$

$$\frac{dF(\tau)}{d\tau} = i(\Delta + i\beta)F(\tau) + \frac{\Omega}{2}G(\tau), \quad (10.85)$$

$$\frac{dH(\tau)}{d\tau} = -i(\Delta - i\beta)F(\tau) + \frac{\Omega}{2}G(\tau), \quad (10.86)$$

with the initial conditions

$$G(0) = \langle S_+(t_0)\sigma_z(t_0)S_-(t_0) \rangle = -\langle S_+(t_0)S_-(t_0) \rangle = -g(0), \quad (10.87)$$

$$F(0) \equiv \langle S_+(t_0)S_+(t_0)S_-(t_0) \rangle = 0, \quad (10.88)$$

$$H(0) \equiv \langle S_+(t_0)S_-(t_0)S_-(t_0) \rangle = 0. \quad (10.89)$$

From (10.80), we immediately notice that

$$g^{(2)}(\tau = 0) = 0, \quad (10.90)$$

thus we see that there is an antibunching effect.

The exact solution, for $\Delta = 0$, is

$$g^{(2)}(\tau) = g(0)^2 \left[1 - \exp\left(-\frac{3\beta\tau}{2}\right) \left(\cos \Omega' \tau + \frac{2\beta}{2\Omega'} \sin \Omega' \tau \right) \right], \quad (10.91)$$

with

$$\Omega' \equiv \sqrt{\Omega^2 - \frac{\beta^2}{4}}. \quad (10.92)$$

The behaviour of

$$\frac{g^{(2)}(\tau)}{g(0)^2} = (g^{(2)}(\tau))_{\text{norm}}, \quad (10.93)$$

is shown in Fig. 10.7, where the solid line corresponds to $\Omega = 5$ and the dotted line to $\Omega = 0.5$. In both cases we took $\beta = 0.5$.

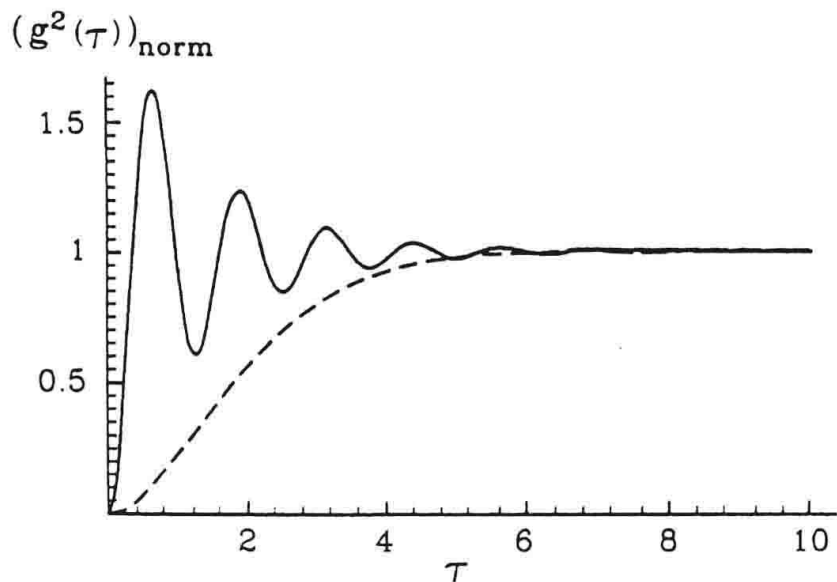


Fig. 10.7. Second-order intensity correlation $(g^{(2)}(\tau))_{\text{norm}}$ versus time, for $\Omega = 5.0$ (solid line), $\Omega = 0.5$ (dashed line). In both cases, $\beta = 0.5$

On the other hand, $[g^{(2)}(\tau)]_{\text{norm}}$ can also be expressed as a photon number correlation:

$$[g^{(2)}(\tau)]_{\text{norm}} = \frac{\langle : n(t)n(t+\tau) :\rangle}{\langle n(t) \rangle^2}. \quad (10.94)$$

For chaotic light, $[g^{(2)}(\tau)]_{\text{norm}} = 2$, that is the correlation is twice the random background correlation, showing the tendency of photons to bunch together.

On the other hand, as we mentioned before, in resonance fluorescence and for $\tau = 0$, antibunching occurs. The physical interpretation of this effect is quite simple. Right after the detection of the first photon the atom is in the lower state and it requires a finite (non-zero) amount of time to get back to the excited state and be able to emit the second photon.

Experiments verifying the antibunching effect in resonance fluorescence were performed by Kimble *et al.* [10.12] and Leuchs *et al.* [10.13].

Lately, the influence of quantum interference on the resonance fluorescent spectrum was studied, when the system is in contact with colored or white noise [10.14, 10.15, 10.16, 10.17, 10.18, 10.19, 10.20, 10.21, 10.22].

Problems

- 10.1. Prove (10.72).
- 10.2. Prove (10.73).
- 10.3. Prove (10.91) for $\Delta = 0$.

11. Quantum Laser Theory. Master Equation Approach

For large fields interacting with atoms, the semiclassical description, that is, considering the atoms quantum mechanically and the field classically, seems to be adequate to describe the most classical features, such as threshold, steady state intensity, etc. However, whenever quantum fluctuations are to be considered, such as in determining the laser linewidth and photon statistics, we require the fully quantized field. The Hamiltonian of a two-level atom interacting with a single-mode (cavity mode) of the field is described by the Jaynes-Cummings Hamiltonian

$$H = \frac{\hbar\omega_{ab}}{2}\sigma_z + \hbar\omega a^\dagger a + \hbar g(\sigma^+ a + \sigma^- a^\dagger), \quad (11.1)$$

within the dipole and rotating-wave approximations. It is convenient to split the Hamiltonian into two terms

$$H = H_1 + H_2, \quad (11.2)$$

where

$$\begin{aligned} H_1 &= \frac{\hbar\omega}{2}\sigma_z + \hbar\omega a^\dagger a, \\ H_2 &= \hbar\frac{\delta}{2}\sigma_z + \hbar g(\sigma^+ a + \sigma^- a^\dagger), \end{aligned} \quad (11.3)$$

with

$$\delta \equiv \omega_{ab} - \omega. \quad (11.4)$$

It is simple to see that $[H_1, H_2] = 0$, and when we go to the interaction picture, the dynamics is governed by $H_2 \equiv V$. The time evolution operator can be exactly computed as

$$\begin{aligned} U(\tau) &= \exp\left(-i\frac{V\tau}{\hbar}\right) = \sum_{n=0}^{\infty} \frac{(-i\tau/\hbar)^n}{n!} V^n \\ &= \sum_{n=0}^{\infty} \frac{(-i\tau)^n}{n!} \begin{bmatrix} \frac{\delta}{2} & ga^\dagger \\ ga^\dagger & -\frac{\delta}{2} \end{bmatrix}^n. \end{aligned} \quad (11.5)$$

It is simple to show that

$$\begin{bmatrix} \frac{\delta}{2} & ga \\ ga^\dagger & -\frac{\delta}{2} \end{bmatrix}^{2m} = \begin{bmatrix} (\varphi + g^2)^m & 0 \\ 0 & (\varphi)^m \end{bmatrix}, \quad (11.6)$$

$$\begin{bmatrix} \frac{\delta}{2} & ga \\ ga^\dagger & -\frac{\delta}{2} \end{bmatrix}^{2m+1} = \begin{bmatrix} \frac{\delta}{2}(\varphi + g^2)^m & g(\varphi + g^2)^m a \\ ga^\dagger(\varphi + g^2)^m & -\frac{\delta}{2}(\varphi)^m \end{bmatrix}$$

where $\varphi \equiv g^2 a^\dagger a + (\frac{\delta}{2})^2$. It then follows that

$$U(\tau) = \begin{bmatrix} \cos(\tau\sqrt{\varphi + g^2}) - \frac{i\delta}{2} \frac{\sin(\tau\sqrt{\varphi + g^2})}{\sqrt{\varphi + g^2}} & -ig \frac{\sin(\tau\sqrt{\varphi + g^2})}{\sqrt{\varphi + g^2}} a \\ -iga^\dagger \frac{\sin(\tau\sqrt{\varphi + g^2})}{\sqrt{\varphi + g^2}} & \cos(\tau\sqrt{\varphi}) + \frac{i\delta}{2} \frac{\sin(\tau\sqrt{\varphi})}{\sqrt{\varphi}} \end{bmatrix}. \quad (11.7)$$

If the initial atom-field density operator is $\rho(0)$, then after an interaction time t , it will be given by

$$\rho(\tau) = U(\tau)\rho(0)U^\dagger(\tau) = U(\tau)\rho_f(0) \begin{bmatrix} 1 & 0 \\ 0 & 0 \end{bmatrix} U^\dagger(\tau),$$

assuming that initially the atom is in the upper state which factorizes with the field. By performing the matrix product and tracing over the atom, that is adding up the diagonal elements, we find

$$\begin{aligned} \rho_f(\tau) &= \cos(\lambda\tau)\rho_f(0)\cos(\lambda\tau) + g^2 a^\dagger \left[\frac{\sin(\lambda\tau)}{\lambda} \right] \rho(0) \left[\frac{\sin(\lambda\tau)}{\lambda} \right] a \quad (11.8) \\ &\equiv M(\tau)\rho(0), \end{aligned}$$

where $\lambda \equiv g\sqrt{a^\dagger a + 1}$, and we assumed zero detuning. M is the gain superoperator acting on ρ .

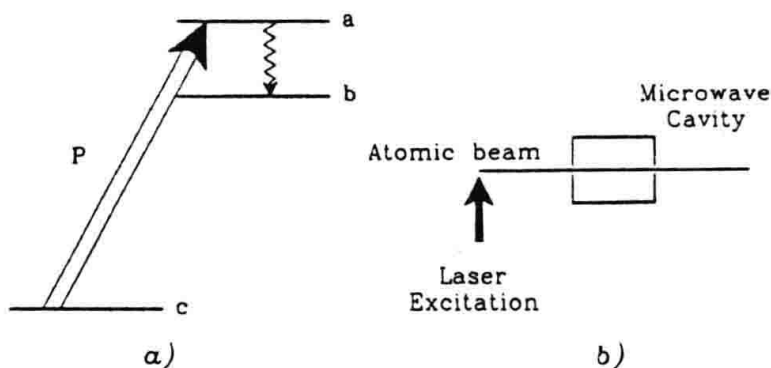


Fig. 11.1. (a) An atom is excited from the level c to the upper level. The lasing transition occurs between the a and b levels. (b) An atomic beam arrives at the excitation region where Rydberg states (micromaser) or excited states (laser) are generated prior to entering the cavity (micromaser) or participating in the laser action (laser)

11.1 Heuristic Discussion of Injection Statistics

We assume that a dense flux of atoms goes through an excitation region, and each atom has a probability p of being excited from the ground state c to the upper level a (see Fig. 11.1). We further assume that the levels a and b are involved in the laser or maser transition, and that the level b remains unpopulated. We also assume that the beam has a regular distribution before arriving at the excitation region, so the number K of the atoms which cross that region, during a time Δt , is given by

$$K = R\Delta t, \quad (11.9)$$

where R is the injection rate and Δt is much larger than the time interval between the arrival of consecutive atoms.

This model may describe a system called a micromaser, in which case one has a beam of highly excited or Rydberg atoms crossing a high-quality microwave cavity, with a couple of energy levels resonant with the microwave field inside the cavity. If we assume that τ is the interaction time of each atom with the cavity field, we may use the same model to describe the excitation process of a laser, in which case τ is related to the atomic lifetime of the lasing levels. In the past, people neglected the effects of pump statistics. However, some recent experiments in micromasers and lasers showed that by controlling the pump noise, one could get a large reduction in photon number fluctuations. The probability for k atoms to be excited during a time Δt is given by

$$P(k, K) = \begin{bmatrix} K \\ k \end{bmatrix} p^k (1-p)^{K-k}. \quad (11.10)$$

The average number of excited atoms and the variance is given by

$$\bar{k} = \sum_{k=0}^{k=K} k P(k, K) = pK = r\Delta t, \quad (11.11)$$

$$\overline{\Delta k^2} = (1-p)\bar{k},$$

with $r \equiv Rp$.

11.2 Master Equation for Generalized Pump Statistics

Let the interaction time between the atom and the field be τ . Also, we assume that the j th atom is “injected” at time t_j . So the field, after interacting with the j th atom, can be written as (we omit the field subindex)

$$\rho(t_j + \tau) = M(\tau)\rho(t_j). \quad (11.12)$$

Now, if k atoms are excited, then

$$\rho^{(k)}(t) = M^k(\tau)\rho(0). \quad (11.13)$$

Of course, if we do not know the exact number of atoms, but only know the number of atoms probabilistically by (11.10), we then have

$$\begin{aligned} \rho(t) &= \sum_{k=0}^K \binom{K}{k} p^k (1-p)^{K-k} M^k(\tau)\rho(0) \\ &= [1 + p(M - 1)]^K \rho(0), \end{aligned} \quad (11.14)$$

with $K = Rt$.

Differentiating (11.14), with respect to time, we get

$$\frac{d\rho(t)}{dt} = \frac{r}{p} \ln [1 + p(M - 1)] \rho(t) + L\rho(t). \quad (11.15)$$

Equation (11.15) is our generalized master equation [11.1], [11.2].

In (11.15) we have added the cavity loss term denoted by $L\rho(t)$. This term can be borrowed from the quantum theory of damping, where the oscillator is our single-mode field interacting with a reservoir, at zero temperature. Thus

$$\begin{aligned} L\rho(t) &= \frac{C}{2}(2a\rho a^\dagger - a^\dagger a\rho - \rho a^\dagger a), \\ C &= \frac{1}{t_{\text{cav}}} = \frac{\omega}{Q}, \end{aligned} \quad (11.16)$$

Q being the cavity quality factor and t_{cav} the photon's lifetime inside the cavity.

If the average photon number is sufficiently large and the distribution narrow, one can expand (11.15) and get

$$\frac{d\rho}{dt} = r(M - 1)\rho(t) - \frac{1}{2}rp(M - 1)^2\rho(t) + L\rho(t). \quad (11.17)$$

If we now use the expression for M given by (11.9), we get

$$\begin{aligned} \frac{d\rho}{dt} &= r(1 + p) \left\{ \cos(\lambda\tau)\rho \cos(\lambda\tau) + g^2 a^\dagger \left[\frac{\sin(\lambda\tau)}{\lambda} \right] \rho \left[\frac{\sin(\lambda\tau)}{\lambda} \right] a \right\} \\ &\quad - r \left(1 + \frac{p}{2} \right) \rho \\ &\quad - \frac{rp}{2} \left\{ \cos^2(\lambda\tau)\rho \cos^2(\lambda\tau) \right. \\ &\quad + g^2 \cos(\lambda\tau)a^\dagger \left[\frac{\sin(\lambda\tau)}{\lambda} \right] \rho \left[\frac{\sin(\lambda\tau)}{\lambda} \right] a \cos(\lambda\tau) \\ &\quad + g^2 a^\dagger \left[\frac{\sin(\lambda\tau)}{\lambda} \right] \cos(\lambda\tau)\rho \cos(\lambda\tau) \left[\frac{\sin(\lambda\tau)}{\lambda} \right] a \\ &\quad \left. + g^4 a^\dagger \left[\frac{\sin(\lambda\tau)}{\lambda} \right] a^\dagger \left[\frac{\sin(\lambda\tau)}{\lambda} \right] \rho \left[\frac{\sin(\lambda\tau)}{\lambda} \right] a \left[\frac{\sin(\lambda\tau)}{\lambda} \right] a \right\} + L\rho. \end{aligned} \quad (11.18)$$

From the above expression, one can calculate ρ_{nn} and $\rho_{n,n+1}$ which will give us the photon statistics and laser linewidth, respectively.

Finally, we notice that the two extreme cases are $p = 0$, while $pR = \text{constant}$, in which case the Bernoulli distribution becomes a Poissonian distribution, corresponding to the random injection case and the usual Scully-Lamb laser theory, while $p = 1$ corresponds to a regular injection of atoms.

The generalized master equation (11.15) was derived under a couple of approximations. First, there is the course graining approximation $\Delta\rho/\Delta t \approx d\rho/dt$, such that during Δt there were many atoms injected into the interaction region, which is normally a good approximation for lasers but could run into problems when dealing with a small photon number, for example in a micromaser. The other approximation is that the loss is independent of the gain which may also lead to erroneous results when $p \neq 0$ [11.3]. This latter assumption is exact in the Poissonian case.

11.3 The Quantum Theory of the Laser. Random Injection ($p = 0$)

In the case of zero detuning, the time evolution operator (11.7) becomes

$$U(\tau) = \begin{bmatrix} \cos g\tau\sqrt{aa^\dagger} & -i \left[\frac{\sin g\tau\sqrt{aa^\dagger}}{\sqrt{aa^\dagger}} \right] a \\ -ia^\dagger \left[\frac{\sin g\tau\sqrt{aa^\dagger}}{\sqrt{aa^\dagger}} \right] & \cos g\tau\sqrt{a^\dagger a} \end{bmatrix}, \quad (11.19)$$

and one can write

$$\begin{aligned} \rho_f(t + \tau) &= \cos(\sqrt{aa^\dagger}\tau)\rho_f(t)\cos(\sqrt{aa^\dagger}\tau) \\ &\quad + a^\dagger \left[\frac{\sin(\sqrt{aa^\dagger}\tau)}{\sqrt{aa^\dagger}} \right] \rho(t) \left[\frac{\sin(\sqrt{aa^\dagger}\tau)}{\sqrt{aa^\dagger}} \right] a. \end{aligned} \quad (11.20)$$

To make a realistic model of a laser, we assume that the atoms have a distribution of time they spend in the cavity. In the case of the two-level atom model, as in this theory, the two levels decay at a rate γ , and the time distribution is

$$P(\tau) = \gamma^{-1} \exp(-\gamma\tau). \quad (11.21)$$

Now, defining again a course time grain $\Delta t \gg \langle \tau \rangle$, we can write

$$\begin{aligned} \left(\frac{d\rho_f}{dt} \right)_{\text{gain}} &\approx \frac{\rho_f(t + \Delta t) - \rho_f(t)}{\Delta t} = r [\rho_f(t + \Delta t) - \rho_f(t)] \\ &= -r\rho_f(t) \\ &\quad + r \int_0^{\Delta t \rightarrow \infty} d\tau \exp(-\gamma\tau) \left[\cos(\sqrt{aa^\dagger}\tau)\rho_f(t)\cos(\sqrt{aa^\dagger}\tau) \right. \\ &\quad \left. + a^\dagger \left[\frac{\sin(\sqrt{aa^\dagger}\tau)}{\sqrt{aa^\dagger}} \right] \rho(t) \left[\frac{\sin(\sqrt{aa^\dagger}\tau)}{\sqrt{aa^\dagger}} \right] a \right]. \end{aligned} \quad (11.22)$$

For a typical laser the arguments of the sine and cosine are small, and one can expand (up to fourth order in g):

$$\cos g\tau\sqrt{aa^\dagger} \approx 1 - \frac{g^2\tau^2}{2}aa^\dagger + \frac{1}{24}g^4\tau^4aa^\dagger aa^\dagger + \dots,$$

$$\left[\frac{\sin g\tau\sqrt{aa^\dagger}}{\sqrt{aa^\dagger}} \right] \approx g\tau - \frac{g^3\tau^3aa^\dagger}{6} + \dots,$$

and substitute into the master equation (11.22), getting

$$\begin{aligned} \frac{d\rho_f}{dt} = & -\frac{\mathcal{A}}{2} \left\{ aa^\dagger \left[\rho_f - \left(\frac{g}{\gamma} \right)^2 (aa^\dagger \rho_f + 3\rho_f aa^\dagger) \right] \right. \\ & + \left[\rho_f - \left(\frac{g}{\gamma} \right)^2 (\rho_f aa^\dagger + 3aa^\dagger \rho_f) \right] aa^\dagger \\ & \left. - 2a^\dagger \left[\rho_f - 2 \left(\frac{g}{\gamma} \right)^2 (aa^\dagger \rho_f + \rho_f aa^\dagger) a \right] \right\} \\ & - \frac{C}{2} (a^\dagger a \rho_f + \rho_f a^\dagger a - 2a \rho_f a^\dagger), \end{aligned} \quad (11.23)$$

where:

$$\begin{aligned} \mathcal{A} &\equiv \frac{2rg^2}{\gamma^2}, \\ \mathcal{B} &\equiv \frac{4g^2}{\gamma^2} \mathcal{A}, \\ C &\equiv \frac{\omega}{Q}. \end{aligned} \quad (11.24)$$

To derive (11.23), we used the following integrals

$$\int \tau^2 \gamma \exp(-\gamma\tau) d\tau = \frac{2}{\gamma^2},$$

$$\int \tau^4 \gamma \exp(-\gamma\tau) d\tau = \frac{24}{\gamma^4}.$$

The coefficient \mathcal{A} is the gain, \mathcal{B} the saturation and C the cavity loss.

11.3.1 Photon Statistics

We go back to the full non-linear theory. We take the nm matrix elements of (11.22), and perform the time integrals, using

$$\begin{aligned} \gamma \int_0^\infty d\tau \exp(-\gamma\tau) &\left(\frac{\cos g\tau\sqrt{n+1} \cos g\tau\sqrt{m+1}}{\sin g\tau\sqrt{n+1} \sin g\tau\sqrt{m+1}} \right) \\ &= \frac{\left(1 + \left(\frac{g}{\gamma} \right)^2 (n+m+2) \right)}{2\left(\frac{g}{\gamma} \right)^2 \sqrt{(n+1)(m+1)}} \\ &= \frac{1 + 2(g/\gamma)^2(n+m+2) + (g/\gamma)^4(n-m)^2}{1 + 2(g/\gamma)^2(n+m+2) + (g/\gamma)^4(n-m)^2}, \end{aligned} \quad (11.25)$$

getting

$$\left(\frac{d\rho}{dt} \right)_{nm} = -\frac{\mathcal{N}'_{nm}\mathcal{A}}{1 + \mathcal{N}_{nm}\mathcal{B}/\mathcal{A}}\rho_{nm} + \frac{\sqrt{nm}\mathcal{A}}{1 + \mathcal{N}_{n-1,m-1}\mathcal{B}/\mathcal{A}}\rho_{n-1,m-1} \\ -\frac{C}{2}(n+m)\rho_{nm} + C\sqrt{(n+1)(m+1)}\rho_{n+1,m+1}, \quad (11.26)$$

where \mathcal{A} and \mathcal{B} have already been defined and:

$$\mathcal{N}'_{nm} = \frac{1}{2}(n+m+2) + \frac{\frac{1}{8}(n-m)^2\mathcal{B}}{\mathcal{A}}, \quad (11.27)$$

$$\mathcal{N}_{nm} = \frac{1}{2}(n+m+2) + \frac{\frac{1}{16}(n-m)^2\mathcal{B}}{\mathcal{A}},$$

and we included, as usual, the cavity losses. This is the Scully–Lamb laser theory [11.4].

For the photon statistics, we take the diagonal element of (11.27), getting

$$\left(\frac{d\rho}{dt} \right)_{nn} = -\frac{\mathcal{A}(n+1)}{1 + (n+1)\mathcal{B}/\mathcal{A}}\rho_{nn} + \frac{n\mathcal{A}}{1 + n\mathcal{B}/\mathcal{A}}\rho_{n-1,n-1} \\ -C(n)\rho_{nn} + C(n+1)\rho_{n+1,n+1}. \quad (11.28)$$

The term $[\mathcal{A}(n+1)/(1 + (n+1)\mathcal{B}/\mathcal{A})]\rho_{nn}$ represents the gain for $\rho_{n+1,n+1}$, due to stimulated emission caused by the presence of the amplifying atoms, and the term $C(n+1)\rho_{n+1,n+1}$ is the loss on this level.

In steady state $(d\rho/dt)_{nn} = 0$, and we get:

$$\rho_{n+1,n+1} = \frac{\mathcal{A}/C}{1 + (n+1)\mathcal{B}/\mathcal{A}}\rho_{nn}, \quad (11.29)$$

and the solution is

$$\rho_{nn} = \rho_{00} \left(\frac{\mathcal{A}}{C} \right)^n \prod_{k=0}^n \left(1 + \frac{k\mathcal{B}}{\mathcal{A}} \right)^{-1}. \quad (11.30)$$

When $\mathcal{A}/C < 1$, the laser is below threshold, since ρ_{nn} is decreasing monotonically with n and the normalization condition gives us: $(k\mathcal{B}/\mathcal{A} \ll 1)$

$$\sum_n \rho_{nn} = 1 = \rho_{00} \sum_n \left(\frac{\mathcal{A}}{C} \right)^n = \frac{\rho_{00}}{1 - \mathcal{A}/C}, \quad (11.31)$$

and if we define $\mathcal{A}/C = \exp(-\hbar\Omega/k_B T)$, then

$$\rho_{nn} = \left(1 - \frac{\mathcal{A}}{C} \right) \left(\frac{\mathcal{A}}{C} \right)^n, \quad (11.32)$$

becomes the Bose–Einstein statistics for the blackbody radiation. That is, the laser below threshold behaves like an incandescent lamp, with a given temperature.

For the case $\mathcal{A}/C > 1$, we use the exact formula (11.29), and get

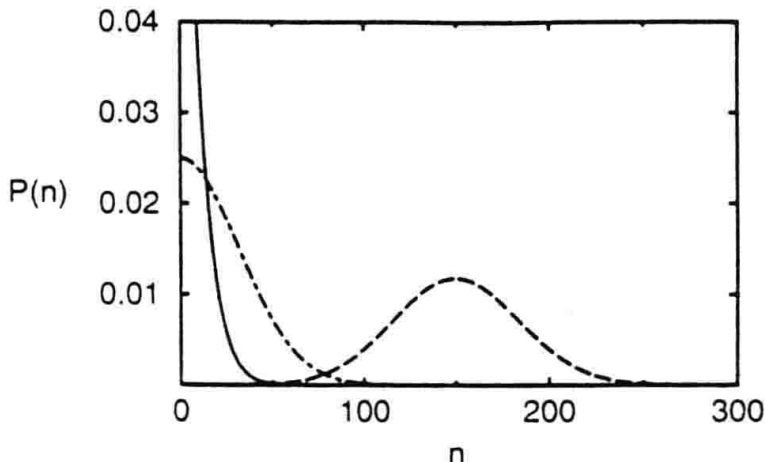


Fig. 11.2. Steady state photon statistics versus n , for the cases: 10% below threshold (solid line); at threshold (dot-dashed line); and 15% above threshold (dashed line). In all cases $B/A = 0.001$

$$\begin{aligned}\rho_{nn} &= \rho_{00} \left(\frac{\mathcal{A}}{C}\right)^n \prod_{k=1}^n \left(1 + \frac{k\mathcal{B}}{\mathcal{A}}\right)^{-1} \\ &= \rho_{00} \left(\frac{\mathcal{A}^2}{BC}\right)^n \prod_{k=1}^n \left(\frac{\mathcal{A}}{B} + k\right)^{-1}\end{aligned}\quad (11.33)$$

We calculate the average photon number

$$\begin{aligned}\langle n \rangle &= \sum_n n \rho_{nn} \\ &= \rho_{00} \sum_n \left(n + \frac{\mathcal{A}}{B} - \frac{\mathcal{A}}{B}\right) \left(\frac{\mathcal{A}^2}{BC}\right)^n \prod_{k=1}^n \left[\frac{1}{(k + \mathcal{A}/B)}\right] \\ &= \rho_{00} \frac{\mathcal{A}^2}{BC} \sum_n \left(\frac{\mathcal{A}^2}{BC}\right)^{n-1} \prod_{k=1}^{n-1} \left[\frac{1}{(k + \mathcal{A}/B)}\right] - \frac{\mathcal{A}}{B} \sum_{n=1}^{\infty} \rho_{nn} \\ &= \frac{\mathcal{A}^2}{BC} - \frac{\mathcal{A}}{B}(1 - \rho_{00}) = \frac{\mathcal{A}}{B} \left(\frac{\mathcal{A}}{C} - 1\right) + \frac{\mathcal{A}}{B} \rho_{00}.\end{aligned}\quad (11.34)$$

Well over the threshold $\langle n \rangle \rightarrow A^2/BC$ and the photon statistics obey

$$\rho_{nn} \approx \frac{(\exp - \langle n \rangle)(\langle n \rangle)^n}{n!} \quad (11.35)$$

which corresponds to Poisson statistics.

The change in photon statistics below and above threshold is illustrated in Fig. 11.2. We notice that for $B/\mathcal{A} \ll 1$,

$$\rho_{nn} = \rho_{00} \prod_{k=1}^n \left[\frac{\mathcal{A}^2}{BC(\mathcal{A}/B + k)}\right],$$

$$\rho_{nn} = \rho_{00} \prod_{k=1}^n \left[\frac{\mathcal{A}}{C(1 + k\mathcal{B}/\mathcal{A})}\right],$$

$$\rho_{nn} \approx \rho_{00} \prod_{k=1}^n \left(\frac{A - k\mathcal{B}}{C} \right).$$

11.3.2 The Fokker–Planck Equation. Laser Linewidth

We start with the approximate master equation (11.23), and neglecting the non-linear terms, we can use the rules described in (9.46), to write a Fokker–Planck equation in terms of the Glauber P -distribution as

$$\frac{\partial P}{\partial t} = -\frac{A - C}{2} \left(\frac{\partial}{\partial \alpha} \alpha + \frac{\partial}{\partial \alpha^*} \alpha^* \right) P + A \frac{\partial^2 P}{\partial \alpha \partial \alpha^*}. \quad (11.36)$$

The non-linear term can be included in the Fokker–Planck equation, using the clever trick [11.5] of observing that (11.36) is modified, according to (11.23), by replacing $P \rightarrow P [1 - 4g^2/\gamma^2 | \alpha |^2]$, getting

$$\begin{aligned} \frac{\partial P}{\partial t} &= -\frac{1}{2} \frac{\partial}{\partial \alpha} \left\{ \left[(A - C) - 4A \frac{g^2}{\gamma^2} |\alpha|^2 \right] \alpha P - A \frac{\partial P}{\partial \alpha^*} \right\} \\ &\quad - \frac{1}{2} \frac{\partial}{\partial \alpha^*} \left\{ \left[(A - C) - 4A \frac{g^2}{\gamma^2} |\alpha|^2 \right] \alpha^* P - A \frac{\partial P}{\partial \alpha} \right\}. \end{aligned} \quad (11.37)$$

This equation has been extensively studied, particularly in connection with the no-lasing–lasing phase transition [11.6], [11.7].

For linewidth purposes, the linear Fokker–Planck equation (11.36) is sufficient. We go to polar coordinates

$$\alpha = r \exp \varphi$$

and get, neglecting radial variations,

$$\frac{\partial P(\theta, t)}{\partial t} = \frac{A}{4\langle n \rangle} \frac{\partial^2}{\partial \theta^2} P(\theta, t) \equiv \frac{D}{2} \frac{\partial^2}{\partial \theta^2} P(\theta, t). \quad (11.38)$$

D is the phase diffusion constant and corresponds, as we shall see from the Langevin theory, precisely to the Schawlow–Townes laser linewidth, when $A \approx C$, which is not far from threshold. The present fourth-order expansion loses its validity well above threshold. It is interesting to observe that C is the empty cavity linewidth, thus the formula

$$D = \frac{C}{2\langle n \rangle} \quad (11.39)$$

shows that the linewidth is decreased by a factor $\langle n \rangle^{-1}$.

These results were also calculated by Lax [11.7], Gordon [11.8] and Haken [11.9].

11.3.3 Alternative Derivation of the Laser Linewidth

We present, in this section, a different approach to the laser linewidth which is related to the off-diagonal elements of the field density matrix. The expressions obtained here will be useful in calculating the quantum phase fluctuations in a laser (Chap. 15).

We begin by rewriting the equation of motion of the off-diagonal elements $\rho_{n,n+k}$, in a form related to the diagonal elements. We introduce the following notation

$$\rho_{n,n'} = \rho_{n,n+k} \equiv \phi_n(k, t), \quad (11.40)$$

where k is the distance from the main diagonal. From (11.26), and expanding to the lowest order in B/A , we get

$$\begin{aligned} \dot{\phi}_n(k, t) = & -\frac{k^2}{8} B \phi_n(k, t) \\ & - \left(n + 1 + \frac{k}{2} \right) \left[A - B \left(n + 1 + \frac{k}{2} \right) \right] \phi_n(k, t) \\ & + [n(n+k)]^{1/2} \left[A - B \left(n + \frac{k}{2} \right) \right] \phi_{n-1}(k, t) \\ & - C \left(n + \frac{k}{2} \right) \phi_n(k, t) \\ & + [(n+1)(n+k+1)]^{1/2} \phi_{n+1}(k, t). \end{aligned} \quad (11.41)$$

The first three terms represent the gain and the last two the loss in the cavity.

We assume a general solution of the form

$$\phi_n(k, t) = \sum_s \varphi_s(n, k) \exp[-\mu_s^{(k)} t], \quad (11.42)$$

where the $\mu_s^{(k)}$ are the eigenvalues and $\varphi_s(n, k)$ the eigenvectors. As we shall see, the eigenvalues are either positive or zero.

In the case $k = 0$ (diagonal elements) the fact that the steady state solution exists implies that

$$\mu_0^{(0)} = 0. \quad (11.43)$$

For the off-diagonal elements, one finds that $\mu_s^{(k)} > 0$, implying that the solution (for $k \neq 0$) obeys

$$\phi_n(k, t) \xrightarrow[t \rightarrow \infty]{} 0. \quad (11.44)$$

Now, for the laser far above threshold, the lowest eigenvalue $\mu_0^{(k)}$ will be small, and we look for a solution of the form

$$\begin{aligned} \phi_n(k, t) &= N_k \left[\prod_{l=0}^n \left(\frac{A-lB}{C} \right) \prod_{m=0}^{n+k} \left(\frac{A-mB}{C} \right) \right]^{1/2} \exp(-\mu_0^{(k)} t) \\ &\approx \sqrt{\rho_{n,n} \rho_{n+k,n+k}} \exp(-\mu_0^{(k)} t). \end{aligned} \quad (11.45)$$

One finds [11.4] that to a very good approximation, the above differential equation is satisfied for

$$\mu_0^{(k)} = \frac{1}{2}k^2 D, \quad (11.46)$$

for

$$D = \frac{C}{2\langle n \rangle}. \quad (11.47)$$

Thus, the off-diagonal elements of the laser field are given by

$$\rho_{n,n+k}(t) = \rho_{n,n+k}(0) \exp(-\mu_0^{(k)} t), \quad (11.48)$$

which, back in the Schrödinger picture, becomes

$$\rho_{n,n+k}(t) = \rho_{n,n+k}(0) \exp(-i\omega t - \mu_0^{(k)} t). \quad (11.49)$$

As in Chap. 8, a one-mode stationary field can be written as

$$E(t) = \varepsilon(a + a^\dagger) \sin kz, \quad (11.50)$$

so the statistical average will be

$$\begin{aligned} E(t) &= \varepsilon \sum_n (\rho_{n,n+1}(t) \sqrt{n+1} + cc) \sin kz \\ &= \varepsilon \sum_n (\rho_{n,n+1}(0) \sqrt{n+1} \exp(-i\omega t - \mu_0^{(k)} t) + cc) \sin kz \\ &= E_0 \cos(\omega t + \varphi) \exp\left(-\frac{D}{2}t\right), \end{aligned} \quad (11.51)$$

where

$$E_0 = 2\varepsilon A, \quad (11.52)$$

and

$$\sum_n \rho_{n,n+1}(0) \sqrt{n+1} = A \exp(-i\varphi). \quad (11.53)$$

The decay of the electric field can be understood as a result of a random walk of the ensemble average electric field due to the stochastic process that influences the system. After a certain amount of time, the phase of the field will have diffused to cover uniformly the whole range 2π . This will be seen in more detail in Chap. 15, when dealing with the quantum phase.

Finally, the Fourier transform of the average electric field gives the laser spectrum

$$\begin{aligned} |E(\Omega)|^2 &= \left| \int_0^\infty dt \exp(-i\Omega t) E_0 \cos(\Omega t + \varphi) \exp\left(-\frac{Dt}{2}\right) \right|^2 \\ &= \frac{E_0^2}{4} \left[\frac{1}{(\omega - \Omega)^2 + (\frac{D}{2})^2} \right], \end{aligned} \quad (11.54)$$

which is a Lorenzian with a full width at half maximum of D .

As a final note on this issue, the stochasticity of the phase of the laser field has its origin in the spontaneous emission. Thus, if one could somehow control this spontaneous emission, it would be possible to decrease the linewidth by a substantial amount.

This subject will be treated in some detail in Chap. 13, when dealing with the correlated emission laser and the methods of quenching the phase diffusion in a laser.

11.4 Quantum Theory of the Micromaser. Random injection ($p = 0$)

As we have seen in the previous chapter, one of the simplest and most fundamental systems to study radiation-matter coupling is a single two-level atom interacting with the one-mode electromagnetic field. For a long time, this model remained only a theoretical scheme, since it was not possible to test experimentally the effects predicted by the model. These effects, among others, are for example the modification of the spontaneous emission rates of a single atom in a resonant cavity, the oscillatory exchange of energy between the atom and the field, the disappearance and quantum revival of the Rabi mutation.

However, the situation has changed over the last decade mainly because of two important factors. The introduction of highly tunable dye lasers, which can excite large populations of highly excited atomic states, with a high principal quantum number n , called Rydberg states. These atoms are also referred to as Rydberg atoms.

Such excited atoms are very suitable for atom-radiation experiments because they are very strongly coupled to the radiation field, since the transition rates between neighbouring levels scale with n^4 . Also these transitions are in the microwave region, where photons can live longer, thus allowing longer interaction times. Finally, Rydberg atoms have long lifetimes, with respect to spontaneous decay [11.10], [11.11], [11.12]. The strong coupling of the Rydberg atom with the field can be physically understood since the dipole moment scales with the atomic radius which scales with n^2 . Thus when dealing with $n \sim 70$, we are talking about very large dipole moments.

To understand how the spontaneous emission rate is modified by a cavity, one has to study the effects of the cavity walls on the mode density. The continuum is replaced by a discrete set of modes, one of which may be resonant with the atom. In this case, the spontaneous decay rate is enhanced by a factor

$$\frac{\gamma_{\text{cav}}}{\gamma_f} = \frac{2\pi Q}{v_c \omega_{ab}^3}, \quad (11.55)$$

with γ_{cav} , γ_f being the spontaneous decay rate with the cavity and in free space, respectively. However, when the cavity is detuned, the decay rate will decrease. The atom cannot emit, since it is not resonant with the cavity. Both effects of reduction and enhancement of spontaneous emission have been observed.

The reduction was observed by Drexhage *et al.* [11.13], where the fluorescence of an active medium is observed, near a mirror. Also, similar effects were observed by De-Martini *et al.* [11.14] and Gabrielse and Dehmelt [11.15].

11.4.1 The Micromaser

A one-atom maser is described in Fig. 11.3. A collimated beam of rubidium atoms is passed through a velocity selector. Before entering a high- Q superconducting microwave cavity, the atom is excited to a high n -level and converted to a Rydberg atom. Micromaser cavities are made of niobium and cooled down to a small fraction of a degree Kelvin.

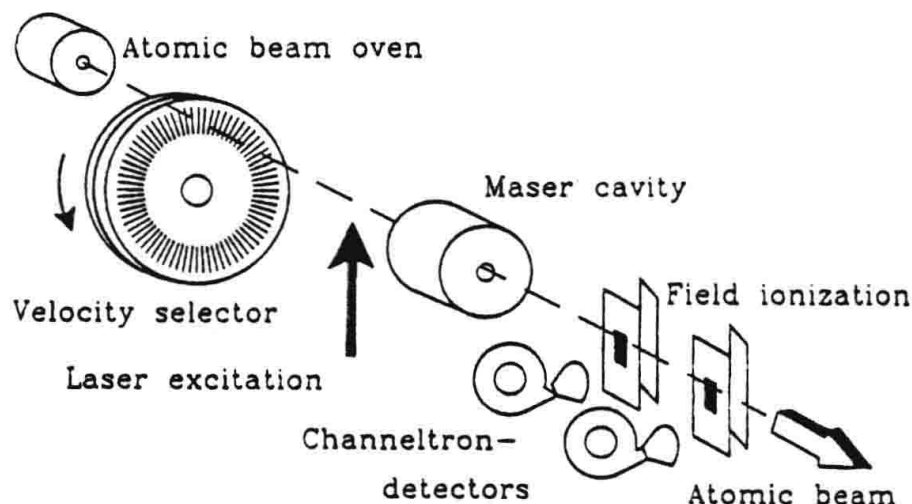


Fig. 11.3. The experimental setup of a micromaser. (After [11.10])

The Rydberg atoms are detected in the upper or lower maser levels by two field ionization detectors and the fields are adjusted so that in the first detector, only the atoms in the upper state are ionized. Maser operation was demonstrated by tuning the cavity to the maser transition and recording, simultaneously, the flux of atoms in the excited state [11.10]. As shown in Fig. 11.4, on resonance, a reduction of the signal is observed, for relatively small atomic fluxes (1750 at s^{-1}). Higher fluxes produce power broadening and a small frequency shift. Also, the two-photon micromaser was experimentally demonstrated [11.16].

In the quantum theory of the micromaser [11.17], the atomic spontaneous emission rate into the free space modes is neglected. Also, since high-quality cavities have been built, one assumes that the photon lifetime is much longer

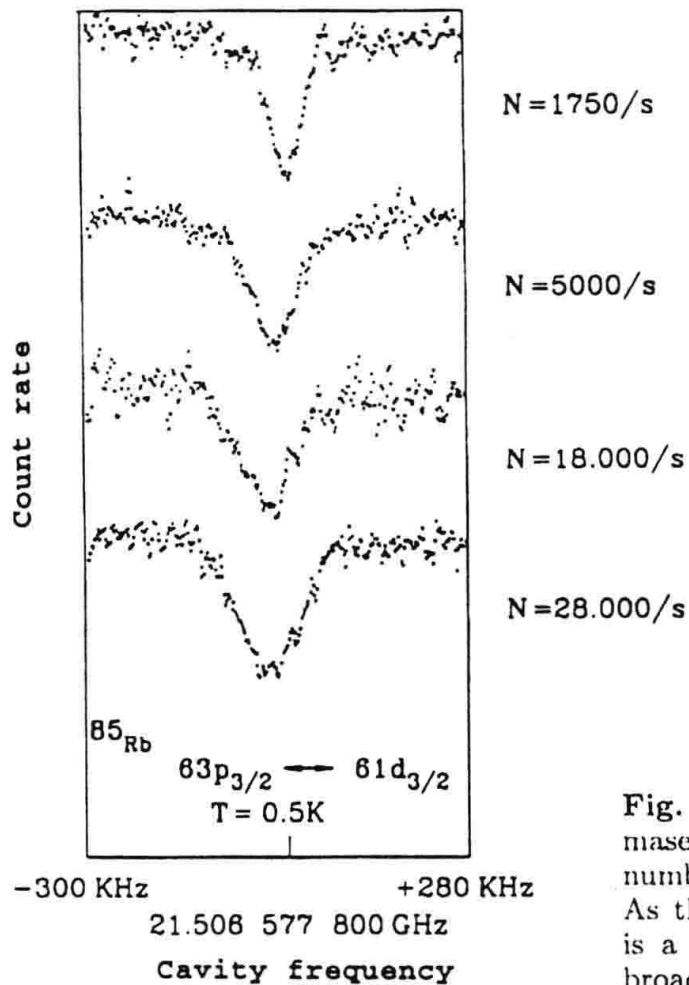


Fig. 11.4. Maser action of a one-atom maser is manifested as a decrease of the number of atoms in the excited state. As the atomic flux is increased, there is a small frequency shift and power broadening (after [11.10])

than the transit time through the cavity, implying that we may neglect the cavity damping while the atom is in the cavity. Also, since the flux is kept low, the time interval between the atoms is much longer than the flight time and hence the cavity is empty most of the time.

Mathematically, the time evolution of the field in the micromaser is given by (11.18). For simplicity, we study the case $p = 0$. In this case, for the diagonal matrix elements, the master equation becomes ($\rho_{nn}(t) = p(n, t)$)

$$\frac{dp(n, t)}{dt} = r [-\sin^2(g\sqrt{n+1}\tau)p(n, t) + \sin^2(g\sqrt{n}\tau)p(n-1, t)] + C(\langle n \rangle_{\text{th}} + 1) [(n+1)p(n+1, t) - np(n, t)] + C\langle n \rangle_{\text{th}} [np(n-1, t) - (n+1)p(n, t)], \quad (11.56)$$

where $\langle n \rangle_{\text{th}}$ is the average thermal photon number.

At steady state, and considering detailed balance,

$$\begin{aligned} & [r \sin^2(g\sqrt{n+1}\tau) + C\langle n \rangle_{\text{th}}(n+1)] p_0(n) \\ & = C(\langle n \rangle_{\text{th}} + 1)(n+1)p_0(n+1), \end{aligned} \quad (11.57)$$

where $p_0(n)$ is the steady state solution of (11.56).

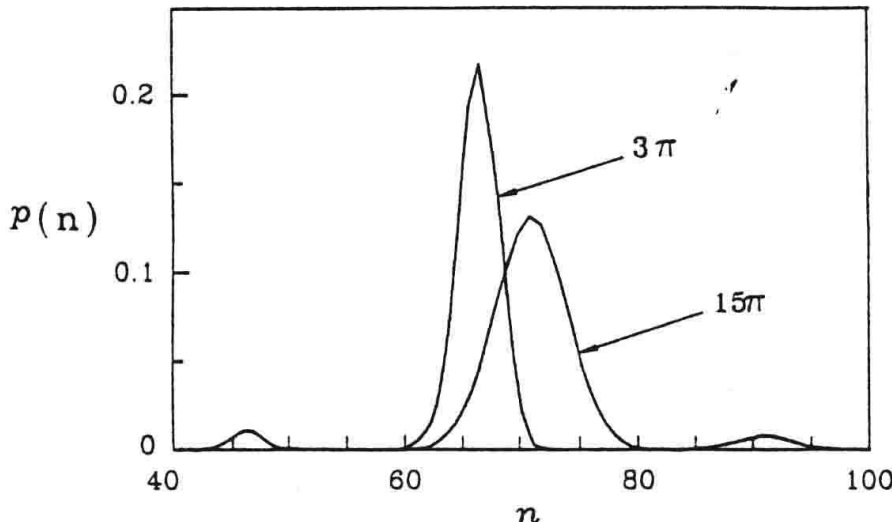


Fig. 11.5. Steady state photon statistics, for $n_{\text{ex}} = 200$, $\langle n \rangle_{\text{th}} = 0.1$ and $\theta = 3\pi, 15\pi$ (after [1.17])

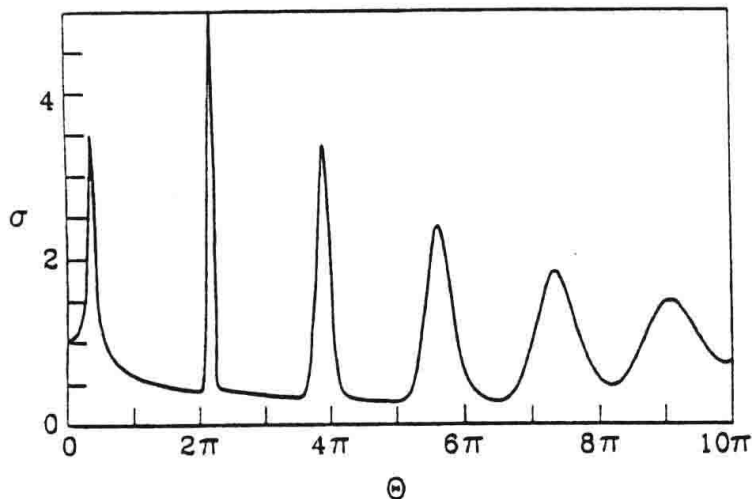


Fig. 11.6. Normalized standard deviation $\sigma = \sqrt{(\Delta n)^2 / \langle n \rangle}$ as a function of θ . A Poissonian distribution corresponds to $\sigma = 1$, $n_{\text{ex}} = 200$ (after [1.17])

The solution of the recursion relation (11.57) is [11.17]

$$p_0(n) = p_0(0) \left(\frac{\langle n \rangle_{\text{th}}}{\langle n \rangle_{\text{th}} + 1} \right)^n \prod_{k=1}^n \left[1 + \frac{n_{\text{ex}} \sin^2(\theta \sqrt{\frac{k}{n_{\text{ex}}}})}{k \langle n \rangle_{\text{th}}} \right], \quad (11.58)$$

where $p_0(0)$ is the normalization constant determined by the condition

$$\sum_{n=0}^{\infty} p_0(n) = 1,$$

$$\theta \equiv \sqrt{n_{\text{ex}}} g \tau,$$

$$n_{\text{ex}} \equiv \frac{r}{C}.$$

A typical photon number distribution is shown in Fig. 11.5. Also, with $p_0(n)$, we can get the variance, which is shown in Fig. 11.6. The sub-Poissonian regions are due to the multipeak structure of the photon distribution.

11.4.2 Trapping States

Under the Jaynes–Cummings dynamics, the time evolution of the atom–field coupling is given, in the interaction picture (on resonance), by [11.17]

$$\begin{aligned}
 & \sum_n S_n |n\rangle (\alpha |a\rangle + \beta |b\rangle) \\
 \rightarrow & \sum_n S_n U(\tau) |n\rangle (\alpha |a\rangle + \beta |b\rangle) \\
 = & \sum_n S_n \begin{bmatrix} \cos(g\tau\sqrt{aa^\dagger}) & -i \left[\frac{\sin(g\tau\sqrt{aa^\dagger})}{\sqrt{aa^\dagger}} \right] a \\ -ia^\dagger \left[\frac{\sin(g\tau\sqrt{aa^\dagger})}{\sqrt{aa^\dagger}} \right] & \cos(g\tau\sqrt{a^\dagger a}) \end{bmatrix} \begin{bmatrix} \alpha \\ \beta \end{bmatrix} |n\rangle \\
 = & |a\rangle \sum_n S_n \left\{ \alpha \cos(g\tau\sqrt{n+1}) |n\rangle \right. \\
 & \left. - i\beta\sqrt{n} \left[\frac{\sin(g\tau\sqrt{n})}{\sqrt{n}} \right] |n-1\rangle \right\} \\
 & + |b\rangle \sum_n S_n [\beta \cos g\tau\sqrt{n} |n\rangle - i\alpha \sin(g\tau\sqrt{n+1}) |n+1\rangle] . \\
 \equiv & |f_a\rangle |a\rangle + |f_b\rangle |b\rangle .
 \end{aligned} \tag{11.59}$$

If, for some $n = N$, we have $g\tau\sqrt{N} = q\pi$, q an integer, then the downward coupling from $|N\rangle \rightarrow |N-1\rangle$ vanishes, and the regions above and below $|N\rangle$ are disconnected. This state is referred to as the downtrapping state.

Similarly, for an integer number p , the condition

$$\sqrt{M+1}g\tau = p\pi \tag{11.60}$$

corresponds to the upwards trapping condition.

Trapping states separate the whole Fock space into disconnected blocks, and, if the initial state of the field is within one of these blocks, the whole dynamics will take place within the block. However, this is a simple picture without losses, and having only no atoms, or at most one atom inside the cavity. Both co-operative and dissipative effects will result in leaks in the trapping blocks, which, after some time, are no longer able to trap.

Pure states can be generated, at steady state, within these blocks, by the field mode. To see this, we assume for the field a pure state within the trapping block

$$|f\rangle = \sum_{n=N}^{n=M} S_n |n\rangle, \tag{11.61}$$

where the number states $|N\rangle$ and states $|M\rangle$ are the lower and upper bounds of the trapping block. Now, we look for possible steady states for the field. This means, that after the interaction with the next atom crossing the cavity, the state of the field will be the same, up to some global phase factor

$$|f\rangle (\alpha |a\rangle + \beta |b\rangle) \implies \exp i\phi |f\rangle (\alpha' |a\rangle + \beta' |b\rangle), \tag{11.62}$$

and making use of (11.59) we get

$$\begin{aligned}\alpha' \exp i\phi |f\rangle &= |f_a\rangle, \\ \beta' \exp i\phi |f\rangle &= |f_b\rangle,\end{aligned}\quad (11.63)$$

which yields the following recursion relations

$$\begin{aligned}S_n &= \frac{i\beta \sin(g\tau\sqrt{n+1})}{\alpha' \exp i\phi - \alpha \cos(g\tau\sqrt{n+1})} S_{n+1}, \\ S_n &= -i \frac{\beta' \exp i\phi - \beta \cos(g\tau\sqrt{n+1})}{\alpha \sin(g\tau\sqrt{n+1})} S_{n+1}.\end{aligned}\quad (11.64)$$

Equations (11.64) have to be satisfied simultaneously, for all n within the block. These relations are satisfied under two possible sets of conditions:

$$\begin{aligned}(a) \quad \exp i\phi &= \pm 1, \\ \alpha' &= -\alpha, \\ \beta' &= \beta.\end{aligned}\quad (11.65)$$

$$\begin{aligned}(b) \quad \exp i\phi &= \pm 1, \\ \alpha' &= \alpha, \\ \beta' &= -\beta.\end{aligned}\quad (11.66)$$

The conditions (a) and (b) lead to different recursion relations. In case (a)

$$S_n = i \frac{\alpha}{\beta} \cot\left(\frac{g\tau\sqrt{n}}{2}\right) S_{n-1}, \quad (11.67)$$

and in case (b)

$$S_n = -i \frac{\alpha}{\beta} \tan\left(\frac{g\tau\sqrt{n}}{2}\right) S_{n-1}. \quad (11.68)$$

The two states are referred to as the cotangent and tangent states respectively.

It is simple to verify that if one takes into account the boundaries of the block in phase space, for the cotangent states

$$\begin{aligned}\sqrt{N}g\tau &= q\pi, \quad \text{for } q \text{ even,} \\ \sqrt{M+1}g\tau &= p\pi, \quad \text{for } p \text{ odd,}\end{aligned}\quad (11.69)$$

and the reverse is true for the tangent states.

From the recursion relation (11.67), a cotangent state can be written as

$$\begin{aligned}|\cot\rangle &= \sum_{n=N}^{n=M} S_n |n\rangle \\ &= C(i)^n \left(\frac{\alpha}{\beta}\right)^n \prod_{j=1}^n \cot\left(\frac{g\tau\sqrt{j}}{2}\right).\end{aligned}\quad (11.70)$$

One of the most interesting properties of the cotangent states is that they are squeezed [11.18].

Since, in practice, the initial conditions include the vacuum state, the cotangent states are the more interesting ones. We take $N = 0$ ($q = 0$) and some odd integer number for p , representing a $2\pi p$ rotation of an initially excited atom. Since the state is exactly known, it is straightforward to compute the quadrature fluctuations.

In Fig. 11.7 we show the variation of the two quadratures for a cotangent state for $N = 0$, $M = 20$ and $p = 1(a)$ and $p = 3(b)$, as a function of the probability of the upper state $|\alpha|^2$. The maximum squeezing is obtained for large α . Also, the squeezing increases with the size of the trapping block.

Trapping states provide a way to build up Fock states or a superposition of Fock states in cavities. It is important, though, to remark that our discussion is somewhat idealized, even in the case of the trapped vacuum state, which does not require the assumption of zero dissipation. The trapping states were found in a recent experiment, using Rubidium atoms in a Rydberg state [11.22].

Actually, the atoms leaving the oven have a Poissonian arrival distribution, so that there is always a finite probability of having two atoms simultaneously in the cavity. This co-operative effect produces a great disruption in the trapping states, even for a very low density beam, with a probability of having two atoms less than 1% [11.19], [11.20].

Finally, recent experiments show that one can also have microlasers, that is laser oscillations with one atom in the optical region [11.21]. In these experiments, a beam of Ba atoms is first excited by a laser pulse, before entering the optical cavity. Laser oscillations were observed, with an average photon number ranging from a fraction of a photon to 11. The rapid increase of the photon number with the pump, when the average number of atoms approaches 1, departing from the linear regime, may be attributed to co-operative effects.

11.5 Quantum Theory of the Laser and the Micromaser with Pump Statistics ($p \neq 0$)

We take the diagonal matrix elements of (11.18), and get

$$\begin{aligned} \frac{d\rho_{nn}}{dt} = & r [-\sin^2(g\sqrt{n+1}\tau)\rho_{nn} + \sin^2(g\sqrt{n}\tau)\rho_{n-1,n-1}] \\ & + \frac{rp}{2} [\{\sin^4(g\sqrt{n}\tau) + \sin^2(g\sqrt{n}\tau)\sin^2(g\sqrt{n+1}\tau)\}\rho_{n-1,n-1} \\ & - \sin^2(g\sqrt{n}\tau)\sin^2(g\sqrt{n-1}\tau)\rho_{n-2,n-2} \\ & - \sin^4(g\sqrt{n+1}\tau)\rho_{nn}] + (L\rho)_{nn}. \end{aligned} \quad (11.71)$$

Now, we can calculate the equation of motion for $\langle n \rangle$ (including the cavity loss term)

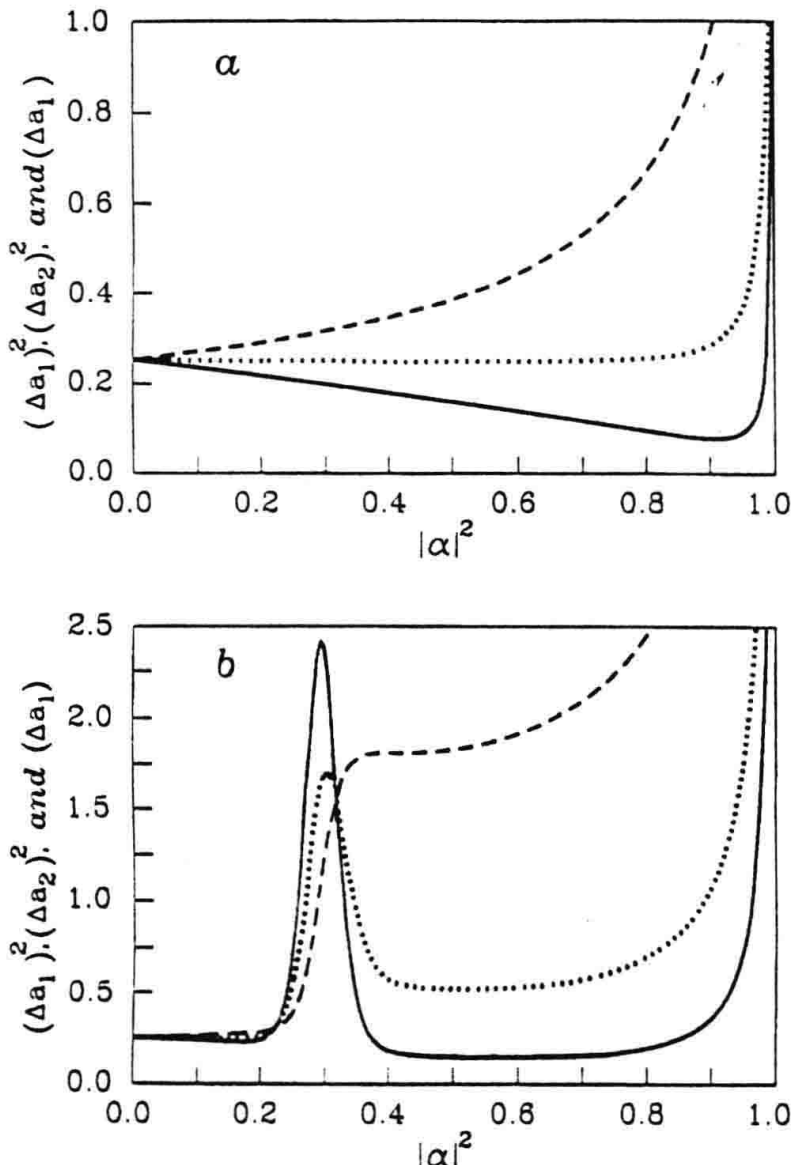


Fig. 11.7. Squeezing of a cotangent state with $p = 1$ (a) and $p = 3$ (b) bound between $N = 0$ and $M = 20$, as a function of $|\alpha|^2$. The solid line corresponds to $(\Delta a_1)^2$, the dashed line to $(\Delta a_2)^2$ and the dotted line to the product $(\Delta a_1)(\Delta a_2)\phi = \pi/2$

$$\frac{d\langle n \rangle}{dt} = \sum_n n \frac{d\rho_{nn}}{dt} = r \sum_n \alpha_n \rho_{nn} - C\langle n \rangle = r\langle \alpha_n \rangle - C\langle n \rangle, \quad (11.72)$$

with

$$\alpha_n = \sin^2(g\sqrt{n+1}\tau) \left\{ 1 + \frac{p}{2} \left[\sin^2(g\sqrt{n+1}\tau) - \sin^2(g\sqrt{n+2}\tau) \right] \right\}. \quad (11.73)$$

We notice that for $n \gg 1, g\tau$, the gain α_n is just its semiclassical expression

$$\alpha_n = \sin^2(g\sqrt{n+1}\tau), \quad (11.74)$$

and is independent of the pump statistics. On the other hand, the variance $v = \langle n^2 \rangle - \langle n \rangle^2$ is readily obtained as

$$\begin{aligned} \frac{dv}{dt} &= 2r\langle \alpha_n \Delta n \rangle + r\langle (\alpha_n - p \sin^2(g\sqrt{n+1}\tau) \sin^2(g\sqrt{n+2}\tau)) \rangle \\ &\quad - 2Cv + C\langle n \rangle, \end{aligned} \quad (11.75)$$

where

$$\Delta n \equiv n - \langle n \rangle.$$

For $n \gg 1$, one has

$$\frac{dv}{dt} = 2r\langle \alpha_n \Delta n \rangle + r\langle (\alpha_n - p\alpha_n^2) \rangle - 2Cv + C\langle n \rangle. \quad (11.76)$$

The steady state value for the average photon number is

$$r\langle \alpha_n \rangle = Cn_{ss}, \quad (11.77)$$

which can be seen graphically as the intersection of the gain curve with the loss (straight line); see Fig. 11.8.

It is not difficult to see that the steady state value n_{ss} is only stable if the slope of the gain curve is smaller than the slope of the loss, that is

$$r \left(\frac{d\alpha_n}{dn} \right)_{n_{ss}} < C. \quad (11.78)$$

To see this, we expand the gain around the intersection point

$$\alpha_n \approx (\alpha_n)_{n_{ss}} + \left(\frac{d\alpha_n}{dn} \right)_{n_{ss}} (n - n_{ss}) + \dots \quad (11.79)$$

Now, if n is slightly larger than n_{ss}

$$n \geq n_{ss}, \quad (11.80)$$

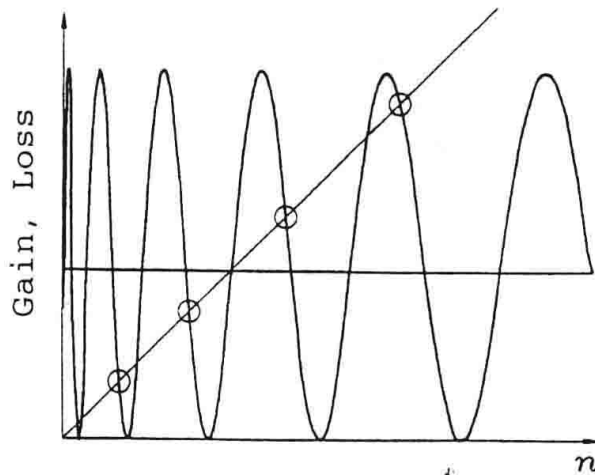


Fig. 11.8. The steady state photon number found as an intersection of the gain curve with the loss straight line

$$\Delta n = n - n_{ss} > 0,$$

then one can write

$$\begin{aligned}\frac{d\langle n \rangle}{dt} &= r \left[\langle \alpha_n \rangle_{n_{ss}} + \left(\frac{d\alpha_n}{dn} \right)_{n_{ss}} \Delta n \right] - C [n_{ss} + \Delta n] \\ &= \left[r \left(\frac{d\alpha_n}{dn} \right)_{n_{ss}} - C \right] \Delta n,\end{aligned}\quad (11.81)$$

and if the equilibrium is stable, $d\langle n \rangle/dt$ should be negative in order to go back to the equilibrium point, so the condition given by (11.78) is satisfied.

Defining a normalized photon number $\eta_n \equiv n/n_{ex}$, where $n_{ex} \equiv r/C$ is the number of excited atoms entering the cavity, during the cavity damping time, we can see from (11.77) that $0 \leq \eta \leq 1$, and the stability condition can be written now as

$$\left(\frac{d\alpha_n}{d\eta_n} \right)_{n=n_{ss}} < 1. \quad (11.82)$$

Now we assume that the photon distribution is highly peaked around a single maximum, and we can expand α_n around n_{ss} . Then we find (using (11.76) in steady state)

$$v = \left(\frac{d\alpha_n}{d\eta_n} \right)_{n=n_{ss}} v + \frac{n_{ex}}{2} \langle \alpha_n \rangle - \frac{pr}{2C} \langle \alpha_n^2 \rangle + \frac{\langle n \rangle}{2}, \quad (11.83)$$

or

$$v = \frac{1}{1 - (d\alpha_n/d\eta_n)_{n=n_{ss}}} \left\langle n - \frac{pn_{ex}}{2} \alpha_n^2 \right\rangle. \quad (11.84)$$

The above expression exhibits the role of the pump statistics on the photon number noise. For the case of the micromaser, one gets a sub-Poissonian distribution, even if $p \rightarrow 0$, if $(d\alpha_n/d\eta_n)_{n=n_{ss}} < 0$. As p is increased, this behaviour is enhanced even further.

A somewhat simpler expression can be obtained for the variance, in the case $n_{ss} \gg 1$, in which case $\langle \alpha_n^2 \rangle \approx \langle \alpha_n \rangle^2$, and we get

$$v \cong \frac{n_{ss} (1 - p\eta_s/2)}{1 - (d\alpha_n/d\eta_n)_{n=n_{ss}}}, \quad (11.85)$$

where η_s is its value at steady state. Choosing $p = \eta_s = 1$, one has a 50% photon noise reduction due to the regularity of the pump, when compared with the same micromaser with a Poissonian pump.

Now we turn our attention to the laser case. Averaging over the atomic lifetimes, we get

$$\alpha_n^{\text{laser}} = \int_0^\infty d\tau \exp(-\gamma\tau) \sin^2(g\sqrt{n}\tau) = \frac{2g^2 n}{\gamma^2 + 4g^2 n}, \quad (11.86)$$

and according to (11.77)

$$\eta_s = \frac{2g^2 n_{ss}}{\gamma^2 + 4g^2 n_{ss}}, \quad (11.87)$$

thus η_s is always smaller than 1/2, approaching this value for large n_{ss} . From (11.86), we get:

$$\left(\frac{d\alpha_n}{d\eta_n} \right)_{n=n_{ss}} = 1 - 2\eta_s \geq 0. \quad (11.88)$$

Substituting (11.88) into (11.85), we get

$$v = \frac{(1 - p\eta_s/2)}{2\eta_s} n_{ss}. \quad (11.89)$$

Now we can discuss the influence of the pump fluctuations over the photon-number variance in the laser. In the case of a Poissonian distribution of the incoming atoms ($p = 0$), the variance is always larger than the mean number of photons, only approaching this value well above threshold, and indeed, when $\eta_s \rightarrow 1/2$, $v \rightarrow n_{ss}$, as it should. On the other hand, if we go to the regular pumping limit ($p = 1$), we can get a considerable noise reduction well above threshold, when $\eta_s \rightarrow 1/2$, getting $v = (3/4)n_{ss}$, thus getting up to 25% noise reduction.

Finally, it is possible to show [11.2] that the phase diffusion constant is not affected by the pump statistics.

Problems

- 11.1. Prove (11.7).
- 11.2. Prove (11.18).
- 11.3. Prove (11.23).
- 11.4. Prove (11.37) from (11.23).

12. Quantum Laser Theory. Langevin Approach

In the previous chapter, we studied the influence of the pump statistics on the amplitude and phase fluctuations of the laser radiation, making use of the master equation approach. We thus derived a generalized master equation in terms of a parameter p that represented the probability for an atom to be excited to the upper level, before entering into the cavity. The two extreme cases were $p \rightarrow 0$ (Poisson statistics) and $p \rightarrow 1$ (regular statistics). What we found was that the pump statistics had no influence on the phase fluctuations or linewidth, but had a strong influence on the photon number fluctuations.

In the present chapter, we discuss the influence of the pump statistics from a different point of view. We use the Langevin formalism [12.1], including generalized noise operators so as to include the effects of the pump noise [12.2]. We show here that again the photon number fluctuations can be reduced by simply reducing the pump fluctuations. Furthermore, we generalize the arguments of the previous chapter, allowing for different atomic decay constants from the two levels.

12.1 Quantum Langevin Equations

Our physical system is described again in Fig. 11.1, where the atoms are prepared initially in the upper level $|a\rangle$. The two levels $|a\rangle$ and $|b\rangle$ constitute the lasing transition, which is coupled to one mode of the radiation field, inside the cavity. The Hamiltonian of this system, in the rotating-wave approximation, is given by

$$H = \hbar\omega a^\dagger a + \sum_{j=1}^N (\epsilon_a |a\rangle\langle a| + \epsilon_b |b\rangle\langle b| + \epsilon_c |c\rangle\langle c|)_j + \hbar g \sum_j \Theta(t - t_j) (a^\dagger \sigma^j + \sigma^{j\dagger} a), \quad (12.1)$$

where $\Theta(t)$ is the usual step function.

In the above Hamiltonian, $\sigma^j = (|b\rangle\langle a|)_j$ represents the polarization operator for the j th atom. The cavity losses as well as the atomic decay are modelled in the usual way, coupling the system to heat reservoirs. We find the following equations of motion

$$\dot{a} = -i\omega_a a - \frac{C}{2}a - ig \sum_j \Theta(t - t_j) \sigma^j + F_C, \quad (12.2)$$

$$\dot{\sigma}^j = -i\omega_{ab}\sigma^j - \gamma\sigma^j + ig\Theta(t - t_j)(\sigma_{aa}^j + \sigma_{bb}^j)a + F_{ba}^j, \quad (12.3)$$

$$\dot{\sigma}_{aa}^j = -\gamma\sigma_{aa}^j + ig\Theta(t - t_j)(a^\dagger\sigma^j - \sigma^{j\dagger}a) + F_{aa}^j, \quad (12.4)$$

$$\dot{\sigma}_{bb}^j = -\gamma\sigma_{bb}^j - ig\Theta(t - t_j)(a^\dagger\sigma^j + \sigma^{j\dagger}a) + F_{bb}^j, \quad (12.5)$$

where $\sigma_{aa}^j = (|a\rangle\langle a|)_j$, $\sigma_{bb}^j = (|b\rangle\langle b|)_j$ and $\omega_{ab} = (\epsilon_a - \epsilon_b)/\hbar$.

For now and for the sake of simplicity, we have assumed that the two atomic decay constants are equal with value γ . However, this assumption will be relaxed later.

Now we look at the noise terms. From the damped harmonic oscillator, we have already seen that

$$\begin{aligned} \langle F_C^\dagger(t)F_C(t') \rangle &= C\langle n \rangle_{\text{th}}\delta(t - t') \\ &= 0 \quad \text{at } T = 0, \end{aligned} \quad (12.6)$$

$$\begin{aligned} \langle F_C(t)F_C^\dagger(t') \rangle &= C(1 + \langle n \rangle_{\text{th}})\delta(t - t') \\ &= C\delta(t - t') \quad \text{at } T = 0, \end{aligned} \quad (12.7)$$

$$\langle F_C(t) \rangle = 0. \quad (12.8)$$

For the atomic noise correlation functions, we first derive the Einstein relations.

12.1.1 Generalized Einstein Relations

We write a quantum Langevin equation, in the absence of atom-field interaction (for a general discussion on stochastic processes, see Appendix D):

$$\dot{A}_\mu = D_\mu(t) + F_\mu(t), \quad (12.9)$$

where $D_\mu(t)$ is the drift operator for $A_\mu(t)$ and $F_\mu(t)$ is the corresponding noise operator with zero reservoir average $\langle F_\mu(t) \rangle = 0$. We also write the two-time average for the noise operator as

$$\langle F_\mu(t)F_\nu(t') \rangle = 2\langle D_{\mu\nu} \rangle \delta(t - t'). \quad (12.10)$$

Now, we start with the identity

$$A_\mu(t) = A_\mu(t - \Delta t) + \int_{t-\Delta t}^t dt' \dot{A}_\mu(t'),$$

in order to obtain the system noise correlation function

$$\begin{aligned}\langle A_\mu(t) F_\nu(t) \rangle &= \langle A_\mu(t - \Delta t) F_\nu(t) \rangle \\ &\quad + \int_{t-\Delta t}^t dt' \langle (D_\mu(t') + F_\mu(t')) F_\nu(t) \rangle,\end{aligned}\tag{12.11}$$

and since $A_\mu(t - \Delta t)$ cannot be affected by the noise term $F_\nu(t)$ at a later time, the first term in (12.12) is zero. The same argument applies to the first term in the integral $\langle D_\mu(t') F_\nu(t) \rangle$, so we are left with only one term

$$\begin{aligned}\langle A_\mu(t) F_\nu(t) \rangle &= \int_{t-\Delta t}^t dt' \langle F_\mu(t') F_\nu(t) \rangle \\ &= \frac{1}{2} \int_{-\infty}^{\infty} dt' \langle F_\mu(t') F_\nu(t) \rangle,\end{aligned}\tag{12.12}$$

and substituting (12.10) into (12.13), we get

$$\langle A_\mu(t) F_\nu(t) \rangle = \langle D_{\mu\nu} \rangle.\tag{12.13}$$

It is simple to prove that, also

$$\langle F_\nu(t) A_\mu(t) \rangle = \langle D_{\mu\nu} \rangle.\tag{12.14}$$

Now we write

$$\begin{aligned}\frac{d}{dt} \langle A_\mu(t) A_\nu(t) \rangle &= \langle \dot{A}_\mu(t) A_\nu(t) \rangle + \langle A_\mu(t) \dot{A}_\nu(t) \rangle \\ &= \langle D_\mu(t) A_\nu(t) \rangle + \langle F_\mu(t) A_\nu(t) \rangle \\ &\quad + \langle A_\mu(t) D_\nu(t) \rangle + \langle A_\mu(t) F_\nu(t) \rangle,\end{aligned}$$

and using (12.13), (12.14), we get the generalized Einstein relations

$$2\langle D_{\mu\nu} \rangle = -\langle A_\mu(t) D_\nu(t) \rangle - \langle D_\mu(t) A_\nu(t) \rangle + \frac{d}{dt} \langle A_\mu(t) A_\nu(t) \rangle.\tag{12.15}$$

12.1.2 Atomic Noise Moments

From the Einstein relations, one can easily calculate the atomic noise moments. Let us take as an example $\langle F_{ba}^\dagger(t) F_{ba}(t') \rangle$, so we take $A_\mu = \sigma^\dagger$ and $A_\nu = \sigma$. From (12.15), we get, neglecting the g -terms,

$$\begin{aligned}2\langle D_{\sigma^\dagger\sigma} \rangle &= -\langle \sigma^\dagger (-\gamma\sigma) \rangle - \langle -\gamma\sigma^\dagger\sigma \rangle + \frac{d}{dt} \langle \sigma_{aa} \rangle \\ &= \gamma \langle \sigma_{aa} \rangle,\end{aligned}\tag{12.16}$$

where we have used the property $\sigma^\dagger\sigma = \sigma_{aa}$ and (12.3). We leave it as an exercise to the reader to verify the rest of the atomic correlations

$$\langle F_{ba}^{\dagger j}(t) F_{ba}^j(t') \rangle = \gamma \langle \sigma_{aa}^j \rangle \delta(t - t'),\tag{12.17}$$

$$\langle F_{ll}^j(t) F_{ll}^j(t') \rangle = \gamma \langle \sigma_{ll}^j \rangle \delta(t - t'), \quad l = a, b\tag{12.18}$$

$$\langle F_{ba}^j(t) F_{aa}^j(t') \rangle = \gamma \langle \sigma^j \rangle \delta(t - t'),\tag{12.19}$$

$$\langle F_{ba}^{\dagger j}(t)F_{bb}^j(t') \rangle = \gamma \langle \sigma^{j\dagger} \rangle \delta(t - t'). \quad (12.20)$$

We now proceed to eliminate the fast-varying terms in (12.2), (12.3), (12.4), (12.5). For simplicity, we assume resonance $\omega_{ab} = \omega$ and define

$$\widetilde{a}(t) = \exp(i\omega t)a(t), \quad \widetilde{\sigma}^j(t) = \exp(i\omega t)\sigma^j(t). \quad (12.21)$$

It is quite evident that the equations of motion for \tilde{a} and $\tilde{\sigma}^j$ are the same as for a and σ^j with the only difference that the terms proportional to ω_{ab} and ω are omitted.

The following step in this theory is to define the collective operators summed over all the atoms. This is very convenient with the adiabatic approximation we are going to make. Thus, we define

$$M(t) = -i \sum_j \Theta(t - t_j) \sigma^j(t), \quad (12.22)$$

$$N_a(t) = \sum_j \Theta(t - t_j) \sigma_{aa}^j(t), \quad (12.23)$$

$$N_b(t) = \sum_j \Theta(t - t_j) \sigma_{bb}^j(t). \quad (12.24)$$

The operators M, N_a, N_b represent the macroscopic polarization and the populations in the a and b levels, respectively.

With the above definitions, the equation of motion for the field now becomes

$$\dot{a} = -\frac{C}{2}a + Mg + F_\gamma. \quad (12.25)$$

On the other hand, for the atomic operator N_a , we differentiate (12.23) and substitute (12.4), getting

$$\begin{aligned} \dot{N}_a &= \sum_j \Theta(t - t_j) \dot{\sigma}_{aa}^j + \delta(t - t_j) \sigma_{aa}^j \\ &= \sum_j \delta(t - t_j) \sigma_{aa}^j(t_j) - \gamma N_a - g(a^\dagger M + M^\dagger a) \\ &\quad - i \sum_j \Theta(t - t_j) F_{ba}^j(t). \end{aligned} \quad (12.26)$$

The first term in the right-hand side of (12.26) corresponds to the pumping of the atoms to the excited state. This can be seen as follows:

$$\begin{aligned} \left\langle \sum_j \delta(t - t_j) \sigma_{aa}^j(t_j) \right\rangle &= \left\langle \sum_j \delta(t - t_j) \langle \sigma_{aa}^j(t_j) \rangle \right\rangle_s \\ &= \left\langle \sum_j \delta(t - t_j) \right\rangle_s. \end{aligned} \quad (12.27)$$

In the above result, we used the fact that the atoms are initially prepared in the upper state, so that $\langle \sigma_{aa}^j(t_j) \rangle = 1$. Also, there is a second bracket with a subscript S, showing that a statistical average has been performed over all the terms that depend on the random injection times t_j .

Assuming an average injection rate of atoms R , then one can write

$$\begin{aligned} \left\langle \sum_j \delta(t - t_j) \sigma_{aa}^j(t_j) \right\rangle &= \left\langle \sum_j \delta(t - t_j) \right\rangle_S \\ &= R \int_{-\infty}^{\infty} dt_j \delta(t - t_j) \\ &= R. \end{aligned} \quad (12.28)$$

In order to separate the drift from the noise terms, we add and subtract R , getting

$$\dot{N}_a = R - \gamma N_a - g(a^\dagger M + M^\dagger a) + F_a, \quad (12.29)$$

with

$$F_a(t) = \sum_j \Theta(t - t_j) F_{aa}^j(t) + \sum_j \delta(t - t_j) \sigma_{aa}^j(t_j) - R. \quad (12.30)$$

In a similar way, one derives the other operator equations

$$\dot{N}_b = -\gamma N_b + g(a^\dagger M + M^\dagger a) + F_b, \quad (12.31)$$

$$\dot{M} = -\gamma M + g(N_a - N_b)a + F_M, \quad (12.32)$$

with

$$F_b(t) = \sum_j \Theta(t - t_j) F_{bb}^j(t) + \sum_j \delta(t - t_j) \sigma_{bb}^j(t_j), \quad (12.33)$$

$$F_M(t) = -i \sum_j \Theta(t - t_j) F_{ba}^j(t) - i \sum_j \delta(t - t_j) \sigma_{ba}^j(t_j). \quad (12.34)$$

Now, we calculate the atomic noise correlation functions. As an example, we calculate $\langle F_a(t) F_a(t') \rangle$.

$$\begin{aligned} \langle F_a(t) F_a(t') \rangle &= \left\langle \sum_{j,k} \Theta(t - t_j) \Theta(t' - t_k) \langle F_{aa}^j(t) F_{aa}^k(t') \rangle \right\rangle_S \\ &\quad + \left\langle \sum_{j,k} \delta(t - t_j) \delta(t' - t_k) \langle \sigma_{aa}^j(t) \sigma_{aa}^k(t') \rangle \right\rangle_S - R^2 \rho_{aa}^2. \end{aligned} \quad (12.35)$$

We notice, once again, that in the above expression, two types of average have been considered.

On one hand, we have the usual quantum mechanical average over the bath variables, and on the other hand, we have the statistical average, symbolized by the subscript S. We also replaced the symbol $\langle \sigma_{aa}^j(t) \rangle$ by ρ_{aa} , just

to differentiate the various terms appearing in the following analysis. Later we will set $\rho_{aa} = 1$, consistent with the initial preparation of the atoms.

In the first term of (12.35), only terms with $j = k$ contribute, since the atoms are independent of each other. Also, we separate the second term into two contributions, one with $j = k$ and the other one with $j \neq k$. In this second term, we can write products of the type $\langle \sigma_{aa}^j(t_j) \sigma_{aa}^k(t_k) \rangle$ as ρ_{aa}^2 . We get the following result

$$\begin{aligned}\langle F_a(t)F_a(t') \rangle &= \left\langle \sum_{j,k} \Theta(t - t_j) \gamma \langle \sigma_{aa}^j(t) \rangle \right\rangle_S \delta(t - t') \\ &\quad + \left\langle \sum_j \delta(t - t_j) \delta(t' - t_j) \rho_{aa} \right\rangle_S \\ &\quad + \left[\left\langle \sum_{j \neq k} \delta(t - t_j) \delta(t' - t_k) \right\rangle_S - R^2 \right] \rho_{aa}^2,\end{aligned}$$

or, in final form

$$\begin{aligned}\langle F_a(t)F_a(t') \rangle &= \gamma \langle N_a \rangle \delta(t - t') + \left\langle \sum_j \delta(t - t_j) \right\rangle_S \rho_{aa} \delta(t - t') \quad (12.36) \\ &\quad + \left[\left\langle \sum_{j \neq k} \delta(t - t_j) \delta(t' - t_k) \right\rangle_S - R^2 \right] \rho_{aa}^2.\end{aligned}$$

In the Appendix C, we derive

$$\left[\left\langle \sum_{j \neq k} \delta(t - t_j) \delta(t' - t_k) \right\rangle_S - R^2 \right] \rho_{aa}^2 = -pR\delta(t - t'), \quad (12.37)$$

and show that

$$\langle F_a(t)F_a(t') \rangle = [\langle \gamma N_a \rangle + R(1 - p)] \delta(t - t'). \quad (12.38)$$

The rest of the correlation functions are calculated in a similar way. The result is, for the non-vanishing terms,

$$\langle F_M^\dagger(t)F_M(t') \rangle = [\langle \gamma N_a \rangle + R] \delta(t - t'). \quad (12.39)$$

$$\langle F_b(t)F_b(t') \rangle = \langle \gamma N_b \rangle \delta(t - t'). \quad (12.40)$$

$$\langle F_b(t)F_M(t') \rangle = \langle \gamma M \rangle \delta(t - t'). \quad (12.41)$$

The differential equations for the field and the atomic variables plus the noise correlation values completely describe the laser under arbitrary pump statistics.

12.2 C-Number Langevin Equations

In order to solve the present problem, we have to convert the four operator equations into *c*-number equations. To do that in a unique way, we have to define a prescribed ordering, the choice of which is completely arbitrary. We choose the following ordering: $a^\dagger, M^\dagger, N_a, N_b, M, a$. We now derive the equations of motion for their *c*-number versions $\varepsilon, \mathcal{M}, \mathcal{N}_a, \mathcal{N}_b$. Since the equations (12.25), (12.29), (12.31), (12.33) are already in the chosen normal order, we can write directly

$$\dot{\varepsilon} = -\frac{C}{2}\varepsilon + g\mathcal{M} + \mathcal{F}_C, \quad (12.42)$$

$$\dot{\mathcal{M}} = -\gamma\mathcal{M} + g(\mathcal{N}_a - \mathcal{N}_b)\varepsilon + \mathcal{F}_M, \quad (12.43)$$

$$\dot{\mathcal{N}}_a = R - \gamma\mathcal{N}_a - g(\varepsilon^*\mathcal{M} + \mathcal{M}^*\varepsilon) + \mathcal{F}_a, \quad (12.44)$$

$$\dot{\mathcal{N}}_b = -\gamma\mathcal{N}_b + g(\varepsilon^*\mathcal{M} + \mathcal{M}^*\varepsilon) + \mathcal{F}_b, \quad (12.45)$$

The Langevin forces \mathcal{F} have the following properties

$$\langle \mathcal{F}_k(t) \rangle = 0, \quad (12.46)$$

$$\langle \mathcal{F}_k(t)\mathcal{F}_l(t') \rangle = 2D_{kl}\delta(t-t'). \quad (12.47)$$

The diffusion coefficients D_{kl} are determined in such a way that the second moments calculated from the *c*-number equations agree with those calculated from the operator equations. To illustrate this procedure, we calculate D_{MM} .

From (12.32) we get

$$\begin{aligned} \frac{d}{dt} \langle M(t)M(t) \rangle &= -2\gamma\langle M \rangle + \langle MF_M \rangle \\ &\quad + \langle F_MM \rangle + g[\langle (N_a - N_b)Ma \rangle + \langle M(N_a - N_b)a \rangle] \end{aligned} \quad (12.48)$$

We notice that the second term in the square bracket is not in the normal form, therefore we use the commutation relation

$$[M, N_a - N_b] = 2M,$$

also the second and third terms vanish, so

$$\frac{d}{dt} \langle M(t)M(t) \rangle = -2\gamma\langle M \rangle + 2g\langle (N_a - N_b)Ma \rangle + 2g\langle Ma \rangle. \quad (12.49)$$

We now obtain the corresponding *c*-number equation

$$\frac{d}{dt} \langle \mathcal{M}\mathcal{M} \rangle = -2\gamma\langle \mathcal{M}\mathcal{M} \rangle + 2g[\langle (\mathcal{N}_a - \mathcal{N}_b)\mathcal{M}\varepsilon \rangle] + 2D_{MM}. \quad (12.50)$$

By comparing the right-hand sides of (12.49), (12.50), we readily get

$$2D_{MM} = 2g\langle \mathcal{M}\varepsilon \rangle. \quad (12.51)$$

In a similar way, we can calculate the rest of the diffusion coefficients as follows

$$\begin{aligned} 2D_{M^*M} &= \gamma\langle N_a \rangle + R \\ 2D_{MM} &= 2g\langle M\varepsilon \rangle \\ 2D_{N_bM} &= \gamma\langle M \rangle \\ 2D_{N_aN_a} &= \gamma\langle N_a \rangle + R(1-p) - g(\langle \varepsilon^* M + \varepsilon M^* \rangle) \\ 2D_{N_bN_b} &= \gamma\langle N_b \rangle - g(\langle \varepsilon^* M + \varepsilon M^* \rangle) \\ 2D_{N_aN_b} &= g(\langle \varepsilon^* M + \varepsilon M^* \rangle). \end{aligned}$$

12.2.1 Adiabatic Approximation

We now want to solve (12.42)–(12.45). Typically, in laser problems, the atomic decay constant γ is much larger than the photon decay C , or in other words, we have two very different time scales in the problem: a short time corresponding to a typical variation of the atomic variables and a much longer time over which there is a sizeable variation of the field. Under these conditions, we can use the adiabatic approximation, where we neglect the time derivatives of the atomic variables, thus calculating N_a, N_b, M , in terms of the field. The result is

$$M = \frac{g}{\gamma}(N_a - N_b)\varepsilon + \frac{\mathcal{F}_M}{\gamma}, \quad (12.52)$$

$$N_a = \frac{R \left(1 + \frac{2g^2}{\gamma^2} I\right) + \left(1 + \frac{2g^2}{\gamma^2} I\right) \mathcal{G}_a + \frac{2g^2}{\gamma^2} I \mathcal{G}_b}{\gamma(1 + \frac{4g^2}{\gamma^2} I)}, \quad (12.53)$$

$$N_b = \frac{R \frac{2g^2}{\gamma^2} I + \left(1 + \frac{2g^2}{\gamma^2} I\right) \mathcal{G}_b + \frac{2g^2}{\gamma^2} I \mathcal{G}_a}{\gamma(1 + \frac{4g^2}{\gamma^2} I)}, \quad (12.54)$$

where $I \equiv \varepsilon\varepsilon^*$ is the intensity of the field and the noise functions \mathcal{G}_a and \mathcal{G}_b are defined as

$$\mathcal{G}_a = \mathcal{F}_a - \frac{g}{\gamma}(\mathcal{F}_M^* \varepsilon + \varepsilon^* \mathcal{F}_M), \quad (12.55)$$

$$\mathcal{G}_b = \mathcal{F}_b + \frac{g}{\gamma}(\mathcal{F}_M^* \varepsilon + \varepsilon^* \mathcal{F}_M). \quad (12.56)$$

Now, if we replace the results of (12.52), (12.53), (12.54) in the equation of motion for ε (12.44) we get

$$\dot{\varepsilon} = -\frac{C}{2}\varepsilon + \frac{\mathcal{A}}{2} \left[\frac{1}{\left(1 + \frac{\beta}{\mathcal{A}I}\right)} \right] \varepsilon + \mathcal{F}_\varepsilon \quad (12.57)$$

where the parameters \mathcal{A} and β are the gain and saturation coefficient, defined as

$$\mathcal{A} = \frac{2g^2 R}{\gamma^2}, \quad \mathcal{B} = \frac{8g^4 R}{\gamma^4}, \quad (12.58)$$

and

$$\mathcal{F}_\varepsilon = \mathcal{F}_C + \frac{g}{\gamma} \mathcal{F}_M + \frac{g^2}{\gamma^2} \left[\frac{1}{(1 + \mathcal{B}/\mathcal{A}I)} \right] (\mathcal{G}_a - \mathcal{G}_b) \varepsilon. \quad (12.59)$$

The noise force \mathcal{F}_ε is characterized by the correlation functions

$$\langle \mathcal{F}_\varepsilon(t) \rangle = 0 \quad (12.60)$$

$$\langle \mathcal{F}_\varepsilon^*(t) \mathcal{F}_\varepsilon(t') \rangle = 2 \langle D_{\varepsilon^* \varepsilon} \rangle \delta(t - t'), \quad (12.61)$$

$$\langle \mathcal{F}_\varepsilon(t) \mathcal{F}_\varepsilon(t') \rangle = 2 \langle D_{\varepsilon \varepsilon} \rangle \delta(t - t'). \quad (12.62)$$

The diffusion coefficients $D_{\varepsilon^* \varepsilon}$ and $D_{\varepsilon \varepsilon}$ determine the strength of the noise and can be calculated, directly from the definition of $\mathcal{F}_\varepsilon(t)$. We leave it to the reader to verify that

$$2D_{\varepsilon \varepsilon} = -\mathcal{A} \left[\frac{1}{1 + \mathcal{B}/\mathcal{A}I} \right]^2 \frac{\mathcal{B}\varepsilon^2}{4\mathcal{A}} \left[3 + \frac{p}{2} + \left(\frac{\mathcal{B}}{\mathcal{A}I} \right) \right], \quad (12.63)$$

$$2D_{\varepsilon^* \varepsilon} = \mathcal{A} \left[\frac{1}{1 + \mathcal{B}/\mathcal{A}I} \right]^2 \left[1 + \left(\frac{\mathcal{B}I}{4\mathcal{A}} \right) \left(3 - \frac{p}{2} + \frac{\mathcal{B}}{\mathcal{A}I} \right) \right]. \quad (12.64)$$

With the above results, we are now ready to calculate the phase and intensity fluctuations in the laser, in terms of the various parameters, including the pump statistics.

12.3 Phase and Intensity Fluctuations

In this section, we analyse the fluctuation properties of the phase and intensity of the field. For this purpose, we write the field amplitude in polar coordinates, that is

$$\varepsilon = \sqrt{I} \exp i\varphi. \quad (12.65)$$

From (12.57), we now derive two differential equations for I and φ :

$$\dot{\varphi} = F_\varphi, \quad (12.66)$$

$$\dot{I} = -CI + \frac{\mathcal{A}}{1 + \mathcal{B}/\mathcal{A}I} I + F_I. \quad (12.67)$$

In (12.67), we neglected the small contribution to the drift due to noise.

The diffusion coefficients corresponding to the noise forces F_I and F_φ are found to be

$$D_{\varphi \varphi} = \frac{\mathcal{A}}{4I} \left[\frac{1}{1 + \mathcal{B}/\mathcal{A}I} \right] \left(1 + \frac{\mathcal{B}}{2\mathcal{A}} I \right), \quad (12.68)$$

and

$$D_{II} = \frac{\mathcal{A}}{(1 + \mathcal{B}/\mathcal{A}I)^2} \left[1 - p \frac{\mathcal{B}}{4\mathcal{A}} I \right] I. \quad (12.69)$$

12.4 Discussion

The quantum mechanical description of the amplitude and phase and their measurement has turned out to be troublesome and it is still a matter of discussion [12.3]. Early attempts to introduce the amplitude and phase operators in a quantum formalism goes back to Dirac in 1927. However, if the photon number is large, we can bypass the above complications and state that the phase in (12.65) is in excellent agreement with the measured phase of the electromagnetic field, and we can identify φ with the phase of the radiation field.

As far as the intensity I is concerned, we have to be careful, since this classical quantity was originally associated with normally ordered operators. For the photon number average, there is no ordering problem, and one has

$$\langle n \rangle = \langle a^\dagger a \rangle = \langle I \rangle; \quad (12.70)$$

however, for the photon number fluctuations

$$\begin{aligned} \langle (\Delta n)^2 \rangle &= \langle a^\dagger a a^\dagger a \rangle - \langle a^\dagger a \rangle^2 \\ &= \langle a^\dagger a^\dagger a a \rangle - \langle a^\dagger a \rangle^2 + \langle a^\dagger a \rangle \\ &= \langle I^2 \rangle - \langle I \rangle^2 + \langle I \rangle \\ &= \langle (\Delta I)^2 \rangle + \langle I \rangle. \end{aligned} \quad (12.71)$$

The steady state intensity is easily found by setting the drift term in (12.67) equal to zero, thus getting

$$I_0 = \frac{\mathcal{A}(\mathcal{A} - C)}{\mathcal{B}C}. \quad (12.72)$$

We now turn our attention to the phase diffusion. Using (12.66), we can write

$$\begin{aligned} \frac{d}{dt} \langle \varphi^2 \rangle &= \frac{d}{dt} \int_0^t dt' \int_0^t dt'' \langle \dot{\varphi}(t') \dot{\varphi}(t'') \rangle \\ &= \frac{d}{dt} \int_0^t dt' \int_0^t dt'' \langle F_\varphi(t') F_\varphi(t'') \rangle \\ &= \langle 2D_{\varphi\varphi} \rangle. \end{aligned} \quad (12.73)$$

If we now substitute the expression for $D_{\varphi\varphi}$ into (12.73), and integrate, we get

$$\langle \varphi^2 \rangle = \frac{1}{4I_0} + \frac{\mathcal{A} + C}{4I_0} t. \quad (12.74)$$

The integration constant $1/4I_0$ comes from the vacuum fluctuations, and can be considered an added noise to the one generated by the spontaneous emission, which corresponds to the second term in (12.74). This last result is the well-known Schawlow–Townes result [12.4], which states that the laser phase diffuses linearly in time. An important observation is that the phase diffusion is independent of the pump parameter p . Therefore, the phase of the electromagnetic field is completely independent of the particular pump mechanism. On the other hand, the intensity diffusion depends on p and hence we expect the photon number fluctuations to also depend on the pump parameter.

Now, we proceed to study the intensity fluctuations around its steady state value. For that purpose, we define $\Delta I = I - I_0$, and linearizing (12.67), we get

$$\frac{d}{dt}(\Delta I) = -C \frac{\mathcal{A} - C}{\mathcal{A}} \Delta I + F_I. \quad (12.75)$$

Equation (12.75) describes a simple Markov process. This type of stochastic differential equation, with a linear drift term, is called an Ornstein–Uhlenbeck differential equation (for an introduction to the subject, see Appendix D [12.5], [12.6]).

The steady state variance of an Ornstein–Uhlenbeck process is given by

$$\langle (\Delta I)^2 \rangle = \frac{D_{II}}{C(\mathcal{A} - C)/\mathcal{A}}. \quad (12.76)$$

Combining (12.69), (12.71) and (12.76), we readily get

$$\langle (\Delta n)^2 \rangle = \left(\frac{\mathcal{A}}{\mathcal{A} - C} - \frac{p}{4} \right) n_0, \quad (12.77)$$

where $n_0 = I_0$ is the average photon number inside the cavity. As pointed out in the last chapter, the photon number fluctuations crucially depend on the particular pump mechanism. In the case of Poisson statistics ($p = 0$), the variance of the photon number is always greater than the mean photon number, and in the high-intensity limit, both quantities tend to be equal, which, as seen in the last chapter, corresponds to a Poisson distribution for the photons.

On the other hand, for a pump noise suppressed laser ($p > 0$), the photon number variance can be smaller than n_0 , which corresponds to sub-Poissonian photon statistics. The optimum noise reduction corresponds to the high-intensity limit ($\mathcal{A} \gg C$) with a regular injection ($p = 1$), in which case

$$\langle (\Delta n)^2 \rangle = 0.75n_0, \quad (12.78)$$

which corresponds to a 25% noise reduction in the photon number fluctuations, with respect to the Poissonian case.

In this theory, we assumed for simplicity that the atomic decay times of both levels were equal, $\gamma_a = \gamma_b = \gamma$. This may not be true in some laser

systems. For the more general case, the decay constants for N_a, N_b, M are γ_a, γ_b and Γ respectively. A calculation completely analogous to the present one gives:

$$\langle (\Delta n)^2 \rangle = \left[\frac{A}{A - C} - \frac{\gamma_a}{\gamma_b + \gamma_a} \frac{p}{2} \right] n_0. \quad (12.79)$$

As we can see from (12.79), in the high-intensity limit and in the case $\gamma_b \ll \gamma_a$, if the injection is regular, we may reduce the photon number variance by 50% with respect to the Poissonian case. (Some publications speak of 50% photon number squeezing; we prefer to use this word only in relation to quadratures, to avoid confusion [12.7].)

Finally, lasers with a small active medium volume were recently developed, like vertical cavity surface emitting semiconductor lasers [12.8, 12.9], heterostructure diode lasers [12.10], microdroplets [12.11], high-Q Fabry Perot microcavity lasers [12.12]. A quantum theory of the thresholdless laser was developed by Protschenko *et al.* [12.13] based on the Heisenberg-Langevin equations of motion for the atomic and field operators.

Problems

- 12.1 Verify the atomic noise correlations given by (12.17)–(12.20).
- 12.2. Prove (12.39)–(12.41).
- 12.3. Prove (12.63) and (12.64).
- 12.4. Prove (12.68) and (12.69).

13. Quantum Noise Reduction I

In many areas of modern physics, ultrasmall displacements are detected optically. The small displacement is converted into a change of optical path length in an interferometer. This detection scheme is usually done in two ways:

- (1) In a passive detection scheme, laser light, generated outside, is sent through a cavity and the change in the path length results in a phase shift. The shift is then detected by homodyning the output beam with a reference beam. This phase shift is generally small, since the light spends only a finite time in the cavity, limited by the cavity lifetime. In this type of measurement, the limiting noise source is the photon-counting error or shot noise, reflecting the photon number fluctuations at the detector.
- (2) In the so-called active detection scheme, the laser light is generated inside the cavity and the operating frequency of the system changes due to the change in the path length, which results in a phase shift proportional to the measurement time, leading in general to a bigger signal as compared to the first case. The shift is then detected by heterodyning the output light with that from a reference beam. The limiting quantum noise source, in this case, is the spontaneous fluctuations of the relative phase between the two lasers, or in other words, the relative phase diffusion noise.

The question posed in the first part of this chapter is: Can one possibly quench the spontaneous emission quantum noise from the relative phase of two lasers? The whole subject of the correlated emission laser (CEL) is directed to answering this particular question.

A geometrical representation of the CEL is shown in Fig. 13.1, where $\delta\epsilon_1$ and $\delta\epsilon_2$ are the contributions to the fields 1 and 2 by spontaneous emission of a photon in the two respective modes. To get an intuitive picture of the effect, consider three-level atoms in a double cavity, interacting with two quantum fields, E_1 and E_2 , and a classical microwave field E_3 , resonant with the upper two levels and originating the necessary correlation between the spontaneous emission into the fields 1 and 2 (Fig. 13.2). In this case, the spontaneously emitted fields 1 and 2 are strongly correlated. To see this, consider a state vector given by [13.1]

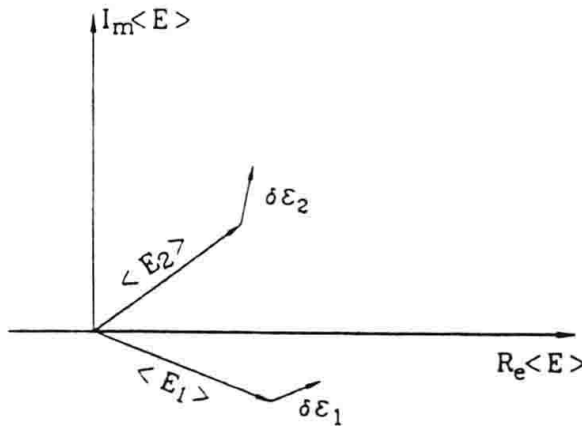


Fig. 13.1. Geometrical representation of the correlated emission laser. $\delta\epsilon_1$ and $\delta\epsilon_2$ are the contributions of a spontaneously emitted photon in modes 1 and 2, respectively

$$|\psi\rangle = \alpha \exp(-i\phi_a) |a, 0\rangle + \beta \exp(-i\phi_b) |b, 0\rangle + \gamma_1 |c, 1_1\rangle + \gamma_2 |c, 1_2\rangle, \quad (13.1)$$

where $1_i, i = 1, 2$, correspond to a photon emitted into the fields 1 and 2, respectively. Now, the expectation value of the fields

$$E_i = \epsilon_i a_i \exp(i(\mathbf{k}_i \cdot \mathbf{r} - \nu_i t)), \quad i = 1, 2 \quad (13.2)$$

vanishes, due to the orthogonality of the atomic states. However, the crossed term does not vanish:

$$\langle \psi | E_1^\dagger E_2 | \psi \rangle = \epsilon_1 \epsilon_2 \gamma_1^* \gamma_2 \exp[-i(\mathbf{k}_1 - \mathbf{k}_2) \cdot \mathbf{r} + i(\nu_1 - \nu_2)t], \quad (13.3)$$

thus giving a clear indication that the spontaneously emitted photons at frequencies ν_1 and ν_2 are correlated.

Strongly motivated by the above arguments, we are led to investigate the diffusion of the relative phase angle between the two modes, in a system where the lasing three-level atoms are placed in a double cavity.

13.1 Correlated Emission Laser (CEL) Systems: The Quantum Beat Laser

13.1.1 The Model

We consider the system described in Fig. 13.2, in which three-level atoms are being pumped into a state $|a\rangle$ at a rate r_a . The external field at frequency ν_3 is characterized by a Rabi frequency Ω . The Hamiltonian is

$$H = H_0 + V, \quad (13.4)$$

where

$$H_0 = \sum_{i=a,b,c} \hbar\omega_i |i\rangle\langle i| + \hbar\nu_1 a_1^\dagger a_1 + \hbar\nu_2 a_2^\dagger a_2, \quad (13.5)$$

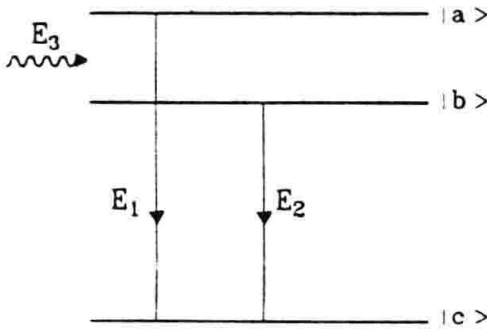


Fig. 13.2. In the three-level atom, the two upper levels a and b are coupled to a classical microwave field of frequency ν_3 . The emissions from the $b-c$ and $a-c$ transitions are strongly correlated

and

$$\begin{aligned} V = & \hbar g_1 (a_1 |a\rangle\langle c| + a_1^\dagger |c\rangle\langle a|) \\ & + \hbar g_2 (a_2 |b\rangle\langle c| + a_2^\dagger |c\rangle\langle b|) \\ & - \frac{\hbar\Omega}{2} (\exp(-iv_3t - i\phi) |a\rangle\langle b| + \exp(iv_3t + i\phi) |b\rangle\langle a|). \end{aligned} \quad (13.6)$$

It is convenient to use the interaction picture

$$V_I = \exp\left(\frac{i}{\hbar}H_0t\right)(V)\exp\left(-\frac{i}{\hbar}H_0t\right). \quad (13.7)$$

After a direct calculation, one finds that

$$V_I = V_1 + V_2, \quad (13.8)$$

with

$$V_1 = -\frac{\hbar\Omega}{2} \begin{pmatrix} 0 & \exp(-i\phi) & 0 \\ \exp(i\phi) & 0 & 0 \\ 0 & 0 & 0 \end{pmatrix}, \quad (13.9)$$

and

$$V_2 = \hbar \begin{bmatrix} 0 & 0 & g_1 a_1 \exp(i\Delta_1 t) \\ 0 & 0 & g_2 a_2 \exp(i\Delta_2 t) \\ g_1 a_1^\dagger \exp(-i\Delta_1 t) & g_2 a_2^\dagger \exp(-i\Delta_2 t) & 0 \end{bmatrix}. \quad (13.10)$$

In (13.10), we introduced the definitions

$$\Delta_1 = \omega_a - \omega_c - v_1; \quad \Delta_2 = \omega_b - \omega_c - v_2. \quad (13.11)$$

In the future, we will assume that $\Delta_1 = \Delta_2 = \Delta$ and that the driving field is resonant with the $a-b$ transition.

Our next goal is to approximate our Hamiltonian model so as to end up with a time-independent Hamiltonian after some sort of rotating-wave approximation. This is most easily achieved by introducing a second interaction picture [13.2]

$$V_{II} = \exp\left(\frac{i}{\hbar}V_1 t\right)V_2 \exp\left(-\frac{i}{\hbar}V_1 t\right). \quad (13.12)$$

One can easily check the following properties of V_1 :

$$(V_1)^{2n} = \left(\frac{\hbar\Omega}{2}\right)^{2n} \begin{bmatrix} 1 & 0 & 0 \\ 0 & 1 & 0 \\ 0 & 0 & 0 \end{bmatrix}, \quad (13.13)$$

$$(V_1)^{2n+1} = \left(\frac{\hbar\Omega}{2}\right)^{2n} (V_1).$$

With the above expressions, one can calculate the transformation explicitly:

$$\exp\left(\pm\frac{i}{\hbar}V_1 t\right) = \begin{bmatrix} \cos(\frac{\Omega}{2})t & \mp i \sin(\frac{\Omega}{2})t \exp(-i\phi) & 0 \\ \mp i \sin(\frac{\Omega}{2})t \exp(i\phi) & \cos(\frac{\Omega}{2})t & 0 \\ 0 & 0 & 1 \end{bmatrix}. \quad (13.14)$$

and now one can calculate explicitly the interaction Hamiltonian

$$V_{II} = \begin{pmatrix} 0 & 0 & V_{ac} \\ 0 & 0 & V_{bc} \\ V_{ac}^\dagger & V_{bc}^\dagger & 0 \end{pmatrix}, \quad (13.15)$$

where

$$V_{ac} = \frac{1}{2} \left(\exp\left[i\left(\Delta + \frac{\Omega}{2}\right)t\right] (g_1 a_1 - g_2 a_2 \exp(-i\phi)) \right) + \exp\left[i\left(\Delta - \frac{\Omega}{2}\right)t\right] (g_1 a_1 + g_2 a_2 \exp(-i\phi)), \quad (13.16)$$

$$V_{bc} = \frac{1}{2} \left(-\exp\left[i\left(\Delta + \frac{\Omega}{2}\right)t\right] (g_1 a_1 \exp(i\phi) - g_2 a_2) + \exp\left[i\left(\Delta - \frac{\Omega}{2}\right)t\right] (g_1 a_1 \exp(i\phi) + g_2 a_2) \right).$$

The condition on CEL found in reference [13.3] was $\Delta = \Omega/2$. We immediately see that this condition is appealing, since one of the time dependences disappears and the other term proportional to $\exp 2\Delta t$ can be neglected in a rotating-wave approximation. The conditions of validity of this approximation will be discussed later.

We define, for convenience, a non-Hermitian operator A

$$A \equiv \frac{g_1 a_1 \exp(i\phi) + g_2 a_2 \exp(-i\phi)}{\sqrt{g_1^2 + g_2^2}}, \quad (13.17)$$

so that it is easy to verify that

$$[A, A^\dagger] = 1, \quad (13.18)$$

and

$$V_{II} = \hbar g \begin{pmatrix} 0 & 0 & A \exp(-i\frac{\phi}{2}) \\ 0 & 0 & A \exp(i\frac{\phi}{2}) \\ A^\dagger \exp(i\frac{\phi}{2}) & A^\dagger \exp(-i\frac{\phi}{2}) & 0 \end{pmatrix}, \quad (13.19)$$

with $g \equiv \frac{1}{2} \sqrt{g_1^2 + g_2^2}$.

13.1.2 The Solution

We are now going to develop the non-linear theory of the quantum beat laser, whose Hamiltonian is given in (13.19). Schrödinger's equation, in the second interaction picture, is

$$i\hbar \frac{\partial \psi}{\partial t} = V_{II}\psi. \quad (13.20)$$

Here, ψ is a column vector with three components, ψ_a, ψ_b, ψ_c . We get the following coupled equations

$$\begin{aligned} i \frac{\partial \psi_a}{\partial t} &= gA\psi_c - i\frac{\gamma}{2}\psi_a, \\ i \frac{\partial \psi_b}{\partial t} &= gA\psi_c - i\frac{\gamma}{2}\psi_b, \\ i \frac{\partial \psi_c}{\partial t} &= gA^\dagger\psi_a + gA^\dagger\psi_b - i\frac{\gamma}{2}\psi_c. \end{aligned} \quad (13.21)$$

In (13.21), ϕ was eliminated by a trivial transformation: $\psi_a \exp(i\phi/2) \rightarrow \psi_a, \psi_b \exp(-i\phi/2) \rightarrow \psi_b$. Also, we have introduced the phenomenological decay constant γ which, for simplicity, is the same for all three levels.

The solution is

$$\begin{aligned} \psi_a = \psi_b &= \frac{1}{\sqrt{2}} \exp -\frac{\gamma}{2}(t - t_0) \cos [g\sqrt{2AA^\dagger}(t - t_0)] \psi_f(t_0), \\ \psi_c &= -i \exp -\frac{\gamma}{2}(t - t_0) A^{-1} (AA^\dagger)^{\frac{1}{2}} \sin [g\sqrt{2AA^\dagger}(t - t_0)] \psi_f(t_0), \end{aligned} \quad (13.22)$$

where we have taken the initial condition with the atom injected in the excited state, that is $\psi_a(t_0) = \psi_f(t_0)$, a function of the field variables only.

13.1.3 The Master Equation

For the second interaction picture, one can write

$$\frac{d\rho}{dt} = -\frac{i}{\hbar} [V_{II}, \rho]. \quad (13.23)$$

The reduced density operator for the field is $\rho_f = \text{Tr}\rho$. Making use of (13.19), one can write

$$\frac{d\rho_f}{dt} = -ig \{ [A, (\rho_{ca} + \rho_{cb})] + [A^\dagger, (\rho_{ac} + \rho_{bc})] \} + L, \quad (13.24)$$

where L is the loss term to be specified later. We need to calculate $(\rho_{ac} + \rho_{bc})$. We adopt the following procedure [13.4]: we first calculate the one-atom contribution injected at time t_0 into the upper level $|a\rangle$ and then add all the contributions from $t - \gamma^{-1}$ to t :

$$\begin{aligned}
& (\rho_{ac} + \rho_{bc}) \\
&= r_a \int_{t-\gamma^{-1}}^t dt_0 [\psi_a(t, t_0) + \psi_b(t, t_0)] \psi_c^\dagger(t, t_0) \\
&= \sqrt{2}i r_a \int_{t-\gamma^{-1}}^t dt_0 \exp -\gamma(t-t_0) \cos [g\sqrt{2}(AA^\dagger)^{\frac{1}{2}}(t-t_0)] \rho_f(t) \\
&\quad \times \sin [g\sqrt{2}(AA^\dagger)^{\frac{1}{2}}(t-t_0)] (AA^\dagger)^{\frac{1}{2}}(A^\dagger)^{-1}.
\end{aligned} \tag{13.25}$$

In this expression, we replaced $\rho_f(t_0) \rightarrow \rho_f(t)$, an assumption that is true only if the cavity time is much longer than the atomic characteristic times, and if during the interaction time ρ_f does not change appreciably. Then we extend the lower limit to $-\infty$ since, due to the exponential damping factor in the integrand, the contribution from $t_0 < t - \gamma^{-1}$ is negligible.

Now, taking the nn' matrix elements, and substituting $(A^\dagger)^{-1} \rightarrow (AA^\dagger)^{-1}A$, when acting on the right, one gets

$$(\rho_{ac} + \rho_{bc})_{n,n'} = ir_a g(R_{n+1,n'}^+ - R_{n+1,n'}^-) \rho_{fn,n'-1}, \tag{13.26}$$

where

$$R_{n,n'}^\pm = \frac{(\sqrt{n} \pm \sqrt{n'})^2}{\gamma^2 + 2g^2(\sqrt{n} \pm \sqrt{n'})^2}. \tag{13.27}$$

Next, we specify the loss term in the usual way

$$\begin{aligned}
L = & -\frac{\nu_1}{2Q_1}(a_1^\dagger a_1 \rho_f + \rho_f a_1^\dagger a_1 - 2a_1 \rho_f a_1^\dagger) \\
& -\frac{\nu_2}{2Q_2}(a_2^\dagger a_2 \rho_f + \rho_f a_2^\dagger a_2 - 2a_2 \rho_f a_2^\dagger).
\end{aligned} \tag{13.28}$$

For convenience, we now introduce a B -mode

$$B \equiv \frac{g_2 a_1 - g_1 a_2}{(g_1^2 + g_2^2)^{\frac{1}{2}}}, \tag{13.29}$$

with the properties

$$[B, B^\dagger] = 1, \quad [A, B] = [A, B^\dagger] = 0, \tag{13.30}$$

that is, the A and B modes are independent. One can write a_1 and a_2 in terms of A and B and use it in (13.29).

Finally, using (13.26) and its Hermitian conjugate, (13.29), and substituting them into (13.24), we obtain the master equation for the field density operator (for simplicity, we skip the subindex f)

$$\begin{aligned}
\frac{d\rho_{n_A,n_B}}{dt} = & \left[\left(\frac{\sqrt{n_A n'_A} \mathcal{A}}{1 + \mathcal{N}_{n_A-1,n'_A-1} \frac{\mathcal{B}}{\mathcal{A}}} \right) \rho_{n_A-1,n_B} \right. \\
& \left. - \left(\frac{\mathcal{N}'_{n_A,n'_A} \mathcal{A}}{1 + \mathcal{N}_{n_A,n'_A} \frac{\mathcal{B}}{\mathcal{A}}} \right) \rho_{n'_A,n_B} \right]
\end{aligned} \tag{13.31}$$

$$\begin{aligned}
& -\frac{\gamma_c}{2} \left\{ (n_A + n'_A + n_B + n'_B) \rho_{n_A, n_B} \right. \\
& - 2\sqrt{(n_A + 1)(n'_A + 1)} \rho_{n_A+1, n_B} \\
& \left. - 2\sqrt{(n_B + 1)(n'_B + 1)} \rho_{n_A, 1+n_B} \right\}.
\end{aligned}$$

Here, for simplicity, we assumed that $\nu_1/Q_1 = \nu_2/Q_2 \equiv \gamma_c$, and the definitions of \mathcal{A} , \mathcal{B} , \mathcal{N} , \mathcal{N}' are given in (11.27), (11.24).

Since the A and B modes are independent, the solution of the master equation must be separable:

$$\rho_{n_A, n_B}^{(A)}(t) = \rho_{n_A, n'_A}^{(A)}(t) \rho_{n_B, n'_B}^{(B)}(t). \quad (13.32)$$

13.1.4 Photon Statistics

We take the steady state case, that is for $d/dt = 0$, and the diagonal terms only, to determine the photon statistics. It is quite apparent that there is no gain term in the B -mode, which just damps away. The solution is

$$\rho_{n_B, n'_B}^{(B)} = \delta_{n_B, 0}. \quad (13.33)$$

On the other hand, the A -mode satisfies the usual one-mode, two-level laser difference equation

$$\left(\frac{n\mathcal{A}}{1 + \mathcal{N}_{n-1, n-1}\mathcal{B}/\mathcal{A}} \right) \rho_{n-1, n-1}^{(A)} - \left[\frac{(n+1)\mathcal{A}}{1 + \mathcal{N}_{n, n}\mathcal{B}/\mathcal{A}} \right] \rho_{n, n}^{(A)} \quad (13.34)$$

$$-\gamma_c \left[n\rho_{n, n}^{(A)} - (n+1)\rho_{n+1, n+1}^{(A)} \right] = 0. \quad (13.35)$$

As we can see, in terms of the composite mode A , the quantum beat laser exhibits the same type of behaviour, as far as photon statistics, threshold or saturation properties are concerned, as the one-mode laser.

Phase Diffusion. In this section we will prove that there is, for the quantum beat laser, a complete noise quenching of the relative phase of the two quantum modes. We start by defining a beat signal as

$$\begin{aligned}
BS &= \text{Re} \left\{ \exp [i(\nu_1 - \nu_2)t] \text{Tr} \left\{ a_1^\dagger a_2 \rho \right\} \right\} \\
&= \text{Re} \left\{ \exp i\nu_3 t \text{Tr} [(A^\dagger A - B^\dagger B + AB^\dagger - A^\dagger B)\rho] \right\},
\end{aligned} \quad (13.36)$$

where we assumed for simplicity $g_1 = g_2$.

Now, performing the separation indicated in (13.32), we get two time-dependent master equations

$$\begin{aligned} \frac{d\rho_{n,n'}^{(A)}}{dt} = & \left[\frac{\sqrt{nn'}\mathcal{A}}{1 + \mathcal{N}_{n-1,n'-1}(\mathcal{B}/\mathcal{A})} \right] \rho_{n-1,n'-1}^{(A)} \\ & - \left[\frac{\mathcal{N}'_{n,n'}\mathcal{A}}{1 + \mathcal{N}_{n,n'}(\mathcal{B}/\mathcal{A})} \right] \rho_{n,n'}^{(A)} \\ & - \frac{\gamma_c}{2} \left[(n+n')\rho_{n,n'}^{(A)} - 2\sqrt{(n+1)(n'+1)}\rho_{n+1,n'+1}^{(A)} \right], \end{aligned} \quad (13.37)$$

$$\frac{d\rho_{n,n'}^{(B)}}{dt} = -\frac{\gamma_c}{2} \left[(n+n')\rho_{n,n'}^{(B)} - 2\sqrt{(n+1)(n'+1)}\rho_{n+1,n'+1}^{(B)} \right]. \quad (13.38)$$

Looking at the time-dependent solutions of (13.37), one writes the general solution in the form [13.4]

$$\rho_{n,n+p} = \sum_{j=0}^{\infty} \phi_j(n,p) \exp(-\mu_j^{(p)} t). \quad (13.39)$$

As we have already seen from the laser theory, the lowest eigenvalue is $\mu_0^{(0)} = 0$, thus giving a non-vanishing stationary solution for the diagonal elements. Also, $\mu_j^{(p)} > 0$ for $p \neq 0$, so that the off-diagonal elements of the field density matrix go to zero for long times.

In the case of an ordinary two-mode laser, the density matrix corresponding to the two modes factorizes as

$$\rho^{(1,2)} = \rho^1 \rho^2, \quad (13.40)$$

so that the beat signal is

$$\text{Re}\langle a_1^\dagger a_2 \rangle_{\text{OL}} = \frac{1}{2} \left[\sum_{n,n'} \rho_{n,n+1}^{(1)}(t) \rho_{n',n'-1}^{(2)}(t) \sqrt{(n+1)n'} + \text{cc} \right], \quad (13.41)$$

and according to (13.39) the above expression vanishes at a rate $\mu_0^{(1)}$. This defines the phase diffusion coefficient as

$$\mu_0^{(1)} = \frac{D}{2}, \quad (13.42)$$

where D is the Schawlow–Townes linewidth.

In the case of the quantum beat laser, this does not happen, since (13.36) contains diagonal elements in $A^\dagger A$, so

$$\text{Re}\langle a_1^\dagger a_2 \rangle_{\text{QBL}} \sim \sum_n n \rho_{n,n}^{(A)} + \dots, \quad (13.43)$$

and since $\mu_0^{(0)} = 0$, there is always a non-zero part of the beat signal.

If we keep the definition of the diffusion coefficient as twice the lowest decay rate, then we conclude that $D = 0$, for the relative phase of the two modes.

A more formal and longer derivation can be done, using Glauber's P -representation to obtain a Fokker–Planck equation in α and α^* , which can

be converted into polar form, in terms of the two amplitudes ρ_1 and ρ_2 and the two phases θ_1 and θ_2 of the two modes. Then one finds that the phase difference $\theta \equiv \theta_1 - \theta_2$ locks to zero and $D(\theta) = 0$. (The details of this rather long calculation can be found in reference [13.2].)

13.2 Other CEL Systems

The active medium can also be prepared in a coherent superposition of the $|a\rangle$ and $|b\rangle$ states which decay to the state $|c\rangle$, via emission of different polarization states. This is the Hanle effect and it can be achieved with a polarization-sensitive mirror to couple the doubly resonant cavity.

Another CEL system is a ring laser whose counter-propagating modes are coupled by a spatial modulation in the gain medium. This is the holographic laser [13.5], where each beam is reflected in part by the thin atomic layers of the gain medium. When the reflected light interferes constructively with the light of the counter-propagating beam, noise quenching is achieved.

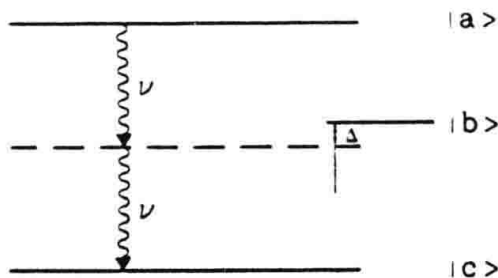


Fig. 13.3. The two-photon correlated emission laser. The active medium consists of three-level atoms in a cascade configuration. The cavity is tuned at ν and the intermediate level is off resonance with respect the centre of the transition

A last example is the two-photon CEL [13.6], which is the extension of the CEL principle in a system where the active medium consists in three-level atoms in the cascade configuration driving a cavity resonant with $\nu_1 = (\omega_a - \omega_c)/2$ as shown in Fig. 13.3. We are again interested in investigating the role of the atomic coherence between the most distant levels a and c in quenching the noise. As it turns out, this system is not only capable of quenching the quantum noise of an active system, but also under certain conditions, reduces the phase noise below the shot noise level, producing a squeezed output. We shall not go into the theoretical details of these systems, since they operate under the same basic principle.

Problems

13.1. Prove (13.13), (13.15), (13.16).

13.2 Show, for the quantum beat laser, that the relative phase diffusion coefficient is given by

$$D(\theta) = \frac{g^2 r}{4\gamma^2 \langle n \rangle} (1 - \cos \theta) - \frac{g^4 r}{\gamma^4} (1 - \cos 2\theta),$$

where γ is the atomic decay and g the same coupling constant for the two modes with the respective transitions. Notice that for $\theta = 0$, $D(\theta) = 0$ [13.2].

13.3. Prove that the drift coefficient of the Fokker–Planck equation $d(\theta)$ vanishes for $\theta = 0$, thus giving the required phase locking to achieve $D(\theta) = 0$ [13.2].

14. Quantum Noise Reduction II

In this chapter we will cover the area of theory and relevant experiments in the generation of squeezed states. Prior to discussing the parametric oscillator, we offer a brief introduction to non-linear optics and input-output theory. Finally, we will discuss other important experiments that generate squeezed states.

14.1 Introduction to Non-linear Optics

Light of a given frequency, falling on an atomic system, can give rise to different frequencies. Even stronger effects can be obtained if, instead of an atomic system, one has a large number of atoms or some particular crystal like quartz, ADP, KDP, etc. One of the early experiments [14.1] generated, with a ruby laser falling onto a quartz crystal, blue light of $\lambda = 3472 \text{ \AA}$, starting from the original red light of $\lambda = 6943 \text{ \AA}$. This experiment demonstrated for the first time the non-linear optical effect of second harmonic generation. Since then, the growth of the field of non-linear optics has been explosive [14.2], [14.3], [14.4], [14.5].

We will be interested in some quantum non-linear effects related to the generation of squeezed states. In order to explore the origin of these phenomena, we go back to the atom-radiation interaction model, to study multiple photon transitions.

14.1.1 Multiple Photon Transitions

The atom-radiation interaction Hamiltonian can be written as [14.6]

$$H = H_0 + H_1, \quad (14.1)$$

where H_0 is the Hamiltonian of the uncoupled radiation H_r plus the bound electrons H_e

$$H_0 = H_r + H_e, \quad (14.2)$$

and, in the dipole approximation, H_1 is the interaction term

$$H_1 = -e\mathbf{r} \cdot \mathbf{E}(\mathbf{r}, t). \quad (14.3)$$

If the initial state of the system is $|\phi(t_0)\rangle$, at time t it will be

$$|\phi(t)\rangle = \exp\left[-\left(\frac{iH(t-t_0)}{\hbar}\right)\right]|\phi(t_0)\rangle. \quad (14.4)$$

On the other hand, let $|i\rangle$ and $|f\rangle$ be eigenstates of the unperturbed energy

$$H_0|i\rangle = \hbar\omega_i|i\rangle, \quad (14.5)$$

$$H_0|f\rangle = \hbar\omega_f|f\rangle.$$

Then, if

$$|\phi(t_0)\rangle = |i\rangle, \quad (14.6)$$

that is, initially the system is in an eigenstate of the unperturbed Hamiltonian H_0 , then the probability for the system to be in $|f\rangle$ at time t is

$$P_{if} = \left| \left\langle f \left| \exp\left(-\frac{iH(t-t_0)}{\hbar}\right) \right| i \right\rangle \right|^2. \quad (14.7)$$

Of course the transition rate of the system from $|i\rangle$ to $|f\rangle$ is the time derivative of the above expression.

In general, there is a range of final states in an experimental observation. Thus one can define a transition rate as

$$\frac{1}{\tau} = \frac{d}{dt} \sum_f \left| \left\langle f \left| \exp\left(-\frac{iH(t-t_0)}{\hbar}\right) \right| i \right\rangle \right|^2. \quad (14.8)$$

The above expression is not very practical, since the relevant term for transitions in the Hamiltonian is H_1 , which does not commute with H_0 . However, we make use of the following trick:

$$\begin{aligned} & \exp\left(\frac{iH_0t}{\hbar}\right) H_1 \exp\left(-\frac{iHt}{\hbar}\right) \\ &= i\hbar \frac{d}{dt} \left\{ \exp\left(\frac{iH_0t}{\hbar}\right) \exp\left(-\frac{iHt}{\hbar}\right) \right\}. \end{aligned} \quad (14.9)$$

The above relation can be easily verified by performing the derivative on the right-hand side of (14.9). Next, we integrate both sides

$$\begin{aligned} & \int_{t_0}^t \exp\left(\frac{iH_0t_1}{\hbar}\right) H_1 \exp\left(-\frac{iHt_1}{\hbar}\right) dt_1 \\ &= i\hbar \left\{ \exp\left(\frac{iH_0t}{\hbar}\right) \exp\left(-\frac{iHt}{\hbar}\right) - \exp\left(\frac{iH_0t_0}{\hbar}\right) \exp\left(-\frac{iHt_0}{\hbar}\right) \right\}, \end{aligned}$$

so

$$\begin{aligned} \exp\left(-\frac{iHt}{\hbar}\right) &= \exp\left(-\frac{iH_0t}{\hbar}\right) \left\{ \exp\left(\frac{iH_0t_0}{\hbar}\right) \exp\left(-\frac{iHt_0}{\hbar}\right) \right. \\ &\quad \left. - \frac{i}{\hbar} \int_{t_0}^t \exp\left(\frac{iH_0t_1}{\hbar}\right) H_1 \exp\left(-\frac{iHt_1}{\hbar}\right) dt_1 \right\}. \end{aligned} \quad (14.10)$$

If one is interested in steady state transitions, we can assume that $t_0 \rightarrow -\infty$, and $H_1(t_0) = 0$.

Also, if one wants the interaction to be switched on in a smooth way, we introduce an $\exp(\varepsilon t_1)$ term, which we can conveniently eliminate at the end of the calculation by setting $\varepsilon \rightarrow 0$. Then:

$$\begin{aligned} \exp\left(-\frac{iHt}{\hbar}\right) &= \exp\left(-\frac{iH_0t}{\hbar}\right) \\ &\times \left\{ 1 - \frac{i}{\hbar} \int_{t_0}^t \exp\left(\frac{iH_0t_1}{\hbar}\right) H_1 \exp(\varepsilon t_1) \exp\left(-\frac{iHt_1}{\hbar}\right) dt_1 \right\}. \end{aligned} \quad (14.11)$$

The right-hand side can be developed as a power series in H_1 by iteration.

Zeroth Order

$$\langle f | \exp\left(-\frac{iH_0t}{\hbar}\right) | i \rangle = \exp(-i\omega_i t) \langle f | i \rangle = 0, \quad \text{for } i \neq j.$$

First Order

$$\begin{aligned} &-\frac{i}{\hbar} \langle f | \exp\left(-\frac{iH_0t}{\hbar}\right) \int_{-\infty}^t \exp\left(\frac{iH_0t_1}{\hbar}\right) H_1 \exp(\varepsilon t_1) \\ &\quad \times \exp\left(-\frac{iH_0t_1}{\hbar}\right) dt_1 | i \rangle \\ &= -\frac{i}{\hbar} \langle f | H_1 | i \rangle \exp(-i\omega_f t) \int_{-\infty}^t \exp t_1 (-i\omega_i + \varepsilon) dt_1 \\ &= \frac{\langle f | H_1 | i \rangle}{\hbar} \left[\frac{\exp t(i\omega_f - i\omega_i + \varepsilon)}{-\omega_f + \omega_i + i\varepsilon} \right], \end{aligned}$$

so the transition to first order is

$$\frac{1}{\tau} = \frac{d}{dt} \sum_f \frac{|\langle f | H_1 | i \rangle|^2}{\hbar^2} \frac{\exp 2\varepsilon t}{(-\omega_f + \omega_i)^2 + \varepsilon^2}, \quad (14.12)$$

$$\frac{1}{\tau} = \frac{2}{\hbar^2} \sum_f |\langle f | H_1 | i \rangle|^2 \frac{\varepsilon \exp 2\varepsilon t}{(-\omega_f + \omega_i)^2 + \varepsilon^2}, \quad (14.13)$$

and when $\varepsilon \rightarrow 0$, we get

$$\frac{1}{\tau} = \frac{2\pi}{\hbar^2} \sum_f |\langle f | H_1 | i \rangle|^2 \delta(\omega_i - \omega_f), \quad (14.14)$$

which is the Fermi golden rule.

Second Order. This is obtained by a first iteration of (14.11), thus getting

$$\begin{aligned} & -\frac{1}{\hbar^2} \langle f | \exp \left(-\frac{iH_0 t}{\hbar} \right) \\ & \quad \times \int_{-\infty}^t dt_1 \int_{-\infty}^{t_1} dt_2 \exp \left(\frac{iH_0 t_1}{\hbar} \right) H_1 \exp(\varepsilon t_1) \exp \left(-\frac{iH_0 t_1}{\hbar} \right) \\ & \quad \times \exp \left(\frac{iH_0 t_2}{\hbar} \right) H_1 \exp(\varepsilon t_2) \exp \left(-\frac{iH_0 t_2}{\hbar} \right) | i \rangle. \end{aligned}$$

and introducing a complete set of eigenstates of H_0 , $\sum_l | l \rangle \langle l | = 1$, we get:

$$\begin{aligned} & -\frac{1}{\hbar^2} \sum_l \exp(-i\omega_f t) \langle f | H_1 | l \rangle \langle l | H_1 | i \rangle \int_{-\infty}^t dt_1 \int_{-\infty}^{t_1} dt_2 \\ & \quad \times \exp[i\omega_f t + \varepsilon t_1 + \varepsilon t_1 - i\omega_l(t_1 - t_2) + \varepsilon t_2 - i\omega_i t_2] \\ & = \sum_l \frac{\langle f | H_1 | l \rangle \langle l | H_1 | i \rangle \exp(2\varepsilon t - i\omega_l t)}{\hbar^2(\omega_i - \omega_l + i\varepsilon)(\omega_i - \omega_f + 2i\varepsilon)}. \end{aligned}$$

Adding the two contributions, we get ($\varepsilon \rightarrow \varepsilon/2$):

$$\frac{1}{\hbar} \left[\frac{\exp(\varepsilon t - i\omega_l t)}{\omega_i - \omega_f + i\varepsilon} \right] \left[\langle f | H_1 | i \rangle + \sum_l \frac{\langle f | H_1 | l \rangle \langle l | H_1 | i \rangle}{\hbar(\omega_i - \omega_l + \varepsilon/2)} \right] \quad (14.15)$$

and the transition rate, up to second order, is

$$\begin{aligned} \frac{1}{\tau} &= \frac{2\pi}{\hbar^2} \sum_f |\langle f | H_1 | i \rangle \\ &+ \frac{1}{\hbar} \sum_l \left| \frac{\langle f | H_1 | l \rangle \langle l | H_1 | i \rangle}{\omega_i - \omega_l} \right|^2 \delta(\omega_i - \omega_f). \end{aligned} \quad (14.16)$$

nth Order

$$\begin{aligned} \frac{1}{\tau} &= \frac{2\pi}{\hbar^2} \sum_f |\langle f | H_1 | i \rangle \\ &+ \frac{1}{\hbar} \sum_l \frac{\langle f | H_1 | l \rangle \langle l | H_1 | i \rangle}{\omega_i - \omega_l} \delta(\omega_i - \omega_f) + \dots \\ &+ \frac{1}{\hbar^{n-1}} \sum_{l_1} \dots \sum_{l_{n-1}} \left| \frac{\langle f | H_1 | l_1 \rangle \langle l_1 | H_1 | l_2 \rangle \dots \langle l_{n-1} | H_1 | i \rangle}{(\omega_i - \omega_{l_1})(\omega_i - \omega_{l_2}) \dots (\omega_i - \omega_{l_{n-1}})} \right|^2 \\ &\times \delta(\omega_i - \omega_f). \end{aligned} \quad (14.17)$$

The states $| l_1 \rangle, | l_2 \rangle, \dots$ are virtual states.

The first-order term represents a direct transition

$$|i\rangle \rightarrow |f\rangle,$$

while in the higher order terms, the transitions are

$$|i\rangle \rightarrow |l_{n-1}\rangle \rightarrow |l_{n-2}\rangle \dots \rightarrow |f\rangle,$$

where there is no requirement to be met by the difference $\omega_i - \omega_l$, except that if the difference is very large it generates a large denominator, contributing very little to the final result.

The various non-linear optical phenomena are contained in this generalized Fermi golden rule. For example, in light scattering, where one photon is absorbed and one is emitted, the second-order term is required. In second harmonic generation, where two photons are absorbed and one photon with double frequency emitted, a third-order process is required, and so on.

14.2 Parametric Processes Without Losses

The fundamental process known as parametric amplification plays an important role in many physical effects. These include, for example, Raman and Brillouin effects. In the case of the Raman coherent effect, a monochromatic light wave incident on a Raman active medium gives rise to a parametric coupling between an optical vibrational mode and the mode of the radiation field, the so-called Stokes mode. In the case of Brillouin scattering, there is a similar coupling, where the vibrations are at acoustical, rather than optical frequencies.

In the case of parametric amplification, an intense light wave in a non-linear dielectric medium couples pairs of field modes, the idler mode and the signal mode, whose frequencies add up to the frequency of the original strong light wave, the pump mode. This effect is shown in Fig. 14.1.

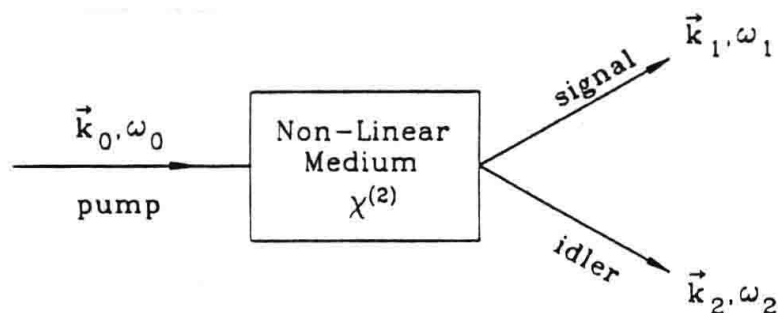


Fig. 14.1. A typical parametric amplifier, where a pump mode splits into a signal and an idler mode, these modes obeying the conservation of energy and momentum

The Hamiltonian describing the non-degenerate ($\omega_1 \neq \omega_2$) parametric amplifier is described by the following effective Hamiltonian

$$H = \hbar\omega_0 a_0^\dagger a_0 + \hbar\omega_1 a_1^\dagger a_1 + \hbar\omega_2 a_2^\dagger a_2 - \frac{i\chi'\hbar}{2} (a_0^\dagger a_1 a_2 - a_0 a_1^\dagger a_2^\dagger), \quad (14.18)$$

where the first three terms correspond to the energies of the pump, signal and idler modes, respectively, and the last term describes the non-linear interaction, where the term $a_0 a_1^\dagger a_2^\dagger$ represents the destruction of a pump photon and the creation of an idler and a signal photon.

A particularly simple case is that of the degenerate parametric amplifier, where a pump photon at frequency 2ω splits into two photons, each of frequency ω .

If we also assume that the pump is intense and classical [14.7], then we have

$$H = \hbar\omega a^\dagger a - i\hbar\frac{\chi}{2} (a^2 \exp(2i\omega t) - a^{\dagger 2} \exp(-2i\omega t)), \quad (14.19)$$

where we have included in χ the non-linear susceptibility and the classical amplitude.

If we go to the interaction picture, we readily get

$$H = -i\hbar\frac{\chi}{2} (a^2 - a^{\dagger 2}). \quad (14.20)$$

The Heisenberg equations of motion for this system are

$$\frac{da}{dt} = \frac{1}{i\hbar} [a, H] = \chi a^\dagger, \quad (14.21)$$

$$\frac{da^\dagger}{dt} = \frac{1}{i\hbar} [a^\dagger, H] = \chi a, \quad (14.22)$$

and the solution can be easily calculated as

$$a(t) = a(0) \cosh \chi t + a^\dagger(0) \sinh \chi t. \quad (14.23)$$

Also, if we combine the two differential equations (14.21), (14.22), we get

$$\frac{dX}{dt} = \chi X, \quad (14.24)$$

$$\frac{dY}{dt} = -\chi Y, \quad (14.25)$$

getting, as solutions

$$X(t) = X(0) \exp(\chi t), \quad (14.26)$$

$$Y(t) = Y(0) \exp(-\chi t), \quad (14.27)$$

$$\langle (\Delta X)^2 \rangle(t) = \exp(2\chi t) \langle (\Delta X)^2 \rangle(0). \quad (14.28)$$

$$\langle (\Delta Y)^2 \rangle(t) = \exp(-2\chi t) \langle (\Delta Y)^2 \rangle(0). \quad (14.29)$$

If the field is initially in the vacuum state, that is

$$\langle(\Delta X)^2\rangle(0) = \langle(\Delta Y)^2\rangle(0) = \frac{1}{4}, \quad (14.30)$$

then

$$\langle(\Delta X)^2\rangle(t) = \frac{1}{4} \exp(2\chi t), \langle(\Delta Y)^2\rangle(t) = \frac{1}{4} \exp(-2\chi t),$$

and the deamplified quadrature (Y) is squeezed at the expense of the other one, the product satisfying the minimum uncertainty relation

$$\langle(\Delta X)^2\rangle(t)\langle(\Delta Y)^2\rangle(t) = \frac{1}{16}. \quad (14.31)$$

The amount of squeezing, from the above results, is proportional to the interaction time, the non-linear parameter and the pump amplitude.

Actually, the theory presented here is a bit naive, since no loss mechanism is present, and one always has fluctuations in the pump intensity, in the case of a parametric amplifier, or if we place the non-linear crystal in a cavity, then we would have cavity losses in the parametric oscillator.

Since, for the case of the parametric oscillator, only the outside field is available for detection, we have to connect the field inside the cavity with the field outside. Input–output theory is quite suitable for this type of problem. This is the subject of the next section.

14.3 Input–Output Theory

In quantum mechanics, S -matrix theory relates input and output fields, having in mind situations such as scattering experiments. Input–output theory is a particular model [14.8], [14.9] that assumes a heat bath coupled to a system, with the following assumptions:

- (a) We consider a particular class of system–bath interaction that is linear in the bath operators. The vast majority of the models in quantum optics satisfy the above requirement.
- (b) We make the rotating-wave approximation.
- (c) The spectrum of the bath is flat, that is independent of frequency.

These assumptions are quite common, and we have already made them when dealing with the damped harmonic oscillator.

Next, we will define the “input” and “output” operators in terms of the bath operators, evaluated at the remote past and future. Then, we can derive quantum Langevin equations for the system and bath operators.

We start by considering the system–bath Hamiltonian

$$H = H_{\text{sys}} + H_B + H_{\text{Int}}, \quad (14.32)$$

$$H_B = \hbar \int_{-\infty}^{\infty} d\omega \omega b^\dagger(\omega) b(\omega), \quad (14.33)$$

$$H_{\text{Int}} = i\hbar \int_{-\infty}^{\infty} d\omega K(\omega) [b^\dagger(\omega)c - b(\omega)c^\dagger], \quad (14.34)$$

where $b(\omega)$ are the boson annihilation operators for the bath, satisfying

$$[b(\omega), b^\dagger(\omega')] = \delta(\omega - \omega'), \quad (14.35)$$

and c is any system operator.

Of course the real frequency range is $(0, \infty)$, but for convenience we have extended it to $(-\Omega, \infty)$, which is acceptable if one goes to a rotating frame with angular frequency Ω , and then takes Ω larger than a typical bandwidth.

We now follow the same procedure as in the quantum theory of damping. We write the Heisenberg equation for an arbitrary system operator a and $b(\omega)$:

$$\dot{b}(\omega, t) = -i\omega b(\omega, t) + K(\omega)c, \quad (14.36)$$

$$\dot{a} = -\frac{i}{\hbar} [a, H_{\text{sys}}] + \int_{-\infty}^{\infty} d\omega K(\omega) \{ b^\dagger(\omega, t) [a, c] - [a, c^\dagger] b(\omega, t) \}, \quad (14.37)$$

and integrating (14.36), we get:

$$\begin{aligned} b(\omega, t) &= \exp[-i\omega(t - t_0)] b(\omega, t_0) \\ &\quad + \int_{t_0}^t K(\omega) \exp[-i\omega(t - t')] c(t') dt'. \end{aligned} \quad (14.38)$$

Now, we substitute $b(\omega)$ in (14.37), obtaining

$$\begin{aligned} \dot{a} &= -\frac{i}{\hbar} [a, H_{\text{sys}}] \\ &\quad + \int_{-\infty}^{\infty} d\omega K(\omega) \{ \exp[i\omega(t - t_0)] b^\dagger(\omega, t_0) [a, c] \\ &\quad - [a, c^\dagger] \exp[-i\omega(t - t_0)] b(\omega, t_0) \} \\ &\quad + \int_{-\infty}^{\infty} d\omega K(\omega)^2 \int_{t_0}^t dt' \{ \exp[i\omega(t - t')] c^\dagger(t') [a, c] \\ &\quad - [a, c^\dagger] \exp[-i\omega(t - t')] c(t') \}. \end{aligned} \quad (14.39)$$

So far our Heisenberg equation of motion is exact. But not for long.

We introduce now the first Markov approximation:

$$K(\omega) = \sqrt{\gamma}, \quad (14.40)$$

which is the broad-band assumption mentioned at the beginning. Also, we make use of the properties of the δ -function:

$$\int_{-\infty}^{\infty} d\omega \exp[-i\omega(t - t')] = 2\pi\delta(t - t'), \quad (14.41)$$

$$\int_{t_0}^t c(t') \delta(t - t') dt' = \frac{1}{2} c(t),$$

to get

$$\begin{aligned}\dot{a} = & -\frac{i}{\hbar} [a, H_{\text{sys}}] - [a, c^\dagger] \left[\frac{\gamma}{2} c + \sqrt{\gamma} a_{\text{IN}}(t) \right] \\ & - \left[\frac{\gamma}{2} c^\dagger + \sqrt{\gamma} a_{\text{IN}}^\dagger(t) \right] [a, c],\end{aligned}\quad (14.42)$$

where we defined the input field as

$$a_{\text{IN}}(t) = - \int_{-\infty}^{\infty} d\omega \exp[-i\omega(t - t_0)] b(\omega, t_0). \quad (14.43)$$

We notice that $\gamma c/2$ and $-\gamma c^\dagger/2$ are the damping terms. Also, the $a_{\text{IN}}(t)$ and $a_{\text{IN}}^\dagger(t)$ terms represent the noise, since they depend on the bath operators at the initial time t_0 .

We may assume that at this initial time, the system and bath density operators factorize and a typical bath state correspond to a thermal state. In the case that the bath state corresponds to a coherent or squeezed state, we no longer can no longer interpret these terms as noise.

For the particular case $c = a$, we get

$$\dot{a} = -\frac{i}{\hbar} [a, H_{\text{sys}}] - \frac{\gamma}{2} a + \sqrt{\gamma} a_{\text{IN}}(t). \quad (14.44)$$

Now, if we take $t_1 > t$, we can integrate (14.36) again, getting

$$\begin{aligned}b(\omega, t) = & \exp[-i\omega(t - t_0)] b(\omega, t_1) \\ & - \int_{t_0}^t K(\omega) \exp[-i\omega(t - t')] c(t') dt',\end{aligned}\quad (14.45)$$

and we define an ‘output field’

$$a_{\text{OUT}}(t) = \int_{-\infty}^{\infty} d\omega \exp[-i\omega(t - t_1)] b(\omega, t_1). \quad (14.46)$$

If we follow the same procedure as with the input field, we readily get

$$\begin{aligned}\dot{a} = & -\frac{i}{\hbar} [a, H_{\text{sys}}] - [a, c^\dagger] \left[-\frac{\gamma}{2} c + \sqrt{\gamma} a_{\text{OUT}}(t) \right] \\ & - \left[-\frac{\gamma}{2} c^\dagger + \sqrt{\gamma} a_{\text{OUT}}^\dagger(t) \right] [a, c],\end{aligned}\quad (14.47)$$

and for the case $a = c$

$$\dot{a} = -\frac{i}{\hbar} [a, H_{\text{sys}}] + \frac{\gamma}{2} a - \sqrt{\gamma} a_{\text{OUT}}(t). \quad (14.48)$$

By comparing (14.48) with (14.44), we get

$$\sqrt{\gamma} a(t) = a_{\text{IN}} + a_{\text{OUT}}. \quad (14.49)$$

Equation (14.48) can be interpreted as a boundary condition relating the input, output and internal field, at the mirrors of the cavity.

Although this analysis refers to a system driven by a bath, this is not necessarily a theory about noise, since no assumption was made about the bath, except for the broad spectrum.

For a linear system, (14.44) and (14.48) can be cast in a convenient matrix form

$$\begin{aligned}\frac{da}{dt} &= \left(A - \frac{\gamma}{2} \mathbf{1} \right) a + \sqrt{\gamma} a_{\text{IN}}(t), \\ &= \left(\left[A + \frac{\gamma}{2} \mathbf{1} \right] \right) - \sqrt{\gamma} a_{\text{OUT}}(t),\end{aligned}\quad (14.50)$$

where

$$a = \begin{pmatrix} a \\ a^\dagger \end{pmatrix}, \quad (14.51)$$

and A is a matrix.

It is convenient to define the Fourier transform

$$\tilde{a}(\omega) = \frac{1}{2\pi} \int_{-\infty}^{\infty} \exp(i\omega t) a(t) dt. \quad (14.52)$$

Now, (14.50) can be written as

$$\begin{aligned}-i\omega \tilde{a}(\omega) &= \left(A - \frac{\gamma}{2} \mathbf{1} \right) \tilde{a}(\omega) + \sqrt{\gamma} \tilde{a}(\omega)_{\text{IN}}, \\ &= \left(A + \frac{\gamma}{2} \mathbf{1} \right) \tilde{a}(\omega) - \sqrt{\gamma} \tilde{a}(\omega)_{\text{OUT}},\end{aligned}\quad (14.53)$$

where

$$\tilde{a}(\omega) = \begin{pmatrix} \tilde{a}(\omega) \\ \tilde{a}^\dagger(-\omega) \end{pmatrix}. \quad (14.54)$$

From the above equations, we can eliminate the internal field and relate the input and output fields. Since

$$- \left[A + \left(i\omega - \frac{\gamma}{2} \right) \mathbf{1} \right] \tilde{a}(\omega) = \sqrt{\gamma} \tilde{a}(\omega)_{\text{IN}} \quad (14.55)$$

$$- \left[A + \left(i\omega + \frac{\gamma}{2} \right) \mathbf{1} \right] \tilde{a}(\omega) = -\sqrt{\gamma} \tilde{a}(\omega)_{\text{OUT}}, \quad (14.56)$$

we get

$$\left[A + \left(i\omega - \frac{\gamma}{2} \right) \mathbf{1} \right]^{-1} \tilde{a}(\omega)_{\text{IN}} = - \left[A + \left(i\omega + \frac{\gamma}{2} \right) \mathbf{1} \right]^{-1} \tilde{a}(\omega)_{\text{OUT}},$$

or, finally

$$\tilde{a}(\omega)_{\text{OUT}} = - \left[A + \left(i\omega + \frac{\gamma}{2} \right) \mathbf{1} \right] \left[A + \left(i\omega - \frac{\gamma}{2} \right) \mathbf{1} \right]^{-1} \tilde{a}(\omega)_{\text{IN}}. \quad (14.57)$$

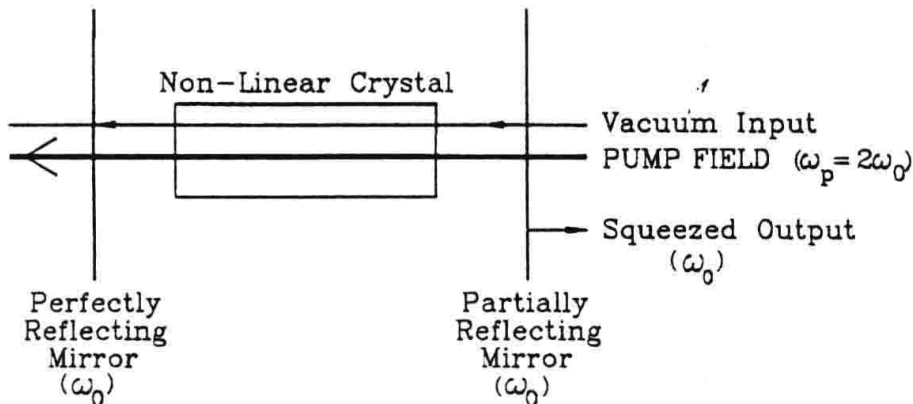


Fig. 14.2. Physical setup of the parametric oscillator

14.4 The Degenerate Parametric Oscillator

The physical system is described in Fig. 14.2. A non-linear crystal acts as the amplifying medium inside an optical cavity, with two mirrors chosen with the following properties:

- (a) both mirrors are almost 100% transmitting at the pump frequency $\omega_p = 2\omega_0$;
- (b) one of the end mirrors is 100% reflecting at ω_0 and the other one (right mirror) is partially transmitting at ω_0 .

The input-output theory developed in the last section is quite suitable to be used in this example.

The Hamiltonian of the degenerate parametric oscillator can be written as

$$H_{\text{sys}} = \hbar\omega_0 a^\dagger a + \frac{i\hbar [\varepsilon \exp(-i\omega_p t) a^{\dagger 2} - \varepsilon^* \exp(i\omega_p t) a^2]}{2}, \quad (14.58)$$

where ε is the classical pump amplitude (including the non-linear coefficient) and $\omega_p = 2\omega_0$ is the pump frequency.

The equation of motion for the internal field is

$$\begin{aligned} \frac{da}{dt} = & -i\omega_0 a + \varepsilon \exp(-i\omega_p t) a^\dagger - \frac{1}{2}(\gamma_1 + \gamma_2)a \\ & + \sqrt{\gamma_1} a_{1\text{IN}}(t) + \sqrt{\gamma_2} a_{2\text{IN}}(t), \end{aligned} \quad (14.59)$$

where γ_1 and γ_2 are the two damping coefficients of the two mirrors and $a_{1\text{IN}}(t)$, $a_{2\text{IN}}(t)$ are the two respective input fields.

Now we go to a rotating frame

$$\begin{aligned} a &\rightarrow a \exp\left(i\frac{\omega_p t}{2}\right), \\ a_{1\text{IN}}(t) &\rightarrow \exp\left(i\frac{\omega_p t}{2}\right) a_{1\text{IN}}(t), \\ a_{2\text{IN}}(t) &\rightarrow \exp\left(i\frac{\omega_p t}{2}\right) a_{2\text{IN}}(t). \end{aligned}$$

If we give the new fields the same symbols as the old ones, we write

$$\frac{da}{dt} = \left[A - \frac{1}{2}(\gamma_1 + \gamma_2)\mathbf{1} \right] \mathbf{a} + \sqrt{\gamma_1} a_{1\text{IN}}(t) + \sqrt{\gamma_2} a_{2\text{IN}}(t), \quad (14.60)$$

with

$$\begin{aligned} A &= \begin{bmatrix} 0 & |\varepsilon| \exp(i\theta) \\ |\varepsilon| \exp(-i\theta) & 0 \end{bmatrix}, \\ \mathbf{a}(t) &= \begin{bmatrix} a \\ a^\dagger \end{bmatrix}, \\ a_{i\text{IN}}(t) &= \begin{bmatrix} a_{i\text{IN}} \\ a_{i\text{IN}}^\dagger \end{bmatrix}, \quad i = 1, 2. \end{aligned} \quad (14.61)$$

Now, performing the Fourier transform and using the property $a^\dagger(\omega) = [a(-\omega)]^\dagger$, we get

$$\begin{aligned} \tilde{\mathbf{a}}(\omega) &= - \left[A + \left(i\omega - \frac{1}{2}(\gamma_1 + \gamma_2) \right) \mathbf{1} \right]^{-1} \\ &\quad \times \left[\sqrt{\gamma_1} \tilde{a}_{1\text{IN}}(\omega) + \sqrt{\gamma_2} \tilde{a}_{2\text{IN}}(\omega) \right]. \end{aligned} \quad (14.62)$$

From the above vector relation, the upper component of $\tilde{\mathbf{a}}(\omega)$ is given by (after matrix inversion):

$$\begin{aligned} \tilde{a}(\omega) &= \frac{(-i\omega + \frac{1}{2}(\gamma_1 + \gamma_2)) \left[\sqrt{\gamma_1} \tilde{a}_{1\text{IN}}(\omega) + \sqrt{\gamma_2} \tilde{a}_{2\text{IN}}(\omega) \right]}{(i\omega - \frac{1}{2}(\gamma_1 + \gamma_2))^2 - |\varepsilon|^2} \\ &\quad + \frac{\varepsilon \left[\sqrt{\gamma_1} \tilde{a}_{1\text{IN}}^\dagger(-\omega) + \sqrt{\gamma_2} \tilde{a}_{2\text{IN}}^\dagger(-\omega) \right]}{(i\omega - \frac{1}{2}(\gamma_1 + \gamma_2))^2 - |\varepsilon|^2}. \end{aligned} \quad (14.63)$$

From (14.49), we get the output field

$$\begin{aligned} a_{\text{OUT}}(\omega) &= \frac{[(\gamma_1/2)^2 - (\gamma_2/2 - i\omega)^2 + |\varepsilon|^2] \tilde{a}_{1\text{IN}}(\omega) + \varepsilon \gamma_1 \tilde{a}_{1\text{IN}}^\dagger(-\omega)}{(i\omega - \frac{1}{2}(\gamma_1 + \gamma_2))^2 - |\varepsilon|^2} \\ &\quad + \frac{\sqrt{\gamma_2 \gamma_1} [(\gamma_1 + \gamma_2)/2 - i\omega] \tilde{a}_{2\text{IN}}(\omega) + \varepsilon \sqrt{\gamma_2 \gamma_1} \tilde{a}_{2\text{IN}}^\dagger(-\omega)}{(i\omega - \frac{1}{2}(\gamma_1 + \gamma_2))^2 - |\varepsilon|^2}. \end{aligned} \quad (14.64)$$

We are mostly interested in the quadrature fluctuations.

It takes a little algebra to show that

$$\langle :X_{1\text{OUT}}(\omega), X(\omega')_{1\text{OUT}} :\rangle \quad (14.65)$$

$$= \frac{|\varepsilon| \gamma_1/2}{\left[\frac{1}{2}(\gamma_1 + \gamma_2) - |\varepsilon|\right]^2 + \omega^2} \delta(\omega + \omega'),$$

$$\langle :Y_{1\text{OUT}}(\omega), Y(\omega')_{1\text{OUT}} :\rangle \quad (14.66)$$

$$= -\frac{|\varepsilon| \gamma_1/2}{\left[\frac{1}{2}(\gamma_1 + \gamma_2) + |\varepsilon|\right]^2 + \omega^2} \delta(\omega + \omega'),$$

where

$$\langle a, b \rangle \equiv \langle ab \rangle - \langle a \rangle \langle b \rangle,$$

and the definitions of x and y are the same as in (5.1). The maximum squeezing is obtained for $\frac{1}{2}(\gamma_1 + \gamma_2) = |\varepsilon|$, getting

$$\langle :Y_{1\text{OUT}}(\omega), Y(\omega')_{1\text{OUT}} :\rangle = -\frac{\gamma_1}{4} \frac{(\gamma_1 + \gamma_2)}{(\gamma_1 + \gamma_2)^2 + \omega^2} \delta(\omega + \omega'). \quad (14.67)$$

The normally ordered spectrum of $Y_{1\text{OUT}}(\omega)$ is the coefficient of the above formula

$$:S_{Y1\text{OUT}}(\omega) := -\frac{\gamma_1}{4} \frac{(\gamma_1 + \gamma_2)}{(\gamma_1 + \gamma_2)^2 + \omega^2}. \quad (14.68)$$

Two important cases are

(a) $\gamma = \gamma_1 = \gamma_2$, the double ended cavity, for which, at resonance

$$:S_{Y1\text{OUT}}(0) := -\frac{1}{8}. \quad (14.69)$$

(b) $\gamma_2 = 0$, single-ended cavity

$$:S_{Y1\text{OUT}}(0) := -\frac{1}{4}. \quad (14.70)$$

We notice that the single-ended cavity has perfect squeezing in the output signal.

14.5 Experimental Results

Quadrature squeezing, and also other non-linear effects such as second harmonic generation [14.10], [14.11], optical bistability [14.12], and four-wave mixing [14.13] have been observed experimentally in parametric oscillators. Squeezing greater than 50% relative to the vacuum noise level was obtained by Wu *et al.* [14.14], using degenerate parametric down-conversion in an optical cavity. The diagram of the experimental setup is shown in Fig. 14.3. The

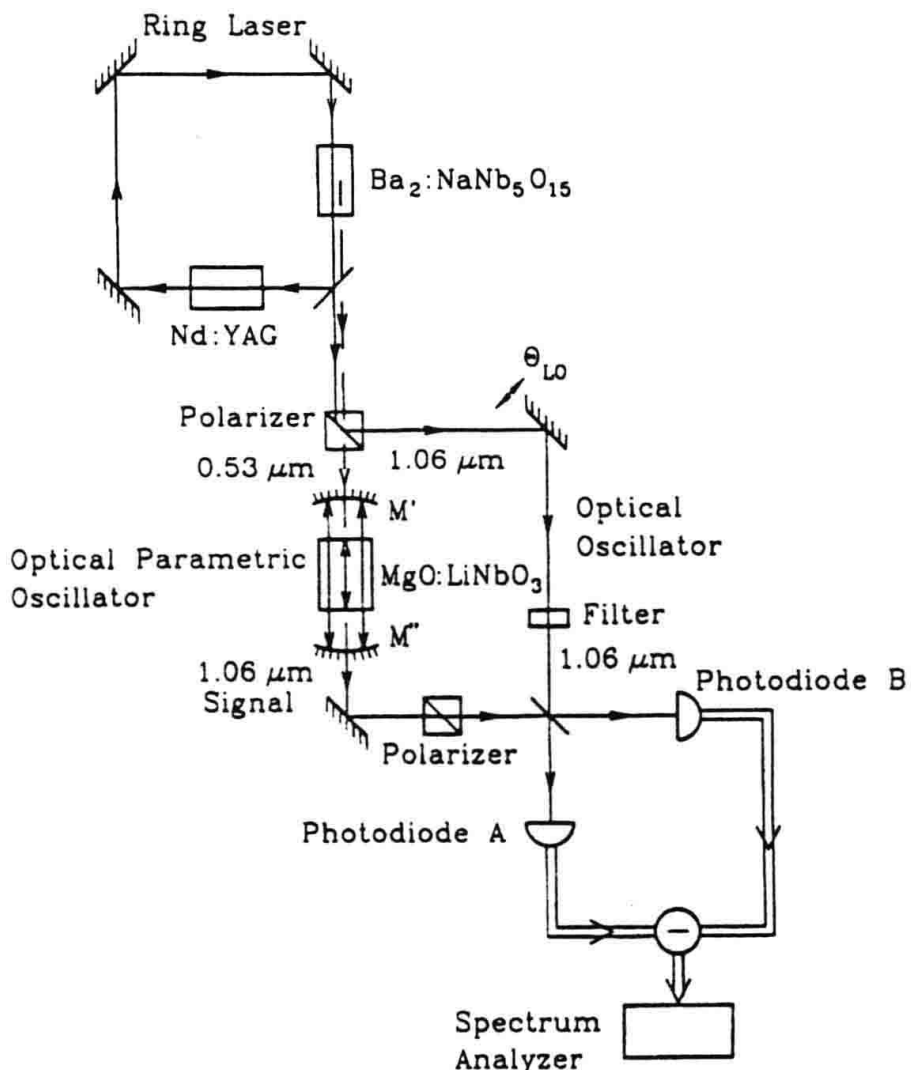


Fig. 14.3. Diagram of the experimental setup of the parametric oscillator that generates squeezes states

down-conversion occurs in the cavity $M'M''$ which contains the non-linear crystal MgO:LiNbO₃, phase matched at 98 °C. The pump for the parametric oscillator is a Nd:YAG laser, whose frequency was doubled from 1.06 μm to 0.53 μm, using a Ba₂NaNb₅O₁₅ crystal inside the laser cavity. The pump field enters the OPO cavity through the mirror M' with a transmission coefficient of 3.5% at 0.53 μm, and 0.06% at 1.06 μm. On the other hand, M'' is coated for low transmission at 0.53 μm and either 4.3% or 7.3% transmission at 1.06 μm.

A fraction of the down-converted light from OPO exits through M'' and combines with the original Nd:YAG laser, which acts as a strong local oscillator at one of the ports of a balanced homodyne detector and the squeezed light enters through the other port. The squeezed signal is observed from the spectra of the intensity difference of the photocurrents coming from detectors A and B .

In Fig. 14.4, we display the noise voltage $V(\theta)$ from the detector, as a function of the phase θ , of the local oscillator. With the OPO input blocked, the vacuum field entering the signal port of the detector produces the noise drawn as a dotted line, with no θ dependence. With the OPO unblocked, there are several dips below the vacuum level, some of which correspond to a reduction of 50%.

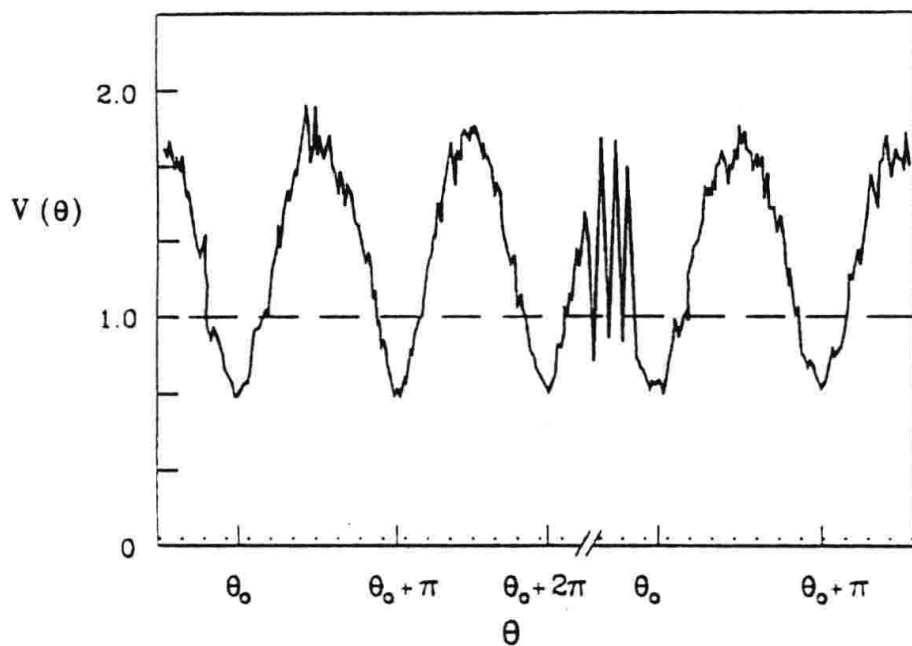


Fig. 14.4. Phase dependence of the rms noise voltage $V(\theta)$ from a balanced homodyne detector as a function of the local oscillator phase θ at a fixed analysis frequency 1.8 MHZ. The dashed line corresponds to the vacuum noise voltage, with the OPO blocked and no phase dependence (after [14.14])

Problems

- 14.1. Show that after matrix inversion, $\tilde{a}(\omega)$ is given by (14.63).
- 14.2. Show that the optimum normally ordered squeezing spectrum for Y is given by (14.68).
- 14.3. Using input-output theory, show that

$$[a(t), a_{\text{IN}}(t')] = u(t - t') \sqrt{\gamma} [a(t), c(t')],$$

$$[a(t), a_{\text{OUT}}(t')] = u(t' - t) \sqrt{\gamma} [a(t), c(t')],$$

where $u(t)$ is the step function, defined as

$$u(t) = \begin{cases} 1, & t > 0 \\ \frac{1}{2}, & t = 0 \\ 0, & t < 0. \end{cases}$$

14.4. Light scattering by a two-level atom. For a weak incident beam on a two-level atom, the usual interaction Hamiltonian is

$$H_1 = \mathbf{e} \cdot \mathbf{d} \cdot \mathbf{E}(0).$$

The initial state of the system consists of photons at frequency ω and wavevector \mathbf{k} . The scattered photons (by the two-level atom) will have a frequency ω_s and a wavevector \mathbf{k}_s , and the fields are characterized by the annihilation operators a and a_s respectively. Also, we assume that the atom is initially in its lower state $|b\rangle$, with zero energy and left in some final atomic state $|f\rangle$ with an energy $\hbar\omega_f$. If the incident field has n photons, then we make use of (14.17) with $|f\rangle_{at-f} = |n-1, 1, f\rangle$ and $|i\rangle_{at-f} = |n, 0, b\rangle$, where the first number refers to the number of photons in the beam, the second number to the number of photons in the scattered field and the third index is the atomic state, and write (up to second order)

$$\frac{1}{\tau} = \frac{2\pi}{\hbar^2} \sum_f |\langle n-1, 1, f | H_1 | n, 0, b \rangle| \\ + \frac{1}{\hbar} \sum_l \left| \frac{\langle n-1, 1, f | H_1 | l \rangle \langle l | H_1 | n, 0, b \rangle}{\omega_i - \omega_l} \right|^2 \delta(\omega - \omega_s - \omega_f).$$

(a) Prove that the linear term does not contribute and that the contributions of the quadratic terms come from the aa_s^\dagger term with the relevant $|l\rangle = |n, 1, j\rangle$, $\omega_l = (n)\omega + \omega_s + \omega_j$ and the $a_s^\dagger a$ term with the relevant $|l\rangle = |n-1, 0, j\rangle$, $\omega_l = (n-1)\omega + \omega_j$.

(b) Show that

$$\frac{1}{\tau} = \sum_f \sum_{\mathbf{k}_s} \frac{\pi e^4 \omega_s \omega n}{2\hbar\varepsilon_0^2 v^2} \left| \sum_j \frac{(\boldsymbol{\varepsilon}_s \cdot \mathbf{d}_{fj})(\boldsymbol{\varepsilon} \cdot \mathbf{d}_{jf})}{\omega_j - \omega} + \frac{(\boldsymbol{\varepsilon} \cdot \mathbf{d}_{fj})(\boldsymbol{\varepsilon}_s \cdot \mathbf{d}_{jf})}{\omega_j + \omega_s} \right|^2 \\ \times \delta(\omega - \omega_s - \omega_f).$$

(c) Converting the sum over \mathbf{k}_s into an integral, and using the notion of cross-section, usually defined as the ratio:

$$\frac{\text{Energy removed from the beam}}{\text{Energy rate crossing a unit area perpendicular to the beam}},$$

or

$$\sigma = \frac{\hbar\omega/\tau}{c\hbar n\omega/v} = \frac{v}{\tau n c},$$

show that

$$\frac{d\sigma}{d\Omega} = \sum_f^{\omega_f < \omega} \frac{e^4}{16\pi^2 \hbar^2 \varepsilon_0^2 c^4} \left| \sum_j \frac{(\boldsymbol{\varepsilon}_s \cdot \mathbf{d}_{fj})(\boldsymbol{\varepsilon} \cdot \mathbf{d}_{jf})}{\omega_j - \omega} \right. \\ \left. + \frac{(\boldsymbol{\varepsilon} \cdot \mathbf{d}_{fj})(\boldsymbol{\varepsilon}_s \cdot \mathbf{d}_{jf})}{\omega_j - \omega_f + \omega} \right|^2.$$

This is the Kramer-Heisenberg formula. The cross section includes the elastic Rayleigh scattering, corresponding to the $f = b$ term, $\omega_f = 0$, and the inelastic Raman scattering, corresponding to the rest [14.6].

14.5. Prove that for elastic Raman scattering (refer to Problem 14.4) one has:

$$\frac{d\sigma}{d\Omega} = \sum_f^{\omega_f < \omega} \frac{e^4(\omega - \omega_f)^3 \omega}{16\pi^2 \hbar^2 \epsilon_0^2 c^4} \left| \sum_j \omega_j \{ (\boldsymbol{\epsilon}_s \cdot \mathbf{d}_{bj}) (\boldsymbol{\epsilon} \cdot \mathbf{d}_{jb}) \right.$$

$$\left. + (\boldsymbol{\epsilon} \cdot \mathbf{d}_{bj}) (\boldsymbol{\epsilon}_s \cdot \mathbf{d}_{jb}) \} \right|^2,$$

in the limit $\omega \gg \omega_j$, when ω is much larger than the atomic excitation frequencies [14.6].

15. Quantum Phase

Dirac was the first to postulate the existence of a Hermitian phase variable in the early days of quantum electrodynamics [15.1].

15.1 The Dirac Phase

Comparison with classical mechanics led Dirac to assume a commutation relation of the number and phase operator

$$[\Phi_D, n] = -i, \quad (15.1)$$

which immediately leads to the uncertainty relation

$$\Delta n \Delta \Phi_D \geq \frac{1}{2}. \quad (15.2)$$

There are some obvious difficulties with the above commutation rule. If we take matrix elements between n and n' , we get

$$(n - n')\langle n' | \Phi_D | n \rangle = -i\delta_{nn'}, \quad (15.3)$$

which is inconsistent when $n = n'$, giving $0 = -i$. Also, trying to write the polar decomposition of the annihilation operator:

$$a = \exp(i\Phi_D) \sqrt{n} = \sqrt{n+1} \exp(i\Phi_D), \quad (15.4)$$

$$a^\dagger = \sqrt{n} \exp(-i\Phi_D) = \exp(-i\Phi_D) \sqrt{n+1},$$

leads to difficulties, since if one assumes that Φ_D is a Hermitian operator, as any respectable observable should be, then $\exp(i\Phi_D)$ is not unitary, and therefore $\exp(-i\Phi_D) \neq [\exp(i\Phi_D)]^\dagger$. These difficulties were pointed out by Dirac himself and also by Susskind and Glogower [15.2].

Another difficulty is that the uncertainty relation (15.2) implies, for small Δn , that $\Delta \Phi_D$ can have values larger than 2π , which makes no physical sense, and basically does not take into account the periodic nature of the phase.

If one inverts the relations (15.4), we define

$$\exp(i\Phi_D) = (n + 1)^{-1/2} a, \quad (15.5)$$

$$\exp(-i\Phi_D) = a^\dagger (n + 1)^{-1/2},$$

and from (15.5), it follows that:

$$[\exp(\pm i\Phi_D), n] = \pm \exp(\pm i\Phi_D). \quad (15.6)$$

15.2 The Louisell Phase

Louisell [15.3] tried to solve the problem of periodicity, by defining trigonometric functions of the Dirac phase

$$\begin{aligned}\cos \Phi_D &= \frac{1}{2} [\exp(i\Phi_D) + \exp(-i\Phi_D)], \\ \sin \Phi_D &= \frac{1}{2i} [\exp(i\Phi_D) - \exp(-i\Phi_D)],\end{aligned}\tag{15.7}$$

leading to the commutation relation

$$\begin{aligned}[\cos \Phi_D, n] &= i \sin \Phi_D \\ [\sin \Phi_D, n] &= -i \cos \Phi_D.\end{aligned}\tag{15.8}$$

Thus n and $\sin \Phi_D$ or $\cos \Phi_D$ obey the uncertainty relations

$$\begin{aligned}\Delta n \Delta \cos \Phi_D &\geq \frac{1}{2} |\langle \sin \Phi_D \rangle|, \\ \Delta n \Delta \sin \Phi_D &\geq \frac{1}{2} |\langle \cos \Phi_D \rangle|.\end{aligned}\tag{15.9}$$

Both the approaches of Dirac and Louisell have a common difficulty in that $\exp(i\Phi_D)$ is not unitary, and (15.4) do not define a Hermitian phase operator [15.4].

15.3 The Susskind–Glogower Phase

Susskind and Glogower[15.2] have a phase definition which is similar to Dirac's:

$$\begin{aligned}a &= A\sqrt{n}, \quad A = \exp(i\Phi_S), \\ a^\dagger &= \sqrt{n}A^\dagger, \quad A^\dagger = [\exp(i\Phi_S)]^\dagger,\end{aligned}\tag{15.10}$$

where A and A^\dagger do not commute. As a matter of fact

$$\begin{aligned}A &= a(n)^{-1/2} = (n+1)^{-1/2}a, \\ A^\dagger &= (n)^{-1/2}a^\dagger = a^\dagger(n+1)^{-1/2}.\end{aligned}\tag{15.11}$$

We see that

$$AA^\dagger = (n+1)^{-1/2}aa^\dagger \cdot (n+1)^{-1/2} = 1,\tag{15.12}$$

but, on the other hand

$$\begin{aligned}
A^\dagger A &= a^\dagger (n+1)^{-1/2} \cdot (n+1)^{-1/2} a \\
&= \sum_{m=0}^{\infty} a^\dagger |m\rangle \langle m| (n+1)^{-1} a \\
&= \sum_{m=0}^{\infty} \sqrt{m+1} |m+1\rangle \langle m+1| (m+1)^{-1} \sqrt{m+1} \\
&= \sum_{m=0}^{\infty} |m+1\rangle \langle m+1| = 1 - |0\rangle \langle 0|.
\end{aligned}$$

Thus

$$[A, A^\dagger] = |0\rangle \langle 0|. \quad (15.13)$$

The two operators A and A^\dagger do not commute and they are not unitary. However, these two operators act like raising and lowering operators

$$a |n\rangle = \sqrt{n} |n-1\rangle = A \sqrt{n} |n\rangle = A \sqrt{n} |n\rangle, \quad (15.14)$$

and therefore

$$A |n\rangle = |n-1\rangle, \quad (15.15)$$

and similarly

$$A^\dagger |n\rangle = |n+1\rangle. \quad (15.16)$$

Equation (15.15) has one exception. In order not to create a Fock state with a negative photon number, we must have

$$A |0\rangle = 0, \quad (15.17)$$

which is the mathematical origin of the non-unitary character of A and A^\dagger . Thus

$$\begin{aligned}
\langle n-1 | A | n \rangle &= 1, \\
\langle n+1 | A^\dagger | n \rangle &= 1,
\end{aligned} \quad (15.18)$$

and all the other matrix elements are zero.

One can also write

$$A = |0\rangle \langle 1| + |1\rangle \langle 2| + |2\rangle \langle 3| + \dots \quad (15.19)$$

One can also show, similarly to the Dirac phase, that

$$\begin{aligned}
[A, n] &= A, \\
[A^\dagger, n] &= -A^\dagger.
\end{aligned} \quad (15.20)$$

We can define the trigonometric functions

$$\begin{aligned}
\cos \Phi_S &= \frac{1}{2}(A + A^\dagger), \\
\sin \Phi_S &= \frac{1}{2i}(A - A^\dagger),
\end{aligned} \quad (15.21)$$

where the non-vanishing elements are

$$\begin{aligned}\langle n-1 | \cos \Phi_S | n \rangle &= \langle n | \cos \Phi_S | n-1 \rangle = \frac{1}{2}, \\ \langle n-1 | \sin \Phi_S | n \rangle &= -\langle n | \sin \Phi_S | n-1 \rangle = \frac{1}{2i}.\end{aligned}\quad (15.22)$$

The reader can readily verify that the condition for a Hermitian operator $\langle n | O | n' \rangle = \langle n' | O | n \rangle^*$ is satisfied by both $\cos \Phi_S$ and $\sin \Phi_S$.

From the commutation relations (15.20), one can verify that

$$\begin{aligned}[\mathbf{n}, \cos \Phi_S] &= -i \sin \Phi_S, \\ [\mathbf{n}, \sin \Phi_S] &= i \cos \Phi_S,\end{aligned}\quad (15.23)$$

which implies that \mathbf{n} and $\cos \Phi_S$ or $\sin \Phi_S$ cannot both be precisely specified. The results of measurements of amplitude and phase are governed by the uncertainty relations

$$\begin{aligned}\Delta n \Delta \cos \Phi_S &\geq \frac{1}{2} |\langle \sin \Phi_S \rangle|, \\ \Delta n \Delta \sin \Phi_S &\geq \frac{1}{2} |\langle \cos \Phi_S \rangle|.\end{aligned}\quad (15.24)$$

One can also prove that the operators $\cos \Phi_S$ and $\sin \Phi_S$ do not commute:

$$\begin{aligned}[\cos \Phi_S, \sin \Phi_S] &= \frac{1}{4i} [\mathbf{A} + \mathbf{A}^\dagger, \mathbf{A} - \mathbf{A}^\dagger] \\ &= -\frac{1}{2i} |0\rangle\langle 0|.\end{aligned}\quad (15.25)$$

The last property, that $\cos \Phi_S$ and $\sin \Phi_S$ do not commute, is rather strange. Normally, in classical mechanics or electromagnetism, the phase is a simple quantity and it is not necessary to define separately both the cosine and the sine of that phase. Of course the above property, as well as the failure of \mathbf{A} and \mathbf{A}^\dagger to commute, is directly related to the vacuum state.

If one has to take the average of these commutation relations, with classical strong fields, for which the probability of being in the vacuum is very small, then all the difficulties vanish, which shows that the real problems arise only when one is dealing with highly quantum mechanical field states with low photon numbers.

We can calculate the expectation values of these trigonometric functions, taking a coherent state [15.5] $|\alpha\rangle$ with $\alpha = |\alpha| \exp(i\theta)$:

$$\begin{aligned}\langle \alpha | \cos \Phi_S | \alpha \rangle &= \frac{1}{2} [\langle \alpha | \mathbf{A} | \alpha \rangle + \langle \alpha | \mathbf{A}^\dagger | \alpha \rangle], \\ \langle \alpha | \cos'^2 \Phi_S | \alpha \rangle &= \frac{1}{4} [\langle \alpha | \mathbf{A}^2 | \alpha \rangle + \langle \alpha | \mathbf{A} \mathbf{A}^\dagger \\ &\quad + \mathbf{A}^\dagger \mathbf{A} | \alpha \rangle + \langle \alpha | \mathbf{A}^{\dagger 2} | \alpha \rangle], \\ \langle \alpha | \sin \Phi_S | \alpha \rangle &= \frac{1}{2i} [\langle \alpha | \mathbf{A} | \alpha \rangle - \langle \alpha | \mathbf{A}^\dagger | \alpha \rangle],\end{aligned}\quad (15.26)$$

$$\begin{aligned}\langle \alpha | \sin^2 \Phi_S | \alpha \rangle = -\frac{1}{4} & [\langle \alpha | A^2 | \alpha \rangle - \langle \alpha | AA^\dagger \\ & + A^\dagger A | \alpha \rangle + \langle \alpha | A^{\dagger 2} | \alpha \rangle].\end{aligned}$$

After some algebraic work, one can show the following properties:

$$\begin{aligned}\langle \alpha | \cos \Phi_S | \alpha \rangle &= \cos \theta \left(1 - \frac{1}{8 |\alpha|^2} + \dots \right), \\ \langle \alpha | \cos^2 \Phi_S | \alpha \rangle &= \cos^2 \theta - \frac{\cos^2 \theta - \frac{1}{2}}{2 |\alpha|^2} + \dots,\end{aligned}\tag{15.27}$$

valid only for $|\alpha|^2 \gg 1$. Also:

$$\langle \alpha | \cos^2 \Phi_S + \sin^2 \Phi_S | \alpha \rangle = 1 - \frac{\exp(-|\alpha|^2)}{2}\tag{15.28}$$

valid for all α . It is interesting to notice that when $|\alpha| \rightarrow 0$, $\langle \alpha | (\cos^2 \Phi_S + \sin^2 \Phi_S) | \alpha \rangle \rightarrow \frac{1}{2}$, which again is a strange property.

As a conclusion of this section, we note that the Susskind–Glogower formalism of the quantum phase is a fairly consistent one, where the main difficulties are not mathematical but with the physical interpretation of $\cos \Phi_S$ and $\sin \Phi_S$ and their relationship with the actual experiments. Finally, a long time ago F. London defined a phase state:

$$|\phi\rangle = \frac{1}{\sqrt{2\pi}} \sum_{n=0}^{\infty} \exp(in\phi) |n\rangle.\tag{15.29}$$

The functions are not orthogonal and cannot be normalized. However, as we shall see, it can be useful to define probability distributions that can be normalized. [15.6], [15.7]. The shortcomings of the above phase operators have led a number of investigators to explore different possibilities [15.8]–[15.25].

15.4 The Pegg–Barnett Phase

A phase state $|\theta\rangle$ is defined in a finite $(s+1)$ -dimensional space, in the limit $s \rightarrow \infty$, as follows [15.13], [15.14], [15.15], [15.16]:

$$|\theta\rangle = \text{Lim}_{s \rightarrow \infty} (s+1)^{-1/2} \sum_{n=0}^s \exp(in\theta) |n\rangle.\tag{15.30}$$

The way to operate the limit is to perform the calculation in a finite space, and after the physical averages are calculated, one is to take the limit $s \rightarrow \infty$.

The parameter θ can take any values between 0 and 2π . Thus, there is an infinite number of these states, which are overcomplete and non-orthogonal. However, one can construct a set of orthogonal states if one picks only specified values of $\theta = \theta_m$

$$\theta_m = \theta_0 + \frac{2\pi m}{s+1}.\tag{15.31}$$

Thus, if one starts from a reference state $|\theta_0\rangle$, one can find a complete set of $s+1$ orthonormal states

$$|\theta_m\rangle = \exp i \left[n \left(\frac{m2\pi}{s+1} \right) \right] |\theta_0\rangle, \quad m = 0, 1, 2, \dots, s. \quad (15.32)$$

The above equation is simple to verify, since

$$\exp(i n \gamma) |n\rangle = |n + \gamma\rangle.$$

The orthonormal condition can be seen as follows:

$$\begin{aligned} \langle \theta_p | \theta_m \rangle &= \langle \theta_0 | \exp \left[-in \left(\frac{p2\pi}{s+1} \right) \right] \exp \left[in \left(\frac{m2\pi}{s+1} \right) \right] |\theta_0\rangle \quad (15.33) \\ &= \text{Lim}_{s \rightarrow \infty} \frac{1}{s+1} \sum_{q,r=0}^s \langle q | \exp(-iq\theta_0) \exp \left[-in \left(\frac{p2\pi}{s+1} \right) \right] \\ &\quad \times \exp i \left[n \left(\frac{m2\pi}{s+1} \right) \right] \exp(ir\theta_0) |r\rangle, \end{aligned}$$

where $|q\rangle$ and $|r\rangle$ are Fock states. Thus

$$\begin{aligned} \langle \theta_p | \theta_m \rangle &= \text{Lim}_{s \rightarrow \infty} \frac{1}{s+1} \sum_{q=0}^s \langle q | q \rangle \exp \left[i \frac{2\pi}{s+1} q(m-p) \right] \quad (15.34) \\ &= \delta_{mp}. \end{aligned}$$

The Hermitian phase operator is defined as

$$\Phi_\theta = \sum_{m=0}^s \theta_m |\theta_m\rangle \langle \theta_m|, \quad (15.35)$$

or

$$\Phi_\theta = \theta_0 + \frac{2\pi}{s+1} \sum_{m=0}^s m |\theta_m\rangle \langle \theta_m|. \quad (15.36)$$

We notice that Φ_θ depends on an arbitrary reference phase θ_0 , which also happens in its classical counterpart. Clearly, the phase operator defined by (15.35) is Hermitian and satisfies the eigenvalue equation

$$\Phi_\theta |\theta_m\rangle = \theta_m |\theta_m\rangle. \quad (15.37)$$

One of the problems with Dirac's phase was that the matrix element $\langle n' | \Phi_D | n \rangle$ was undefined. In the Pegg–Barnett formalism, that problem is not present.

We start from

$$|\theta_m\rangle \langle \theta_m| = (s+1)^{-1} \sum_{n,n'=0}^s \exp [i(n'-n)\theta_m] |n'\rangle \langle n|; \quad (15.38)$$

thus the phase operator can be written as

$$\begin{aligned}\Phi_\theta &= \theta_0 + \frac{2\pi}{s+1} \sum_{m=0}^s m(s+1)^{-1} \sum_{n,n'=0}^s \exp[i(n'-n)\theta_m] |n'\rangle\langle n| \quad (15.39) \\ &= \theta_0 + \frac{2\pi}{s+1} + \frac{2\pi}{s+1} \sum_{n \neq n'}^s \frac{\exp[i(n'-n)\theta_0]}{\exp[i(n'-n)2\pi/(s+1)] - 1} |n'\rangle\langle n|.\end{aligned}$$

Now, taking matrix elements of Φ_θ :

$$\begin{aligned}\langle n | \Phi_\theta | n \rangle &= \theta_0 + \frac{2\pi s}{s+1}, \\ \langle n' | \Phi_\theta | n \rangle &= \frac{2\pi}{s+1} \frac{\exp[i(n'-n)\theta_0]}{\exp[i(n'-n)2\pi/(s+1)] - 1}, \quad n \neq n'.\end{aligned}\quad (15.40)$$

From the above formula, we observe that the matrix elements of Φ_θ are well defined, implying that the commutator $[\Phi, n] = -i$ must be incorrect.

From (15.40), we immediately see that

$$\begin{aligned}\langle n | [n, \Phi_\theta] | n \rangle &= 0, \\ \langle n' | [n, \Phi_\theta] | n \rangle &= \frac{2\pi(n' - n)}{s+1} \frac{\exp[i(n'-n)\theta_0]}{\exp[i(n'-n)2\pi/(s+1)] - 1}, \quad n \neq n'.\end{aligned}\quad (15.41)$$

If we take ‘finite’ or ‘physical’ states with $n, n' \ll s$, then we get approximately

$$\begin{aligned}\langle n' | \Phi_\theta | n \rangle &\approx \frac{-i}{n - n'} \exp[i(n'-n)\theta_0]. \\ \langle n' | [n, \Phi_\theta] | n \rangle &\approx -i(1 - \delta_{nn'}) \exp[i(n'-n)\theta_0].\end{aligned}\quad (15.42)$$

If $\theta_0 = 0$, and for $n \neq n'$, we get

$$[n, \Phi_\theta]_{n'n} = -i, \quad (15.43)$$

which resembles the Dirac commutator.

Now, we concentrate on the exponential operators $\exp(\pm i\Phi_\theta)$. They are both eigenstates of $|\theta_m\rangle$:

$$\exp(\pm i\Phi_\theta) |\theta_m\rangle = \exp(\pm i\theta_m) |\theta_m\rangle. \quad (15.44)$$

The action of $\exp(\pm i\Phi_\theta)$ on the Fock states is

$$\exp(i\Phi_\theta) |n\rangle = \exp\left(i \sum_{m=0}^s \theta_m |\theta_m\rangle\langle\theta_m|\right) |n\rangle, \quad (15.45)$$

but since

$$|n\rangle = \sum_{p=0}^s |\theta_p\rangle\langle\theta_p| |n\rangle = (s+1)^{-1/2} \sum_{p=0}^s \exp(-in\theta_p) |\theta_p\rangle, \quad (15.46)$$

then substituting (15.46) in (15.45), we get

$$\exp(i\Phi_\theta) |n\rangle = (s+1)^{-1} \sum_{m=0}^s \exp[-i(n-1)\theta_m] |\theta_m\rangle = |n-1\rangle, \quad (15.47)$$

for $n > 0$.

For $n = 0$, we get the unphysical state $| -1 \rangle$, but we can call that state $| s \rangle$, thus

$$(s+1)^{-1} \sum_{m=0}^s \exp(i\theta_m) |\theta_m\rangle = (s+1)^{-1} \exp[i\theta_0(s+1)] \quad (15.48)$$

$$\sum_{m=0}^s \exp(-is\theta_m) |\theta_m\rangle = \exp[i\theta_0(s+1)] |s\rangle.$$

Thus the number state representation of $\exp(i\Phi_\theta)$ is

$$\begin{aligned} \exp(i\Phi_\theta) = & |0\rangle\langle 1| + |1\rangle\langle 2| + \dots \\ & + |s-1\rangle\langle s| + \exp[i\theta_0(s+1)] |s\rangle\langle 0|. \end{aligned} \quad (15.49)$$

The above expansion is similar to that of Susskind and Glogower, except for the last term, which makes the exponential operator unitary.

Finally, in the Pegg–Barnett phase, the trigonometric functions behave in a more normal way. The reader may verify the following properties

$$\cos^2 \Phi_\theta + \sin^2 \Phi_\theta = 1, \quad (15.50)$$

$$[\cos \Phi_\theta, \sin \Phi_\theta] = 0, \quad (15.51)$$

$$\langle n | \cos^2 \Phi_\theta | n \rangle + \langle n | \sin^2 \Phi_\theta | n \rangle = 1. \quad (15.52)$$

A drawback in the Pegg–Barnett formalism is that the state space is finite, thus

$$[a, a^\dagger] \neq 1. \quad (15.53)$$

This can be easily seen as follows

$$\begin{aligned} a &= \exp(i\Phi_\theta)\sqrt{n} = |0\rangle\langle 1| + \sqrt{2}|1\rangle\langle 2| + \dots + \sqrt{s}|s-1\rangle\langle s|, \\ a^\dagger &= \sqrt{n}\exp(-i\Phi_\theta) = |1\rangle\langle 0| + \sqrt{2}|2\rangle\langle 1| + \dots + \sqrt{s}|s\rangle\langle s-1|, \end{aligned} \quad (15.54)$$

so

$$[a, a^\dagger] = 1 - (s+1)|s\rangle\langle s|. \quad (15.55)$$

15.4.1 Applications

Fock states. The Fock states should be states with random phase. This is actually also true for any mixed state of the field with only diagonal elements in the density matrix. The expectation value of Φ_θ is

$$\begin{aligned} \langle n | \Phi_\theta | n \rangle &= \sum_{m=0}^s \theta_m |\langle \theta_m | n \rangle|^2 \\ &= \frac{1}{s+1} \sum_{m=0}^s \theta_m \\ &= \theta_0 + \frac{\pi s}{s+1}. \end{aligned} \quad (15.56)$$

We notice that when $s \rightarrow \infty$

$$\langle n | \Phi_\theta | n \rangle = \theta_0 + \pi. \quad (15.57)$$

On the other hand

$$\begin{aligned} \langle n | \Phi_\theta^2 | n \rangle &= \sum_{m=0}^s \theta_m^2 | \langle \theta_m | n \rangle |^2 \\ &= \frac{1}{s+1} \sum_{m=0}^s \theta_m^2 \\ &= \theta_0^2 + \frac{2\pi\theta_0 s}{s+1} + \frac{4\pi^2 s(s+\frac{1}{2})}{3(s+1)^2}, \end{aligned}$$

and when $s \rightarrow \infty$

$$\langle n | \Phi_\theta^2 | n \rangle = \theta_0^2 + 2\pi\theta_0 + \frac{4\pi^2}{3}, \quad (15.58)$$

and

$$(\Delta\Phi_\theta^2)_n = \frac{\pi^2}{3}. \quad (15.59)$$

This corresponds exactly to the classical result. If one has a uniform phase distribution, corresponding to a random phase, then

$$\begin{aligned} \langle \phi \rangle &= \frac{1}{2\pi} \int_{\theta_0}^{\theta_0+2\pi} \phi d\phi = \theta_0 + \pi, \\ \langle \phi^2 \rangle &= \frac{1}{2\pi} \int_{\theta_0}^{\theta_0+2\pi} \phi^2 d\phi = \theta_0^2 + 2\pi\theta_0 + \frac{4\pi^2}{3}, \\ (\Delta\phi^2)_{\text{class}} &= \frac{\pi^2}{3}. \end{aligned} \quad (15.60)$$

Coherent states

$$\langle \alpha | \Phi_\theta | \alpha \rangle = \sum_{m=0}^s \theta_m | \langle \theta_m | \alpha \rangle |^2, \quad (15.61)$$

$$\langle \alpha | \Phi_\theta^2 | \alpha \rangle = \sum_{m=0}^s \theta_m^2 | \langle \theta_m | \alpha \rangle |^2. \quad (15.62)$$

We have to calculate $\langle \theta_m | \alpha \rangle$:

$$\langle \theta_m | \alpha \rangle = \exp\left(-\frac{r^2}{2}\right) (s+1)^{-\frac{1}{2}} \sum_{n=0}^{\infty} \left(\frac{r^n}{\sqrt{n!}}\right) \exp[in(\phi - \theta_m)], \quad (15.63)$$

$$\alpha = r \exp(i\phi),$$

and

$$\begin{aligned} |\langle \theta_m | \alpha \rangle|^2 &= \frac{1}{s+1} \\ &+ \left[\frac{2 \exp(-r^2)}{s+1} \right] \sum_{n>n'} \frac{r^n r^{n'}}{\sqrt{n! n'!}} \cos[(n-n')(\phi - \theta_m)], \end{aligned} \quad (15.64)$$

and choosing for convenience $(\phi - \theta_0) = \pi s/s + 1$, and defining $\mu \equiv m-s/2$, so $-s/2 \leq \mu \leq s/2$, then when $s \rightarrow \infty$, the above summations can be converted into integrals, getting [15.17]

$$\begin{aligned} \langle \Phi_\theta \rangle_\alpha &= \phi, \\ \langle \Delta \hat{\Phi}_\theta^2 \rangle_\alpha &= \frac{\pi^2}{3} + 4 \exp(-r^2) \left[\sum_{n>n'} \frac{(-1)^{n+n'} r^n r^{n'}}{\sqrt{n! n'! (n-n')^2}} \right], \end{aligned} \quad (15.65)$$

which can be evaluated numerically, giving the result shown in Fig. 15.1.

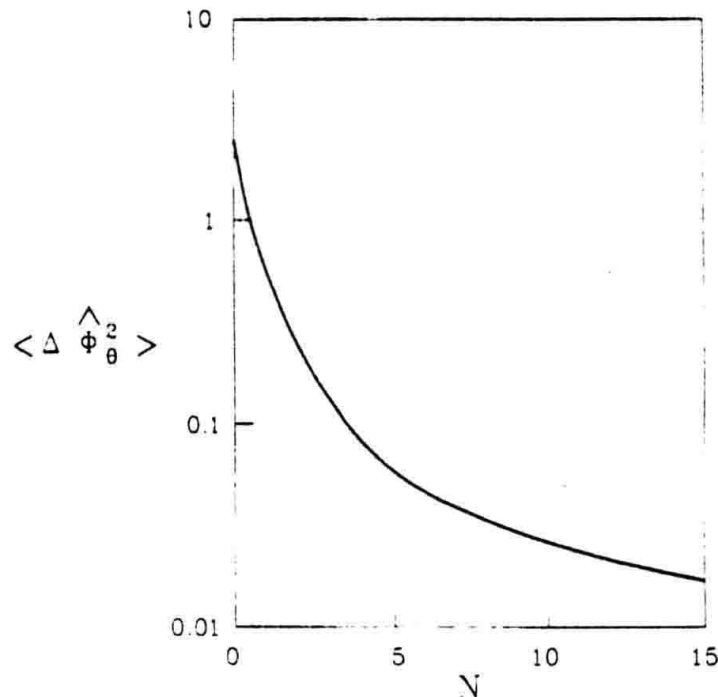


Fig. 15.1. Phase fluctuations of a coherent state versus number of photons

15.5 Phase Fluctuations in a Laser

From the quantum theory of the laser, in the master equation approach the off-diagonal matrix elements of the field density operator can be written as [15.26]

$$\rho_{n,n+k} = \sqrt{\rho_{n,n} \rho_{n+k,n+k}} \exp(-\mu_k t), \quad (15.66)$$

where, according to the Scully-Lamb theory,

$$\mu_k = \frac{1}{2} k^2 D, \quad (15.67)$$

D being the phase diffusion coefficient

$$D = \frac{C}{2\langle n \rangle}, \quad (15.68)$$

and we have assumed that $\rho_{n,n}$ and $\rho_{n+k,n+k}$ are the steady state diagonal elements of the field density operator. Now, assuming that we start from a coherent state $|\alpha\rangle$, one can write [15.26]

$$\begin{aligned} \rho(t) &= \exp(-r^2) \sum_{n,l=0}^s \left\{ \frac{r^n r^l}{\sqrt{n! l!}} \exp \left[i\xi_0(n-l) - \frac{Dt(n-l)^2}{2} \right] \right. \\ &\quad \times |n\rangle \langle l| \}, \quad \alpha = r \exp(i\xi_0). \end{aligned} \quad (15.69)$$

Now we calculate the variance of the Pegg–Barnett phase operator:

$$\langle \Delta \Phi_\theta^2 \rangle_{\text{Laser}} = \sum_m \theta_m^2 \langle \theta_m | \rho | \theta_m \rangle - \left[\sum_m \theta_m \langle \theta_m | \rho | \theta_m \rangle \right]^2. \quad (15.70)$$

From (15.69), we calculate

$$\begin{aligned} &\langle \theta_m | \rho | \theta_m \rangle \\ &= \exp(-r^2) \sum_{n,l=0}^s \frac{r^n r^l}{\sqrt{n! l!}} \exp \left[i\xi_0(n-l) - \frac{Dt(n-l)^2}{2} \right] \\ &\quad \times \langle \theta_m | n \rangle \langle l | \theta_m \rangle \\ &= \frac{\exp(-r^2)}{s+1} \sum_{n,l=0}^s \frac{r^n r^l}{\sqrt{n! l!}} \exp \left[i(\xi_0 - \theta_m)(n-l) - \frac{Dt(n-l)^2}{2} \right] \\ &= \frac{1}{s+1} \left[1 + 2 \exp(-r^2) \sum_{n=1}^s \sum_{l=0}^{n-1} \frac{r^n r^l}{\sqrt{n! l!}} \cos[(\xi_0 - \theta_m)(n-l)] \right. \\ &\quad \left. \times \exp \left(-\frac{Dt(n-l)^2}{2} \right) \right]. \end{aligned} \quad (15.71)$$

Now, we take the continuous limit $s \rightarrow \infty$, $\theta_m \rightarrow \theta$, and get the probability density distribution

$$\begin{aligned} P(\theta)^{(\xi_0)} &= \frac{s+1}{2\pi} \langle \theta | \rho | \theta \rangle \\ &= \frac{1}{2\pi} \left[1 + 2 \exp(-r^2) \sum_{n=1}^{\infty} \sum_{l=0}^{n-1} \frac{r^n r^l}{\sqrt{n! l!}} \cos[(\xi_0 - \theta)(n-l)] \right. \\ &\quad \left. \times \exp \left(-\frac{Dt(n-l)^2}{2} \right) \right]. \end{aligned} \quad (15.72)$$

The above distribution is normalized in the range $[0, 2\pi]$, which corresponds to the entire range of θ_m , when $s \rightarrow \infty$. Furthermore, this probability density is invariant under

$$\xi_0 \rightarrow \xi_0 + 2\pi k, \quad k = 0, 1, 2, \dots . \quad (15.73)$$

For computational convenience, we use the following Gaussian approximation

$$P(k) = \exp(-r^2) \frac{r^{2k}}{k!} \approx \frac{1}{(2\pi r^2)^{1/2}} \exp\left[-\frac{(r^2 - k)^2}{2r^2}\right], \quad (15.74)$$

and substituting $\sqrt{P(k)}$ in (15.72), and replacing summations by integrals, we write

$$P(\theta)^{(\xi_0)} = \frac{1}{2\pi} \left[\frac{1}{(2\pi r^2)^{\frac{1}{2}}} \int_0^\infty dn \int_0^\infty dl \right] \exp \left\{ \frac{-1}{4r^2} [(r^2 - n)^2 + (r^2 - l)^2] + i(\xi_0 - \theta)(n - l) - \frac{Dt(n - l)^2}{2} \right\}$$

or

$$P(\theta)^{(\xi_0)} = \frac{1}{[2\pi(\frac{1}{4r^2} + Dt)]^{1/2}} \exp\left[-\frac{(\xi_0 - \theta)^2}{2(\frac{1}{4r^2} + Dt)}\right]. \quad (15.75)$$

The above probability density is normalized in the θ range $[-\infty, \infty]$, and it is a Gaussian with a variance increasing in time.

We would like to have, instead, a probability distribution in the $[\theta_0, \theta_0 + 2\pi]$ range. Adding an infinite number of Gaussians with the same width, with their centre displaced by $2\pi k$, k integer, we obtain a probability density that is normalized in the desired range and is periodic:

$$P(\theta, \xi_0) = \sum_{k=-\infty}^{\infty} P(\theta)^{(\xi_0 + 2\pi k)} = \frac{1}{[\pi a^2]^{1/2}} \sum_{k=-\infty}^{\infty} \exp\left[-\frac{(\xi_0 + 2\pi k - \theta)^2}{2(\frac{1}{4r^2} + Dt)}\right], \quad (15.76)$$

with

$$a^2 = 2 \left(\frac{1}{4r^2} + Dt \right). \quad (15.77)$$

One can show [15.26] that the phase variance can be written in terms of error functions:

$$\begin{aligned} \langle (\Delta\Phi_\theta)^2 \rangle &= \left(\frac{1}{4r^2} + Dt \right) + \sum_{k=1}^{\infty} k^2 \left\{ \Phi\left[\frac{-\pi + 2\pi(k+1)}{a^2}\right] \right. \\ &\quad \left. - \Phi\left[\frac{-\pi + 2\pi k}{a^2}\right] \right\} \\ &- 4(\pi a^2)^{\frac{1}{2}} \sum_{k=1}^{\infty} \left\{ \exp\left[-\frac{(-\pi + 2\pi k)^2}{a^2}\right] \right. \\ &\quad \left. - \exp\left[-\frac{(-\pi + 2\pi(k+1))^2}{a^2}\right] \right\}, \end{aligned} \quad (15.78)$$

where Φ is the error function. The results are shown in Fig. 15.2.

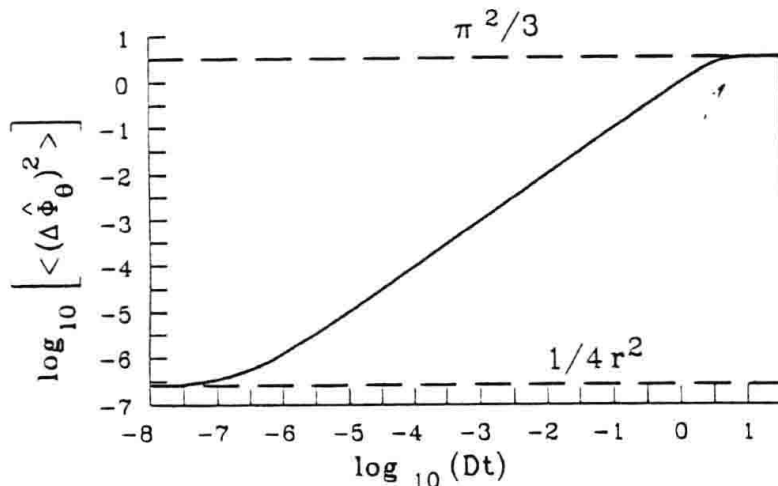


Fig. 15.2. Phase fluctuations of a laser versus time (after [15.26])

We notice from Fig. 15.2 that at the lower end, for $Dt \ll 1$, the phase fluctuations correspond to the shot noise $1/4r^2$, and at the upper end, $Dt \gg 1$, they correspond to a random phase $\pi^2/3$. There is an extensive region of Dt where there is linear dependence. In this last region, the phase diffusion model is valid, and the slope of the curve is the well-known Schawlow-Townes phase diffusion coefficient.

Problems

15.1. Show that

$$\langle n | \cos \phi_D | n \rangle = \langle n | \sin \phi_D | n \rangle = 0,$$

and

$$\begin{aligned} \langle n | \cos^2 \phi_D | n \rangle &= \langle n | \sin^2 \phi_D | n \rangle \\ &= \begin{cases} \frac{1}{2}, & n \neq 0 \\ \frac{1}{4}, & n = 0. \end{cases} \end{aligned}$$

15.2. Prove that

$$[\cos \phi_D, \sin \phi_D] = \frac{\{a^\dagger(n+1)^{-1}a - 1\}}{2i},$$

and hence all the matrix elements are zero except for

$$\langle 0 | [\cos \phi_D, \sin \phi_D] | 0 \rangle = -\frac{1}{2i}.$$

15.3. Prove (15.6).

15.4. Prove (15.27).

15.5 Verify the properties given by (15.50), (15.51), (15.52).

15.6 Prove (15.65).

16. Quantum Trajectories

Einstein, in his classical paper on the A and B coefficients for spontaneous and stimulated emission, assumed the existence of quantum jumps, which greatly stimulated quantum mechanics. However, up until very recently, quantum jumps played practically no role in various theories coupling radiation and matter, and these types of interactions are well described by the Schrödinger wavefunction describing the properties of an ensemble, rather than individual systems. Now, in all the examples we have seen of systems coupled to reservoirs, we have followed the procedure of starting from the Liouville equation for the system coupled to the reservoir, then we trace or average over the reservoir variables and, after a Markovian approximation, end up with a master equation of the form

$$\frac{d\rho_S}{dt} = \frac{i}{\hbar} [\rho_S, H_S] + L_{\text{relax}}(\rho_S), \quad (16.1)$$

where

$$L_{\text{relax}}(\rho_S) = -\frac{1}{2} \sum_m (C_m^\dagger C_m \rho_S + \rho_S C_m^\dagger C_m + 2C_m \rho_S C_m^\dagger). \quad (16.2)$$

The above form, normally called the Lindblad form, describes many systems coupled to reservoirs.

For example, if we want to describe the spontaneous emission in a two-level atomic system, then $C_1 = \sqrt{\gamma}\sigma^-$, and $L_{\text{relax}}(\rho_S) = -\frac{1}{2}\gamma(\sigma^\dagger\sigma\rho_S + \rho_S\sigma^\dagger\sigma + 2\sigma\rho_S\sigma^\dagger)$, γ being the inverse lifetime of the atomic transition. Similarly, if we are describing a damped harmonic oscillator, then the same applies after replacing $\sigma^\dagger \rightarrow a^\dagger$, $\sigma \rightarrow a$.

We now present a method based on the wavefunction to describe such a system. In general, we are not allowed to use the Schrödinger equation to describe system-reservoir type interactions, since even if we start initially with a pure state, the coupling to the bath will produce statistical mixtures, and we traditionally are forced to go to the Liouville equation. However two alternatives have been recently proposed:

- (1) The system evolves with a non-Hermitian Hamiltonian, interrupted once in a while by instantaneous quantum jumps. Carmichael called this process ‘quantum trajectories’, and it is also called the Monte Carlo wavefunction method [16.1], [16.2], [16.3].

- (2) Schrödinger's equation is reinterpreted as representing an individual system following stochastic dynamics of the diffusive type. We will write a stochastic Schrödinger equation

16.1 Monte Carlo Wavefunction Method

We calculate the change of the wavefunction $|\phi(t)\rangle \rightarrow |\phi(t+\delta t)\rangle$ in two steps:

- (a) Calculate $|\phi^1(t + \delta t)\rangle$ obtained from the evolution of $|\phi(t)\rangle$ with a non-Hermitian Hamiltonian given by

$$H = H_s - \frac{i\hbar}{2} \sum_m C_m^\dagger C_m. \quad (16.3)$$

For δt small, we get

$$|\phi^1(t + \delta t)\rangle = \left(1 - \frac{iH\delta t}{\hbar}\right) |\phi(t)\rangle. \quad (16.4)$$

Since H is non-Hermitian, $|\phi^1(t + \delta t)\rangle$ is not normalized. Thus

$$\begin{aligned} \langle \phi^1(t + \delta t) | \phi^1(t + \delta t) \rangle &= \langle \phi(t) | \left(1 + \frac{iH^\dagger \delta t}{\hbar}\right) \left(1 - \frac{iH\delta t}{\hbar}\right) |\phi(t)\rangle \\ &\equiv 1 - \delta p, \end{aligned} \quad (16.5)$$

$$\delta p = \delta t \frac{i}{\hbar} \langle \phi(t) | H - H^\dagger | \phi(t) \rangle \equiv \sum_m \delta p_m, \quad (16.6)$$

$$\delta p_m \equiv \delta t \langle \phi(t) | C_m^\dagger C_m | \phi(t) \rangle \geq 0.$$

We can always adjust δt such that $\delta p \ll 1$.

- (b) The second step corresponds to a gedanken experiment of a measurement process. We consider the possibility of a quantum jump. In order to decide whether a quantum jump has occurred, we define a random number ε uniformly distributed between zero and one and compare it to δp . Two cases may arise:

- (I) $\varepsilon \geq \delta p$. This will be the vast majority of cases, since $\delta p \ll 1$. In this case there is no quantum jump and $|\phi(t + \delta t)\rangle = |\phi^1(t + \delta t)\rangle / \sqrt{1 - \delta p}$.
- (II) $\varepsilon < \delta p$. A quantum jump occurs to one of the states $C_m |\phi(t)\rangle$ according to the relative probability among the various possible types of jumps, $\Pi_m = \delta p_m / \delta p$ (notice that $\sum_m \Pi_m = 1$). So

$$|\phi(t + \delta t)\rangle = \frac{C_m |\phi(t)\rangle}{\sqrt{\delta p_m / \delta p}}. \quad (16.7)$$

Milburn *et al.* [16.10] showed that a mode of the electromagnetic field in a cavity at $T' = 0$ is described by a quantum jump equation if the outgoing light is detected directly by a photodetector. We will generalize these arguments in the next sections.

16.1.1 The Monte Carlo Method is Equivalent, on Average, to the Master Equation

We define $\bar{\sigma}(t) = \text{Av}[\sigma(t) = |\phi(t)\rangle\langle\phi(t)|]$, where Av means the average of many Monte Carlo results at time t , all of them starting from $|\phi(0)\rangle$. We will now show that $\bar{\sigma}(t)$ coincides with ρ_S . We calculate $\bar{\sigma}(t + \delta t)$:

$$\begin{aligned}\bar{\sigma}(t + \delta t) &= (1 - \delta p) \frac{|\phi^1(t + \delta t)\rangle\langle\phi^1(t + \delta t)|}{\sqrt{1 - \delta p}\sqrt{1 - \delta p}} \\ &\quad + \delta p \sum_m \pi_m \frac{C_m |\phi(t)\rangle\langle\phi(t)| C_m^\dagger}{\sqrt{\delta p_m/\delta p}\sqrt{\delta p_m/\delta p}}\end{aligned}\quad (16.8)$$

or:

$$\begin{aligned}\bar{\sigma}(t + \delta t) &= \left(1 - \frac{i\hbar}{2} \left(H_s - \frac{i\hbar}{2} \sum_m C_m^\dagger C_m \right) \right) |\phi(t)\rangle\langle\phi(t)| \\ &\quad \times \left[1 + \frac{i\delta t}{\hbar} \left(H_s + \frac{i\hbar}{2} \sum_m C_m^\dagger C_m \right) \right] \\ &\quad + \delta t \sum_m C_m |\phi(t)\rangle\langle\phi(t)| C_m^\dagger,\end{aligned}$$

which can be put as

$$\begin{aligned}\bar{\sigma}(t + \delta t) &= \sigma(t) + \frac{i\delta t}{\hbar} \left\{ \sigma \left(H_s + \frac{i\hbar}{2} \sum_m C_m^\dagger C_m \right) \right. \\ &\quad \left. - (H_s - \frac{i\hbar}{2} \sum_m C_m^\dagger C_m) \sigma \right\} \\ &\quad + \delta t \sum_m C_m \sigma C_m^\dagger \\ &= \sigma + \frac{i\delta t}{\hbar} [\sigma, H_s] + \delta t L_{\text{relax}}(\sigma).\end{aligned}\quad (16.9)$$

Finally, if we average over a large number of trajectories, we recover the master equation (16.1).

Similarly to the master equation methods, one is interested in computing averages of interesting observables. Here, for each trajectory we get $\langle\phi^i(t) | A | \phi^i(t)\rangle$ for many solutions $|\phi^i(t)\rangle$, thus $\langle A \rangle_n = \frac{1}{n} \sum_n \langle\phi^i(t) | A | \phi^i(t)\rangle$ and $\langle A \rangle_n \rightarrow \langle A \rangle$ as $n \rightarrow \infty$.

The equivalence between the master equation and the Monte Carlo method is valid as long as $\eta_i \delta t \ll 1$, where $\eta_i \hbar$ is a typical energy eigenvalue of the system. An example to illustrate the procedure is the one-atom Raman laser [16.4], [16.5]. It consists in a three-level atom interacting with two quantum fields and a classical coherent pump, as shown in Fig. 16.1.

The Hamiltonian of the system is

$$H = i\hbar g_{ab}(a\sigma_{ab} - a^\dagger\sigma_{ba}) + i\hbar g_{bc}(b\sigma_{bc} - b^\dagger\sigma_{cb}) + i\hbar\Omega(\sigma_{ac} - \sigma_{ca}), \quad (16.10)$$

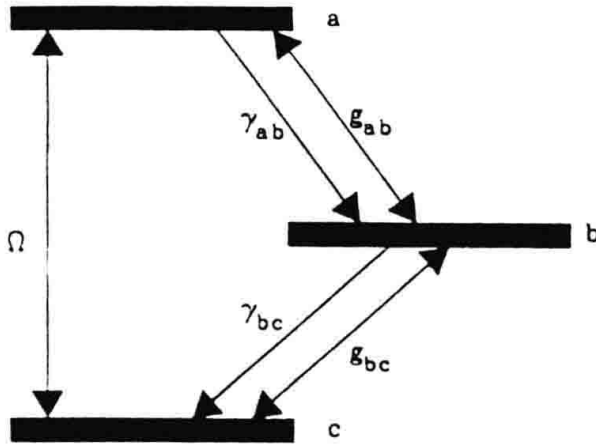


Fig. 16.1. Three-level atom inside a double cavity

and the damping terms are

$$\begin{aligned}
 L_{\text{relax}}(\rho_S) = & \frac{\gamma_{ab}}{2}(2\sigma_{ba}\rho_S\sigma_{ab} - \sigma_{ab}\sigma_{ba}\rho_S - \rho_S\sigma_{ab}\sigma_{ba}) \\
 & + \frac{\gamma_{bc}}{2}(2\sigma_{cb}\rho_S\sigma_{bc} - \sigma_{bc}\sigma_{cb}\rho_S - \rho_S\sigma_{bc}\sigma_{cb}) \\
 & + \frac{\gamma_a}{2}(2a\rho_S a^\dagger - a^\dagger a \rho_{\text{sys}} - \rho_{\text{sys}} a^\dagger a) \\
 & + \frac{\gamma_b}{2}(2b\rho_{\text{sys}} b^\dagger - b^\dagger b \rho_{\text{sys}} - \rho_{\text{sys}} b^\dagger b).
 \end{aligned} \tag{16.11}$$

In Fig. 16.2 we show $\langle n \rangle$ and the Mandel parameter $Q_{\text{Mandel}} \equiv (\langle (\Delta n)^2 \rangle - \langle n \rangle)/\langle n \rangle$ as a function of time. The results were obtained by averaging over

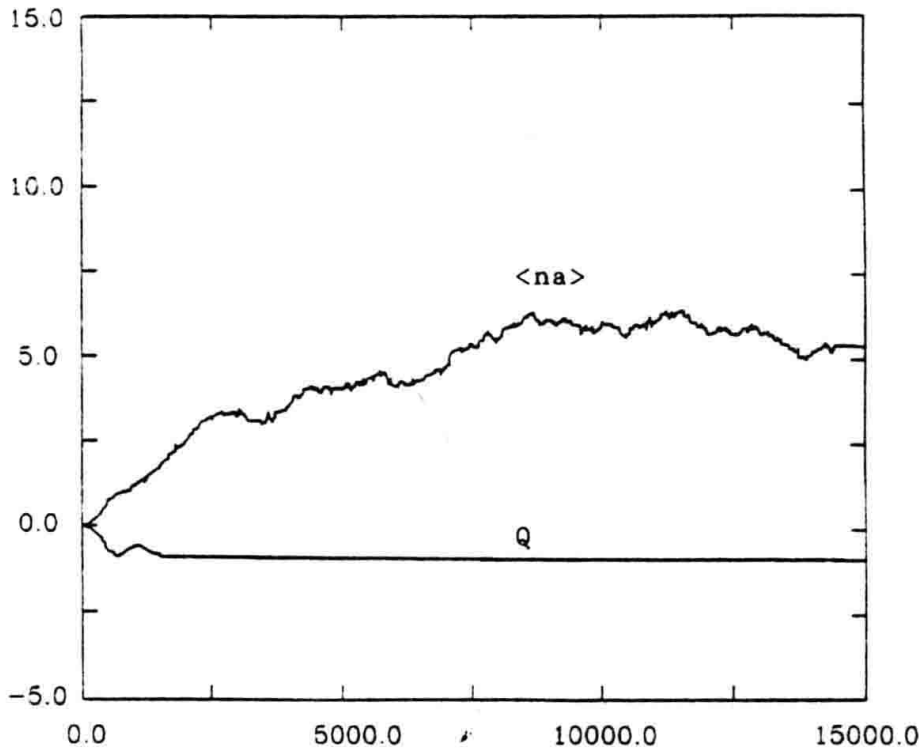


Fig. 16.2. Average photon number (upper curve) and Mandel's Q parameter as a function of time. The parameters taken are $g_{ab} = g_{bc} = 1$, $\Omega = 1$, $\gamma_a = 0.5$, $\gamma_b = 3$, $\gamma_{ab} = 0$, $\gamma_{bc} = 1$. We also added a detuning $\delta_a = -\delta_b = 1.41$.

50 trajectories. We notice that for a certain set of parameters we get a Q value very close to -1 , implying that we are generating an almost pure Fock state.

16.2 The Stochastic Schrödinger Equation

If an open system with a density operator ρ starts initially as a pure state and evolves into a mixed state, as a result of the interaction with the reservoir, there can be no deterministic equation for $|\phi\rangle$, but one could define a stochastic equation, as one would expect, given the probabilistic nature of the interaction with the environment. Gisin and Percival [16.6], [16.7], [16.8] proposed the following equation

$$|d\phi\rangle = |v\rangle \delta t + \sum_j |u_j\rangle \langle u_j| d\xi_j, \quad (16.12)$$

where the first term on the right-hand side of (16.12) represents the drift and the second one the diffusion. Also $d\xi_j$ is a complex stochastic Wiener process, such that

$$\begin{aligned} M(\text{Re}(d\xi_j)\text{Re}(d\xi_k)) &= M(\text{Im}(d\xi_j)\text{Im}(d\xi_k)) = \delta_{jk} \frac{\delta t}{2}, \\ M\text{Re}(d\xi_j) &= M(\text{Im}(d\xi_j)\text{Re}(d\xi_j)) = 0, \end{aligned} \quad (16.13)$$

which is equivalent to writing

$$M((d\xi_j)^*(d\xi_k)) = \delta_{jk} \delta t. \quad (16.14)$$

For normalization purposes, we set $\langle \phi | u_j \rangle = 0$, and take the mean value of both $|d\phi\rangle$ and $|d\phi\rangle\langle d\phi|$:

$$M |d\phi\rangle = |v\rangle \delta t, \quad (16.15)$$

$$M |d\phi\rangle\langle d\phi| = 2 \sum_j |u_j\rangle\langle u_j| \delta t.$$

We notice that (16.15) was obtained to order δt and also using (16.14), that is $d\xi_k$ is of order $\sqrt{\delta t}$ and therefore we have to keep second-order differentials. This is the characteristic of the Ito algebra.

Now, we can write

$$d\rho = M(|\phi\rangle\langle d\phi| + |d\phi\rangle\langle\phi| + |d\phi\rangle\langle d\phi|), \quad (16.16)$$

$$\frac{d\rho}{dt} = |\phi\rangle |v\rangle + |v\rangle\langle\phi| + 2 \sum_j |u_j\rangle\langle u_j|, \quad (16.17)$$

and we try to obtain the diffusion and drift term and relate them to the Master equation.

Multiplying (16.17) on the left and right sides by the projector $(1 - |\phi\rangle\langle\phi|)$, we get

$$(1 - |\phi\rangle\langle\phi|) \frac{d\rho}{dt} (1 - |\phi\rangle\langle\phi|) = 2 \sum_j |u_j\rangle\langle u_j|. \quad (16.18)$$

Now for the drift part, we take (16.17) and multiply it by $\frac{1}{2}\langle\phi|$ on the left and $|\phi\rangle$ on the right. We readily get

$$\frac{1}{2} \left\langle \phi \left| \frac{d\rho}{dt} \right| \phi \right\rangle = \text{Re}\langle\phi|v\rangle, \quad (16.19)$$

and multiplying (16.17) by $|\phi\rangle$, we also get

$$\frac{d\rho}{dt} |\phi\rangle = |\phi\rangle\langle v|\phi\rangle + |v\rangle. \quad (16.20)$$

By combining (16.19), (16.20), we finally get

$$|v\rangle = \frac{d\rho}{dt} |\phi\rangle - \left(\frac{1}{2}\langle\phi| \frac{d\rho}{dt} |\phi\rangle + ic \right) |\phi\rangle, \quad (16.21)$$

where c is a non-physical imaginary phase determined by the convention that this equation has to agree with the conventional Schrödinger equation in the absence of coupling to the environment, and corresponds to $\text{Im}\langle\phi|v\rangle$.

As we can see, we have obtained both the diffusion (16.18) and the drift (16.21) in terms of $d\rho/dt$, so all that is left is to replace the master equation (16.3), (16.4) in both terms, to arrive at the stochastic Schrödinger equation

$$\begin{aligned} d|\phi\rangle &= -\frac{i}{\hbar}H|\phi\rangle\delta t \\ &+ \sum_m \left(\langle C_m \rangle_\phi C_m - \frac{1}{2}C_m^\dagger C_m - \frac{1}{2}\langle C_m^\dagger \rangle_\phi \langle C_m \rangle_\phi \right) |\phi\rangle\delta t \\ &+ \sum_m (C_m - \langle C_m \rangle_\phi) |\phi\rangle d\xi_m. \end{aligned} \quad (16.22)$$

An equivalent stochastic Schrödinger equation, interpreted as homodyne measurement, for $T = 0$, can be derived [16.10], with a noise that is real rather than complex:

$$\begin{aligned} d|\phi\rangle &= -\frac{i}{\hbar}H|\phi\rangle\delta t \\ &+ \left\{ \left(-\frac{\gamma}{2}a^\dagger a + 2\gamma\langle X(t)\rangle_\phi \right) \delta t \right. \\ &\quad \left. + \sqrt{\gamma}\Delta W(t)a \right\} |\phi\rangle, \end{aligned} \quad (16.23)$$

where the ΔW is a Wiener increment, satisfying

$$\langle \Delta W \rangle = 0, \quad (16.24)$$

$$\langle (\Delta W)^2 \rangle = \Delta t. \quad (16.25)$$

In the next few sections, we will generalize these arguments for $T \neq 0$. We will also show a physical realization, in the context of cavity QED, of both the Monte Carlo and stochastic Schrödinger methods.

16.3 Stochastic Schrödinger Equations and Dissipative Systems

As we mentioned at the begining of this chapter, a wide class of master equations describing the evolution of dissipative quantum systems can be written in the Lindblad form [16.12]

$$\dot{\rho}_S = \mathcal{L}\rho_S, \quad (16.26)$$

where

$$\mathcal{L} = \mathcal{L}_0 + \sum_n \mathcal{L}_n, \quad (16.27)$$

$$\mathcal{L}_0\rho_S = \frac{i}{\hbar}[\rho_S, H_S], \quad (16.28)$$

$$\mathcal{L}_n\rho_S = -\frac{1}{2}[C_n^\dagger C_n \rho_S + \rho_S C_n^\dagger C_n] + \sum_n C_n \rho_S C_n^\dagger, \quad (16.29)$$

ρ_S is the reduced density operator for the ‘small’ system S (obtained by tracing out the degrees of freedom of the reservoir R from the density operator for the full system $S + R$), and H_S describes the Hamiltonian evolution of the small system S in the interaction picture. The operators C_n act on the space of states of the small system S , and express the interaction of S with the reservoir R . The number of them depends on the nature of the problem. We follow here the reference [16.13].

An example of such an equation is the master equation for a field in a lossy cavity, at temperature T , given in the interaction picture by

$$\begin{aligned} \frac{d\rho_f}{dt} = & \gamma\langle n \rangle_{\text{th}} \left(a^\dagger \rho_f a - \frac{1}{2}aa^\dagger \rho_f - \frac{1}{2}\rho_f aa^\dagger \right) \\ & + \gamma(1 + \langle n \rangle_{\text{th}}) \left(a\rho_f a^\dagger - \frac{1}{2}a^\dagger a\rho_f - \frac{1}{2}\rho_f a^\dagger a \right), \end{aligned} \quad (16.30)$$

where a and a^\dagger are the photon annihilation and creation operators, respectively, $\langle n \rangle_{\text{th}}$ is the average number of thermal photons, given by Planck’s distribution, and $\gamma = 1/t_{\text{cav}}$, where t_{cav} is the damping time. In this case, one could set

$$C_1 \equiv \sqrt{\gamma(1 + \langle n \rangle_{\text{th}})}a, \quad C_2 \equiv \sqrt{\gamma\langle n \rangle_{\text{th}}}a^\dagger. \quad (16.31)$$

A formal solution of (9.4) is

$$\rho(t) = \exp(\mathcal{L}t)\rho(0). \quad (16.32)$$

Let us define

$$J_n \rho = C_n \rho C_n^\dagger, \quad (16.33)$$

and write

$$\rho(t) = \exp \left\{ \mathcal{L}_0 + \sum_n [J_n + (\mathcal{L}_n - J_n)] t \right\} \rho(0). \quad (16.34)$$

Note that

$$(\mathcal{L}_n - J_n) \rho_S = -\frac{1}{2} (C_n^\dagger C_n \rho_S + \rho_S C_n^\dagger C_n). \quad (16.35)$$

Applying Dyson's expansion to (16.34), we get

$$\begin{aligned} \rho(t) &= \sum_{m=0}^{\infty} \int_0^t dt_m \int_0^{t_m} dt_{m-1} \dots \int_0^{t_2} dt_1 \\ &\quad \{ S(t - t_m) \left(\sum_n J_n \right) S(t_m - t_{m-1}) \\ &\quad \times \dots \times \left(\sum_n J_n \right) S(t_1) \} \rho(0), \end{aligned} \quad (16.36)$$

where

$$S(t) = \exp \left\{ \left[\mathcal{L}_0 + \sum_n (\mathcal{L}_n - J_n) \right] t \right\}. \quad (16.37)$$

Equation (16.36) may be rewritten in the following way

$$\begin{aligned} \rho(t) &= \sum_{m=0}^{\infty} \sum_{\{n_i\}} \int_0^t dt_m \int_0^{t_m} dt_{m-1} \dots \int_0^{t_2} dt_1 \\ &\quad \{ S(t - t_m) J_{n_m} S(t_m - t_{m-1}) \\ &\quad \times \dots \times J_{n_1} S(t_1) \} \rho(0). \end{aligned} \quad (16.38)$$

Each term in the above double sum can be considered as a quantum trajectory, the reduced density operator at time t being given by the sum over all possible quantum trajectories. For each of these trajectories, (16.38) shows that the evolution of the system can be considered as a succession of quantum jumps, associated with the operators J_n , interspersed by smooth time evolutions, associated with the operators $S(t)$. The probability of each trajectory is given by the trace of the corresponding term in (16.38).

From (16.35) and (16.37), we can write

$$S(t)\rho = N(t)\rho N(t)^\dagger, \quad (16.39)$$

where

$$N(t) = \exp \left[-\frac{i}{\hbar} H_S t - \frac{t}{2} \sum_n (C_n^\dagger C_n) \right]. \quad (16.40)$$

Therefore, if ρ is a pure state, then $S(t)\rho$ is also a pure state. The same is true for $J_n\rho$, with J_n defined by (16.33). This implies that a pure state remains pure when a single quantum trajectory is considered. Note also that the evolution between jumps is given by the non-unitary operator $N(t)$.

It is clear from (16.34) that different choices of the jump operators are possible. These different choices correspond to different decompositions in terms of quantum trajectories of the time evolution of the density operator ρ_S and, eventually, to different experimental schemes leading to the continuous monitoring of the evolution of the system. It is precisely due to this continuous monitoring that an initial pure state remains pure, since no information is lost in this situation: for a field in a cavity, this continuous monitoring amounts to accounting for every photon gained or lost by the field, due to its interaction with the reservoir [16.13].

We will discuss now two different ways of looking at the reservoir for a field in a cavity, which will lead to a Monte Carlo quantum jump approach, for the first case, and to a Schrödinger equation with stochastic terms, for the second one.

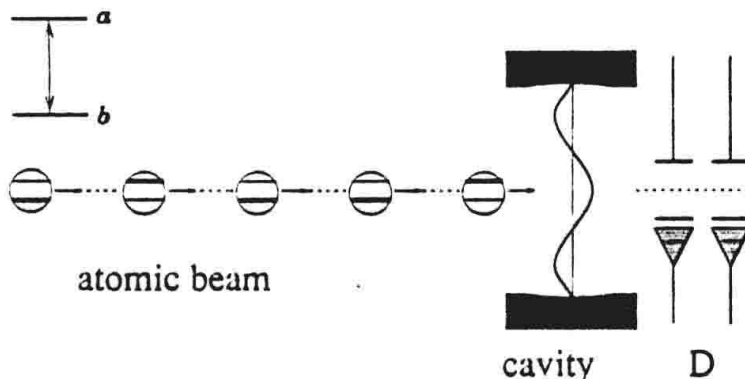


Fig. 16.3. Physical realization of a quantum jump trajectory. A beam of two-level atoms crosses a resonant cavity

16.4 Simulation of a Monte Carlo SSE

We exhibit in this section a physical realization of the Monte Carlo method [16.13]. The corresponding experimental scheme is shown in Fig. 16.3. A monokinetic atomic beam plays the role of a reservoir R and crosses a lossless cavity, interacting with one mode of the electromagnetic field. The cavity mode plays the role of a small system S . The atoms, regularly spaced along the atomic beam, are prepared in one of two Rydberg states: an upper state $|a\rangle$ or a lower state $|b\rangle$. The transition frequency ω between these two states is assumed to be resonant with the cavity mode. A similar model of the reservoir was adopted in Sect. 16.1 of [16.14].

The state of the atoms is measured by a detector just at the exit of the cavity. The ratio between the flux of the upper state atoms r_a and the lower state atoms r_b before their entrance into the cavity is chosen so that

$$\frac{r_a}{r_b} = e^{-\hbar\omega/k_B T} \equiv \frac{\langle n \rangle_{\text{th}}}{1 + \langle n \rangle_{\text{th}}}, \quad (16.41)$$

where $\hbar\omega$ is the difference in energy between $|a\rangle$ and $|b\rangle$ and, as will be shown in the next few paragraphs, T is the reservoir temperature.

We analyse now the time evolution of the state vector $|\Psi(t)\rangle$ of S , under the continuous measurement of the atoms after they leave the cavity. We also assume that one knows the state of each atom before it interacts with the cavity. This may be achieved by selectively exciting the atoms to $|a\rangle$ or $|b\rangle$, according to the proportion given by (16.41). We will adopt the following simplifying assumptions: (a) the atom-field interaction time τ is the same for all atoms; (b) the spatial profile of the electric field is constant; (c) the cavity is perfect, i.e., the field state is changed only by the atoms; (d) the atom-field coupling constant g and the interaction time τ are both small, so that the atomic state rotation is very small; (e) the rotating-wave and dipole approximations will be used; and (f), according to statements (d) and (e), quantum cooperative effects will be neglected. In this case the interaction Hamiltonian in the interaction picture will be

$$H = \hbar g (|b\rangle\langle a|a^\dagger + |a\rangle\langle b|a). \quad (16.42)$$

The operators a and a^\dagger are annihilation and creation operators, acting on the space of states of the field mode. Just before the i th atom enters the cavity, the state describing the combined system (atom i + field) is given by

$$|\Psi_{a-f}(t_i)\rangle = |\Psi(t_i)\rangle \otimes |\Psi_a(t_i)\rangle. \quad (16.43)$$

Here $|\Psi_a(t_i)\rangle = |a\rangle$ or $|\Psi_a(t_i)\rangle = |b\rangle$, depending on the state to which the atom was excited just prior to entering the cavity.

At time $t_i + \tau$, the atom-field state vector, up to second order in τ , is given by

$$|\tilde{\Psi}_{a-f}(t_i + \tau)\rangle = \left(1 - ig\tau|b\rangle\langle a|a^\dagger - ig\tau|a\rangle\langle b|a - \frac{g^2\tau^2}{2}|b\rangle\langle b|a^\dagger a - \frac{g^2\tau^2}{2}|a\rangle\langle a|aa^\dagger \right) |\Psi_{a-f}(t_i)\rangle, \quad (16.44)$$

where the tilde indicates that the state vector is not normalized. The expansion (16.44) should be very good in view of condition (d). We assume that $(r_a + r_b)\tau < 1$, so that there is at most one atom inside the cavity at each instant of time. After this atom exits the cavity and is detected, one of the following four cases will be realized:

- (i) The atom enters the cavity in state $|b\rangle$ and is detected in the same state. In this case, according to (16.44), the state of S at time $t = t_i + \tau$ will be given by

$$|\tilde{\Psi}(t_i + \tau)\rangle = \left(1 - \frac{g^2\tau^2}{2}a^\dagger a\right)|\Psi(t_i)\rangle. \quad (16.45)$$

- (ii) The atom enters the cavity in state $|a\rangle$ and it is detected in the same state $|a\rangle$. In this case,

$$|\tilde{\Psi}(t_i + \tau)\rangle = \left(1 - \frac{g^2\tau^2}{2}aa^\dagger\right)|\Psi(t_i)\rangle. \quad (16.46)$$

- (iii) The atom enters the cavity in the state $|b\rangle$ and it is detected in the state $|a\rangle$. In this case,

$$|\tilde{\Psi}(t_i + \tau)\rangle = -ig\tau a|\Psi(t_i)\rangle. \quad (16.47)$$

- (iv) The atom enters the cavity in the state $|a\rangle$ and it is detected in the state $|b\rangle$. Then,

$$|\tilde{\Psi}(t_i + \tau)\rangle = -ig\tau a^\dagger|\Psi(t_i)\rangle. \quad (16.48)$$

Note that in the cases (i) and (ii) a small change in the state of S takes place, while in the cases (iii) and (iv) a big change may happen (a quantum jump). However, these last two cases are very rare, due to the small change of the atomic state during the interaction time.

We consider now the change of $|\Psi\rangle$ from t to $t + \delta t$, where the time interval δt is large enough so that many atoms go through the cavity during this time interval ($n_a = r_a \delta t \gg 1$, $n_b = r_b \delta t \gg 1$), and also much smaller than $t_{\text{cav}}/\langle n \rangle_{\text{th}}\langle n \rangle$, where $\langle n \rangle$ is the average number of photons in the state. This last condition, as will be seen later, implies that the probability of a quantum jump during δt is very small. In most of the time intervals δt the atoms will be detected at the same state they came in, since the transition probability is very small. The evolution of $|\Psi\rangle$ during these intervals will be given by

$$\begin{aligned} |\tilde{\Psi}(t + \delta t)\rangle &= \left(1 - \frac{g^2\tau^2}{2}aa^\dagger\right)^{n_a} \\ &\quad \times \left(1 - \frac{g^2\tau^2}{2}a^\dagger a\right)^{n_b} |\Psi(t)\rangle \\ &= \left(1 - \frac{n_a g^2 \tau^2}{2}aa^\dagger - \frac{n_b g^2 \tau^2}{2}a^\dagger a\right) |\Psi(t)\rangle. \end{aligned} \quad (16.49)$$

This result does not depend on the ordering of the upper-state and lower-state atoms. We also note that in the interaction picture the state vector does not evolve when there is no atom inside the cavity, since the only source of field dissipation is the interaction with the atomic beam.

Equation (16.49) displays the interesting property that the wavefunction of the system (and, consequently, the mean energy) may change even when there is no exchange of energy between the system and the measurement apparatus (represented by the atoms in the present case). An easy way to understand this effect physically is to imagine that all atoms are sent into the cavity in the lower state, and are detected in the same state after exiting the cavity, for a given realization of the system, which starts with a coherent state in the cavity. Then, even though there is no exchange of energy between the atoms and the field in the cavity, as time evolves the ground state component of the initial state should also increase, since the results of the measurements lead to an increasing probability that there is a vacuum state in the cavity. In other words, the fact that there is no quantum jump, for that specific trajectory, provides us with information about the quantum state of the system, and this information leads to an evolution of the state [16.13]. This is closely related to the quantum theory of continuous measurement [16.15], [16.16] and also to quantum non-demolition measurement schemes proposed recently [16.17]. This problem is also very similar to that of a Heisenberg microscope in which even the unsuccessful events of light scattering produce a change in the quantum-mechanical state of the particle [16.18].

We introduce now the following definitions

$$\gamma \equiv (r_b - r_a)g^2\tau^2 = \frac{r_b}{1 + \langle n \rangle_{\text{th}}} g^2\tau^2 = \frac{r_a}{\langle n \rangle_{\text{th}}} g^2\tau^2, \quad (16.50)$$

$$C_1 \equiv \sqrt{\gamma(1 + \langle n \rangle_{\text{th}})} a, \quad C_2 \equiv \sqrt{\gamma\langle n \rangle_{\text{th}}} a^\dagger. \quad (16.51)$$

Using these definitions and (16.41), (16.49) may be rewritten in the following way:

$$|\tilde{\Psi}(t + \delta t)\rangle = \left[1 - \frac{\delta t}{2} \sum_m C_m^\dagger C_m \right] |\Psi(t)\rangle. \quad (16.52)$$

If an atom enters the cavity in state $|a\rangle$ and is detected in state $|b\rangle$, the state vector of S suffers a ‘quantum jump’, and one photon is added to that system. On the other hand, a de-excitation in S occurs if an atom which entered in $|b\rangle$ is detected in state $|a\rangle$. The probability of this event occurring may be calculated by using (16.51) and (16.47) or (16.48); thus, the probability of an excitation (action of a^\dagger) occurring between t and $t + \delta t$ is given by

$$\delta p_1 = \delta t \langle \Psi(t) | C_1^\dagger C_1 | \Psi(t) \rangle. \quad (16.53)$$

The probability of a de-excitation (action of a) during this time interval is

$$\delta p_2 = \delta t \langle \Psi(t) | C_2^\dagger C_2 | \Psi(t) \rangle. \quad (16.54)$$

The probabilities δp_1 and δp_2 are very low, so that the joint probability of having one excitation and one de-excitation during the same time interval δt is negligible. One may therefore write

$$|\tilde{\Psi}(t + \delta t)\rangle = C_1^{\delta N_1} C_2^{\delta N_2} \left[1 - \frac{\delta t}{2} \sum_m C_m^\dagger C_m \right] |\Psi(t)\rangle. \quad (16.55)$$

where δN_1 and δN_2 are equal to one or zero, with probabilities δp_1 and δp_2 for δN_1 and δN_2 to be equal to one, respectively. This may be represented by writing the statistical mean $M(\delta N_m) = \langle C_m^\dagger C_m \rangle \delta t$. Also, $\delta N_m \delta N_n = \delta N_m \delta_{nm}$. One should note that the instants of time in which the quantum jumps occur during the time interval δt are irrelevant, since the jump operators can be commuted through the no-jump evolution, the commutation producing an overall phase which goes away upon renormalization of the state. This can be easily seen by rewriting the no-jump evolution, during a time interval $\delta t_j < \delta t$, as an exponential

$$1 - \frac{\delta t_j}{2} \sum_m C_m^\dagger C_m = \exp \left(-\frac{\delta t_j}{2} \sum_m C_m^\dagger C_m \right) + O[(\delta t_j)^2], \quad (16.56)$$

and using the relation

$$C_i \exp \left(-\frac{\delta t_j}{2} \sum_m C_m^\dagger C_m \right) = \exp \left(-\frac{\delta t_j}{2} \sum_m C_m^\dagger C_m \right) C_i e^{\lambda_i}, \quad (16.57)$$

where $\lambda_1 = -(\delta t_j/2)\gamma(1 + \langle n \rangle_{\text{th}})$ and $\lambda_2 = (\delta t_j/2)\gamma\langle n \rangle_{\text{th}}$.

The results of the measurement may be simulated by picking up random numbers. The state vector in (16.55) may be normalized as follows:

$$|\psi(t + \delta t)\rangle = \left\{ \begin{aligned} & \frac{C_1}{\sqrt{C_1^\dagger C_1}} \delta N_1 + \frac{C_2}{\sqrt{C_2^\dagger C_2}} \delta N_2 \\ & + (1 - \delta N_1)(1 - \delta N_2) \left(1 - \frac{\delta t}{2} \sum_m C_m^\dagger C_m \right) \\ & \times \left(1 - \delta t \sum_m \langle C_m^\dagger C_m \rangle \right)^{-1/2} \end{aligned} \right\} |\psi(t)\rangle. \quad (16.58)$$

In this equation, the first two terms represent the possible jumps, each normalized, as in the Monte Carlo method, and the last term is the no-jump evolution contribution, normalized with the corresponding prefactor that rules out the jumps. From (16.58) one gets for $|\mathrm{d}\psi(t)\rangle \equiv |\psi(t + \delta t)\rangle - |\psi(t)\rangle$

$$|\mathrm{d}\psi(t)\rangle = \left\{ \begin{aligned} & \sum_m \left[\frac{C_m}{\sqrt{C_m^\dagger C_m}} - 1 \right] \delta N_m \\ & - \frac{\delta t}{2} \sum_m (C_m^\dagger C_m - \langle C_m^\dagger C_m \rangle) \end{aligned} \right\} |\psi(t)\rangle. \quad (16.59)$$

16.5 Simulation of the Homodyne SSDE

We now show that, by a suitable modification of the atomic configuration, it is also possible to interpret physically diffusion-like Schrödinger equations in terms of continuous measurements made on atoms [16.13], which cross the cavity containing the field. The corresponding scheme is shown in Fig. 16.4: a beam of three-level atoms with a degenerate lower state (states b and c) crosses the cavity, the field in the cavity being resonant with a transition between one of the two lower levels (say, level b) and the upper atomic state a , while a strong classical field connects the other lower state with the upper level (one may assume that both fields are circularly polarized, so that the cavity field cannot connect a and c , while the strong field does not induce transitions between a and b). We also assume that the atom is prepared in either a coherent superposition of the two lower levels:

$$|\psi_{\text{atom}}\rangle = \frac{1}{\sqrt{2}}(|b\rangle + |c\rangle), \quad (16.60)$$

or in the upper one, following a Boltzmann distribution corresponding to a temperature T for the atoms, which act as a reservoir for the quantum field in the cavity.

In the interaction picture, one can write

$$\begin{aligned} H = & \hbar g_{ac}(\varepsilon |a\rangle\langle c| + \varepsilon |c\rangle\langle a|) \\ & + \hbar g_{ab}(a^\dagger |b\rangle\langle a| + a |a\rangle\langle b|). \end{aligned} \quad (16.61)$$

We assume for simplicity that $g_{ac} = g_{ab} = g$, and that ε is real. The time evolution of the wave function, to second order in the coupling constant, is

$$|\psi(t+\tau)\rangle = \left[1 - \frac{iH\tau}{\hbar} - \frac{H^2\tau^2}{2\hbar^2}\right] |\psi(t)\rangle. \quad (16.62)$$

As in the previous model, there are two possible quantum jump processes. The first one corresponds to the atom entering the cavity in the coherent

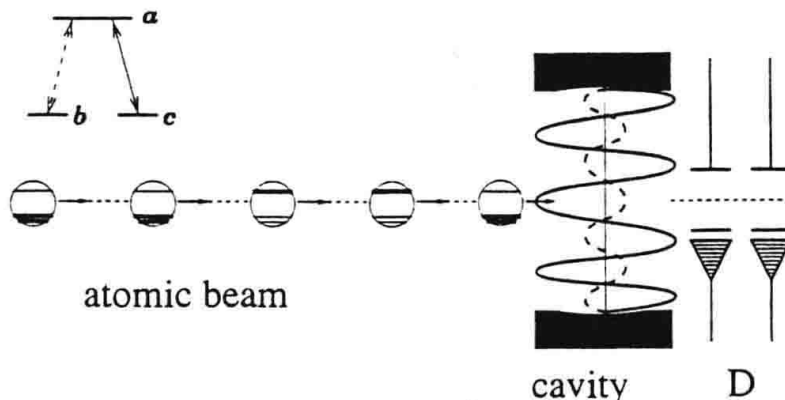


Fig. 16.4. Physical realization of the homodyne stochastic Schrödinger trajectory. A beam of three-level atoms crosses a resonant cavity, being subjected to an external classical field

superposition of lower states, and being detected in the upper state. After the measurement, the state of the field is given, by

$$|\psi(t+\tau)\rangle_f^{(b,c \rightarrow a)} = \frac{-ig\tau}{\sqrt{2}}(\varepsilon + a) |\psi(t)\rangle_f. \quad (16.63)$$

The corresponding probability of detecting an atom in $|a\rangle$, after a time interval δt , starting from the initial superposition state, is given by

$$\delta p_1 = n_b \frac{g^2 \tau^2}{2} \langle \psi_f(t) | (\varepsilon + a^\dagger)(\varepsilon + a) | \psi_f(t) \rangle, \quad (16.64)$$

where $n_b \equiv r_b \delta t$, r_b being the rate of atoms injected in the superposition of the lower states.

The second jump process corresponds to the atom entering the cavity in the upper state $|a\rangle$, and being detected in the superposition of lower states. Then, the state of the field after the measurement is

$$|\psi(t+\tau)\rangle_f^{(a \rightarrow b,c)} = \frac{-ig\tau}{\sqrt{2}}(\varepsilon + a^\dagger) |\psi(t)\rangle_f. \quad (16.65)$$

The corresponding probability is given by

$$\delta p_2 = n_a \frac{g^2 \tau^2}{2} \langle \psi_f(t) | (\varepsilon + a)(\varepsilon + a^\dagger) | \psi_f(t) \rangle, \quad (16.66)$$

where $n_a = r_a \delta t$ is the number of atoms which enter the cavity in state $|a\rangle$, during the time interval δt .

This analysis suggests that the quantum jump operators corresponding to these two processes should be, respectively,

$$\begin{aligned} C_1 &= \sqrt{\gamma(1 + \langle n \rangle_{th})}(\varepsilon + a), \\ C_2 &= \sqrt{\gamma \langle n \rangle_{th}}(\varepsilon + a^\dagger), \end{aligned} \quad (16.67)$$

where

$$\gamma \equiv (r_b - r_a) \frac{g^2 \tau^2}{2} = \frac{r_b}{1 + \langle n \rangle_{th}} \frac{g^2 \tau^2}{2} = \frac{r_a}{\langle n \rangle_{th}} \frac{g^2 \tau^2}{2}. \quad (16.68)$$

Formally, these jump operators are retrieved by rewriting the master equation (16.30) in the following equivalent form

$$\begin{aligned} \frac{d\rho_f}{dt} &= (J_1 + J_2)\rho_f - \frac{\gamma(1 + \langle n \rangle_{th})}{2} [(a^\dagger a + 2\varepsilon a + \varepsilon^2)\rho_f \\ &\quad + \rho_f(a^\dagger a + 2\varepsilon a^\dagger + \varepsilon^2)] - \frac{\gamma \langle n \rangle_{th}}{2} [(aa^\dagger + 2\varepsilon a^\dagger + \varepsilon^2)\rho_f \\ &\quad + \rho_f(aa^\dagger + 2\varepsilon a + \varepsilon^2)] \end{aligned} \quad (16.69)$$

with

$$J_i = C_i \rho C_i^\dagger, \quad i = 1, 2 \quad (16.70)$$

being associated with the jumps, the operators C_i now being given by (16.67).

We now derive the stochastic Schrödinger equation that describes the present measurement scheme. With the above jump operators, and using the expansion given by (16.38), we show in Appendix E that the joint probability of getting m_1 and m_2 jumps corresponding respectively to the first and second processes described above is given by the following expression

$$\begin{aligned} P_{m_1, m_2}(\Delta t) &= \left(\exp(\mu_1) \frac{(\mu_1)^{m_1}}{m_1!} \right) \left(\exp(\mu_2) \frac{(\mu_2)^{m_2}}{m_2!} \right) \\ &\times \text{Tr} \left\{ \exp(\beta') \left[1 + \frac{1}{\varepsilon} (m_1 a + m_2 a^\dagger) \right] \rho \right. \\ &\times \left. \left[1 + \frac{1}{\varepsilon} (m_1 a^\dagger + m_2 a) \right] \exp(\beta'^*) \right\}, \end{aligned} \quad (16.71)$$

where

$$\begin{aligned} \mu_1 &= \gamma \Delta t \varepsilon^2 (1 + \langle n \rangle_{\text{th}}), \\ \mu_2 &= \gamma \Delta t \varepsilon^2 (\langle n \rangle_{\text{th}}), \\ \beta' &= -\frac{\gamma \Delta t}{2} [a^\dagger a (2\langle n \rangle_{\text{th}} + 1) + 2\varepsilon a (\langle n \rangle_{\text{th}} + 1) + 2\varepsilon a^\dagger \langle n \rangle_{\text{th}} + \langle n \rangle_{\text{th}}]. \end{aligned} \quad (16.72)$$

From (16.71) and (16.72), one can readily find $\langle m_i \rangle$ and $\langle m_i^2 \rangle$ for $i = 1, 2$. Up to order $\varepsilon^{-3/2}$, one finds

$$\begin{aligned} \langle m_i \rangle &= \mu_i \left(1 + \frac{2}{3} \langle X_1 \rangle \right), \\ \langle m_i^2 \rangle &= \mu_i, \end{aligned} \quad (16.73)$$

with

$$X_1 \equiv \frac{a + a^\dagger}{2}. \quad (16.74)$$

Going back to the definition of $S(t)$, one may write

$$S(\Delta t) = N(\Delta t) \rho N^\dagger(\Delta t), \quad (16.75)$$

in terms of a smooth evolution operator N that preserves pure states. This operator N is given by (16.40), with the jump operators C_m now given by (16.67). Now, if we consider a sequence of jumps (of the two kinds, in the present analysis) and evolutions, the state vector of the field will evolve according to

$$\begin{aligned} |\tilde{\psi}\rangle_f(\Delta t) &= N(\Delta t - t_m) C_2 N(t_m - t_{m-1}) C_1 \dots |\psi\rangle_f(0) \\ &= N(\Delta t) C_2^{m_2} C_1^{m_1} |\psi\rangle_f(0). \end{aligned} \quad (16.76)$$

In the last step, in deriving (16.76), we used the fact that the commutators between the jump operators and the no-jump evolution produce overall phases, like in the Monte Carlo evolution given by (16.55).

Now, we consider m_i , $i = 1, 2$, as a couple of random variables with non-zero average, and write them as:

$$m_i = \langle m_i \rangle + \Delta W_i \frac{\sigma_i}{\sqrt{\Delta t}}, \quad (16.77)$$

where the ΔW_i are two real and independent Wiener increments, with

$$\langle \Delta W_i^2 \rangle = \Delta t, \quad i = 1, 2. \quad (16.78)$$

From (16.76), (16.77) and up to order $\varepsilon^{-3/2}$, we get the following homodyne stochastic Schrödinger differential equation (HSSDE)

$$\begin{aligned} & \Delta^{m_1, m_2} |\tilde{\psi}\rangle_f(\Delta t) \\ &= |\tilde{\psi}\rangle_f(\Delta t) - |\psi\rangle_f(0) \\ &= \left\{ \left[-\frac{\gamma}{2}(1 + \langle n \rangle_{\text{th}})a^\dagger a - \frac{\gamma}{2}(\langle n \rangle_{\text{th}})aa^\dagger + 2\gamma\langle X_1 \rangle(a(1 + \langle n \rangle_{\text{th}}) \right. \right. \\ & \quad \left. \left. + a^\dagger \langle n \rangle_{\text{th}}) \right] \Delta t + a^\dagger \sqrt{\gamma \langle n \rangle_{\text{th}}} \Delta W_2 \right. \\ & \quad \left. + a \sqrt{\gamma(1 + \langle n \rangle_{\text{th}})} \Delta W_1 \right\} |\psi\rangle_f(0). \end{aligned} \quad (16.79)$$

At zero temperature, a typical quantum trajectory in this homodyne scheme is as follows:

- (a) If one starts from a coherent state, the quantum jumps will only produce a multiplicative factor in the wavefunction of the field, a factor that can be absorbed in the normalization. On the other hand, during the ‘no-click’ periods, the nature of the coherent state is preserved, changing only the coherent amplitude, all the way to the vacuum.
This situation will be studied in Chap. 18 [16.19] in the context of continuous measurement theory, applied to three-level atoms and two resonant fields, with the difference that there the number of detections is a pre-determined quantity. However, the net result of the preservation of the coherent nature of the state of the field, along the trajectory, is the same [16.13].
- (b) If we start with a Fock state, the quantum jumps will invariably produce a mixture of various Fock states, while the waiting or ‘no-click’ periods will only generate numerical factors in front of those Fock states.
In the finite-temperature case, the situation is more complex, since there will be also creation of photons, which will disturb an initial coherent state and produce further mixtures in the Fock state case.

A more detailed analysis of these various cases is described in the next section, devoted to numerical simulation.

16.6 Numerical Results and Localization

We present now the numerical calculations corresponding to the two equations associated with the two measurement schemes discussed above [16.13]. We consider in these calculations the general case in which the temperature of the reservoir is taken to be different from zero.

16.6.1 Evolution of Quantum Jumps

We consider first an example in which the initial state of the system is a Fock state with three photons. We assume that the temperature of the reservoir corresponds to an average number of photons also equal to three. The corresponding evolutions is exhibited in Fig. 16.5.

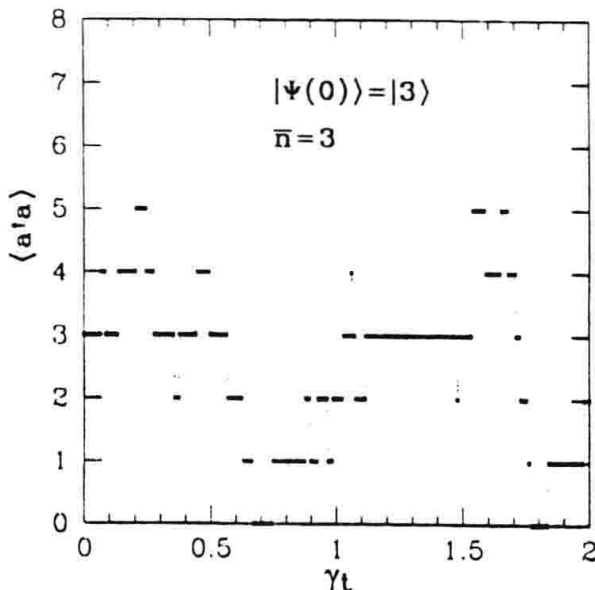


Fig. 16.5. Quantum jump for an initial Fock state with $n = 3$, the number of thermal photons being also equal to three (after [16.13])

The state of the system remains a Fock state, with a number of photons which keeps jumping between several values, in such a way that the average number of photons is equal to three. We have verified that the probability distribution for the number of photons is a Bose-Einstein distribution, as long as the observation is done over a sufficiently long time.

Fig. 16.6 displays two different views of the evolution of the photon number population $|a_n|^2$ of an initial coherent state. These figures clearly exhibit the dual nature of the system dynamics, with quantum jumps interspersed by non-unitary evolutions. In the case illustrated, the vacuum component of the state increases until the first quantum jump occurs. This jump corresponds to the addition of a thermal photon to the system, leading to the disappearance of the vacuum component. The second jump corresponds to the absorption of a photon from the cavity field, leading to the reappearance of the vacuum state. The combination of the non-unitary evolution with the quantum jumps finally leads to a Fock state, which under the action of the reservoir keeps jumping in such a way that the photon number distribution over a long time span reproduces the Bose-Einstein distribution. This process is illustrated in Fig. 16.7, which displays the time evolution of the Q distribution for the field, defined for each realization as $Q = |\langle \alpha | \psi \rangle|^2 / \pi$, where $|\alpha\rangle$ is a coherent state with amplitude α .

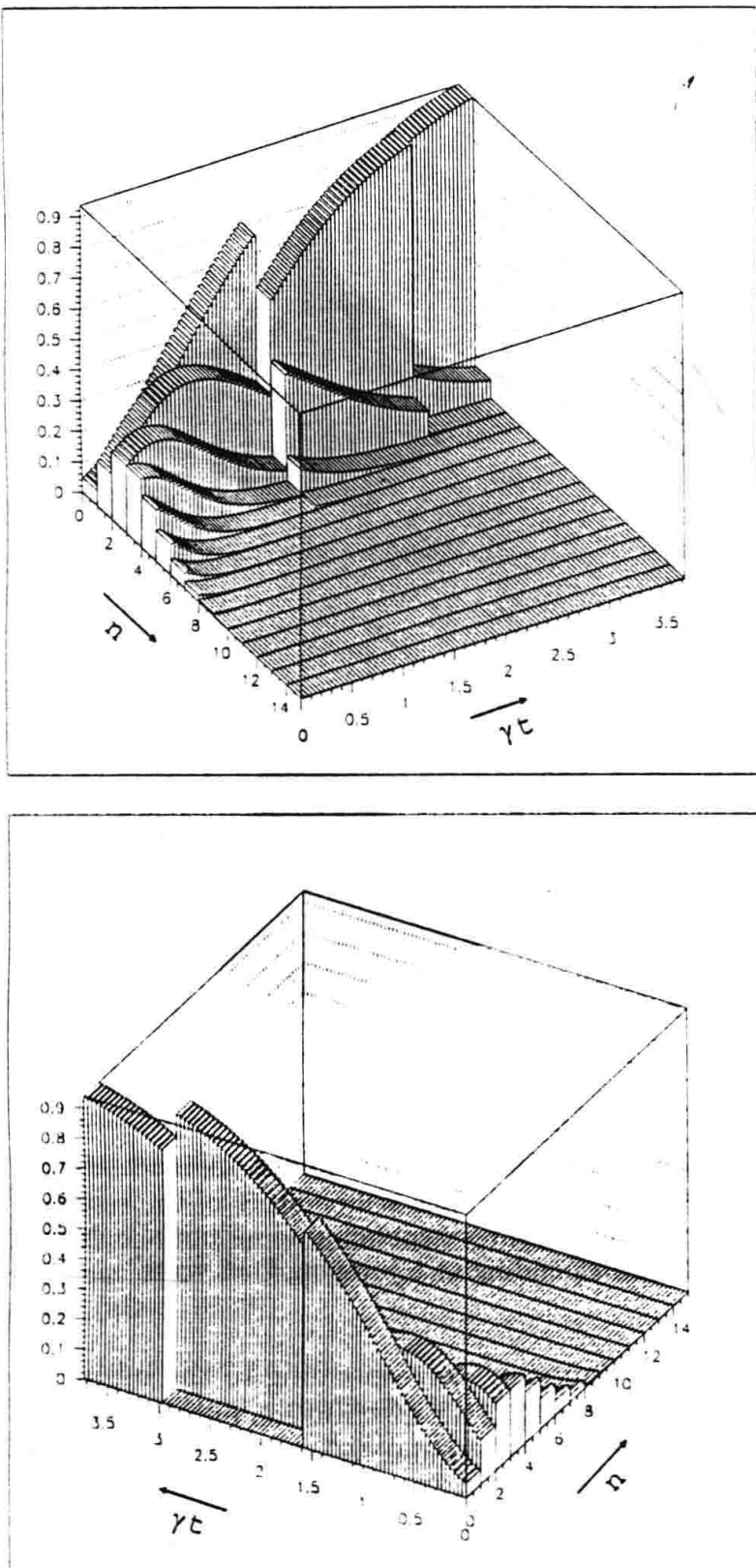


Fig. 16.6. Two views of the evolution of an initial coherent state (average photon number equal to three), in the quantum jump approach. The temperature of the reservoir corresponds to a number of thermal photons equal to 0.2. At around $\gamma t = 1.52$, a photon is absorbed by the cavity mode, while at around $\gamma t = 3$, a photon is lost by the cavity. Before the first jump, the amplitude of the coherent state decreases exponentially. After several jumps, the state becomes a jumping Fock state (after [16.13])

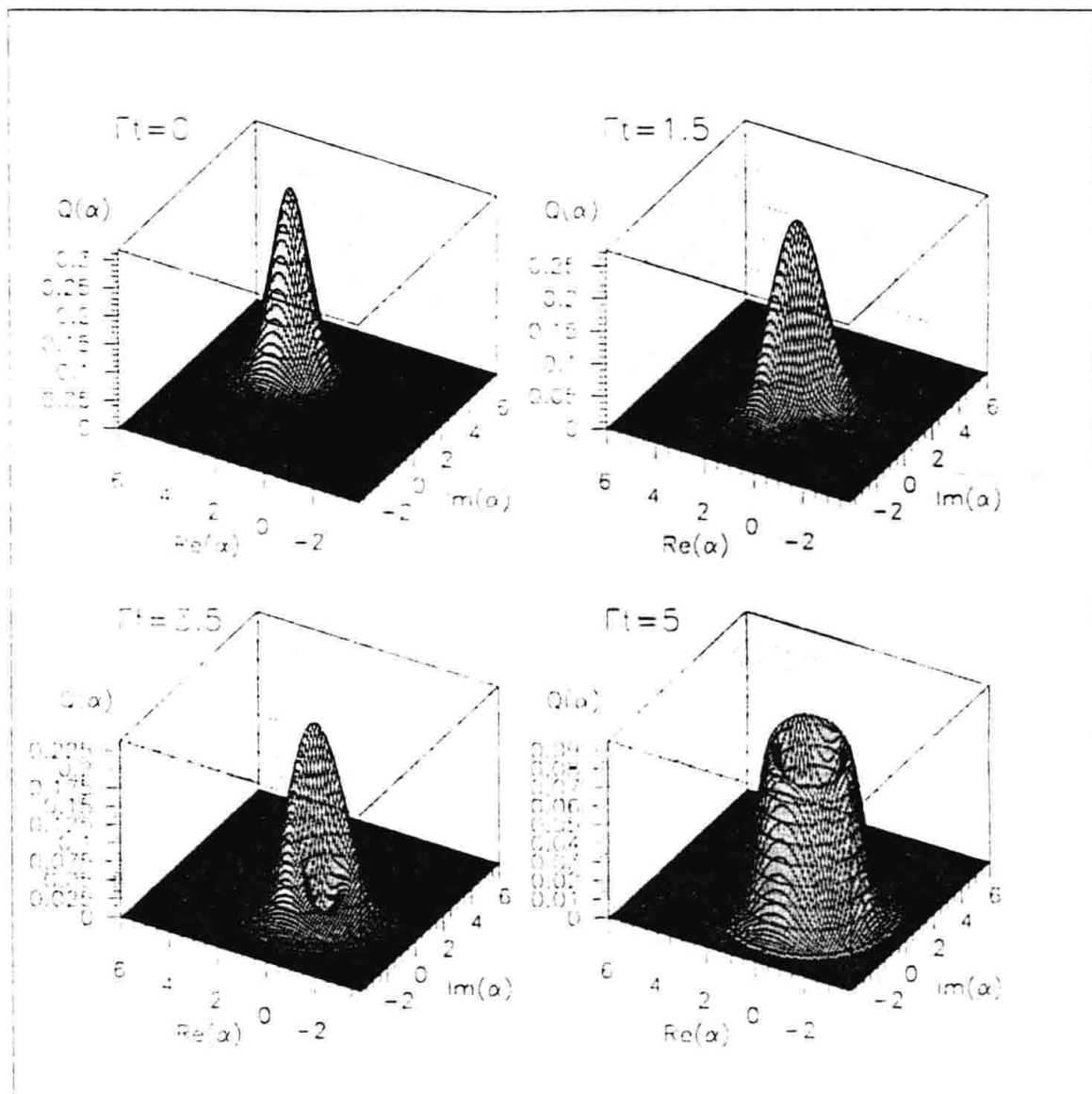


Fig. 16.7. Evolution of the Q -function for the quantum jumps approach and an initial coherent state, with $\alpha_0 = \sqrt{15/2}(1 + i)$. The temperature of the reservoir corresponds to $\langle n \rangle_{\text{th}} = 2$. The initial Gaussian corresponding to an initial coherent state evolves into the distribution corresponding to a jumping Fock state

The initial Q distribution is a Gaussian, corresponding to the initial coherent state $|\alpha_0\rangle$, with $\alpha_0 = \sqrt{15/2}(1 + i)$. This distribution evolves into the one corresponding to a Fock state, with a number of photons which keeps jumping around the thermal value $\langle n \rangle_{\text{th}} = 2$, in the same way as shown in Fig. 16.5.

16.6.2 Diffusion-like Evolution

We consider now the evolution corresponding to the situation displayed in Fig. 16.4. We consider as initial state the same coherent state as in Fig. 16.8, the reservoir temperature being also the same as before ($\langle n \rangle_{\text{th}} = 2$). In this

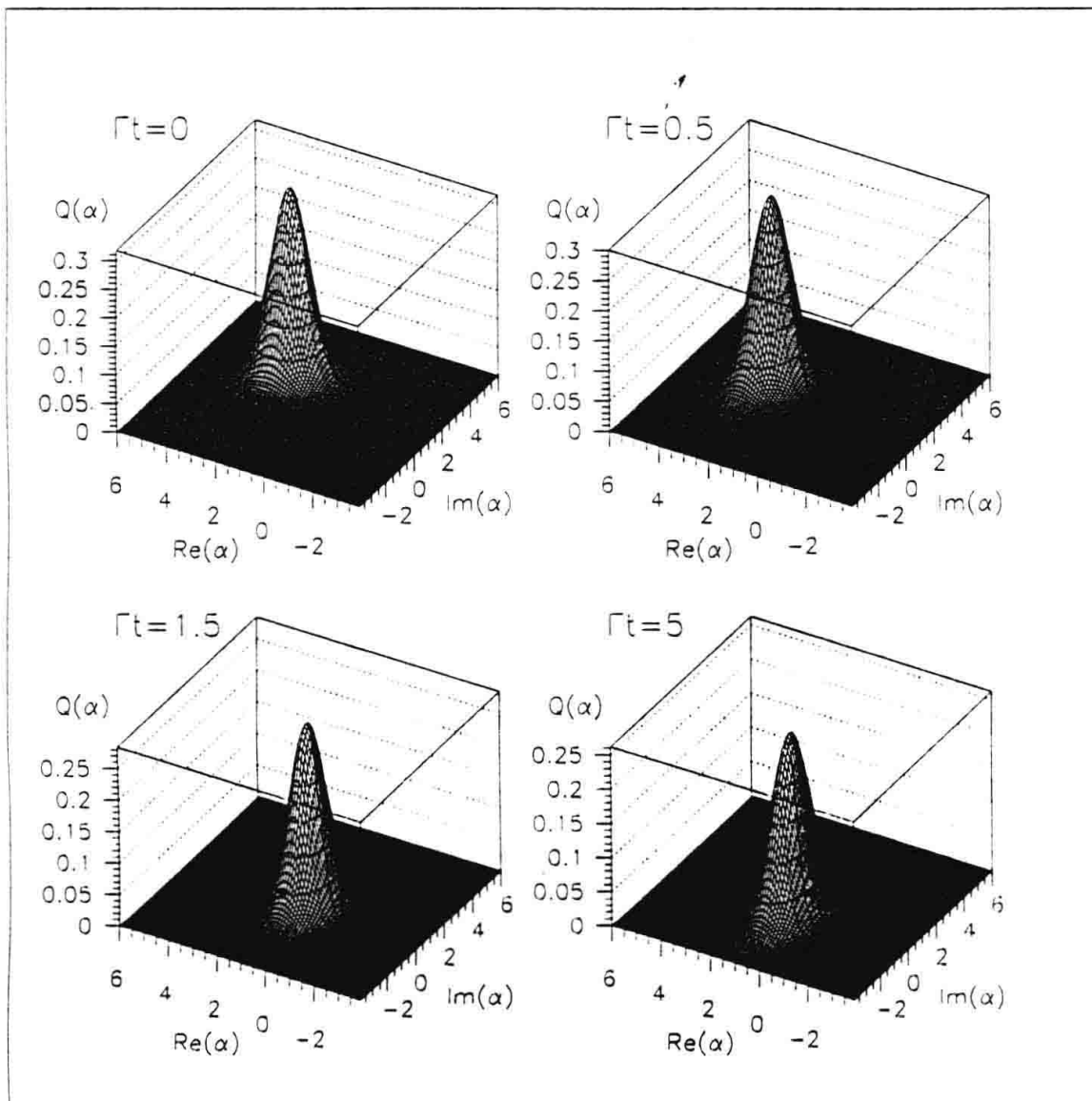


Fig. 16.8. Evolution of the Q function, for the quantum jump approach, and an initial coherent state, with $\alpha_0 = \sqrt{15/2}(1 + i)$. The reservoir temperature corresponds to two thermal photons(average). The initial Gaussian, corresponding to a coherent state, evolves into a distorted Gaussian, whose centre diffuses in phase space (after [16.13])

case, the system evolves according to the homodyne stochastic Schrödinger equation given by (16.80). After some time, the Q function approaches a distorted Gaussian, with a mild amount of squeezing along the direction of the axis corresponding to the real part of α . The centre of this Gaussian keeps diffusing in phase space, so that after a long time span the time-averaged distribution coincides with the Bose–Einstein distribution.

16.6.3 Analytical Proof of Localization

For the quantum jump situation, it is actually possible to demonstrate that the system evolves towards a Fock state, for non-zero temperatures [16.13].

We first define two kind of variances, for an arbitrary operator O . For the Hermitian case

$$\langle \Delta O^2 \rangle = \langle O^2 \rangle - \langle O \rangle^2, \quad (16.80)$$

and for the non-Hermitian case

$$\begin{aligned} |\Delta O|^2 &= (O^\dagger - \langle O^\dagger \rangle)(O - \langle O \rangle) \\ &= O^\dagger O - \langle O^\dagger \rangle O - O^\dagger \langle O \rangle - \langle O^\dagger \rangle \langle O \rangle, \end{aligned} \quad (16.81)$$

so that

$$\langle |\Delta O|^2 \rangle = \langle O^\dagger O \rangle - \langle O^\dagger \rangle \langle O \rangle. \quad (16.82)$$

In particular, we are interested in the two quantities

$$Q_1 = \langle |\Delta a|^2 \rangle, \quad (16.83)$$

$$Q_2 = \langle |\Delta n|^2 \rangle, \quad (16.84)$$

which measure the distance of the state from being a coherent or a Fock state, respectively.

We start with the quantum jump equation

$$\begin{aligned} |d\psi\rangle &= -\frac{i}{\hbar}H|\psi\rangle\delta t \\ &\quad -\frac{1}{2}\sum_m(C_m^\dagger C_m - \langle C_m^\dagger \rangle \langle C_m \rangle)|\psi\rangle\delta t \\ &\quad + \sum_m \left(\frac{C_m}{\sqrt{C_m^\dagger C_m}} - 1 \right) |\psi\rangle\delta N_m, \end{aligned} \quad (16.85)$$

with

$$M(\delta N_m) = \langle C_m^\dagger C_m \rangle \delta t, \quad (16.86)$$

$$\delta N_m \delta N_m = \delta N_n \delta_{n,m}. \quad (16.87)$$

We will calculate, using Ito's rule of calculus, Q_1 and Q_2 for $T = 0$ ($C = \sqrt{T}a$) and $T > 0$ ($C_1 = \sqrt{(\langle n \rangle_{\text{th}} + 1)}\gamma a$, $C_2 = \sqrt{\gamma \langle n \rangle_{\text{th}}}a^\dagger$).

We first develop some general expressions, which will be applied to calculate the above variances.

$$\begin{aligned} d\langle O \rangle &= \langle d\psi | O | \psi \rangle + \langle \psi | O | d\psi \rangle + \langle d\psi | O | d\psi \rangle \\ &= -\frac{i}{\hbar}\langle [O, H] \rangle \delta t - \frac{1}{2}\langle \{O, C^\dagger C\} \rangle \delta t + \langle O \rangle \langle C^\dagger C \rangle \delta t \\ &\quad + \frac{(\langle C^\dagger O C \rangle - \langle C^\dagger C \rangle \langle O \rangle)}{\langle C^\dagger C \rangle} \delta N, \end{aligned} \quad (16.88)$$

and similarly for the case in which several jump operators are present.

For the variance of a non-Hermitian operator, we have

$$d(\langle |\Delta O|^2 \rangle) = d\langle O^\dagger O \rangle - \langle O \rangle d\langle O^\dagger \rangle - \langle O^\dagger \rangle d\langle O \rangle - d\langle O^\dagger \rangle d\langle O \rangle. \quad (16.89)$$

After a simple calculation, one gets

$$\begin{aligned} d(\langle |\Delta O|^2 \rangle) = & -\frac{i}{\hbar} \langle [|\Delta O|^2, H] \rangle \delta t \\ & -\frac{1}{2} \langle \{|\Delta O|^2, C^\dagger C\} \rangle \delta t \\ & + \langle |\Delta O|^2 \rangle \langle C^\dagger C \rangle \delta t - \langle |\Delta O|^2 \rangle \delta N \\ & + \frac{\langle C^\dagger O^\dagger O C \rangle \langle C^\dagger C \rangle - \langle C^\dagger O^\dagger C \rangle \langle C^\dagger O C \rangle}{\langle C^\dagger C \rangle \langle C^\dagger C \rangle} \delta N. \end{aligned} \quad (16.90)$$

In the Hermitian case, on the other hand, we get

$$\begin{aligned} d(\langle \Delta O^2 \rangle) = & -\frac{i}{\hbar} \langle [\Delta O^2, H] \rangle \delta t - \frac{1}{2} \langle \{ \Delta O^2, C^\dagger C \} \rangle \delta t \\ & + \langle \Delta O^2 \rangle \langle C^\dagger C \rangle \delta t - \langle \Delta O^2 \rangle \delta N \\ & + \frac{\langle C^\dagger O^2 C \rangle \langle C^\dagger C \rangle - \langle C^\dagger O C \rangle \langle C^\dagger O C \rangle}{\langle C^\dagger C \rangle \langle C^\dagger C \rangle} \delta N. \end{aligned} \quad (16.91)$$

Now we specialize to several cases.

- (a) $T = 0, O = a; C = \sqrt{\gamma}a; H = \hbar\omega a^\dagger a$.

Using the above general expressions, we write

$$\begin{aligned} d(\langle |\Delta a|^2 \rangle) = & [-\gamma \langle a^\dagger a a^\dagger a \rangle - 2\gamma \langle a^\dagger a \rangle \langle a^\dagger \rangle \langle a \rangle \\ & + \gamma \langle a^\dagger a \rangle \langle a^\dagger a \rangle + \frac{\gamma}{2} \langle a^\dagger a^\dagger a \rangle \langle a \rangle + \frac{\gamma}{2} \langle a^\dagger a a^\dagger \rangle \langle a \rangle \\ & + \frac{\gamma}{2} \langle a a^\dagger a \rangle \langle a^\dagger \rangle + \frac{\gamma}{2} \langle a^\dagger a a \rangle \langle a^\dagger \rangle] \delta t \\ & - \langle a^\dagger a \rangle \delta N + \langle a^\dagger \rangle \langle a \rangle \delta N \\ & + \frac{\langle a^\dagger a^\dagger a a \rangle \langle a^\dagger a \rangle - \langle a^\dagger a^\dagger a \rangle \langle a^\dagger a a \rangle}{\langle a^\dagger a \rangle \langle a^\dagger a \rangle} \delta N. \end{aligned} \quad (16.92)$$

The above results are neither strictly positive or negative, so we cannot draw any conclusion. However, for the statistical mean

$$\begin{aligned} M \frac{d(\langle |\Delta a|^2 \rangle)}{dt} = & -\gamma \langle |\Delta a|^2 \rangle \\ & - \frac{\gamma \langle (\Delta a^\dagger) a^\dagger a \rangle \langle a^\dagger a \Delta a \rangle}{\langle a^\dagger a \rangle} \leq 0, \end{aligned} \quad (16.93)$$

so, in the mean, the system goes to a coherent state, which, in this case, is the vacuum.

- (b) $T > 0; O = a; C_1 = \sqrt{(\langle n \rangle_{\text{th}} + 1)\gamma}a, C_2 = \sqrt{\gamma \langle n \rangle_{\text{th}}}a^\dagger, H = \hbar\omega a^\dagger a$.
The reader can easily verify, with a little algebra, that in this case neither $d(\langle |\Delta a|^2 \rangle)$ nor $M d(\langle |\Delta a|^2 \rangle)$ are strictly negative.
- (c) $T > 0, O = a^\dagger a; C_1 = \sqrt{(\langle n \rangle_{\text{th}} + 1)\gamma}a, C_2 = \sqrt{\gamma \langle n \rangle_{\text{th}}}a^\dagger, H = \hbar\omega a^\dagger a$.
In this case, as shown in Appendix F, $d(\langle \Delta a^\dagger a \rangle^2)$ is not negative, but $M d(\langle \Delta a^\dagger a \rangle^2)$ is

$$\begin{aligned}
M \frac{d\langle(\Delta a^\dagger a)^2\rangle}{dt} &= -\gamma(\langle n \rangle_{\text{th}} + 1) \frac{\langle(\Delta a^\dagger a)a^\dagger a\rangle\langle a^\dagger a(\Delta a^\dagger a)\rangle}{\langle a^\dagger a \rangle} \\
&\quad - \gamma(\langle n \rangle_{\text{th}}) \frac{\langle(\Delta a a^\dagger)aa^\dagger\rangle\langle aa^\dagger(\Delta a a^\dagger)\rangle}{\langle aa^\dagger \rangle} \\
&\leq 0.
\end{aligned} \tag{16.94}$$

So Q_2 is strictly decreasing in the mean, even at $T > 0$. Since Q_1 is not, the final state will not be the vacuum. It is easy to show from (16.94) that $M[d\langle(\Delta a^\dagger a)^2\rangle/dt] = 0$ if and only if the state of the system is a Fock state. This result shows therefore that any initial state eventually approaches a Fock state $|n\rangle$, with n fluctuating with mean $\langle n \rangle_{\text{th}}$.

16.7 Conclusions

The dynamics of dissipative quantum systems is often described through master equations for the reduced density matrix, obtained by tracing the degrees of freedom of the reservoir and making the usual Markov–Born approximation. However, in recent years monitoring single quantum systems has become a reality in Paul traps, micromasers, etc., so new methods have been sought through the evolution of state vectors.

The two methods discussed in this chapter are the Monte Carlo wavefunction or quantum jump method, involving random finite discontinuities, and the stochastic Schrödinger equation characterized by a diffusive term added to the equation for the state vector, generally associated to a homodyne measurement.

We propose here a physical interpretation of the quantum jump approach and the homodyne stochastic Schrödinger differential equation, using as an example the damping of one field mode in a cavity at temperature T . This field damping mechanism can be modelled as an atomic beam, whose upper and lower population ratio is given by the Boltzmann factor, crossing a lossless cavity.

The quantum jump trajectory can be interpreted as a continuous monitoring of the outgoing two-level atoms, which are resonant with the cavity mode. We show both numerically and analytically that this continuous measurement on the reservoir leads, for each trajectory, to a pure Fock state. At a later time and due to the non-zero temperature, a thermal photon may produce a jump to a different Fock state, thus leading, as time goes on, to a series of Fock states, whose statistics will reproduce the thermal distribution.

In the case of the homodyne stochastic Schrödinger differential equation, the proposed damping mechanism consists of a three-level atomic beam, with a split ground state, whose population ratio of the upper and lower levels is given by the Boltzmann factor. The atoms again cross a lossless cavity, being resonant with the mode of the field under consideration. A second field

is externally applied, with the same frequency but different polarization, so that each of the two fields connects the upper atomic state with a different lower sublevel. If this external field is a strong classical field, we show analytically that the stochastic Schrödinger equation describing the behaviour of the quantum field in the cavity corresponds precisely to the homodyne stochastic Schrödinger equation.

The beam is then continuously monitored as it exits the cavity. Numerically, one observes, for low temperatures, that the state of the field goes to a mildly squeezed state, centred around a value of α which diffuses in phase space, in such a way that the time-averaged distribution again reproduces the thermal state.

Recently, the Monte Carlo simulation has been used to describe spontaneous emission [16.20], two-photon processes [16.21]. Also, there has been several publications related to quantum diffusion and localization [16.22, 16.23, 16.24, 16.25, 16.26, 16.27].

Problems

16.1. The Lindblad form of the master equation is not unique.

Show that if we transform

$$D_m = T^\dagger C_m T,$$

where T is a unitary transformation, the master equation is unchanged. However, the nature of the jumps has changed, since now the system may jump to one of the states

$$D_m |\phi(t)\rangle,$$

with a probability

$$\delta p_m^D = \langle\phi| D_m^\dagger D_m |\phi\rangle \delta t.$$

16.2. Derive a linear stochastic equation equivalent to the master equation.

Hint: See [16.11].

17. Atom Optics

Atom optics [17.1], in analogy with electron or neutron optics, deals with manipulation of matter waves. As such, they are characterized by a wavelength, which is the de Broglie wavelength $\lambda_{dB} \equiv h/p$ and the momentum $p = mv$. The momentum of a typical atom is larger than that of a typical photon, absorbed or emitted by that atom. There are several advantages of using atoms instead of photons for optical experiments:

- Atoms have a non-zero rest mass, which is interesting when, for example, we want to detect gravitational waves.
- Atoms, as opposed to neutrons or electrons, are less susceptible to stray fields, but cannot be manipulated as easily as charged particles.
- Atoms have variable velocities, and as a result, one can in principle, control their de Broglie wavelengths.
- Atoms are easy and cheap to produce, as compared, for instance, to neutrons.
- A very important aspect of the atom optics, is that atoms have internal structure, which can be probed and modified using light.

17.1 Optical Elements

In general, a typical atom optics experiment will consist of a source, optical elements and a detector. Sources, in general, provide a well-collimated, monochromatic atomic beam. Sources can be fast or slow. Among the sources of slow atoms are thermal expansions, with a Maxwellian velocity distribution. These type of sources are in general easy to operate and have a large flux. Within the fast type, when the reservoir pressure is increased, supersonic sources can be created, with a narrow longitudinal velocity distribution, typically a Gaussian distribution.

For some experiments, a better controlled atomic source is required. These slow beams are produced by loading atoms from thermal sources into an atomic trap, and then releasing them in a controlled fashion. Since these atoms are extremely cold ($30 \mu\text{K}$), we may have a small velocity spread and large de Broglie wavelength.

A large number of different schemes have been used for the detection of atomic beams. A neutral atom can be collected using a hot wire detector which absorbs the atom briefly and ionizes it. The ions are then detected as a current proportional to the incident atomic flux. On the other hand, atoms in a metastable state can be detected by ionization followed by Auger neutralization. Another versatile detection method in atom optics is laser-induced fluorescence. In recent years, a large amount of effort has been put into developing optical elements, such as mirrors (for example, reflection of sodium atoms from evanescent waves, [17.2], [17.3]), lenses, beam splitters, etc.

It is interesting to note that although atom optics experiments belong to the decades of the 1980s and 1990s, the diffraction of atoms was actually performed as early as 1929, by Stern *et al.* [17.4].

17.2 Atomic Diffraction from an Optical Standing Wave

The diffraction of an atomic beam by an optical standing wave can be easily visualized as follows: the standing wave acts as a phase grating for the atoms, splitting the incoming plane wave into a series of plane waves, separated by an integer number of photon momentum units hk (see Fig. 17.1).

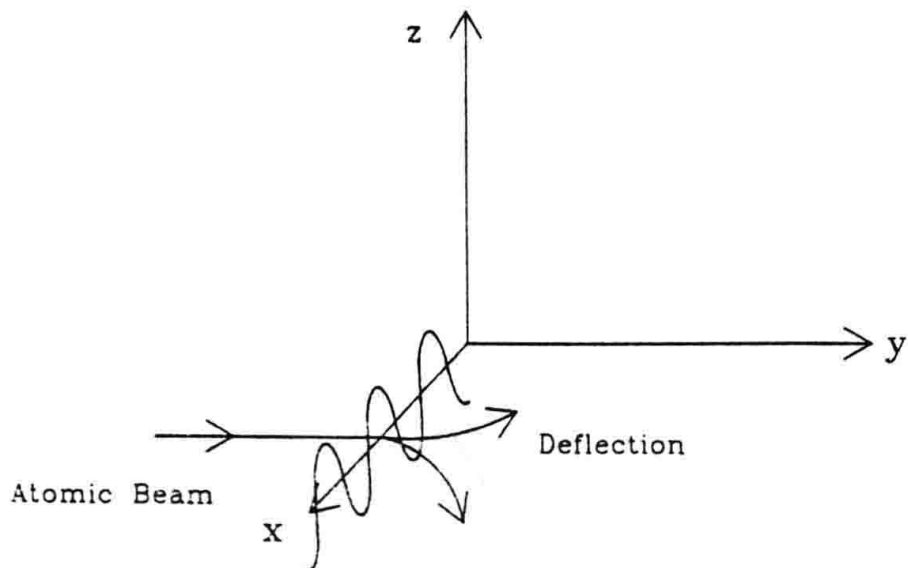


Fig. 17.1. Atomic beam crossing and being deflected by a standing wave

In the present theoretical treatment, we will be using the Raman-Nath approximation which consists in neglecting the transverse kinetic energy of the atoms. We will also assume near-resonance between the field and a couple of atomic levels. One of the first experimental observations of this effects was achieved by Moskowitz *et al.* [17.5], in 1983. An improved version was done

by Martin *et al.* in 1987 [17.6]. In this experiment, low-velocity sodium atoms (2 m s^{-1}) are diffracted by a near-resonant standing wave of light. There have also been several other experiments [17.7], [17.8], [17.9], [17.10].

17.2.1 Theory

The deflection of atoms by standing waves has been, for some years, a subject of considerable interest, in particular, in connection with atomic interferometers. When the standing wave is intense, classical fields are adequate. However, with modern experimental tools, we may observe in the near future diffraction from a few photons, where quantum effects are important. Also, spontaneous emission plays a role. In this particular treatment, we will assume the detuning to be sufficiently large, as to neglect this effect altogether.

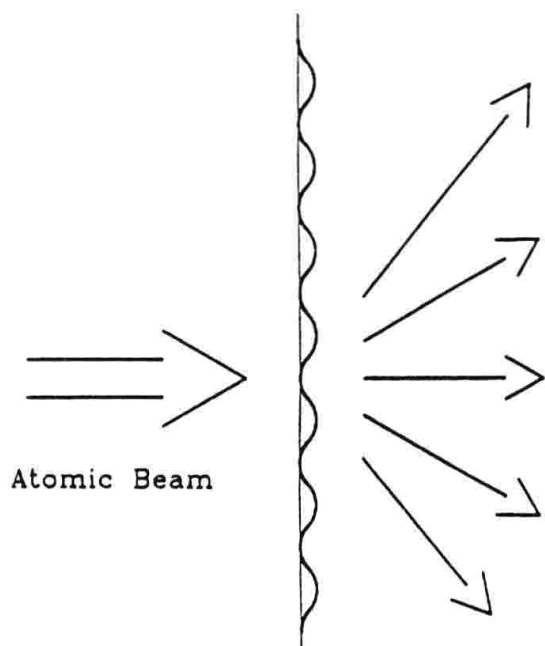


Fig. 17.2. Atomic diffraction by a standing wave light field

Now, consider a collimated atomic beam travelling in the y -direction (see Fig. 17.2). The individual atoms are deflected by the photons. The field induces absorption and emission. As a result of this interaction, the atomic transverse momentum spreads. This behaviour can be understood in terms of travelling waves. The atom absorbs a photon, thus gaining $\hbar k$ transverse momentum from one of the travelling waves and can emit a photon into the other travelling wave, thus changing its own momentum by $2\hbar k$. This is shown in Fig. 17.3.

Actually, the above argument is only approximate, since there is a difference between a standing wave and two travelling waves. In principle, in two travelling waves, the momentum exchange between the field and the atom can only be finite, limited by the number of photons available. On the other

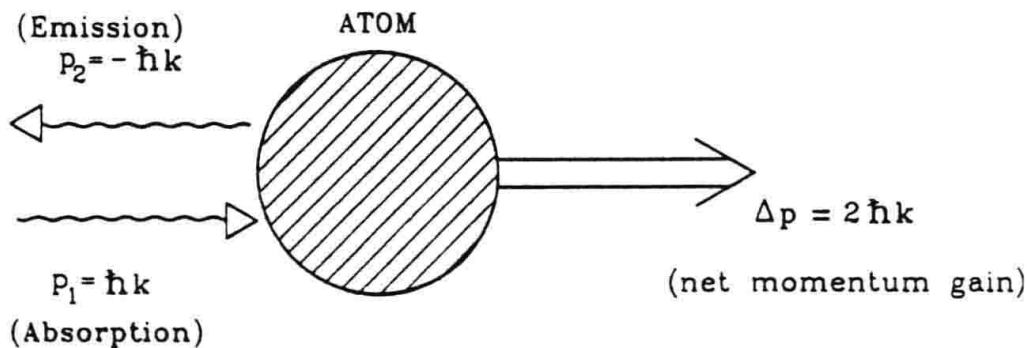


Fig. 17.3. Change of the atom's momentum after an absorption and emission event. As a result, the atom gains two units of the photon's momentum

hand, in the standing wave, there is an inseparable quantum unit, with zero average momentum. Here an important role is played by the fixed mirrors, which act as an infinite sink of momentum, and the amount of momentum exchanged between the standing wave and the atom is no longer limited. An interesting discussion on this point is found in Shore et al. [17.11].

The Hamiltonian of the system is

$$H = \frac{p^2}{2m} + \hbar\omega a^\dagger a + \hbar\omega_0 \sigma_z + \hbar g(a^\dagger \sigma_- + a^\dagger \sigma_+) \cos kx, \quad (17.1)$$

where the first term in (17.1) represents the atomic centre-of-mass motion; the second and third terms are the free field and the internal energy of the two-level atom respectively. The last term represents the atom-standing-wave interaction, where $\sigma_z, \sigma_+, \sigma_-$ are the usual Pauli spin matrices.

The total kinetic energy can be split into a transverse and a longitudinal part:

$$\frac{p^2}{2m} = \frac{p_x^2}{2m} + \frac{p_y^2}{2m}, \quad p_y \gg p_x, \quad (17.2)$$

and the transverse kinetic energy can be written as

$$\frac{p_x^2}{2m} = \hbar \left(\frac{\hbar k^2}{2m} \right) S_z^2, \quad (17.3)$$

where we defined

$$S_z \equiv \frac{p_x}{\hbar k}, \quad (17.4)$$

where S_z is just the transverse momentum change, in units of the photon momentum. Normally (although this is not really necessary) one assumes that initially the transverse momentum is zero, and we define an $|m\rangle$ basis, with m integer, such that

$$S_z |m\rangle = m |m\rangle. \quad (17.5)$$

We also define

$$S^\pm \equiv \exp(\pm ikx). \quad (17.6)$$

It is simple to see that

$$\begin{aligned}[S^+, S^-] &= 0, \\ [S_z, S^\pm] &= \pm S^\pm.\end{aligned}\quad (17.7)$$

As we can see, the S^+ , S^- operators are the step operators for the centre-of-mass momentum of the atom, such that:

$$\begin{aligned}S^+ |m\rangle &= |m+1\rangle, \\ S^- |m\rangle &= |m-1\rangle.\end{aligned}\quad (17.8)$$

The Hamiltonian can now be written as:

$$H = \hbar\epsilon_R S_z^2 + \frac{p_y^2}{2m} + \hbar\omega a^\dagger a + \frac{\hbar\omega_0 \sigma_z}{2} + \frac{\hbar g}{2} (a^\dagger \sigma_- + a^\dagger \sigma_+) (S^+ + S^-). \quad (17.9)$$

Now, the quantity $\hbar\omega(a^\dagger a + \sigma_z)$ is a constant of the motion, since it commutes with the total Hamiltonian. Also, the longitudinal kinetic energy is very large and can be considered approximately as a constant, so these three terms can be eliminated from the energy, getting

$$H = \hbar\epsilon_R S_z^2 + \frac{\hbar\Delta \sigma_z}{2} + \frac{\hbar g}{2} (a^\dagger \sigma_- + a^\dagger \sigma_+) (S^+ + S^-). \quad (17.10)$$

Now, we use the $|n\rangle |m\rangle$ basis, and since $\sigma_z + a^\dagger a$ is a constant of the motion, we write the wavefunction as

$$|\Psi\rangle = \sum_{m=-\infty}^{m=+\infty} \left[C_{nm}^+ |n\rangle |m\rangle \begin{pmatrix} 1 \\ 0 \end{pmatrix} + C_{n+1,m}^- |n+1\rangle |m\rangle \begin{pmatrix} 0 \\ 1 \end{pmatrix} \right]. \quad (17.11)$$

We now write the Schrödinger equation as

$$\begin{aligned}i\hbar \frac{\partial |\Psi\rangle}{\partial t} &= H |\Psi\rangle \\ &= i\hbar \sum_{m=-\infty}^{m=+\infty} \left[\frac{dC_{nm}^+}{dt} |n\rangle |m\rangle \begin{pmatrix} 1 \\ 0 \end{pmatrix} \right. \\ &\quad \left. + \frac{dC_{n+1,m}^-}{dt} |n+1\rangle |m\rangle \begin{pmatrix} 0 \\ 1 \end{pmatrix} \right] \\ &= \frac{\hbar\Delta}{2} \sum_{m=-\infty}^{m=+\infty} \left[C_{nm}^+ |n\rangle |m\rangle \begin{pmatrix} 1 \\ 0 \end{pmatrix} \right. \\ &\quad \left. - C_{n+1,m}^- |n+1\rangle |m\rangle \begin{pmatrix} 0 \\ 1 \end{pmatrix} \right] \\ &\quad + \hbar\epsilon_R \sum_{m=-\infty}^{m=+\infty} m^2 \left[C_{nm}^+ |n\rangle |m\rangle \begin{pmatrix} 1 \\ 0 \end{pmatrix} \right. \\ &\quad \left. + C_{n+1,m}^- |n+1\rangle |m\rangle \begin{pmatrix} 0 \\ 1 \end{pmatrix} \right]\end{aligned}\quad (17.12)$$

$$\begin{aligned}
& + \frac{\hbar g}{2} \sum_{m=-\infty}^{m=+\infty} [C_{nm}^+ \sqrt{n+1} |n+1\rangle \\
& \times (|m+1\rangle + |m-1\rangle) \begin{pmatrix} 0 \\ 1 \end{pmatrix} \\
& + C_{n+1,m}^- \sqrt{n+1} |n\rangle \\
& \times (|m+1\rangle + |m-1\rangle) \begin{pmatrix} 1 \\ 0 \end{pmatrix}] .
\end{aligned}$$

Finally, by comparing the $\begin{pmatrix} 1 \\ 0 \end{pmatrix}$ and $\begin{pmatrix} 0 \\ 1 \end{pmatrix}$ terms, we get

$$\begin{aligned}
i \frac{dC_{nm}^+}{dt} & = (\frac{\Delta}{2} + \epsilon_R m^2) C_{nm}^+ \\
& + \frac{g}{2} \sqrt{n+1} [C_{n+1,m-1}^- + C_{n+1,m+1}^-] ,
\end{aligned} \tag{17.13}$$

$$\begin{aligned}
i \frac{dC_{n+1,m}^-}{dt} & = (-\frac{\Delta}{2} + \epsilon_R m^2) C_{n+1,m}^- \\
& + \frac{g}{2} \sqrt{n+1} [C_{n,m-1}^+ + C_{n,m+1}^+] .
\end{aligned} \tag{17.14}$$

Equations (17.13, 17.15) are quite general and exact.

17.2.2 Particular Cases

(a) $\Delta = 0, p_x^2 \approx 0$.

This is the Raman–Nath regime with no detuning. If we also assume that $n \gg 1$, so that $g\sqrt{n+1} = \text{constant}$, then (17.13) reduce to

$$i \frac{dC_m}{dt} = \frac{g}{2} \sqrt{n+1} [C_{m-1} + C_{m+1}] . \tag{17.15}$$

The difference-differential equation for the Bessel functions is

$$2 \frac{d}{dz} J_n(z) = J_{n-1}(z) - J_{n+1}(z) . \tag{17.16}$$

Thus, by direct comparison between (17.15) and (17.16), we get

$$C_m = (-i)^m J_m(\Omega t) , \tag{17.17}$$

with $\Omega \equiv g\sqrt{n+1}$, or

$$P_{n,m}(t) = J_m^2(g\sqrt{n+1}t) . \tag{17.18}$$

If instead of having initially a Fock state, we have a general superposition of Fock states, distributed with probability W_n , we get

$$P_m(t) = \sum_{n=0}^{n=\infty} W_n J_m^2(g\sqrt{n+1}t) . \tag{17.19}$$

Equation (17.19) gives the probability distribution for the transverse momentum of an atom after an interaction time t with a standing wave-light field for any given initial field distribution. The momentum distribution of the atom is a signature of the field this atom interacted with.

Figures 17.4 and 17.5 show $P_m(t)$ for $gt = 10$ and $gt = 100$, for a Fock state with $n = 9$. We notice that the maximum of the Bessel function $J_m(g\sqrt{n+1}t)$ happens when $m \approx g\sqrt{n+1}t$ and then it sharply drops to zero, as we see from these figures [17.12].

We also show the momentum distribution for a squeezed state in Figs. 17.6 and 17.7. We notice that the case $\Delta = 0$ is not very realistic, since spontaneous emission has not been considered [17.13, 17.14]. However, for large Δ , the model, again, is reasonable.

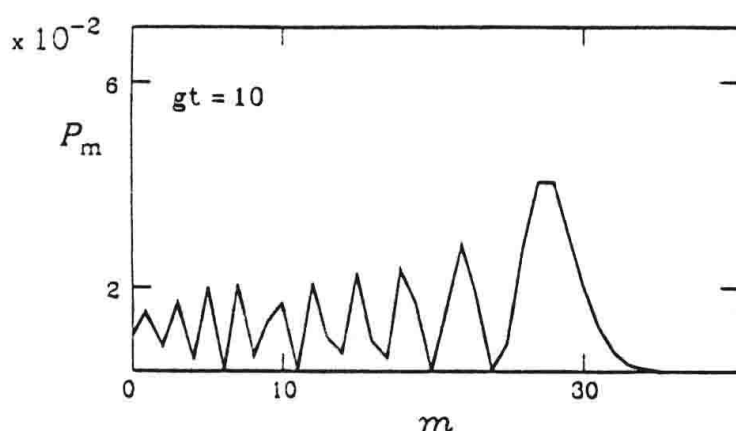


Fig. 17.4. Momentum distribution of atoms scattered off a Fock state $n = 9$, and $gt = 10$ (after [17.12])

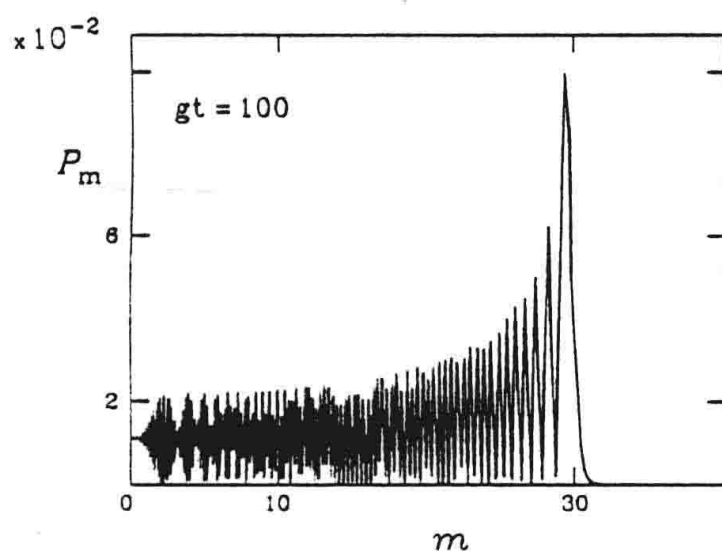


Fig. 17.5. Momentum distribution of atoms scattered off a Fock state with $n = 9$ for $gt = 100$ (after [17.12])

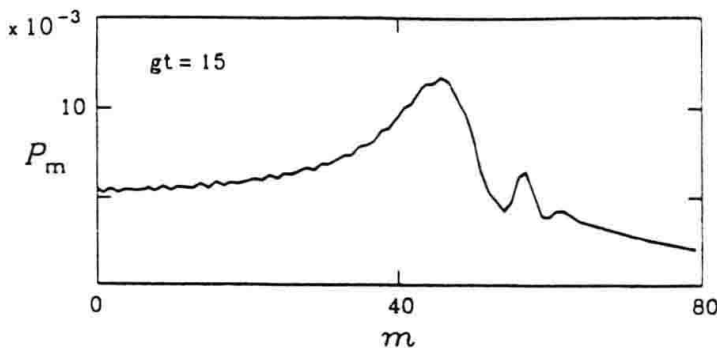


Fig. 17.6. Momentum distribution for the atoms interacting with a squeezed state with $\alpha^2 = 9$ and $r = 50$ and $gt = 15$ (after [17.12])

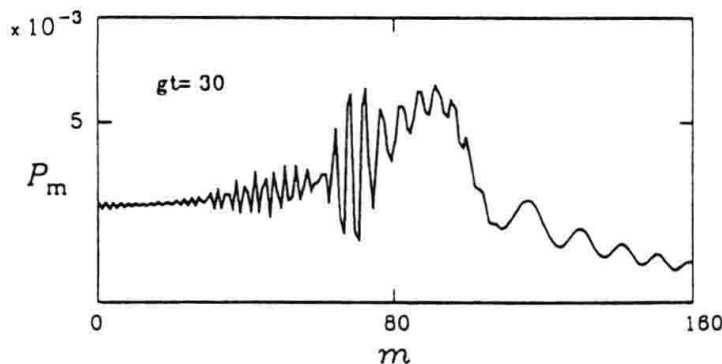


Fig. 17.7. Momentum distribution for the atoms interacting with a squeezed state with $\alpha^2 = 9$ and $r = 50$ and $gt = 30$ (after [17.12])

(b) $\Delta \gg g\sqrt{n}, \epsilon_R m^2$.

If we consider the Raman–Nath approximation ($p_x^2/2m \sim 0$), it is not difficult to show that for large detuning, one can write an approximate effective Hamiltonian:

$$V_{\text{eff}} = \frac{\hbar g^2}{\Delta} \sigma_z a^\dagger a \left(\frac{S^+ + S^-}{2} \right), \quad (17.20)$$

where this time $S^\pm \equiv \exp(\pm 2ikx)$, $S_z \equiv p_x/2\hbar kx$. Notice, that this definition is similar to that of the previous case, except that the transitions are in steps of two photon momentum units. We also notice in this case, that both σ_z and $a^\dagger a$ are constants of the motion and therefore there is only one index left $m = p_x/2\hbar k$, and

$$|\Psi\rangle = \sum_m C_m |m\rangle \begin{pmatrix} 1 \\ 0 \end{pmatrix}, \quad (17.21)$$

and Schrödinger's equation can be written as

$$2i \frac{dC_m}{d\tau} = \frac{|g|^2 n}{2\Delta} (C_{m-1} + C_{m+1}), \quad (17.22)$$

where $\tau \equiv |g|^2 tn/2\Delta$ is an adimensional scaled time and the procedure to arrive at (17.22) is the same as that used in the previous section. The solution of (17.22) is

$$C_{n,m} = (-i)^m J_m \left(\frac{|g|^2 n}{2\Delta} \tau \right), \quad (17.23)$$

where the formula (17.23) is valid only for even m .

In Fig. 17.8 we show a comparison of the theoretical predictions presented here with experimental observation.

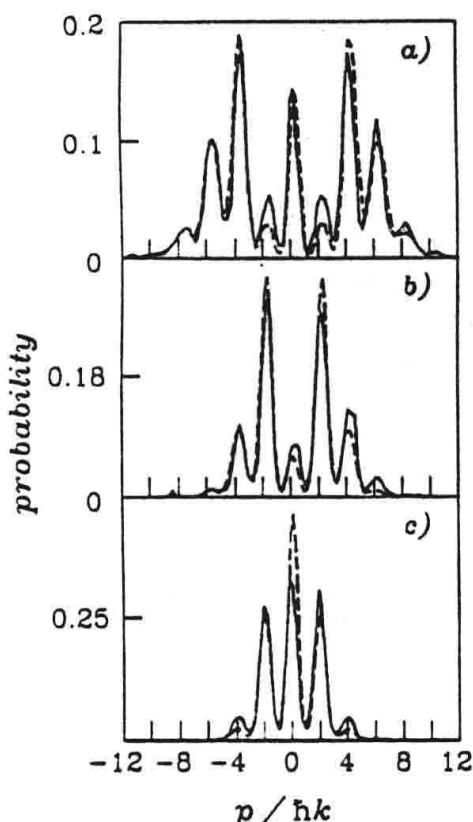


Fig. 17.8. Diffraction patterns for different velocities v_x , which can be obtained experimentally by tilting the standing wave with respect to the atomic beam. (a) $v_x = 0.06 \text{ m s}^{-1}$, (b) $v_x = 1.22 \text{ m s}^{-1}$, (c) $v_x = 1.68 \text{ m s}^{-1}$ (Solid line represents experimental data; dashed line represents theory; after [17.6])

17.3 Atomic Focusing

Lenses are important elements in many optical systems. In atomic optics, possible applications of lenses for atoms are found in the fields of microscopy and lithography. The typical resolution of a diffraction-limited microscope is determined by the wavelength. The instant success, for instance, of electron microscopy is that wavelengths much smaller than optical can be achieved. A particle with a kinetic energy E , has a de Broglie wavelength $\lambda_{dB} = h/\sqrt{2mE}$. Atomic resolution is possible, but in the keV range, which may damage the sample.

On the other hand, for atoms, with much larger mass, the same resolution is possible but with much lower energies.

Another important application of lenses is in atomic lithography, where atoms are deposited onto a surface with a very high resolution. An example of such an experiment is that by McClelland *et al.* [17.15] (see Fig. 17.9).

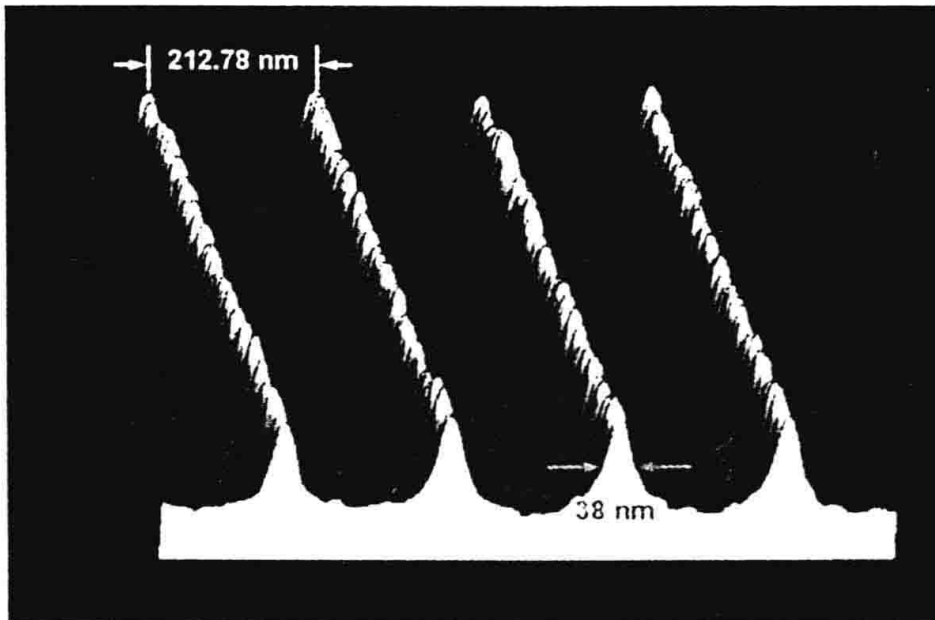


Fig. 17.9. A typical image of chromium lines created by atomic deposition (after [17.15])

17.3.1 The Model

We consider a collimated beam of atoms of mass m moving in the xz plane along $x = \kappa > 0$. We will assume that the atoms are prepared in such a way that they can be modelled by two-level atoms [17.16], [17.17]. In the interaction region $-L < z < 0$ (or interaction time $T = L/v_z$), the atoms cross an orthogonal one-mode standing light wave detuned by Δ . The longitudinal velocity v_z of the atoms along the beam axis (z -axis) is considered to be sufficiently large so that the spatial dependence of the field in z can be replaced by a time dependence $t = z/v_z$.

The Hamiltonian is [17.18]

$$H = \frac{p^2}{2m} + \hbar\omega a^\dagger a + \frac{\hbar\omega_0}{2}\sigma_z + \hbar(a^\dagger\sigma_- g(x) + a^\dagger\sigma_+ g^*(x)). \quad (17.24)$$

In (17.24), $g(x)$ is the space-dependent dipole of the atomic transition. In the limit of high detuning, and keeping the kinetic energy, we have

$$H_{\text{eff}} = \frac{p_x^2}{2m} + \frac{\hbar |g(x)|^2}{\Delta}\sigma_z a^\dagger a. \quad (17.25)$$

In the above limit, again, $\sigma_z, a^\dagger a$ are constants and we neglect the effects of spontaneous emission.

We consider a relatively narrow atomic beam, so that the usual sinusoidal coupling constant can be expanded

$$|g(x)|^2 = |G \sin\left(\frac{2\pi x}{\lambda}\right)|^2 \cong \left(\frac{2\pi G}{\lambda}\right)^2 x^2. \quad (17.26)$$

We now expand the quantum mechanical states in the following basis

$$\sum_{j=-,+} \sum_{n=0}^{\infty} \int_{-\infty}^{+\infty} dx' |j, n, x', t\rangle \langle j, n, x', t| = 1, \quad (17.27)$$

$$\langle j, n, x', t | k, m, x'', t\rangle = \delta_{jk} \delta_{nm} \delta(x' - x'').$$

and we notice that if the atoms are in the lower state at $t = 0$, they remain there for all time. Thus, for $\Delta < 0$, we get a harmonic oscillator

$$i\hbar \frac{d}{dt} \langle -, n, x', t | \Psi \rangle = \left\langle -, n, x', t \left| \frac{p_x^2}{2m} + \frac{m\omega_n^2 x^2}{2} \right| \Psi \right\rangle, \quad (17.28)$$

for each n , with frequency

$$\omega_n^2 = -\frac{2\hbar}{\Delta m} \left(\frac{2\pi G}{\lambda}\right)^2 n. \quad (17.29)$$

17.3.2 Initial Conditions and Solution

In a real experiment, the lateral velocity of the atoms, before entering the interaction region, is in general not exactly zero. Also, the orthogonal alignment between the beam and the standing wave has a certain deviation from orthogonality, etc. All these effects can be included in the fluctuation of the lateral position κ as well as the initial lateral momentum p . Therefore, we will model all these effects by a Gaussian

$$\begin{aligned} & \langle -, n, x', t = -T | \Psi \rangle \\ &= w_n \frac{1}{\sqrt{\sqrt{\pi} d}} \exp\left(-\frac{1}{2} \left(\frac{x' - \kappa}{d}\right)^2 - \frac{i}{\hbar} p(x' - \kappa)\right), \end{aligned} \quad (17.30)$$

where w_n is the initial field amplitude, assumed to be a pure state $\sum w_n |n\rangle$.

During the time the atom is going through the interaction region (from $t = -T$ to $t = 0$), the dynamics is that of a Gaussian wave packet in a harmonic potential [17.19]. After traversing the interaction region, the atom becomes free again (from $t = 0$ to $t > 0$). By applying the free propagator to the previous result, one gets a time-dependent Gaussian

$$\begin{aligned} & |\langle -, n, x', t | \Psi \rangle|^2 \\ &= \frac{|w_n|^2}{\sqrt{\pi} D_n(t)} \exp\left\{-\left[\frac{x' - x'_n(T) + v'_n(T)t}{D_n(t)}\right]^2\right\}, \end{aligned} \quad (17.31)$$

whose width $D_n(t)$ is

$$D_n(t) = d \left[\left(\frac{\hbar}{d^2 m \omega_n} \right)^2 (\omega_n t \cos(\omega_n T) + \sin(\omega_n T))^2 + (\cos(\omega_n T) - \omega_n t \sin(\omega_n T))^2 \right]^{1/2} \quad (17.32)$$

The definitions of $x'_n(T), v'_n(T)$ are

$$\begin{aligned} x'(T) &= \kappa \frac{\cos(\omega T + \phi)}{\cos(\phi)}, \\ p'(T) &= p \frac{\sin(\omega T + \phi)}{\sin(\phi)}, \\ \tan \phi &= \frac{p}{m \omega \kappa}. \end{aligned} \quad (17.33)$$

The physical picture emerging from these results is quite simple. A classical mass subject to the harmonic potential, after the interaction time T , has as solutions $x'(T), p'(T)$ with initial conditions $x'(0) = \kappa, p'(0) = p$.

17.3.3 Quantum and Classical Foci

From (17.32), we see that the classical trajectory of the n th wave packet is

$$x' = x'_n(T) - v'_n(T)t, \quad (17.34)$$

and in the paraxial approximation ($\phi \ll 1$), the incoming atoms all intersect at

$$\begin{pmatrix} x_n^{\text{cf}} \\ z_n^{\text{cf}} \end{pmatrix} = \begin{pmatrix} -\frac{p}{m \omega_n} \csc(\omega_n T) \\ \frac{v_z}{\omega_n} \cot(\omega_n T) \end{pmatrix}, \quad (17.35)$$

which we call the classical focus.

On the other hand, from (17.33), one can write D_n as

$$D_n = d \left[\left(\frac{\cos^2 \varphi_n}{\chi^2 \varphi_n^2} + \sin^2 \varphi_n \right) (\omega_n t - \omega_n t_n^{\text{qf}})^2 + \frac{1}{\cos^2 \varphi_n + \chi^2 \varphi_n^2 \sin^2 \varphi_n} \right]^{\frac{1}{2}}, \quad (17.36)$$

with

$$\omega_n t_n^{\text{qf}} \equiv \sin \varphi_n \cos \varphi_n \frac{\chi^2 \varphi_n^2 - 1}{\cos \varphi_n^2 + \chi^2 \varphi_n^2 \sin^2 \varphi_n}, \quad (17.37)$$

$$\chi \equiv \frac{md^2}{\hbar T}, \quad \varphi_n = \omega_n T.$$

From (17.37) and (17.37) it is clear that the beam converges at the position

$$z_n^{\text{qf}} = v_z t_n^{\text{qf}}, \quad (17.38)$$

and we define the quantum focus at this position. The value of D_n at the quantum focus becomes

$$D(t_n^{qf}) = \frac{d}{\sqrt{\cos \varphi_n^2 + \chi^2 \varphi_n^2 \sin^2 \varphi_n}}. \quad (17.39)$$

If one is restricted to photon numbers

$$n > \frac{-\Delta\hbar}{2d^4m} \left(\frac{\lambda}{2\pi G} \right)^2,$$

then $\chi^2 \varphi_n^2 > 1$, and we have focusing, in the sense that $D(t_n^{qf}) < d$.

17.3.4 Thin versus Thick Lenses

In many experimental situations, the particle trajectories are only slightly deflected, which in the present notation means that $\varphi_n \ll 1$, for all relevant n values. This is the thin lens condition. According to (17.35), different rays coming with the same p but different κ all intersect at

$$\left(\frac{x_n^{cf}}{z_n^{cf}} \right) \approx \frac{1}{\varphi_n^2} \left(-\frac{p}{m} \right) T, \quad (17.40)$$

which implies that the focal length z_n^{cf} goes as $1/n$.

If we assume classical light, that is a coherent state

$$|w_n|^2 = \frac{\langle a^\dagger a \rangle^n}{n!} \exp -\langle a^\dagger a \rangle, \quad (17.41)$$

with large $\langle a^\dagger a \rangle$, the single classical focus corresponding to each n will be distributed over a distance characterized by $\sqrt{\langle a^\dagger a \rangle}$, that is the focal spot along z will have a size of the order of

$$\frac{-\Delta m v_z \lambda^2}{8\hbar T \pi^2 G^2 \langle a^\dagger a \rangle^{3/2}}$$

centred at

$$z_{\langle n \rangle}^{cf} = \frac{-\Delta m v_z \lambda^2}{8\hbar T \pi^2 G \langle a^\dagger a \rangle}.$$

The spot width in x will be

$$D_{\langle n \rangle}(t_{\langle n \rangle}^{cf}) = \frac{-\Delta \lambda^2}{8\pi^2 G^2 d T \langle a^\dagger a \rangle}, \quad (17.42)$$

which does not contain \hbar nor the atomic mass m .

The thin lens is convergent. However, if $\varphi_n > \pi/2$, the classical focus becomes negative and we speak of a divergent lens.

17.3.5 The Quantum Focal Curve

If we introduce (17.37) in (17.34), we have the quantum focus

$$\begin{pmatrix} x_n^{qf} \\ z_n^{qf} \end{pmatrix} = \begin{pmatrix} \kappa \xi_n \\ \chi L \zeta_n \end{pmatrix}, \quad (17.43)$$

where x and z have been parametrized by

$$\begin{aligned} \xi_n &= \kappa \frac{c_n}{c_n^2 + l_n^2 s_n^2}, \\ \zeta_n &= v_z \frac{c_n s_n}{\omega_n} \frac{l_n^2 - 1}{c_n^2 + l_n^2 s_n^2}, \\ c_n &= \cos \omega_n T, \quad s_n = \sin \omega_n T, \quad l_n = \frac{d^2 m \omega_n}{\hbar}. \end{aligned} \quad (17.44)$$

Equation (17.43) is the parametrized focal curve. For large χ , as $n \rightarrow \infty$, it approaches

$$\left(|\xi_n| - \frac{1}{2} \right)^2 + \zeta_n^2 = 1. \quad (17.45)$$

Equation (17.45) describes a double circular lobe (see Fig. 17.10).

Let us assume that $\chi \varphi_n \gtrsim 1$. Then one can easily check that

$$|t_n^{cf}| \geq |t_n^{qf}|,$$

and the classical and quantum foci become real, for the same value of n . Since they both lie on the trajectory line (17.34), it is evident from the geometry that they should essentially coincide in position, when close to the z -axis. In this case, and if $\chi^2 \varphi_n^2 \sin^2 \varphi_n \geq |\cos \varphi_n|$,

$$|\chi_n^{qf}| \ll \kappa. \quad (17.46)$$

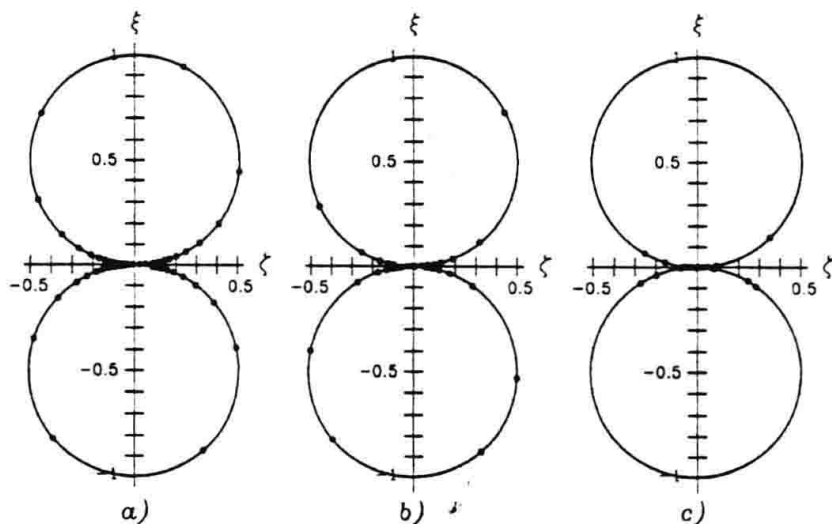


Fig. 17.10. Quantum focal distribution for $\chi = 0.4$ (a), $\chi = 1$ (b), $\chi = 4$ (c). For large χ , all foci concentrate close to the origin (after [17.18])

Classical and quantum foci will then be equally distributed, at

$$z_n^{qf} \approx v_z T \frac{\cos \varphi_n}{\varphi_n \sin \varphi_n} \approx z_n^{cf},$$

and we will introduce the superscript f to refer to both.

In the case of thin lenses, and more generally, whenever $|\varphi_n - m\pi| \ll 1$ holds, for a given $m = 0, 1, 2, \dots$, and if (17.46) is satisfied, the focal position becomes

$$z_n^f \approx \frac{L}{\varphi_n(\varphi_n - m\pi)}, \quad (17.47)$$

and

$$z_n^f - z_{n+1}^f \approx \frac{L}{2n}. \quad (17.48)$$

17.3.6 Aberrations

Chromatic. Chromatic aberration arises from the velocity spread in the incident beam. In other words, instead of having a plane wave with velocity v_z , we may assume an incoherent superposition of plane waves with different velocities. This implies different interaction times of the atoms. If we consider a velocity shift $v_z \rightarrow v_z + \delta v_z$, it will produce a shift $z_n \rightarrow z_n + \delta z_n$

$$\delta z_n \approx \delta v_z \frac{dz_n}{dv_z} = \delta v_z T \left[\frac{2z_n}{L} + \frac{1}{\sin^2 \varphi_n} \right], \quad (17.49)$$

for the n th focus. Unfortunately, the quantity in parentheses is positive and the lens cannot be made achromatic.

Isotopic. When the atomic species used in the beam consists of various isotopes, the exact focal length will vary with the mass. For a mass difference between isotopes δm , the focal shift is

$$\delta z_n^f \approx \delta m \frac{dz_n^f}{dm} = \frac{L \delta m}{2m} \left[\frac{z_n^f}{L} + \frac{1}{\sin^2 \varphi_n} \right]. \quad (17.50)$$

The isotopic aberration could be used to create lines made of different isotopes.

Spherical. If we want to take into account the anharmonicity of the potential, we have to consider quartic terms or the full sinusoidal potential. Both problems are rather difficult. The sinusoidal potential leads to Mathieu functions.

Problems

17.1. Show that

$$S^+ |m\rangle = |m+1\rangle,$$

$$S^- |m\rangle = |m-1\rangle,$$

where

$$S^\pm = \exp(\pm i k x).$$

17.2. Show that for the Hamiltonian given by (17.9), the quantity

$$C = \hbar\omega(a^\dagger a + \sigma_z),$$

is a constant of the motion.

17.3. Justify the fact that neglecting spontaneous emission in atomic diffraction is only reasonable if $\Delta \gg g\sqrt{n}$.

17.4. Prove (17.31), (17.32).

18. Measurements, Quantum Limits and all That

In the present chapter we study the various quantum limits. We also deal with quantum non-demolition (QND) as well as continuous measurements.

18.1 Quantum Standard Limit

18.1.1 Quantum Standard Limit for a Free Particle

We want, in this section, to study the motion of a free particle, or even better, we want to monitor its position during a time τ , confining ourselves to only two measurements [18.1], [18.2]. We assume, at $t = 0$, that we measure a free particle's position with an error $(\Delta x_{\text{measure}})_1$, which, according to the uncertainty principle, produces a perturbation in the momentum

$$(\Delta p)_{\text{pert}} \geq \frac{\hbar}{2(\Delta x_{\text{measure}})_1}. \quad (18.1)$$

A second measurement is now performed at time $t = \tau$, and the momentum perturbation will produce an additional uncertainty in the position

$$(\Delta x)_{\text{add}} = \frac{(\Delta p)_{\text{pert}}\tau}{m} \geq \frac{\hbar\tau}{2m(\Delta x_{\text{measure}})_1}. \quad (18.2)$$

Now, if these contributions superpose incoherently, and we assume an error in the second measurement $(\Delta x_{\text{measure}})_2$, then

$$(\Delta x(\tau))^2 = (\Delta x_{\text{measure}})_1^2 + (\Delta x_{\text{measure}})_2^2 + (\Delta x_{\text{add}})^2, \quad (18.3)$$

and substituting (18.2) in (18.3), we can minimize the above expression, making

$$\frac{d(\Delta x(\tau))^2}{d(\Delta x_{\text{measure}})_1^2} = 0. \quad (18.4)$$

The optimum occurs when $(\Delta x_{\text{measure}})_1 = \sqrt{\hbar\tau/2m}$, thus giving an optimum for $(\Delta x(\tau))$ (if $(\Delta x_{\text{measure}})_2^2 = 0$)

$$(\Delta x(\tau)) = \Delta x_{\text{SQL}} = \sqrt{\frac{\hbar\tau}{m}}. \quad (18.5)$$

Also, we get for Δp

$$\Delta p_{SQL} = \sqrt{\frac{m\hbar}{2\tau}}. \quad (18.6)$$

On the other hand, if one could prepare the state of the system, then we repeat the argument and

$$x(\tau) = x(0) + \frac{p(0)\tau}{m}, \quad (18.7)$$

whose variance is

$$\begin{aligned} (\Delta x(\tau))^2 &= (\Delta x(0))^2 + \frac{(\Delta p(0))^2\tau^2}{m^2} \\ &\quad + \langle \Delta x(0)\Delta p(0) + \Delta p(0)\Delta x(0) \rangle \frac{\tau}{m}, \end{aligned} \quad (18.8)$$

and if we prepared the system in a contractive state, such that

$$\langle \Delta x(0)\Delta p(0) + \Delta p(0)\Delta x(0) \rangle < 0, \quad (18.9)$$

then one could beat the standard quantum limit [18.3].

18.1.2 Standard Quantum Limit for an Oscillator

Consider a harmonic oscillator with a mass m and angular frequency ω , with

$$H_0 = \frac{p^2}{2m} + \frac{1}{2}m\omega^2x^2, \quad (18.10)$$

and number of quanta

$$N = \frac{H_0}{\hbar\omega} - \frac{1}{2}. \quad (18.11)$$

Since the harmonic oscillator is quantum mechanical, one has

$$[x, p] = i\hbar, \quad (18.12)$$

$$\Delta x \Delta p \geq \frac{\hbar}{2}.$$

When such an oscillator is in the ground state, the variance of x and p have the minimum allowed by the uncertainty principle

$$\Delta x = \frac{\Delta p}{m\omega} = \sqrt{\frac{\hbar}{2m\omega}}, \quad (18.13)$$

which is the half-width of the oscillator ground state. Even more generally, in a coherent state one has the same uncertainties.

18.1.3 Thermal Effects

Now, we may think that these quantum limits are not very relevant if one has large classical thermal fluctuations. When the measurement time τ is larger than the oscillator relaxation time τ^*

$$\tau > \tau^*, \quad (18.14)$$

then the criterion for neglecting thermal fluctuations is

$$k_B T \leq \frac{\hbar\omega}{2}. \quad (18.15)$$

This criterion could correspond to extremely low temperatures.

For short measurements ($\tau < \tau^*$), the condition is less stringent on the temperature. As a matter of fact, the above condition is not valid since the energy exchange with the oscillator, on the average, is only a fraction $(\tau/\tau^*)k_B T$.

One can show that the thermally induced fluctuations for $\tau \ll \tau^*$ are

$$\Delta x_{\text{thermal}} = \sqrt{\frac{k_B T \tau}{m \omega^2 \tau^*}}. \quad (18.16)$$

Direct comparison of the above limit with the quantum standard limit for the oscillator gives us a criterion for deciding if a system is classical or quantum mechanical. The system behaves quantum mechanically, in the case of short measurements, if

$$k_B T \frac{\tau}{\tau^*} \ll \frac{\hbar\omega}{2}. \quad (18.17)$$

In order to verify the above discussion, we borrow a result from the chapter on the damped harmonic oscillator

$$\Delta x \Delta p = \frac{\hbar}{2} [1 + 2\langle n \rangle_{\text{th}} [1 - \exp(-\gamma\tau)]], \quad (18.18)$$

and, defining $\gamma = \tau^{*-1}$, we have two regimes

(a) $\tau/\tau^* \gg 1$. Then

$$\Delta x \Delta p = \frac{\hbar}{2} (1 + 2\langle n \rangle_{\text{th}}) \quad (18.19)$$

and, for the oscillator to be in a quantum regime, the 1 in the above equation must be much larger than $\langle n \rangle_{\text{th}}$

$$1 \gg 2\langle n \rangle_{\text{th}} = 2 \frac{1}{\exp(\hbar\omega/k_B T) - 1}, \quad (18.20)$$

which implies

$$\frac{\hbar\omega}{2} \gg k_B T. \quad (18.21)$$

(b) $\tau/\tau^* \ll 1$. Then

$$\Delta x \Delta p = \frac{\hbar}{2} \left(1 + \left[2\langle n \rangle_{\text{th}} \frac{\tau}{\tau^*} \right] \right). \quad (18.22)$$

The quantity in the square brackets in (18.22) should be much less than one, for the system to behave quantum mechanically. That condition implies

$$k_B T \frac{\tau}{\tau^*} \ll \frac{\hbar \omega}{2}, \quad (18.23)$$

proving the above assertion.

18.2 Quantum Non-demolition (QND) Measurements

18.2.1 The Free System

The problem of measuring classical signals [18.2] which are very weakly coupled to detectors was originally of interest in research in gravitational wave detection. In the case of large bar detectors, with masses of the order of ten tonnes, the gravitational waves interact so weakly with these detectors that they produce a typical displacement of the order of 10^{-19} cm. With such a small signal, the actual position measurement will introduce a momentum uncertainty that will feed back in extra position uncertainty, as discussed in the last section, leading to a quantum standard limit

$$\Delta x_{\text{SQL}} = \sqrt{\frac{\hbar \tau}{m}} \approx 5 \times 10^{-19} \text{ cm}, \quad (18.24)$$

for a typical gravitational wave period of 10^{-3} s. As we can see, the minimum uncertainty introduced in the first measurement has made it impossible to detect with certainty if the gravitational wave has or has not acted on the detector.

On the other hand, if one tries to detect p rather than x , something non-trivial from the experimental point of view, the error in p produces an added uncertainty in x , according to the uncertainty principle. However, this added noise will not feed back to p , since for a free particle, p is a constant of the motion. Therefore, a second measurement of p can be made, with the same accuracy as the first one. This is an example of a quantum non-demolition measurement, to avoid the back action of the measurement on the observed variable.

QND experiments have been performed in the optical domain [18.4], [18.5], [18.6], [18.7], based on the Kerr coupling of a signal field to be measured with a probe field, whose phase is changed linearly with the number of photons of the signal.

Here, we will discuss another proposal [18.8], where photons are stored in a microwave resonant cavity and they are detected by measuring the phase

shift of the electric dipoles of non-resonant Rydberg atoms crossing the cavity. In this way, weak fields (with a small photon number) can be monitored continuously, with no back action on the number of photons. In this example, the detector is the atomic beam crossing the microwave cavity.

As we have already mentioned, the original research on QND measurements was triggered by the desire for monitoring a very weak force, acting on a harmonic oscillator, with an accuracy better than the quantum standard limit. Braginsky *et al.* [18.9] proposed what they called a quantum non-demolition measurement, where one monitors an observable of the oscillator, which has to be measured many times, with each measurement being completely determined by the result of an initial precise measurement. We call such an observable a ‘quantum non-demolition observable’.

To fix ideas, let us assume that we have a system described by a Hamiltonian H_S and we want to measure an observable (Hermitian operator) A_S that could be, for example, the number of quanta of the harmonic oscillator, to monitor a classical force produced, in this particular example, by the gravitational wave. In the optical case, A_S could be the photon number of a field. The measurement of A_S , however, is not made directly, but via the detection of a probe observable A_P , conveniently coupled to the system, during the measurement. The above definition of a QND observable can be used to derive its condition.

For the moment, we neglect the interaction with the probe, or measuring apparatus. Now we assume a sequence of measurements of A_S , assuming that we have no control over the state of the system. Also, we denote by $|A_S, \alpha_S\rangle$ the normalized eigenstate of $A_S(t_0)$, with

$$A_S |A_S, \alpha_S\rangle = A_S |A_S, \alpha_S\rangle, \quad (18.25)$$

where α_S labels the degeneracy index. As a result of the first measurement, one gets the eigenvalue A_0 of $A_S(t_0)$, and the eigenstate, after this measurement, is

$$|\psi(t_0)\rangle = \sum_{\alpha} C_{\alpha} |A_0, \alpha\rangle. \quad (18.26)$$

In the interval between the first and second measurement, in the Heisenberg picture $|\psi(t)\rangle = |\psi(t_0)\rangle$, that is the state does not change. If a second measurement at $t = t_1$ is to produce a predictable result, it means that all the states $|A_0, \alpha\rangle$ must be eigenstates of $A_S(t_1)$, but in general, with different eigenvalues:

$$A_S(t_1) |A_0, \alpha\rangle = f_1(A_0) |A_0, \alpha\rangle. \quad (18.27)$$

Since the above result is true for all the eigenvalues of $A_S(t_0)$, we must have

$$A_S(t_1) = f_1(A_S(t_0)). \quad (18.28)$$

For a QND measurement at times $t = t_0, t_1, \dots, t_n$, one must have:

$$A_S(t_k) = f_k(A_S(t_0)), \quad k = 1, 2, \dots, n, \quad (18.29)$$

where f_k is a real function.

For a continuous measurement, or at arbitrary times, one writes

$$\mathbf{A}_S(t) = f(\mathbf{A}_S(t_0); t, t_0). \quad (18.30)$$

The above condition is satisfied by a constant of the motion, which in the absence of interactions, satisfies

$$\frac{d\mathbf{A}_S(t)}{dt} = -\frac{i}{\hbar} [\mathbf{A}_S(t), H_S] + \frac{\partial \mathbf{A}_S(t)}{\partial t}. \quad (18.31)$$

In a harmonic oscillator, \mathbf{x} and \mathbf{p} are not QND observables. However N is conserved. In the case of a free particle, \mathbf{x} is not a QND variable but \mathbf{p} is.

Another way of expressing the QND condition (18.30) is

$$[\mathbf{A}_S(t), \mathbf{A}_S(t')] = 0. \quad (18.32)$$

18.2.2 Monitoring a Classical Force

Once we have defined a continuous QND observable, and a QND measurement, satisfying the condition given in (18.32), we consider its application to monitoring a classical force $F(t)$. The procedure is the following: we make a sequence of QND measurements and detect the changes the classical force produced in the precisely predictable values of the QND variable, in the absence of the force.

We would like to go even further and actually monitor the time dependence of the force with arbitrary accuracy, satisfying the following conditions [18.2]:

- (a) The measuring apparatus and its coupling to the system can produce arbitrarily precise measurements.
- (b) The $(k+1)$ th measurement at time t_k must be uniquely determined as a result of an initial measurement at time t_0 and the history of $F(t)$ between t_0 and t_k .

For condition (b) to be satisfied, one must have

$$\mathbf{A}(t) = f(\mathbf{A}(t_0); F(t'); t, t_0), \quad t_0 < t' < t. \quad (18.33)$$

In the above condition, $\mathbf{A}(t)$ is a Heisenberg operator evolving with a Hamiltonian that includes a coupling term to the apparatus.

- (c) From the history of the measured values of $\mathbf{A}(t)$, one should in principle, derive $F(t)$. This implies that the above condition (18.33) should be invertible.

Now we concentrate in the measuring apparatus and its interaction with the system.

18.2.3 Effect of the Measuring Apparatus or Probe

We assume that we want to measure a quantum observable A_S of the system S , by detecting it indirectly, that is by measuring the change in an observable of a probe A_P , during a time interval T . We notice that here we talk about measuring a quantum observable A_S , thus generalizing the argument of monitoring a classical force of the previous section.

The Hamiltonian of the system coupled to the probe is

$$H = H_S + H_P + H_I, \quad (18.34)$$

where H_S and H_P are the free terms for the system and probe respectively, and H_I is their interaction. To do this measurement, the interaction Hamiltonian must depend on A_S , that is

$$\frac{\partial H_I}{\partial A_S} \neq 0. \quad (18.35)$$

On the other hand, if we are doing this measurement indirectly via another quantum observable A_P , and if furthermore, we want to monitor it with several measurements, then A_P must respond to Heisenberg's equation, as a dynamic variable, or in other words, we require that

$$[A_P, H_I] \neq 0. \quad (18.36)$$

Finally, and most importantly, we have the original QND restriction given by (18.32), which, in this model, implies

$$[A_S, H_I] = 0, \quad (18.37)$$

in the particular case when there is no explicit time dependence of the variables ($\partial A_S / \partial t = 0$).

Equations (18.35), (18.36), (18.37) describe a QND measurement completely, and they will be instrumental in describing a particular QND measurement scheme in an optical system, presented in the next section.

18.3 QND Measurement of the Number of Photons in a Cavity

18.3.1 The Model

An interesting example of a time-independent QND measurement is the one involving cavity quantum electrodynamics [18.8]. We assume a beam of three-level atoms interacting non-linearly and non-resonantly with a signal field. What we want to measure as accurately as possible is the photon number of the signal field and the probe is the atomic beam.

In order to do this detection efficiently, the atoms are prepared in Rydberg states, that is with large dipole moments, and the signal is a microwave field,

in a high- Q cavity, nearly resonant with a couple of adjacent atomic energy levels, as shown in Fig. 18.1, where the three levels are denoted by a , b , c and the atoms cross a microwave cavity with frequency ω , with a relative detuning δ

$$\delta = \omega - \omega_{ab}, \quad (18.38)$$

with $\omega_{ab} = (E_a - E_b)/\hbar$. We also assume that $g^2 n / \delta^2 \ll 1$, where $g(r)$ is a position-dependent coupling constant (the position of the atom within the cavity).

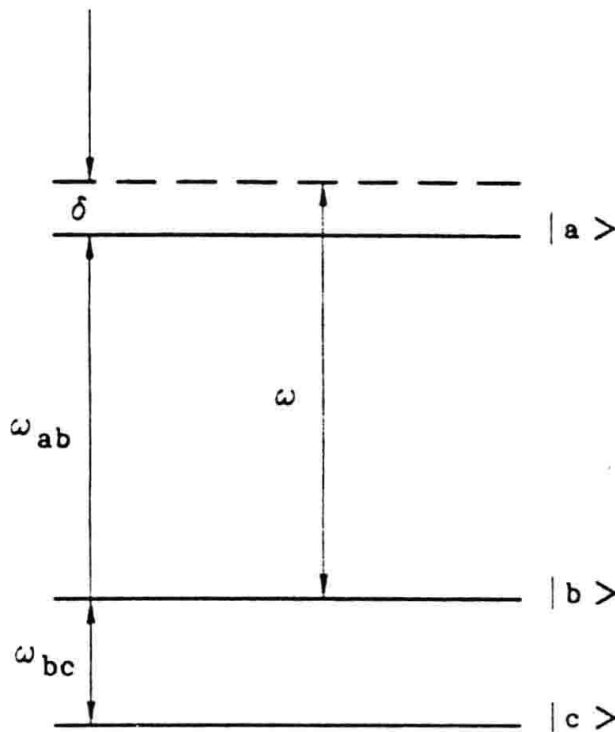


Fig. 18.1. Three-level atom used in the QND measurement of the photon number in the cavity

If one has the combined atom-field state $|b, n\rangle$, with an unperturbed energy $E_b + \hbar\omega(n + 1/2)$, this level suffers an energy Stark shift

$$\hbar\Delta_b = \frac{\hbar g^2(r)n}{\delta}, \quad (18.39)$$

for $E_b < E_a$, and

$$\hbar\Delta_b = -\frac{\hbar g^2(r)(n + 1)}{\delta}, \quad (18.40)$$

for $E_b > E_a$. Here we consider the level scheme of Fig. 18.1, with $E_b < E_a$.

18.3.2 The System–Probe Interaction

We will assume that the off-resonant level $|c\rangle$ is not affected by this field and will be used for the measurement only. For QND measurement purposes, we concentrate now on the subspace with atomic levels $|b\rangle$ and $|c\rangle$.

The atomic Hamiltonian, in this subspace, is

$$H_{\text{at}}^{(b,c)} = \hbar\omega_{bc} |b\rangle\langle b|, \quad (18.41)$$

and, in the presence of the field, the effective Hamiltonian is (a detailed derivation of such an effective Hamiltonian is found in Chap. 19)

$$H_{\text{I}} = \hbar \left[\omega_{bc} + \frac{g^2 n}{\delta} \right] |b\rangle\langle b|. \quad (18.42)$$

As we mentioned before, we consider the atom as probe to measure the photon number of the field.

The Hamiltonian for the S–P coupling is from (18.42) (noting that n is the photon number corresponding to the $a_S^\dagger a_S$ field)

$$\begin{aligned} H_{\text{at}}^{(b,c)\text{eff}} &= \frac{\hbar g^2}{\delta} a_S^\dagger a_S |b\rangle\langle b| \\ &= \frac{\hbar g^2}{\delta} a_S^\dagger a_S (D_{bc}^\dagger D_{bc}), \end{aligned} \quad (18.43)$$

where

$$D_{bc} = |c\rangle\langle b|.$$

The probe observable is defined as the atomic dipole operator:

$$A_P^{\text{at}} = \frac{1}{2i} (D_{bc}^\dagger - D_{bc}), \quad (18.44)$$

which is a quantity sensitive to the atomic phase, something that one could measure.

If the field contains n photons, the change of atomic phase, after a time interval t , is

$$\Delta\varphi = \left[\omega_{bc} + \frac{g^2 n}{\delta} \right] t. \quad (18.45)$$

One can easily check that in this system and probe, all the QND measurement criteria are satisfied.

18.3.3 Measuring the Atomic Phase with Ramsey Fields

Now a device is needed to measure the atomic phase shift $\Delta\varphi$. An interesting possibility is the Ramsey method of two oscillating fields R_1 and R_2 as shown in Fig. 18.2. Before entering the cavity, each atom is prepared by a laser in a Rydberg level $|b\rangle$. Then the atom interacts with the first Ramsey field

(R_1) , which is a microwave field at frequency ω_r , quasi-resonant with the b - c transition. The atom, after this interaction, leaves in a linear superposition of the $|b\rangle$ and $|c\rangle$ states. Then it crosses the cavity and outside the cavity, it interacts with a second Ramsey microwave field (R_2) , with frequency ω_r .

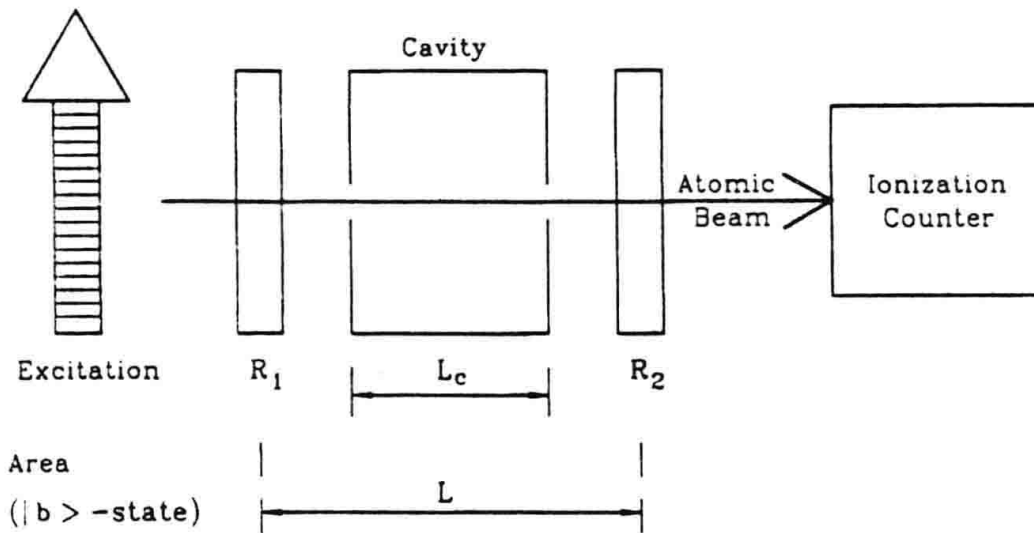


Fig. 18.2. Experimental setup for a QND measurement of photon number in the cavity. The atoms are initially excited into a Rydberg state $|b\rangle$ by a laser. They cross the cavity between the two Ramsey fields R_1 and R_2 . After that, an ionization detector determines the velocity and state of the atom

In the absence of photons, the atomic dipole phase shift introduced by the two Ramsey fields is

$$\varphi_0 = (\omega_r - \omega_{bc}) \frac{L}{v_0}, \quad (18.46)$$

where v_0 is the atomic velocity. With n photons in the cavity, this shift becomes

$$\varphi_n = \varphi_0 - n\epsilon, \quad (18.47)$$

where ϵ represents the spatial average of the phase shift per photon, that is

$$\epsilon = \frac{\overline{g(r)^2}}{\delta} \frac{L_c}{v_0} = \frac{g(0)^2 L_c}{2\delta v_0}, \quad (18.48)$$

where we have assumed that $g(r)$ has a sinusoidal dependence that when averaged ($\overline{g^2}$) gives the extra factor $1/2$.

We now analyze the interaction in some detail. Assume that the cavity contains n photons. The atom-field wavefunction, in the unperturbed representation, can be written as

$$|\psi^{\text{atom-field}}\rangle = b_b(n, t) |b, n\rangle + b_c(n, t) |c, n\rangle, \quad (18.49)$$

where b_b, b_c are time-dependent functions due to the R_1 and R_2 fields, with initial conditions

$$b_b(n, 0) = 1, \quad b_c(n, 0) = 0. \quad (18.50)$$

During the passage of the atom through R_1 , we have the typical couple of differential equations corresponding to a two-level atom interacting with a single mode resonant field. If δL is the length of each zone, the interaction time τ is $\tau = \delta L/v$, and we have

$$\begin{aligned} \dot{b}_b(n, t) &= \frac{\Omega_r}{2} b_b(n, t), \\ \dot{b}_c(n, t) &= -\frac{\Omega_r}{2} b_c(n, t), \end{aligned} \quad (18.51)$$

Ω_r being the corresponding Rabi frequency.

The solutions, satisfying the initial conditions, are

$$\begin{aligned} b_b(n, t) &= \cos \frac{\Omega_r}{2} \tau, \\ b_c(n, t) &= -\sin \frac{\Omega_r}{2} \tau. \end{aligned} \quad (18.52)$$

After the atom passes through the cavity, b_b suffers a phase shift while b_c remains the same.

The initial conditions, before entering the second Ramsey zone, are

$$b_b(n) = \exp \left(-in\varepsilon \frac{v_0}{v} \right) \cos \frac{\Omega_r}{2} \tau, \quad (18.53)$$

$$b_c(n) = -\sin \frac{\Omega_r}{2} \tau, \quad (18.54)$$

with v_0/v expressing the dependence of the phase shift on time or the inverse velocity.

In the second zone, the differential equations are the same as the first one, except for the added phase $\pm\varphi_0 v_0/v$ which takes account of the shifts between the two Ramsey fields

$$\begin{aligned} \dot{b}_b(n, t) &= \frac{\Omega_r}{2} \exp \left(-i\varphi_0 \frac{v_0}{v} \right) b_b(n, t) \\ \dot{b}_c(n, t) &= -\frac{\Omega_r}{2} \exp \left(i\varphi_0 \frac{v_0}{v} \right) b_c(n, t). \end{aligned} \quad (18.55)$$

After the second Ramsey zone, the solutions are

$$b_b(n) = \exp \left(-in\varepsilon \frac{v_0}{v} \right) \cos^2 \frac{\Omega_r}{2} \tau - \sin^2 \frac{\Omega_r}{2} \tau \exp \left(-i\varphi_0 \frac{v_0}{v} \right) \quad (18.56)$$

$$b_c(n) = -\frac{1}{2} \sin \Omega_r \tau \left(1 + \exp i(\varphi_0 - n\varepsilon) \frac{v_0}{v} \right).$$

Finally, if we set $\Omega_r \tau = \pi/2$, we get

$$|\psi_{\text{atom-field}}\rangle_{\text{final}} = b_b(n, v; \varphi_0, \varepsilon) |b, n\rangle + b_c(n, v; \varphi_0, \varepsilon) |c, n\rangle, \quad (18.57)$$

with

$$\begin{aligned} b_b(n, v; \varphi_0, \varepsilon) &= \exp(-i\varphi_0 \frac{v_0}{v}) \left[\cos^2 \frac{\pi v_0}{4v} \exp(i\varphi_n \frac{v_0}{v}) - \sin^2 \frac{\pi v_0}{4v} \right], \\ b_c(n, v; \varphi_0, \varepsilon) &= -\frac{1}{2} \sin \frac{\pi v_0}{2v} \left(1 + \exp \left(i\varphi_n \frac{v_0}{v} \right) \right). \end{aligned} \quad (18.58)$$

The atoms are detected when they leave the second Ramsey zone, by a field-ionization detector which determines whether the atom is in state $|b\rangle$ or $|c\rangle$ and also, synchronizing it with that laser excitation, one can determine the velocity v .

The probability P_c of being at c is

$$\begin{aligned} P_c(n, v; \varphi_0, \varepsilon) &= 1 - P_b \\ &= |b_c|^2 \\ &= \sin^2 \frac{\pi v_0}{2v} \cos^2 \varphi_n \frac{v_0}{2v}. \end{aligned} \quad (18.59)$$

If instead of a pure $|n\rangle$ state in the cavity, we have a photon distribution $P(n)$, then:

$$P_c(p(n), \varphi_0, \varepsilon) = \sum_n p(n) P_c(n, v; \varphi_0, \varepsilon). \quad (18.60)$$

We may also average over a Maxwellian velocity distribution $D(v)$ thus getting:

$$P_c(n, \varphi_0, \varepsilon) = \int D(v) P_c(n, v; \varphi_0, \varepsilon) dv. \quad (18.61)$$

$P_c(n, \varphi_0, \varepsilon)$ is shown in Fig. 18.3 for $\varepsilon = 2\pi$, for a Fock state (a), a coherent state (b), and a thermal state (c), with $\bar{n} = 3$.

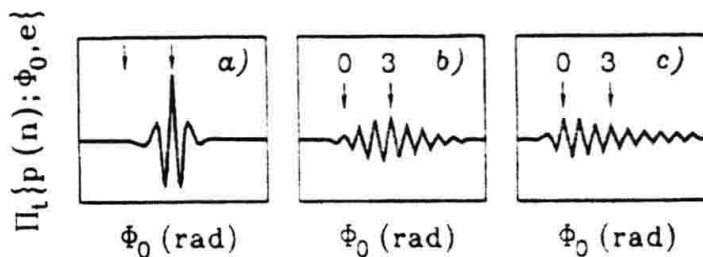


Fig. 18.3. $P_f(p(n), \varphi_0, \varepsilon)$ versus φ_0 for a Fock state (a), a coherent state (b), and a thermal state (c) (after [18.8])

The different fringe patterns allow us in principle to distinguish between the various photon statistics. Since these are probabilities, experimentally we should detect, for each φ_0 , a large number of atoms and the average. This of course implies that the field should be prepared in an initial state with photon statistics $p(n)$, before each atom crosses the cavity, which can be rather cumbersome. It would be more attractive if we had a scheme involving only one realization of the system, using basically the same experimental set-up.

18.3.4 QND Measurement of the Photon Number

We assume a large Q -factor for the cavity and that a bunch of atoms cross it. At the output, each atom's velocity and internal state is detected by the counter. The state of the atom-field system at the entry of the $(k+1)$ atom is given by the density operator

$$\rho_{k+1}^{\text{field+atom}} = \sum_{n,n'} |b,n\rangle\langle b,n| \rho_{k,n,n'}, \quad (18.62)$$

and, after going through the apparatus, will become

$$\begin{aligned} \rho_{k+1}^{\text{field+atom}} &= \sum_{n,n'} (b_b(n, v; \varphi_0, \varepsilon) |b,n\rangle + b_c(n, v; \varphi_0, \varepsilon) |c,n\rangle) \\ &\quad \times \rho_{k,n,n'} (b_b^*(n', v; \varphi_0, \varepsilon) \langle b,n'| + b_c^*(n', v; \varphi_0, \varepsilon) \langle c,n'|). \end{aligned} \quad (18.63)$$

After the atomic measurement, the density operator collapses and it is projected, giving $\langle \alpha n | \rho_{k+1}^{\text{field+atom}} | \alpha n' \rangle$, so ($\alpha = b, c$)

$$\rho_{k+1,n,n'}^{(\alpha,v)} = \frac{b_\alpha(n, v, \varphi_0, \varepsilon) b_\alpha^*(n', v, \varphi_0, \varepsilon)}{\sum_n |b_\alpha(n, v, \varphi_0, \varepsilon)|^2} \rho_{k,n,n'}, \quad (18.64)$$

where we have introduced the normalizing denominator, since normalization was lost after the state collapse.

This denominator is nothing but $P_\alpha(p(n), v, \varphi_0, \varepsilon)$, the probability for the atom to be found in the $|\alpha\rangle$ state, at a given velocity and for a given photon statistics. In other words, for an $|\alpha\rangle$ and v measurement

$$\rho_{k+1,n,n'}^{(\alpha,v)} = \frac{b_\alpha(n, v, \varphi_0, \varepsilon) b_\alpha^*(n', v, \varphi_0, \varepsilon)}{P_\alpha(p(n), v, \varphi_0, \varepsilon)} \rho_{k,n,n'}. \quad (18.65)$$

If only the atomic velocity is detected

$$\rho_{k+1,n,n'}^{(\alpha=? , v)} = \sum_{\alpha=b,c} b_\alpha(n, v, \varphi_0, \varepsilon) b_\alpha^*(n', v, \varphi_0, \varepsilon) \rho_{k,n,n'}, \quad (18.66)$$

and if the atom is not detected at all

$$\rho_{k+1,n,n'}^{(\alpha=? , v=?)} = \int D(v) dv \sum_{\alpha=b,c} b_\alpha(n, v, \varphi_0, \varepsilon) b_\alpha^*(n', v, \varphi_0, \varepsilon) \rho_{k,n,n'}. \quad (18.67)$$

If one is only interested in the photon number distribution, then only the diagonal part of the field density operator is relevant. Letting $\rho_{nn} = p_n$, we have several cases.

(a) The atom is detected with velocity v and at the level α :

$$p_{k+1}^{(\alpha,v)}(n) = \frac{P_\alpha(n, v, \varphi_0, \varepsilon)}{P_\alpha(p_k(n), v, \varphi_0, \varepsilon)} p_k(n). \quad (18.68)$$

(b) The atomic level is not detected:

$$p_{k+1}^{(\alpha=?,\nu=?)}(n) = [P_e(n, \nu, \varphi_0, \varepsilon) + P_f(n, \nu, \varphi_0, \varepsilon)] p_k(n) = p_k(n), \quad (18.69)$$

and the original photon distribution is not changed at all.

(c) If the atom is undetected then again

$$p_{k+1}^{(\alpha=?,\nu=?)}(n) = p_k(n). \quad (18.70)$$

It is interesting to note that the unread atom does not alter the photon statistics of the field. As we shall see in the next section, this in general is not true for any type of measurement and it is a signature of the QND nature of this measurement. Also, the fact that we are getting, via the probe atom, information about the field, modifies the field, in spite of the fact that no energy exchange took place. If we start the field in a pure Fock state $p_k(n) = \delta(n - n_k)$, then

$$P_\alpha(p(n), \nu, \varphi_0, \varepsilon) = P_\alpha(n, \nu, \varphi_0, \varepsilon), \quad (18.71)$$

and no change occurs in the photon statistics

$$p_{k+1}^{(\alpha,\nu)}(n) = p_k(n). \quad (18.72)$$

Now we proceed with the numerical simulation of a continuous QND measurement of the field, initially with a distribution $p_0(n)$. First, we take a velocity v_1 randomly, and compute $P_\alpha(p(n), \nu, \varphi_0, \varepsilon)$ from (18.60). Then we decide the result of the measurement of α (energy level) by comparing this probability to a random number between 0 and 1. Next, we multiply $p_0(n)$ by $P_\alpha(n, \nu, \varphi_0, \varepsilon)$ and normalize, obtaining $p_1(n)$, and so on. This iteration leads to

$$p_k(n) = \frac{\prod_{p=1}^k P_{\alpha_p}(n, v_p, \varphi_0, \varepsilon) p_0(n)}{\sum_{n'} p_0(n') \prod_{p=1}^k P_{\alpha_p}(n', v_p, \varphi_0, \varepsilon)}. \quad (18.73)$$

This simulation can be carried out for different values of φ_0, ε .

Starting from a coherent or thermal distribution, one finds a collapse to a Fock state, as shown in Fig. 18.4. As we can see from the figure, a decimation process takes place as we increase the number of detected atoms, until a pure Fock state is reached. This final state is not *a priori* predictable, since the whole process depends on random variables that mimic the measurement process. So, if we repeat this experiment many times, and considering that we are dealing with QND measurements, the statistics of the result will coincide with the initial photon statistics $p_0(n)$.

What we have just described in this section is a particular continuous measurement without back-action on the measured observable, in this case the photon number in a cavity. In general, in a non-QND measurement, the back-action is present and typically a Fock state after repeated measurements, becomes a different state. This will be described in detail in the next section.

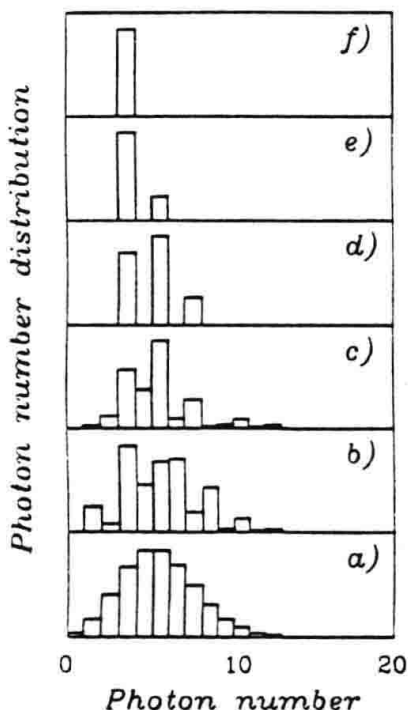


Fig. 18.4. Photon number distribution in a QND sequence. The initial state is coherent with $\bar{n} = 5$ (a). The figures (b), (c), (d), (e) and (f) correspond to the detection of 1, 3, 6, 10 and 15 atoms, respectively. This run collapses in the Fock state $n = 3$ (after [18.8])

18.4 Quantum Theory of Continuous Photodetection Processes

In a series of recent publications, Ueda and coworkers [18.10], [18.11], showed that the quantum properties of the field are generally affected by yes and no results, that is a photodetection event or the absence of it, modifying the statistics of the field. We start our study with a simple model of a two-level atom detector interacting resonantly with a one-mode field, ruled by the Jaynes-Cummings Hamiltonian

$$H = \hbar g(a\sigma^\dagger + \sigma a^\dagger). \quad (18.74)$$

The time evolution of the state vector is

$$|\psi(\tau)\rangle = \left[1 - \frac{iH\tau}{\hbar} - \frac{H^2\tau^2}{2\hbar^2} + \dots \right] |\psi(0)\rangle. \quad (18.75)$$

Let the initial state of the detector-field system be ($|b\rangle$ is the lower state and $|f\rangle$ an unspecified field state)

$$|\psi(0)\rangle = |b\rangle |f\rangle. \quad (18.76)$$

After we measure a photon absorption event, the state vector is projected onto the $|a\rangle$ atomic state, that is (to the lowest approximation)

$$\begin{aligned}\langle a | \psi(\tau) \rangle &= -\frac{i g \tau}{\hbar} \langle a | a \sigma^\dagger + \sigma a^\dagger | b \rangle | f \rangle \\ &= -\frac{i g \tau}{\hbar} a | f \rangle.\end{aligned}\quad (18.77)$$

So, the field density operator, after a photodetection event, and up to a normalization constant, changes as

$$\rho_f \rightarrow a \rho_f a^\dagger. \quad (18.78)$$

On the other hand, if there is no photodetection, during the time interval τ , then the final atomic state remains in $|b\rangle$, and we have

$$\begin{aligned}\langle b | \psi(\tau) \rangle &= \langle b | \left[1 - \frac{i H \tau}{\hbar} - \frac{H^2 \tau^2}{2 \hbar^2} + \dots \right] | \psi(0) \rangle \\ &= |f\rangle - \frac{\tau^2 g^2}{2} \langle b | [\sigma^\dagger \sigma a a^\dagger + \sigma \sigma^\dagger a^\dagger a] |b\rangle |f\rangle \\ &\approx \exp\left(-\frac{\tau^2 g^2}{2} a^\dagger a\right) |f\rangle,\end{aligned}\quad (18.79)$$

where, in the last step, we assumed that the interaction time is short enough so as to have

$$\frac{\tau^2 g^2}{2} \langle a^\dagger a \rangle \ll 1. \quad (18.80)$$

As we can see, up to a normalization constant, the initial field density operator, after a no-absorption event, changes to

$$\rho_f \rightarrow \exp\left(-\frac{\tau^2 g^2}{2} a^\dagger a\right) \rho_f \exp\left(-\frac{\tau^2 g^2}{2} a^\dagger a\right). \quad (18.81)$$

Now, we assume that the ‘yes’ events are detected at times $0, t_1, t_2, \dots, t_n$ and no events in between, with our photodetector being continuously monitored. Each period is subdivided into N small intervals τ , so for example at $t_1 = N\tau$,

$$\begin{aligned}\rho_f(t_1) &= \exp\left(-\frac{N \tau^2 g^2}{2} a^\dagger a\right) \rho_f \exp\left(-\frac{N \tau^2 g^2}{2} a^\dagger a\right) \\ &= \exp(-2Rt_1 a^\dagger a) \rho_f \exp(-2Rt_1 a^\dagger a),\end{aligned}\quad (18.82)$$

with $R = g^2 \tau / 4$.

The sequence shown in Fig. 18.5 corresponds to the transformation of the field density matrix operator, as shown

$$\begin{aligned}\rho_f &\rightarrow \dots [\exp(-2R(t_2 - t_1)a^\dagger a)] a [\exp(-2Rt_1 a^\dagger a)] a \rho_f(0) \\ &\quad a^\dagger [\exp(-2Rt_1 a^\dagger a)] a^\dagger [\exp(-2R(t_2 - t_1)a^\dagger a)] \dots\end{aligned}\quad (18.83)$$

We can group all the a ’s on one side and the a^\dagger ’s on the other, giving us numerical factors that can be included in the renormalization constant. The result is

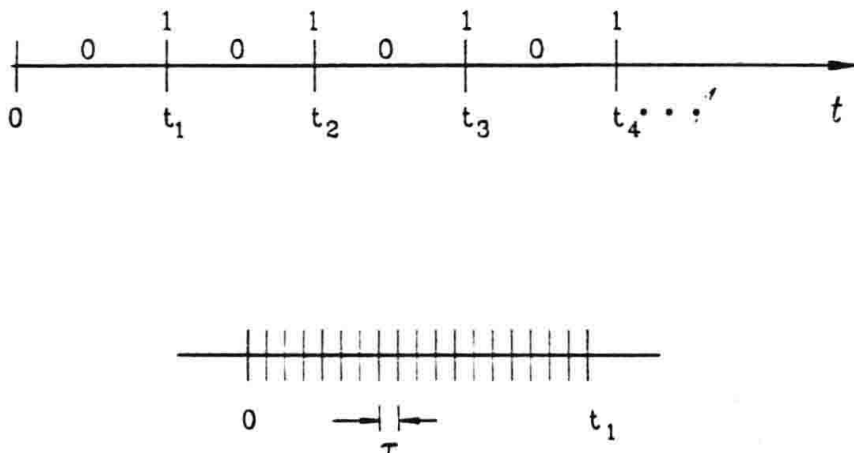


Fig. 18.5. Photodetection sequence at times $0, t_1, t_2, \dots$. In between these times, no absorption is detected. The interval between 0 and t_1 is subdivided into smaller τ intervals

$$\rho_f \rightarrow \frac{[\exp(-2Rta^\dagger a)] a^m \rho_f a^{+m} [\exp(-2Rta^\dagger a)]}{\text{Tr} [\exp(-2Rta^\dagger a)] a^m \rho_f a^{+m} [\exp(-2Rta^\dagger a)]}, \quad (18.84)$$

which corresponds to the modified density operator after m yes counts, t being the total measurement time.

We notice immediately that if the initial state of the field is either a coherent or a Fock state, their nature doesn't change, but the state does, that is

$$\begin{aligned} |\alpha\rangle &\rightarrow |\alpha \exp(-2Rt)\rangle, \\ |N\rangle &\rightarrow |N - m\rangle. \end{aligned} \quad (18.85)$$

18.4.1 Continuous Measurement in a Two-Mode System. Phase Narrowing

We consider now the interaction of a three-level Λ system with a two-mode radiation field, in a high- Q cavity, as shown in Fig. 18.6. We assume that the Λ system is initially prepared in a superposition of the split lower states $|b\rangle$ and $|b'\rangle$:

$$|\psi_A(0)\rangle = \frac{1}{\sqrt{2}} [|b\rangle + \exp(-i\varphi) |b'\rangle]. \quad (18.86)$$

Also, we assume that the $|b'\rangle \rightarrow |a\rangle$ transition is resonant with the cavity field (field b) and that the $|b\rangle \rightarrow |a\rangle$ transition is driven by a coherent field $|\alpha\rangle$.

The relevant Hamiltonian in this system is

$$H_I = \hbar g(a_1 |a\rangle\langle b| + a_2 |a\rangle\langle b'| + \text{hc}), \quad (18.87)$$

Outside the high- Q cavity, there is an ionization detector that will tell us if the atom is in the excited state or in one of the lower states ($|b\rangle$ or $|b'\rangle$).

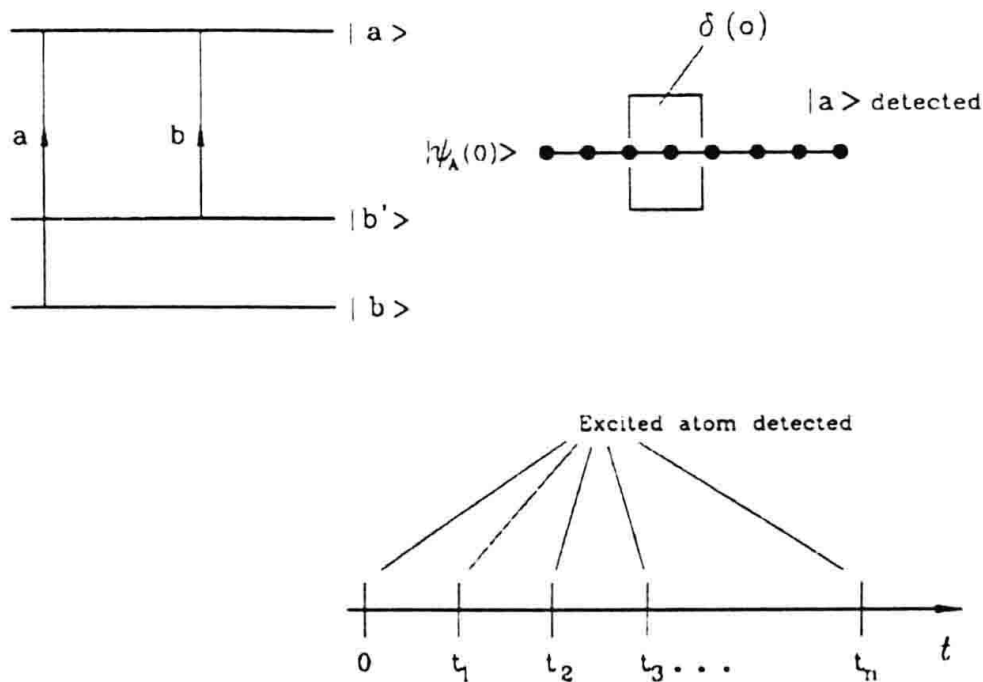


Fig. 18.6. Diagram of the proposed continuous measurement scheme

Following a similar argument to the previous section, it is simple to show that after the atom is detected in the excited state $|a\rangle$, the field changes as

$$\rho_f(\tau) = \frac{g^2\tau^2}{\hbar^2} A \rho_f(0) A^\dagger, \quad (18.88)$$

with

$$A = \frac{1}{\sqrt{2}} [a_1 + a_2 \exp(-i\varphi)]. \quad (18.89)$$

On the other hand, if the detected atom is not in the excited state, during the measurement period τ , then the field changes as

$$\rho_f(t) = \exp(-2RtA^\dagger A)\rho_f(0)\exp(-2RtA^\dagger A). \quad (18.90)$$

Once more, if we have n detections in a total measurement time t , then

$$\rho_f^{(n)}(t) = \frac{\exp(-2RtA^\dagger A)A^n\rho_f(0)A^{\dagger n}\exp(-2RtA^\dagger A)}{\text{Tr}(\exp(-2RtA^\dagger A)A^n\rho_f(0)A^{\dagger n}\exp(-2RtA^\dagger A))}. \quad (18.91)$$

We notice that in the ordering process we used the relation

$$\exp(xA^\dagger A)(A)\exp(-xA^\dagger A) = A\exp(-x), \quad (18.92)$$

which adds an extra factor which can be included in the normalization of $\rho_f^{(n)}(t)$.

As an example, we assume that initially, both fields are coherent:

$$\rho(0) = |\alpha, \beta\rangle\langle\alpha, \beta|, \quad (18.93)$$

so that

$$A |\alpha, \beta\rangle = \frac{1}{\sqrt{2}} [\alpha + \beta \exp(-i\varphi)] |\alpha, \beta\rangle, \quad (18.94)$$

and the density matrix, after n detections becomes

$$\rho_f^{(n)}(t) = \frac{\exp(-2RtA^\dagger A) |\alpha, \beta\rangle \langle \alpha, \beta| \exp(-2RtA^\dagger A)}{\text{Tr} \{ \exp(-2RtA^\dagger A) |\alpha, \beta\rangle \langle \alpha, \beta| \exp(-2RtA^\dagger A) \}}. \quad (18.95)$$

We notice that

$$\rho_f^{(n)}(t) = \rho_f^{(0)}(t), \quad (18.96)$$

since for a coherent state the A^n factor becomes a numerical one, which can be absorbed in the normalization constant. In this case, we may say only no counts count. [18.12]

Now, we want to simplify the expression given in (18.19). We define an operator B

$$B = \frac{1}{\sqrt{2}} (a_1 - a_2 \exp(-i\varphi)), \quad (18.97)$$

with

$$[A, B] = [A, B^\dagger] = 0, \quad (18.98)$$

$$[B, B^\dagger] = 1.$$

We look at the effect of the a_1 and a_2 operators on $\exp(-2RtA^\dagger A) |\alpha, \beta\rangle$:

$$\begin{aligned} & a_2 \exp(-2RtA^\dagger A) |\alpha, \beta\rangle \\ &= \left(\frac{A - B}{\sqrt{2}} \right) \exp(i\varphi) \exp(-2RtA^\dagger A) |\alpha, \beta\rangle \\ &= \exp(-2RtA^\dagger A) \exp(2RtA^\dagger A) \\ &\quad \times \left(\frac{A - B}{\sqrt{2}} \right) \exp(i\varphi) \exp(-2RtA^\dagger A) |\alpha, \beta\rangle \\ &= \exp(-2RtA^\dagger A) \\ &\quad \times \left[\frac{A \exp(-2Rt) - B}{\sqrt{2}} \right] \exp(i\varphi) |\alpha, \beta\rangle, \end{aligned} \quad (18.99)$$

where in the last step, we used the identity given by (18.92).

Now, from (18.99), we observe that $\exp(-2RtA^\dagger A) |\alpha, \beta\rangle$ is an eigenstate of a_2 with eigenvalue $\tilde{\beta}$:

$$\begin{aligned} & a_2 \exp(-2RtA^\dagger A) |\alpha, \beta\rangle = \tilde{\beta} \exp(-2RtA^\dagger A) |\alpha, \beta\rangle, \\ & \tilde{\beta} = \left[\left(\frac{\alpha \exp(i\varphi) + \beta}{2} \right) \exp(-2Rt) - \frac{1}{2} (\alpha \exp(i\varphi) - \beta) \right]. \end{aligned} \quad (18.100)$$

Similarly, one can show that

$$\begin{aligned} & a_1 \exp(-2RtA^\dagger A) |\alpha, \beta\rangle = \tilde{\alpha} \exp(-2RtA^\dagger A) |\alpha, \beta\rangle, \\ & \tilde{\alpha} = \left\{ \left[\frac{\alpha + \beta \exp(-i\varphi)}{2} \right] \exp(-2Rt) - \frac{1}{2} [\alpha - \beta \exp(-i\varphi)] \right\}. \end{aligned} \quad (18.101)$$

So

$$\rho_f^{(n)}(t) = |\tilde{\alpha}, \tilde{\beta}\rangle \langle \tilde{\alpha}, \tilde{\beta}|. \quad (18.102)$$

As we can see, as a result of the continuous measurement process, a coherent state, say $|\beta\rangle$, has become a new coherent state with a modified amplitude $|\tilde{\beta}\rangle$. Thus, there is a phase noise reduction or phase narrowing if $|\tilde{\beta}|^2 > |\beta|^2$.

On the other hand, if one of the fields is classical (a_1), that is $|\alpha| \gg |\beta|$, then approximately

$$|\tilde{\beta}| = \frac{|\alpha|}{2} [1 - \exp(-2Rt)]. \quad (18.103)$$

Writing the phase state

$$|\theta\rangle = \sum_{n=0}^{\infty} \exp(in\theta) |n\rangle, \quad (18.104)$$

one can write an expression for the phase distribution

$$P^n(\theta) = \langle \theta | \tilde{\beta} \rangle \langle \tilde{\beta} | \theta \rangle. \quad (18.105)$$

This distribution has been numerically evaluated for $\alpha = 10$, $\beta = 1$, and various times $Rt = 0$ (a), $Rt = 0.5$ (b), $Rt = 1$ (c), $Rt = 1.5$ (d). In Fig. 18.7, we observe a striking phase narrowing, which can have interesting applications in small-signal detection.

We can also look at the steady state, when one of the fields (say a_2) is in the vacuum, that is $\beta = 0$. Then, for $t \rightarrow \infty$,

$$|0\rangle_{a_2} \rightarrow |-\frac{\alpha}{2} \exp(i\varphi)\rangle. \quad (18.106)$$

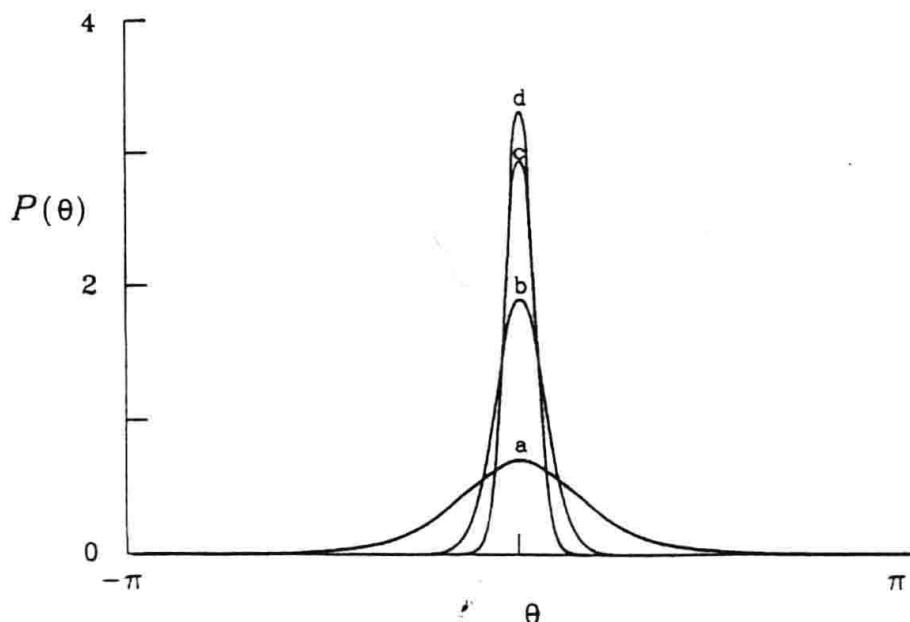


Fig. 18.7. Phase distribution for various times (a) $Rt = 0$; (b) $Rt = 0.5$; (c) $Rt = 1$; (d) $Rt = 1.5$. The parameters are $\alpha = 10$, $\beta = 1$ (after [18.12])

We may say that we have transferred the coherence from the a_1 to the a_2 mode.

Furthermore, this result is independent of the number of clicks (independent of n); that is, the coherence transfer occurs even if we never find an atom in the excited state [18.13].

Problems

- 18.1. Verify the solution for the atom-field state given by (18.57), (18.58).
- 18.2. Prove that the reordering procedure of the creation and annihilation operators gives the result (18.84).
- 18.3. Show that

$$\exp(xA)A\exp(-xA) = A\exp(-x)$$

(Hint: see Appendix A).

- 18.4. Show that the standard quantum limit for the energy of an oscillator is

$$\Delta E_{SQL} = \sqrt{\hbar\omega E},$$

where E is the oscillator's mean energy.

- 18.5. Suppose that instead of wanting to monitor the position of an oscillator, as we did in Sect. 18.1.3, we wanted to monitor its energy, and derive a condition for the thermal effects. Prove that for short time measurements

$$\Delta E = \sqrt{\hbar\omega E \frac{\tau}{\tau^*}},$$

and if $\Delta E \leq \hbar\omega$, then

$$\left(n + \frac{1}{2}\right) \frac{k_B T \tau}{\tau^*} \leq \hbar\omega.$$

In other words, to monitor the resonator's energy at level $\hbar\omega$ requires a temperature smaller by a factor $2(n + 1/2)$ than the temperature required to set the condition that the oscillator behaves quantum mechanically [18.1].

- 18.6. Prove that the standard quantum limit for the measurement of an impulsive force, using an oscillator, is

$$F = \frac{1}{\tau_F} \sqrt{\frac{\hbar\omega m}{2}},$$

where τ_F is the duration of the pulse.

19. Trapped Ions

In this chapter we study the Paul trap [19.1] for ions. We also analyse the various interactions between the ion's internal and centre-of-mass degrees of freedom with light waves.

19.1 Paul Trap

This is a trap that confines charged particles in a quadrupole potential, modulated by a radio-frequency field (Fig. 19.1). One generates a potential difference U between the two hyperboloid end caps and a ring of radius r_0 , located at z_0 from the upper end cap (the origin is at the centre of the ring). We assume a configuration described by the following potential:

$$\phi(x, y, z) = A(x^2 + y^2 - 2z^2), \quad (19.1)$$

and, from Fig. 19.1,

$$\phi(r_0, 0, 0) - \phi(0, 0, z_0) = U. \quad (19.2)$$

From the two equations above, we can calculate

$$A = \frac{U}{r_0^2 + 2z_0^2}, \quad (19.3)$$

or

$$\phi(x, y, z) = \frac{U}{r_0^2 + 2z_0^2}(x^2 + y^2 - 2z^2). \quad (19.4)$$

Unfortunately, one cannot confine a charged particle in three dimensions with a constant electric field, since this electric field would converge from all directions and a net flux would be present, violating the equation $\nabla \cdot \mathbf{E} = 0$. What we can do, instead, is to modulate the field with a harmonic term proportional to $\cos \Omega t$, thus getting

$$\phi(x, y, z, t) = \frac{V_0}{r_0^2 + 2z_0^2}(x^2 + y^2 - 2z^2) \cos \Omega t, \quad (19.5)$$

where we replaced U by $V_0 \cos \Omega t$. If we neglect the \mathbf{B} field and let

$$\mathbf{E} = -\nabla \phi = A' \cos \Omega t (-2x, -2y, 4z), \quad (19.6)$$

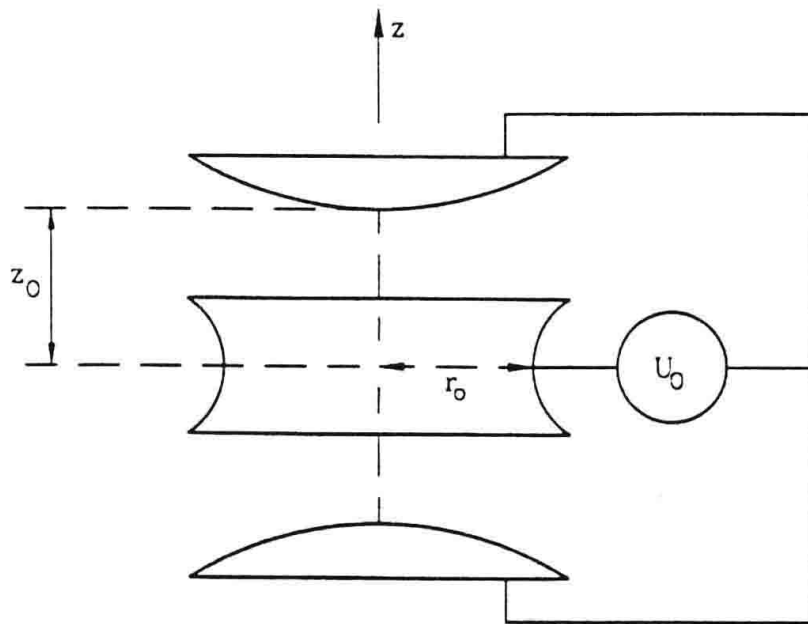


Fig. 19.1. Paul trap to confine charged particles

with

$$A' = \frac{V_0}{r_0^2 + 2z_0^2}, \quad (19.7)$$

then the classical equations of motion for a charged particle in this field are

$$\ddot{x} = -\frac{2A'q \cos \Omega t}{m} x, \quad (19.8)$$

$$\ddot{y} = -\frac{2A'q \cos \Omega t}{m} y, \quad (19.9)$$

$$\ddot{z} = \frac{4A'q \cos \Omega t}{m} z, \quad (19.10)$$

where m and q are the mass and charge of the particle.

The above equations can be written in the compact form:

$$\ddot{x}_i = C_i x_i \cos \Omega t, \quad (19.11)$$

with

$$C_1 = C_2 = -\frac{2A'q}{m} \quad (19.12)$$

$$C_3 = \frac{4A'q}{m},$$

and $x_1 = x, x_2 = y, x_3 = z$.

Now we decompose the motion into fast and slow time-varying parts:

$$x_i = \bar{x}_i + \xi_i, \quad (19.13)$$

where \bar{x}_i is the slow term, varying with a frequency ω_i , still to be determined, and ξ_i is the fast term changing with frequency $\Omega \gg \omega_i$. So, we can now write

$$\ddot{\bar{x}}_i + \ddot{\xi}_i = C_i \bar{x}_i \cos \Omega t + C_i \xi_i \cos \Omega t. \quad (19.14)$$

Now, we want to satisfy

$$|\bar{x}_i| \gg |\xi_i|, \quad (19.15)$$

$$|\ddot{\bar{x}}_i| \ll |\ddot{\xi}_i|,$$

which is possible due to the difference in the frequencies. Then we have

$$\ddot{\xi}_i = C_i \bar{x}_i \cos \Omega t. \quad (19.16)$$

For a time scale of the order of $1/\Omega$, \bar{x}_i is basically constant, and we have

$$\xi_i = -\frac{C_i}{\Omega^2} \bar{x}_i \cos \Omega t. \quad (19.17)$$

As we can see, the acceleration and position of ξ_i have opposite signs, so there is a restoring force, similar to a harmonic oscillator, and independent of the sign of C_i , so this is true for all three spatial directions.

If we substitute (19.16), (19.17) in (19.14), we get

$$\ddot{\bar{x}}_i + \frac{C_i^2}{\Omega^2} \cos^2 \Omega t \bar{x}_i = 0. \quad (19.18)$$

Now, if again, we average over a time scale $1/\Omega$, the \cos^2 averages to $1/2$, and we get a three-dimensional harmonic oscillator

$$\ddot{\bar{x}}_i + \frac{C_i^2}{2\Omega^2} \bar{x}_i = 0, \quad (19.19)$$

with the corresponding frequencies

$$\omega_x = \omega_y = \frac{|C_1|}{\sqrt{2}\Omega} = \frac{\sqrt{2}A'q}{m\Omega}, \quad (19.20)$$

$$\omega_z = \frac{|C_3|}{\sqrt{2}\Omega} = \frac{2\sqrt{2}A'q}{m\Omega}.$$

Thus, one can write the effective potential energy

$$V_{\text{eff}} = \sum_i \frac{mC_i^2}{4\Omega^2} \dot{x}_i^2. \quad (19.21)$$

As we can see, in the limit $\Omega \gg \omega_i$, the motion of the charged particle is well described by an effective potential corresponding to a three-dimensional harmonic oscillator, superposed with a small amplitude and rapidly varying ξ . This is shown pictorially in Fig. 19.2.

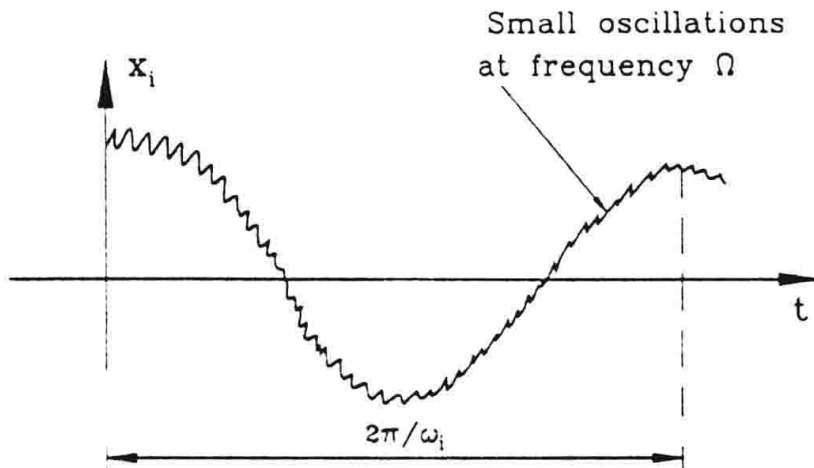


Fig. 19.2. Motion of a charged particle in a Paul trap

19.1.1 Stability Analysis

One can easily verify that if a static field is added to U , that is

$$U = U_0 + V_0 \cos \Omega t, \quad (19.22)$$

or

$$\phi(x, y, z, t) = \frac{U_0 + V_0 \cos \Omega t}{r_0^2 + 2z_0^2} (x^2 + y^2 - 2z^2), \quad (19.23)$$

then the effective potential energy becomes

$$\begin{aligned} V'_{\text{eff}} &= \frac{q^2 V_0^2}{m \Omega^2 (r_0^2 + 2z_0^2)^2} (\bar{x}^2 + \bar{y}^2 + 4 \bar{z}^2) \\ &\quad + \frac{q U_0}{r_0^2 + 2z_0^2} (\bar{x}^2 + \bar{y}^2 - 2 \bar{z}^2), \end{aligned} \quad (19.24)$$

which becomes isotropic if

$$U_0 = \frac{q V_0^2}{m \Omega^2 (r_0^2 + 2z_0^2)}. \quad (19.25)$$

One can also have essentially a one-dimensional harmonic oscillator, along the z -axis, if one chooses U_0 to be large and negative.

In general for any value of U_0 and V_0 , the equations of motion for x and z are

$$\begin{aligned} \ddot{x} &= \frac{-2q}{m(r_0^2 + 2z_0^2)} [U_0 + V_0 \cos \Omega t] x, \\ \ddot{z} &= \frac{4q}{m(r_0^2 + 2z_0^2)} [U_0 + V_0 \cos \Omega t] z. \end{aligned} \quad (19.26)$$

We now perform the change of variables

$$\Omega t = 2\tau, \quad (19.27)$$

$$\begin{aligned} x_1 &= x, \quad x_2 = y, \quad x_3 = z, \\ a_3 &\equiv \frac{-16qU_0}{m\Omega^2(r_0^2 + 2z_0^2)} = -2a_1 = -2a_2, \\ q_3 &\equiv \frac{8qV_0}{m\Omega^2(r_0^2 + 2z_0^2)} = -2q_1 = -2q_2. \end{aligned}$$

With the above definitions, the equations of motion now read

$$\frac{d^2x_i}{d^2\tau} + [a_i - 2q_i \cos 2\tau] x_i = 0, \quad i = 1, 2, 3. \quad (19.28)$$

Equation (19.28) is Mathieu's equation, with a periodic coefficient, with period π . Thus, if $x(\tau)$ is a solution of Mathieu's equation, then $x(\pi + \tau)$ is also a solution.

Now, we explore the possibility of finding solutions of Mathieu's equation, where

$$x(\pi + \tau) = \mu x(\tau), \quad (19.29)$$

μ being a complex number to be determined later (Floquet's Theorem).

Now, let $h(\tau)$ and $g(\tau)$ be two independent solutions of Mathieu's equation. Since this equation is linear, then

$$x(t) = Ag(\tau) + Bh(\tau), \quad (19.30)$$

is also a solution. Furthermore

$$\begin{aligned} g(\tau + \pi) &= \alpha_1 g(\tau) + \alpha_2 h(\tau), \\ h(\tau + \pi) &= \beta_1 g(\tau) + \beta_2 h(\tau). \end{aligned} \quad (19.31)$$

Now, substituting (19.30), (19.31) in (19.29), we get

$$\begin{aligned} x(\pi + \tau) &= Ag(\tau + \pi) + Bh(\tau + \pi) \\ &= A[\alpha_1 g(\tau) + \alpha_2 h(\tau)] + B[\beta_1 g(\tau) + \beta_2 h(\tau)] \\ &= (A\alpha_1 + B\beta_1)g(\tau) + (A\alpha_2 + B\beta_2)h(\tau) \\ &= \mu Ag + \mu Bh, \end{aligned} \quad (19.32)$$

or

$$\begin{aligned} (\alpha_1 - \mu)A + \beta_1 B &= 0, \\ \alpha_2 A + (\beta_2 - \mu)B &= 0. \end{aligned} \quad (19.33)$$

For non-trivial solutions, the determinant of the coefficients must vanish, giving us two possible values for μ :

$$\begin{aligned} x_1(\pi + \tau) &= \mu_1 x_1(\tau), \\ x_2(\pi + \tau) &= \mu_2 x_2(\tau). \end{aligned} \quad (19.34)$$

If we define the two quantities

$$\begin{aligned}\exp \sigma_i \pi &\equiv \mu_i \\ F_i(\tau) &\equiv x_i(\tau) \exp(-\sigma_i \tau),\end{aligned}\tag{19.35}$$

then it is simple to show that $F_i(\tau)$ is π -periodic:

$$\begin{aligned}F_i(\tau + \pi) &= x_i(\tau + \pi) \exp(-\sigma_i \tau) \exp(-\sigma_i \pi) \\ &= x_i(\tau) \exp(\sigma_i \pi) \exp(-\sigma_i \tau) \exp(-\sigma_i \pi) \\ &= x_i(\tau) \exp(-\sigma_i \tau) \\ &= F_i(\tau).\end{aligned}\tag{19.36}$$

From the last line of (19.36), we write

$$x_i(\tau) = (\mu_i)^{\tau/\pi} F_i(\tau),\tag{19.37}$$

with $F_i(\tau)$ being a periodic function, with period π .

Some properties of μ_1 and μ_2

If x_1 and x_2 are solutions of the Mathieu equation, one can easily prove that

$$\ddot{x}_1 x_2 - \ddot{x}_2 x_1 = 0,$$

or

$$\frac{d(x_1 \dot{x}_2 - \dot{x}_1 x_2)}{d\tau} = 0,\tag{19.38}$$

leading to

$$\dot{x}_1 x_2 - \dot{x}_2 x_1 = c.\tag{19.39}$$

But, since

$$\begin{aligned}x_1(\pi + \tau) &= \mu_1 x_1(\tau); \\ x_2(\pi + \tau) &= \mu_2 x_2(\tau),\end{aligned}$$

then

$$\begin{aligned}\dot{x}_1(\pi + \tau) x_2(\pi + \tau) - \dot{x}_2(\pi + \tau) x_1(\pi + \tau) &= c \\ &= \mu_1 \mu_2 (\dot{x}_1 x_2 - \dot{x}_2 x_1) \\ &= (\dot{x}_1 x_2 - \dot{x}_2 x_1),\end{aligned}$$

thus

$$\mu_1 \mu_2 = 1.\tag{19.40}$$

We can clearly distinguish two cases:

(a) μ_1 and μ_2 are reals. Then

$$\mu_1 = (\mu_2)^{-1} = \exp \sigma_1 \pi, \quad (19.41)$$

and since σ is real, we get a stable and an unstable solution

$$\begin{aligned} x_1(\tau) &= \exp(\sigma_1 \tau) F_1(\tau), \\ x_2(\tau) &= \exp(-\sigma_1 \tau) F_2(\tau). \end{aligned}$$

So, in this case, one always has an unstable solution.

(b) $\mu_1 = \mu_2^*, |\mu_{1,2}|^2 = 1$. So, if $\mu_1 = \exp(i\beta\pi)$, $\mu_2 = \exp(-i\beta\pi)$, then

$$\begin{aligned} x_1(\tau) &= \exp(i\beta\tau) F_1(\tau), \\ x_2(\tau) &= \exp(-i\beta\tau) F_2(\tau), \end{aligned} \quad (19.42)$$

which are both stable solutions.

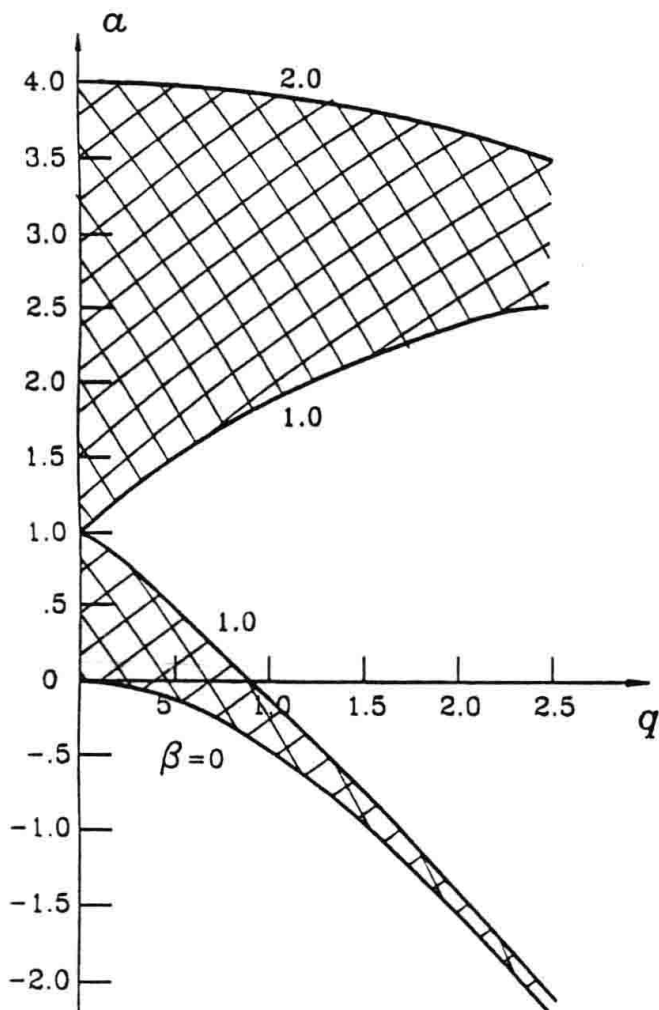


Fig. 19.3. Parameter space of Mathieu's equation separating the stable region (with lines) from the unstable one

Boundary Between Stable and Unstable Regions

$\mu = \exp(i\beta\pi)$ becomes real for

$$\beta = 0 \rightarrow \mu_1 = \mu_2 = 1,$$

$$\beta = 1 \rightarrow \mu_1 = \mu_2 = -1,$$

in which case the solutions are periodic functions of τ , with period π ($\beta = 0$) or 2π ($\beta = 1$). One can plot [19.2] the values of a and q that admit periodic solutions, with period 2π . This curve separates the stable region from the unstable region in parameter space (Fig. 19.3).

19.2 The Trapped Ion in the Raman Scheme

Recently, single quantum systems have been investigated, based on advances in low temperature [19.3] and confinement techniques. For example, in the case of single trapped ions, much work has been devoted to the coupling of a few internal electronic levels with the centre-of-mass motion of the ion. These couplings, in the case of ion traps, can be achieved by direct transition [19.4], [19.5], or non-resonant Raman transition. In the latter case, this coupling is via two optical fields [19.6], [19.7], [19.8].

Several proposals have been presented for experiments leading to observation of non-classical states such as the generation of Fock and squeezed vibrational states, and also vibrational Schrödinger cats [19.9]. In most cases, these proposals use an effective interaction between the internal and external degrees of freedom of the ion. Single trapped ions have also led to the observation of quantum jumps [19.5], antibunching in resonance fluorescence, and quantum Zeno effects [19.10].

19.2.1 The Model and the Effective Hamiltonian

The basic level scheme is shown in Fig. 19.4. The electronic levels $|a\rangle$ and $|b\rangle$ are assumed to be metastable, separated by $\hbar\omega_0$ and coupled by stimulated Raman transition via two classical optical fields

$$E_i = E_{0i} [\exp i(\mathbf{k}_i \cdot \mathbf{x} - \omega_i t + \phi_i) + cc], \quad (19.43)$$

where \mathbf{x} is the position operator associated with the centre-of-mass motion, and $\omega_1 - \omega_2 = (k_1 - k_2)c = \omega_0 + \delta$, δ being of the order of ω , the vibrational frequency of the ion. Both fields 1 and 2 are detuned from the $b-c$ and $a-c$ transition by Δ and $\Delta - \delta$ respectively. A fourth level $|d\rangle$ is introduced for detecting electronic states and precooling, as will be shown later.

We assumed that the ion is trapped in a harmonic potential. The center-of-mass position operator can be written as

$$\mathbf{x}_i = \sqrt{\frac{\hbar}{2m\omega_i}}(a_i + a_i^\dagger), \quad i = 1, 2, 3, \quad (19.44)$$

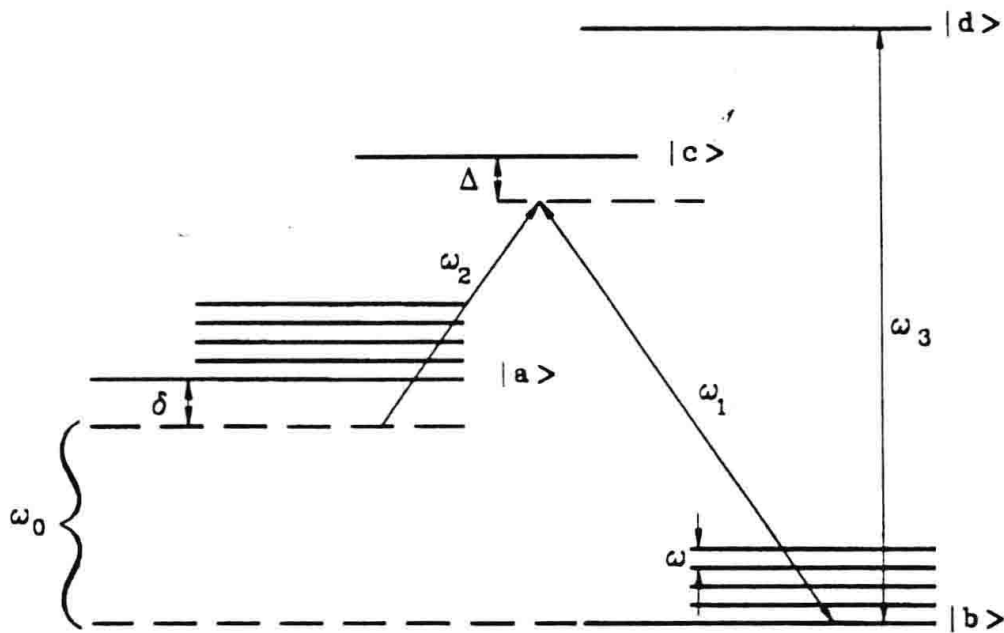


Fig. 19.4. Energy level diagram. A Raman stimulated transition is induced between the levels $|a\rangle$ and $|b\rangle$ by laser beams 1 and 2. Detection of the electronic state is provided by the scattered photons resulting from the cycling transition $|b\rangle$ and $|d\rangle$, produced by a resonant pulse 3

where ω_i is the oscillatory frequency along the i direction. The Hamiltonian that describes the system between detections (so the level $|d\rangle$ does not participate in the dynamics) can be written as

$$H = H_0 + H_1, \quad (19.45)$$

with

$$H_0 = \sum_{i=x,y,z} \hbar\omega_i a_i^\dagger a_i + \hbar\omega_a |a\rangle\langle a| + \hbar\omega_b |b\rangle\langle b| + \hbar\omega_c |c\rangle\langle c|, \quad (19.46)$$

and

$$\begin{aligned} H_1 = & \hbar g_1 \exp[-i(\mathbf{k}_1 \cdot \mathbf{x} - \omega_1 t + \phi_1)] |b\rangle\langle c| \\ & + \hbar g_2 \exp[-i(\mathbf{k}_2 \cdot \mathbf{x} - \omega_2 t + \phi_2)] |a\rangle\langle c| + \text{hc}. \end{aligned} \quad (19.47)$$

For shorthand notational purposes, if we set

$$g_1 \exp[i\mathbf{k}_1 \cdot \mathbf{x} - \omega_1 t + \phi_1] \rightarrow g_1,$$

$$g_2 \exp[i\mathbf{k}_2 \cdot \mathbf{x} - \omega_2 t + \phi_2] \rightarrow g_2,$$

and

$$\omega_{cb} - \omega_1 = \Delta, \quad (19.48)$$

$$\omega_{ca} - \omega_2 = \Delta - \delta, \quad (19.49)$$

then the Hamiltonian H_0 can be written as

$$H_0 = \sum_{i=x,y,z} \hbar\omega_i a_i^\dagger a_i + \hbar(\omega_b + \Delta) |b\rangle\langle b| + \hbar[\omega_a + (\Delta - \delta)] |a\rangle\langle a| + \hbar\omega_c |c\rangle\langle c| - \hbar\Delta |b\rangle\langle b| - \hbar(\Delta - \delta) |a\rangle\langle a|, \quad (19.50)$$

so that the time-dependent factor is eliminated in the interaction picture, since

$$\omega_c - (\omega_b + \Delta) = \omega_1, \quad (19.51)$$

$$\omega_c - (\omega_a + \Delta - \delta) = \omega_2. \quad (19.52)$$

The Hamiltonian in the interaction picture now reads

$$H' = -\hbar\Delta |b\rangle\langle b| - \hbar(\Delta - \delta) |a\rangle\langle a| + \hbar(g_1 |c\rangle\langle b| + g_1^* |b\rangle\langle c|) + \hbar(g_2 |c\rangle\langle a| + g_2^* |a\rangle\langle c|). \quad (19.53)$$

Now we proceed to calculate the effective Hamiltonian for the a and b levels only, by adiabatic elimination of the c level [19.11]. Starting from the Liouville equation

$$\dot{\rho} = -\frac{i}{\hbar} [H, \rho], \quad (19.54)$$

we can write

$$\begin{aligned} \dot{\rho} = & i\Delta [|b\rangle\langle b|, \rho] + i(\Delta - \delta) [|a\rangle\langle a|, \rho] \\ & - i[g_1 |c\rangle\langle b| + g_1^* |b\rangle\langle c|, \rho] \\ & - i[g_2 |c\rangle\langle a| + g_2^* |a\rangle\langle c|, \rho]. \end{aligned} \quad (19.55)$$

Writing the Liouville equation in terms of its matrix elements, we get

$$\dot{\rho}_{cc} = -ig_1\rho_{bc} + ig_1^*\rho_{cb} - ig_2\rho_{ac} + ig_2^*\rho_{ca}, \quad (19.56)$$

$$\dot{\rho}_{bb} = ig_1\rho_{bc} - ig_1^*\rho_{cb}, \quad (19.57)$$

$$\dot{\rho}_{aa} = ig_2\rho_{ac} - ig_2^*\rho_{ca}, \quad (19.58)$$

$$\dot{\rho}_{ca} = -i(\Delta - \delta)\rho_{ca} - ig_2\rho_{aa} + ig_2\rho_{cc} - ig_1\rho_{ba}, \quad (19.59)$$

$$\dot{\rho}_{cb} = -i\Delta\rho_{cb} - ig_1\rho_{bb} + ig_1\rho_{cc} - ig_2\rho_{ab}, \quad (19.60)$$

$$\dot{\rho}_{ab} = i\Delta\rho_{ab} + i(\Delta - \delta)\rho_{ab} + ig_1\rho_{ac} - ig_2^*\rho_{cb}. \quad (19.61)$$

Now, we take $\Delta \gg \delta$ and set ρ_{ca}, ρ_{cb} to the steady state:

$$\rho_{cb} = \frac{1}{i\Delta} [ig_1(\rho_{cc} - \rho_{bb}) - ig_2\rho_{ab}], \quad (19.62)$$

$$\rho_{ca} = \frac{1}{i\Delta} [ig_2(\rho_{cc} - \rho_{aa}) - ig_1\rho_{ba}], \quad (19.63)$$

and substituting (19.62), (19.63) in (19.56) we get

$$\dot{\rho}_{cc} = 0,$$

so, if $\rho_{cc}(0) = 0$, then $\rho_{cc}(t) = 0$.

The rest of the equations become

$$\dot{\rho}_{bb} = \frac{ig_1^*g_2}{\Delta}\rho_{ab} - \frac{ig_2^*g_1}{\Delta}\rho_{ba}, \quad (19.64)$$

$$\dot{\rho}_{aa} = \frac{ig_2^*g_1}{\Delta}\rho_{ba} - \frac{ig_1^*g_2}{\Delta}\rho_{ab}, \quad (19.65)$$

$$\dot{\rho}_{ab} = -i(\delta')\rho_{ab} - \frac{ig_2^*g_1}{\Delta}(\rho_{aa} - \rho_{bb}), \quad (19.66)$$

with

$$\delta' = \left(\delta + \frac{|g_1|^2}{\Delta} - \frac{|g_2|^2}{\Delta} \right). \quad (19.67)$$

We notice that δ' differs from δ by the Stark shifts $|g_1|^2/\Delta$ and $|g_2|^2/\Delta$.

Now, if we write the effective Hamiltonian in the following form

$$H = \hbar\alpha \frac{|a\rangle\langle a| - |b\rangle\langle b|}{2} + \hbar\beta |a\rangle\langle b| + \hbar\beta^* |b\rangle\langle a|, \quad (19.68)$$

then the Liouville equation gives us

$$\dot{\rho}_{bb} = -i\beta^*\rho_{ab} + i\beta\rho_{ba}, \quad (19.69)$$

$$\dot{\rho}_{aa} = -i\beta\rho_{ba} + i\beta^*\rho_{ab}, \quad (19.70)$$

$$\dot{\rho}_{ab} = -i\alpha\rho_{ab} + i\beta(\rho_{aa} - \rho_{bb}). \quad (19.71)$$

By direct comparison of the above equations with (19.64), (19.65) and (19.66) we get

$$\alpha = \delta', \quad (19.72)$$

$$\beta = -\frac{g_2^*g_1}{\Delta}.$$

The final effective Hamiltonian is

$$H = \sum_{i=x,y,z} \hbar\omega_i a_i^\dagger a_i + \hbar\delta'\sigma_3 - \frac{\hbar\Omega_0}{2} [|a\rangle\langle b| \exp[i(k_1 - k_2)x + i\phi] + \text{hc}], \quad (19.73)$$

with

$$\Omega_0 \equiv \left(\frac{2|g_1g_2|}{\Delta} \right), \quad \sigma_3 \equiv \left(\frac{|a\rangle\langle a| - |b\rangle\langle b|}{2} \right).$$

In terms of the phonon raising and lowering operators, we can also write this as

$$H = \sum_{i=x,y,z} \hbar\omega_i a_i^\dagger a_i + \hbar\delta' \sigma_3 - \frac{\hbar\Omega_0}{2} \left[|a\rangle\langle b| \exp \left(i \sum_i \eta_i (a_i + a_i^\dagger) + i\phi \right) + \text{hc} \right], \quad (19.74)$$

where η_i is the Lamb-Dicke parameter, defined as

$$\eta_i \equiv \delta k_i \sqrt{\frac{\hbar}{2m\omega_i}}, \quad (19.75)$$

$$\delta k_i \equiv (k_1 - k_2). \quad (19.76)$$

We notice that according to the definition of η_i , η_i^2 is the ratio between the recoil energy and the quantum vibrational energy, both taken in the i th direction.

In the rest of this chapter, we are going to assume, for the sake of simplicity, that only vibrations in a given i -direction are excited, which could be the case if ω_i is much larger than the other frequencies or if $\delta\mathbf{k}$ is in the i -direction. Then the Hamiltonian is

$$H = \hbar\omega a^\dagger a + \hbar\delta' \sigma_3 - \frac{\hbar\Omega_0}{2} [|a\rangle\langle b| \exp [i\eta(a + a^\dagger) + i\phi] + \text{hc}]. \quad (19.77)$$

Expanding the exponential and using the BCH identity (see Appendix A), we get

$$\exp [i\eta(a + a^\dagger)] = \exp \left(-\frac{\eta^2}{2} \right) \sum_{l,l'} \frac{(i\eta)^{l+l'}}{l!l'} a^{\dagger l} a^{l'}, \quad (19.78)$$

and

$$H = \hbar\omega a^\dagger a + \hbar\delta' \sigma_3 - \frac{\hbar\Omega_0}{2} \left[|a\rangle\langle b| \exp \left(-\frac{\eta^2}{2} \right) \sum_{l,l'} \frac{(i\eta)^{l+l'}}{l!l'} a^{\dagger l} a^{l'} \exp(i\phi) + \text{hc} \right]. \quad (19.79)$$

In the interaction picture, the Hamiltonian becomes

$$H_I = -\frac{\hbar\Omega_0}{2} \left[|a\rangle\langle b| \exp \left(-\frac{\eta^2}{2} + i\phi \right) \times \sum_{l,l'} \frac{(i\eta)^{l+l'}}{l!l'} a^{\dagger l} a^{l'} \exp(it) [(l - l')\omega + \delta'] + \text{hc} \right]. \quad (19.80)$$

Let $k = l' - l$, so that

$$\Delta_k \equiv \delta' - k\omega, \quad (19.81)$$

and define

$$\Omega_k \equiv \frac{\Omega_0}{2} \exp\left(-\frac{\eta^2}{2} + i\phi\right) (i\eta)^k \sum_l \frac{(i\eta)^{2l}}{l!(l+k)!} a^{\dagger l} a^l. \quad (19.82)$$

Considering now a near-resonant condition, where for a particular value of k , $\Delta_k \ll k\omega$, and neglecting the fast rotating terms, one can write approximately

$$H_I = -\hbar \begin{pmatrix} 0 & \Omega_k \exp(i\Delta_k t) a^k \\ a^{\dagger k} \Omega_k^\dagger \exp(-i\Delta_k t) & 0 \end{pmatrix}. \quad (19.83)$$

19.2.2 The Lamb–Dicke Expansion and Raman Cooling

In the Lamb–Dicke limit $\eta\sqrt{n} \ll 1$, we mention several interesting cases (in this section we will neglect the Stark shifts, thus δ' reduces to δ). We concentrate on the time-independent case, that is for $\Delta_k = 0$, or $\delta' = k\omega$.

Carrier Transition. This case corresponds to $\delta = 0$, $k = 0$, and the lowest-order Hamiltonian term in η is

$$H_I = -\frac{\hbar\Omega_0}{2} (\exp(i\phi)\sigma_+ + \exp(-i\phi)\sigma_-). \quad (19.84)$$

This Hamiltonian produces Rabi oscillations between vibrational sublevels of the same degree of excitation as shown in Fig. 19.5.

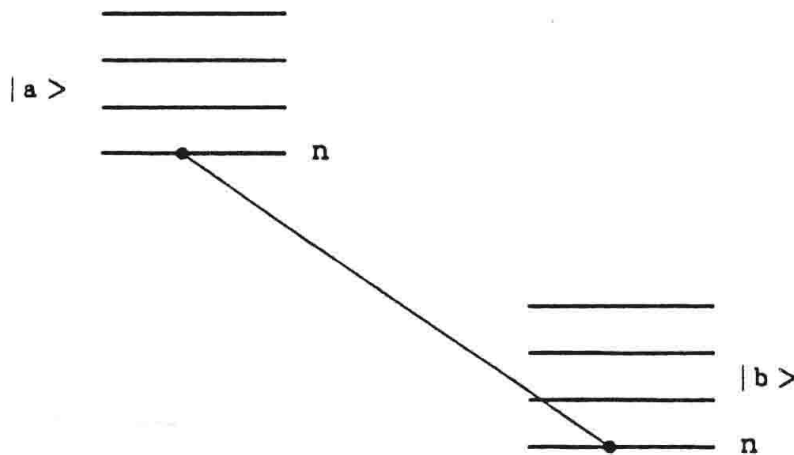


Fig. 19.5. Rabi oscillation between two vibrational sublevels of the same degree of excitation. This case corresponds to $k = 0 = \delta$

First Red Sideband. This case corresponds to

$$\delta = \omega, \quad k = 1 \quad (19.85)$$

and we get, to lowest order in η ,

$$H_I = -i\eta\hbar \frac{\Omega_0}{2} (a\sigma_+ \exp i\phi - a^\dagger \sigma_- \exp -i\phi), \quad (19.86)$$

which is the Jaynes–Cummings Hamiltonian. The vibrational transitions described by this Hamiltonian are shown in Fig. 19.6.

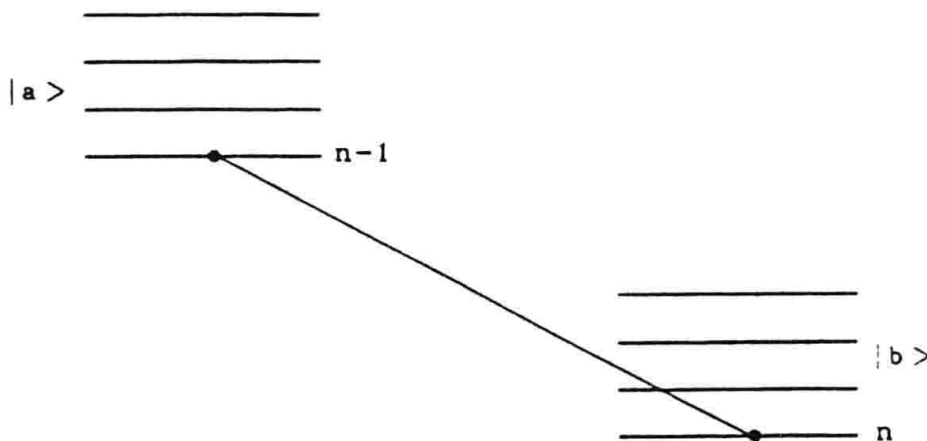


Fig. 19.6. First sideband vibrational transition for the case $\delta = \omega$, $k = 1$, which corresponds to Jaynes-Cummings dynamics. The upwards transition ($b \rightarrow a$) produces a vibrational cooling from n to $n - 1$

Similarly, there is a first blue sideband, corresponding to an anti-Jaynes-Cummings model and higher-order sidebands corresponding to non-linear optical models. For example, $\delta = 2\omega$ or $k = 2$ corresponds to the two-photon Jaynes-Cummings model

$$H_1 = \frac{\eta^2 \hbar}{2} (a^2 \sigma_+ \exp(i\phi) + a^{\dagger 2} \sigma \exp(-i\phi)), \quad (19.87)$$

and so on.

Recent experimental results [19.8] have reported that the first red sideband has been used for cooling purposes. However, if they just tuned the $\delta = \omega$ transition, one can go from n to $n - 1$, but the reverse process is also possible and on the average, no cooling occurred [19.12]. In order to achieve resolved sideband stimulated Raman cooling, they needed the following sequence. First a π red sideband pulse, producing the $|b\rangle|n\rangle \rightarrow |a\rangle|n-1\rangle$ transition. Second, an additional repumper pulse populates the $|c\rangle$ level, followed by spontaneous emission, to the same $|n-1\rangle$ level, but now associated with the $|b\rangle$ electronic state. This is shown in Fig. 19.7. In order to have a quantitative understanding of the above effects, we require the study of the dynamics of our system [19.13], [19.11].

19.2.3 The Dynamical Evolution

An exact solution for the time evolution operator can be derived in some simple cases, like the Hamiltonian given by (19.83). We show here the detailed calculation to illustrate the method.

We have to solve the equation

$$i\hbar \frac{dU}{dt} = HU, \quad (19.88)$$

or

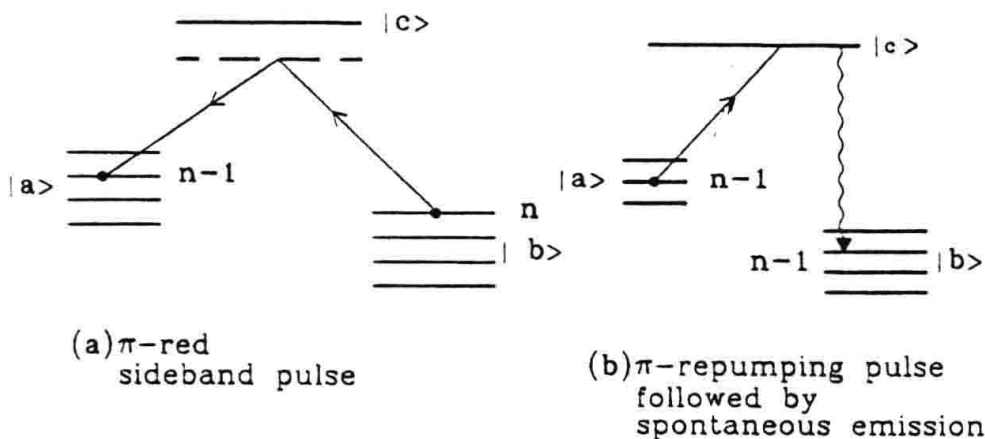


Fig. 19.7. Resolved side band stimulated Raman Stimulated Raman cooling. First a red side band π pulse produces the $|a\rangle|n\rangle \rightarrow |b\rangle|n-1\rangle$ transition. A second π repumping pulse followed by spontaneous emission produces the $|b\rangle|n-1\rangle \rightarrow |a\rangle|n-1\rangle$ transition having a net cooling effect

$$i \begin{pmatrix} \dot{U}_{aa} & \dot{U}_{ab} \\ \dot{U}_{ba} & \dot{U}_{bb} \end{pmatrix} = \begin{pmatrix} 0 & -\Omega_k \exp(i\Delta_k t) a^k \\ -a^{tk} \Omega_k^\dagger \exp(-i\Delta_k t) & 0 \end{pmatrix} \begin{pmatrix} U_{aa} & U_{ab} \\ U_{ba} & U_{bb} \end{pmatrix}, \quad (19.89)$$

giving us the set of equations

$$i \dot{U}_{aa} = -\Omega_k \exp(i\Delta_k t) a^k U_{ba}, \quad (19.90)$$

$$i \dot{U}_{ba} = -a^{\dagger k} \Omega_k^\dagger \exp(-i\Delta_k t) U_{aa}, \quad (19.91)$$

$$i \dot{U}_{ab} = -\Omega_k \exp(i\Delta_k t) a^k U_{bb}, \quad (19.92)$$

$$i \dot{U}_{bb} = -a^{\dagger k} \Omega_k^\dagger \exp(-i\Delta_k t) U_{ab}. \quad (19.93)$$

We can easily eliminate the time-dependent factors with the transformation

$$\overline{U_{ba}} = \exp i \frac{\Delta_k t}{2} U_{ba}, \quad (19.94)$$

$$\overline{U_{aa}} = \exp -i \frac{\Delta_k t}{\hbar} U_{aa}, \quad (19.95)$$

$$\overline{U_{ab}} = \exp -i \frac{\Delta_k t}{\hbar} U_{ab}, \quad (19.96)$$

$$\overline{U_{bb}} = \exp i \frac{\Delta_k t}{2} U_{bb}. \quad (19.97)$$

It is simple to verify that the differential equations for the various matrix elements are

$$\overleftrightarrow{U_{bb}} + \bar{\mu}^2 \overleftarrow{U_{bb}} \equiv 0, \quad (19.98)$$

$$\overline{\overline{U_{ba}}} + \bar{\mu}^2 \overline{U_{ba}} = 0, \quad (19.99)$$

$$\overline{\overline{U_{aa}}} + \mu^2 \overline{U_{aa}} = 0, \quad (19.100)$$

$$\overline{\overline{U_{ab}}} + \mu^2 \overline{U_{ab}} = 0, \quad (19.101)$$

where

$$\mu^2 = \frac{\Delta_k^2}{4} + \Omega_k a^k a^{\dagger k} \Omega_k^\dagger, \quad (19.102)$$

$$\bar{\mu}^2 = \frac{\Delta_k^2}{4} + a^{\dagger k} \Omega_k^\dagger \Omega_k a^k. \quad (19.103)$$

The reader may verify that the solutions of the above equations, for the initial conditions $U_{bb}(0) = U_{aa}(0) = 1$ and $U_{ab}(0) = U_{ba}(0) = 0$ are [19.14]:

$$U_{aa}(t) = \exp\left(i\frac{\Delta_k t}{2}\right) \left(\cos \mu t - i\frac{\Delta_k}{2\mu} \sin \mu t \right), \quad (19.104)$$

$$U_{ab}(t) = \exp\left(i\frac{\Delta_k t}{2}\right) i\frac{\sin \mu t}{\mu} \Omega_k a^k, \quad (19.105)$$

$$U_{ba}(t) = \exp\left(-i\frac{\Delta_k t}{2}\right) i\frac{\sin \bar{\mu} t}{\bar{\mu}} a^{\dagger k} \Omega_k^\dagger, \quad (19.106)$$

$$U_{bb}(t) = \exp\left(-i\frac{\Delta_k t}{2}\right) \left(\cos \bar{\mu} t + i\frac{\Delta_k}{2\bar{\mu}} \sin \bar{\mu} t \right). \quad (19.107)$$

For the resonant case ($\Delta_k = 0$) we can expand these results in η (the Lamb–Dicke regime), getting

$$\Omega_k \approx \frac{\Omega_0}{2} \exp\left[i\left(\phi + \frac{k\pi}{2}\right)\right] \eta^k \left[1 - \eta^2 \left(\frac{a^\dagger a}{(k+1)!} + \frac{1}{2} + \dots \right) \right], \quad (19.108)$$

$$\mu^2 \approx \frac{\Omega_0^2}{4} \eta^{2k} a^k a^{k\dagger} \left[1 - 2\eta^2 \left(\frac{a^\dagger a}{(k+1)!} + \frac{1}{2} \right) + \dots \right], \quad (19.109)$$

$$\bar{\mu}^2 \approx \frac{\Omega_0^2}{4} \eta^{2k} a^{k\dagger} a^k \left[1 - 2\eta^2 \left(\frac{a^\dagger a}{(k+1)!} + \frac{1}{2} \right) + \dots \right], \quad (19.110)$$

$$U_{aa}(t) = \cos \mu t, \quad U_{bb}(t) = \cos \bar{\mu} t, \quad (19.111)$$

$$U_{ab}(t) = i\frac{\sin \mu t}{\mu} \Omega_k a^k, \quad U_{ba}(t) = i\frac{\sin \bar{\mu} t}{\bar{\mu}} a^{\dagger k} \Omega_k^\dagger.$$

For the Jaynes–Cummings model, applied for cooling, $k = 1$, and initially, with the ion in the state $|n\rangle |b\rangle$, after some time t

$$|\psi(t)\rangle = \begin{pmatrix} \cos \mu t & i \frac{\sin \mu t}{\mu} \Omega_1 a \\ i \frac{\sin \bar{\mu} t}{\bar{\mu}} a^\dagger \Omega_1^\dagger & \cos \bar{\mu} t \end{pmatrix} \begin{pmatrix} 0 \\ 1 \end{pmatrix} |n\rangle, \quad (19.112)$$

$$|\psi(t)\rangle = \left[\left(i \frac{\sin \mu t}{\mu} \Omega_1 a \right) |b\rangle + \cos \bar{\mu} t |a\rangle \right] |n\rangle. \quad (19.113)$$

In lowest order, $\bar{\mu} \approx \mu \approx \Omega_0/2\eta\sqrt{n}$. A π pulse corresponds to $\Omega_0\eta\sqrt{n}t = \pi$, and the net effect of such a pulse is to change the state

$$|n\rangle |b\rangle \rightarrow i \frac{\Omega_1 \sqrt{n}}{\mu} |n-1\rangle |a\rangle, \quad (19.114)$$

which corresponds to the experimental situation described in the previous section.

19.2.4 QND Measurements of Vibrational States

We assume [19.15], [19.16], in this case, that $\delta = k = 0$, and if

$$|\psi(0)\rangle = \sum_n C_n |n\rangle |b\rangle, \quad (19.115)$$

then at a later time t

$$|\psi(t)\rangle_b = \sum_n C_n \left[\left(i \exp(i\phi) \sin \frac{\Omega_n}{2} t \right) |a\rangle + \cos \frac{\Omega_n}{2} t |b\rangle \right], \quad (19.116)$$

where $\Omega_n = 2\mu_{nn} = 2\bar{\mu}_{nn} = \Omega_0 [1 - \eta^2(n + 1/2) + \dots]$ is the usual Rabi frequency. In the case when the ion is initially in the $|a\rangle$ electronic state, at time t it will be in

$$|\psi(t)\rangle_a = \sum_n C_n \left[\left(i \exp(-i\phi) \sin \frac{\Omega_n}{2} t \right) |b\rangle + \cos \frac{\Omega_n}{2} t |a\rangle \right]. \quad (19.117)$$

The linear dependence of Ω_n with n is the basis for the QND measurement of the vibrational population for the trapped ion. We proceed as follows.

The ion is submitted to a Raman pulse of duration τ , resonant with the electronic transition, so that the vibrational occupation number is not changed. This time τ is assumed to be much smaller than the lifetimes of the electronic states or the vibrational states. Right after the pulse, the electronic state of the ion is detected, by resonant excitation of the $|b\rangle \rightarrow |d\rangle$ transition with circularly polarized light. This is the way the experimental detection was reported in reference [19.9].

We assume that the area of this pulse is sufficiently large, so that at this stage, a large number of photons are scattered by the ion, thus generating a detection efficiency close to one. This determines the electronic state of the ion. A fluorescent signal implies that the ion is in the $|b\rangle$ state, and therefore, as a consequence of the measurement, the ion is projected into this state, while the absence of fluorescence projects the ion into the $|a\rangle$ state.

We notice that in the Lamb-Dicke regime, each photon scattering leads to a negligible recoil ($\eta \propto \Delta k$). However, for many photons, appreciable heating is possible, spoiling our QND procedure, based on the fact that approximately no energy exchange takes place during the measurement. This puts an upper limit on the photon number scattered by the ion.

A rough estimate of this limitation goes as follows. Let ΔE be the recoil energy of a single scattering process. Then we must assume, for a near QND measurement, that

$$N\Delta E \ll \hbar\omega, \quad (19.118)$$

N being the number of scattered photons, and since $\eta^2 = \Delta E/\hbar\omega$, the condition becomes:

$$N \ll \eta^{-2}. \quad (19.119)$$

For a typical experimental value, $\eta \sim 0.1$ so $N \ll 100$.

On the other hand, for a saturating cycling process, $N \approx \Gamma T/2$, where Γ is the width of the $|d\rangle$ level and T the duration of the pulse, so one must have $T \ll 200/\Gamma$ and for $\Gamma/2\pi = 20$ MHz, we get

$$T < 2\mu\text{s}. \quad (19.120)$$

If the above conditions are satisfied, then very little heating takes place, and so it can be neglected, and if $|\psi_\varepsilon^{(1)}\rangle$ is the state of the ion after the first measurement, where $\varepsilon = 1$ corresponds to the case in which the detected electronic state coincides with the initial one, and $\varepsilon = 0$ otherwise, then

$$|\psi_\varepsilon^{(1)}\rangle = \frac{\sum_n C_n \sin(\Omega_n \tau/2 + \varepsilon\pi/2)}{\sqrt{\sum_{n=0}^{\infty} |C_n|^2 \sin^2(\Omega_n \tau/2 + \varepsilon\pi/2)}}. \quad (19.121)$$

Equation (19.121) shows that the original vibrational distribution $P(n) = |C_n|^2$, after the measurement, is modified to

$$P_\varepsilon^{(1)}(n) = \frac{P(n) \sin^2(\Omega_n \tau/2 + \varepsilon\pi/2)}{\sum_{n'=0}^{\infty} P(n') \sin^2(\Omega_{n'} \tau/2 + \varepsilon\pi/2)}. \quad (19.122)$$

This implies a decimation of the population, depending on the phase $\theta(\tau) = \eta^2 \tau \Omega_0/2$.

To enhance the n dependence of Ω_n , we choose a pulse duration τ such that $\theta(\tau) = \pi$. On the other hand, the term $\Omega_{n'} \tau/2$ is a large number, but independent of both n or η and produces an irrelevant phase shift.

After the first sequence of Raman pulse and detection, a new cycle is initiated with a different pulse area $\Omega_0 \tau$, thus multiplying the original $P(n)$ -distribution by sines and cosines. After the i th cycle

$$P_\varepsilon^{(i)}(n) = \frac{P^{(i-1)}(n) \sin^2(\Omega_n \tau_i/2 + \varepsilon\pi/2)}{\sum_{n'=0}^{\infty} P^{(i-1)}(n') \sin^2(\Omega_{n'} \tau_i/2 + \varepsilon\pi/2)}, \quad (19.123)$$

where τ_i is the duration of the i th Raman cycle, and we defined $P_\varepsilon^{(0)} = P(n)$, and $P^{(i-1)}(n)$ is the probability distribution of vibronic excitations of the previous cycle.

The numerical simulation of this procedure shows that this may result in a decimation of more and more population, until a Fock state is reached, and then the state no longer changes. If this procedure is done in all three directions, a three-dimensional Fock state is formed. Since this process depends on the random nature of the detected state, which Fock state is obtained is something that cannot be predicted *a priori*. This experiment can be turned into a numerical experiment, by feeding the computer with data about the successive state detection and pulse duration.

We notice here an interesting point. Doing the experiment many times gives us a different Fock state every time, thus building up a distribution of vibrational states. Since the QND measurement did not change the vibrational states and adding all possible measurements implies no measurement at all, this vibrational distribution should be identical to the original distribution $P(n)$. Also, the probability of detecting an ion in the $|a\rangle$ or $|b\rangle$ state, at the end of the i th cycle, is

$$P_\varepsilon^{(i)}(n) = \sum_{n'=0}^{\infty} P^{(i-1)}(n') \sin^2 \left(\frac{\Omega_{n'} \tau_i}{2} + \frac{\varepsilon \pi}{2} \right), \quad (19.124)$$

where, as above, $\varepsilon = 1$ or 0 depending on whether this state does or does not coincide with the electronic state at the beginning of the cycle.

In order to do the numerical experiment, we choose a random number with a flat distribution, between 0 and 1 , and according to the above probabilities of being in the $|a\rangle$ or $|b\rangle$ state, we decide the outcome of the measurement every time. The result is shown in Fig. 19.8.

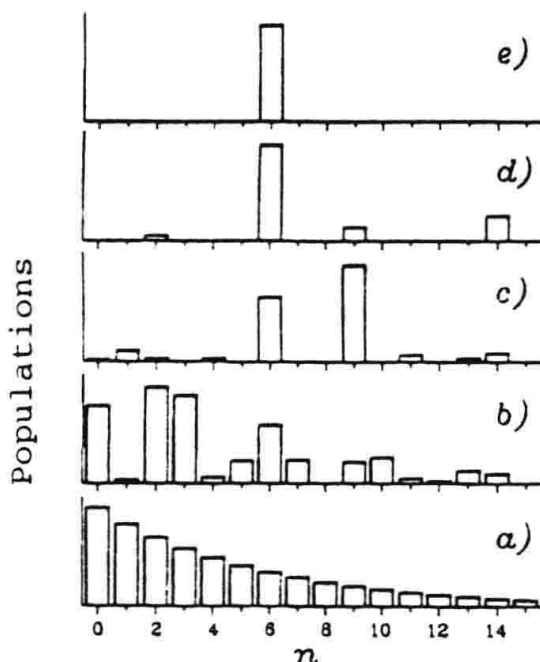


Fig. 19.8. Population distribution as a function of the vibronic excitation number, for $\eta = 0.1$, and (a) initial state, which was chosen to be a thermal distribution with $\langle n \rangle = 5$; (b) after the first cycle; (c) after the fifth cycle; (d) after the tenth cycle; (e) after the thirteenth cycle. θ was chosen at random, and the level that was detected was chosen according to the probability distribution

19.2.5 Generation of Non-classical Vibrational States

Generation and detection of vibrational Fock, coherent and squeezed states was recently achieved, with a single ${}^9\text{Be}^+$ ion, confined in an rf Paul trap, with a frequency $\omega/2\pi = 11.2$ MHz, along the x -axis and $\eta = 0.2$. Once the ion is prepared in the $|b\rangle|0\rangle$ state, a high n -Fock state can be created by simply applying a sequence of π -pulses of laser radiation on the first blue sideband ($k = -1$), the first red sideband ($k = 1$) and carrier ($k = 0$).

For example we want to generate the $|a\rangle|2\rangle$ state. This can be achieved by the following sequence

$$|b\rangle|0\rangle \xrightarrow[\text{blue sideband}]{\pi\text{-pulse}} |a\rangle|1\rangle \xrightarrow[\text{red sideband}]{\pi\text{-pulse}} |b\rangle|2\rangle \xrightarrow[\text{carrier}]{\pi\text{-pulse}} |a\rangle|2\rangle$$

which can also be seen in Fig. 19.9.

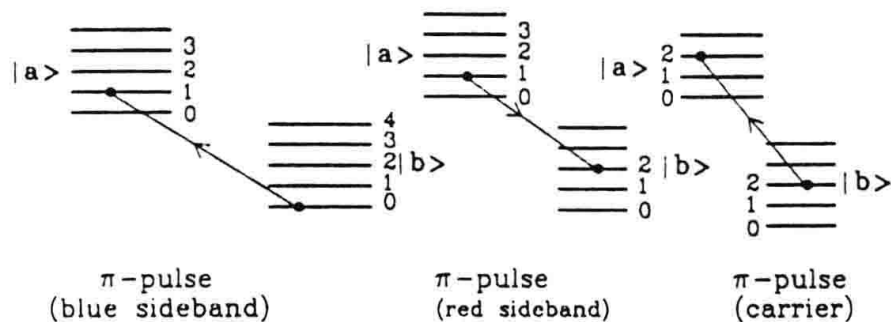


Fig. 19.9. $|n\rangle$ state created by applying a sequence of Rabi π -pulses, first on the blue sideband ($k = -1$), next on the red sideband ($k = 1$) and finally on the carrier frequency ($k = 0$)

Coherent states can be produced by a classical driving field, oscillating at the trap frequency. We can also apply a two-photon Raman coupling within one atomic state, with $k = 1$ ($\delta = \omega$). Starting from $n = 0$, the vibronic excitation number diffuses upwards. It can be shown that applying this sequence of pulses is equivalent to applying the displacement operator $|0\rangle \rightarrow |\alpha\rangle$, with $\alpha = \eta\Omega_0\tau$.

Finally, Zoller *et al.* [19.17] proposed the preparation of squeezed states of motion in an ion trap with a combination of standing and travelling-wave light fields.

Also, one can irradiate the ion in the $|n = 0\rangle$ state with two Raman beams that differ by 2ω , driving transitions between even- n levels and creating a squeezed vacuum state. The interested reader can check the references for more details [19.18].

Furthermore, there has been recently interesting advances in creating arbitrary superpositions of coherent states [19.22], entangled states with two trapped ions [19.23, 19.24] and laser cooling with two trapped ions [19.25].

Problems

19.1. Consider a single two-level ion moving in a one-dimensional Paul trap and interacting with a classical laser field [19.19]. The corresponding Hamiltonian is

$$H(t) = H_{\text{cm}} + H_a + H_{\text{In}},$$

where H_{cm} represents the centre-of-mass motion, H_a is the ion's internal energy and H_{In} is the interaction term. The three parts of the Hamiltonian can be written as

$$H_{\text{cm}} = \frac{p^2}{2m} + \frac{1}{2}\omega(t)^2x^2,$$

$$H_a = \frac{\hbar\omega_a}{2}\sigma_z,$$

$$H_{\text{In}} = \hbar g (\sigma^+ \exp[-i(\omega_L t - kx)] + \text{hc}),$$

where

$$\omega^2(t) = \frac{\Omega^2}{4} [a + 2q \cos \Omega t].$$

The parameters a and q are proportional to the applied DC and AC fields of the trap and Ω is the frequency of the AC field.

Show that in the interaction picture

$$H_{\text{INT}} = \hbar g(\sigma^+ \exp(-i\Delta t) D[\alpha(t)] + \text{hc}).$$

where

$$\Delta = \omega_L - \omega_a,$$

$$\alpha(t) = i\eta\varepsilon(t),$$

$$\eta = k\sqrt{\frac{\hbar}{2m\omega_r}},$$

and $\varepsilon(t)$ satisfies Mathieu's differential equation [19.21]

$$\ddot{\varepsilon} + \omega(t)^2\varepsilon = 0.$$

$D[\alpha(t)]$ is Glauber's displacement operator

$$D(\alpha) = \exp [\alpha b^+ - \alpha^* b],$$

with:

$$\hat{x} = \sqrt{\frac{\hbar}{2m\omega_r}} (\varepsilon^*(t)b + \varepsilon(t)b^+),$$

and b, b^+ , ω_r are annihilation, creation operator and frequency of the time independent reference harmonic oscillator. Notice that ω_r is an arbitrary real parameter.

19.2. In problem 19.1, the interaction involves multiphoton transitions.

To make this more evident, prove that

$$H_{\text{INT}} = \sum_{n=0}^{\infty} \sum_{s=-n}^{\infty} \hbar \Omega^{(n,n+s)}(t) \sigma^+ |n\rangle \langle n+s | + \text{hc},$$

where the generalized Rabi frequency is defined as

$$\begin{aligned} \Omega^{(n,n+s)}(t) &= g \sqrt{\frac{n!}{(n+s)!}} \exp(-i\Delta t) [i\eta\varepsilon^*(t)]^s \\ &\times \exp\left[-\frac{\eta^2}{2}\varepsilon(t)^2\right] L_n^s(\eta |\varepsilon(t)|^2) \end{aligned}$$

for $s \geq 0$, and

$$\begin{aligned} \Omega^{(n,n+s)}(t) &= g \sqrt{\frac{(n+s)!}{n!}} \exp(-i\Delta t) [i\eta\varepsilon(t)]^{-s} \\ &\times \exp\left[-\frac{\eta^2}{2}\varepsilon(t)^2\right] L_{n+s}^{-s}(\eta |\varepsilon(t)|^2) \end{aligned}$$

for $-n \leq s < 0$.

Hint: use the relations [19.20]

$$\begin{aligned} \langle n | D(\alpha(t)) | m \rangle &= \sqrt{\frac{m!}{n!}} \exp\left(-\frac{1}{2} |\alpha|^2\right) \alpha^{n-m} L_m^{n-m}(|\alpha|^2), \quad m \leq n, \\ \langle n | D(\alpha(t)) | m \rangle &= \sqrt{\frac{n!}{m!}} \exp\left(-\frac{1}{2} |\alpha|^2\right) (-\alpha^*)^{m-n} L_n^{m-n}(|\alpha|^2), \quad m \geq n. \end{aligned}$$

20. Decoherence

Quantum mechanics is a very successful theory that explains a huge number of physical phenomena. Quantum states evolve according to Schrödinger's equation, which is linear. As such, the superposition principle plays a major role. An important factor is that macroscopic systems are coupled to the environment, and therefore we are dealing in general with open systems where the Schrödinger equation is no longer applicable, or, to put it in a different way, the coherence leaks out of the system into the environment, and, as a result, we have decoherence [20.1], [20.2], [20.3].

Niels Bohr [20.4] proposed that, according to the Copenhagen interpretation of quantum mechanics, classical apparatus was necessary to carry out the measurements, thus implying a sharp borderline between the classical and the quantum worlds. Traditionally, classical systems are associated with the macroscopic and quantum systems with the microscopic [20.1], but this distinction is actually not very adequate, considering recently studied effects of macroscopic systems that behave quantum mechanically. We also have non-classical squeezed states with large numbers of photons, etc.

As opposed to Bohr, von Neumann [20.5] considered quantum measurements. Let us assume that we have a system with states $|a\rangle$ and $|b\rangle$ and a meter that can be in the states $|d_a\rangle$ and $|d_b\rangle$. If the detector is initially in the $|d_b\rangle$ state, we assume that it switches when the system is in the $|a\rangle$ state and does not change if the system is in the $|b\rangle$ state, that is

$$|a\rangle |d_b\rangle \rightarrow |a\rangle |d_a\rangle, \quad (20.1)$$

$$|b\rangle |d_b\rangle \rightarrow |b\rangle |d_b\rangle.$$

If, on the other hand, we assume that the system is in a superposition state

$$|\psi_{\text{initial}}\rangle = \alpha |a\rangle + \beta |b\rangle, \quad (20.2)$$

with

$$|\alpha|^2 + |\beta|^2 = 1, \quad (20.3)$$

then

$$|\psi_{\text{initial}}\rangle = (\alpha |a\rangle + \beta |b\rangle) |d_b\rangle \quad (20.4)$$

$\xrightarrow{\text{after}}$
 $\xleftarrow{\text{meas}}$

$$\alpha |a\rangle |d_a\rangle + \beta |b\rangle |d_b\rangle \equiv |\Psi^c\rangle,$$

where the state $|\Psi^c\rangle$ is a correlated one, and this process can be achieved, as we will soon see, just with Schrödinger's equation, with an appropriate interaction. Thus, if the detector is in the $|d_a\rangle$ state, one can be certain that the system is in the $|a\rangle$ state.

However, we are ignorant about the quantum state of the system and it is more realistic to approach the system in a statistical way, with the density matrix. According to von Neumann, besides the unitary evolution that rules the dynamics of quantum phenomena, there is also a non-unitary reduction of the wavefunction $|\Psi^c\rangle$ that takes the pure state density matrix $|\Psi^c\rangle\langle\Psi^c|$ and converts it into a mixed state, by eliminating the off-diagonal elements

$$\begin{aligned}\rho^c &= |\Psi^c\rangle\langle\Psi^c| \\ &= |\alpha|^2|a\rangle\langle a||d_a\rangle\langle d_a| + |\beta|^2|b\rangle\langle b||d_b\rangle\langle d_b| \\ &\quad + \alpha^*\beta|b\rangle\langle a||d_b\rangle\langle d_a| + \alpha\beta^*|a\rangle\langle b||d_a\rangle\langle d_b| \\ &\xrightarrow[\text{unitary}]{\text{Non}} \\ \rho^r &= |\alpha|^2|a\rangle\langle a||d_a\rangle\langle d_a| + |\beta|^2|b\rangle\langle b||d_b\rangle\langle d_b|.\end{aligned}\tag{20.5}$$

The difference between the original ρ^c and the after the measurement reduced density matrix ρ^r , is that since in the latter case the off-diagonal elements are missing, one could safely describe the system with alternative states ruled by classical probabilities $|\alpha|^2$ and $|\beta|^2$.

On the other hand, in the quantum case (ρ^c) things are more complicated, since we may use a different basis, say:

$$\begin{aligned}|c\rangle &= \frac{1}{\sqrt{2}}(|a\rangle + |b\rangle), \\ |d\rangle &= \frac{1}{\sqrt{2}}(|a\rangle - |b\rangle),\end{aligned}\tag{20.6}$$

and choosing $\alpha = -\beta = 1/\sqrt{2}$, we write

$$\begin{aligned}|\Psi^c\rangle &= \frac{1}{\sqrt{2}}(|a\rangle|d_a\rangle - |b\rangle|d_b\rangle) \\ &= \frac{1}{\sqrt{2}}\left[\frac{1}{\sqrt{2}}(|c\rangle + |d\rangle)|d_a\rangle - \frac{1}{\sqrt{2}}(|c\rangle - |d\rangle)|d_b\rangle\right] \\ &= \frac{1}{\sqrt{2}}[|c\rangle|d_c\rangle - |d\rangle|d_d\rangle],\end{aligned}\tag{20.7}$$

where

$$\begin{aligned}|d_c\rangle &= \frac{1}{\sqrt{2}}(|d_a\rangle - |d_b\rangle), \\ |d_d\rangle &= \frac{1}{\sqrt{2}}(|d_a\rangle + |d_b\rangle).\end{aligned}\tag{20.8}$$

We see that the diagonal elements of ρ^c give us different alternatives. In the first basis:

$$(\rho^c)_{\text{diag}} = \frac{1}{2} |a\rangle\langle a| |d_a\rangle\langle d_a| + \frac{1}{2} |b\rangle\langle b| |d_b\rangle\langle d_b|, \quad (20.9)$$

while in the second basis:

$$(\rho^c)_{\text{diag}} = \frac{1}{2} |c\rangle\langle c| |d_c\rangle\langle d_c| + \frac{1}{2} |d\rangle\langle d| |d_d\rangle\langle d_d|. \quad (20.10)$$

The problem, once more, is that we do not know the quantum state of the system.

Now, as we mentioned before, the first step of the measurement is to obtain the correlated wavefunction $|\Psi^c\rangle$, which can be achieved via a unitary operator. The second step, however, was the von Neumann non-unitary reduction. Can this step be achieved in a different way? Perhaps, by another unitary operator?

The answer to this question is ‘yes’ [20.1], and the way to do it is by coupling the system-detector pair to the environment, in order to dispose of the extra information. We call the environment states $|\varepsilon\rangle$. Then

$$\begin{aligned} |\Psi^c\rangle |\varepsilon_0\rangle &= (\alpha |a\rangle |d_a\rangle + \beta |b\rangle |d_b\rangle) |\varepsilon_0\rangle \\ &\rightarrow \\ (\alpha |a\rangle |d_a\rangle |\varepsilon_a\rangle + \beta |b\rangle |d_b\rangle |\varepsilon_b\rangle) &= |\psi\rangle. \end{aligned} \quad (20.11)$$

where the correlation has been extended from the system-detector to system-detector-environment, getting a chain of states.

If the environment states $|\varepsilon_a\rangle$ and $|\varepsilon_b\rangle$, corresponding to the detector states $|d_a\rangle$ and $|d_b\rangle$ respectively, are orthogonal, then we can trace (average) over the environment variables

$$\rho_{\text{SD}} = \text{Tr}_\varepsilon |\psi\rangle\langle\psi| = \sum_i \langle\varepsilon_i|\psi\rangle\langle\psi|\varepsilon_i\rangle = \rho^r, \quad (20.12)$$

getting precisely the von Neumann reduced density matrix, but this time by only unitary transformations, without *ad hoc* assumptions.

20.1 Dynamics of the Correlations

Here we discuss in more detail [20.6] the chain of states mentioned in the previous section. We assume that the system is coupled to the environment by a Hamiltonian of the following form

$$H_{\text{int}} = \hbar \sum_n |n\rangle\langle n| A_n, \quad (20.13)$$

where A_n are n -dependent operators acting on the Hilbert space of the environment and $|n\rangle$ is an eigenstate of a system observable to be measured.

The environment acquires the information about the state $|n\rangle$, in the sense that it changes according to

$$\begin{aligned} |n\rangle |\phi_0\rangle &\xrightarrow{t} \exp\left(-i\frac{H_{\text{int}}}{\hbar}t\right) |n\rangle |\phi_0\rangle = |n\rangle \exp(-iA_n t) |\phi_0\rangle \\ &= |n\rangle |\phi_n(t)\rangle. \end{aligned} \quad (20.14)$$

We notice that here the measurement is made not in the sense of von Neumann, but rather as a dynamical evolution of the joint system, according to Schrödinger's equation, with the appropriate coupling. The resulting environment states $|\phi_n(t)\rangle$ are called pointer states. In case the environment is interpreted as the measuring apparatus, they would correspond to particular apparatus states.

From the linearity of Schrödinger's equation, one can also write

$$\sum_n C_n |n\rangle |\phi_0\rangle \xrightarrow{t} \sum_n C_n |n\rangle |\phi_n(t)\rangle, \quad (20.15)$$

that is, we get a correlated state. The density matrix of the system changes according to

$$\begin{aligned} \rho_S &= \text{Tr}_{\text{envir}} \sum_{n,m} C_n C_m^* |n\rangle \langle m| |\phi_n(t)\rangle \langle \phi_m(t)| \\ &= \sum_{n,m} C_n C_m^* |n\rangle \langle m| \langle \phi_n(t)| \phi_m(t)\rangle, \end{aligned} \quad (20.16)$$

and for orthogonal states

$$\langle \phi_n(t) | \phi_m(t) \rangle = \delta_{nm}, \quad (20.17)$$

the system density matrix becomes diagonal

$$\rho_S \rightarrow \sum_n |C_n|^2 |n\rangle \langle n|. \quad (20.18)$$

During this evolution, the interference was destroyed and the system appears to be classical with respect to the quantum number n . If the above evolution is viewed as a model of system-apparatus coupling, unfortunately, the apparatus, being macroscopic, will invariably interact with the environment ε . By the same mechanism, the information about the measurement is rapidly transferred to the environment:

$$\sum_n C_n |n\rangle |\phi_n\rangle |\varepsilon_0\rangle \xrightarrow{t} \sum_n C_n |n\rangle |\phi_n\rangle |\varepsilon_n\rangle, \quad (20.19)$$

and if the environment states are orthogonal, then

$$\rho_{\text{system-apparatus}} = \sum_n |C_n|^2 |n\rangle \langle n| |\phi_n\rangle \langle \phi_n|. \quad (20.20)$$

Once more, we have defined the interaction of the apparatus with the environment by a Hamiltonian of the form given by (20.13), defining in this way, the pointer states $|\phi_n\rangle$.

20.2 How Long Does it Take to Decohere?

As discussed in the two previous sections, both measurement and coupling the system to an environment has, as a net effect, the loss of coherence, that is, the off-diagonal elements of the density matrix of our system vanish. In this section, we want to find out, in one particular example, the damped harmonic oscillator, how long it takes for the coherence to vanish.

We start with an initial condition for the oscillator that consists of a superposition of two coherent states, and we study its evolution to discover that actually two very different time scales are present. One is the time it takes for the coherent amplitude to decay, γ^{-1} , while the off-diagonal elements of the density matrix, or the quantum coherence, decays much faster, with a characteristic time (in the case when the initial superposition is proportional to $(|\alpha\rangle + |-\alpha\rangle)$):

$$t_c = \frac{\gamma^{-1}}{2 |\alpha|^2}.$$

We first study the harmonic oscillator without losses, with an initial state [20.7]

$$|\psi(0)\rangle = N (|\alpha_1\rangle + |\alpha_2\rangle), \quad (20.21)$$

where N is just a normalization factor. Since the Hamiltonian is: $H = \hbar\omega a^\dagger a$, at time t it will evolve to

$$\begin{aligned} |\psi(t)\rangle &= U(t) |\psi(0)\rangle \\ &= \exp(-i\omega a^\dagger a t) N (|\alpha_1\rangle + |\alpha_2\rangle) \\ &= N [|\alpha_1 \exp(-i\omega t)\rangle + |\alpha_2 \exp(-i\omega t)\rangle]. \end{aligned} \quad (20.22)$$

To derive last line of the above relation, we used the property

$$\begin{aligned} \exp(-i\omega a^\dagger a t) |\alpha\rangle &= \exp\left(-\frac{|\alpha|^2}{2}\right) \sum_n \frac{\alpha^n}{\sqrt{n!}} \exp(-i\omega t n) |n\rangle \\ &= \exp\left(-\frac{|\alpha|^2}{2}\right) \sum_n \frac{(\alpha \exp(-i\omega t))^n}{\sqrt{n!}} |n\rangle \\ &= |\alpha \exp(-i\omega t)\rangle. \end{aligned} \quad (20.23)$$

Thus,

$$\rho(t) = N^2 \sum_{i,j=1}^2 |\alpha_i(t)\rangle \langle \alpha_j(t)|, \quad (20.24)$$

with

$$\alpha_i(t) = \alpha_i \exp(-i\omega t). \quad (20.25)$$

On the other hand, we look at the position representation of the coherent states

$$\langle q' | \alpha \rangle = \left(\frac{\omega}{\pi \hbar} \right)^{1/4} \exp \left[-\frac{\omega}{2\hbar} q'^2 + \sqrt{\frac{2\omega}{\hbar}} \alpha q' - \frac{\alpha^2 + |\alpha|^2}{2} \right], \quad (20.26)$$

so that:

$$\begin{aligned} \langle q' | \rho(t) | q' \rangle &= N^2 [|\langle q' | \alpha_1(t) \rangle|^2 + |\langle q' | \alpha_2(t) \rangle|^2 \\ &\quad + 2 \operatorname{Re} \langle q' | \alpha_1(t) \rangle \langle \alpha_2(t) | q' \rangle]. \end{aligned} \quad (20.27)$$

Since $\alpha_i(t)$ is a complex number, one can separate the real and imaginary parts of $\langle q' | \alpha \rangle$:

$$\begin{aligned} \langle q' | \alpha \rangle &= \left(\frac{\omega}{\pi \hbar} \right)^{1/4} \exp \left[- \left(\sqrt{\frac{\omega}{2\hbar}} q' - \alpha \cos \omega t \right)^2 \right] \\ &\quad \times \exp i \left[- \sqrt{\frac{2\omega}{\hbar}} \alpha q' \sin \omega t + \frac{\alpha^2}{2} \sin 2\omega t \right], \end{aligned} \quad (20.28)$$

so we can write, in the case $\alpha_1 = \alpha, \alpha_2 = -\alpha$,

$$|\langle q' | \alpha_{1,2} \rangle|^2 = \left(\frac{\omega}{\pi \hbar} \right)^{1/2} \exp \left[- \left(\sqrt{\frac{\omega}{\hbar}} q' \pm \sqrt{2}\alpha \cos \omega t \right)^2 \right] \equiv I_{1,2}^2, \quad (20.29)$$

and

$$2 \operatorname{Re} \langle q' | \alpha_1(t) \rangle \langle \alpha_2(t) | q' \rangle = 2I_1 I_2 \cos \theta(t), \quad (20.30)$$

so finally

$$\langle q' | \rho(t) | q' \rangle = N^2 [I_1^2 + I_2^2 + 2I_1 I_2 \cos \theta(t)], \quad (20.31)$$

with

$$\theta(t) = 2 \sqrt{\frac{2\omega}{\hbar}} \alpha q' \sin \omega t. \quad (20.32)$$

As we can see, the quantum interference term $2I_1 I_2 \cos \theta(t)$ is present.

Now, it is interesting to study the effects of damping. This will give us information about the characteristic decoherence time due to the interaction with the environment. The master equation for the damped harmonic oscillator, at zero temperature, is given by

$$\frac{d\rho}{dt} = \frac{\gamma}{2} (2a\rho a^\dagger - a^\dagger a\rho - \rho a^\dagger a). \quad (20.33)$$

The normally ordered characteristic function is defined as

$$X_N(\eta, t) = \operatorname{Tr}(\rho(t) \exp(\eta a^\dagger) \exp(-\eta^* a)). \quad (20.34)$$

One can write [20.8]

$$\begin{aligned}
\frac{\partial X_N(\eta, t)}{\partial t} &= \text{Tr} \left[\frac{d\rho}{dt} \exp(\eta a^\dagger) \exp(-\eta^* a) \right] \\
&= \frac{\gamma}{2} \text{Tr} [(2a\rho a^\dagger - a^\dagger a\rho - \rho a^\dagger a) \exp(\eta a^\dagger) \exp(-\eta^* a)] \\
&= \frac{\gamma}{2} \text{Tr} [2\rho a^\dagger \exp(\eta a^\dagger) \exp(-\eta^* a)a - \rho \exp(\eta a^\dagger) \exp(-\eta^* a)a^\dagger a \\
&\quad - \rho a^\dagger a \exp(\eta a^\dagger) \exp(-\eta^* a)] \\
&= -\frac{\gamma}{2} [\eta \text{Tr}(\rho a^\dagger \exp(\eta a^\dagger) \exp(-\eta^* a)) \\
&\quad - \eta^* \text{Tr}(\rho \exp(\eta a^\dagger) \exp(-\eta^* a)a)] \\
&= -\frac{\gamma}{2} \left[\eta \frac{\partial X_N(\eta, t)}{\partial \eta} + \eta^* \frac{\partial X_N(\eta, t)}{\partial \eta^*} \right]. \tag{20.35}
\end{aligned}$$

In the last steps, we used the following properties

$$[a, f(a, a^\dagger)] = \frac{\partial f(a, a^\dagger)}{\partial a^\dagger}, \tag{20.36}$$

$$[a^\dagger, f(a, a^\dagger)] = -\frac{\partial f(a, a^\dagger)}{\partial a}, \tag{20.37}$$

$$\begin{aligned}
[a^\dagger a, \exp(\eta a^\dagger) \exp(-\eta^* a)] &= \eta a^\dagger \exp(\eta a^\dagger) \exp(-\eta^* a) \\
&\quad + \eta^* \exp(\eta a^\dagger) \exp(-\eta^* a)a. \tag{20.38}
\end{aligned}$$

One can show that the solution to (20.35) is

$$X_N(\eta, t) = X_N \left(\eta \exp \left(-\frac{\gamma t}{2} \right), 0 \right) = X_N(\eta(t), 0). \tag{20.39}$$

We can check the above result as follows (considering η as a complex number):

$$\begin{aligned}
\frac{\partial X_N(\eta, t)}{\partial t} &= \frac{\partial X_N(\eta, t)}{\partial \eta(t)} \frac{\partial \eta(t)}{\partial t} + \frac{\partial X_N(\eta, t)}{\partial \eta^*(t)} \frac{\partial \eta^*(t)}{\partial t} \\
&= -\frac{\gamma}{2} \left[\eta \frac{\partial X_N(\eta, t)}{\partial \eta} + \eta^* \frac{\partial X_N(\eta, t)}{\partial \eta^*} \right].
\end{aligned}$$

Now, the initial condition is

$$\begin{aligned}
X_N(\eta, 0) &= \text{Tr} [\rho(0) \exp(\eta a^\dagger) \exp(-\eta^* a)], \\
&= N^2 \text{Tr} \sum_{i,j} [|\alpha_i\rangle \langle \alpha_j| \exp(\eta a^\dagger) \exp(-\eta^* a)] \\
&= N^2 \sum_{i,j} [\langle \alpha_j | \exp(\eta a^\dagger) \exp(-\eta^* a) | \alpha_i \rangle] \\
&= N^2 \sum_{i,j} [\langle \alpha_j | \alpha_i \rangle \exp(\eta \alpha_j^* - \eta^* \alpha_i)], \tag{20.40}
\end{aligned}$$

So

$$X_N(\eta, t) = N^2 \sum_{i,j} \left[\langle \alpha_j | \alpha_i \rangle \exp(\eta \alpha_j^* - \eta^* \alpha_i) \exp\left(-\frac{\gamma t}{2}\right) \right]. \quad (20.41)$$

It is not difficult to show that the corresponding density matrix ρ is given by

$$\begin{aligned} \rho = & N^2 \sum_{i,j=1}^2 \langle \alpha_i | \alpha_j \rangle^{(1-\exp(-\gamma t))} \\ & \times \left| \alpha_j \exp\left(-\frac{\gamma t}{2}\right) \right\rangle \left\langle \alpha_i \exp\left(-\frac{\gamma t}{2}\right) \right|. \end{aligned} \quad (20.42)$$

In the particular case $\alpha_1 = \alpha; \alpha_2 = -\alpha$ we have

$$\langle \alpha | -\alpha \rangle = \exp(-2 |\alpha|^2), \quad (20.43)$$

and

$$\begin{aligned} \rho = & N^2 \left[\left| \alpha \exp\left(-\frac{\gamma t}{2}\right) \right\rangle \left\langle \alpha \exp\left(-\frac{\gamma t}{2}\right) \right| \right. \\ & + \left. \left| -\alpha \exp\left(-\frac{\gamma t}{2}\right) \right\rangle \left\langle -\alpha \exp\left(-\frac{\gamma t}{2}\right) \right| \right] \\ & + N^2 \exp[-2 |\alpha|^2 (1 - \exp(-\gamma t))] \\ & \times \left\{ \left| \alpha \exp\left(-\frac{\gamma t}{2}\right) \right\rangle \left\langle -\alpha \exp\left(-\frac{\gamma t}{2}\right) \right| \right. \\ & \left. + \left| -\alpha \exp\left(-\frac{\gamma t}{2}\right) \right\rangle \left\langle \alpha \exp\left(-\frac{\gamma t}{2}\right) \right| \right\} \end{aligned} \quad (20.44)$$

If $\gamma t \ll 1$, then the relevant exponential factor multiplying the crossed terms becomes

$$\exp(-2 |\alpha|^2 \gamma t) \equiv \exp\left(-\frac{t}{t_c}\right), \quad (20.45)$$

where

$$t_c = \frac{\gamma^{-1}}{2 |\alpha|^2}, \quad (20.46)$$

and

$$\langle q' | \rho(t) | q' \rangle = N^2 \left[I_1^2 + I_2^2 + 2I_1 I_2 \cos \theta(t) \exp\left(-\frac{t}{t_c}\right) \right], \quad (20.47)$$

where all the definitions are the same as before, except that $\alpha \rightarrow \alpha \exp(-\gamma t/2)$, so

$$I_{1,2}^2 = \left(\frac{\omega}{\pi \hbar} \right)^{1/2} \exp \left[- \left(\sqrt{\frac{\omega}{\hbar}} q' \pm \sqrt{2} \alpha \exp\left(-\frac{\gamma t}{2}\right) \cos \omega t \right)^2 \right], \quad (20.48)$$

which is a Gaussian distribution, whose centre is oscillating, the amplitude of which decreases in a timescale γ^{-1} . On the other hand, the quantum interference term $2I_1I_2 \cos \theta(t) \exp(-t/t_c)$ will vanish, for $|\alpha|^2 \gg 1$, in a much shorter time t_c . This may explain the difficulties in observing the quantum coherence in a macroscopic situation.

It has been shown [20.9] that the decay time of the quantum coherence, in a phase sensitive-reservoir, for an initial superposition of $|\alpha\rangle$ and $|- \alpha\rangle$ is given by

$$t_c^{(\text{sq})} = \frac{\gamma^{-1}}{2[N + 2\alpha^2(N - M + 1/2)]}, \quad (20.49)$$

where the notation is the same as in Chap. 9. In the vacuum reservoir, $M = N = 0$, the result coincides with (20.46).

On the other hand, it is interesting to notice that for an ideally squeezed reservoir ($|M|^2 = N(N + 1)$), with $M > 0$, the decay rate of the quantum coherence is significantly suppressed, and for large N is independent of α , namely

$$t_c^{(\text{sq})} = \frac{\gamma^{-1}}{2[N]}, \quad (20.50)$$

which means that the decay rate of the quantum coherence (off-diagonal terms in the density matrix) is of the same order of magnitude as the decay rate of the energy (diagonal part of the density matrix). Also, if $M < 0$, the decay rate of the coherence increases.

As we can see, one could in principle control the decay rate of the quantum coherence by monitoring the phase of the squeezing parameter of the reservoir [20.9], [20.10], [20.11], [20.12], which may have interesting applications in quantum computing.

Finally, there are some recent publications on decoherence in the non-classical motion of trapped ions [20.13, 20.14, 20.15].

Problems

20.1. Prove (20.42).

20.2. Show that for a phase-sensitive reservoir, one has

$$t_c^{(\text{sq})} = \frac{\gamma^{-1}}{2[N + 2\alpha^2(N - M + \frac{1}{2})]}.$$

Hint: see ref. [20.9].

A. Operator Relations

A.1 Theorem 1

Let A and B be two non-commuting operators, then [A.1]

$$\exp(\alpha A)B \exp(-\alpha A) = B + \alpha [A, B] + \frac{\alpha^2}{2!} [A, [A, B]] + \dots \quad (\text{A.1})$$

Proof. Let

$$f_1(\alpha) = \exp(\alpha A)B \exp(-\alpha A). \quad (\text{A.2})$$

Then, one can expand f_1 in a Taylor series about the origin. We first evaluate the derivatives

$$f'_1(\alpha) = \exp(\alpha A)(AB - BA) \exp(-\alpha A),$$

so

$$f'_1(0) = [A, B]. \quad (\text{A.3})$$

Similarly

$$f''_1(\alpha) = \exp(\alpha A)(A[A, B] - [A, B]A) \exp(-\alpha A),$$

so that

$$f''_1(0) = [A, [A, B]]. \quad (\text{A.4})$$

Now, we write the Taylor expansion

$$f_1(\alpha) = f_1(0) + \alpha f'_1(0) + \frac{\alpha^2}{2!} f''_1(0) + \dots \quad (\text{A.5})$$

or

$$\exp(\alpha A)B \exp(-\alpha A) = B + \alpha [A, B] + \frac{\alpha^2}{2!} [A, [A, B]] + \dots \quad (\text{A.6})$$

A particular case is when $[A, B] = c$, where c is a c -number. Then

$$\exp(\alpha A)B \exp(-\alpha A) = B + \alpha c, \quad (\text{A.7})$$

in which case $\exp(\alpha A)$ acts as a displacement operator.

A.2 Theorem 2.

The Baker–Campbell–Haussdorf Relation

Let A and B be two non-commuting operators such that:

$$[A, [A, B]] = [B, [A, B]] = 0. \quad (\text{A.8})$$

Then

$$\begin{aligned} \exp[\alpha(A + B)] &= \exp\alpha A \exp\alpha B \exp\left[-\frac{\alpha^2}{2}[A, B]\right] \\ &= \exp\alpha B \exp\alpha A \exp\left[\frac{\alpha^2}{2}[A, B]\right]. \end{aligned} \quad (\text{A.9})$$

Proof. Define

$$f_2(\alpha) \equiv \exp\alpha A \exp\alpha B. \quad (\text{A.10})$$

Then

$$\begin{aligned} \frac{df_2(\alpha)}{d\alpha} &= (A + \exp(\alpha A)B \exp(-\alpha A))f_2(\alpha) \\ &= (A + B + \alpha[A, B])f_2(\alpha), \end{aligned} \quad (\text{A.11})$$

where in the last step, we used (A.6). Also, from the definition of $f_2(\alpha)$, we can write

$$\begin{aligned} \frac{df_2(\alpha)}{d\alpha} &= \exp(\alpha A)A \exp\alpha B + \exp(\alpha A)\exp(\alpha B)B \\ &= \exp\alpha A \exp\alpha B [\exp(-\alpha B)A \exp\alpha B + B] \\ &= f_2(\alpha)(A + B + \alpha[A, B]). \end{aligned} \quad (\text{A.12})$$

By comparing (E.6) and (A.12), we can see that $f_2(\alpha)$ commutes with $(A + B + \alpha[A, B])$. Thus one can integrate as a *c*-number differential equation, getting

$$\begin{aligned} f_2(\alpha) &= \exp\left[(A + B)\alpha + \frac{\alpha^2}{2}[A, B]\right] \\ &= \exp\alpha(A + B) \exp\frac{\alpha^2}{2}[A, B]. \end{aligned} \quad (\text{A.13})$$

thus obtaining the desired result.

Theorem 1 can also be applied to the case

$$\begin{aligned} A &= aa^\dagger, \\ B &= a \text{ or } a^\dagger. \end{aligned} \quad (\text{A.14})$$

Since

$$[n, a] = -a \quad (\text{A.15})$$

and the higher-order commutators also give a with alternating signs, then

$$\exp(\alpha n)a \exp(-\alpha n) = a - \alpha a + \frac{\alpha^2}{2}a + \dots = \exp(-\alpha)a. \quad (\text{A.16})$$

Similarly

$$\exp(\alpha n)a^\dagger \exp(-\alpha n) = \exp(\alpha)a^\dagger. \quad (\text{A.17})$$

A.3 Theorem 3. Similarity Transformation

$$\exp(\alpha A)f(B)\exp(-\alpha A) = f(\exp(\alpha A)(B)\exp(-\alpha A)). \quad (\text{A.18})$$

Proof. We start with the identity

$$\begin{aligned} [\exp(\alpha A)(B)\exp(-\alpha A)]^n &= \exp(\alpha A)B\exp(-\alpha A)\exp(\alpha A)B\exp(-\alpha A) \\ &= \exp(\alpha A)B^n\exp(-\alpha A). \end{aligned}$$

Then, Theorem 3 follows for any function $f(B)$ that can be expanded in a power series.

As an interesting application, let us calculate

$$\begin{aligned} &\exp(-\alpha a^\dagger + \alpha^* a) f(a, a^\dagger) \exp(\alpha a^\dagger - \alpha^* a) \\ &= f(\exp(-\alpha a^\dagger + \alpha^* a) a \exp(\alpha a^\dagger - \alpha^* a)), \\ &\exp(-\alpha a^\dagger + \alpha^* a) a^\dagger \exp(\alpha a^\dagger - \alpha^* a)) \\ &= f(a + \alpha, a^\dagger + \alpha^*). \end{aligned}$$

Also

$$\exp(-\alpha a^\dagger) f(a, a^\dagger) \exp(\alpha a^\dagger) = f(a + \alpha, a^\dagger), \quad (\text{A.19})$$

$$\exp(\alpha^* a) f(a, a^\dagger) \exp(-\alpha^* a) = f(a, a^\dagger + \alpha^*), \quad (\text{A.20})$$

$$\exp(\alpha n) f(a, a^\dagger) \exp(-\alpha n) = f(a \exp(-\alpha), a^\dagger \exp(\alpha)). \quad (\text{A.21})$$

Other properties can be listed as follows. One can easily show that

$$[a, a^{\dagger l}] = la^{\dagger l-1} = \frac{da^{\dagger l}}{da^\dagger}, \quad (\text{A.22})$$

$$[a^\dagger, a^l] = -la^{l-1} = -\frac{da^l}{da}.$$

A more general version of the above relations is, for a function $f(a, a^\dagger)$ which may be expanded in a power series in a and a^\dagger ,

$$[a, f(a, a^\dagger)] = \frac{\partial f(a, a^\dagger)}{\partial a^\dagger}, \quad (\text{A.23})$$

$$[a^\dagger, f(a, a^\dagger)] = -\frac{\partial f(a, a^\dagger)}{\partial a}. \quad (\text{A.24})$$

B. The Method of Characteristics

We have a first-order partial differential equation [B.1]:

$$Pp + Qq = R, \quad (\text{B.1})$$

where $P = P(x, y, z)$, $Q = Q(x, y, z)$, $R = R(x, y, z)$, and

$$p \equiv \frac{\partial z}{\partial x}, \quad q \equiv \frac{\partial z}{\partial y}, \quad (\text{B.2})$$

and we wish to find a solution of (B.1), of the form

$$z = f(x, y). \quad (\text{B.3})$$

The general solution of (B.1) is

$$F(u, v) = 0, \quad (\text{B.4})$$

where F is an arbitrary function, and

$$u(x, y, z) = c_1, \quad v(x, y, z) = c_2, \quad (\text{B.5})$$

is a solution of the equations

$$\frac{dx}{P} = \frac{dy}{Q} = \frac{dz}{R}. \quad (\text{B.6})$$

Proof. If (B.5) are solutions of (B.6), then the equations

$$\frac{\partial u}{\partial x} dx + \frac{\partial u}{\partial y} dy + \frac{\partial u}{\partial z} dz = 0, \quad (\text{B.7})$$

and

$$\frac{dx}{P} = \frac{dy}{Q} = \frac{dz}{R},$$

must be compatible, thus we must have

$$Pu_x + Qu_y + Ru_z = 0, \quad (\text{B.8})$$

and similarly for v :

$$Pv_x + Qv_y + Rv_z = 0. \quad (\text{B.9})$$

On the other hand, if x and y are independent variables and $z = z(x, y)$, then from (B.5), we get

$$\begin{aligned} u_x + u_z \frac{\partial z}{\partial x} &= 0, \\ u_y + u_z \frac{\partial z}{\partial y} &= 0. \end{aligned} \tag{B.10}$$

and substituting (B.10) into (B.8) we get

$$\left[-P \frac{\partial z}{\partial x} - Q \frac{\partial z}{\partial y} + R \right] \frac{\partial u}{\partial z} = 0,$$

and (B.1) is satisfied.

The second part of the proof is to show that the general solution of (B.1) is

$$F(u, v) = 0. \tag{B.11}$$

From (B.11), one writes

$$\frac{\partial F}{\partial x} = \frac{\partial F}{\partial u} \left(\frac{\partial u}{\partial x} + \frac{\partial u}{\partial z} \frac{\partial z}{\partial x} \right) + \frac{\partial F}{\partial v} \left(\frac{\partial v}{\partial x} + \frac{\partial v}{\partial z} \frac{\partial z}{\partial x} \right) = 0, \tag{B.12}$$

$$\frac{\partial F}{\partial y} = \frac{\partial F}{\partial u} \left(\frac{\partial u}{\partial y} + \frac{\partial u}{\partial z} \frac{\partial z}{\partial y} \right) + \frac{\partial F}{\partial v} \left(\frac{\partial v}{\partial y} + \frac{\partial v}{\partial z} \frac{\partial z}{\partial y} \right) = 0. \tag{B.13}$$

We finally notice that (B.13) are satisfied by considering (B.10).

Example. Find the general solution of the equation

$$x^2 \frac{\partial z}{\partial x} + y^2 \frac{\partial z}{\partial y} = (x + y)z. \tag{B.14}$$

In this case

$$\begin{aligned} P &= x^2, \\ Q &= y^2, \\ R &= (x + y)z, \end{aligned} \tag{B.15}$$

and we have to find the solution of

$$\frac{dx}{x^2} = \frac{dy}{y^2} = \frac{dz}{(x + y)z}. \tag{B.16}$$

Integrating, first

$$\frac{dx}{x^2} = \frac{dy}{y^2},$$

we get

$$x^{-1} + y^{-1} = c_1'. \tag{B.17}$$

On the other hand

$$\frac{dx - dy}{x^2 - y^2} = \frac{(x^2/y^2 - 1)dy}{x^2 - y^2} = \frac{dy}{y^2} = \frac{dz}{(x + y)z},$$

from where we get

$$\frac{x-y}{z} = c_2 = v. \quad (\text{B.18})$$

Combining (B.17) and (B.18), we get

$$\frac{xy}{z} = c_1 = u, \quad (\text{B.19})$$

so the general solution can be written as

$$F\left(\frac{xy}{z}, \frac{x-y}{z}\right) = 0, \quad (\text{B.20})$$

or, if we write (B.20) in the equivalent form

$$u = g(v), \quad (\text{B.21})$$

then the solution is

$$\frac{xy}{z} = g\left(\frac{x-y}{z}\right). \quad (\text{B.22})$$

C. Proof of Eq. (12.37)

In this appendix, we derive the equation

$$\left[\left\langle \sum_{j \neq k} \delta(t - t_j) \delta(t' - t_k) \right\rangle_S - R^2 \right] \rho_{aa}^2 = -pR\delta(t - t'). \quad (\text{C.1})$$

For regular pumping, one can put $t_j = t_0 + j\tau$, where τ is the constant time interval between the atoms and t_0 some arbitrary time origin [C.1].

In this case, there are no pumping fluctuations and therefore there are no correlations between the products of delta functions, that is

$$\begin{aligned} \sum_{j,k} \langle \delta(t - t_j) \delta(t' - t_k) \rangle_S &= \sum_j \langle \delta(t - t_j) \rangle_S \sum_k \langle \delta(t' - t_k) \rangle_S \\ &= R^2. \end{aligned} \quad (\text{C.2})$$

Now, we split the left-hand side of the above equation into two parts

$$\begin{aligned} \sum_{j \neq k} \langle \delta(t - t_j) \delta(t' - t_k) \rangle_S + \sum_{j=k} \langle \delta(t - t_j) \delta(t' - t_k) \rangle_S &= R^2, \\ \sum_{j \neq k} \langle \delta(t - t_j) \delta(t' - t_k) \rangle_S + R\delta(t - t') &= R^2, \end{aligned} \quad (\text{C.3})$$

thus proving the relation

$$\left[\left\langle \sum_{j \neq k} \delta(t - t_j) \delta(t' - t_k) \right\rangle_S - R^2 \right] \rho_{aa}^2 = -pR\delta(t - t')$$

for $p = 1$.

In the Poissonian case, t_j and t_k are totally uncorrelated ($j \neq k$), so

$$\sum_{j \neq k} \langle \delta(t - t_j) \delta(t' - t_k) \rangle_S = \sum_j \langle \delta(t - t_j) \rangle_S \sum_k \langle \delta(t' - t_k) \rangle_S = R^2, \quad (\text{C.4})$$

which proves (C.1) for $p = 0$.

Notice that in the above result, we are missing an atom in the second summation, so the above result is approximate, the approximation being very good when $R \gg 1$. (The error is of the order of R compared to R^2).

A more general proof can be found in reference [C.2].

D. Stochastic Processes in a Nutshell

D.1 Introduction

Classical mechanics gives a deterministic view of the dynamical variables of a system. This of course is true when one is not in a chaotic regime. On the other hand, in many cases the system under study is only described by the time evolution of probability distributions.

To explore these ideas with an example, we take a look at the random walk in one dimension, which is by now a classical problem [D.1]. A person moves in a line, taking random steps forward or backward, with equal probability, at fixed time intervals τ . Denoting the position $x_n = na$, then the probability that it occupies the site x_n at time t is $P(x_n | t)$ and obeys the equation

$$P(x_n | t + \tau) = \frac{1}{2} P(x_{n-1} | t) + \frac{1}{2} P(x_{n+1} | t). \quad (\text{D.1})$$

Now, we go to the continuum limit, letting τ and a become small, but with finite a^2/τ . Then

$$\begin{aligned} P(x | t + \tau) &= P(x | t) + \tau \frac{\partial}{\partial t} P(x | t) + \dots \\ P(x_{n\pm 1} | t) &= P(x \pm a | t) \\ &= P(x | t) \pm a \frac{\partial}{\partial x} P(x | t) \\ &\quad + \frac{a^2}{2} \frac{\partial^2}{\partial x^2} P(x | t) + \dots, \end{aligned} \quad (\text{D.2})$$

and inserting the above expansions in (D.1), we get

$$\tau \frac{\partial}{\partial t} P(x | t) + \mathcal{O}(\tau^2) = \frac{a^2}{2} \frac{\partial^2}{\partial x^2} P(x | t) + \mathcal{O}(a^4) + \dots \quad (\text{D.3})$$

Now, letting $\tau, a \rightarrow 0$ with

$$D \equiv \frac{a^2}{\tau}, \quad (\text{D.4})$$

D being the diffusion coefficient, we get a diffusion or Fokker–Planck equation:

$$\frac{\partial}{\partial t} P(x | t) = \frac{D}{2} \frac{\partial^2}{\partial x^2} P(x | t). \quad (\text{D.5})$$

D.2 Probability Concepts

Let us call ω an event and let A describe a set of events. Thus

$$\omega \in A, \quad (\text{D.6})$$

meaning that the event ω belongs to the set of events A [D.2]. Also, we call Ω the set of all events and \emptyset the set of no events.

We now introduce the probability of A , $P(A)$, satisfying the following axioms

- (i) $P(A) \geq 0$ for all A .
- (ii) $P(\Omega) = 1$.
- (iii) If A_i ($i = 1, 2, 3, \dots$) is a countable collection of non-overlapping sets, such that

$$A_i \cap A_j = \emptyset, \quad i \neq j. \quad (\text{D.7})$$

then

$$P(\cup_i A_i) = \sum_i P(A_i). \quad (\text{D.8})$$

Now, we are ready to define the joint and conditional probabilities.

Joint Probability

$$P(A \cap B) = P\{\omega \in A \text{ and } \omega \in B\}. \quad (\text{D.9})$$

Conditional Probability

$$P(A | B) = \frac{P(A \cap B)}{P(B)}, \quad (\text{D.10})$$

which satisfies the intuitive idea of a conditional probability that $\omega \in A$ (given that we know that $\omega \in B$) is given by the joint probability of A and B divided by the probability of B .

Now, suppose we have a collection of sets B_i , such that

$$B_i \cap B_j = \emptyset, \quad (\text{D.11})$$

$$\cup_i (A \cap B_i) = A \cap (\cup_i B_i) = A. \quad (\text{D.12})$$

Now, by axiom (iii)

$$\sum_i P(A \cap B_i) = P(\cup_i (A \cap B_i)) = P(A), \quad (\text{D.13})$$

thus

$$\sum_i P(A, B_i) = \sum_i P(A | B_i)P(B_i) = P(A), \quad (\text{D.14})$$

or, put it in words, if we sum the joint probability over the mutually exclusive events B_i , it eliminates that variable. These ideas will be useful later in deriving the Chapman–Kolmogorov equation.

D.3 Stochastic Processes

If we have a time-dependent random variable $X(t)$ and measure the values x_1, x_2, x_3, \dots , at times t_1, t_2, t_3, \dots , then the joint probability densities

$$P(x_1, t_1; x_2, t_2; \dots)$$

completely describe the system, which is referred to as a stochastic process.

One can also define the conditional probability densities as

$$\begin{aligned} P(x_1, t_1; x_2, t_2; \dots | y_1, \tau_1; y_2, \tau_2; \dots) \\ = \frac{P(x_1, t_1; x_2, t_2; \dots, y_1, \tau_1; y_2, \tau_2; \dots)}{P(y_1, \tau_1; y_2, \tau_2; \dots)}, \end{aligned} \quad (\text{D.15})$$

where the time sequence increases as

$$t_1 \geq t_2 \geq \dots \geq \tau_1 \geq \tau_2 \geq \dots$$

we give some simple examples.

- (a) Complete independence. In this case $X(t)$ is completely independent of the past and future, or

$$P(x_1, t_1; x_2, t_2; \dots) = \prod_i P(x_i, t_i). \quad (\text{D.16})$$

- (b) The next simplest case is the Markov process, where the conditional probability is entirely determined by the knowledge of the most recent condition, that is

$$\begin{aligned} P(x_1, t_1; x_2, t_2; \dots | y_1, \tau_1; y_2, \tau_2; \dots) \\ = P(x_1, t_1; x_2, t_2; \dots | y_1, \tau_1). \end{aligned} \quad (\text{D.17})$$

It is simple to show that for the Markovian case an arbitrary joint probability can be written as

$$\begin{aligned} P(x_1, t_1; x_2, t_2; \dots, x_n, t_n) \\ = \prod_{i=1}^{n-1} P(x_i, t_i | x_{i-1}, t_{i-1}) P(x_n, t_n). \end{aligned} \quad (\text{D.18})$$

D.3.1 The Chapman–Kolmogorov Equation

As we saw in the previous section, summing over all mutually exclusive variables, eliminates that variable. In other words

$$\sum_B P(A \cap B \cap C \dots) = P(A \cap C \dots). \quad (\text{D.19})$$

Now, we apply this idea to a stochastic process

$$\begin{aligned} P(x, t | x_0, t_0) &= \int dy P(x, t; y, s | x_0, t_0) \\ &= \int dy P(x, t | y, s; x_0, t_0) P(y, s | x_0, t_0). \end{aligned} \quad (\text{D.20})$$

Next, we apply the Markov condition, in order to get the Chapman–Kolmogorov equation

$$P(x, t | x_0, t_0) = \int dy P(x, t | y, s) P(y, s | x_0, t_0). \quad (\text{D.21})$$

In the above analysis, t_0 is any initial time for which $x(t_0) = x_0$, and s is an intermediate time $t_0 \leq s \leq t$, and $x(s) = y$.

At this point, we observe that $P(x, t | x_0, t_0)$ is a probability density, satisfying the initial condition

$$P(x, t | x_0, t_0) |_{t=t_0} = \delta(t - t_0), \quad (\text{D.22})$$

and the normalization condition

$$\int dx P(x, t | x_0, t_0) = 1. \quad (\text{D.23})$$

Now, going back to (D.21), we write $t = s + \Delta t$, and expand in Δt :

$$\begin{aligned} P(x, s + \Delta t | x_0, t_0) &= \int dy \left\{ P(x, s | y, s) + \Delta t \frac{\partial P(x, t | y, s)}{\partial t} \Big|_{t=s} \right\} \\ &\quad \times P(y, s | x_0, t_0), \end{aligned}$$

or

$$\begin{aligned} P(x, s + \Delta t | x_0, t_0) &= P(x, s | x_0, t_0) \\ &\quad + \Delta t \int dy W(x | y) P(y, s | x_0, t_0), \end{aligned} \quad (\text{D.24})$$

where $W(x | y)$ is the transition rate, defined as

$$W(x | y) = \frac{\partial P(x, s | y, s)}{\partial t} \Big|_{t=s}. \quad (\text{D.25})$$

Letting $\Delta t \rightarrow 0$, (D.25) becomes

$$\frac{\partial P(x, t | x_0, t_0)}{\partial t} = \int dy W(x | y) P(y, t | x_0, t_0). \quad (\text{D.26})$$

This is the forward Chapman–Kolmogorov equation.

By integrating (D.26), one can easily verify that

$$\int dx W(x | y) = 0. \quad (\text{D.27})$$

The transition probability can be split into two parts: one that does not change, plus the change, that is

$$W(x | y) = W_0(x) \delta(x - y) + W_1(x | y). \quad (\text{D.28})$$

and integrating the above equation in x and using (D.27), we get

$$W_0(y) = - \int W_1(x | y) dx,$$

so the forward Chapman–Kolmogorov equation now reads as

$$\begin{aligned} \frac{\partial P(x, t | x_0, t_0)}{\partial t} &= \int dy W_1(x | y) P(y, t | x_0, t_0) \\ &\quad - \int dy W_1(y | x) P(x, t | x_0, t_0), \end{aligned} \quad (\text{D.29})$$

which has the form of a rate equation.

If the random variable X can take discrete values, the forward Chapman–Kolmogorov equation can be written as

$$\frac{\partial P(x_i, t)}{\partial t} = \sum_j [W_{ij} P(x_j, t) - W_{ji} P(x_i, t)]. \quad (\text{D.30})$$

This equation is known as the master equation.

Many stochastic processes are of a special type called ‘birth and death process’ or one-step process [D.3]. They correspond to

$$W_{ij} = r_j \delta_{i,j-1} + g_j \delta_{i,j+1}, \quad (i \neq j) \quad (\text{D.31})$$

which permits jumps to adjacent sites.

Also, for the diagonal part

$$W_n = -(r_n + g_n), \quad (\text{D.32})$$

so the master equation becomes

$$\dot{P}_n = r_{n+1} P_{n+1} + g_{n-1} P_{n-1} - (r_n + g_n) P_n, \quad (\text{D.33})$$

where r_n represents the probability per unit time to jump from $n \rightarrow n - 1$, and g_n is the probability per unit time to go from $n \rightarrow n + 1$.

Typically, one-step processes occur in atomic transitions via one photon (emission and absorption), nuclear excitation and de-excitation, fission, etc. An interesting example is the Poisson process, defined as

$$r_n = 0, \quad (\text{D.34})$$

$$g_n = q,$$

$$P_n(0) = \delta_{n,0},$$

and the master equation is

$$\dot{P}_n = q(P_{n-1} - P_n). \quad (\text{D.35})$$

This is a one-sided random walk.

To solve it, we use the characteristic function:

$$G(s, t) = \langle \exp(ins) \rangle = \sum_n P_n(t) \exp(ins), \quad (\text{D.36})$$

with boundary condition $G(s, 0) = 1$.

Multiplying the master equation by $\exp(is)$ and summing over n , we get

$$\sum_n \exp(is) \dot{P}_n = q \sum_n (P_{n-1} \exp(is) - P_n \exp(is)),$$

or

$$\frac{\partial G(s, t)}{\partial t} = q(\exp(is) - 1)G(s, t). \quad (\text{D.37})$$

It is simple to verify that the solution of (D.37) is

$$\begin{aligned} G(s, t) &= \exp\{tq[\exp(is) - 1]\} \\ &= \exp(-tq) \sum_n \frac{[\exp(is)]^n (tq)^n}{n!}, \end{aligned} \quad (\text{D.38})$$

thus comparing with (D.36), we finally get

$$P_n(t) = \exp(-tq) \frac{(tq)^n}{n!}, \quad (\text{D.39})$$

which is a Poisson distribution with $\langle n \rangle = tq$.

D.4 The Fokker–Planck Equation

Sometimes, instead of discrete jumps, one chooses to describe the random process as a continuous one. If we take, for example, in the Chapman–Kolmogorov equation [D.1]:

$$\Phi(w | x) \equiv W(x + w | x), \quad (\text{D.40})$$

then

$$\begin{aligned} \frac{\partial P(x, t | x_0, t_0)}{\partial t} &= \int dw \Phi(w | x - w) P(x - w, t | x_0, t_0) \\ &= \int \exp\left(-w \frac{\partial}{\partial x}\right) [\Phi(w | x) P(x, t | x_0, t_0)] dw \\ &= \int \left[1 - w \frac{\partial}{\partial x} + \frac{1}{2} w^2 \frac{\partial^2}{\partial x^2} + \dots\right] \\ &\quad \times [\Phi(w | x) P(x, t | x_0, t_0)] dw, \end{aligned} \quad (\text{D.41})$$

and since $\int dw \Phi(w | x) = 0$, we get

$$\frac{\partial P(x, t | x_0, t_0)}{\partial t} = \sum_{n=1}^{\infty} \frac{(-1)^n}{n!} \frac{\partial^n}{\partial x^n} [Q_n(x) P(x, t | x_0, t_0)], \quad (\text{D.42})$$

with

$$Q_n(x) = \int w^n \Phi(w | x) dw. \quad (\text{D.43})$$

In many cases, the above equation is truncated, keeping only the first two terms, getting the Fokker–Planck Equation.

In one dimension, with $Q_1 = A, Q_2 = B$, we get

$$\begin{aligned}\frac{\partial P(x, t \mid x_0, t_0)}{\partial t} &= -\frac{\partial}{\partial x} [A(x, t)P(x, t \mid x_0, t_0)] \\ &\quad + \frac{1}{2} \frac{\partial^2}{\partial x^2} [B(x, t)P(x, t \mid x_0, t_0)].\end{aligned}\quad (\text{D.44})$$

A simple generalization to more variables leads to the Fokker–Planck equation

$$\begin{aligned}\frac{\partial P(\mathbf{x}, t \mid \mathbf{x}_0, t_0)}{\partial t} &= -\sum_i \frac{\partial}{\partial x_i} [\mathbf{A}_i(\mathbf{x}, t)P(\mathbf{x}, t \mid \mathbf{x}_0, t_0)] \\ &\quad + \frac{1}{2} \sum_{i,j} \frac{\partial^2}{\partial x_i \partial x_j} [\mathbf{B}_{ij}(\mathbf{x}, t)P(\mathbf{x}, t \mid \mathbf{x}_0, t_0)],\end{aligned}\quad (\text{D.45})$$

where \mathbf{A} is the drift vector and \mathbf{B} the diffusion matrix. This equation can also be written as

$$\frac{\partial P(\mathbf{x}, t \mid \mathbf{x}_0, t_0)}{\partial t} + \sum_i \frac{\partial}{\partial x_i} \mathbf{J}_i(\mathbf{x}, t) = 0, \quad (\text{D.46})$$

$$\begin{aligned}\mathbf{J}_i(\mathbf{x}, t) &= [\mathbf{A}_i(\mathbf{x}, t)P(\mathbf{x}, t \mid \mathbf{x}_0, t_0)] \\ &\quad - \frac{1}{2} \sum_j \frac{\partial}{\partial x_j} [\mathbf{B}_{ij}(\mathbf{x}, t)P(\mathbf{x}, t \mid \mathbf{x}_0, t_0)].\end{aligned}\quad (\text{D.47})$$

$\mathbf{J}_i(\mathbf{x}, t)$ is interpreted as a probability current.

Let us take a one-dimensional example.

D.4.1 The Wiener Process

We take the particular case $A = 0, B = 1$, so the Fokker–Planck equation now reads [D.2]

$$\frac{\partial P(w, t \mid w_0, t_0)}{\partial t} = \frac{1}{2} \frac{\partial^2}{\partial w^2} [P(w, t \mid w_0, t_0)]. \quad (\text{D.48})$$

Once more, we use the characteristic function

$$\phi(s, t) = \int dw \exp(isw)P(w, t \mid w_0, t_0). \quad (\text{D.49})$$

The differential equation for ϕ is

$$\frac{\partial \phi}{\partial t} = -s^2 \phi. \quad (\text{D.50})$$

We also notice that since $P(w, t \mid w_0, t_0) \mid_{t=t_0} = \delta(w - w_0)$, so $\phi(s, t_0) = \exp(isw_0)$, and the solution is

$$\phi(s, t) = \exp \left[i s w_0 - \frac{1}{2} s^2 (t - t_0) \right], \quad (\text{D.51})$$

which is a Gaussian, whose inverse transform is also a Gaussian

$$P(w, t | w_0, t_0) = \frac{1}{\sqrt{2\pi(t - t_0)}} \exp \left(-\frac{(w - w_0)^2}{2(t - t_0)} \right). \quad (\text{D.52})$$

The first two moments are

$$\begin{aligned} \langle W \rangle &= w_0, \\ \langle (\Delta W)^2 \rangle &= t - t_0. \end{aligned} \quad (\text{D.53})$$

This distribution spreads in time and corresponds precisely to Einstein's model for Brownian motion.

An important characteristic of Wiener's process is the independence of the increments, which is interesting for stochastic integration purposes. We saw that, in general, for Markov processes, one has

$$\begin{aligned} P(w_n, t_n; w_{n-1}, t_{n-1}; \dots; w_0, t_0) &\quad (\text{D.54}) \\ &= \prod_{i=0}^{n-1} P(w_{i+1}, t_{i+1} | w_i, t_i) P(w_0, t_0) \\ &= \prod_{i=0}^{n-1} \left\{ [2\pi(t_{i+1} - t_i)]^{-1/2} \exp \left[-\frac{(w_{i+1} - w_i)^2}{2(t_{i+1} - t_i)} \right] \right\} P(w_0, t_0). \end{aligned}$$

Now we define the Wiener increments as

$$\Delta W_i = W(t_i) - W(t_{i-1}), \quad (\text{D.55})$$

and

$$\Delta t_i = t_i - t_{i-1},$$

so the joint probability density for the increments is

$$\begin{aligned} P(\Delta w_n; \Delta w_{n-1}; \dots; \Delta w_1; w_0) &\\ &= \prod_{i=1}^n \left\{ [2\pi \Delta t_i]^{-1/2} \exp \left[-\frac{(\Delta w_i)^2}{2(\Delta t_i)} \right] \right\} P(w_0, t_0). \end{aligned} \quad (\text{D.56})$$

Thus they are statistically independent.

If we define the mean and autocorrelation functions as

$$\langle \mathbf{W}(t) | \mathbf{W}_0, t_0 \rangle = \int d\mathbf{w} P(\mathbf{w}, t | \mathbf{w}_0, t_0) \mathbf{w}, \quad (\text{D.57})$$

$$\begin{aligned} \langle \mathbf{W}(t) \mathbf{W}(t_0)^T | \mathbf{W}_0, t_0 \rangle &= \int d\mathbf{w} d\mathbf{w}_0 P(\mathbf{w}, t; \mathbf{w}_0, t_0) \mathbf{w} \mathbf{w}_0^T \\ &= \int d\mathbf{w}_0 \langle \mathbf{W}(t) | \mathbf{W}_0, t_0 \rangle \mathbf{w}_0^T P(\mathbf{w}_0, t_0). \end{aligned}$$

then for the Wiener process

$$\langle W(t)W(s) | W_0, t_0 \rangle = \langle [W(t) - W(s)] W(s) | W_0, t_0 \rangle + \langle W(s)^2 \rangle, \quad (\text{D.58})$$

and due to the independence of the increments, the first term is zero and

$$\langle W(t)W(s) | W_0, t_0 \rangle = w_0^2 + \min(t - t_0, s - t_0). \quad (\text{D.59})$$

D.4.2 General Properties of the Fokker–Planck Equation

The general Fokker–Planck equation is

$$\begin{aligned} \frac{\partial P(\mathbf{x}, t | \mathbf{x}_0, t_0)}{\partial t} &= - \sum_i \frac{\partial}{\partial x_i} [\mathbf{A}_i(\mathbf{x}, t) P(\mathbf{x}, t | \mathbf{x}_0, t_0)] \\ &\quad + \frac{1}{2} \sum_{i,j} \frac{\partial^2}{\partial x_i \partial x_j} [\mathbf{B}_{ij}(\mathbf{x}, t) P(\mathbf{x}, t | \mathbf{x}_0, t_0)]. \end{aligned} \quad (\text{D.60})$$

As we mentioned before, the first term in the right-hand side is the drift term, which will rule the deterministic motion, and the second one is the diffusion term which will cause the probability to broaden. These different roles of the two terms can be easily seen if we calculate $\langle x_i \rangle$ and $\langle x_i x_j \rangle$. One can easily show that

$$\begin{aligned} \frac{d\langle x_i \rangle}{dt} &= \langle \mathbf{A}_i \rangle, \\ \frac{d\langle x_i x_j \rangle}{dt} &= \langle x_i \mathbf{A}_j \rangle + \langle x_j \mathbf{A}_i \rangle + \frac{1}{2} \langle \mathbf{B}_{ij} + \mathbf{B}_{ji} \rangle. \end{aligned} \quad (\text{D.61})$$

D.4.3 Steady State Solution

Very often in optics and other areas of physics, one is not really interested in the time dependent solution of the Fokker–Planck equation, but rather in the steady state. Thus we set the time derivative to zero and get

$$\begin{aligned} \sum_i \frac{\partial}{\partial x_i} &[-\mathbf{A}_i(\mathbf{x}, t) P(\mathbf{x}, t | \mathbf{x}_0, t_0) \\ &\quad + \frac{1}{2} \sum_j \frac{\partial}{\partial x_j} [\mathbf{B}_{ij}(\mathbf{x}, t) P(\mathbf{x}, t | \mathbf{x}_0, t_0)]] \\ &= 0, \end{aligned} \quad (\text{D.62})$$

and if the constant current is set to zero (detailed balance), one gets

$$\mathbf{A}_i(\mathbf{x}, t) P(\mathbf{x}, t | \mathbf{x}_0, t_0) = \frac{1}{2} \sum_j \frac{\partial}{\partial x_j} [\mathbf{B}_{ij}(\mathbf{x}, t) P(\mathbf{x}, t | \mathbf{x}_0, t_0)] \quad (\text{D.63})$$

or

$$\begin{aligned} 2\mathbf{A}_i - \sum_j \frac{\partial \mathbf{B}_{ij}}{\partial x_j} &= \sum_j \mathbf{B}_{ij} \frac{1}{P(\mathbf{x}, t \mid \mathbf{x}_0, t_0)} \frac{\partial P(\mathbf{x}, t \mid \mathbf{x}_0, t_0)}{\partial x_j} \\ &= \sum_j \mathbf{B}_{ij} \frac{\partial \ln(P(\mathbf{x}, t \mid \mathbf{x}_0, t_0))}{\partial x_j}, \end{aligned}$$

and defining a potential function $V(\mathbf{x})$ by $P(\mathbf{x}, t \mid \mathbf{x}_0, t) = N \exp(-V(\mathbf{x}))$, we get for V

$$-\frac{\partial V(\mathbf{x})}{\partial x_i} = 2 \sum_j \mathbf{B}_{ij}^{-1} \mathbf{A}_j - \sum_{j,k} \mathbf{B}_{ij}^{-1} \frac{\partial \mathbf{B}_{jk}}{\partial x_k}. \quad (\text{D.64})$$

Integrating (D.64), we get for the probability distribution

$$P_{\text{SS}}(\mathbf{x}) = N \exp \left[\int \sum_{i,j} 2 \mathbf{B}_{ij}^{-1} \mathbf{A}_j d\mathbf{x}_i - \int \sum_{i,j,k} \mathbf{B}_{ij}^{-1} \frac{\partial \mathbf{B}_{jk}}{\partial x_k} d\mathbf{x}_i \right]. \quad (\text{D.65})$$

In particular, for $\mathbf{B}_{ij} = D\delta_{ij}$, we get

$$P_{\text{SS}}(\mathbf{x}) = N \exp \int \frac{2}{D} \mathbf{A}(\mathbf{x}) \cdot d\mathbf{x}. \quad (\text{D.66})$$

D.5 Stochastic Differential Equations

One way of treating the motion of a Brownian particle, or any other problem with a random force, is via a Langevin or Stochastic differential equation

$$\dot{V} = -\gamma V + L(t), \quad (\text{D.67})$$

where, in the case of a Brownian particle, the right-hand side is the force of the fluid over the particle and is made up of two components:

- (a) the damping force $-\gamma V$;
- (b) a rapidly varying force $L(t)$, independent of the particle's velocity, which accounts for the collisions of the water molecules with the Brownian particle, whose average is zero. Thus

$$\langle L(t) \rangle = 0 \quad (\text{D.68})$$

$$\langle L(t)L(t') \rangle = D\delta(t-t').$$

$\langle L(t)L(t') \rangle$ is referred to as the two-time correlation function.

If one defines the spectrum as the Fourier transform of the two-time correlation function

$$S(\omega) = \int_{-\infty}^{+\infty} d\tau \exp(i\omega\tau) \langle L(t+\tau)L(t) \rangle, \quad (\text{D.69})$$

we immediately notice that since the Fourier transform of a delta function is a constant, $L(t)$ has a flat spectrum or it corresponds to white noise.

Let us assume that the initial velocity of the Brownian particle is deterministic and given by $V(0) = V_0$. Then for $t > 0$, for each sample path

$$V(t) = V_0 \exp(-\gamma t) + \exp(-\gamma t) \int_0^t \exp(\gamma t') L(t') dt'. \quad (\text{D.70})$$

Using the properties of L , we can calculate $\langle V \rangle$ and $\langle V^2 \rangle$:

$$\langle V(t) | V_0, t_0 \rangle = V_0 \exp(-\gamma t), \quad (\text{D.71})$$

$$\begin{aligned} \langle V^2(t) | V_0, t_0 \rangle &= V_0^2 \exp(-2\gamma t) \\ &\quad + \exp(-2\gamma t) \int_0^t dt' \int_0^{t'} dt'' \exp \gamma(t' + t'') \langle L(t') L(t'') \rangle \\ \langle V^2(t) | V_0, t_0 \rangle &= V_0^2 \exp(-2\gamma t) + \frac{D}{2\gamma} [1 - \exp(-2\gamma t)]. \end{aligned} \quad (\text{D.72})$$

When $t \rightarrow \infty$

$$\langle V^2(t) | V_0, t_0 \rangle = \frac{D}{2\gamma}, \quad (\text{D.73})$$

On the other hand, for short times

$$\langle (\Delta V)^2(t_0 + \Delta t) | V_0, t_0 \rangle = D \Delta t + \mathcal{O}(\Delta t)^2. \quad (\text{D.74})$$

We also notice that in this case the drift and diffusion coefficients are

$$A = \frac{\langle \Delta V \rangle}{\Delta t} = \frac{\langle (V - V_0) \rangle|_{t=t_0+\Delta t}}{\Delta t} = -\gamma V, \quad (\text{D.75})$$

$$B = \frac{\langle (\Delta V)^2 \rangle}{\Delta t} = D, \quad (\text{D.76})$$

so that the corresponding Fokker-Planck equation is

$$\frac{\partial P(V, t)}{\partial t} = \gamma \frac{\partial}{\partial V} (VP) + \frac{D}{2} \frac{\partial^2 P}{\partial V^2}. \quad (\text{D.77})$$

The above equation describes the so-called Ornstein-Uhlenbeck process, corresponding to a linear drift and a constant diffusion term.

We now calculate the power spectrum of V . We first need the two-time correlation function

$$\begin{aligned} \langle V(t)V(t') \rangle &= V_0^2 \exp[-\gamma(t+t')] \\ &\quad + \exp[-\gamma(t+t')] \int_0^t dt'' \int_0^{t'} dt''' \exp[\gamma(t''+t''')] \\ &\quad \times \langle L(t'')L(t''') \rangle \\ &= V_0^2 \exp[-\gamma(t+t')] \\ &\quad + \exp[-\gamma(t+t')] D \int_0^{t'} dt''' \exp[2\gamma t'''] \end{aligned}$$

$$\begin{aligned}\langle V(t)V(t') \rangle &= V_0^2 \exp[-\gamma(t+t')] \\ &\quad + \exp[-\gamma(t+t')] \frac{D}{2\gamma} [\exp(2\gamma t') - 1].\end{aligned}\quad (\text{D.78})$$

In steady state, for $t, t' \rightarrow \infty$ but with $t - t' = \tau$, we get

$$\langle V(t+\tau)V(t) \rangle = \frac{D}{2\gamma} \exp(-\gamma |\tau|). \quad (\text{D.79})$$

Finally, taking the Fourier transform, we get the power spectrum of V :

$$\begin{aligned}\phi_V(\omega) &= \frac{1}{2\pi} \int \exp(i\omega\tau) \langle V(t+\tau)V(t) \rangle d\tau \\ &= \frac{1}{2\pi} \frac{D}{\omega^2 + \gamma^2}.\end{aligned}\quad (\text{D.80})$$

D.5.1 Ito versus Stratonovich Calculus

A more general type of Langevin equation can be written as

$$\frac{dx}{dt} = a(x, t) + b(x, t)L(t), \quad (\text{D.81})$$

where the previous D factor can be absorbed in b , so that

$$\begin{aligned}\langle L(t)L(t') \rangle &= \delta(t-t'), \\ \langle L \rangle &= 0.\end{aligned}\quad (\text{D.82})$$

Now we define

$$W(t) = \int_0^t L(t') dt', \quad (\text{D.83})$$

assumed to be continuous, so that

$$\langle W(t + \Delta t) - W_0(t) | W_0, t \rangle = \left\langle \int_t^{t+\Delta t} ds L(s) \right\rangle = 0, \quad (\text{D.84})$$

$$\begin{aligned}\langle [W(t + \Delta t) - W_0(t)]^2 | W_0, t \rangle &= \left\langle \int_t^{t+\Delta t} ds_1 \int_t^{t+\Delta t} ds_2 L(s_1)L(s_2) \right\rangle \\ &= \int_t^{t+\Delta t} ds_1 \int_t^{t+\Delta t} ds_2 \delta(s_1 - s_2) \\ &= \Delta t.\end{aligned}\quad (\text{D.85})$$

Therefore, one could write a Fokker–Planck equation for W with

$$A = 0, \quad B = 1,$$

which corresponds to a Wiener process, and $Ldt = dW$ becomes a Wiener increment.

The stochastic differential equation (D.81) is not fully defined unless one specifies how to integrate it. Normally, this would not be a problem and the rules of ordinary calculus apply. However, here we must be careful since we are dealing with a rapidly varying function of time, $L(t)$.

Thus we define the integral as the mean square limit of a Riemann–Stieltjes sum

$$\int_{t_0}^t f(t') dW(t') = ms \lim_{n \rightarrow \infty} \sum_{i=1}^n f(\tau_i) [W(t_i) - W(t_{i-1})], \quad (\text{D.86})$$

where $t_{i-1} \leq \tau_i \leq t_i$, and we have divided the time interval from $t_0 \rightarrow t$ into n intermediate times t_1, t_2, \dots, t_n .

One can verify that *it does matter which $f(\tau_i)$ we choose*. Two popular choices are:

- (a) Ito calculus with $\tau_i = t_{i-1}$;
- (b) Stratonovich calculus : $f(\tau_i) = \frac{1}{2}(f(t_i) + f(t_{i-1}))$.

From the above assumptions, one learns how to calculate things with Ito and Stratonovich calculus.

For Stratonovich calculus, we have for example

$$\begin{aligned} S \int_{t_0}^t W(t') dW(t') \\ &= ms \lim_{n \rightarrow \infty} \sum_{i=1}^n \left[\frac{W(t_i) + W(t_{i-1})}{2} \right] [W(t_i) - W(t_{i-1})] \\ &= \frac{1}{2} ms \lim_{n \rightarrow \infty} \sum_{i=1}^n [W^2(t_i) - W^2(t_{i-1})] \\ &= \frac{1}{2} (W^2(t) - W^2(t_0)), \end{aligned}$$

which obeys the rules of ordinary calculus.

On the other hand, for Ito calculus

$$\begin{aligned} I \int_{t_0}^t W(t') dW(t') \\ &= ms \lim_{n \rightarrow \infty} \sum_{i=1}^n [W(t_{i-1})] [W(t_i) - W(t_{i-1})] \\ &= ms \lim_{n \rightarrow \infty} \sum_{i=1}^n [W(t_{i-1}) \Delta W(t_i)] \\ &= ms \lim_{n \rightarrow \infty} \frac{1}{2} \sum_{i=1}^n [(W(t_{i-1}) + \Delta W(t_i))^2 - W(t_{i-1})^2 - \Delta W(t_i)^2] \\ &= \frac{1}{2} [W(t)^2 - W(t_0)^2] - ms \lim_{n \rightarrow \infty} \frac{1}{2} \sum_{i=1}^n \Delta W(t_i)^2, \end{aligned}$$

and since

$$ms \lim_{n \rightarrow \infty} \frac{1}{2} \sum_{i=1}^n \Delta W(t_i)^2 = t - t_0,$$

we finally get

$$I \int_{t_0}^t W(t') dW(t') = \frac{1}{2} [W(t)^2 - W(t_0)^2 - (t - t_0)]. \quad (\text{D.87})$$

Finally, for the Ito integration one can prove that

$$\begin{aligned} dW(t)^2 &= dt, \\ dW(t)^{2+N} &= 0, \quad N = 1, 2, 3, \dots \end{aligned} \quad (\text{D.88})$$

The details and proof of the above properties can be found in Gardiner's book [D.2].

From these properties, we can see that $dW \sim \sqrt{dt}$ and we have to keep terms up to $(dW)^2$, which differs from ordinary calculus.

D.5.2 Ito's Formula

Consider a function $f[x(t)]$. We will derive the basic formula for Ito's calculus:

$$\begin{aligned} df[x(t)] &= f[x(t) + dx] - f[x(t)] \\ &= f'[x(t)] dx + \frac{1}{2} f''[x(t)] dx^2 + \dots \\ &= f'[x(t)] \{a(x, t) + b(x, t)dW\} \\ &\quad + \frac{1}{2} f''[x(t)] \{b(x, t)dW^2 + \dots\} \end{aligned}$$

and using (D.88), we get

$$\begin{aligned} df[x(t)] &= \left\{ a(x, t)f'[x(t)] + \frac{1}{2} b(x, t)f''[x(t)] \right\} dt \\ &\quad + b(x, t)f'[x(t)] dW. \end{aligned} \quad (\text{D.89})$$

The above formula can be easily generalized to many dimensions.

Now, we take the average of Ito's formula:

$$\begin{aligned} \frac{d\langle f(x) \rangle}{dt} &= \int dx \partial_t P(x, t) f(x) \\ &= \int dx \left[a \partial_x f + \frac{b}{2} \partial_x^2 f \right] P(x, t). \end{aligned}$$

and integrating by parts and discarding the surface terms, we get

$$\int dx f(x) \partial_t P(x, t) = \int dx f(x) \left[-\partial_x a P + \frac{1}{2} \partial_x^2 b P \right],$$

thus getting the Ito Fokker-Planck equation

$$\partial_t P(x, t | x_0, t_0) = -\partial_x [a(x, t)P(x, t | x_0, t_0)] \quad (\text{D.90})$$

$$+ \frac{1}{2} \partial_x^2 [b(x, t)P(x, t | x_0, t_0)]. \quad (\text{D.91})$$

Similarly, for many variables, if one has an Ito stochastic differential equation

$$(I)d\mathbf{x} = \mathbf{a}(x, t) + \mathbf{b}(x, t)d\mathbf{W}, \quad (\text{D.92})$$

where $d\mathbf{W}$ is an n -component Wiener process, then the corresponding Ito's Fokker–Planck equation is:

$$\partial_t P(\mathbf{x}, t | \mathbf{x}_0, t_0) = - \sum_i \partial_i [\mathbf{a}_i(\mathbf{x}, t)P(\mathbf{x}, t | \mathbf{x}_0, t_0)] \quad (\text{D.93})$$

$$+ \frac{1}{2} \sum_{i,j} \partial_i \partial_j [\mathbf{b}\mathbf{b}^T(x, t)]_{ij} P(\mathbf{x}, t | \mathbf{x}_0, t_0). \quad (\text{D.94})$$

Thus, from our previous notation

$$\mathbf{B} = \mathbf{b}\mathbf{b}^T. \quad (\text{D.95})$$

Similarly, for Stratonovich calculus

$$(S)d\mathbf{x} = \mathbf{a}^S(x, t) + \mathbf{b}^S(x, t)d\mathbf{W}, \quad (\text{D.96})$$

we get a Stratonovich Fokker–Planck equation

$$\partial_t P(\mathbf{x}, t | \mathbf{x}_0, t_0) = - \sum_i \partial_i [\mathbf{a}_i^S(\mathbf{x}, t)P(\mathbf{x}, t | \mathbf{x}_0, t_0)] \quad (\text{D.97})$$

$$+ \frac{1}{2} \sum_{i,j,k} \partial_i [\mathbf{b}_{ik}^S \partial_j \mathbf{b}_{jk}^{ST}(x, t)] P(\mathbf{x}, t | \mathbf{x}_0, t_0).$$

By simple comparison between the two Fokker–Planck equations, we get

$$\mathbf{a}_i^S = \mathbf{a}_i - \frac{1}{2} \sum_{j,k} \mathbf{b}_{kj} \partial_k \mathbf{b}_{ij}^T, \quad (\text{D.98})$$

$$\mathbf{b}_{ik}^S = \mathbf{b}_{ik}.$$

This last relation tells us that if we have a given Fokker–Planck equation, it corresponds to a Langevin equation to be integrated the Ito way, with a and b as drift and diffusion coefficients, and to a Langevin equation integrated the Stratonovich way with \mathbf{a}^S and \mathbf{b}^S as the corresponding drift and diffusion coefficients. The relation between the two sets of coefficients is given by (D.98).

D.6 Approximate Methods

Non-linear Langevin equations are difficult to solve exactly. We present here the Ω -expansion of van Kampen [D.4], where Ω is the size or number of

particles of our system. We consider a variable X which is proportional to the particle number, and define

$$x = \frac{X}{\Omega}. \quad (\text{D.99})$$

The key point in van Kampen's expansion is that we can separate D.4:

$$x(t) = x_0(t) + \sqrt{\epsilon}y(t), \quad (\text{D.100})$$

where $x_0(t)$ is the deterministic part, $y(t)$ represents the fluctuations with $\epsilon = 1/\Omega$. This decomposition is based on the central limit theorem that says that for large Ω , the fluctuations of X around its mean value go as Ω . Of course, this expansion fails, as we shall see, near an instability point.

We also assume that in the stochastic equation, the small parameter $\sqrt{\epsilon}$ is the noise strength, so we write

$$dx = a(x)dt + \sqrt{\epsilon}dW(t), \quad (\text{D.101})$$

and

$$x(t) = x_0(t) + \sqrt{\epsilon}x_1(t) + \epsilon x_2(t) + \dots \quad (\text{D.102})$$

Differentiating x and expanding $a(x)$ around x_0 , we get

$$\begin{aligned} & dx_0(t) + \sqrt{\epsilon}dx_1(t) + \epsilon dx_2(t) + \dots \\ &= a(x_0)dt + a'(x_0)(x - x_0)dt + \frac{1}{2}a''(x_0)(x - x_0)^2dt \\ &\quad + \dots + \sqrt{\epsilon}dW(t) \\ &= a(x_0)dt + a'(x_0)[\sqrt{\epsilon}x_1(t) + \epsilon x_2(t) + \dots] dt \\ &\quad + \frac{1}{2}a''(x_0)[\epsilon x_1^2 + \dots] dt + \sqrt{\epsilon}dW(t), \end{aligned}$$

and by comparing different orders of ϵ we get

$$dx_0(t) = a(x_0)dt, \quad (\text{D.103})$$

$$dx_1(t) = a'(x_0)x_1(t)dt + dW(t), \quad (\text{D.104})$$

$$dx_2(t) = a'(x_0)x_2(t)dt + \frac{1}{2}a''(x_0)x_1^2dt, \quad (\text{D.105})$$

and so on. The initial conditions for x_1, x_2, x_3, \dots , are

$$x_1(0) = 0, x_2(0) = 0, \text{etc} \quad (\text{D.106})$$

Now, we take a non-trivial example. A particle, in one dimension, moves under the action of a double well potential

$$a(x) = -\frac{dV}{dx}, \quad (\text{D.107})$$

with:

$$V = -\frac{\gamma}{2}x^2 + \frac{g}{4}x^4. \quad (\text{D.108})$$

The stochastic differential equation is in this case

$$dx(t) = (\gamma x - gx^3)dt + \sqrt{\epsilon}dW(t). \quad (D.109)$$

The shape of the potential is described in Fig. D.1

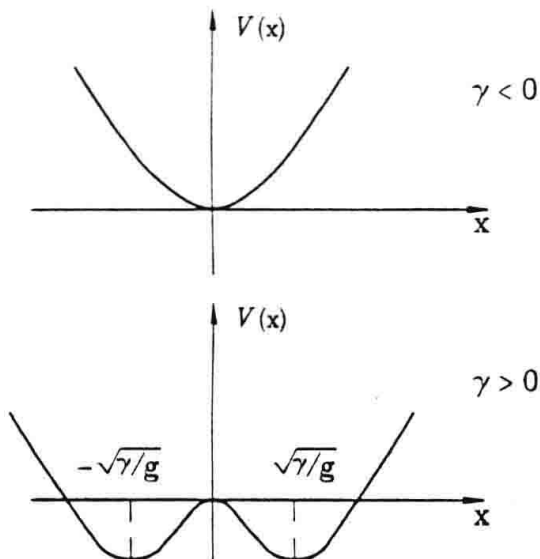


Fig. D.1. Double well potential for the cases $\gamma < 0$ (upper curve) and $\gamma > 0$ (lower curve)

We will consider the case $\gamma > 0$. Near the equilibrium positions, the drift is practically zero and the noise term in the stochastic equation is quite important. On the other hand, very far from the equilibrium positions, the motion is dominated by a large drift and is practically a deterministic one.

For $\gamma > 0$, $x = 0$ is an unstable equilibrium position and $x = \pm\sqrt{\gamma/g}$ are stable ones. Applying our method in this example, we get

$$dx_0 = (\gamma x_0 - gx_0^3)dt, x_0(0) = h, \quad (D.110)$$

$$dx_1 = (\gamma - 3gx_0^2)x_1 dt + dW, \quad x_1(0) = 0, \quad (D.111)$$

$$dx_2 = [(\gamma - 3gx_0^2)x_2 - 3gx_0x_1^2] dt, \quad x_2(0) = 0, \quad (D.112)$$

The solution, for the deterministic motion is

$$x_0(t) = \frac{h \exp(\gamma t)}{\sqrt{1 + (g/\gamma)h^2(\exp(2\gamma t) - 1)}}, \quad (D.113)$$

so that if we choose the unstable equilibrium point, that is the initial condition $h = 0$, then we get $x_0(t) = 0$, and for the stable equilibrium points, $h = \pm\sqrt{\gamma/g}$, we get $x_0(t) = \pm\sqrt{\gamma/g}$, as it should be.

For the first case, $h = x_0(t) = 0$, we get

$$dx_1 = \gamma x_1 dt + dW(t), \quad (D.114)$$

$$dx_2 = \gamma x_2 dt, \quad (D.115)$$

and the solution to the above equations are

$$\begin{aligned}x_1(t) &= \int_0^\infty \exp[\gamma(t-t')] dW(t'), \\x_2(t) &= 0.\end{aligned}\tag{D.116}$$

In the stable case $x_0 = h = \pm\sqrt{\gamma/g}$, we get

$$\begin{aligned}dx_1(t) &= -2\gamma x_1 dt + dW(t), \\dx_2(t) &= \left(-2\gamma x_2 \mp 3g\sqrt{\frac{\gamma}{g}}x_1^2 \right) dt,\end{aligned}\tag{D.117}$$

and the solutions are

$$\begin{aligned}x_1(t) &= \int_0^t dW(t') \exp[-2\gamma(t-t')] \\x_2(t) &= \mp 3g\sqrt{\frac{\gamma}{g}} \int_0^t dt' x_1^2(t') \exp[-2\gamma(t-t')].\end{aligned}\tag{D.118}$$

Now, we notice that in all cases $\langle x_1 \rangle = 0$, so

$$\langle x^2(t) \rangle = x_0^2 + \epsilon (\langle x_1^2 \rangle + 2x_0 \langle x_2 \rangle) + \dots\tag{D.119}$$

and in the two cases we can write

$$\begin{aligned}\langle x^2(t) \rangle_{\text{uns}} &= \frac{\epsilon}{2\gamma} [\exp(2\gamma t) - 1], \\ \langle x^2(t) \rangle_{\text{stable}} &= \frac{\gamma}{g} + \frac{\epsilon}{4\gamma} [1 - \exp(-4\gamma t)] - \frac{3\epsilon}{4\gamma} [1 - \exp(-2\gamma t)]^2 + \dots\end{aligned}\tag{D.120}$$

In the limit $t \rightarrow \infty$, $\langle x^2(\infty) \rangle_{\text{uns}}$ diverges, while

$$\langle x^2(t) \rangle_{\text{stable}} \rightarrow \frac{\gamma}{g} - \frac{\epsilon}{2\gamma}.$$

As we can see, the perturbative expansion gives the correct answer when starting from stable equilibrium points but it diverges when starting from an unstable equilibrium. In this last case, the perturbative expansion is no longer valid.

E. Derivation of the Homodyne Stochastic Schrödinger Differential Equation

Here we present the detailed derivation of the homodyne stochastic Schrödinger differential equation. We start from the expansion given by (16.36), which in the two-jump situation, and neglecting the commutators between the jump operators and the no-jump evolution, can be expressed as

$$\rho(\Delta t) = \sum_{m_1, m_2=0}^{\infty} \frac{(\Delta t)^{m_1+m_2}}{m_1! m_2!} S(\Delta t) J_2^{m_2} J_1^{m_1} \rho(0). \quad (\text{E.1})$$

The probability of m_1 and m_2 quantum jumps of the respective types is given by

$$P_{m_1, m_2}(\Delta t) = \frac{(\Delta t)^{m_1+m_2}}{m_1! m_2!} \text{Tr} \{ S(\Delta t) J_2^{m_2} J_1^{m_1} \rho(0) \}. \quad (\text{E.2})$$

The master equation of the field, corresponding to a lossy cavity at temperature T , may be written as

$$\begin{aligned} \frac{d\rho}{dt} &= (J_1 + J_2)\rho - \frac{\gamma}{2}\rho [a^\dagger a(1 + 2\langle n \rangle_{\text{th}}) + 2\varepsilon(1 + \langle n \rangle_{\text{th}})a^\dagger \\ &\quad + 2\varepsilon\langle n \rangle_{\text{th}}a + \langle n \rangle_{\text{th}} + \varepsilon^2(1 + 2\langle n \rangle_{\text{th}})] \\ &\quad - \frac{\gamma}{2} [a^\dagger a(1 + 2\langle n \rangle_{\text{th}}) + 2\varepsilon(1 + \langle n \rangle_{\text{th}})a + 2\varepsilon\langle n \rangle_{\text{th}}a^\dagger \\ &\quad + \langle n \rangle_{\text{th}} + \varepsilon^2(1 + 2\langle n \rangle_{\text{th}})] \rho \end{aligned} \quad (\text{E.3})$$

Therefore, according to the discussion given in Chap. 16, one possible way of writing $S(\Delta t)$ is

$$S(\Delta t)\rho = N(\Delta t)\rho N(\Delta t)^\dagger, \quad (\text{E.4})$$

with

$$\begin{aligned} N(\Delta t) &= \exp \left\{ -\frac{\gamma(\Delta t)}{2} [a^\dagger a(1 + 2\langle n \rangle_{\text{th}}) + 2\varepsilon(1 + \langle n \rangle_{\text{th}})a^\dagger \right. \\ &\quad \left. + 2\varepsilon\langle n \rangle_{\text{th}}a + \langle n \rangle_{\text{th}} + \varepsilon^2(1 + 2\langle n \rangle_{\text{th}})] \right\}. \end{aligned} \quad (\text{E.5})$$

Using (E.2) and (E.5), we can write

$$\begin{aligned}
P_{m_1, m_2}(\Delta t) &= \left[\frac{\exp \mu_1(\mu_1)^{m_1}}{m_1!} \right] \left[\frac{\exp \mu_2(\mu_2)^{m_2}}{m_2!} \right] \\
&\times \text{Tr} \left[\exp(\beta') \left(1 + \frac{a^\dagger}{\varepsilon} \right)^{m_2} \left(1 + \frac{a}{\varepsilon} \right)^{m_1} \rho \left(1 + \frac{a^\dagger}{\varepsilon} \right)^{m_1} \right. \\
&\left. \times \left(1 + \frac{a}{\varepsilon} \right)^{m_2} \exp(\beta'^*) \right], \tag{E.6}
\end{aligned}$$

where

$$\mu_1 = \gamma \Delta t \varepsilon^2 (1 + \langle n \rangle_{\text{th}}), \tag{E.7}$$

$$\mu_2 = \gamma \Delta t \varepsilon^2 \langle n \rangle_{\text{th}},$$

$$\begin{aligned}
\beta' &= -\frac{-\gamma \Delta t}{2} \left\{ a^\dagger a (1 + 2 \langle n \rangle_{\text{th}}) \right. \\
&\left. + 2 [\varepsilon (1 + \langle n \rangle_{\text{th}}) a + \varepsilon \langle n \rangle_{\text{th}} a^\dagger] + \langle n \rangle_{\text{th}} \right\}.
\end{aligned}$$

From (E.6), we can now calculate $\langle m_i \rangle$ and $\sigma_i^2 = \langle m_i^2 \rangle - \langle m_i \rangle^2$ up to order $(1/\varepsilon)^{3/2}$. The result is

$$\begin{aligned}
\langle m_i \rangle &= \mu_i (1 + \frac{2}{\varepsilon} \langle X \rangle), \\
\sigma_i^2 &= \mu_i. \tag{E.8}
\end{aligned}$$

Now, we turn to the final step of this calculation, which yields the time evolution of the state vector. After repeated jump and no-jump events, the unnormalized wavefunction for the field can be written as

$$|\tilde{\psi}\rangle_f(\Delta t) = N(\Delta t - t_m) C_2 N(t_m - t_{m-1}) C_1 N.. |\psi\rangle_f(0),$$

or, except for an overall phase factor,

$$|\tilde{\psi}\rangle_f(\Delta t) = N(\Delta t) C_2^{m_2} C_1^{m_1} |\psi\rangle_f(0), \tag{E.9}$$

where the symbol \sim indicates that the state vector is not normalized.

Using (E.2) and (E.2), one can write, up to a normalization constant,

$$\begin{aligned}
|\tilde{\psi}\rangle_f(\Delta t) &= \exp \left(-\frac{\gamma(\Delta t)}{2} \left\{ a^\dagger a (1 + \langle n \rangle_{\text{th}}) \right. \right. \\
&\left. \left. + 2 [\varepsilon (1 + \langle n \rangle_{\text{th}}) a^\dagger + \varepsilon \langle n \rangle_{\text{th}} a] \right\} \right) \\
&\times \left(1 + \frac{a^\dagger}{\varepsilon} \right)^{m_2} \left(1 + \frac{a}{\varepsilon} \right)^{m_1} |\psi\rangle_f(0), \tag{E.10}
\end{aligned}$$

or, expanding up to $\varepsilon^{-3/2}$,

$$\begin{aligned}
|\tilde{\psi}\rangle_f(\Delta t) &= \left[1 - \frac{\gamma \Delta t}{2} (a^\dagger a (1 + \langle n \rangle_{\text{th}}) + a a^\dagger \langle n \rangle_{\text{th}}) \right. \\
&\left. - \gamma \Delta t \varepsilon (a (1 + \langle n \rangle_{\text{th}}) + a^\dagger \langle n \rangle_{\text{th}}) \right] \\
&\times \left[1 + \frac{1}{\varepsilon} (m_1 a + m_2 a^\dagger) \right] |\psi\rangle_f(0). \tag{E.11}
\end{aligned}$$

We are interested in the limit $\varepsilon \rightarrow \infty$. In deriving (E.11), we considered ε large, $\gamma\Delta t \sim \varepsilon^{-3/2}$, and $m_1, m_2, \mu_1, \mu_2 \sim \varepsilon^{1/2}$. Now, we consider two random numbers with non-zero average m_1 and m_2

$$\begin{aligned} m_1 &= \langle m_1 \rangle + \frac{\sigma_1}{\sqrt{\Delta t}} \Delta W_1, \\ m_2 &= \langle m_2 \rangle + \frac{\sigma_2}{\sqrt{\Delta t}} \Delta W_2, \end{aligned} \quad (\text{E.12})$$

which satisfy

$$\langle (\Delta W_1)^2 \rangle = \langle (\Delta W_2)^2 \rangle = \Delta t. \quad (\text{E.13})$$

We notice that ΔW_i are two independent Wiener processes.

Finally, (E.11) can be written as

$$\begin{aligned} \Delta^{m_1, m_2} |\tilde{\psi}\rangle_f(\Delta t) &= |\tilde{\psi}\rangle_f(\Delta t) - |\psi\rangle_f(0) \\ &= \left\{ \left[-\frac{\gamma}{2}(1 + \langle n \rangle_{\text{th}})a^\dagger a - \frac{\gamma}{2}(\langle n \rangle_{\text{th}})aa^\dagger \right. \right. \\ &\quad + 2\gamma\langle X \rangle(a(1 + \langle n \rangle_{\text{th}}) \\ &\quad \left. \left. + a^\dagger\langle n \rangle_{\text{th}}) \right] \Delta t + a^\dagger \sqrt{\gamma\langle n \rangle_{\text{th}}} \Delta W_2 \right. \\ &\quad \left. + a \sqrt{\gamma(1 + \langle n \rangle_{\text{th}})} \Delta W_1 \right\} |\psi\rangle_f(0). \end{aligned} \quad (\text{E.14})$$

which is the desired result.

F. Fluctuations

We want to calculate $d\langle(\Delta a^\dagger a)^2\rangle$ and $M d\langle(\Delta a^\dagger a)^2\rangle$. We do it first in the simple case $T = 0$, $O = a^\dagger a$; $C = \sqrt{\gamma}a$; $H = \hbar\omega a^\dagger a$:

$$\begin{aligned} d\langle(\Delta a^\dagger a)^2\rangle &= \gamma\delta t\{-\langle a^\dagger aa^\dagger aa^\dagger a\rangle + 2\langle a^\dagger aa^\dagger a\rangle\langle a^\dagger a\rangle \\ &\quad - 2\langle a^\dagger a\rangle\langle a^\dagger a\rangle\langle a^\dagger a\rangle + \langle a^\dagger aa^\dagger a\rangle\langle a^\dagger a\rangle\} \\ &\quad - \langle a^\dagger aa^\dagger a\rangle\delta N + \langle a^\dagger a\rangle\langle a^\dagger a\rangle\delta N \\ &\quad + \frac{\langle a^\dagger a^\dagger aa^\dagger aa\rangle\langle a^\dagger a\rangle - \langle a^\dagger a^\dagger aa\rangle\langle a^\dagger a^\dagger aa\rangle}{\langle a^\dagger a\rangle\langle a^\dagger a\rangle}\delta N, \end{aligned} \quad (\text{F.1})$$

or

$$\begin{aligned} d\langle(\Delta a^\dagger a)^2\rangle &= -\gamma\delta t\langle(\Delta a^\dagger a)(\Delta a^\dagger a)(\Delta a^\dagger a)\rangle \\ &\quad - \langle(\Delta a^\dagger a)^2\rangle\delta N \\ &\quad + \frac{\langle a^\dagger a^\dagger aa^\dagger aa\rangle\langle a^\dagger a\rangle - \langle a^\dagger a^\dagger aa\rangle\langle a^\dagger a^\dagger aa\rangle}{\langle a^\dagger a\rangle\langle a^\dagger a\rangle}\delta N. \end{aligned} \quad (\text{F.2})$$

Now, we apply the above results to the more interesting case $T > 0$, $O = a^\dagger a$; $C_1 = \sqrt{(\langle n \rangle_{\text{th}} + 1)}\gamma a$, $C_2 = \sqrt{\gamma\langle n \rangle_{\text{th}}}a^\dagger$; $H = \hbar\omega a^\dagger a$:

$$\begin{aligned} d\langle(\Delta a^\dagger a)^2\rangle &= -\gamma(\langle n \rangle_{\text{th}} + 1)\langle(\Delta a^\dagger a)(\Delta a^\dagger a)(\Delta a^\dagger a)\rangle dt \\ &\quad - \langle(\Delta a^\dagger a)^2\rangle\delta N_1 \\ &\quad + \frac{\langle a^\dagger aa^\dagger aa^\dagger a\rangle\langle a^\dagger a\rangle - \langle a^\dagger aa^\dagger a\rangle\langle a^\dagger aa^\dagger a\rangle}{\langle a^\dagger a\rangle\langle a^\dagger a\rangle}\delta N_1 \\ &\quad + \gamma\langle n \rangle_{\text{th}}dt[-\langle aa^\dagger aa^\dagger aa^\dagger \rangle + 2\langle aa^\dagger aa^\dagger \rangle - \langle aa^\dagger \rangle \\ &\quad + 2\langle aa^\dagger aa^\dagger \rangle\langle a^\dagger a\rangle - 2\langle aa^\dagger \rangle\langle a^\dagger a\rangle - \langle aa^\dagger \rangle\langle a^\dagger a\rangle\langle a^\dagger a\rangle \\ &\quad + \langle a^\dagger aa^\dagger a\rangle\langle aa^\dagger \rangle - \langle a^\dagger a\rangle\langle a^\dagger a\rangle\langle aa^\dagger \rangle] \\ &\quad - \langle(\Delta a^\dagger a)^2\rangle\delta N_2 \\ &\quad + \frac{\langle aa^\dagger aa^\dagger aa^\dagger \rangle\langle aa^\dagger \rangle - \langle aa^\dagger aa^\dagger \rangle\langle aa^\dagger aa^\dagger \rangle}{\langle aa^\dagger \rangle\langle aa^\dagger \rangle}\delta N_2. \end{aligned} \quad (\text{F.3})$$

In the above expression, neither the deterministic or the stochastic term is definitely non-increasing. But in the mean it does decrease:

$$\begin{aligned}
 M \frac{d\langle(\Delta a^\dagger a)^2\rangle}{dt} &= -\gamma(\langle n \rangle_{\text{th}} + 1) \frac{\langle(\Delta a^\dagger a)a^\dagger a\rangle\langle a^\dagger a(\Delta a^\dagger a)\rangle}{\langle a^\dagger a\rangle} \\
 &\quad -\gamma\langle n \rangle_{\text{th}} \frac{\langle(\Delta aa^\dagger)aa^\dagger\rangle\langle aa^\dagger(\Delta aa^\dagger)\rangle}{\langle aa^\dagger\rangle} \\
 &\leq 0.
 \end{aligned} \tag{F.4}$$

Hints for Solutions of Problems

Chapter 1

- 1.1 Use (1.11) and (1.12).
- 1.2 Calculate $\langle n^2 \rangle$.
- 1.3 Verify the solution using (1.3).

Chapter 2

- 2.1 Use (2.36).

Chapter 3

- 3.1 Iterate (3.27) many times.
- 3.2 See Appendix A.
- 3.3 See Appendix A.
- 3.4 Follow the text from (3.39) to (3.45).
- 3.5 Use (3.44) and:

$$\frac{\partial}{\partial z} \delta_{11}^T(\rho) = \frac{\partial}{\partial z} \delta(\rho) + \frac{i}{(2\pi)^3} \int_{-\infty}^{\infty} \frac{k_3 k_1^2}{k^2} \exp(i\mathbf{k} \cdot \rho) d\mathbf{k}$$
$$\frac{\partial}{\partial x} \delta_{13}^T(\rho) = \frac{i}{(2\pi)^3} \int_{-\infty}^{\infty} \frac{k_3 k_1^2}{k^2} \exp(i\mathbf{k} \cdot \rho) d\mathbf{k}.$$

Chapter 4

- 4.1 Define

$$a^\dagger |\beta\rangle = \beta |\beta\rangle,$$

and follow the same procedure as in (4.2) to (4.6).

- 4.2 Use

$$|\alpha\rangle = \exp\left(-\frac{\alpha\alpha^*}{2}\right) \exp(\alpha a^\dagger) |0\rangle,$$

and write

$$|\alpha\rangle\langle\alpha| = \exp(-\alpha\alpha^*)\exp(\alpha a^\dagger)|0\rangle\langle 0| \exp(\alpha^*a).$$

- 4.3 Use (4.6).
- 4.4 Convert the sums into integrals.
- 4.5 Use (4.31) and (4.32).
- 4.6 Start from (4.2).
- 4.7 To prove the last property, use the second one for continuous spectrum.
- 4.8 Use the results of Problem (4.7).

Chapter 5

- 5.1 Use a procedure similar to the one leading to (5.27).
- 5.2 Use the results of Problem (5.1).
- 5.3 See Reference [5.1].
- 5.4 See Reference [5.1].
- 5.5 Use the results of Problem (5.1).

Chapter 6

- 6.1 Calculate $\langle n^2 \rangle$ as we did for $\langle n \rangle$ in (6.95).

Chapter 7

- 7.1 Use (4.16).
- 7.2 Use (3.19).
- 7.3 Use the commutation relation

$$[a, a^{\dagger n}] = n a^{\dagger(n-1)}.$$

- 7.4 Use the equations (A.23) and (A.24).

- 7.5 First show that

$$a^l F^{(n)}(a^\dagger, a) = \mathcal{N}(a + \frac{\partial}{\partial a^\dagger})^l F^{(n)}(a^\dagger, a),$$

$$F^{(n)}(a^\dagger, a) a^{\dagger l} = \mathcal{N}(a^\dagger + \frac{\partial}{\partial a})^l F^{(n)}(a^\dagger, a).$$

Chapter 8

- 8.1 Find the eigenvalues and eigenvectors of H_n .
- 8.2 Use (8.46) and (8.38).
- 8.3 Approximate (8.55).

Chapter 9

- 9.2 Verify the definitions, using the results of Problem (9.1).
 9.3 Use the rules given by (9.49).
 9.4 Use the rules given by (9.49).
 9.5 Use the rules given by (9.49).
 9.6 Find $\langle a^2 \rangle$ and $\langle a^{\dagger 2} \rangle$ from an equation similar to (9.21).

Chapter 10

- 10.1 Use (10.59)–(10.61).
 10.2 Calculate the Fourier Transform of the result of Problem (10.1).
 10.3 Use (10.84)–(10.86).

Chapter 11

- 11.1 Use (11.5) and (11.6).
 11.2 Use (11.8).
 11.3 Start from (11.22) and approximate the trigonometric functions.
 11.4 Start from (11.23).

Chapter 12

- 12.1 Use the Generalized Einstein relations.
 12.2 Use a procedure similar to (12.35)–(12.38).
 12.3 See Reference [12.1].
 12.4 Take ε^2 and differentiate with respect to time and use (12.65).

Chapter 13

- 13.1 Start from (13.12).
 13.2 Use (13.24) and follow the rules given by (9.49). Then one gets a Fokker Planck equation in terms of α_1 and α_2 . To go to polar coordinates, define

$$\alpha_1 = \rho_1 \exp(i\theta_1); \alpha_2 = \rho_2 \exp(i\theta_2),$$

then, one has

$$\frac{\partial}{\partial \alpha_1} = \frac{1}{2} \exp(-i\theta_1) \frac{\partial}{\partial \rho_1} + \frac{1}{2i} \frac{\exp(-i\theta_1)}{\rho_1} \frac{\partial}{\partial \theta_1},$$

$$\frac{\partial}{\partial \alpha_2} = \frac{1}{2} \exp(-i\theta_2) \frac{\partial}{\partial \rho_2} + \frac{1}{2i} \frac{\exp(-i\theta_2)}{\rho_2} \frac{\partial}{\partial \theta_2},$$

$$\frac{\partial}{\partial \theta_1} = \frac{1}{2} \frac{\partial}{\partial \mu} +,$$

$$\frac{\partial}{\partial \theta_2} = \frac{1}{2} \frac{\partial}{\partial \mu} - \frac{\partial}{\partial \theta},$$

where

$$\mu = \frac{\theta_1 + \theta_2}{2},$$

$$\theta = \frac{\theta_1 - \theta_2}{2}.$$

13.3 Use the results of the Problem (13.2).

Chapter 14

14.1 Start from (14.62).

14.2 Start from (14.66).

14.3 Integrate (14.38) over ω .

14.4 Part (b). Use the quadratic part of the formula for $\frac{1}{\tau}$.

14.5 Use the results of the Problem (14.4) for the case $\omega \gg \omega_j$.

Chapter 15

15.1 Use (15.5)-(15.7).

15.2 Use (15.7).

15.3 Use (15.5).

15.4 See Reference [15.5].

15.5 Use (15.49).

15.6 See Reference [15.17].

Chapter 16

16.1 See Reference [16.27].

16.2 See Reference [16.11].

Chapter 17

17.1 Use (17.7).

17.2 Verify that $[H, c] = 0$.

17.4 See Reference [17.18].

Chapter 18

- 18.1 Use (18.49) and (18.50).
- 18.2 Use (A.16) and (A.17).
- 18.3 See Appendix A.
- 18.4 See Reference [18.1].
- 18.5 See Reference [18.1].
- 18.6 See Reference [18.1].

Chapter 19

- 19.1 See Reference [19.19].
- 19.2 See Reference [19.19].

Chapter 20

- 20.1 Use (20.34),(20.41) to verify (20.42).
- 20.2 See References [20.9–12].

References

Preface

- [P.1] P. Neruda, *Antología Fundamental* (Pehuen Editores, Santiago, Chile, 1988).

Chapter 1

- [1.1] A. Einstein, Phys.Z. **18**, 121 (1917).
- [1.2] M. Planck, Verh. Deutsch. Phys. Ges. **2**, 202 (1900).
- [1.3] A. Einstein, Ann. Phys. **17**, 132 (1905).
- [1.4] A. Einstein, *The Old Quantum Theory* (Pergamon, London, 1967).
- [1.5] R. Loudon, *The Quantum Theory of Light* (Clarendon Press, Oxford, 1983).
- [1.6] L.M. Narducci, N.B. Abraham, *Laser Physics and Laser Instabilities* (World Scientific, Singapore, 1988).

Further Reading

- H. Haken, *Light Vol 1* (North-Holland, Amsterdam, 1981).
- H. Haken, *Light Vol 2* (North-Holland, Amsterdam, 1985).
- L. Mandel, E. Wolf, *Optical Coherence and Quantum Optics* (Cambridge University Press, Cambridge, 1995).
- P. Meystre, M. Sargent III, *Elements of Quantum Optics* (Springer, Berlin, Heidelberg, 1993).
- M. Sargent III, M.O. Scully, W.L. Lamb, *Laser Physics* (Addison Wesley, Reading, MA, 1974).
- M.O. Scully, M.S. Zubairy, *Quantum Optics* (Cambridge University Press, Cambridge, 1997).

Chapter 2

- [2.1] K. Thyagarajan, A.K. Ghatak, *Lasers, Theory and Applications* (Plenum Press, New York, 1981).
- [2.2] R. Loudon, *The Quantum Theory of Light* (Clarendon Press, Oxford, 1983).
- [2.3] P. Meystre, M. Sargent III, *Elements of Quantum Optics* (Springer, Berlin, Heidelberg, 1990).
- [2.4] S. Stenholm, *Lasers in Applied and Fundamental Research* (Adam Hilger, Bristol, 1985); also: S. Stenholm, *Foundations of Laser Spectroscopy* (Wiley, New York, 1983).
- [2.5] H.M. Gibbs, Phys. Rev. A **8**, 446 (1973).

Further Reading

- H.M. Nussenzveig *Introduction to Quantum Optics* (Gordon and Breach, London, 1973)

Chapter 3

[3.1] P.A.M. Dirac, Proc. Roy. Soc. A **114**, 243 (1927).

Further Reading

- C. Cohen-Tannoudji, J. Dupont-Roc, G. Grynberg, *Photons and Atoms. Introduction to Quantum Electrodynamics* (Wiley, New York, 1989).
- C. Cohen-Tannoudji, J. Dupont-Roc, G. Grynberg, *Atom-Photon Interaction* (Wiley, New York, 1992).
- C.W. Gardiner, *Quantum Noise* (Springer, Berlin, Heidelberg, 1991).
- W. Heitler, *The Quantum Theory of Radiation*, 2nd ed (Fir Lawn, NJ, 1944).
- C. Itzykson, J.B. Zuber, *Quantum Field Theory* (McGraw-Hill, New York, 1980).
- J.R. Klauder, E.C.G. Sudarshan, *Fundamentals of Quantum Optics* (W.A. Benjamin, New York, 1970).
- R. Loudon, *The Quantum Theory of Light* (Clarendon Press, Oxford, 1983).
- W.H. Louisell, *Quantum Statistical Properties of Radiation* (Wiley, New York, 1973)
- L. Mandel, E. Wolf, *Optical Coherence and Quantum Optics* (Cambridge University Press, Cambridge, 1995).
- P.W. Milonni (1994), *The Quantum Vacuum: An Introduction to Quantum Electrodynamics* (Academic Press, New York, 1994).
- J. Perina, *Quantum Statistics of Linear and Nonlinear Phenomena* (Reidel, Dordrecht, 1984).
- E.A. Power, *Introductory Quantum Electrodynamics* (Longman, London, 1964).
- B.W. Shore, *The Theory of Coherent Atomic Excitation* Vols 1 and 2 (Wiley, New York, 1990).
- W. Vogel, D.G. Welsch, *Lectures on Quantum Optics* (Akademie Verlag, Berlin, 1994).
- D.F. Walls, G.J. Milburn, *Quantum Optics* (Springer, Berlin, Heidelberg, 1994)

Chapter 4

- [4.1] R.J. Glauber, Phys. Rev. **130**, 2529 (1963); R.J. Glauber, Phys. Rev. **131**, 2766 (1963); R.J. Glauber, Phys. Rev. Lett. **10**, 84 (1963).
- [4.2] E.C.G. Sudarshan, Phys. Rev. Lett. **10**, 277 (1963).
- [4.3] W.H. Louisell, *Quantum Statistical Properties of Radiation* (Wiley, New York, 1973).

Further Reading

- R.J. Glauber, in *Quantum Optics and Electronics*, Les Houches, edited by C. De-Wit, A. Blandin, C. Cohen-Tannoudji (Gordon and Breach, New York, 1965).

Chapter 5

- [5.1] A good review of squeezed states can be found in: R. Loudon, P. Knight, J. Mod. Opt. **34**, 709 (1989); also: D.F. Walls, Nature **306**, 141 (1983).
- [5.2] D. Stoler, Phys. Rev. D **1**, 3217 (1970); D. Stoler, Phys. Rev. D **4**, 1925 (1971).
- [5.3] H.P. Yuen, Phys. Lett. A **51**, 1 (1975); H.P. Yuen, Phys. Rev. A **13**, 2226 (1976).
- [5.4] This definition, which is slightly different from that given by Yuen and Stoler, is due to C. Caves; see for example: C.M. Caves, Phys. Rev. Lett. **45**, 75 (1980); C.M. Caves, Phys. Rev. D **23**, 1693 (1982).

- [5.5] O. Hirota, *Squeezed Light* (Elsevier, Amsterdam, 1992).
- [5.6] H.P. Yuen, Phys. Rev. A **13**, 2226 (1976),
- [5.7] H.P. Yuen, J.H. Shapiro, IEEE Trans. Inf. Theory **26**, 78 (1980).
- [5.8] H.P. Yuen, J.H. Shapiro, IEEE Trans. Inf. Theory **24**, 657 (1978).
- [5.9] H.P. Yuen, J.H. Shapiro, J.A. Machado, Mata. IEEE Trans Inf. Theory **25**, 179 (1979).
- [5.10] H.P. Yuen, V.W. Chan, Opt. Lett. **8**, 177 (1983).
- [5.11] J.H. Shapiro, IEEE J. Quantum. Elect. **QE21**, 237 (1985).
- [5.12] B.L. Schumaker, Opt. Lett. **9**, 189 (1984).

Chapter 6

- [6.1] R.J. Glauber, Phys. Rev. **130**, 2529 (1963); R.J. Glauber, Phys. Rev. **131**, 2766 (1963); R.J. Glauber, Phys. Rev. Lett. **10**, 84 (1963).
- [6.2] L. Mandel, Phys. Rev. Lett. **49**, 136 (1982).
- [6.3] L. Mandel, Proc. Phys. Soc. (London) **72**, 1037 (1958).
- [6.4] L. Mandel, E.C.G. Sudarshan, E. Wolf, Proc. Phys. Soc. (London) **84**, 435 (1964).
- [6.5] C.L. Mehta, in *Progress in Optics*, Vol 8, 373, edited by E. Wolf (North-Holland, Amsterdam, 1970).
- [6.6] R. Loudon, *The Quantum Theory of Light* (Clarendon Press, Oxford, 1983).
- [6.7] P.L. Kelley, W.H. Kleiner, Phys. Rev. A **136**, 316 (1964).

Further Reading

- M. Born, E. Wolf, *Principles of Optics*, 2nd ed (Pergamon, London, 1965)

Chapter 7

- [7.1] M.O. Hillery, R.F. O'Connell, M.O. Scully, E.P. Wigner, Phys. Rep. **106**, 121 (1984).
- [7.2] E.P. Wigner, Phys. Rev. **40**, 749 (1932).

Further Reading

- R. Loudon, *The Quantum Theory of Light* (Clarendon Press, Oxford, 1983).
- W.H. Louisell, *Quantum Statistical Properties of Radiation* (John Wiley, New York, 1973).
- D.F. Walls, G.J. Milburn, *Quantum Optics* (Springer, Berlin, Heidelberg, 1994).

Chapter 8

- [8.1] E.A. Power, *Introductory Quantum Electrodynamics* (Longman, London, 1964).
- [8.2] C. Cohen-Tannoudji, J. Dupont-Roc, Grynberg, *Photons and Atoms. Introduction to Quantum Electrodynamics* (Wiley, New York, 1989).
- [8.3] P. Meystre, M. Sargent III, *Elements of Quantum Optics* (Springer, Berlin, Heidelberg, 1991).
- [8.4] B.W. Shore, P.L. Knight, J. Mod. Optics **40**, 1195 (1993).
- [8.5] F.W. Cummings, Phys. Rev. **140**, A1051 (1965).
- [8.6] S.M. Barnett, P. Filipowicz, J. Javanainen, P. Knight, in *Frontiers in Quantum Optics*, edited by E.R. Pike, S. Sarkar (Adam Hilger, London, 1986).
- [8.7] J.H. Eberly, N.B. Narozny, J.J. Sanchez-Mondragon, Phys. Rev. Lett. **44**, 1323 (1980).

- [8.8] J.H. Eberly, N.B. Narozhny, J.J. Sanchez-Mondragon, Phys. Rev. Lett. **44**, 1323 (1980).
- [8.9] N.B. Narozhny, J.J. Sanchez-Mondragon, J.H. Eberly, Phys. Rev. A **23**, 236 (1981).
- [8.10] H.I. Yoo, J.H. Eberly, Phys. Rep. **118**, 239 (1985).
- [8.11] W. Vogel, R.L. MatosFilho, Phys. Rev. A **52**, 4214 (1995).
- [8.12] D.M. Meekhof, C. Monroe, B.E. King, W.M. Itano, D.J. Wineland, Phys. Rev. Lett. **76**, 1796 (1996).
- [8.13] S.C. Gou, P.L. Knight, Phys. Rev. A **54**, 1682 (1996).
- [8.14] Y. Wu, X. Yang, Phys. Rev. Lett. **78**, 30861 (1997).
- [8.15] S. Wallentowitz, W. Vogel, Phys. Rev. A **58**, 679 (1998).

Further Reading

- L. Allen, J.H. Eberly, *Optical Resonance and Two-Level Atoms* (Wiley, New York, 1975).
- C. Cohen-Tannoudji, J. Dupont-Roc, G. Grynberg, *Atom-Photon Interaction* (Wiley, New York, 1992).
- C.W. Gardiner, *Quantum Noise* (Springer, Berlin, Heidelberg, 1991).
- W. Heitler, *The Quantum Theory of Radiation*, 2nd ed (Fir Lawn, NJ, 1944).
- C. Itzykson, J.B. Zuber, *Quantum Field Theory* (McGraw-Hill, New York, 1980).
- E.T. Jaynes, F.W. Cummings, Proc. IEEE **51**, 89 (1963).
- J.R. Klauder, E.C.G. Sudarshan, *Fundamentals of Quantum Optics* (W.A. Benjamin, New York, 1970).
- P.L. Knight, P.W. Milonni, Phys. Rep. **66**, 21 (1980).
- W.H. Louisell, *Quantum Statistical Properties of Radiation* (Wiley, New York, 1973).
- R. Loudon, *The Quantum Theory of Light* (Clarendon Press, Oxford, 1983).
- L. Mandel, E. Wolf, *Optical Coherence and Quantum Optics* (Cambridge University Press, Cambridge, 1995).
- P.W. Milonni, *The Quantum Vacuum: An Introduction to Quantum Electrodynamics* (Academic Press, New York, 1994).
- H.M. Nussenzveig, *Introduction to Quantum Optics* (Gordon and Breach, London, 1973).
- J. Perina, *Quantum Statistics of Linear and Nonlinear Phenomena* (Reidel, Dordrecht, 1984).
- M. Sargent III, M.O. Scully, W.E. Lamb, *Laser Physics* (Addison Wesley, Reading, MA, 1974).
- M.O. Scully, M.S. Zubairy, *Quantum Optics* (Cambridge University Press, Cambridge, 1997).
- B.W. Shore, *The Theory of Coherent Atomic Excitation*, Vols 1 and 2 (Wiley, New York, 1990).
- S. Stenholm, *Foundations of Laser Spectroscopy* (Wiley, New York, 1984).
- S. Stenholm, Phys. Rep. **6**, 1 (1973).
- W. Vogel, D.G. Welsch, *Lectures on Quantum Optics* (Akademie Verlag, Berlin, 1994).
- D.F. Walls, G.J. Milburn, *Quantum Optics* (Springer, Berlin, Heidelberg, 1994)

Chapter 9

- [9.1] W.H. Louisell (1973), *Quantum Statistical Properties of Radiation* (Wiley, New York, 1973).
- [9.2] L.M. Narducci, WPI Lecture Notes (unpublished) (1973).

- [9.3] I. Sneddon, *Elements of Partial Differential Equations* (McGraw-Hill, New York, 1957).
- [9.4] V. Bargmann, Commun. Pure. Appl. Math. **14**, 187 (1962).
- [9.5] H. Risken, *The Fokker-Planck Equation* (Springer, Berlin, Heidelberg, 1984).
- [9.6] C.W. Gardiner, *Handbook of Stochastic Methods* (Springer, Berlin, Heidelberg, 1983).
- [9.7] P. Meystre, M. Sargent III, *Elements of Quantum Optics* (Springer, Berlin, Heidelberg, 1990).
- [9.8] V. Weisskopf, E. Wigner, Z. Phys. **63**, 54 (1930).
- [9.9] M.J. Collett, Gardiner, Phys. Rev. A **30**, 1386 (1984).
- [9.10] C.W. Gardiner (1986), Phys. Rev. Lett. **56**, 1917 (1986).

Further Reading

- M. Lax, Phys. Rev. **145**, 110 (1966).
- H. Haken, *Laser Theory* (Springer, Berlin, Heidelberg, 1970).
- M. Sargent III, M.O. Scully, W.E. Lamb, *Laser Physics* (Addison-Wesley, Reading, MA, 1974).
- M.O. Scully, M.S. Zubairy, *Quantum Optics* (Cambridge University Press, Cambridge, 1997)

Chapter 10

- [10.1] V. Weisskopf, E. Wigner, Z. Phys. **63**, 54 (1930).
- [10.2] B.R. Mollow, Phys. Rev. **188**, 1969 (1969).
- [10.3] C. Cohen-Tannoudji, S. Reynaud, J. Phys. B **10**, 3451 (1976).
- [10.4] P.L. Knight, P.W. Milonni, Phys. Rep. **66**, 21 (1980).
- [10.5] A.L. Newstein, Phys. Rev. **167**, 89 (1968).
- [10.6] A.L. Burshtein, Sov. Phys. J. E.T.P. **21**, 567 (1965); *ibid* **22**, 939 (1966).
- [10.7] F.Y. Yu, R.E. Grove, S. Ezekiel, Phys. Rev. Lett. **35**, 1426 (1975); also: R.E. Grove, F.Y. Yu, S. Ezekiel, Phys. Rev. A **15**, 227 (1977).
- [10.8] F. Schuda, C.R. Stroud, M. Hercher, J. Phys. B, Atom. Mol. Phys. **7**, L198 (1975).
- [10.9] H. Walther, Bull. Am. Phys. Soc. II **20**, 1467 (1975);
also: W. Hartig, W. Rasmussen, R. Schieder, H. Walther, Z. Physik A **278**, 205 (1976).
- [10.10] R. Handbury Brown, R.Q. Twiss, Nature **177**, 27 (1956).
- [10.11] H.J. Carmichael, D.F. Walls, J. Phys. B, Atom. Mol. Phys. **9**, 1199 (1976).
- [10.12] H.J. Kimble, M. Dagenais, L. Mandel, Phys. Rev. Lett. **39**, 691 (1977);
Phys. Rev. A **18**, 201 (1978).
- [10.13] J.D. Cresser, J. Hager, G. Leuchs, F.M. Rateike, H. Walther, in *Dissipative Systems in Quantum Optics*, edited by R. Bonifacio (Springer, Berlin, Heidelberg, 1982).
- [10.14] S.Y. Zhu, L.M. Narducci, M.O. Scully, Phys. Rev. A **52**, 4791 (1995).
- [10.15] H.R. Xia, C.Y. Ye, S.Y. Zhu, Phys. Rev. Lett. **77**, 1032 (1996).
- [10.16] S.Y. Zhu, M.O. Scully, Phys. Rev. Lett. **76**, 388 (1996).
- [10.17] P. Zhou, S. Swain, Phys. Rev. Lett. **77**, 3995 (1996).
- [10.18] P. Zhou, S. Swain, Phys. Rev. Lett. **78**, 832 (1997).
- [10.19] E. Paspalakis, C.H. Keitel, P.L. Knight, Phys. Rev. A **58**, 4868 (1998).
- [10.20] W.S. Smyth, S. Swain, Phys. Rev. A **59**, R2583 (1999).
- [10.21] P. Zhou, S. Swain, Phys. Rev. A **59**, 1603 (1999).

- [10.22] F. Li, S.Y. Zhu, Phys. Rev. A **59**, 2330 (1999).

Line Narrowing in Fluorescence

- L.M. Narducci, M.O. Scully, G.L. Oppo, P. Ru, J.R. Tredice, Phys. Rev. A **42**, 1630 (1990).
- C.H. Keitel, L.M. Narducci, M.O. Scully, Appl. Phys. B **60**, 5153 (1995).
- C.H. Keitel, J. Mod. Opt. **43**, 1555 (1996).

Discussion on the Physical Spectrum

- J.H. Eberly, K. Wodkiewicz, J. Opt. Soc. Am. B **67**, 1252 (1977).

Chapter 11

- [11.1] Yu.M. Golubev, I.V. Sokolov, Zh. Eksp. Teor. Fiz. **87**, 408 (1984); Sov. Phys. JETP **60**, 234.
- [11.2] J. Bergou, L. Davidovich, M. Orszag, C. Benkert, M. Hillery, M.O. Scully, Opt. Comm. **72**, 82 (1989); J. Bergou, L. Davidovich, M. Orszag, C. Benkert, M. Hillery, M.O. Scully, Phys. Rev. A **40**, 5073 (1989); also: F. Haake, S.M. Tan, D. Walls, Phys. Rev. A **40**, 7121 (1989).
- [11.3] An excellent discussion on this point, as well as on noise suppression in quantum optical systems, can be found in: L. Davidovich, Rev. Mod. Phys. **68**, 127 (1996).
- [11.4] M.O. Scully, W.E. Lamb, Phys. Rev. **159**, 208 (1967); also: M. Sargent III, M.O. Scully, W.E. Lamb, *Laser Physics* (Addison Wesley, Reading, MA, 1974); M.O. Scully, W.E. Lamb, Phys. Rev. **159**, 208 (1967); M.O. Scully, W.E. Lamb, Phys. Rev. **179**, 368 (1969).
- [11.5] S. Stenholm, Phys. Rep. **6**, 1 (1973).
- [11.6] V. Degiorgio, M.O. Scully, Phys. Rev. **2**, 1170 (1970).
- [11.7] R. Graham, H. Haken, Z. Physik **237**, 31 (1970).
- [11.7] M. Lax, Phys. Rev. **157**, 213 (1967).
- [11.8] J.P. Gordon, Phys. Rev. **161**, 367 (1967).
- [11.9] H. Haken, Z. Physik **190**, 327 (1966).
- [11.10] H. Walther, Phys. Rep. **219**, 263 (1992).
- [11.11] S. Haroche, J.M. Raimond, in *Advances in Atomic and Molecular Physics*, Vol 20, p 350, edited by D. Bates, B. Benderson (Academic Press, New York, 1985).
- [11.12] J.A.C. Gallas, G. Leuchs, H. Walther, H. Figger, in *Advances in Atomic and Molecular Physics*, Vol 20, p 413, edited by D. Bates, B. Benderson (Academic Press, New York, 1985).
- [11.13] K.H. Drexhage, in *Progress in Optics*, Vol 12, edited by E. Wolf (North-Holland, Amsterdam, 1974).
- [11.14] F. De-Martini, G. Innocenti, G. Jacobitz, D. Mantolini, Phys. Rev. Lett. **29**, 2955 (1987).
- [11.15] G. Gabrielse, H. Dehmelt, Phys. Rev. Lett. **55**, 67 (1985).
- [11.16] M.S. Brune, J.M. Raimond, P. Goy, L. Davidovich, S. Haroche, Phys. Rev. Lett. **59**, 1899 (1987).
- [11.17] P. Filipowicz, J. Javanainen, P. Meystre, Phys. Rev. A **34**, 3077 (1986).
- [11.18] J.J. Slosser, P. Meystre, Phys. Rev. A **41**, 3867 (1990).
- [11.19] M. Orszag, R. Ramirez, J.C. Retamal, C. Saavedra, Phys. Rev. A **49**, 2933 (1994).
- [11.20] E. Wehner, R. Seno, N. Sterpi, B.G. Englert, H. Walther, Opt. Comm. **110**, 655 (1994).
- [11.21] K. An, J.J. Childs, R.R. Dasari, M. Feld, Phys. Rev. Lett. **73**, 3375 (1994).

- [11.22] M. Weidinger, B.T.H. Varcoe, R. Heerlein, H. Walther, Phys. Rev. Lett. **82**, 3795 (1999).

Further Reading

- F.T. Arecchi, A.M. Ricca, Phys. Rev. A **15**, 308 (1977).
- F. Casagrande, L.A. Lugiato, Phys. Rev. A **14**, 778 (1976).
- R. Graham, W.A. Smith, Opt. Comm. **7**, 289 (1973).
- L.A. Lugiato, Physics **81A**, 565 (1976).
- H. Risken, Z. Phys. **191**, 186 (1965).
- H. Risken, H.D. Vollmer, Z. Phys. **201**, 323 (1967).
- M.O. Scully, in *Proceedings of the International School of Physics ‘Enrico Fermi’ Course XLII*, edited by R. Glauber (Academic Press, New York, 1969).
- M.O. Scully, M.S. Zubairy, *Quantum Optics* (Cambridge University Press, Cambridge, 1977).

Chapter 12

- [12.1] C. Benkert, M.O. Scully, J. Bergou, L. Davidovich, M. Hillery, M. Orszag, Phys. Rev. A **41**, 2756 (1990).
- [12.2] For a different approach to pump noise, see: S. Machida, Y. Yamamoto, Y. Itaya, Phys. Rev. Lett. **58**, 100 (1987); M. Marte, H. Ritsch, D.F. Walls, Phys. Rev. Lett. **61**, 1093 (1988).
- [12.3] For many papers on the various interpretations of the quantum phase, see for example: *Quantum Phase and Quantum Phase Measurements*, edited by W.P. Schleich, S.M.W. Barnett, Physica Scripta **T48** (1993).
- [12.4] A.L. Schawlow, C.H. Townes, Phys. Rev. **112**, 1940 (1958).
- [12.5] N.G. Van Kampen, *Stochastic Processes in Physics and Chemistry* (North-Holland, Amsterdam, 1981).
- [12.6] C.W. Gardiner, *Handbook of Stochastic Processes* (Springer, Berlin, Heidelberg, 1985).
- [12.7] M.T. Fontenelle, L. Davidovich, Phys. Rev. A **51**, 2560 (1995).
- [12.8] F.S. Choa, M.H. Shih, J.Y. Fan, G.J. Simonis, P.L. Liu, T. Tanburn-Ek, R.A. Logan, W.T. Trang, A.M. Sargent, App. Phys. Lett. **67**, 2777 (1995).
- [12.9] D.L. Huffaker, J. Shin, D.G. Deppe, App. Phys. Lett. **66**, 1723 (1995); D.L. Huffaker, H. Deng, Q. Deng, D.G. Deppe, App. Phys. Lett. **69**, 3477 (1997).
- [12.10] Z. Feit, M. McDonald, R.J. Woods, V. Archambault, P. Mak, App. Phys. Lett. **68**, 738 (1996).
- [12.11] H. Taniguchi, H. Tomisawa, J. Kido, App. Phys. Lett. **66**, 1578 (1995); S. Tanosaki, H. Taniguchi, K. Tsujita, H. Inaba, App. Phys. Lett. **69**, 719 (1996).
- [12.12] K. An, J.J. Childs, R.R. Desari, M.S. Feld, Phys. Rev. Lett. **73**, 3375 (1994).
- [12.13] I. Protsenko, P. Domokos, V. Lefevre-Seguin, J. Hare, J.M. Raimond, L. Davidovich, Phys. Rev. A **59**, 1667 (1999).

Further Reading

- C.W. Gardiner, *Quantum Noise* (Springer, Berlin, Heidelberg, 1991).
- H. Haken, *Laser Theory* (Springer, Berlin, Heidelberg, 1970).
- H. Haken, *Light*, Vols 1 and 2 (Springer, Berlin, Heidelberg, 1981).
- M. Lax, in *Physics of Quantum Electronics*, edited by P.L. Kelley, B. Lax, P.E. Tannenwald (McGraw-Hill, New York, 1966).
- M. Lax, in *Statistical Physics, Phase Transition and Superconductivity*, Vol II, edited by M. Chretien, E.P. Gross, S. Dreser (Gordon and Breach, New York, 1968).

- H. Risken, *The Fokker-Planck Equation* (Springer, Berlin, Heidelberg, 1984).
- M. Sargent III, M.O. Scully, W.E. Lamb, *Laser Physics* (Addison Wesley, Reading, MA, 1974).
- M.O. Scully, M.S. Zubairy, *Quantum Optics* (Cambridge University Press, Cambridge, 1997)

Chapter 13

- [13.1] M.O. Scully, Phys. Rev. Lett. **55**, 2802 (1985).
- [13.2] J.A. Bergou, M. Orszag, M.O. Scully, Phys. Rev. A **38**, 754 (1988). For a general review of the subject of correlated emission laser, see also: M. Orszag, J.A. Bergou, W. Schleich, M.O. Scully, in *Squeezed and Non-classical Light*, edited by P. Tombesi, E.R. Pike (Plenum, NY, 1989).
- [13.3] M.O. Scully, M.S. Zubairy, Phys. Rev. A **35**, 752 (1987).
- [13.4] M.O. Scully, W.E. Lamb, Phys. Rev. **159**, 208 (1967); also: M. Sargent III, M.O. Scully, W.E. Lamb, *Laser Physics* (Addison Wesley, Reading, MA, 1974).
- [13.5] J. Krause, M.O. Scully, Phys. Rev. A **36**, 1771 (1987).
- [13.6] M.O. Scully, K. Wodkiewicz, S. Zubairy, J. Bergou, N. Lu, J. Meyer ter Vehn, Phys. Rev. Lett. **60**, 1832 (1988).

Further References

- K. Zaheer, M.S. Zubairy, Phys. Rev. A **38**, 5227 (1988).

CEL Experiments

- M. Ohtsu, K.Y. Liou, App. Phys. Lett. **52**, 10 (1988).
- M.P. Winters, J.L. Hall, P.E. Toschek, Phys. Rev. Lett. **65**, 3116 (1990).

The Largest Phase Diffusion Noise Reduction

- I. Steiner, P.E. Toschek, Phys. Rev. Lett. **74**, 4639 (1995).

A Different View of CEL

- W. Schleich, M.O. Scully, Phys. Rev. A **37**, 1261 (1988).

A General Review of CEL

- B.J. Dalton, in *New Frontiers in Quantum Electrodynamics and Quantum Optics*, edited by A.O. Barut (Plenum, New York, 1990)

Chapter 14

- [14.1] P.A. Franken, A.E. Hill, C. Peters, G. Weinreich, Phys. Rev. Lett. **7**, 118 (1961).
- [14.2] N. Bloembergen, *Nonlinear Optics* (Benjamin, New York, 1965).
- [14.3] F.A. Hopf, G. Stegeman, *Applied Classical Electrodynamics*, Vol 2 (Wiley, New York, 1986).
- [14.4] Y.R. Shen, *Principles of Nonlinear Optics* (Wiley, New York, 1984).
- [14.5] S. Kielich, *Nonlinear Molecular Optics* (Nauk, Moscow, 1981).
- [14.6] R. Loudon, *The Quantum Theory of Light* (Clarendon Press, Oxford, 1983).
- [14.7] D.F. Walls, G. Milburn, *Quantum Optics* (Springer, Berlin, Heidelberg, 1994).
- [14.8] M.J. Collett, C.W. Gardiner, Phys. Rev. A **30**, 1386 (1984).
- [14.9] C.W. Gardiner, M.J. Collett, Phys. Rev. A **31**, 3761 (1985).
- [14.10] S.F. Pereira, M. Xiao, H.J. Kimble, Phys. Rev. A **38**, 4931 (1989).
- [14.11] A. Sizman, R. Horowicz, G. Wagner, G. Leuchs, Opt. Comm. **80**, 138 (1990).

- [14.12] The theoretical approach of the generation of squeezed states in dispersive optical bistability can be found in: P.D. Drummond, D.F. Walls, J. Phys. A **13**, 725 (1980).
- [14.13] R.E. Slusher, L.W. Hollberg, B. Yurke, H.J.C. Mertz, J.F. Valley, Phys. Rev. Lett. **55**, 2409 (1985).
- [14.14] L.A. Wu, H.J. Kimble, J.L. Hall, H. Wu, Phys. Rev. Lett. **57**, 2520 (1986)

Chapter 15

- [15.1] P.A.M. Dirac, Proc. Roy. Soc. Lond. A **114**, 243 (1927).
- [15.2] L. Susskind, I. Glogower, Physics **1**, 49 (1964).
- [15.3] W.H. Louisell, Phys. Lett. **7**, 60 (1963).
- [15.4] W. Vogel, D.G. Welsch, *Lectures on Quantum Optics* (Akademie Verlag, Berlin, 1994).
- [15.5] P. Carruthers, M.M. Nieto, Phys. Rev. Lett. **14**, 387 (1965).
- [15.6] F. London, Z. Phys. **37**, 915 (1926).
- [15.7] F. London, Z. Phys. **40**, 193 (1926).
- [15.8] E.C. Lerner, Nuovo Cimento B **56**, 183 (1968).
- [15.9] J. Zak, Phys. Rev. **187**, 1803 (1969).
- [15.10] L.A. Turski, Physics **57**, 432 (1972).
- [15.11] H. Paul, D. Forts, Physik **22**, 657 (1974).
- [15.12] M. Schubert, W. Vogel, Phys. Lett. **68A**, 321 (1978).
- [15.13] S.M. Barnett, D.T. Pegg, J. Phys. A **19**, 3849 (1986).
- [15.14] S.M. Barnett, D.T. Pegg, J. Mod. Opt. **36**, 7 (1989).
- [15.15] D.T. Pegg, S.M. Barnett, Europhys. Lett. **6**, 483 (1988).
- [15.16] D.T. Pegg, S.M. Barnett, J. Phys. Rev. A **39**, 1665 (1986).
- [15.17] R. Lynch, Phys. Rev. A **41**, 2841 (1990).
- [15.18] J.H. Shapiro, S.R. Shepard, N.C. Wong, Phys. Rev. Lett. **62**, 2377 (1989).
- [15.19] W. Schleich, R.J. Horowitz, S. Varro, Phys. Rev. A **40**, 7405 (1989).
- [15.20] A. Bandilla, H. Paul, H.H. Ritze, Quant. Opt. **3**, 267 (1991).
- [15.21] W. Vogel, W. Schleich, Phys. Rev. A **44**, 7642 (1991).
- [15.22] J.W. Noh, A. Fougieres, L. Mandel, Phys. Rev. Lett. **67**, 1426 (1991).
- [15.23] J.W. Noh, A. Fougieres, L. Mandel, Phys. Rev. A **45**, 424 (1992a).
- [15.24] J.W. Noh, A. Fougieres, L. Mandel, Phys. Rev. A **46**, 2840 (1992b).
- [15.25] J.W. Noh, A. Fougieres, L. Mandel, Phys. Rev. Lett. **71**, 2579 (1993).
- [15.26] M. Orszag, C. Saavedra, Phys. Rev. A **43**, 554 (1991).

Further References

- R. Loudon, *The Quantum Theory of Light* (Clarendon Press, Oxford, 1973)

Chapter 16

- [16.1] H.J. Carmichael, *An Open System Approach to Quantum Optics*, Lecture Notes in Physics (Springer, Berlin, Heidelberg, 1993); also: L. Tian, H.J. Carmichael, Phys. Rev. A **46**, 6801 (1992).
- [16.2] J. Dalibard, Y. Castin, K. M  lmer, Phys. Rev. Lett. **68**, 580 (1992).
- [16.3] K. M  lmer, Y. Castin, J. Dalibard, J. Opt. Soc. Am. A **10**, 524 (1993).
- [16.4] F. Haake, M.J. Kolobov, C. Fabre, E. Giacobino, S. Reynaud, Phys. Rev. Lett. **71**, 995 (1993).
- [16.5] T. Pellizzari, H. Ritsch, Phys. Rev. Lett. **72**, 3973 (1994).
- [16.6] N. Gisin, I.C. Percival, J. Phys. A **25**, 5677 (1992).
- [16.7] N. Gisin, I.C. Percival, J. Phys. A **26**, 2233 (1993a).
- [16.8] N. Gisin, I.C. Percival, J. Phys. A **26**, 2245 (1993b).

- [16.9] Also, for earlier work, see: D. Bohm, J. Bub, Rev. Mod. Phys. **38**, 453 (1966); D. Pearl, Phys. Rev. D **13**, 857 (1976); L.J. Diosi, J. Phys. A **21**, 2885 (1988).
- [16.10] H.M. Wiseman, G.J. Milburn, Phys. Rev. A **47**, 642 (1993); also: H.M. Wiseman, G.J. Milburn, Phys. Rev. A **47**, 1652 (1993).
- [16.11] P. Goetsch, R. Graham, F. Haake, Quant. Semiclass. Opt. **8**, 1571 (1996)
- [16.12] G. Lindblad, Commun. Math. Phys. **48**, 119 (1976).
- [16.13] T.B. Kist, M. Orszag, T. Brun, L. Davidovich, J. Optics B **1**, 251 (1999).
- [16.14] M. Sargent III, M.O. Scully, W.E. Lamb, Jr., *Laser Physics* (Addison-Wesley, New York, 1974).
- [16.15] E.B. Davies, M.D. Srinivas, Opt. Acta **28**, 981 (1981).
- [16.16] T. Ogawa, M. Ueda, N. Imoto, Phys. Rev. Lett. **66**, 1046 (1991); Phys. Rev. A **43**, 6458 (1991); M. Ueda *et al.*, Phys. Rev. A **46**, 2859 (1992).
- [16.17] M. Brune *et al.*, Phys. Rev. A **45**, 5193 (1992); S. Haroche, M. Brune, J.M. Raimond, J. Phys. (Paris) **2**, 659 (1992).
- [16.18] R.H. Dicke, Am. J. Phys. **49**, 925 (1981).
- [16.19] G.S. Agarwal, M. Graf, M. Orszag, M.O. Scully, H. Walther, Phys. Rev. A **49**, 4077 (1994).
- [16.20] R. Dum, P. Zoller, H. Ritsch, Phys. Rev. A **45**, 4879 (1992).
- [16.21] B.M. Garraway, P.L. Knight, Phys. Rev. A **49**, 1266 (1994).
- [16.22] I. Percival, *Quantum State Diffusion* (Cambridge University Press, Cambridge, 1998).
- [16.23] N. Gisin, J. Mod. Opt. **40**, 2313 (1993).
- [16.24] N. Gisin, I. Percival, in *Experimental Metaphysics* (Kluwer, Dordrecht, 1997).
- [16.25] I.C. Percival, W.T. Strutz, J. Phys. A **31**, 1815 (1998).
- [16.26] M. Rigo, F. Mota-Furtado, G. Alber, P.F. O'Mahony, Phys. Rev. A **55**, 1165 (1997).
- [16.27] K. Mølmer, Y. Castin, Quantum. Semiclass. Opt. **8**, 49 (1996).

Further Reading

Quantum Jumps

- C. Cohen-Tannoudji, J. Dalibard, Europhys. Lett. **1**, 441 (1986).
- P. Zoller, M. Marte, D.F. Walls, Phys. Rev. A **35**, 198 (1987).

Quantum Jumps in Lasing Without Inversion

- C. Cohen-Tannoudji, B. Zambon, E. Arimondo, *Compte Rendu de l'Academie des Sciences. Serie II* **314**, 1139 (1992).
- C. Cohen-Tannoudji, B. Zambon, E. Arimondo, *Compte Rendu de l'Academie des Sciences. Serie II* **314**, 1293 (1992).
- C. Cohen-Tannoudji, B. Zambon, E. Arimondo, J. Opt. Soc. Am. B **10**, 2107 (1993).

Quantum Jumps in Laser Cooling

- Y. Castin, Mølmer, Phys. Rev. Lett. **74**, 3772 (1995).
- P. Marte, R. Dum, R. Taieb, P.D. Lett, P. Zoller, Phys. Rev. Lett. **71**, 1335 (1993).
- P. Marte, R. Dum, R. Taieb, P. Zoller, Phys. Rev. A **47**, 1378 (1993).

Quantum Jumps and Quantum Zeno Effect

- B. Misra, E.C.G. Sudarshan, J. Math. Phys. **18**, 756 (1977).

Quantum Jumps and Resonance Fluorescence

- W.L. Power, J. Mod. Optics **42**, 913 (1995).
- W.L. Power, P.L. Knight, Phys. Rev. A **53**, 1052 (1996).

- A. Beige, G.C. Hegerfeld, Phys. Rev. A **53**, 53 (1996).
- A. Beige, G.C. Hegerfeld, Quant. Optics **8**, 999 (1996); also: V. Frerichs, A. Schenzle, Phys. Rev. A **44**, 1962 (1991).
- C.W. Gardiner, A.S. Parkins, P. Zoller, Phys. Rev. A **46**, 4363 (1992).

Review Papers

- P. Zoller, C.W. Gardiner, *Lecture Notes of Les Houches Summer School on Quantum Fluctuations* (Elsevier, Amsterdam, 1995)
- P. Knight, B.M. Garraway, *Quantum Dynamics of Simple Systems, Proceedings of the 44th Scottish Universities Summer School in Physics*, edited by G.L. Oppo, S.M. Barnett, M. Wilkinson (Institute of Physics, Bristol, 1996).
- K. Molmer, Y. Castin, Quant. Opt. **8**, 49 (1996).
- M.B. Plenio, P. Knight (Los Alamos Preprint quant-ph\9702007).

Chapter 17

- [17.1] K.H. Baldwin, J. Aust, J. Phys. **49**, 855 (1996).
- [17.2] J.V. Hajnal, K.G.H. Baldwin, P.T.H. Fisk, H.A. Bachor, G.I. Opat, Opt. Comm. **73**, 331 (1989).
- [17.3] K.G.H. Baldwin, J.V. Hajnal, P.T.H. Fisk, H.A. Bachor, G.I. Opat, J. Mod. Opt. **37**, 1839 (1990).
- [17.4] O. Stern, Naturwissensch. **17**, 391 (1929).
- [17.5] P.E. Moskowitz, P.L. Gould, S.R. Atlas, D.E. Pritchard, Phys. Rev. Lett. **51**, 370 (1983).
- [17.6] P.J. Martin, P.L. Gould, B.G. Oldaker, A.H. Miklich, D.E. Pritchard, Phys. Rev. A **36**, 2495 (1987).
- [17.7] C. Tanguy, S. Reynaud, C. Cohen-Tannoudji, J. Phys. B **17**, 4623 (1984).
- [17.8] P.L. Gould, G.A. Ruff, D.E. Pritchard, Phys. Rev. Lett. **56**, 827 (1986).
- [17.9] P.J. Martin, B.G. Oldaker, A.H. Miklich, D.E. Pritchard, Phys. Rev. A **60**, 515 (1988).
- [17.10] P.L. Gould, P.G. Martin, G.A. Ruff, R.E. Stoner, L. Pique, D.E. Pritchard, Phys. Rev. A **43**, 585 (1991).
- [17.11] B. Shore, P. Meystre, S. Stenholm, J. Opt. Soc. Am. B **8**, 903 (1991).
- [17.12] V.M. Akulin, Le Kien. Fam, W.P. Schleich, Phys. Rev. A **44**, R1642 (1991).
- [17.13] S.M. Tan, D.F. Walls, Phys. Rev. A **44**, R2779 (1991).
- [17.14] M. Wilkens, E. Schumacher, P. Meystre, Opt. Comm. **86**, 34 (1991).
- [17.15] J.J. McClelland, R.E. Scholten, E.C. Palm, R.J. Celotta, Science **262**, 877 (1993).
- [17.16] I.Sh. Averbukh, V.M. Akulin, W.P. Schleich, Phys. Rev. Lett. **72**, 437 (1994).
- [17.17] E. Mayr, D. Krähmer, A.M. Herkommer, V.M. Akulin, W.P. Schleich, Acta Physica Polonica, Proceedings of Quantum Optics III (1994)
- [17.18] B. Rohwedder, M. Orszag, Phys. Rev. A **54**, 5076 (1996).
- [17.19] D.S. Saxon, *Elementary Quantum Mechanics* (Holden-Day, San Francisco, CA, 1968).
- [17.20] J.J. McClelland, R. Gupta, Z.J. Jabbour, R.J. Celotta, Aust. J. Phys. **49**, 555 (1996).

Chapter 18

- [18.1] V.B. Braginsky, F.Y. Khalil, *Quantum Measurements* (Cambridge University Press, Cambridge, 1992).

- [18.2] C. Caves, K.S. Thorne, R.W.P. Drever, V.D. Sandberg, M. Zimmermann, Rev. Mod. Phys. **52**, 341 (1980).
- [18.3] M. Ozawa, in *Squeezed and Nonclassical Light*, edited by P. Tombesi, E.R. Pike (Plenum, New York, 1988).
- [18.4] M.D. Levenson, R.M. Shelby, M. Reid, D.F. Walls, Phys. Rev. Lett. **57**, 2473 (1986).
- [18.5] N. Imoto, S. Watkins, Y. Sasaki, Opt. Comm. **61**, 159 (1987).
- [18.6] A. LaPorta, R.E. Slusher, B. Yurke, Phys. Rev. Lett. **62**, 28 (1989).
- [18.7] P. Grangier, J.F. Roch, G. Roger, Phys. Rev. Lett. **66**, 1418 (1991).
- [18.8] M. Brune, S. Haroche, J.M. Raimond, L. Davidovich, N. Zagury, Phys. Rev. A **45**, 5193 (1992); also: M. Brune, S. Haroche, V. Lefebvre, J.M. Raimond, N. Zagury, Phys. Rev. Lett. **65**, 976 (1990).
- [18.9] V.B. Braginsky, Y.I. Vorontsov, Sov. Phys. Usp. **17**, 644 (1975).
- [18.10] M. Ueda, N. Imoto, H. Nagaoka, T. Ogawa, Phys. Rev. A **46**, 2859 (1992).
- [18.11] T. Ogawa, M. Ueda, N. Imoto, Phys. Rev. Lett. **66**, 1046 (1991); Phys. Rev. A **43**, 6458 (1991).
- [18.12] G.S. Agarwal, M.O. Scully, H. Walther, Physica Scripta, **148**, 128 (1993).
- [18.13] G.S. Agarwal, M. Graf, M. Orszag, M.O. Scully, H. Walther, Phys. Rev. A **49**, 4077 (1994).

Further Reading

- V.B. Braginsky, Y.I. Vorontsov, K.S. Thorne, Science **209**, 5471 (1980).
- G.J. Milburn, D.F. Walls, Phys. Rev. A **28**, 2065 (1983).
- N. Imoto, H.A. Haus, Y. Yamamoto, Phys. Rev. A **32**, 2287 (1985).
- B. Yurke, J. Opt. Soc. Am. B **2**, 732 (1985).

Chapter 19

- [19.1] C. Cohen-Tannoudji, Cours de Physique Atomique et Moléculaire (notes, 1986).
- [19.2] E.L. Ince, *Ordinary Differential Equations* (Dover, New York, 1956).
- [19.3] J. Javanainen, J. Opt. Soc. Am. B **5**, 73 (1988).
- [19.4] F. Dietrich, J.C. Bergquist, W.M. Itano, D.J. Wineland, Phys. Rev. Lett. **62**, 403 (1989).
- [19.5] W. Nagourney, J. Sandberg, H.G. Dhemelt, Phys. Rev. Lett. **56**, 2797 (1986); T.H. Sauter, W. Neuhauser, R. Blatt, P. Toschek, Phys. Rev. Lett. **57**, 1696 (1986); J.C. Berquist, R.G. Hulet, I.W.M. Itano, D.J. Wineland, Phys. Rev. Lett. **57**, 1699 (1986).
- [19.6] M. Kasevich, S. Chu, Phys. Rev. Lett. **69**, 1741 (1992).
- [19.7] D.J. Heinzen, D.J. Wineland, Phys. Rev. A **42**, 2977 (1990).
- [19.8] C. Monroe, D.M. Meekhof, B.E. King, S.R. Jefferts, W.M. Itano, J.M. Wineland, P. Gould, Phys. Rev. Lett. **75**, 4011 (1995); C. Monroe, D.M. Meekhof, B.E. King, W.M. Itano, J.M. Wineland, Phys. Rev. Lett. **75**, 4714 (1995).
- [19.9] C. Monroe, D.M. Meekhof, B.E. King, J.M. Wineland, Science **272**, 1131 (1996).
- [19.10] W.M. Itano, D.J. Heinzen, J.J. Bollinger, D.J. Wineland, Phys. Rev. A **41**, 2295 (1990).
- [19.11] J.C. Retamal, notes and private communication.
- [19.12] C. Monroe, Lecture notes, Swieca School, Rio de Janeiro (1996).
- [19.13] I. Marzoli, J.I. Cirac, R. Blatt, P. Zoller, Phys. Rev. A **49**, 2771 (1994).
- [19.14] J.C. Retamal, N. Zagury, Phys. Rev. A **55**, 2387 (1997).
- [19.15] L. Davidovich, M. Orszag, N. Zagury, Phys. Rev. A **54**, 5118 (1996).

- [19.16] W. Vogel, R.L. deMathos Filho, Phys. Rev. Lett. **22**, 4608 (1996).
- [19.17] J.I. Cirac, A.S. Parkins, R. Blatt, P. Zoller, Phys. Rev. Lett. **70**, 556 (1993).
- [19.18] D.M. Meekhof, C. Monroe, B.E. King, W.M. Itano, J.M. Wineland, P. Gould, Phys. Rev. Lett. **76**, 1796 (1996).
- [19.19] P.J. Bardroff, C. Leichtle, G. Schrade, W.P. Schleich, Acta Phys. Slov. **46**, 231 (1996).
- [19.20] K.E. Cahill, R.J. Glauber, Phys. Rev. **177**, 1857 (1969).
- [19.21] J.I. Cirac, L.J. Garay, R. Blatt, A.S. Parkins, P. Zoller, Phys. Rev. A **49**, 421 (1994).
- [19.22] H. Moya-Cessa, S. Wallentowitz, V.W. Vogel, Phys. Rev. A **59**, 2920 (1999).
- [19.23] Q.A. Turchette, C.S. Wood, B.E. King, C.J. Myatt, D. Leibfried, W.M. Itano, C. Monroe, D.J. Wineland, Phys. Rev. Lett. **81**, 3631 (1998).
- [19.24] E. Solano, R.L. de Matos Filho, N. Zagury, Phys. Rev. A **59**, R2539 (1999).
- [19.25] G. Morigi, J. Eschner, J.I. Cirac, P. Zoller, Phys. Rev. A **59**, 3797 (1999).

Observation of Quantum Jumps on Single Ions :

- W. Nagourney, J. Sandberg, H. Dhemelt, Phys. Rev. Lett. **56**, 2797 (1986).
- Th. Sauter, W. Neuhauser, R. Blatt, P.E. Toschek, Phys. Rev. Lett. **57**, 1696 (1986).
- J.C. Bregquist, R.G. Hulet, W.M. Itano, D.J. Wineland, Phys. Rev. Lett. **57**, 1699 (1986).

Photon Antibunching in Single Ions

- F. Dietrich, H. Walther, Phys. Rev. Lett. **58**, 203 (1987)

Chapter20

- [20.1] W.H. Zurek, Physics Today **44**, 36 (1991).
- [20.2] W.H. Zurek, Phys. Rev. A **24**, 1516 (1981).
- [20.3] W.H. Zurek, Phys. Rev. A **26**, 1862 (1982).
- [20.4] N. Bohr, Nature **121**, 580 (1928).
- [20.5] J. Von Neumann, *Matematische Grundlagen der Quantenmechanik* (Springer, Berlin, Heidelberg, 1932).
- [20.6] D. Giulini, E. Joos, C. Kiefer, J. Kupsch, I.O. Stamatescu, H.D. Zeh, *Decoherence and the Appearance of the Classical World in Quantum Theory* (Springer, Berlin, Heidelberg, 1997).
- [20.7] D.F. Walls, G.J. Milburn, Phys. Rev. A **31**, 2403 (1985).
- [20.8] D.F. Walls, G.J. Milburn, *Quantum Optics* (Springer, Berlin, Heidelberg, 1994).
- [20.9] V. Buzek, P.L. Knight, in *Progress in Optics* Vol XXXIV, 1, edited by E. Wolf (Elsevier, Amsterdam, 1995).
- [20.10] M.S. Kim, V. Buzek, Phys. Rev. A **46**, 4239 (1992).
- [20.11] M.S. Kim, V. Buzek, J. Mod. Opt. **39**, 1609 (1992).
- [20.12] M.S. Kim, V. Buzek, Phys. Rev. A **47**, 610 (1993).
- [20.13] S. Schneider, G.J. Milburn, Phys. Rev. A **57**, 3748 (1998).
- [20.14] M. Munrao, P.L. Knight, Phys. Rev. A **58**, 663 (1998).
- [20.15] S. Schneider, G.J. Milburn, Phys. Rev. A **59**, 3766 (1999).

Quantum Coherence in Cavity QED

- L. Davidovich, M. Brune, J.M. Raimond, S. Haroche, Phys. Rev. A **53**, 1295 (1996).

Appendix A

- [A.1] W.H. Louisell, *Quantum Statistical Properties of Radiation* (Wiley, New York, 1973)

Appendix B

- [B.1] I. Sneddon, *Elements of Partial Differential Equations* (McGraw-Hill, New York, 1957)

Appendix C

- [C.1] An excellent discussion on this point, as well and on noise suppression in quantum optical systems, can be found in: L. Davidovich, Rev. Mod. Phys. **68**, 127 (1996).
- [C.2] C. Benkert, M.O. Scully, J. Bergou, L. Davidovich, M. Hillery, M. Orszag, Phys. Rev. A **41**, 2756 (1990).

Appendix D

- [D.1] S. Stenholm, in *Quantum Optics, Experimental Gravitation and Measurement Theory*, edited by P. Meystre, M.O. Scully (Plenum, New York, 1983).
- [D.2] C.W. Gardiner, *Handbook of Stochastic Methods* (Springer, Berlin, Heidelberg, 1983).
- [D.3] N.G. Van Kampen, *Stochastic Processes in Physics and Chemistry* (North-Holland, Amsterdam, 1981).
- [D.4] N.G. Van Kampen, Can. J. Phys. **39**, 551 (1961).
- [D.5] P. Tombesi, in *Stochastic Processes Applied to Physics and Other Related Fields*, edited by B. Gomez, S.M. Moore, A.M. Rodriguez-Vargas, A. Rueda (World Scientific, Singapore, 1983).

Index

A and *B* coefficients
- spontaneous and stimulated emission 1
aberrations
- chromatic, atomic focusing 245
- isotopic, atomic focusing 245
- spherical, atomic focusing 245
absorption 1, 2
adiabatic approximation, laser theory 158
annihilation operator 24
- generalized 41
antinormal ordering, *Q*-representation 71
atom-field interaction, semiclassical theory 11
atom optics 231
- diffraction 232
- experiments in diffraction 233
- optical elements 231
- sources 231
- theory of diffraction 234
atomic lifetime 5
atomic decay 18
atomic diffraction
- large detuning 237
- no detuning 236
atomic focusing 239
- chromatic aberrations 245
- classical focus 243
- experiment 240
- isotopic aberrations 245
- quantum focal curve 244
- quantum focus 243
- spherical aberrations 245
- theory 240
-- initial conditions and solution 241
- thin versus thick lenses 243
atomic noise correlation functions 155
atomic noise moments 153
atomic phase, measurement 255

Baker-Campbell-Haussdorf relation 31, 302
birth and death process 315
blackbody energy 3
Bloch equations 16, 17
Boltzmann factor 34
Boltzmann distribution 3
Bose-Einstein distribution 4
boundary conditions
- exponential 22
- input-output theory 181
- sinusoidal 22
broad-band spectrum 14
Chapman-Kolmogorov equation 313
- forward 314
characteristic function 74
- defined in an antinormal way 74
- defined in a normal way 74
- defined in the symmetric way 74
- normally ordered 76
chromatic aberration, atom focusing 245
coherence
- first-order 59, 60
- *n*-th-order 60
- second-order 60
-- classical 60
-- quantum mechanical 62
-- quantum theory 62
- second-order effects 60
coherence function
- first-order 52
- *n*-th-order 52
coherent squeezed state 42
coherent state 29
- coordinate representation 33
- displacement operator 31
- minimum uncertainty state 30, 40
- non-orthogonality 30
- normalization 29
- overcompleteness 31

- photon statistics 32
- Poisson statistics 32
- coincidence rate, n -th fold 56
- collapse time 89
- collapse and revivals 88
- commutation relation
 - between the electric field and the vector potential 26
 - between two different components of the electric field 27
 - between two different components of the magnetic field 27
 - between two different components of the vector potential 27
 - Dirac's commutator 197
 - Loisell's trigonometric functions 192
 - number-phase 191
 - Susskind-Glogower phase 193
- commutation relations 23, 24, 26, 27
- conditional probability 312
- continuous measurements 261
 - phase narrowing 263, 266
- coordinate representation of a coherent state 33
- correlated emission laser 163
- correlated emission laser (CEL) systems
 - 164
 - holographic laser 171
 - two-photon laser 171
- correlation function
 - atomic noise 155
 - classical 61
 - first-order 58, 59
 - general properties 56
 - n -th-order 56
 - second-order 60, 63
 - examples 63
- correlations
 - dynamics of 293
 - intensity, resonance fluorescence 123
 - second-order 60
- Coulomb gauge 21, 82
- creation operator 24
- damping, quantum theory 93
- decay
 - between levels 18
 - to unobserved levels 17
- decimation 260
 - in vibrational states 287
- decoherence
 - how long it takes 295
 - in phase-sensitive reservoirs 299
 - non-classical motion 299
 - decoherence time 298
 - degenerate parametric oscillator
 - input-output theory 183
 - quadrature fluctuations, input-output theory 184
 - density matrix
 - multimode thermal state 35
 - time evolution of elements 98
 - density of modes 26
 - density operator
 - in P -representation 100
 - in terms of the Q -function 73
 - modified with continuous measurements 263
 - thermal state 34
 - detailed balance 319
 - detectors
 - ideal 51
 - n -atom 55
 - one-atom 52
 - diffusion coefficients 157
 - dipole approximation 83, 173
 - detrapping state 144
 - dressed states 85, 87
 - drift and diffusion coefficients 321
 - Dyson's time ordering operator 55
 - Dyson's expansion 212
 - Einstein relations (generalized) 152
 - Einstein's theory of atom-radiation interaction 1
 - electric dipole approximation 12
 - electric field
 - per photon 83
 - positive frequency component 58
 - emission
 - spontaneous 1, 2
 - stimulated 1, 2
 - energy
 - ground state 24
 - multimode radiation field 23
 - zero-point 24
 - energy density 2
 - ergodic hypothesis 67
 - events 312
 - evolution, diffusion-like 224
 - Fermi golden rule 175
 - generalized 177
 - fluctuations
 - of intensity 159

- of phase 159
- Fock states 24
- Fokker-Planck equation 311, 317
 - damped harmonic oscillators 101, 103
 - for the Glauber-Sudarshan representation 100
 - general properties 319
 - several dimensions 317
 - steady-state solution 319
 - time-dependent solution 101
- free radiation field 81
- gain, laser theory 158
- generalized Einstein relations 152
- generating function 66
- generation of non-classical vibrational states 288
- Hamiltonian
 - A system with two-mode radiation field 263
 - to realize a stochastic Schrödinger equation 218
 - atom in thermal bath 105
 - atom-field interaction 52, 81
 - atom-radiation interaction 173
 - atomic diffraction 234
 - large detuning 238
 - atomic focusing 240
 - degenerate parametric oscillator 183
 - dipole approximation 81, 83
 - effective 276
 - free atom 12, 52
 - free field 52
 - interaction of quantum beat laser 166
 - Jaynes-Cummings 85, 88, 129
 - non-degenerate parametric amplifier 178
 - atom-field interaction 52
 - one-atom Raman laser 207
 - quantum beat laser 164
 - resonance fluorescence 114
 - trapped ion in the Raman scheme 276, 277
- harmonic oscillator, quantization rule 23
- Heisenberg picture 27
- Heisenberg equations
 - damped harmonic oscillator 103
 - non-degenerate parametric amplifier 178
- resonance fluorescence 115
- system-bath Hamiltonian 180
- Hermite polynomial of degree n 44
- Hermitian phase operator 196
- homodyne stochastic Schrödinger differential equation 218, 329
- ideal photon counter 55
- injection statistics, heuristic discussion 131
- input field, definition 181
- input-output theory 179
- isotopic aberration, atomic focusing 245
- Ito versus Stratonovich 322
- Ito's Fokker-Planck equation 324
- Ito's formula 324
- Jaynes-Cummings Hamiltonian 85, 88, 129, 261
- Jaynes-Cummings model 144
 - two photon 282
- joint probability 312
- Kramer-Heisenberg formula 189
- Lamb-Dicke expansion 281
- Lamb-Dicke parameter 280
- Langevin equations 103
 - of the damped harmonic oscillator 104
 - Langevin quantum laser theory 151
 - laser theory 4
 - diffusion coefficients 157
 - elementary 5
 - Langevin equations, normal ordering 157
 - linewidth 137
 - - alternative derivation 138
 - master equation approach 129
 - population inversion 6
 - quantum beat laser 168, 169
 - - phase diffusion 160
 - - photon statistics 169
 - Raman laser 208
 - random injection 133
 - rate equations 6
 - stability analysis 7
 - steady-state intensity 160
 - steady-state 6
 - threshold condition 6
 - with pump statistics 146
 - laser theory, quantum mechanical

- *c*-number Langevin equations 157
- adiabatic approximation 158
- atomic noise correlation 155
- Fokker Planck equation 137
- general Master equation 133
- injection statistics, heuristic discussion 131
- Langevin equations 155
- noise reduction 150
- noise suppression via pump statistics 161
- phase and intensity fluctuations 159
- phase diffusion 137
- photon statistics 134
- light
 - Poissonian 63, 64
 - sub-Poissonian 63, 64
 - super-Poissonian 63, 64
- Liouville equation 95
- Liouville's equation 94
- Liouville's equation
 - trapped ion in the Raman scheme 278
- localization 221
 - analytical proof 225
- Markoffian assumption 95
- Markov approximation 105
- Markov stochastic processes 313
- Master equation 95, 205, 315
 - atom in thermal bath 106
 - damped harmonic oscillator 96
 - damped oscillator in squeezed bath 107
 - generalized with pump statistics 132
 - laser and micromaser with pump statistics 146
 - Lindblad form 205
 - micromaser 142
 - quantum beat laser 168, 170
 - two-level atom in thermal bath 106
- Maxwell's equations 21
- Maxwellian velocity distribution 258
- measurements 247
 - atomic phase 255
 - continuous 261
 - in a dynamical sense 294
 - two-mode system 263
 - Von Neumann 291
- method of characteristics 99, 305
- micromaser 131
- cooperative effects 146
- Master equation 142
- noise reduction 149
- operation 141
- photon statistics 143
- quantum theory 140
- squeezing in trapping states 146
- tangent and cotangent trapping states 145
- trapping condition 144
- trapping states 144
- minimum uncertainty states 30
- mixed state 33
 - density operator for thermal state 34
 - thermal distribution 34
- momentum distribution, atomic diffraction 237
- momentum generating function $Q(s)$ 63
- Monte Carlo method 213
- Monte Carlo wavefunction method 206
- multimode radiation field, energy 23
- multimode squeezed state 44
- multiple photon transitions 173
- n*-atom-detector 55
- noise operator, damped harmonic oscillator 105
- non-commuting operators 301
- non-classical vibrational states 288
- non-Hermitian Hamiltonian 206
- non-linear Langevin equation 325
- non-linear optics 173
- normal modes in a cavity 25
- normal ordering, *P*-representation 74
- normalized correlation function
 - first-order 59
 - second-order 60
- normally ordered products, average 75
- one-atom laser
 - Hamiltonian 207
 - Raman 207
- one-atom detector 52
- optical Bloch equations 17
- optical nutation 18
- Ornstein-Uhlenbeck process 321
- orthogonality condition 22
- orthonormality condition 12
- output field, definition 181

- P*-representation 71, 74
 - averages of normally ordered products 75
 - coherent state 77
 - examples 76
 - Fourier transform 75
 - normalization 74
 - number state 77
- parametric amplification 177
- parametric amplifier
 - degenerate 178
 - non-degenerate 177
 - quadrature fluctuations, ideal case 178
- parametric oscillator, degenerate 183
- Paul trap 269
 - boundary between stable and unstable solutions 275
 - equations of motion 270
 - general properties 269
 - Mathieu's equation 273
 - oscillation frequencies 271
 - stability analysis 272
- Pauli matrices 83
- phase
 - Dirac 191
 - Louisell 192
 - Pegg Barnett 195
 - Susskind-Glogower 192
- phase fluctuations
 - Pegg and Barnett
 - coherent state 200
 - Fock state 199
 - laser 202
- phase operator, Hermitian 196
- phinholes 58
- photoelectric effect 65
- photoelectric emission, fluctuations 67
- photoelectron distribution 67
- photoemission 66
- photon
 - antibunching 60, 64
 - - resonance fluorescence 126
 - bunching 60, 64
- photon count distribution 68
 - chaotic state 69
 - coherent state 69
 - quantum-mechanical 68
- photon counting 65
- photon number, differential equation 105
- photon statistics, thermal state 34
- photons 1
 - spontaneously emitted 17
- plane waves 22
- Poisson distribution of incoming atoms 62
- Poisson statistics of the coherent state 32
- population inversion 4
- potential condition 320
- power spectrum in resonance fluorescence 121
- Q*-representation 71
 - examples 72
 - anti-normally ordered products 72
 - density operator 73
 - normalization 71
 - of a coherent state 72
 - of a number state 72
 - of a thermal state 72
- quadrature operators 39
- quadrature squeezing in degenerate parametric oscillator, experimental evidence 185
- quantization rule for the harmonic oscillator 23
- quantum and classical foci 242
- quantum beat laser 164
 - Master equation 168
 - photon statistics 169
 - rotating wave approximation 165
- quantum diffusion 229
- quantum efficiency 48, 65
- quantum jumps 205, 206, 222
- quantum non-demolition measurements 250
 - condition 252
 - effect of measuring apparatus 253
 - experiments 250
 - in cavity QED 251, 253
 - of the number of photons in a cavity 259
 - of photon number 259
 - of vibrational states 285
- quantum non-demolition observable 252
- quantum phase
 - Dirac 191
 - Louisell 192
 - Pegg and Barnett
 - - coherent states 199
 - - Fock states 198
 - - hermitian phase operator 196
 - - orthonormal states 196

- phase state 195
- properties 198
- Susskind-Glogower 191, 192
- expectation values 194
- quantum standard limit 247
- for a free particle 247
- for an oscillator 248
- quantum trajectories 205

- Rabi oscillations 16
 - dressed state picture 85
 - quantum mechanical 87
- Raman cooling 281, 282
- Raman effect 177
- Raman Nath approximation, atomic diffraction 238
- Raman scattering 189
- Ramsey fields 255
 - to measure the atomic phase 255
- random walk, one-sided 315
- rate equations 2, 5
- Rayleigh scattering 114
- revival 91
- rotating-wave approximation 85
- Rydberg atoms 140, 141
- Rydberg states 140

- saturation coefficient, laser theory 158
- Schawlow-Townes linewidth 161
- Schrödinger equation 53
 - atomic diffraction 235
 - stochastic 210, 211
 - time-dependent 12
 - two-dimensional harmonic oscillator 102
- Schrödinger operator 24
- Schrödinger picture 24, 27
- second harmonic generation, early experiment 173
- spectral energy 14
- spectrum 14
 - broad band 14
 - emission from driven two-level atoms 120
 - three-peaked
 - resonance fluorescence 123
- spherical aberration
 - atomic focusing 245
- spherical waves 58
- spontaneous decay in squeezed bath 109
- squeeze operator 41
- squeezed states
 - balanced detection 45
 - balanced homodyne detection 47
 - calculation of moments 42
 - detection 39
 - direct detection 45
 - eigenstate of A 42
 - general properties 39
 - heterodyne detection 45, 48
 - minimum uncertainty state 40
 - ordinary homodyne detection 45, 46
 - photon statistics 44
 - pictorial representation 42
 - quadrature fluctuations 43
 - second-order correlation function 64
 - squeeze operator 41
- squeezed states
 - calculation of moments 42
 - multimode 44
- squeezing
 - degenerate parametric oscillator 185
 - double ended cavity 185
 - single ended cavity 185
 - spectrum
 - degenerate parametric oscillator 185
 - standard quantum limit 248
 - harmonic oscillator 248
 - thermal effects 249
 - states of the electromagnetic field 29
 - steady-state photon statistics
 - above threshold 136
 - below threshold 135
 - stochastic differential equations 320
 - stochastic equation, instability point 326
 - stochastic processes 313
 - Chapman-Kolmogorov equation 313
 - independence 313
 - Markov process 313
 - stochastic Schrödinger equation 206, 209, 210, 211
 - Stratonovich's Fokker-Planck equation 325
 - sub-Poissonian 64
 - super-Poissonian 64
 - system-apparatus coupling 294

 - thermal energy 3
 - thermal equilibrium 3, 34
 - thermal radiation 33, 34

- time evolution operator 55
- transition probability 51, 54, 55
- transverse momentum change, atom optics 234
- trapped ions 276
 - effective Hamiltonian 278
 - observation of non-classical vibrational states 276
 - theory 276
- trapping block 144
- trapping states
 - micromaser 144
 - tangent and cotangent states 145
- two-mode squeeze operator 45
- two-level atom 14, 83
- upwards trapping condition 144
- Van Kampen's expansion 326
- vector potential 22
- visibility 59
- white noise 320
- Wiener increments 318
- Wiener process 209, 317, 322, 331
- Wiener-Kinchine theorem 118
- Wigner representation 71, 77
 - moments 78
 - symmetric ordering 77
- Wigner-Weisskopf theory for spontaneous emission 107
- Young interference 58
- zero-point energy 23

Images have been losslessly embedded. Information about the original file can be found in PDF attachments. Some stats (more in the PDF attachments):

```
{  
  "filename": "NDA3MTIxMjQuemlw",  
  "filename_decoded": "40712124.zip",  
  "filesize": 55350200,  
  "md5": "a3a0d210626c0ab1f37aa1fad5eed220",  
  "header_md5": "4ea43d17f98008ef280525ed2b4b2e28",  
  "sha1": "e238ddf0343e3e2840f642fd489863e9e34d552f",  
  "sha256": "b543792264fa858eefa7f8e238a6e38458c808c07b23b0725c16285a4596db4f",  
  "crc32": 2354756974,  
  "zip_password": "",  
  "uncompressed_size": 55259458,  
  "pdg_dir_name": "40712124",  
  "pdg_main_pages_found": 361,  
  "pdg_main_pages_max": 361,  
  "total_pages": 378,  
  "total_pixels": 2131415340,  
  "pdf_generation_missing_pages": false  
}
```